Volume 6, Number 1 January 2011

ISSN:1559-1948 (PRINT), 1559-1956 (ONLINE)

EUDOXUS PRESS,LLC

JOURNAL OF APPLIED FUNCTIONAL ANALYSIS

GUEST EDITORS: HIKMET CAGLAR, LEVENT CUHACI, GURSEL HACIBEKIROGLU and MEHMET OZER

SPECIAL ISSUE I: "CHAOS and COMPLEX SYSTEMS 2010"

SCOPE AND PRICES OF

JOURNAL OF APPLIED FUNCTIONAL ANALYSIS

A quartely international publication of **EUDOXUS PRESS,LLC**

ISSN:1559-1948(PRINT),1559-1956(ONLINE)

Editor in Chief: George Anastassiou
Department of Mathematical Sciences
The University of Memphis
Memphis, TN 38152,USA
E mail: ganastss@memphis.edu

The purpose of the "Journal of Applied Functional Analysis"(JAFA) is to publish high quality original research articles, survey articles and book reviews from all subareas of Applied Functional Analysis in the broadest form plus from its applications and its connections to other topics of Mathematical Sciences. A sample list of connected mathematical areas with this publication includes but is not restricted to: Approximation Theory, Inequalities, Probability in Analysis, Wavelet Theory, Neural Networks, Fractional Analysis, Applied Functional Analysis and Applications, Signal Theory, Computational Real and Complex Analysis and Measure Theory, Sampling Theory, Semigroups of Operators, Positive Operators, ODEs, PDEs, Difference Equations, Rearrangements, Numerical Functional Analysis, Integral equations, Optimization Theory of all kinds, Operator Theory, Control Theory, Banach Spaces, Evolution Equations, Information Theory, Numerical Analysis, Stochastics, Applied Fourier Analysis, Matrix Theory, Mathematical Physics, Mathematical Geophysics, Fluid Dynamics, Quantum Theory. Interpolation in all forms, Computer Aided Geometric Design, Algorithms, Fuzzyness, Learning Theory, Splines, Mathematical Biology, Nonlinear Functional Analysis, Variational Inequalities, Nonlinear Ergodic Theory, Functional Equations, Function Spaces, Harmonic Analysis, Extrapolation Theory, Fourier Analysis, Inverse Problems, Operator Equations, Image Processing, Nonlinear Operators, Stochastic Processes, Mathematical Finance and Economics, Special Functions, Quadrature, Orthogonal Polynomials, Asymptotics, Symbolic and Umbral Calculus, Integral and Discrete Transforms, Chaos and Bifurcation, Nonlinear Dynamics, Solid Mechanics, Functional Calculus, Chebyshev Systems. Also are included combinations of the above topics.

Working with Applied Functional Analysis Methods has become a main trend in recent years, so we can understand better and deeper and solve important problems of our real and scientific world.

JAFA is a peer-reviewed International Quarterly Journal published by Eudoxus Press,LLC.

We are calling for high quality papers for possible publication. The contributor should send four copies of the contribution to the EDITOR in CHIEF in TEX,LATEX double spaced,in ten point type size. They should be sent BY REGULAR MAIL ONLY, NOT REGISTERED MAIL, AND NO E-MAIL SUBMISSIONS [See: Instructions to Contributors]

Journal of Applied Functional Analysis(JAFA)
is published in January,April,July and October of each year by

EUDOXUS PRESS,LLC,
1424 Beaver Trail Drive,Cordova,TN38016,USA,
Tel.001-901-751-3553
anastassioug@yahoo.com
http://www.EudoxusPress.com visit also http://www.msci.memphis.edu/~ganastss/jafa.

Webmaster:Ray Clapsadle

Annual Subscription Current Prices:For USA and Canada,Institutional:Print $400,Electronic $250,Print and Electronic $450.Individual:Print $ 150, Electronic $80,Print &Electronic $200.For any other part of the world add $50 more to the above prices for Print.
Single article PDF file for individual $15.Single issue in PDF form for individual $60.

No credit card payments.Only certified check,money order or international check in US dollars are acceptable.
Combination orders of any two from JoCAAA,JCAAM,JAFA receive 25% discount,all three receive 30% discount.

JAFA is reviewed and abstracted by AMS Mathematical Reviews,MATHSCI,and Zentralblaat MATH.

JAFA IS A JOURNAL OF RAPID PUBLICATION

Journal of Applied Functional Analysis
Editorial Board
Associate Editors

Tel.(+33)(0)3.20.43.42.18
Fax (+33)(0)3.20.43.43.02
Catalin.Badea@math.univ-lille1.fr
Approximation Theory, Functional
Analysis, Operator Theory.

4) Erik J.Balder
Mathematical Institute
Universiteit Utrecht
P.O.Box 80 010
3508 TA UTRECHT
The Netherlands
Tel.+31 30 2531458
Fax+31 30 2518394
balder@math.uu.nl
Control Theory, Optimization,
Convex Analysis, Measure Theory,
Applications to Mathematical
Economics and Decision Theory.

5) Carlo Bardaro
Dipartimento di Matematica e Informatica
Universita di Perugia
Via Vanvitelli 1
06123 Perugia, ITALY
TEL+390755853822
+390755855034
FAX+390755855024
E-mail bardaro@unipg.it
Web site: http://www.unipg.it/~bardaro/
Functional Analysis and Approximation
Theory,
Signal Analysis, Measure Theory, Real
Analysis.

6) Heinrich Begehr
Freie Universitaet Berlin
I. Mathematisches Institut, FU Berlin,
Arnimallee 3,D 14195 Berlin
Germany,
Tel. +49-30-83875436, office
+49-30-83875374, Secretary
Fax +49-30-83875403
begehr@math.fu-berlin.de
Complex and Functional Analytic
Methods in PDEs, Complex Analysis,
History of Mathematics.

7) Fernando Bombal
Departamento de Analisis Matematico
Universidad Complutense
Plaza de Ciencias,3
28040 Madrid, SPAIN
Tel. +34 91 394 5020
Fax +34 91 394 4726
fernando_bombal@mat.ucm.es

Mathematical Institute
Academy of Sciences of Czech Republic
Zitna 25
CZ-115 67 Praha 1
Czech Republic
Tel +420 222 090 743
Fax +420 222 211 638
krbecm@matsrv.math.cas.cz
Function spaces,Real Analysis,Harmonic
Analysis,Interpolation and
Extrapolation Theory,Fourier Analysis.

28) V. Lakshmikantham
Department of Mathematical Sciences
Florida Institute of Technology
Melbourne, FL 32901
e-mail: lakshmik@fit.edu
Ordinary and Partial Differential Equations,
Hybrid Systems, Nonlinear Analysis

29) Peter M.Maass
Center for Industrial Mathematics
Universitaet Bremen
Bibliotheksstr.1,
MZH 2250,
28359 Bremen
Germany
Tel +49 421 218 9497
Fax +49 421 218 9562
pmaass@math.uni-bremen.de
Inverse problems,Wavelet Analysis and
Operator Equations,Signal and Image
Processing.

30) Julian Musielak
Faculty of Mathematics and Computer Science
Adam Mickiewicz University
Ul.Umultowska 87
61-614 Poznan
Poland
Tel (48-61) 829 54 71
Fax (48-61) 829 53 15
Grzegorz.Musielak@put.poznan.pl
Functional Analysis, Function Spaces,
Approximation Theory,Nonlinear Operators.

31) Gaston M. N'Guerekata
Department of Mathematics
Morgan State University
Baltimore, MD 21251, USA
tel:: 1-443-885-4373
Fax 1-443-885-8216
Gaston.N'Guerekata@morgan.edu
Nonlinear Evolution Equations,
Abstract Harmonic Analysis,
Fractional Differential Equations,

Operators on Banach spaces,
Tensor products of Banach spaces,
Polymeasures, Function spaces.

8) Michele Campiti
Department of Mathematics "E.De Giorgi"
University of Lecce
P.O. Box 193
Lecce,ITALY
Tel. +39 0832 297 432
Fax +39 0832 297 594
michele.campiti@unile.it
Approximation Theory,
Semigroup Theory, Evolution problems,
Differential Operators.

9)Domenico Candeloro
Dipartimento di Matematica e Informatica
Universita degli Studi di Perugia
Via Vanvitelli 1
06123 Perugia
ITALY
Tel +39(0)75 5855038
+39(0)75 5853822,
+39(0)744 492936
Fax +39(0)75 5855024
candelor@dipmat.unipg.it
Functional Analysis, Function spaces,
Measure and Integration Theory in
Riesz spaces.

10) Pietro Cerone
School of Computer Science and
Mathematics, Faculty of Science,
Engineering and Technology,
Victoria University
P.O.14428,MCMC
Melbourne,VIC 8001,AUSTRALIA
Tel +613 9688 4689
Fax +613 9688 4050
Pietro.cerone@vu.edu.au
Approximations, Inequalities,
Measure/Information Theory,
Numerical Analysis, Special Functions.

11)Michael Maurice Dodson
Department of Mathematics
University of York,
York YO10 5DD, UK
Tel +44 1904 433098
Fax +44 1904 433071
Mmd1@york.ac.uk
Harmonic Analysis and Applications to
Signal Theory,Number Theory and
Dynamical Systems.

Almost Periodicity & Almost Automorphy.

32) Vassilis Papanicolaou
Department of Mathematics
National Technical University of Athens
Zografou campus, 157 80
Athens, Greece
tel:: +30(210) 772 1722
Fax +30(210) 772 1775
papanico@math.ntua.gr
Partial Differential Equations,
Probability.

33) Pier Luigi Papini
Dipartimento di Matematica
Piazza di Porta S.Donato 5
40126 Bologna
ITALY
Fax +39(0)51 582528
papini@dm.unibo.it
Functional Analysis, Banach spaces,
Approximation Theory.

34) Svetlozar T.Rachev
Chair of Econometrics,Statistics
and Mathematical Finance
School of Economics and
Business Engineering
University of Karlsruhe
Kollegium am Schloss, Bau II,20.12, R210
Postfach 6980, D-76128,
Karlsruhe,GERMANY.
Tel +49-721-608-7535,
+49-721-608-2042(s)
Fax +49-721-608-3811
Zari.Rachev@wiwi.uni-karlsruhe.de
Second Affiliation:
Dept.of Statistics and Applied Probability
University of California at Santa Barbara
rachev@pstat.ucsb.edu
Probability,Stochastic Processes and
Statistics,Financial Mathematics,
Mathematical Economics.

35) Paolo Emilio Ricci
Department of Mathematics
Rome University "La Sapienza"
P.le A.Moro,2-00185
Rome,ITALY
Tel ++3906-49913201 office
++3906-87136448 home
Fax ++3906-44701007
Paoloemilio.Ricci@uniroma1.it
riccip@uniroma1.it
Special Functions, Integral and Discrete

12) Sever S.Dragomir
School of Computer Science and
Mathematics, Victoria University,
PO Box 14428,
Melbourne City,
MC 8001,AUSTRALIA
Tel. +61 3 9688 4437
Fax +61 3 9688 4050
sever@csm.vu.edu.au
Inequalities,Functional Analysis,
Numerical Analysis, Approximations,
Information Theory, Stochastics.

13) Paulo J.S.G.Ferreira
Department of Electronica e
Telecomunicacoes/IEETA
Universidade de Aveiro
3810-193 Aveiro
PORTUGAL
Tel +351-234-370-503
Fax +351-234-370-545
pjf@ieeta.pt
Sampling and Signal Theory,
Approximations, Applied Fourier Analysis,
Wavelet, Matrix Theory.

14) Gisele Ruiz Goldstein
Department of Mathematical Sciences
The University of Memphis
Memphis,TN 38152,USA.
Tel 901-678-2513
Fax 901-678-2480
ggoldste@memphis.edu
PDEs, Mathematical Physics,
Mathematical Geophysics.

15) Jerome A.Goldstein
Department of Mathematical Sciences
The University of Memphis
Memphis,TN 38152,USA
Tel 901-678-2484
Fax 901-678-2480
jgoldste@memphis.edu
PDEs,Semigroups of Operators,
Fluid Dynamics,Quantum Theory.

16) Heiner Gonska
Institute of Mathematics
University of Duisburg-Essen
Lotharstrasse 65
D-47048 Duisburg
Germany
Tel +49 203 379 3542
Fax +49 203 379 1845
gonska@math.uni-duisburg.de
Approximation and Interpolation Theory,
Transforms, Symbolic and Umbral Calculus,
ODE, PDE,Asymptotics, Quadrature,
Matrix Analysis.

36) Silvia Romanelli
Dipartimento di Matematica
Universita' di Bari
Via E.Orabona 4
70125 Bari, ITALY.
Tel (INT 0039)-080-544-2668 office
080-524-4476 home
340-6644186 mobile
Fax -080-596-3612 Dept.
romans@dm.uniba.it
PDEs and Applications to Biology and
Finance, Semigroups of Operators.

37) Boris Shekhtman
Department of Mathematics
University of South Florida
Tampa, FL 33620,USA
Tel 813-974-9710
boris@math.usf.edu
Approximation Theory, Banach spaces,
Classical Analysis.

38) Rudolf Stens
Lehrstuhl A fur Mathematik
RWTH Aachen
52056 Aachen
Germany
Tel ++49 241 8094532
Fax ++49 241 8092212
stens@mathA.rwth-aachen.de
Approximation Theory, Fourier Analysis,
Harmonic Analysis, Sampling Theory.

39) Juan J.Trujillo
University of La Laguna
Departamento de Analisis Matematico
C/Astr.Fco.Sanchez s/n
38271.LaLaguna.Tenerife.
SPAIN
Tel/Fax 34-922-318209
Juan.Trujillo@ull.es
Fractional: Differential Equations-
Operators-
Fourier Transforms, Special functions,
Approximations,and Applications.

40) Tamaz Vashakmadze
I.Vekua Institute of Applied Mathematics
Tbilisi State University,
2 University St. , 380043,Tbilisi, 43,
GEORGIA.
Tel (+99532) 30 30 40 office

22) Hubertus Th. Jongen
Department of Mathematics
RWTH Aachen
Templergraben 55
52056 Aachen
Germany
Tel +49 241 8094540
Fax +49 241 8092390
jongen@rwth-aachen.de
Parametric Optimization, Nonconvex Optimization, Global Optimization.

45) Richard A. Zalik
Department of Mathematics
Auburn University
Auburn University,AL 36849-5310
USA.
Tel 334-844-6557 office
678-642-8703 home
Fax 334-844-6555
zalik@auburn.edu
Approximation Theory,Chebychev Systems, Wavelet Theory.

Preface

These **four** special issues, which constitute the proceedings of the symposium 3rd International Interdisciplinary Chaos Symposium on CHAOS and COMPLEX SYSTEMS - CCS2010 (21-24 May 2010), have tried to create a forum for the exchange of information and experience in the exciting interdisciplinary field of chaos. However the conference was more in the Applied Mathematics, Social Sciences and Physics direction centered.

The view of the organizers concerning international resonance of the conference has been fulfilled: approximatelly 200 scientists from 21 diffrent countries (Algeria, Bulgaria, Croatia, Denmark, France, Germany, Greece, Iran, Italy, Jordan, Lebanon, Malaysia, Pakistan, Republic of Serbia, Russia, Sultanate of Oman, Tunisia, Turkey, Ukraine, United Kingdom and United States of America) have participated. Good relations to research institutes of these countries might be of great importance for science and applications in different fields of Chaos.

On behalf of the Organizing Committee we would like to express our thanks to the Scientific Committee, the Program Committee and to all who have contributed to this conference for their support and advice. We are also grateful to the invited lecturers Prof. Henry D.I. Abarbanel, Prof. David S. Byrne, Prof. George Anastassiou, Prof. Zidong Wang, Prof. Turgut Ozis and Prof. Markus J. Aschwanden.

Special thanks are due to Rector Prof. Dursun Kocer and Vice Rector Prof. Cetin Bolcal for their close support, advice and incentive encouraging.

Our thanks are also due to the Istanbul Kultur University, which was hosting this symposium and provided all of its facilities.

Finally, we are grateful to the Editor-in-Chief, Prof. George Anastassiou for accepting this volume for publication.

Hikmet Caglar, PhD in Mathematics, s.caglar@iku.edu.tr
Levent Cuhaci, PhD in Computer Science, l.cuhaci@iku.edu.tr
Gursel Hacibekiroglu, PhD in Physics, g.hacibekiroglu@iku.edu.tr
Mehmet Ozer, PhD in Physics, m.ozer@iku.edu.tr

Istanbul Kultur University, Faculty of Science and Letters, Istanbul, Turkey

JOURNAL OF APPLIED FUNCTIONAL ANALYSIS, VOL.6, NO.1, 11-16, COPYRIGHT 2011 EUDOXUS PRESS, LLC

CONTROL OF CHAOS IN ROTATIONAL MOTION OF A SATELLITE IN AN ELLIPTIC ORBIT UNDER THE INFLUENCE OF THIRD BODY TORQUE

AYUB KHAN
Department of Mathematics, Zakir Husain College, University of Delhi, New Delhi-110002, India.

MOHAMMAD SHAHZAD
Department of Information Technology, Higher College of Technology, Muscat, Oman.
E-mail: dmsinfinite@gmail.com

ABSTRACT: We have investigated the robust control term to the order of e^2 for the Hamiltonian of rotational motion of a satellite in an elliptic orbit about the central body (earth) under the influence of third body torque, which is due to the influence of the third body (moon). By adding the small and simple control term to the perturbed Hamiltonian, the system of rotational motion of a satellite becomes more regular than the previous one. This control of chaos has been shown computationally through Poincare surface of sections. Practically, we have achieved this by measuring in advance in such a way that our estimated value of the control term (f) is smaller than the perturbation due to the moon experienced by the satellite.

Key words: celestial mechanics; Astronomical methods and techniques: analytical; numerical.

1. INTRODUCTION

The mathematical description of chaos has achieved a mature state during the last decade. By using the tools such as classical phase space, time series analysis, Poincare sections, Lyapunov exponents, etc. Much attention has been paid to control the chaos as it can be harmful in several contexts. Since last decade, inhibition of chaos has become a key challenge in the chaos existing branches of nonlinear sciences. Most of the methods for controlling chaos in the chaotic systems are used by tilting targeted trajectories. For many body experiments (e.g. the magnetic confinement of plasma, satellite's dynamics and the control of turbulent flows, etc.), successful attempts have been made by Pyragas (1992), Ott et al. (1990) and Tsui & Jones (2000) in dealing a high number of trajectories simultaneously.

In the present studies, we focus on the strategy to control transport properties without significantly altering neither the original structure of the system under investigation nor its overall chaotic structure which is based on building barriers by adding a small perturbation localized in phase space therefore, confining all the trajectories. The main motivations behind a localized control are: the control of a physical system can only be performed in some specific regions of phase space. Often, it is sometimes desirable to stabilize only a given region of phase space without modifying the major part of phase space in order to preserve some specific features of the system. This method can be used to bound the motion of particles without changing the perturbation inside (and outside) the barrier. Also, using a localised control means to inject much fewer energy than a global control in order to create isolated barriers of transport. In this direction to control chaos attempts have been made by Ciraolo et al. (2004a, 2004b, 2004c) and Khan & Shahzad (2008).

Here the meaning of control is reduce or suppress chaos by inducing a relevant change in the transport properties by means of a small perturbation so that the original structure of the system under investigation is substantially kept unaltered. It has been shown by Ciraolo et al. (2004a, 2004b, 2004c) and Khan & Shahzad (2008) that a very small and suitably chosen perturbation can indeed be an efficient control for perturbed Hamiltonian systems. Khan & Shahzad (2008) have studied the Hamiltonian system of Mimas-Tethys system (The natural satellites of Saturn) by keeping the original structure of the system unaltered. During their study, they have found that the chaos in the Mimas-Tethys system is suppressed drastically.

Keeping in view the above discussions, we tend to study the chaos control in rotational motion of a satellite in an elliptic orbit under the influence of third body torque. The class of Hamiltonian system of the rotational motion of a satellite can be written in the form of $H = H_0 + eV$ which can be read as a sum of an integrable Hamiltonian H_0 (with an action-angle variable) and a small perturbation eV. The naive choice for a control term would be $f(p,q,v) = -eV$ but this would be useless since it is of the same magnitude of the source of chaotic transport and thus would require a major modification of the physical condition of the system of interest. So for the small perturbation, we have obtained a term to control the chaotic diffusion in the dynamics of the system under consideration. The main advantage of the control term (*f*) is that it is explicit in nature. Due to its explicit nature, we have an opportunity to study simultaneously the dynamics of the system with and without control term (i.e. $H = H_0 + eV + f$ and $H = H_0 + eV$).

For the perturbed Hamiltonian $H = H_0 + eV$, a control term has been estimated Vittot (2004) up to $O(e^2)$. The inclusion of this term in the above tested Hamiltonian gives us the more regular dynamics or less diffusion than the uncontrolled Hamiltonian.

2. FORMULATION OF THE PROBLEM

Let us consider a rigid satellite moving in an elliptic orbit (semi-major axis *a,* eccentricity *e*) about the earth of mass *M* under the influence of the central body and its moon of mass *m* whose orbit is assumed to be circular and coplanar with the elliptic orbit of the satellite. The satellite is assumed to be a triaxial ellipsoid with moments of inertia $A < B < C$, C is the moment of inertia about the spin axis which is perpendicular to the orbital plane. The influence of the moon is obtained by resolving potential of the torque with respect to the r/R ratio, where *r* is the radius of the satellite under investigation and *R* is the radius of the moon's orbit.

For ν_1 the true anomaly, and orientation of the satellite's long axis θ, $\theta-\nu_1=\frac{q}{2}$ measures the orientation of the satellite's long axis related to the satellite's radius vector. Equation of motion of the planar oscillation of a satellite in an elliptic orbit with third body perturbation is (Bhatnagar & Bhardwaj 1994):

$$\left\{1+e\cos\left(\frac{\Omega_1}{\Omega}\nu\right)\right\}\frac{d^2q}{d\nu^2}-\frac{2e\Omega_1}{\Omega}\sin\left(\frac{\Omega_1}{\Omega}\nu\right)\frac{dq}{d\nu}-\frac{4e\Omega_1^2}{\Omega^2}\sin\left(\frac{\Omega_1}{\Omega}\nu\right)+n^2\sin q$$
$$-n^2\varepsilon\sin(\nu-q)=0, \tag{2.1}$$

where $\nu=\Omega t$, $\Omega=2(\Omega_1-\Omega_2)$, $\nu_1\cong\Omega_1 t$, $\nu_2=\Omega_2 t$, $n^2=3\left(\frac{\Omega_1}{\Omega}\right)^2\left(\frac{B-A}{C}\right)$,

$\varepsilon\cong\left(\frac{\Omega_1}{\Omega}\right)^2\frac{m}{M}$, Ω_1 and Ω_2 are the angular orbital velocities of the satellite and moon respectively, (q, p) is the generalized coordinate of Euclidian space and ε is the parameter due to third body effect and it has been taken to the order of e in (2.2) (i.e. $\varepsilon=e\varepsilon_1$).

Using Hamilton's canonical equations, the Hamiltonian of the (2.1), can be written as

$$H=\frac{p^2}{2}-\frac{2\Omega_1}{\Omega}p-n^2\cos q-e\left[p^2\cos\left(\frac{\Omega_1}{\Omega}\nu\right)+n^2\cos q\cos\left(\frac{\Omega_1}{\Omega}\nu\right)\right.$$
$$\left.+n^2\varepsilon_1\cos(q-\nu)\right], \tag{2.2}$$

In order to apply the control theory, we put Hamiltonian (2.2) in an autonomous form. Taking ν as an additional angle whose conjugate action is E, the autonomous Hamiltonian is given by

$$H(p,q,E,\nu)=\frac{p^2}{2}-2\alpha p-n^2\cos q+E-e\left[p^2\cos\alpha\nu+n^2\cos q\cos\alpha\nu\right.$$
$$\left.+n^2\varepsilon_1\cos(q-\nu)\right]. \tag{2.3}$$

Where $\alpha=\frac{\Omega_1}{\Omega}$, the actions are $\mathrm{A}=(p,E)$ and the angles are $\Phi=(q,\nu)$. The unperturbed Hamiltonian H_0 which is used to construct the operators Γ, $\Re$ and N is

$$H_0(p,E)=\frac{p^2}{2}-2\alpha p-n^2\cos q+E, \tag{2.4}$$

The action of $\{H_0\}$, Γ, $\Re$ and N (Ciraolo et al. 2004b) on the function

$V(p,q,E,\nu)=\sum_{k_1,k_2\in Z}V_{k_1,k_2}(p,E)e^{i(k_1q+k_2\nu)}$, $V\in\boldsymbol{\mathcal{A}}$ is given by

$$\{H_0\}V=\sum_{k_1,k_2\in Z}i(k_1p+k_2)V_{k_1,k_2}(p,E)e^{i(k_1q+k_2\nu)},$$

$$\Gamma V=\sum_{k_1,k_2\in Z}\frac{\chi(k_1p+k_2\neq 0)}{i(k_1p+k_2)}V_{k_1,k_2}(p,E)e^{i(k_1q+k_2\nu)},$$

$$\Re V=\sum_{k_1,k_2\in Z}\chi(k_1p+k_2=0)V_{k_1,k_2}(p,E)e^{i(k_1q+k_2\nu)},$$

$\mathrm{N}V = \sum_{k_1,k_2\in Z} \chi(k_1 p + k_2 \neq 0) V_{k_1,k_2}(p,E) e^{i(k_1 q + k_2 \nu)}$, where $\chi(k_1 p + k_2) = 0$ if the proposition is wrong and equal to 1 when the proposition is true.

When $V(q,\nu) = -e\left[p^2 \cos\alpha\nu + n^2 \cos q \cos\alpha\nu + n^2\varepsilon_1 \cos(q-\nu)\right]$ is acted upon by the above operators, we obtain

$$\{H_0\}V = e\left[\alpha p^2 \sin\alpha\nu + \tfrac{1}{2}n^2(p-\alpha)\sin(q+\alpha\nu) + \tfrac{1}{2}n^2(p-3\alpha)\sin(q-\alpha\nu) + n^2\varepsilon_1(p-2\alpha-1)\sin(q-\nu)\right],$$

$$\Gamma V = -e\left[\frac{p^2 \sin\alpha\nu}{\alpha} + \frac{n^2 \sin(q+\alpha\nu)}{2(p-\alpha)} + \frac{n^2 \sin(q-\alpha\nu)}{2(p-3\alpha)} + \frac{n^2\varepsilon_1 \sin(q-\nu)}{(p-2\alpha-1)}\right],$$

$$\Re V = 0,$$

$$\mathrm{N}V = -e\left[p^2 \cos\alpha\nu + \frac{n^2}{2}\cos(q+\alpha\nu) + \frac{n^2}{2}\cos(q-\alpha\nu) + n^2\varepsilon_1 \cos(q-\nu)\right],$$

for $p \neq \alpha, 3\alpha, 1+2\alpha$.

Since $\Re V = 0$, the control term is given by $f(V) = \sum_{s=2}^{\infty} f_s$, where f_s is of the order of e^s and given by $f_s = \frac{1}{s}\{\Gamma V, f_{s-1}\}$, where $f_1 = V$ and the terms in the series are computed by recursion. In particular, the control term (*f*), is given by

$$f(p,q,\nu) = f_2(p,q,\nu) = -\frac{1}{2}\{\Gamma V, V\},$$ where $\{.,.\}$ is the Poisson bracket.

$$f(p,q,\nu) = \frac{e^2}{2}\left[\left\{\frac{2p\sin\alpha\nu}{\alpha} - \frac{n^2\sin(q+\alpha\nu)}{2(p-\alpha)^2} - \frac{n^2\sin(q-\alpha\nu)}{2(p-3\alpha)^2} - \frac{n^2\varepsilon_1\sin(q-\nu)}{(p-2\alpha-1)^2}\right\}\right.$$
$$\times\left\{\frac{n^2}{2}\sin(q+\alpha\nu) + \frac{n^2}{2}\sin(q-\alpha\nu) + n^2\varepsilon_1\sin(q-\nu)\right\} + 2p\cos\alpha\nu$$
$$\left.\times\left\{\frac{n^2\cos(q+\alpha\nu)}{2(p-\alpha)} + \frac{n^2\cos(q-\alpha\nu)}{2(p-3\alpha)} + \frac{n^2\varepsilon_1\cos(q-\nu)}{(p-2\alpha-1)}\right\}\right].$$

The main purpose of the control is to have a control term which is as simple as possible in order to be implemented in the experiment. A possible simplification is to consider the region in between the primary resonances located around $p = \alpha, 3\alpha, 1+2\alpha$. Developing the approximate control term around $p = 2\alpha$, We have

$$f = -\frac{e^2n^4}{2\alpha^2}\left[\sin q\cos\alpha\nu + \alpha\varepsilon_1\sin(q-\nu)\right]^2 - \frac{e^2n^4}{2}\varepsilon_1\left(1-\frac{1}{\alpha}\right)^2 \sin q\cos\alpha\nu\sin(q-\nu)$$
$$+e^2n^2\varepsilon_1\left[(1-\alpha)\cos(q-\nu-\alpha\nu) - (1+\alpha)\cos(q-\nu+\alpha\nu)\right].$$

Furthermore, for small values of *n*, *e*, α and ε_1, the effect of first and second term in f will be negligible. Hence, more practically f may be defined as

$$f = e^2n^2\varepsilon_1\left[(1-\alpha)\cos(q-\nu-\alpha\nu) - (1+\alpha)\cos(q-\nu+\alpha\nu)\right].$$

In order to make the control term more effective, we change the amplitude of the control term by introducing β. Thus, the more effective and the finally approximated control term may be written as:

$$f(p,q,\nu) = e^2 n^2 \beta \varepsilon_1 \left[(1-\alpha)\cos(q-\nu-\alpha\nu) - (1+\alpha)\cos(q-\nu+\alpha\nu)\right].$$

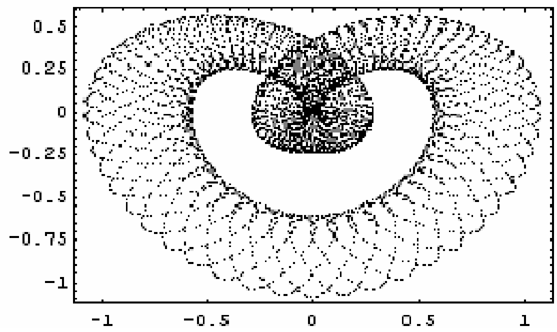

Fig 1: Poincare Surface without control term

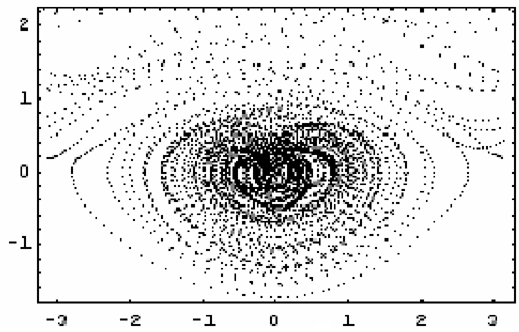

Fig 2: Poincare Surface with control term

For $n = 0.9; e = 0.2; \Omega_1 = 0.01; \Omega = 0.02; \varepsilon_1 = 0.5; \beta = 4; q(0) = 0; p(0) = 0$, figures 1 and 2 depict the dynamics of the system under consideration through the computational tools (Poincare surface of sections) without and with the estimated control term respectively. In figure 2, it is clear that the dynamics of the satellite under investigation becomes more regular including the control term (*f*). The Poincare surface in figure 1 depicts the broken KAM tori whereas the Poincare surface in figure 2 depicts the formation of lots of KAM tori in the vicinity of $p = 2\alpha$, which is the clear indication of chaos control.

3. CONCLUSION

We have provided an effective strategy to control the chaotic diffusion in Hamiltonian dynamics using small perturbations. Due to the explicit formula of the control term, we have compared the dynamics without and with the control term. A Hamiltonian $H_0 + eV$ is controlled by adding a control term (*f*). The naive choice for a control term would be $f(p,q,\nu) = -eV$ but this would be useless since it is of the same magnitude of the source of chaotic transport and thus would require a major modification of the physical condition of the system of interest. The idea of the control is pictorially represented in figure 1, where we have plotted the Poincare surface of section without the control term whereas the Poincare surface of section in figure 2 are with control term. It is clear from the figures that the control term is effective for the system under consideration. Further, our computational studies reveal that although the estimated control term is smaller as compared to the perturbation, yet this control is robust which is clear from the figures displayed. Interestingly our analytical and computational studies are in an excellent agreement.

REFERENCES

1. K. B. Bhatnagar & R. Bhardwaj, Rotational motion of a satellite in an elliptical orbit under the influence of third body torque (I), *Astron. Soc. of India Bul.*, 22, 359-367 (1994).
2. G. Ciraolo, C. Chandre, R. Lima, M. Pettini, M. Vittot, C. Figarella & P. Ghendrih, Controlling chaotic transport in a Hamiltonian model of interest to magnetized plasmas, *J. Phys. A: Math. Gen*., 37, 3589-3597 (2004a).
3. G. Ciraolo, C. Chandre, R. Lima, M. Vittot & M. Pettini, Control of chaos in Hamiltonian systems, *Cel. Mech. & Dyn. Astr*., 90, 3-12 (2004b).
4. G. Ciraolo, F. Briolle, C. Chandre, E. Floriani, R. Lima, M. Vittot, M. Pettini, C. Figarella & P. Ghendrih, Control of Hamiltonian chaos as a possible tool to control anomalous transport in fusion plasmas, *Phys. Rev. E*, 69(4), 056213-056221 (2004).
5. A. Khan & M. Shahzad, Control of chaos in the Hamiltonian system of Mimas-Tethys, *Astronomical J.*, 136, 2201-2203(2008).
6. E. Ott, C. Grebogi & J. A. Yorke, Controlling chaos, *Phys. Rev. Lett.*, 64, 1196-1199 (1990).
7. K. Pyragas, Continuous Control of Chaos by Self-Controlling Feedback, *Phys. Lett. A*, 170, 421-427 (1992).
8. A. P. M. Tsui & A. J. Jones, The control of higher dimensional chaos: comparative results for the chaotic satellite attitude control problem, *Physica D*, 135, 41-62 (2000).
9. M. Vittot, Perturbation Theory and Control in Classical or Quantum Mechanics by an Inversion Formula, *J. Phys. A: Math. Gen.*, 37, 6337-6357 (2004).

JOURNAL OF APPLIED FUNCTIONAL ANALYSIS, VOL.6, NO.1, 17-25, COPYRIGHT 2011 EUDOXUS PRESS, LLC

Error Estimates of Spectral Collocation Method for the Coupled Korteweg-de Vries Equations

Abdur Rashid*and Ahmad Izani Bin Md. Ismail†

Abstract

In this paper, a coupled Korteweg-de Vries (KdV) equation with periodic boundary conditions is considered. Semi discrete and fully discrete spectral collocation schemes are given. In fully discrete case, a three-level spectral collocation scheme is considered. An energy estimation method is used to obtain error estimates for the approximate solutions. Numerical results are presented.

Keywords: Coupled Korteweg-de Vries equations, spectral collocation method, energy estimation method

1 Introduction

We consider the periodic initial-boundary values problem of the coupled KdV equations:

$$\begin{cases} u_t - au_{xxx} - 6auu_x - 2bvv_x = 0, & x \in \mathbb{R}, t > 0, \\ v_t + v_{xxx} - 3uv_x = 0, & x \in \mathbb{R}, t > 0, \\ u(x+2,t) = u(x,t), v(x+2,t) = v(x,t), & x \in \mathbb{R}, t > 0, \\ u(x,0) = u_0(x), v(x,0) = v_0(x), & x \in \mathbb{R}, \end{cases} \tag{1.1}$$

where a and b are constants. The Coupled system (1.1) describes interaction of two long waves with different dispersion relations.

The KdV equation is the simple example of a model equation, which describe the physical phenomena. In 1895 Korteweg and de-Vries [1] published a paper on long wave in a rectangular canal. At that time various dynamical systems governed by the nonlinear partial differential equations have been developed. A few of these equations are found to be a pair of coupled equations.

The KdV type of equations have different application in the field of physical science and engineering. In geophysical fluid dynamics, they describe a long wave in shallow seas and deep oceans [8, 9]. The KdV equations gives rise to the ion acoustic solution in the field of Plasma physics [3, 5, 7]

There has been extensive literature on the coupled KdV equations. For example, In [11] Tam et al. used Hirota method to solve the coupled KdV equation. Kaya and Inan [12] used Adomian decomposition method to find some analytical and numerical travelling solutions. Fan [13] used tanh method to find some travelling solutions of the coupled KdV equations. Assas [15] solved this system using variational iteration method. Abbasbandy [17] used homotopy analysis method to solve the generalized coupled KdV equations.

Spectral methods have become increasingly popular in applied mathematics and scientific computing for the solution of partial differential equations. The main advantage of these methods lies in their accuracy for a given number of unknowns. For problems whose solutions are sufficiently smooth, they exhibit exponential rate of convergence/spectral accuracy. There are three most commonly used spectral versions, namely Galerkin, tau and collocation methods. Among them, the spectral collocation/ pseudospectral method is particularly attractive owing to its economy. Comprehensive discussions on spectral

*Department of Mathematics, Gomal University, Dera Ismail Khan, Pakistan.
†School of Mathematical Sciences, University Sains Malaysia, Penang, Malaysia.

methods can be found in review articles and monographs, see for example (Peyret [6] , Boyd [14], Gottlieb [4]).

When time-dependent partial differential equations are solved numerically by spectral methods, spectral differentiation is used in space, while finite difference method is used in the time direction. In principle, we have to sacrifice spectral accuracy in time, but in practice a small time step with a finite difference formula of order one or higher, often results in satisfactory global accuracy. Small time steps are much more affordable than small space steps, i.e., they affect the computation time, but not the storage. The details are given in (Canuto and Hussaini [18], Trefethen [16], Fornberg [2]).

In this paper we consider the periodic initial boundary-value problem of (1.1). We investigate the second order finite difference approximation in time, combined with spectral collocation in space for solving (1.1). The fully discrete schemes are analyzed and error estimates for both are found. The rate of convergence of the resulting scheme are $O(\tau^2 + N^{-S})$ where N is the number of spatial Fourier modes, τ is the discrete mesh spacing of the time variable t and where S is depending only on the smoothness of the exact solution.

2 Notations and Lemmas

Let $\Omega = [0, 2]$ and $L^2(\Omega)$ denote the set of all square integrable functions with the inner product $(u, v) = \int_0^2 u(x)v(x)dx$ and the norm $\|u\|^2 = (u, u)$. Let $L^\infty(\Omega)$ denote the Lebesgue space with norm $\|u\|_\infty = ess \sup_{x\in\Omega} |u(x)|$ and $H_p^S(\Omega)$ denote the periodic Sobolev space with the norm $\|u\|_S = \left(\sum_{\ell=0}^{S} \left\|\frac{\partial^\ell u}{\partial x^\ell}\right\|^2\right)^{1/2}$, we define

$$L^2\left(0, T; H_p^S(\Omega)\right) = \left\{u(\cdot, t) \in H_p^S(\Omega) : \int_0^T \|u(\cdot, \zeta)\|_S^2 d\zeta < \infty\right\},$$

$$L^\infty\left(0, T; H_p^S(\Omega)\right) = \left\{u(\cdot, t) \in H_p^S(\Omega) : \sup_{0\le\zeta<T} \|u(\cdot, \zeta)\|_S < \infty\right\}.$$

Let $S_N = \text{span}\left\{\psi_k = \frac{1}{\sqrt{2\pi}} e^{ikx} : |k| \le N\right\}$. Suppose $h = \frac{2}{2N+1}$ is the mesh step of variable x. The nodes are then $x_\ell = x_0 + \ell h$, $x_0 = 0$, $\ell = 0, 1, \ldots, 2N$. The discrete inner product and norm in the interval Ω are defined by

$$(u, v)_N = h \sum_{\ell=0}^{2N} u(x_\ell)v(x_\ell), \qquad \|u\|_N = (u, v)_N^{1/2}.$$

Let $P_N : L^2(\Omega) \longrightarrow S_N$ be the orthogonal projection operator i.e.

$$(P_N u, v) = (u, v)\,, \quad \forall v \in S_N.$$

and $P_c : C(\Omega) \longrightarrow S_N$ be the interpolation operator, i.e. such that for all $u \in C(\Omega)$

$$P_c u(x_\ell) = u(x_\ell), \qquad 0 \le \ell \le 2N.$$

For the discretization in the time variable t, let τ be the mesh spacing of t and $R_\tau = \left\{t = k\tau : 0 \le k \le \left[\frac{T}{\tau}\right]\right\}$ and $u^k = u(x, k\tau)$. We define the following difference quotients

$$u_{\hat{t}}^k = \frac{1}{2\tau}(u^{k+1} - u^{k-1})$$

$$\widehat{u}^k = \frac{1}{2}(u^{k+1} + u^{k-1}).$$

Now, we state without proof a set of lemmas which will be useful for the next section.

Lemma 1. *[18] Assume that $u \in H_p^S(\Omega)$, for any $0 \le \mu \le S$, there exists a constant C independent of u and N*

$$\|u - P_N u\|_\mu \le CN^{\mu - S}\|u\|_S.$$

Lemma 2. *[18] Assume that $u \in H_p^S(\Omega)$, for any $0 \le \mu \le S$, there exists a constant C independent of u and N*

$$\|u - P_c u\|_\mu \le CN^{\mu - S}\|u\|_S$$

Lemma 3. *[4] If $u, v \in C(\Omega)$, there exists a constant C independent of u, v and N, such that*

$$(P_c u, P_c v)_N = (P_c u, P_c v) = (u, v)_N.$$

Lemma 4. *[6] If $S \ge 1$, and $u, v \in H^S(\Omega)$, there exists a constant C independent of u, v and N, such that*

$$\|uv\|_S \le C\,\|u\|_S\,\|v\|_S\,.$$

3 Error Estimates of Semi Discrete Scheme

The semi discrete spectral collocation approximation of equation (1.1) consists in finding $u_N, v_N \in S_N$, satisfying

$$\begin{cases} u_{Nt} - au_{Nxxx} - 6aP_c(u_N u_{Nx}) - 2bP_c(v_N v_{Nx}) = 0, & x \in \mathbb{R}, t > 0,\\ v_{Nt} + v_{Nxxx} - 3P_c(u_N v_{Nx}) = 0, & x \in \mathbb{R}, t > 0,\\ u_N(x,0) = P_N u_0(x), \qquad v_N(x,0) = P_N v_0(x), & x \in \mathbb{R}, \end{cases} \tag{3.1}$$

Suppose that (u, v) is the solution of (1.1) and (u_N, v_N) is the solution of (3.1). Setting

$$\begin{aligned} e_1 &= u - u_N = (u - P_N u) + (P_N u - u_N) = \xi_1 + \eta_1,\\ e_2 &= v - v_N = (v - P_N v) + (P_N v - v_N) = \xi_2 + \eta_2. \end{aligned}$$

Note that $(\xi_\ell, w) = 0, \ell = 1, 2, \forall w \in S_N$. Subtracting (3.1) from (1.1), then η_1 and η_2 satisfy the system

$$\begin{cases} (e_{1t}, w) + a(e_{1xx}, w_x) - 6a(uu_x - P_c(u_N u_{Nx}), w) & \\ -2b(vv_x - P_c(v_N v_{Nx}), w) = 0, & x \in \mathbb{R}, t > 0,\\ (e_{2t}, w) + (e_{2xx}, w_x) + 3(uv_x - P_c(u_N v_{Nx}), w) = 0, & x \in \mathbb{R}, t > 0, \end{cases} \tag{3.2}$$

Setting $w = \eta_1$ in the first equation of (3.2), we have

$$\frac{1}{2}\frac{d}{dt}\|\eta_1\|^2 + a\|\eta_{1x}\|^2 - 6a(uu_x - P_c(u_N u_{Nx}), \eta_1) - 2b(vv_x - P_c(v_N v_{Nx}), \eta_1) = 0, \tag{3.3}$$

Now we are going to estimate third and fourth term of (3.3)

$$|6a(uu_x - P_c(u_N u_{Nx}), \eta_1)| \le C(\|uu_x - P_c(u_N u_{Nx})\|^2 + \|\eta_1\|^2), \tag{3.4}$$

where

$$\|uu_x - P_c(u_N u_{Nx})\| \le (\|(I - P_c)(uu_x)\| + \|u_x\|_\infty \|P_c(u - u_N))\| + \|u_N\|_\infty \|P_c(u_x - u_{Nx})\|)$$

By Lemma 1 and Lemma 4 we have

$$\begin{aligned} &\|(I - P_c)(uu_x)\| \le CN^{-S}\|u\|_S\|u_x\|_S,\\ &\|P_c(u - u_N)\| \le CN^{-S}\|u\|_S + \|\eta_1\|,\\ &\|P_c(u_x - u_{Nx})\| \le CN^{-S}\|u\|_S + \|\eta_{1x}\|. \end{aligned}$$

From the above estimates, we obtain

$$\|uu_x - P_c(u_N u_{Nx})\| \leq C(N^{-2S} + \|\eta_1\|^2 + \|\eta_{1x}\|^2), \tag{3.5}$$

Similarly

$$| - 2b(vv_x - P_c(v_N v_{Nx}), \eta_1)| \leq C(N^{-2S} + \|\eta_1\|^2 + \|\eta_2\|^2 + \|\eta_{1x}\|^2 + \|\eta_{2x}\|^2) \tag{3.6}$$

Putting the above estimate into (3.3), we get

$$\frac{1}{2}\frac{d}{dt}\|\eta_1\|^2 + a\|\eta_{1x}\|^2 \leq C(N^{-2S} + \|\eta_1\|^2 + \|\eta_2\|^2 + \|\eta_{1x}\|^2 + \|\eta_{2x}\|^2) \tag{3.7}$$

Setting $w = \eta_2$ in the second equation of (3.2), we have

$$\frac{1}{2}\frac{d}{dt}\|\eta_2\|^2 + \|\eta_{2x}\|^2 + 3(uv_x - P_c(u_N v_{Nx}), \eta_2) = 0, \tag{3.8}$$

Now we are going to estimate third term of (3.8)

$$|3(uv_x - P_c(u_N v_{Nx}), \eta_2)| \leq C(\|uv_x - P_c(u_N v_{Nx})\|^2 + \|\eta_2\|^2),$$

where

$$\begin{aligned}\|uv_x - P_c(u_N v_{Nx})\|^2 &\leq (\|(I - P_c)(uv_x)\| + \|v_x\|_\infty \|P_c(u - u_N))\| + \|u_N\|_\infty \|P_c(v_x - v_{Nx})\|) \\ &\leq C(N^{-2S} + \|\eta_1\|^2 + \|\eta_2\|^2 + \|\eta_{2x}\|^2).\end{aligned}$$

Putting the above estimate into (3.8), we get

$$\frac{1}{2}\frac{d}{dt}\|\eta_2\|^2 + \|\eta_{2x}\|^2 \leq C(N^{-2S} + \|\eta_1\|^2 + \|\eta_2\|^2 + \|\eta_{2x}\|^2). \tag{3.9}$$

Combining (3.7) and (3.9), we get

$$\frac{1}{2}\frac{d}{dt}\|\eta_1\|^2 + \frac{1}{2}\frac{d}{dt}\|\eta_2\|^2 + a\|\eta_{1x}\|^2 + \|\eta_{2x}\|^2 \leq C(N^{-2S} + \|\eta_1\|^2 + \|\eta_{1x}\|^2 + \|\eta_2\|^2 + \|\eta_{2x}\|^2). \tag{3.10}$$

By applying Gronwall's inequality, we obtain

$$\begin{aligned}&\|\eta_1(t)\|^2 + \|\eta_1(t)\|^2 + \|\eta_{1x}(t)\|^2 + \|\eta_{2x}(t)\|^2 \\ &\qquad \leq \|\eta_1(0)\|^2 + \|\eta_2(0)\|^2 + CN^{-2s} + C\int_0^T \left(\|\eta_1(\varphi)\|^2 + \|\eta_1(\phi)\|^2\right).\end{aligned}$$

In fact

$$\|u(t)\|_1^2 = \|u(t)\|^2 + \|\partial_x u(t)\|^2.$$

The initial conditions read as

$$\eta_1(0) = \eta_2(0) = 0.$$

Let

$$E(t) = \|\eta_1(t)\|_1^2 + \|\eta_2(t)\|_1^2.$$

Then we have

$$E(t) \leq CN^{-2s} + C\int_0^T E(\varphi)d\varphi.$$

Theorem 1. *Suppose u and v are solutions of equation (1.1) and assume $u, v \in L^\infty\left(0, T; H_p^s\right)$, Then for u_N and v_N the solution for the spectral collocation scheme (3.1), there exits positive constants C independent of N, the following error estimates holds*

$$\|u(t) - u_N(t)\|_1^2 + \|v(t) - v_N(t)\|_1^2 \leq CN^{-2s}.$$

4 Error Estimates of Fully Discrete Scheme

We consider the fully discrete spectral collocation scheme which consists in finding $u_N^k, v_N^k \in S_N$, such that for $k = 1, \dots, \left[\frac{T}{\tau}\right]$, the equations

$$\begin{cases} u^k_{N\hat{t}} - a\widehat{u}^k_{Nxxx} - 6aP_c(u^k_N\widehat{u}^k_{Nx}) - 2bP_c(v^k_N\widehat{v}^k_{Nx}) = 0, & x \in \mathbb{R}, t > 0, \\ v^k_{N\hat{t}} + \widehat{v}^k_{Nxxx} - 3P_c(u^k_N\widehat{v}^k_{Nx}) = 0, & x \in \mathbb{R}, t > 0, \\ u^0(x) = P_N u_0(x), v^0(x) = P_N v_0(x), & x \in \mathbb{R}, \\ u^1(x) = P_N u_1(x), v^1(x) = P_N v_1(x), & x \in \mathbb{R}, \end{cases} \tag{4.1}$$

are satisfied at $x = x_\ell, \ell = 0, \dots, 2N$. Let

$$\begin{aligned} e^k_1 &= u^k - u^k_N = (u^k - P_N u^k) + (P_N u^k - u^k_N) = \xi^k_1 + \eta^k_1, \\ e^k_2 &= v^k - v^k_N = (v^k - P_N v^k) + (P_N v^k - v^k_N) = \xi^k_2 + \eta^k_2. \end{aligned}$$

Note that $(\xi^k_\ell, w) = 0, \ell = 1, 2, \forall w \in S_N$, subtracting (4.1) from (1.1), then η^k_1 and η^k_2 satisfy the system

$$\begin{cases} (e^k_{1\hat{t}}, w) - a(\widehat{\eta}^k_{1Nxxx}, w) - 6a(P_c(u^k\widehat{u}^k_x - u^k_N\widehat{u}^k_{Nx}), w) & \\ -2b(P_c(v^k\widehat{v}^k_x - v^k_N\widehat{v}^k_{Nx}), w) = (\tau^k_1, w), & x \in \mathbb{R}, t > 0, \\ (e^k_{2\hat{t}}, w) + (\widehat{\eta}^k_{1Nxxx}, w) - 3(P_c(\widehat{u}^k\widehat{v}^k_x - \widehat{u}^k_N\widehat{v}^k_{Nx}), w) = (\tau^k_2, w), & x \in \mathbb{R}, t > 0, \\ u^0(x) = P_N u_0(x), v^0(x) = P_N v_0(x), & x \in \mathbb{R}, \\ u^1(x) = P_N u_1(x), v^1(x) = P_N v_1(x), & x \in \mathbb{R}, \end{cases} \tag{4.2}$$

where τ^k_1 and τ^k_2 are truncation errors. By applying Taylor's theorem and Lemma 3, we get

$$\begin{aligned} \tau^k_1 =& \frac{\tau^2}{12}\left(\frac{\partial^3 u}{\partial t^3}(t^k_1) + \frac{\partial^3 u}{\partial t^3}(t^k_2)\right) - \frac{a\tau^2}{2}\left(\frac{\partial^2 u_{xxx}}{\partial t^2}(t^k_3) + \frac{\partial^2 u_{xxx}}{\partial t^2}(t^k_4)\right) - \frac{6a\tau^2 u^k}{4} \\ & \times \left(\frac{\partial^3}{\partial t^3}(u_x(t^k_5)) + \frac{\partial^3}{\partial t^3}(u_x(t^k_6))\right) - \frac{2b\tau^2 v^k}{4}\left(\frac{\partial^3}{\partial t^3}(v_x(t^k_7)) + \frac{\partial^3}{\partial t^3}(v_x(t^k_8))\right) \\ & + 6a(I - P_c)(u^k\widehat{u}^k_x) + 2b(I - P_c)(v^k\widehat{v}^k_x), \end{aligned}$$

$$\begin{aligned} \tau^k_2 =& \frac{\tau^2}{12}\left(\frac{\partial^3 v}{\partial t^3}(t^k_9) + \frac{\partial^3 v}{\partial t^3}(t^k_{10})\right) - \frac{\tau^2}{2}\left(\frac{\partial^2 v_{xxx}}{\partial t^2}(t^k_{11}) + \frac{\partial^2 v_{xxx}}{\partial t^2}(t^k_{12})\right) - \frac{3\tau^2 u^k}{4} \\ & \times \left(\frac{\partial^3}{\partial t^3}(v_x(t^k_{13})) + \frac{\partial^3}{\partial t^3}(v_x(t^k_{14}))\right) - \frac{3\tau^2 v^k_x}{4}\left(\frac{\partial^3}{\partial t^3}(v_x(t^k_{15})) + \frac{\partial^3}{\partial t^3}(v_x(t^k_{16}))\right) \\ & + 3(I - P_c)(\widehat{u}^k\widehat{v}^k_x), \end{aligned}$$

where $t^{k-1} \le t^k_\ell \le t^{k+1},\ \ell = 1, 2, ..., 16$. Setting $\psi = \widehat{\eta}^k_1$ in the first equation of (4.2)

$$\frac{1}{4\tau}\left(\|\eta^{k+1}_1\|^2 - \|\eta^{k-1}_1\|^2\right) + \|\widehat{\eta}^k_{1x}\|^2 + F^k_1 + F^k_2 = (\tau^k_1, \widehat{\eta}^k_1). \tag{4.3}$$

where

$$\begin{aligned} F^k_1 &= 6a(P_c(u^k\widehat{u}^k_x - u^k_N\widehat{u}^k_{Nx}), \widehat{\eta}^k_1). \\ F^k_2 &= 2b(P_c(v^k\widehat{v}^k_x - v^k_N\widehat{v}^k_{Nx}), \widehat{\eta}^k_1). \end{aligned}$$

Now differentiate first equation of (4.2) with respect to x, setting $\psi = \partial_x\widehat{\eta}^k_1$, we obtain

$$\frac{1}{4\tau}(\|\eta^{k+1}_{1x}\|^2 - \|\eta^{k-1}_{1x}\|^2) + \|\widehat{\eta}^k_{1xx}\|^2 + F^k_5 + F^k_6 = (\tau^k_{1x}, \widehat{\eta}^k_{1x}), \tag{4.4}$$

where

$$\begin{aligned} F^k_3 &= 6a(P_c(u^k\widehat{u}^k_x - u^k_N\widehat{u}^k_{Nx})_x, \widehat{\eta}^k_{1x}). \\ F^k_4 &= 2b(P_c(v^k\widehat{v}^k_x - v^k_N\widehat{v}^k_{Nx})_x, \widehat{\eta}^k_{1x}). \end{aligned}$$

Now setting $w=\widehat{\eta}_2^k$ in the second equation of (4.2), we get

$$\frac{1}{4\tau}(\|\eta_2^{k+1}\|^2-\|\eta_2^{k-1}\|^2)+\|\widehat{\eta}_{2x}^k\|^2+F_5^k=(\tau_2^k,\widehat{\eta}_2^k), \tag{4.5}$$

where

$$F_5^k=-3(P_c(\widehat{u}^k\widehat{v}_x^k-\widehat{u}_N^k\widehat{v}_{Nx}^k),\widehat{\eta}_2^k).$$

Combining (4.3), (4.4) and (4.5), we get

$$\begin{aligned}\frac{1}{4\tau}(\|\eta_1^{k+1}\|^2-\|\eta_1^{k-1}\|^2)+\frac{1}{4\tau}(\|\eta_{1x}^{k+1}\|^2-\|\eta_{1x}^{k-1}\|^2)+\frac{1}{4\tau}(\|\eta_2^{k+1}\|^2-\|\eta_2^{k-1}\|^2)\\+\|\widehat{\eta}_{1x}\|^2+\|\widehat{\eta}_{1xx}\|^2+\|\widehat{\eta}_{2x}\|^2+\sum_{\ell=1}^{5}F_\ell^k=(\tau_1^k,\widehat{\eta}_1^k)+(\tau_{1x}^k,\widehat{\eta}_{1x}^k)+(\tau_2^k,\widehat{\eta}_2^k)\end{aligned} \tag{4.6}$$

Hereafter we shall use C to denote a general positive constant independent of τ and N. It can be different in different cases. Now we are going to estimate $F_\ell^k,\ell=1,\ldots,5$ and right hand side of the equation (4.6). By applying Lemma 1, Lemma 2, Lemma 3, Lemma 4, Cauchy-Schwartz inequality and the algebraic inequality, we get

$$\begin{aligned}|F_1^k|\le&C(\|(P_c(u^k\widehat{u}_x^k-u_N^k\widehat{u}_{Nx}^k)\|^2+\|\widehat{\eta}_1^k\|^2),\\\le&C(\|u^k\|_\infty(CN^{-2S}\|u^k\|_S+\|\widehat{\eta}_{1x}^k\|^2)+\|\widehat{u}_{Nx}^k\|_\infty(CN^{-2S}\|u^k\|_S+\|\widehat{\eta}_1^k\|^2)).\end{aligned}$$

Consequently

$$|F_1^k|\le C(N^{-2S}+\|\widehat{\eta}_{1x}^k\|^2+\|\eta_1^k\|^2+\|\widehat{\eta}_1^k\|^2)),$$

Similarly

$$\begin{aligned}|F_2^k|&\le C(N^{-2S}+\|\widehat{\eta}_{2x}^k\|^2+\|\eta_2^k\|^2+\|\widehat{\eta}_1^k\|^2),\\|F_3^k|&\le C(N^{-2S}+\|\widehat{\eta}_{1xx}^k\|^2+\|\eta_{1x}^k\|^2+\|\widehat{\eta}_{1x}^k\|^2),\\|F_4^k|&\le C(N^{-2S}+\|\widehat{\eta}_{2xx}^k\|^2+\|\eta_{2x}^k\|^2+\|\widehat{\eta}_{1x}^k\|^2),\\|F_5^k|&\le C(N^{-2S}+\|\widehat{\eta}_1^k\|^2+\|\widehat{\eta}_2^k\|^2+\|\widehat{\eta}_{2x}^k\|^2).\end{aligned}$$

The right hand terms of (4.6) can be estimated as

$$\begin{aligned}|(\tau_1^k,\widehat{\eta}_1^k)|&\le C(N^{-2S}+\tau^4+\|\widehat{\eta}_2^k\|^2+\|\widehat{\eta}_1^k\|^2),\\|(\tau_1^k,\widehat{\eta}_{1x}^k)|&\le C(N^{-2S}+\tau^4+\|\widehat{\eta}_{2x}^k\|^2+\|\widehat{\eta}_{1x}^k\|^2),\\|(\tau_2^k,\widehat{\eta}_2^k)|&\le C(N^{-2S}+\tau^4+\|\widehat{\eta}_1^k\|^2+\|\widehat{\eta}_2^k\|^2).\end{aligned}$$

Substituting the above estimate into (4.6), we get

$$\begin{aligned}\frac{1}{4\tau}(\|\eta_1^{k+1}\|^2-\|\eta_1^{k-1}\|^2)+\frac{1}{4\tau}(\|\eta_1^{k+1}\|_1^2-\|\eta_1^{k-1}\|_1^2)+\frac{1}{4\tau}(\|\eta_2^{k+1}\|^2-\|\eta_2^{k-1}\|^2)\\-\|\widehat{\eta}_{1x}^k\|^2+\|\widehat{\eta}_1^k\|^2+\|\widehat{\eta}_{1xx}^k\|^2+\|\widehat{\eta}_2^k\|^2+\|\widehat{\eta}_{2x}^k\|^2\le C(\tau^4+N^{-2S}+\|\eta_1^k\|^2\\+\|\eta_2^k\|^2+\|\widehat{\eta}_1^k\|^2+\|\widehat{\eta}_2^k\|^2+\|\widehat{\eta}_{1x}^k\|^2+\|\widehat{\eta}_{2x}^k\|^2+\|\widehat{\eta}_{1xx}^k\|^2+\|\widehat{\eta}_{2xx}^k\|^2).\end{aligned} \tag{4.7}$$

In fact

$$\|u(t)\|_1^2=\|u(t)\|^2+\|\partial_x u(t)\|^2\quad\text{and}\quad\|\widehat{u}^k\|^2\le\frac{1}{2}\left(\|u^{k+1}\|^2+\|u^{k-1}\|^2\right).$$

Let

$$E^k=\|\eta_1^{k+1}\|_1^2+\|\eta_1^k\|_1^2+\|\eta_2^{k+1}\|_1^2+\|\eta_2^k\|_1^2,$$

By summing up (4.7) for $k = 1, \cdots, n$, we get

$$E^n \leq C(E^0 + \tau^4 + N^{-2S}) + C\tau \sum_{k=1}^{n-1} E^k.$$

Note that

$$\|\eta_1^0\|_1^2 = \|\eta_2^0\|_1^2 = 0, \quad \text{and} \quad \|\eta_1^1\|_1^2 = \|\eta_2^1\|_1^2 \leq C(\tau^4 + N^{-2S}).$$

By applying Grönwall's Lemma, we get

$$C(\tau^4 + N^{-2S}) \leq Me^{-CT}.$$

$$E^n \leq C(\tau^4 + N^{-2S})e^{c(n+1)\tau}, \qquad \forall (n+1)\tau \leq T,$$

where M is the positive constant. Thus we have proved

Theorem 2. *Assume τ is sufficiently small, the solutions $u(x,t)$, $v(x,t)$ of (1.1) satisfy* $\frac{\partial^3 u}{\partial t^3} \in L^\infty(0,T;H^0(\Omega))$, $\frac{\partial^2 u}{\partial t^2} \in L^\infty(0,T;H^2(\Omega))$, $\frac{\partial^3 v}{\partial t^3} \in L^\infty(0,T;H^0(\Omega))$, $\frac{\partial^3 v}{\partial t^3}, \frac{\partial^2 v}{\partial t^2} \in L^\infty(0,T;H^2(\Omega))$, *are the solutions of (4.1). Then there exist constant M, independent of τ and N such that for $k = 0, 1, \cdots, n-1$*

$$\|u^{k+1} - u_N^{k+1}\|_1 + \|v^{k+1} - v_N^{k+1}\|_1 \leq M(\tau^2 + N^{-S}).$$

5 Numerical Simulation

We present some numerical results of our scheme for the coupled KdV equations. We used single solitary wave propagation to test the good accuracy of our method. We define maximum error as follows:

$$\|E(u)\|_\infty = \max_{0 \leq j \leq N} |u(x_j,t) - u_N(x_j,t)|,$$

where $u_N(x_j,t)$ is the solution of numerical scheme (4.1) and $u(x_j,t)$ is the exact solution of (1.1). By using Hirota method [10], the single solitary wave solution of this system is

$$u(x,t) = 2\lambda^2 \mathrm{sech}^2(\xi), \qquad v(x,t) = \frac{1}{2\sqrt{\eta}}\mathrm{sech}(\xi), \tag{5.1}$$

$$\xi = \lambda(x - \lambda^2 t) + \frac{1}{2\log(\eta)}, \quad \eta = \frac{-b}{8(4a+1)\lambda^4} \tag{5.2}$$

We take the value of exact solution (5.1) and (5.2) at $t = 0$ as our initial conditions:

$$u(x,0) = 2\lambda^2 \mathrm{sech}^2(\xi), \qquad v(x,0) = \frac{1}{2\sqrt{\eta}}\mathrm{sech}(\xi),$$

where $\xi = \lambda x + \frac{1}{2\log(\eta)}$

Computation were done with parameters $a = 0.5$, $b = 3$, $\lambda = 0.5$ and $N = 8, 16$. Tables 1-2 show the maximum error for the soliton u and v respectively. It can be seen that the error norm calculated by pseudo-spectral scheme is smaller than that of Ismail [19]. Figs 1-2 plot the single soliton for u and v. The graph of pseudo-spectral method coincide with the exact solution. The reason may be due to that the error order of pseudo-spectral is infinite and on temporal is 2. Our scheme is better than the collocation scheme developed by Ismail [19].

Table 1: Maximum error for single soliton u

	N=8		N=16	
Time	Present Method	Ismail [19]	Present Method	Ismail [19]
0.1	3.5518×10^{-5}	3.0085×10^{-4}	2.4407×10^{-5}	2.9974×10^{-4}
0.3	3.0577×10^{-5}	3.4972×10^{-4}	2.9466×10^{-5}	2.3861×10^{-4}
0.5	3.8579×10^{-5}	4.5155×10^{-4}	2.7468×10^{-5}	3.4044×10^{-4}
0.7	3.6506×10^{-5}	2.9705×10^{-4}	2.5495×10^{-5}	1.8694×10^{-4}
1.0	3.0555×10^{-5}	3.5333×10^{-4}	2.9444×10^{-5}	2.4222×10^{-4}

Table 2: Maximum error for single soliton v

	N=8		N=16	
Time	Present Method	Ismail [19]	Present Method	Ismail [19]
0.1	5.1521×10^{-5}	4.6833×10^{-4}	4.0410×10^{-5}	3.5722×10^{-4}
0.3	6.2302×10^{-5}	4.1610×10^{-4}	5.1291×10^{-5}	8.0509×10^{-4}
0.5	5.7407×10^{-5}	4.0631×10^{-4}	4.6396×10^{-5}	3.9520×10^{-4}
0.7	4.9000×10^{-5}	5.2757×10^{-4}	3.8999×10^{-5}	4.1646×10^{-4}
1.0	4.8310×10^{-5}	5.2378×10^{-4}	3.7209×10^{-5}	4.1267×10^{-4}

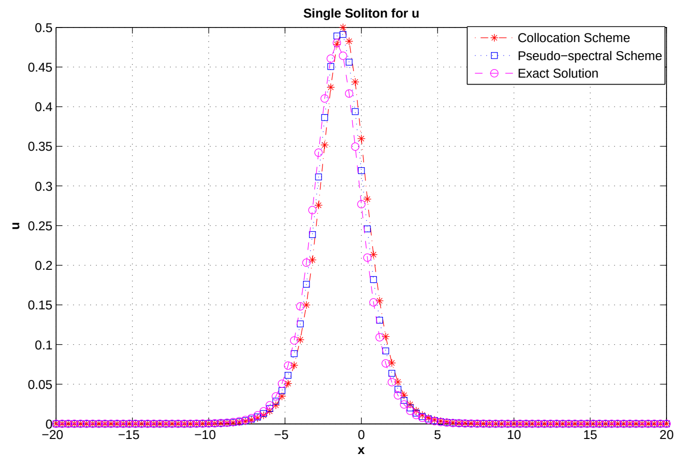

Figure 1: The graph of u soliton at t=1

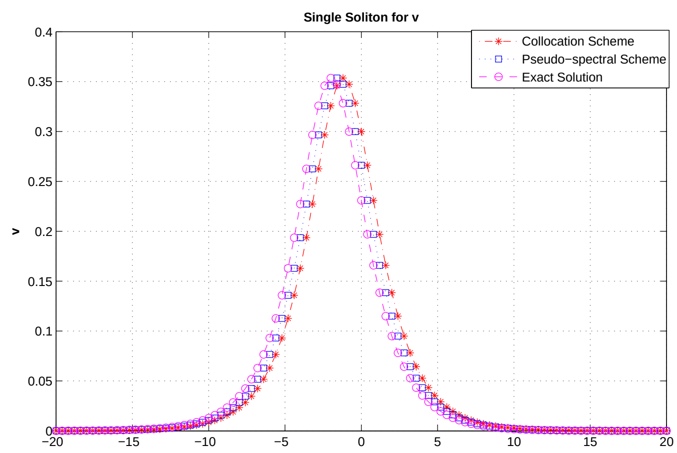

Figure 2: The graph of v soliton at t=1

Acknowledgements The first author would like to acknowledge the financial support of University Sains Malaysia during my stay at School of Mathematical Sciences, USM, Penang, Malaysia.

References

[1] D.J. Korteweg, G.de Vries, On the change of form of long waves advancing in rectangular canal and on a new type of long stationary waves, *Philos. Mag.* 36, 422-443 (1895) .

[2] B. Fornberg, *A Practical Guide to Pseudospectral Methods*, Cambridge University Press, Cambridge, 1998.

[3] Das G. Sarma J. Response to comment on 'A new mathematical approach for finding the solitary waves in dusty plasma,. *Phys Plasma*, 6, 439-447 (1999).

[4] D. Gottlieb and S. A. Orszag, *Numerical Analysis of Spectral Methods: Theory and Applications*, SIAM, Philadelphia, 1977.

[5] Gao YT. Tian B. Ion-acoustic shocks in space and laboratory dusty plasma: Two-dimensional and non-travelling wave observable effects. *Phys Plasma* 8, 314-323 (2001).

[6] R. Peyret, *Spectral methods in incompressible viscous flow*, Springer-Verlag, New York, 2002.

[7] J.H. He, Approximate analytical solution for seepage flow with fractional derivative in porous media. *Comput. Methods Appl. Mech. Eng.* 167, 69-73 (1998).

[8] A. Osborne, The inverse scattering transform: Tools for the nonlinear Fourier analysis and filtering of ocean surface waves. *Choas Solitons and Fractal*, 5, 2623-2637 (1995).

[9] L. Ostrovsky, and Y. Stepanyants, Do interal solution exist in the *ocean. Rev. Geophys.* 27, 293-310 (1989).

[10] R. Hirota and J. Satsuma, Soliton solution of the coupled KdV system, *Phys. Lett. A.*, 85, 407-408 (1981).

[11] H. W. Tam, W. Ma, X.-B. Hu, and D-Wang, The Hirota-Satsuma coupled KdV equation and coupled Ito system Revisited, *J. Phys. Soc. Jpn.*, 69, 45-52 (2000).

[12] D. Kaya and I. Inan, Exact and numerical traveling wave solutions for nonlinear coupled equation using symbolic computation, *Appl. Math. Comput.*, 151, 775-787 (2004).

[13] E. G. Fan, Travelling wave solutions for nonlinear equations using symbolic computation, *Comput. Math. Appl*, 43, 671-680 (2002).

[14] J. P. Boyd, *Chebyshev and Fourier spectral methods*, Springer-Verlag, New York, 2002.

[15] L. M. B. Assas, Variational iteration method for solving coupled KdV equations, *Chaos, Solitons Fractals*, 38, 1225-1228 (2008).

[16] L. N. Trefethen, *Spectral Methods in MATLAB*, SIAM, Philadelphia, 2000.

[17] S. Abbasbandy, The application of homotopy analysis method to solve the generalized Hirota-Satsuma coupled KdV equation, *Phys. Lett. A.*, 361, 478-483 (2007).

[18] C., Canuto, M. Y. Hussaini, A. Quarteroni, and T. A. Zang, *Spectral methods (fundamental in single domains)* Springer-Verlag, Berlin, 2006.

[19] M.S. Ismail, Numerical solution of a coupled Korteweg-de Vries equations by collocation method. *Numer. Methods Partial Differential Equations* 25, 275–291 (2009).

JOURNAL OF APPLIED FUNCTIONAL ANALYSIS, VOL.6, NO.1, 26-36, COPYRIGHT 2011 EUDOXUS PRESS, LLC

Non-ergodic dynamics of Nanosystems.

V.A.Benderskii
Institute of Problems of Chemical Physics, RAS
142432 Moscow Region, Chernogolovka, Russia

E. I. Kats
Laue-Langevin Institute, Grenoble, France and
L. D. Landau Institute for Theoretical Physics, RAS, Moscow, Russia

(Dated: May 27, 2010)

We investigate quantum dynamics of a small system selected state coupled to other discrete dense states of the system. We show that in a generic case with non-constant interlevel spacings and coupling matrix elements, the quantum dynamics of the selected level demonstrates non-trivial fine structures of the recurrence cycles (Loschmidt echo) and cycle mixing leading eventually to irregular, chaotic like longtime evolution. Our results illustrate non-ergodic dynamics of such a system, i.e., system population (or its energy) is not equally distributed over all system states but in a certain time intervals it is concentrated in a few levels. Our approach can be applied to rationalize experiments on femtosecond range vibrational relaxation of a specially selected state (the system) coupled to all other states (the reservoir) of nano-particles, where various regimes of time evolution, varying from exponential decay to irregular oscillations are observed in spectroscopic experimental data within the window $10^{-13} - 10^{-11}\ s$.

PACS numbers: 03.65, 82.20.B, 05.45.-a, 72.10.-d

Keywords: quantum dynamics, discrete spectrum reservoir, ergodicity, chaos

I. INTRODUCTION

In quantum mechanical systems quite often one has to deal with superposition of a given (somehow selected) state wave function with wave functions from continuous spectrum formed by either free states of the same system, separated from the given quasi-stationary state by a potential barrier (like it is the case in α-decay), or by the system environment, we will term reservoir (see the classical papers [1], [2]). Following this, common wisdom ascribes irreversible evolution of quasi-stationary states by coupling to reservoir with continuum spectrum [3], [4]. With a model reservoir formed by a sea of harmonic oscillators, this approach is in the heart of the theory of quantum dissipative systems [5], [6], [7].

The opposite limit is considered in the theory of transition states which is widely used to treat various chemical dynamics problems [8], [9]. In this basically microscopic approach one has to chose properly a set of internal degrees of freedom forming so-called reaction path, and a small number of transverse degrees of freedom which are coupled to the longitudinal reaction coordinate. This microscopic description is feasible in practice up to a few dozens of the transversal degrees of freedom. For larger systems the microscopic approach becomes un-practical and useless (since even for modern computer power for a system with 10^4 transversal degrees of freedom purely computation problems, to find all eigen states to restore multi dimensional potential energy surfaces, is nearly insuperable). However many nano-system with $10^2 - 10^4$ degrees of freedom, interesting from their practical importance and the associated theoretical challenges, belong to this intermediate case when the both mentioned above approaches (macroscopic theory of quantum dissipative systems and microscopic theory of chemical dynamics) do not work. Evidently to cover very complex phenomena occurring in the intermediate region without any small parameter, it is necessary to chose a simplified (but yet not trivial) model. One avenue of research is to borrow concepts from other systems with dense discrete spectra, like nuclei and nuclear reactions. In this realm it was shown [10], [11], [12], [13], [14], that statistical description of such a system does not require the detailed information about its spectrum, but only universal mean spectral characteristics (like interlevel spacing distribution function), which are determined by random Hamiltonian matrix. These approaches are very convenient tools to describe e.g., spectral chaos and many other global features of the behavior, but they say almost nothing about quantum dynamics, we are interested in this paper. Our approach is conceptually distinctive from that. Namely, instead of an approximate solution of a more or less complete quantum model of the phenomenon, we simplify the bare model to a level admitting its exact solution. In this respect we follow a general spirit that the exact solvability of non-trivial quantum mechanical models plays an extraordinary important role.

Our motivation is not a pure curiosity. As a matter of fact quantum dynamics of various systems (ranging from relatively small molecules in a pre-dissociation condition [15], [16] up to large photochromic molecules and their protein complexes [18], [17], [19], [20], [21], [22]), or molecules confined near interfaces [23] (see also [22]). is an active area of experimental researches. The femtosecond spectroscopy data (which allow to study time evolution of one selected initially prepared by optical pumping state) manifest variety of possible regimes including not only weakly damped more or less regular oscillations but also very irregular long time behavior with a number of peaks corresponding to a partial recovering of the initial state population.

Observed in such systems seemingly irregular damped oscillation regimes can not be explained theoretically in the frame work of widely used models with reservoirs possessing continuous spectra [24], [5], [8], [7], [6]. Indeed in the case of a system coupled to the continuous spectrum reservoir, only smooth crossover between coherent oscillations and exponential decay is possible upon increasing of the coupling. Nevertheless, as it was shown in the references above, generic complex dynamics is observed in the systems with characteristic inter-level spacing of the order of $10\,cm^{-1}$, when the measurements are performed in the range of sub-picoseconds, or femtoseconds. To explain these weakly damped oscillations semi-empirical models have been proposed [22], [25], assuming more or less arbitrary that the system interacts not only with the reservoir (in agreement with a common belief possessing continuous spectrum) but also with a few (1-2) weakly damped discrete vibrational levels. However, these models providing in principal possible mechanism for weakly damped oscillations are not able to explain irregular, random-like dynamic evolution. It is worth noting that a generic feature of systems with such irregular behavior is the existence of the dense but discrete vibrational spectra, where in the range of $10^{-13} - 10^{-11}\,s$ there exist $10^2 - 10^3$ levels with characteristic inter-level spacings of the order of $10\,cm^{-1}$. This generic feature is omnipresent in the systems with complex and irregular vibrational relaxation.

Motivated by these observations, our intent here is to propose a simple (but yet non-trivial) model of a system coupled to a reservoir with discrete spectrum, and to examine joint system-reservoir evolution, i.e., recurrence cycles, when the energy is flowing back from the reservoir to the system. Surprisingly for us, scanning the literature we did not find any paper treating theoretically such a model. We do believe that the basic ideas inspiring our work can be applied to a large variety of interesting nano-systems. In a recent short publication [26] such a model of a system coupled to a reservoir with dense discrete spectrum was proposed, and under assumptions put forward by Zwanzig [27] (equidistant spectrum of the reservoir and system-reservoir coupling independent of the reservoir state quantum numbers) its exact analytic was found. For that model we found recurrence cycles (as it should be for any system with discrete spectrum, according to Poincare theorem) with period $2\pi/\Omega$ (Ω is the interlevel spacing), because of equidistant reservoir spectrum. However even for these rather artificial assumptions of the Zwanzig model, long time behavior turns out quite non-trivial and irregular [26]. The fact is that in every cycle of energy or population exchange between the system (we term as a system the specific level selected by optical pumping) and the reservoir levels, occurs not simultaneously for all reservoir levels participating in that exchange. This breaks synchronization of the exchange between the reservoir levels and the systems, and yields to the fine structure of the recurrence cycles or spontaneous Loschmidt echo. The same phenomenom produces broadening of the echo signals, and the Loschmidt echo width increases with time, or what is the same with a cycle number k. As a result of this starting from the critical cycle number, when its width becomes of the order of the period, more and more neighboring components are mixed and time evolution becomes irregular, chaotic-like. To answer a natural question arising from this very unexpected (to say the least) result, namely whether it comes from the very restrictive assumptions of the exactly solvable Zwanzig model, or it illustrates generic behavior of any system with discrete but dense spectrum, is the main aim of the present manuscript.

Details of our basic approach to solve quantum dynamic problem for a state coupled (not necessary independent of quantum numbers) to discrete (not necessary equidistant) spectrum of the orthogonal states of the bare reservoir, are introduced and described in the next section II. In the section III we formulate this problems in terms of recurrence cycle partial amplitudes. Specific models where reservoir interlevel spacings monotonically increase or decrease with level quantum numbers and also the case when the coupling matrix elements decreases with energy are investigated in the section IV. In the last section V, we summarize our results discuss several predictions relevant for vibrational spectroscopy of large molecules.

II. MAIN IDEA OF THE ANALYSIS

Our analysis is based on a simple but very general observation known from the standard quantum mechanics. Namely that for a selected unperturbed energy level ϵ_s^0 (in what follows we will term the level as a system) coupled to a discrete spectrum reservoir (with its unperturbed energy states $\{\epsilon_n^0\}$), the Hamiltonian matrix contains besides the main diagonal, only one row and one line of non-zero matrix elements. Therefore the corresponding secular equation (its roots determine the coupled system-reservoir eigenvalues) has the following deceptively simple form

$$F(\epsilon) = \epsilon - \sum_n \frac{C_n^2}{\epsilon - \epsilon_n^0} = 0 \,, \tag{1}$$

where we count the energy levels from ϵ_s^0, and to get such a compact form for the function $F(\epsilon)$ we chose the orthogonal basis of the reservoir states, i.e., all matrix elements between the reservoir states are zero. Furthermore, because of singularities occurring at $\epsilon = \epsilon_n^0$ in r.h.s. of (1), in each interval $[\epsilon_n^0 \, \epsilon_{n+1}^0]$ there is always one eigenvalue ϵ_n. It is convenient to use as a reference point the eigenvalues known [26] for the Zwanzig model

$$\epsilon_n \equiv n g(n) \,;\, C_n = C h(n) \,, \tag{2}$$

with the functions $g(n)$ and $h(n)$ describing deviations from equidistant reservoir and independent of quantum numbers coupling results. Assuming also that eigenvalues and matrix elements transform under operation $n \to -n$ as

$$\epsilon_n^0 = -\epsilon_{-n}^0 \,;\, C_n^2 = C_{-n}^2 \tag{3}$$

one can show by direct calculations that the secular equation (1) can be solved analytically for the following choices of the function g and h

$$g_{\pm}(n) = (1 + \chi n^2)^{\pm 1/2} \,;\, h(n) = \left(1 + \frac{n^2}{\Delta^2}\right)^{-1/2} \,, \tag{4}$$

where parameters $\Delta \gg 1$ and $\chi \ll 1$ to have many reservoir levels involved into the coupling.

Time dependent wave functions $\Psi_s(t)$ of the Hamiltonian can be expanded over the unperturbed (uncoupled) eigenfunctions of the system Φ_s and of the reservoir states Φ_n

$$\Psi_s(t) = a_s(t)\Phi_s + \sum_n a_n(t)\Phi_n \tag{5}$$

with time dependent amplitudes $a_s(t)$, $a_n(t)$. These time dependent amplitudes satisfy to the corresponding Heisenberg equations of motion

$$i\dot{a}_s = \sum_n C_n a_n \,;\, i\dot{a}_n = C_n a_s + \epsilon_n^0 a_n \,, \tag{6}$$

supplemented by the initial condition

$$a_s(0) = 1 \,;\, a_n(0) = 0 \,. \tag{7}$$

These equations can be solved formally by utilizing the Laplace transform of the amplitudes $a_s(t)$

$$a_s(t) = \frac{1}{2\pi i} \int_{\delta - i\infty}^{\delta + i\infty} dp \frac{\exp(pt)}{p + \sum_n C_n^2 (p + i\epsilon_n^0)^{-1}} \,, \tag{8}$$

where $\delta \to +0$. Replacing $p = i\epsilon$ the (8) is transformed into the Fourier series

$$a_s(t) = \frac{1}{2\pi i} \int_{-\infty}^{+\infty} d\epsilon \frac{\exp(i\epsilon t)}{F(\epsilon)} = 2 \sum_{n=-\infty}^{n=+\infty} \left. \frac{\cos(\epsilon t)}{dF/d\epsilon} \right|_{\epsilon = \epsilon_n} \,. \tag{9}$$

Thus we conclude that the system amplitude $a_s(t)$ is the Fourier series sum over the residues in the simple poles $\epsilon = \epsilon_n$ which are the roots of the secular equation.

III. QUANTUM DYNAMICS IN RECURRENCE CYCLE REPRESENTATION

As in every diagonalization procedure we need to select a well-behaved representation. Fourier series for the system amplitude (9) can be presented as a sum over recurrence cycle partial amplitudes [26]

$$a_s(t) = \sum_{k=-\infty}^{\infty} a_s^{(k)}(\tau_k)\,, \tag{10}$$

where τ_k is a local time for the cycle k which via Poisson summation formulae (see e.g., similar derivation in [28], [29]) depends on the reservoir spectrum and coupling matrix elements. To find this dependence it is convenient to replace ϵ in the secular equation by another variable λ

$$\epsilon = \lambda g(\lambda)\,, \tag{11}$$

and the function g should be chosen to keep the secular equation in a form similar to that [26] for equidistant reservoir spectrum

$$F(\lambda) = P(\lambda)(Q(\lambda) - \cot(\pi\lambda))\,, \tag{12}$$

where the function P and Q are expressed in terms of the reservoir spectrum and coupling matrix elements characteristic functions $g_\pm$ and h (2). Utilizing the Poisson summation formulae

$$\sum_n f(n) = \sum_{k=-\infty}^{+\infty} \int_{-\infty}^{+\infty} f(x)\exp(i2\pi kx)dx\,, \tag{13}$$

and also well known property of the δ-function

$$\delta(f(x)) = \sum_n \left|\frac{df}{dx}\right|^{-1}_{x=x_n} \delta(x - x_n)\,, \tag{14}$$

where x_n are the roots of the equation $f(x) = 0$, we end up with the (12) in mind with the following formal expression for the recurrence cycle partial amplitudes

$$a_s^{(k)} = \pi^{-1}\int_{-\infty}^{+\infty} d\lambda \frac{\exp[i\lambda(\epsilon(\lambda)t/\lambda - 2k\pi)]}{P(\lambda)(1+Q^2(\lambda))}\frac{d\epsilon}{d\lambda}\left(\frac{Q(\lambda+i}{Q(\lambda-i}\right)^k\,. \tag{15}$$

For the Zwanzig model $\lambda \equiv \epsilon$, $P = \pi C^2 \equiv \Gamma$, $Q = \epsilon/\Gamma$ and the local time does not depend on ϵ. It is not the case for non-equidistant spectra, where

$$\tau_k(\lambda) = \frac{\epsilon t}{\lambda} - 2k\pi\,. \tag{16}$$

To calculate entering (15) integral one has to find the residues in the poles inside a close integration contour, including the real axis and large radius semi-circle. Where to put this semi-circle depends on the sign of the local time τ_k. Note first that contributions of the cycles with $k < 0$ are exponentially small for $t > 0$. For the initial cycle $k = 0$ the amplitude is determined by the poles in the upper half-plane. For all other cycles $k \geq 1$ the poles in the upper/lower half-plane are relevant for τ_k positive/negative. For the Zwanzig model there is only one pole in the upper half-plane, therefore all the recurrence cycle partial amplitudes contribute to only forward in time evolution for $\tau_k \geq 0$. However if the functions $g_\pm(n) \neq 1$ and/or $h(n) \neq 1$, the backward in time evolution occurs from the poles in the lower half-plane. Positions of the both kinds of the poles (for forward and backward evolutions) are related to recurrence cycle periods

$$T(\lambda^*) = \frac{2\pi}{\epsilon(\lambda^*)}\,, \tag{17}$$

where λ^* are the poles of the integrand in the (15).

IV. GENERALIZED ZWANZIG MODEL WITH NON-EQUIDISTANT RESERVOIR

A. Reservoirs with increasing interlevel spacings

To move further on smoothly let us consider first the case (see the definition (2) when

$$g(n) = g_+(n)\,;\; h(n) = 1\,. \tag{18}$$

It generalizes the Zwanzig model for the reservoirs with interlevel spacings increasing with energy. Performing tedious but straitforward algebra we find

$$\lambda^2 = \frac{1}{2\chi\Gamma^2}[\sqrt{1+4\chi\epsilon^2} - 1]\,, \tag{19}$$

and the functions $P(\lambda)$ and $Q(\lambda)$ read as

$$P(\lambda) = \frac{\sqrt{1+\chi\lambda^2}}{1+2\chi\lambda^2}\,, \tag{20}$$

whereas

$$Q(\lambda) = \lambda\left(1 + 2\chi\lambda^2 - \frac{\Gamma\sqrt{\chi}}{\sqrt{1+\chi\lambda^2}}\right)\,. \tag{21}$$

In the initial cycle $k = 0$ the poles in the integrand in the recurrence cycle representation are the roots of the equation $Q^2 + 1 = 0$. In the upper half plane its solution gives two pure imaginary poles. In the limit $\chi\Gamma^2 \to 0$, the poles are

$$\lambda_1 = i(1 + \Gamma\sqrt{\chi})\,;\; \lambda_2 = i\frac{(1-\chi\Gamma^2)}{\Gamma\sqrt{\chi}}\,. \tag{22}$$

Upon increasing the controlling behavior parameter $\chi\Gamma^2$, the poles approach to each other, merge at the critical value $\chi_c = 1/(27\Gamma^2)$, and become two complex conjugated poles. Moreover with increase of the parameter $\chi\Gamma^2$ the residue at the λ_2 increases, and the partial amplitude $a_s^{(0)}$ decay becomes non-exponential (!). The effective rate constant

$$\Gamma_{eff} \equiv -\frac{d\ln a_s^{(0)}}{dt} = \frac{\epsilon(\lambda_1)B(\lambda_1)\exp(-\epsilon(\lambda_1)t) - \epsilon(\lambda_2)B(\lambda_2)\exp(-\epsilon(\lambda_2)t)}{B(\lambda_1)\exp(-\epsilon(\lambda_1)t) - B(\lambda_2)\exp(-\lambda_2)t)}\,, \tag{23}$$

where we use notation

$$B(\lambda_{1,2}) = \left(\frac{d\epsilon}{d\lambda}\right)_{\lambda_{1,2}}\frac{1}{P(\lambda_{1,2})}\,, \tag{24}$$

where $i = 1, 2$. We see that the effective rate is not a constant (as one would expect for the usual exponential decay). It is zero when $t \to 0$ and increases with time. However the rate constant decreases with χ when $\Gamma t < 1$. This decrease is because at constant Γ the number of reservoir levels participating in energy exchange with the system, decreases. In long time asymptotics $\Gamma t \gg 1$, the effective rate Γ_{eff} becomes larger than that of the equidistant reservoir. In the limit of the equidistant reservoir spectrum $\chi \to 0$ reservoir levels displacements (due to the coupling with the system) are proportional to n^{-2}, whereas with increase of χ all essential levels, i.e., with $n \leq \Gamma$ giving the principal contributions to the rate, displace more or less equally. Therefore the active levels approach to almost equidistant ones.

There are also two complex conjugated poles in the lower half plane, which are the roots of the equation $Q(\lambda) = i$. These poles are responsible for the backward system evolution (characteristic feature of the non-equidistant reservoir spectra) in the recurrence cycles $k \geq 1$. We show the system amplitude dynamics in the Fig. 1. At $\chi = 0$ the Loschmidt echo appears only for $\tau_k \geq 0$. At $k < k_c \equiv \pi\Gamma$, the system dynamics is regular one, and the Loschmidt echo components are well separated (ratio of the echo width to the cycle period is of the order of k/k_c, i.e., smaller than 1). However for non-equidistant reservoir ($\chi \neq 0$) the echo appears also for $\tau_k < 0$ (backward evolution). From

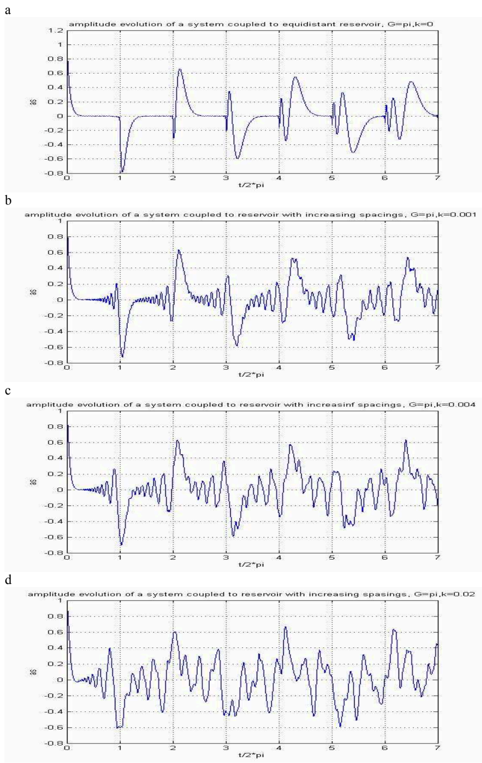

Figure 1: System amplitude time evolution for a model with $h(n) = 1$ and $g(n) = g_+(n)$ (see (2). The parameter $\chi = 0\,,\, 0.001\,,\, 0.004\,,\, 0.002$ for the figures $a - d$, respectively.

(15) we estimate in the limit $\chi\Gamma^2 \ll 1$

$$a_s^{(k)}(\tau_k) \simeq \left(\begin{array}{ll} \exp(-\tau_k(\lambda_1)/2) L_{k-1}^1(\tau_k(\lambda_1)) & ;\, \tau_k > 0 \\ (\chi/\chi_c)^{1/2} \exp(-\tau_k(\lambda_{31})) \cos(\tau_k(\lambda_{32})) & ;\, \tau_k < 0 \end{array} \right. , \tag{25}$$

where $\tau_k(\lambda_1)$ is the local time defined by the smallest among the pole s in the upper half plane, $\tau_k(\lambda_{31})$ and $\tau_k(\lambda_{32})$ correspond to the complex conjugated poles in the lower half plane, $\lambda_3 = \lambda_{31} + i\lambda_{32}$, and L_{k-1}^1 is generalized Laguerre polynomial [30].

It is worth noting that backward evolution occurring only for non-equidistant spectrum reservoirs, modifies considerably cycle mixing conditions. If for $\chi = 0$ the cycles are overlapped at $\tau_k > 0$, when their characteristic width becomes of the order of the recurrence cycle period, the backward echo decreases the threshold for cycle overlapping, which decreases with χ.

B. Generalized Zwanzig model with non constant coupling matrix elements

Let us now add one more new ingredient in a root to more realistic models describing nano-particle relaxation. We will relax in this subsection the assumption on constant coupling matrix elements, namely we chose $h(n) \neq 1$ in the form (3), while keeping the equidistant reservoir spectrum ($g_\pm(n) = 1$). The recurrence cycle partial amplitudes read as

$$a_s^{(k)}(\tau_k) = \int_{-\infty}^{+\infty} du \left(\frac{R(u)+i}{R(u)-i}\right)^k \frac{1+\alpha^2 u^2}{R^2(u)+1} \exp\left[-i\frac{\tau_k u}{2}\right], \tag{26}$$

where $\tau_k = 2\Gamma(t-2k\pi)$ for this model, and we denoted $\alpha = \Gamma\Delta^{-1}\coth(\pi\Delta) \simeq \Gamma\Delta^{-1}$, and $R(u) = (1-\alpha)u + \alpha^2 u^3$. The integrand in (26) has $(k+1)$-th order poles which are the roots of the equations

$$R(u) \pm i = (\alpha u \pm i)(\alpha u^2 \mp iu - 1) = 0, \tag{27}$$

where $\pm$ signs correspond to $k \geq 1$ and $k \leq -1$ respectively ($k = 0$ cycle has the both types of the poles). The roots of the (27) can be easily found

$$u_{1,2}^{\pm} = \pm i u_{1,2}\,;\; u_3^{\pm} = \mp i u_3 \tag{28}$$

and in the explicit forms, the roots are

$$u_{1,2} = \frac{1}{2\alpha}(1 \mp \sqrt{1-4\alpha})\,;\; u_3 = \frac{1}{\alpha}. \tag{29}$$

By a simple inspection of the (29) we find that the root u_1 increases with α, whereas two other roots move from infinity along the imaginary axis. When α exceeds its critical value $\alpha_c = 1/4$, the two roots are complex conjugated ones, while the third root remains pure imaginary one. In this case the integration contour lies in the upper half plane, therefore there is no backward evolution in time. Depending on α one can distinguish three different time evolution regimes. When

$$2u_1 < u_2 - u_1\,;\; 0 \leq \alpha \leq 3/16 \tag{30}$$

system kinetics is determined by the pole u_1 , and qualitatively behavior is similar to that found in [26] for the Zwanzig model. In the region where

$$|u_1 - u_2| < min(2u_1\,,\, |u_1 + u_2|)\,;\; 3/16 < \alpha < 1/2 \tag{31}$$

system kinetics is controlled by two close poles (pure imaginary ones at $\alpha \leq 1/4$ and complex conjugated at $\alpha > 1/4$). Finally there is region where the complex conjugated poles satisfy

$$|u_1 - u_2| > |u_1 + u_2|)\,;\; \alpha > 1/2\,. \tag{32}$$

We illustrate this behavior in Fig. 2. In the region (30) similarly to the Zwanzig model dynamics, there is Loschmidt echo in each recurrence cycle k with its fine structure containing k components, I_{kl} (where $l = 1, 2, ...k$). The total echo width increases with cycle number k, but upon increase of the parameter α, the widths of the echo components $l < k$ (and therefore the total echo width) decrease, whereas the main component I_{kk} intensity remains constant. In this region one can find approximately the following spectrum of the Loschmidt echo

$$a_s^{(k)}(\tau_k) \simeq Res(u_1) = \left(-f_{k2}(u_1)\frac{\tau_k}{k}L_{k-1}^1(u_1\tau_k) + \sum_{n=0}^{k} C_{k-n+1}^k (2u_1)^n f_{k2}^{(n)}(u_1) L_{k-n-1}^n(u_1\tau_k)\right)\exp(-u_1\tau_k/2)\,, \tag{33}$$

where C_{k-n+1}^k stands for the permutative combinatorial coefficient, and

$$f_{k2}(u) \equiv \frac{(u_2+u)^{k-1}(u_3+u)^k}{(u_2-u)^{k+1}(u_3-u)^{k+1}}\,. \tag{34}$$

The first term in the (33) is an order k polynomial of $u_1\tau$, which is the same as that describing the Loschmidt echo signal at $\alpha = 0$ (up to a replacement of τ by $u_1\tau$. In the range $0 \leq u_1\tau \leq 4k$ it includes k components with increasing intensities. For $k \gg 1$ we may approximate

$$f_{k2}^{(n)}(u_1) \simeq f_{k2}(u_1)(2kQ)^n\,, \tag{35}$$

where

$$Q = \frac{4ku_1^2(u_3^2 - u_1u_2)}{u_2(u_2-u_1)u_3(u_3+u_1)}\,. \tag{36}$$

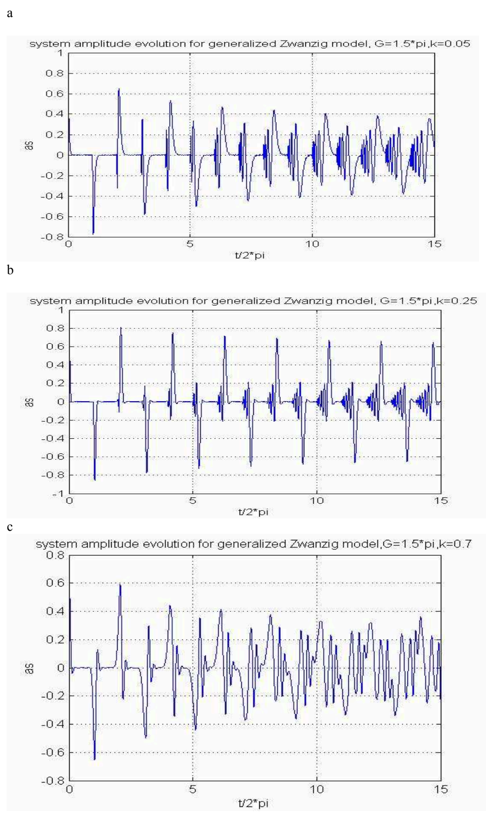

Figure 2: System amplitude time evolution for a model with $g(n) = 1$ and $h(n)$ is given by the (2). The parameter $\alpha \equiv \Gamma/\Delta$ (see (2): $\alpha = 0.05$, 0.25 , 0.7 for the figures $a - c$, respectively.

With (35), (36) in hands we can perform the summation in (33)

$$\sum_{n=1}^{k} \frac{Q^n}{n!} L_{k-n}^{n-1} = (-1)^k \left((1 + Q - u_1\tau)^k - (1 - u_1\tau)k - kQ \right) . \tag{37}$$

In a dramatic contrast with multicomponent Loschmidt echo signals for Zwanzig model, there is only one maximum in (37) at $u_1 \tau_k^* \simeq Q + 2k$. Thus we arrive at the conclusion that upon increase of α and k, the intensity of the main echo component increases whereas all other echo components remain unchanged in the main approximation. Therefore the parameter α reduces effectively the satellite echo components intensities I_{kl} (where $l < k$), and only weak echo components (not the main echo signals) are mixed at $k > k_c$. Similarly at $\alpha = \alpha_c$ only one echo component dominates the spectrum and mixing occurs only when k is several times larger than $k_c = \pi\Gamma$. Only when $\alpha > \alpha_c$ and a_s dynamics is represented as damped oscillations with characteristic time incommensurate with the cycle period, the cycle mixing occurs at $k < k_c$. We shall not proceed further on with the calculations. Since our model is rather crude, the detailed algebra is not worth the effort. Therefore we rationalize time evolution on a qualitative level and illustrate it in Fig 2. In the region (30), the reservoir states not synchronous return their populations back to the system. Thus the system population is recovered only partially. However upon increase of the parameter α the reservoir - system exchange becomes more and more synchronous, and the main component echo intensity approaches to 1 in the region (31). The system evolution in this case is a superposition of ergodic components corresponding to the reservoir eigenfrequencies. This regime resembles conditionally-periodic dynamics [31] and could be termed as quasi -ergodic regime (see also [32], [33]). Finally in the region (32), the reservoir states are mixed already for $k \geq 2$.

C. Reservoirs with decreasing interlevel spacings

In this case according to the (2), $g(n) = g_-(n)$ and $C_n = Ch(n)$, there are no poles of the partial amplitudes in the lower half-plane, and in the upper half-plane there are complex-conjugated poles like for the case with $g(n) = g_+(n)$ and $h(n) = 1$ studied in the subsection IV A. The system evolution in this case is determined by the main echo component and damped satellite oscillations with their amplitudes slowly increasing with the cycle number k (see Fig. 3a). Note that even for not too small values of the parameter Δ, when the interlevel spacing reduces by several times for the active level $n \simeq \Gamma$, the one-component Loschmidt echo period remains practically constant (see Fig. 3b).

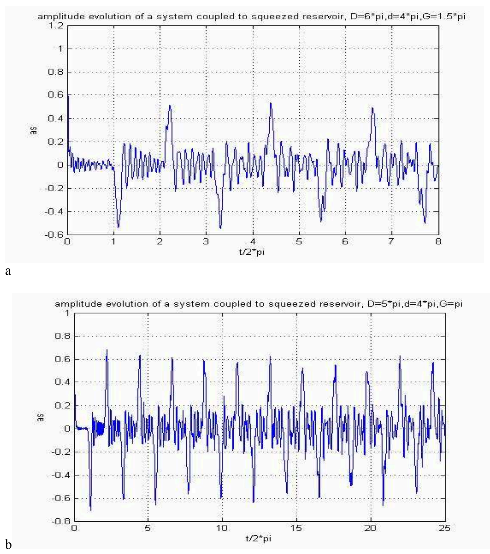

Figure 3: System amplitude time evolution for a model with $h(n) \neq 1$ and $g(n) = g_-(n)$ (see (2). The parameter $\Delta = 4\pi$ and $\chi = (5\pi)^{-2}$, $C = 1$ for the Fig. 3a, and $\Delta = 4\pi$, $\chi = (6\pi)^{-2}$, and $C = 1.5$ for the Fig. 3b.

V. CONCLUSION

To summarize, in this paper we investigated quantum dynamics of a small system selected state coupled to other discrete dense states of the system. This publication represents a substantial extension of the note [26], where only the equidistant reservoir and constant coupling Zwanzig model have been studied. Here we provide a more complete account and investigation of phenomena only briefly addressed in [26], and besides generalize Zwanzig model. We show that in a generic case with non-constant interlevel spacings and coupling matrix elements, the quantum dynamics of the selected level demonstrates non-trivial fine structures of the recurrence cycles (Loschmidt echo) and cycle mixing leading eventually to irregular, chaotic like longtime evolution. Our results illustrate non-ergodic dynamics of such a system, i.e., system population (or its energy) is not equally distributed over all system states but in a certain time intervals it is concentrated in a few levels. Turns out that for a rather broad interlevel spacings and coupling matrix elements distributions, these features of the Zwanzig model [26] remain valid. Mathematically it comes from the fact that system quantum evolution is governed by only a few poles of the system amplitude expansion over partial recurrence cycle amplitudes. For the Zwanzig model (with equidistant reservoir and constant coupling matrix elements) there is only one pole in such a mapping. The additional poles existing for the generalized Zwanzig model investigated in this paper, breaks pure exponential system decay in the initial cycle ($k = 0$) and strongly modify conditions of cycle mixing in the following cycles $k \geq 1$. In the model where coupling matrix elements decrease with energy small amplitude satellites in the Loschmidt echo signal are replaced by damped oscillations, and strongly reduced, while the main echo component remains more or less unchanged.

The generalized Zwanzig model investigated in this paper reflects the spirit of minimalist approaches, in that it is simple yet based on a physical principle. The results presented here are probably less notable in terms of technological applications of nano-systems, than for the progress they could generate in our understanding of their complicated vibrational spectra. Our consideration yields quite reasonable qualitative description of a variety vibrational relaxation regimes and mode selectivity observed in experiments, and the model under investigation appears to be a simplest one demonstrating that relatively small variation of the coupling enables to change qualitatively dynamic behavior. Understanding all its limitations, we nevertheless hope that our crude theory captures the essential elements of vibrational relaxation in nano-systems. Note to the same point that modern femtosecond spectroscopy methods (see e.g., [17] - [22]) indeed demonstrate (in a qualitative agreement with our consideration) remarkably different types of behaviors (exponential decay and complicated oscillation) of relatively close initially excited states. We believe we are the first to explicitely address this issue.

Acknowledgments

It is our pleasure also to acknowledge helpful discussions with Ya.G.Sinai, S.P.Novikov, and W.Miller.

[1] W.F.Weiskopf, E.P.Wigner, Z.Phys., **63**, 54 (1930).
[2] A.J.F.Siegert, Phys. Rev., **56**, 750 (1939).
[3] P.Grigolini, Quantum Mechanical Irreversibility, World Scientific, Singapore (1993).
[4] I.Prigogin, T.Y.Petrovsky, Adv. Chem. Phys., **99**, 1 (1997).
[5] A.J.Leggett, S.Chakravarty, A.T.Dorsey, M.P.A.Fisher, A.Garg, M.Zweger, Rev. Mod. Phys., **59**, 1 (1987).
[6] U.Weiss, Quantum dissipative systems, World Scientific, Singapore (1999).
[7] L.H. Yu, C-P.Sun, Phys. Rev. A, **49**, 592 (1994).
[8] V.A.Benderskii, D.E.Makarov, C.A.Wight, Chemical Dynamics at Low Temperatures, Willey-Interscience, New York (1994).
[9] V.A.Benderskii, E.V.Vetoshkin, I.S.Irgibaeva, H.P.Trommsdorff, Chem. Phys., **262**, 369 (2000); ibid, 393.
[10] G.V.Milnikov, H.Nakamura, Phys. Chem. Chem. Phys., **10**, 1374 (2008).
[11] O.Bohigas, S.Tomsovic, D.Ulmo, Phys. Rep., **223**, 43 (1993).
[12] V.K.B. Kota, Phys. Rep., **347**, 223 (2001).
[13] T.Papenbrock, H.A.Weidenmuller, Rev. Mod. Phys., **79**, 997 (2007).
[14] M.L.Mehta, Random matrices, Academic Press, New York (1968).
[15] E.B.Stechel, E.J.Heller, Ann. Rev. Phys. Chem., **35**, 563 (1984).
[16] R.Schinke, Photodissociation Dynamics, Cambridge Univ. Press., Cambridge (1994).
[17] M.Ben-Nun, T.J.Martinez, Chem. Phys. Lett., **298**, 57 (1998).
[18] M.Joeux, S.C.Farantos, R.Schinke, J.Phys.Chem. A, **106**, 5407 (2002).
[19] T.Vreven, F.Bernardi, M.Caravelli, M.Olivucci, M.Robb, H.B.Schlegel, J. Am. Chem. Soc., **119**, 1267 (1997).
[20] M.Ben-Num, F.Molnar, H.Lu, J.C.Phillips, J.T.Martinez, Farad Discus., **110**, 447 (1998).
[21] S.Hayashi, E.Tajkhorshid, K.Schulten, Biophys. J., **85**, 1440 (2003).
[22] C.J.Fecko, J.D.Eaves, J.J.Loparo, A.Tokmakoff, P.L.Geissler, Science, **301**, 1698 (2003).
[23] A.V.Benderskii, K.B.Eisental, J. Phys. Chem., A, **106**, 7482 (2002).
[24] A.O.Caldeira, A.J.Leggett, Ann. Phys., **149**, 587 (1983).
[25] S.Roy, B.Bagchi, J. Chem. Phys., **99**, 9938 (1993).
[26] V.A.Benderskii, L.A.Falkovsky, E.I.Kats, JETP Lett., **86**, 311 (2007).
[27] R.Zwanzig, Lectures in Theor. Phys., **3**, 106 (1960).
[28] M.Tabor, Chaos and Integrability in Nonlinear Dynamics, J.Wiley, New York (1989).

[29] M.C.Gutzwiller, Chaos in Classical and Quantum Mechanics, Springer, New York (1990).
[30] H.Bateman, A.Erdelyi, Higher Transcendental Functions, vol.2, McGraw Hill, New York (1953).
[31] Ya.G.Sinai, Introduction to Ergodic Theory, Princeton Univ. Press, Princeton (1977).
[32] V.A.Benderskii, E.I.Kats, Phys. Rev. E, **65**, 036217 (2002).
[33] V.A.Benderskii, E.V.Vetoshkin, E.I.Kats, HAIT Journal, **1**, 386 (2004).

JOURNAL OF APPLIED FUNCTIONAL ANALYSIS, VOL.6, NO.1, 37-47, COPYRIGHT 2011 EUDOXUS PRESS, LLC

Strategic System Planning by Experienced Managers

Nasser Fegh-hi Farahmand

Industrial Management Ph.D & Associate Professor of Islamic Azad University – Tabriz Branch

Islamic Republic of IRAN

Email: farahmand@iaut.ac.ir

Abstract

Since the Strategic System Planning (SSP) has been one of the fastest growing executive and energetically debated topics among practitioners and academicians. Which characteristics of Official Organizations (OO) influence whether or not those organizations engage in SSO. The focus is primarily on the environmental characteristics of Experienced Managers (EM) such as education and prior experience rather than those characteristics derived from personality traits. Data are drawn from a survey of the OO in official zones of North West of Islamic Republic of Iran that around ten percent the samples of EM engage in SSP. The EM characteristics showing a significant association with a commitment to SSP include an above average level of education, experience and running organization in sectors outside their previous experience. SSP showed a positive association with those EM with a growth orientation. It is concluded that EM characteristics can be important in explaining the SSP within the OO. This paper is to explore the ways in which certain characteristics of EM of OO generate a tendency to prepare a formal written Executive Plan (EP).
Key words: strategic planning, strategic executive planning, experienced managers, executive plan.

Introduction

Productive Strategic System Planning (SSP) is one of the important factors in executive success. There are arguing that formal written planning may be inappropriate for the Official Organizations (OO) but this seems a minority view. In OO, where an Executive Plan (EP) exists, the preparation of the SSP may have been driven by external forces. However, the EP may serve as a strategic planning document for the managers, entrepreneurs and workers, a plan to guide the executive and serve as a basis for taking strategic decisions and also it may serve as a subsequent monitoring device. In view of its perceived ongoing value to the small OO it might be expected that SSP would be a feature of many, if not most, OO (Deakins, 2003, 329; Feghhi farahmand, 2005, 458).

Official Strategy (OS)

The possible effects of OS on the propensity to prepare executive plans, is expected that organization oriented towards growth will show a greater propensity to undertake Strategic System Planning (SSP). It does not seem unreasonable to argue that an organization with a committed development strategy would have a executive plan. In most cases, this might also be reflected in an aim to increase the size of the customer base (Watts, et al, 2003; Stutely, 2002, 69). Indeed, wherever a strategy of growth required external support either from financial institutions or executive advice agencies, it is likely the external support agencies would require a SSP as a condition of their support. This paper examined the influence of these EM characteristics and OO strategies on the presence/absence of SSP in small organization, whilst controlling out the characteristics of the organization which the EM are operating. The key research questions addressed in this paper are as follows:

1) How prevalent is SSP amongst the EM of OO?

2) Are EM and BS characteristics important in distinguishing between EM with SSP?

3) Which EM and BS characteristics are important?

Strategic System Planning (SSP)

Recent research reviewing corporate coaching programmed that we can see this move from intuition towards rationalized models as complementary and off-setting to developments in strategic management. As management itself becomes more emphatically fast-paced and intuitive, in order to deal with complexity and unpredictability, research is beginning to accumulate showing that coaching formats used in management support are more effective than training in the older logical comprehensive pursuits. Like all scientific enterprises, a period of accumulation of evidence will be required before definitive conclusions may be drawn. However, there are early gleanings that evidence based evaluation research is underway.

In strategic system terms, the organization may be governed by experienced senior managers. In this way, executives systems that require sustained high levels of creative response will reward emotional intelligence over rational intelligence (Feghhi farahmand, 2004, 452). At the top level in all professions and disciplines, both sets of skills are required to perform at the highest levels. To this point, the discussion has focused on the fact that coaching-based intervention strategies assist management in adapting to the more intuitive and

fast-response aspects in its operations. Coaching as an emergent profession, however, is moving in the other direction.
It is progressing from a period in which right-brained intuitive judgments have been dominant to an evidence-based, left-brain rationalist approach.
In corporate settings, where large investments in coaching programmers are underway, evidence is required to justify these expenditures.
Models of development that build logically among different experiences are required. The basic steps of SSP development that they are suitable for all of organizations are as follows (Storey, 1994, 365 and Feghhi farahmand, 2004, 428):

1) Purpose: To develop SSP to strengthen the organization's customer related, operational, and financial performance.

2) Scope: The SSP should include both short-term and long term goals and plans and a method to ensure that the plan is deployed and adhered to should be part of the management review procedure throughout the organization.

3) Self Responsibility: The chief executive usually has control of these developments, deployment, improvement processes and all executive management should be personally involved in these processes.

4) Procedure: It should include the description of the timetable for strategy and SSP development should be including and how the development considers customer requirements, information related to quality, operational performance, and relevant financial data are collected, analyzed, and integrated into the strategy development should be included in this procedure. These should be compared with similar measures of competitors and or appropriate benchmarks.

5) Continuous improvement: Describe the main types of data and information needed to support operations and decision making, and to drive improvement of this executive process. The management and use of key performance measures should include periodic review for continued validity and need, as well as the analysis and use in process improvement. Factors in the evaluation might include completeness, timeliness, effectiveness, and reliability.

6) Instructions: Management responsibility, quality system, document and data control, corrective and preventive action, internal quality audits, training, statistical techniques and continuous improvement. Performance in a management setting means learning to express powerful, even negative, emotions in ways that are received as positive by the organization. Management, in this perspective, becomes a performance-based profession, where the way in which a team leader expresses objectives and values is as important as the targets themselves. Gaining the sustained co-operation of fellow team members requires emotional leadership (Feghhi Farahmand, 2003, 45).
Therefore Strategic is a tern used by some to refer to what might be termed know-when and know-why. Although it seems reasonable to conceive of these as

aspects of doing, it is difficult to envision them as being separate from that doing. In other words, we can separate out strategic knowledge only in the describing, not the doing. Consequently, strategic knowledge is probably best thought of as a subset of declarative knowledge instead of its own category.

Experienced Managers (EM)

The specification and nature of the EM is seen as critical in other aspects of the activities of OO. A selection of the EM characteristics is the potential to influence an owner manager's propensity to undertake SSP. Predictions of the direction in which the variables (Feghhi Farahmand, 2002, 345; Smith, 1967, 145) will operate are inevitably problematic as there is little prior work on the determinants of SSP upon which we can draw:

1) Age: This variable has been identified as important in a number of studies.

2) Experience: It may be strongly linked to age and it could be argued that it might work in two ways. A long number of years running an organization as an EM might increase a propensity to plan future directions for the official or indeed, once the initial phases had passed and funding secured planning might well be less of a priority.

3) Education: In the context of SSP, this variable might seem reasonable to hypothesis that the more highly educated EM will tend to be more aware of the desirability of SSP and thus, organization run by the better educated EM might be more likely to have Executive plans. In contrast, the EM with a more limited education will tend to work outside a formal planning framework.

4) Creativity: A distinction here may be drawn between those for whom the current organization is their first and serial founders.

5) Workers: This was identified as an influence on organization behaviour and in the context of SSP, EM with previous work experience in larger organization, perhaps where SSP was seen as an important part of official behaviour, would tend to encourage SSP in organization.

6) Managerial position: Organization founders are drawn either from operatives or from those with previous managerial experience.

7) Current experience: Here it might be argued that EM moving into a new sector might be encouraged to plan rather more than those who are official were in sectors in which they had considerable prior experience.

8) OO zone: This was introduced into the analysis as it might be expected that local EM, who grew up in the geographical area under study, will tend to be introspective and less receptive to contemporary management practice.

9) Locally: The relationships between OO and their localities have become an important research area and organization with links with local official institutions might be more likely to official plan. The argument here would be that mixing with local official leaders would increase awareness of the value of SSP. Conversely, mixing with other EM of small organization might re-inforce scepticism towards the idea of SSP, especially where SSP was not seen as a key element of official activity.

Methodology

This study is based on a sample of small official organization and the influence of organization characteristics such as SSP of organization have been well explored over the last decades. Sector contrasts between the largest group of organization in official organizations in the sample and size involves employment and turnover variables were included in some of the preliminary analysis but no sector or size effects were detected and OO was defined as one with less than 100 employees. The data relate to a sample drawn from independent plants in North West of Iran listed in directory of official organizations. The random sample was drawn and 34 organizations participated in the survey based on face to face, meeting, advising, questionnaire, participation in consultant sessions and e-mail interviews using a semi structured interview schedule. These organizations represent a response about rate of 62 percent and tests for response bias were possible. Virtually about 68 percent of the interviews were with the EM, the other interviews were experimental managers that they have not scientific management information and were the only viable respondent as they were working for retired managers who had relinquished overall control of the organization but maintained a financial link and in other cases, they worked closely with the managers who were still involved in the official.

These managers could answer the key questions about the environmental and strategic system variables in which interested and thus the use of a small number of senior managers is not as problematic as it would have been if interested in the psychological and personality characteristics of the EM. The interview schedule was designed to collect data on a number of EM and strategic system characteristics in addition to asking about the presence or absence of a SSP and, where appropriate, the time period to which the plan applied. Some organization related characteristics were also included to check for the presence of any uncontrolled organization variables. The data are explored through the analysis of bivariate relationships using non parametric statistics and the relatively small sample size precluded more detailed statistical analysis.

Results

EM were asked whether or not they had a formal SSP for their organization and the period of time to which it applied. Over half the EM (Table 1) had no such plan which fits well with the common perception of the lack of planning in small official organization. Clearly, SSP is not a feature of the majority OO, at least not within this sample of organization within this location. Nevertheless, SSP did exist in just under half (32 percent) of the surveyed organization. Over 75 percent of organizations with formal SSP were planning within a five year time frame.

Table 1: SSP

SSP in organization	**%**
Formal EP	32
No EP	68
All	100
SSP time	**%**
1 year	15
2year	11
3year	19
4year	9
5year	22
>5 year	24
All	100

The characteristics of the EM of the sample OO are summarized in Table 2. EM ranged in age from 20 to over 70 years of age and well over one half was over 45 years of age. In view the age of most of the EM, just over half had been controlling their organization for 15 or more years. Their formal educational levels tended to be high. Amongst these EM, a distinction could be drawn between and those for whom their current official was their first organization and the majority were novice EM. Regardless of the workers, a significant number had gained managerial position before setting up their own organization. They can be contrasted with the remainder of the sample group who had been working more directly in production. A striking feature of these organizations perhaps not surprising in organization based mainly on traditional industries is that 61 percent of the EM had grown up in industrial area.

Table 2: EM and BS characteristics

EM and BS characteristics	%
Age (45 years or more)	51
Total experience (>15 years)	58
Education (University)	55
First organization	66
Workers (100 or less employees)	53
Managerial position	39
Same sector	53
OO zone	61
Locally	45
Customer target	88
Executive Strategy	59

There were striking variations in official strategies. An active search for new Service receivers was characteristic of the majority 59 percent of the organization that admitted to an aim to increase their turnover. Clearly, within this group, there is a sub set of growth oriented EM whose propensity to undertake SSP might be contrasted with those who were content with their current level of official. The latter may well belong to that group of EM often characterized as running lifestyle organization. From this overview of the selected EM characteristics and the strategies of the sampled organization, it is now possible to explore the extent to which these differing characteristics and strategies influence whether or not an organization engages in SSP. The main focus is on the role of EM characteristics in influencing the propensity for SSP.
The results of the bivariate analysis are summarized in Table 3 that age and experience had no significant relationship with SSP the predicted positive relationship between higher levels of education and undertaking SSP was in the expected direction. Those who had extended their education were significantly more likely to plan than those who had not ($p = 0.042$, one tail).

Table 3: SSP, EM and BS characteristics ($P < 0.10$)

EM, BS and SSP	With SSP (Chi-square)
Education	.042
Workers	.041
Different sector	.036
Seeks Service receivers	.023
Growth strategy	.069

Amongst those who had extended their education beyond the minimum age 59 percent had official plan, compared with 37 percent of those with a more limited education (Table 4).

Table 4: SSP and full time education

		SSP and Education	
		Minimum Education	High education
With Plan	n	4	9
	%	21	60
No Plan	n	15	6
	%	79	40
Totals	n	19	15
	%	100	100
N		34	
Chi-square		185	
tail		One	
P		0.042	

Rather surprisingly, those whose previous experience was at operative level were as likely to plan as those who had held managerial positions whilst serial entrepreneurs were no more likely to plan than novice entrepreneurs running their first organization (Table 3). However, an important influence on the SSP amongst those who had previously been employed by another organization was whether or not they had worked previously for a medium or large organization. There was significant propensity to engage in SSP amongst those previously working for a medium/large organization (p = 0.041). Whereas just under two thirds of those formerly working in a medium/large organization were official planners, this was true of only a third of those formerly working in OO (Table 5). This finding suggests these EM from the medium/large organization group had been aware of SSP in their previous employment.

Table 5: SSP and Workers

		SSP and Workers	
		Small (100 or less employees)	Medium/ Large
With Plan	n	10	8
	%	45	67
No Plan	n	12	4
	%	55	33
Totals	n	22	12
	%	100	100
N		34	
Chi-square		6.64	
tail		Two	
P		0.041	

Perhaps the most striking, but understandable finding, was the tendency (p = 0.036) for EM, operating in sectors with which they had little familiarity, to undertake SSP. Whereas two thirds of those moving into a new sector were official planners, this was true of only just over one third of those staying with the sector in which they had experience (Table 6). This tendency to plan by those moving into a new sector to reflect the higher levels of uncertainty the EM faced in operating in an area which was new to them. The degree of engagement with the local official community had no significant influence on SSP.

Table 6: SSP and sector experience

		SSP and sector experience	
		Same Sector	Different Sector
With Plan	n	12	5
	%	67	31
No Plan	n	6	11
	%	33	69
Totals	n	18	16
	%	100	100
N		34	
Chi-square		4.31	
tail		Two	
P		0.036	

The last stage of the analysis focused on the two BS variables. This revealed that both measures of BS had a significant and positive relationship with the presence of SSP amongst the EM of these organizations. The growth orientated EM had a high propensity to have a SSP whether measured by actively seeking new Service receivers ($p = 0.023$) or by expressing an aim to increase their turnover ($p = 0.069$). In part, this may reflect the point noted earlier, that the necessity to raise finance to fund expansion might require the preparation of a SSP for the funding agencies. Of small OO who actively sought new Service receivers, over one half had a SSP whereas this was true of less than one quarter of those who were less proactive in developing their customer base (Table 7).

Table 7: SSP and seeking Service receivers

		SSP and seeking Service receivers	
		Seeking Service receivers	Not Seeking Service receivers
With Plan	n	14	3
	%	58	30
No Plan	n	10	7
	%	42	70
Totals	n	24	10
	%	100	100
N		34	
Chi-square		5.33	
tail		Two	
P		0.023	

Conclusions

Further, the characteristics which have been measured can be grouped into environmental and BS variables rather than those variables which measure attributes of the personality of the EM. It is important to stress that this study is confined to a sample of the EM of OO in one part of the area of OO zone. It is also recognized that the relationships only significant at a relatively low level but this reflects, in part, the small size of our initial sample. Therefore useful conclusions can be drawn as follows:

1) The key EM characteristics, associated with a greater tendency to undertake SSP, are a higher level of education, experience and running a OO. Not unexpectedly, those organizations with growth strategies also tended to be official planners.

2) There was no evidence that previous management experience was linked to a higher propensity to official plan. Those EM with management experience are somewhat cynical of the value of paper exercises and the writing of official plans.

3) SSP is a characteristic of the OO that there still remains a high proportion of EM of OO who does not undertake SSP. EM characteristics and BS variables can be an influence upon whether or not small OO undertakes SSP when controls have been introduced for sector and size.

4) Although this is a study of OO in one zone, this paper has demonstrated that EM characteristics cannot be ignored in trying to understand the extent to which OO display a commitment to SSP.

5) Success is most likely to come from approaches to those EM with the characteristics of planners but who are not yet planners. These are the EM who may be unaware of the benefits of SSP rather than outwardly hostile. However, EM characteristics are rarely in the public domain so such targeting becomes difficult.

6) Where creative responses of many kinds are required, managers will prove to be at the heart of management excellence, which empower their colleagues and clients to expand their OO performance and utilize a higher proportion of the OO potential.

7) Analysis of the environmental and strategic characteristics of EM identified a set of variables.

8) Gaining the sustained co-operation of fellow team members requires emotional leadership. Where such leadership is available, much forgiveness is afforded. Performance creativity in a manager links to conceptual creativity because the corporation’s key competence, its Strategic System Planning Concept Innovation Capability (SSPCIC) index, is the key to success in a knowledge driven economy.

References

1) Deakin, D. & Freel, M. (2003), Entrepreneurship and Executive planning, London, McGraw Hill. pp 230-495

2) Feghhi farahmand, Nasser (2002), Active and dynamic management of organization, Tabriz Iran, Forouzesh. pp 180-369.
3) Feghhi Farahmand, Nasser (2003), Permanent Management of Organization, Tabriz Iran, Frouzesh. pp 18-69.
4) Feghhi farahmand, Nasser (2004), Technology Management of Organization, Tabriz Iran, Frouzesh. pp 241-497.
5) Feghhi farahmand, Nasser (2005), Strategic Management of Organization, Tabriz Iran, Frouzesh. pp125-467.
6) Smith, N. R. (1967), The Entrepreneur and His Organization, University of Michigan: pp 95-180.
7) Storey, D. J. (1994), Understanding the small Executive Sector, London, Rutledge. pp 214-381.
8) Stutely, R. (2002), The Definitive Executive Plan, London, Financial Times, Prentice Hall. pp 45-97.
9) Watts, H. D., Wood, A. M. and Wardle. P. (2003), Making friends or making things?, Urban Studies.

JOURNAL OF APPLIED FUNCTIONAL ANALYSIS, VOL.6, NO.1, 48-56, COPYRIGHT 2011 EUDOXUS PRESS, LLC

On the distribution of zeros of exponential polynomials and Shapiro conjecture *

H. ABBAS and A. HAJJ-DIAB
Department of Mathematics, Lebanese University,
Faculty of Sciences-I, Lebanon
habbas@ul.edu.lb

Abstract

Shapiro conjectured that if two exponential polynomials have infinitely many zeros in common, they have a non trivial common factor. In this paper we prove a result that conducts to prove the conjecture in many particular cases where the coefficients of the polynomials are algebraic and the frequencies are linear combination with rational coefficients of two algebraic numbers.

Keywords. Shapiro conjecture, exponential polynomial.
AMS (MOS) subject classification: 11L03,11L07,11C08.

1 NOTATION AND INTRODUCTION

For an ordinary differential equation or an autonomous dynamical system, the stationary solution is asymptotically stable if and only if all roots of the corresponding characteristic equation of the linearized have negative real parts. Since the characteristic function is a polynomial, the well-known Routh-Hurwitz criterion can be used to determine the negativity of the real parts of the characteristic roots. Similar equivalence holds for delay differential equations. However, the characteristic functions corresponding to the linearized delay differential equations are no longer polynomials, rather, they are *exponential polynomials*. The study of exponential polynomials is of a great importance in many branches of sciences, for instance, in dynamical systems theory, neural networks, automation control, electronics and others (see [4,9,10] and the references cited therein).

* *This work was supported by a grant from the Lebanese University.*

In this paper we denote by E the ring of all exponential polynomials; that is, the set of all functions f of the shape

$$f(z) = \sum_{i=0}^{m} a_i(z) e^{\alpha_i z}$$

where the coefficients a_i belong to $\mathbb{C}[z]$ and the frequencies $\alpha_i \in \mathbb{C}$ are distinct and E_0 denoted the sub-ring of E formed by exponential polynomials with constant coefficients.
In [6], Shapiro proposed the following conjecture:
If two exponential polynomials have infinitely many zeros in common, they are both multiples of some third (entire transcendental) exponential polynomial.

Van der Poorten [8] proved this conjecture in a special case where f is just a simple exponential polynomial with constant coefficients and there exist a complex number α such that every frequency is a rational multiply of α. In [1] Hajj-Diab proved that for any f and g belonging to E there exist h in E dividing f and g, and such that the common zeros of $\frac{f}{h}$ and $\frac{g}{h}$ are zeros of some $\psi \in E_0$. This proves that it sufficient to study the Shapiro conjecture for $f \in E$ and $g \in E_0$ [1]. Also, in the same paper he gave a proof to the conjecture when the frequencies are linear combination of $\mathbb{R}$-linearly independent two complex numbers μ_1 and μ_2 over $\mathbb{R}$.

In this paper we consider the case of two exponential polynomials with frequencies are $\mathbb{Q}$-linearly combination of two non zero algebraic numbers μ_1 and μ_2 and the coefficients are polynomials in z with algebraic coefficients. We shall prove that the Shapiro's conjecture is true if one of the two exponential f and g admits a finite number of zeros in neighborhood of the straight line of equation $Re(\mu_1\ z) = 0$.
We denote by $\overline{\mathbb{Q}}$ the field of algebraic numbers and $\overline{\mathbb{Q}}[X, Y, Z]$ is the ring of polynomials of three indeterminate X, Y and Z over $\overline{\mathbb{Q}}$.
The following theorems are the main results:

Theorem 1 *Let α be a real algebraic irrational number. For any f and g in $\overline{\mathbb{Q}}[e^z, e^{\alpha z}, z]$ there exist $h \in \overline{\mathbb{Q}}[e^z, e^{\alpha z}, z]$ such that h divides f and g and for all $\varepsilon > 0$, the common zeros of $\dfrac{f}{h}$ and $\dfrac{g}{h}$, excepted possibly finitely many of them, are in the region $|Re(z)| < \varepsilon$.*

Theorem 2 *Consider two exponential polynomials* $f(z) = \sum_{i=0}^{m} a_i(z)e^{\alpha_i z}$ *and* $g(z) = \sum_{i=0}^{n} b_i(z)e^{\beta_i z}$ *where* $a_i(z)$ *and* $b_j(z)$ *are polynomials in* z *with algebraic coefficients and the frequencies* α_i *and* β_j *are* $\mathbb{Q}$*-linear combination of two non zero algebraic numbers* μ_1 *and* μ_2*. Then there exist an exponential polynomial* $h \in E$ *such that* h *is a common factor of* f *and* g *and for all* $\varepsilon > 0$*, the common zeros of* $\frac{f}{h}$ *and* $\frac{g}{h}$ *are in the region* $|Re(\ \mu_1 z)| < \varepsilon$*.*

2 DISTRIBUTION OF ZEROS

Let $p(X,Y)$ and $q(X,Y)$ be two polynomials in X and Y over the field of complex numbers $\mathbb{C}$:

$$p(X,Y) = u_0(Y) + u_1(Y)X + ... + u_m(Y)X^m$$
$$q(X,Y) = v_0(Y) + v_1(Y)X + ... + v_n(Y)X^n$$

$l_p(Y)$ is the leading coefficient $u_m(Y)$ of $p(X,Y)$;
$\Omega(p) = \{|\alpha| : \alpha \neq 0 \text{ is a root of } l_p\}$;
$B(a,\delta) = \{z \in \mathbb{C} : |Re(z) - a| < \delta\}$, for $a \in \mathbb{R}$ and $\delta > 0$;
$\Delta = \{\rho \in \Omega(p) : \rho^\lambda \in \Omega(q)\}$;
$H(\delta) = \cup_{\rho\in\Delta} B(\ln\rho, \delta)$.

In what follows, we shall prove the fundamental key lemma.

Lemme 3 *Let* M *be a positive number such that* $e^{-M} < \Omega(p) < e^M$*, then for every positive number* δ*, there exist a positive number* R *such that the zeros of the exponential polynomial* $P(z, e^z)$*, satisfying* $|Re(z)| < M$ *and* $|z| > R$*, are in the region* $\bigcup_{a\in\Omega(p)} B(a,\delta)$*.*

Proof. Firstly, notice that the zeros of the two exponential polynomials $p(z,e^z)$ and $e^{sz}p(z,e^z)$, where s is an integer, are the same. So without loss of generality, we can suppose that the leading coefficient $l_p(e^z) = u_m(e^z)$ can be factorized as

$$l_p(e^z) = \prod_{a\in\Omega(p)} (e^z - a)^{k_a}$$

where k_a is the multiplicity of the root a. Thus the roots are on the straight lines of equations $x = \ln a$. But from the given, we have $-M < \ln a < M$ so by applying the mean value theorem, we obtain

$$|e^z - a| \geq ||e^z| - a\ | \geq |Re(z) - \ln a|e^{-M}.$$

Therefore for $z \in \mathbb{C}$ with $|Re(z) - \ln a| \ > \delta$, we have

$$|l_p(e^z)| = \prod_{a\in\Omega(p)} |(e^z - a)^{k_a}| \geq \prod_{a\in\Omega(p)} |Re(z) - \ln a|^{k_a} e^{-Mk_a}$$

$$\geq \prod_{a\in\Omega(P)} \delta^{n_0} e^{-Mn_0}.$$

where $n_0 = \sum k_a$ is the degree of the polynomial $l_p(x)$. Consequently $l_p(e^z) \neq 0$ for $z \in \mathbb{C}$ and $z \notin \bigcup_{a\in\Omega(p)} B(a,\delta)$. We define now the function

$$\varepsilon(z) = \frac{p(z,e^z)}{u_m(e^z)z^m} - 1 \ \text{ for all } z \notin \textstyle\bigcup_{a\in\Omega(p)} B(a,\delta)\ .$$

The $|u_j(e^z)|$, $1 \leq j \leq m$, are bounded by a number α whenever $Re(z) \in]-M, M[$, Hence

$$|\frac{u_k(e^z)}{u_m(e^z)}| < \frac{\alpha}{\delta^{n_0}}$$

and thus

$$|\varepsilon(z)| \leq \sum \frac{\alpha}{\delta^{n_0}} \frac{1}{|z|^{m-j}}.$$

Therefore for$|z| > 1$, we have $|\varepsilon(z)| \leq \frac{1}{2}$. And by taking $R > max(1, \frac{2\alpha m}{\delta^{n_0}})$, we get

$$|\varepsilon(z)| < \frac{1}{2} \ \text{ and so } \ \varepsilon(z) + 1 \neq 0$$

Finally for $|z| > R$ and $z \notin \bigcup_{a\in\Omega(p)} B(a,\delta)$, we have $p(z,e^z) \neq 0$. That is, the zeros of $p(z,e^z)$ for $|z| > R$ are inside $\bigcup_{a\in\Omega(p)} B(a,\delta)$. ■

3 PRELIMINARIES TO THE PROOF OF MAIN THEOREMS

Before proceeding, it is convenient to prove some essentials theorems and lemmas.

Theorem 4 *If $p(X,Y)$ and $q(X,Y)$ are in the ring $\mathbb{C}[X,Y]$ and if α is a real irrational number then for all positive number δ the two exponential polynomials*

$$p(z,e^z) \text{ and } q(z,e^{\alpha z})$$

have a finite number of common zeros in the region

$$\mathbb{C} - \bigcup_{\rho \in \Delta} B(\ln \rho, \delta).$$

Proof. We prove this theorem in two steps.
Step1: there exist $H > 0$ such that the common zeros of the exponential polynomials $p(z, e^z)$ and $q(z, e^{\alpha} z)$, but finitely many of them, are in the region $-H < Re(z) < H$.
If we denote $G = \mathbb{C}[e^z, e^{\alpha z}]$ then p and q are in $G[z]$. Therefore, it is known [1] that there exist h and ψ in $G[z]$ such that h is a common factor of p and q and the zeros of $\frac{p}{h}$ and $\frac{q}{h}$ are zeros of ψ. But the theorem of factorization of Ritt [5] affirms that $h \in \mathbb{C}[z]$. By consequently the zeros of the exponential polynomials $p(z, e^z)$ and $q(z, e^{\alpha z})$, excepted possibly a finite number, are zeros of ψ. However the zeros of ψ are in the region $-H_1 < Re(z) < H_1$.

Step2: let $H > 0$ such that $H > H_1$. The set $\Omega(p)$ is in the interval $]e^{-H}, e^{H}[$ and $\Omega(p) = \Delta \cup (\Delta - \Omega(p))$.
By using *lemma*.1, for all $\delta > 0$ there exist $R > 0$ such that for $|z| > R$ and $|Re(z)| < H$, the zeros of $p(z, e^z)$ are in $H(\delta) \cup (\cup_{\rho \neq \Delta} B(\ln \rho, \delta))$ and the zeros of $q(z, e^{\alpha z})$ are in $\cup_{\rho' \in \Omega(q)} B(\frac{1}{\alpha} \ln \rho', \delta)$.
Now if ρ is not in Δ then

$$\ln \rho \neq \frac{1}{\alpha} \ln \rho' \quad \forall\ \rho' \in \Omega(q).$$

Hence, for a small convenient $\delta > 0$ the two sets

$$B(\ln \rho, \delta) \quad \text{and} \quad \cup_{\rho' \in \Omega(q)} B(\frac{1}{\alpha} \ln \rho', \delta)$$

are disjoint. Therefore the remainder zeros for $|z| > R$ and $|Re(z)| < H$, excepted a finite number, are in the region $H(\delta)$ and the theorem is proved.
■

Theorem 5 *If $p(X, Y)$ and $q(X, Y)$ are in the ring $\overline{\mathbb{Q}}[X, Y]$ and if α is a real irrational algebraic number, then for all positive number ε, the two exponential polynomials $P(z, e^z)$ and $Q(z, e^{\alpha z})$ have a finite number of common zeros in the region $|Re(z)| > \varepsilon$.*

Proof. It is sufficient to prove that $H(\varepsilon) \subseteq B(0, \varepsilon)$.
If $\Delta = \emptyset$ then $H(\delta) = \emptyset$.
If $\Delta \neq \emptyset$ then $\rho \in \Delta$ is equivalent to

$$\rho^{\alpha} = \rho'$$

which is also equivalent to

$$\alpha \ln \rho = \ln \rho'$$

that is

$$\rho = \rho' = 1.$$

Since if $\rho \neq 1$ and, as α is an irrational algebraic number, we have ρ^{α} is transcendental number, thus by the Gelfand-Schneider theorem [3] (if α is an algebraic number different then 0 and 1 and if β is an algebraic irrational number, then $\alpha^{\beta} = e^{\beta ln \alpha}$ is transcendental), ρ' is a transcendental number which is in contradiction with the fact that it is an algebraic number. By consequently

$$\rho = \rho' = 1$$

and hence

$$H(\varepsilon) = B(0, \varepsilon)$$

and this completes the proof. ■
We also prove the following important lemma.

Lemme 6 *Let A be a factorial ring, p , q be two elements of $A[X]$ of degree greater than or equal to one and $d = gcd(p, q)$ in $A[X]$. Then there exist $a \in A - \{0\}$, u, $v \in A[X]$ verifying*

$$a = u\ \frac{p}{d} + v\ \frac{q}{d}.$$

Proof. Let $\mathbb{K}$ be the quotient field of A, $p_1 = \dfrac{p}{d}$ and $q_1 = \dfrac{q}{d}$. p_1 and q_1 are coprime in the factorial ring $A[X]$ so they are coprime in $\mathbb{K}[X]$ which is principal so, by the Bezout identity, there exist u_1 and v_1 in $\mathbb{K}[X]$ verifying

$$1 = u_1 p_1 + v_1 q_1.$$

Finally, there exist $a \in A - \{0\}$ so that $u = au_1 \in A[X]$ and $v = av_1 \in A[X]$. By consequently

$$a = a\ u_1\ p_1 + a\ v_1\ q_1 = u\ p_1 + v\ q_1 = u\ \frac{p}{d} + v\ \frac{q}{d}.$$

■

4 PROOF OF MAIN THEOREMS

Let W denoted the ring $\overline{\mathbb{Q}}[X,Y,Z]$, $A=\overline{\mathbb{Q}}[Y,Z]$ and $B=\overline{\mathbb{Q}}[X,Z]$. Therefore $W=A[X]=B[Y]$ and A,B and W are unique factorization domains (UFD). Now consider $p(X,Y,Z)$ and $q(X,Y,Z)$ in W and $\alpha\in\mathbb{R}\cap\overline{\mathbb{Q}}$, $\alpha\notin\mathbb{Q}$ and denote

$$f(z)=p(e^z,e^{\alpha z},z),\ \ g(z)=q(e^z,e^{\alpha z},z) \text{ and } \ F=\overline{\mathbb{Q}}[e^z,e^{\alpha z},z].$$

We are now capable to prove our first main theorem

Proof. (**theorem 1**)

We have $f(z)=p(e^z,e^{\alpha z},z)$ and $g(z)=q(e^z,e^{\alpha z},z)$. p and q are in $A[X]$ and $d=gcd(p,q)$ so by the lemma 6, there exist $\psi\in A$ and $u,\ v\in W$ such that

$$\psi=u\ \frac{p}{d}+v\ \frac{q}{d}.$$

By reapplying again the lemma 6 to $\frac{p}{d}$ and $\frac{q}{d}$, which are in $B[Y]$, so there exist $\phi\in B$, $u_1\in W$ and $v\in W$ verifying

$$\phi=u_1\ \frac{p}{d}+v_1\ \frac{q}{d}.$$

By taking $h=d(e^z,e^{\alpha z},z)\in F$ we get, h divides f and g in F and the two relations

$$u_1(z)\ \frac{f(z)}{h(z)}+v_1(z)\ \frac{g(z)}{h(z)}=\phi(e^z,z),$$
$$u(z)\ \frac{f(z)}{h(z)}+v(z)\ \frac{g(z)}{h(z)}=\psi(e^{\alpha z},z).$$

Hence the common zeros of $\frac{f}{h}$ and $\frac{g}{h}$ are also common zeros for $\psi(e^{\alpha z},z)$ and $\phi(e^z,z)$. However, we proved in Theorem 5 that for all $\varepsilon>0$, ϕ and ψ can have a finite number of common zeros in the region $|Re(z)|>\varepsilon$. By consequently, $\frac{f}{h}$ and $\frac{g}{h}$ can only have a finite number of common zeros in the region $|Re(z)|>\varepsilon$. ■

The following is the proof of the second theorem

Proof. (**theorem 2**)

The case where μ_1 and μ_2 are $\mathbb{R}$-linearly independent was proved in [1]. Therefore we study the case where μ_1 and μ_2 are $\mathbb{R}$-linearly dependent and $\mathbb{Q}$-linearly independent. Since the case where μ_1 and μ_2 are $\mathbb{Q}$-linearly dependent is a particular case of the case the simple exponential polynomial proved by A. van der Poorten [8]. We have $\mu_2 = \alpha\mu_1$ where α is a real irrational algebraic number. α_i, β_j are $\mathbb{Q}$-linear combination of two non zero algebraic numbers μ_1 and μ_2, that is,

$$\alpha_i = p_i\ \mu_1 + q_i\mu_2, \quad p_i, q_i \in \mathbb{Q} \ \text{ for } 0 \le i \le n$$

and

$$\beta_i = p'_i\ \mu_1 + q'_i\mu_2, \quad p'_i,\ q'_i \in \mathbb{Q} \ \text{ for } 0 \le j \le m.$$

Let N be the least common multiple of the denominators of $p_i, q_i, p'_j$and q'_j for $0 \le i \le n$ and $0 \le j \le m$. Also, let n_0 be the minimum of the integers Np_i, Nq_i, Np'_j, Nq'_j. Then

$$Np_i - n_0, Nq_i - n_0, Np'_j - n_0, Nq'_j - n_0$$

are non negative integers. By multiplying f and g by the unit

$$e^{-n_0(\frac{\mu_1+\mu_2}{N})z}$$

and by making the change of variable $t = \mu_1 \frac{z}{N}$, we obtain

$$\begin{aligned} e^{-n_0(\frac{\mu_1+\mu_2}{N})z}\ f(z) &= f_1(t), \\ e^{-n_0(\frac{\mu_1+\mu_2}{N})z}\ g(z) &= g_1(t) \end{aligned}$$

where $f_1(t), g_1(t) \in \overline{\mathbb{Q}}[e^t, e^{\alpha t}, t]$. Hence by using Theorem 1, there exist an exponential polynomial $h_1 \in \overline{\mathbb{Q}}[e^t, e^{\alpha t}, t]$ such that h_1 is a common factor of f_1 and g_1 and for all $\varepsilon > 0$, the common zeros of $\frac{f_1}{h_1}$ and $\frac{g_1}{h_1}$ are in the region $|Re(t)| < \varepsilon$. However, there exist a bijection between the zeros of $f(z)$ and $f_1(t)$ as well as $g(z)$ and $g_1(t)$, by consequently there exist $h \in E$ dividing f and g and such that for all $\varepsilon' > 0$, the common zeros of $\frac{f}{h}$ and $\frac{g}{h}$ are in the region $|Re(\ \frac{\mu_1 z)}{N}| < \varepsilon'$. By choosing $\varepsilon' = \frac{\varepsilon}{N}$ we obtain the demanded result. ■

References

[1] A.H.Diab, "Sur les zéros communs des polyômes exponentiels" C.R.Acad.Sc. Paris, 281, A 757-758 (1975).

[2] S. Lang, "Algebra" Addison-Wesley Publishing Company (1978).

[3] I. Niven, " Irrational numbers". The Mathemtical association of America (1956).

[4] L.S. Pontryagin, "On the zeros of some elementary transcendental functions". Amer. Math. Soc. Transl. (2),1, pp.95-110 (1955).

[5] J.F. Ritt," On the zeros of exponential polynomials" trans. Amer. Math. Soc., Vol. 29, pp. 680-686 (1929).

[6] H.S. Shapiro, "The expansion of mean-periodic functions in series of exponentials" Comm. Pure and Appl. Math., 11, pp.1-21 (1958).

[7] A.J. Van der Poorten, " Factorization in fractional powers". Acta. Arith.(1995).

[8] A.J. Van der Poorten, "A note on the zeros of exponential polynomials" Compositio. Math. 31, pp.109-113 (1975).

[9] J. Wei, S. Ruan, T. Zhang, "On the zeros of transcendental functions with applications to stability of delay differential equations with two delays" Dynamics of Continuous , Discrete and Impulsive Systems Series A: Mathematics Analysis 10 pp.863-874, (2003) .

[10] T. Zhang, H. Jiang, Z. Teng, "On the distribution of the roots of the fifth degree exponential polynomial with application to a delayed neural network model " Neurocomputing 72 pp.1098-1104 (2009).

JOURNAL OF APPLIED FUNCTIONAL ANALYSIS, VOL.6, NO.1, 57-64, COPYRIGHT 2011 EUDOXUS PRESS, LLC

Electrodeposition of silver-indium alloys: An example of non-linear dynamic process

Ts. Dobrovolska[1], I. Krastev[1], P. Zabinski[2], R. Kowalik[2], and A. Zielonka[3]

[1] Rostislaw Kaischew Institute of Physical Chemistry, BAS, 1113 Sofia,Bulgaria
[2] Physical Chemistry and Electrochemistry Laboratory, Faculty of Non-Ferrous Metals, AGH, University of Science and Technology, 30-059, Krakow, Poland
[3] Forschungsinstitut für Edelmetalle und Metallchemie, 73525 Schwäbisch Gmünd, Germany

tsvetina@ipc.bas.bg

Abstract

During electrodeposition of silver-indium alloys the patterned coatings with spatio-temporal structures similar to those observed during Belousov-Zhabotinsky reaction are observed. This electrochemical system could be used as a model in the investigations of the non-linear dynamic behavior of complex systems. It was shown, the applied magnetic filed with a intensity of up to 0.3 T parallel to the electrode surface does not influence significantly the formation and the growth of the observed spatio-temporal structures of Ag-In electrodeposited alloy.

1 Introduction

Non-linear phenomena are everywhere around - changes of leaf colours or rhythms, such as heartbeat, pattern formation in many geological and biological systems. The idea of self-organization is central in the description of a lot of systems from the subcellular to the ecosystem level. Pattern formation could be observed in liquid-phase reactions, in heterogeneous catalysis, in non-linear optics and etc. [1-5].

The most nonlinear phenomena are observed in chemical systems [6,7]. The Belousov–Zhabotinsky reaction and the oxidation reaction of CO on Pt single crystals became paradigmatic chemical systems for studies of spatiotemporal dynamics. Their mechanisms are well understood and satisfactory theoretical models of their kinetics are available. The general aspects of the nonlinear wave propagation in reaction–diffusion systems and its control can be well illustrated on the basis of these examples [7].

The relatively simple production and the unique structure and morphology of the electrodeposited materials are the reasons for the wide application of the electrodeposition technique. The experimental electrodeposition conditions of those systems can be reversibly and quickly changed by altering external parameters, different from the chemical parameters [8-10].

In 1938, when E. Raub for first time observed spiral formation during electrodeposition of silver–indium alloys the phenomenon was not attributed to the class of non–linear dynamical systems [11]. Later the spiral formation observed during electrodeposition of Ag-Sb alloys was recognized as a self-organization phenomenon [12-14] and similar effects were re-discovered in the Ag-In system [15,16]. Pattern formation has been observed on solid electrodes also during electrodeposition of some other alloys, such as Ag-Bi [17], Ag-Sn [18] and Ag-Cd [19]. The pattern in the electrodeposited alloys represent a very attractive and rare phenomenon, where they are constituted of metals and alloys, in contradiction to other systems where they are soft materials.

In the recent years, the efforts in the investigations of the silver-indium electrodeposited alloys were devoted to some technological aspects – stabilization of clear electrolytes [20], establishment of the conditions for reproducible pattern formation [15]; investigation of the physical-chemical properties of the alloys, such as internal stress, hardness, roughness, abrasion resistance, electrical contact resistance and etc. [21]. The phase compositions of the alloys and of the different zones of the spatio-temporal structures were also determined and compared by anodic linear sweep voltammetry and conventional X-ray technique [22,23]. It was shown that the process of patterned silver-indium electrodeposition proceeds over very complicated reaction-diffusion-convection mechanism, which includes the typical characteristics of the well known non-linear dynamic processes [24].

In the Zhabotinsky personal web-page is written ”The BZ reaction makes it possible to observe development of complex patterns in time and space by naked eye on a very convenient human time scale of dozens of seconds and space scale of several millimeters”.

We consider that this formulation is completely suitable for the spatio-temporal structures observed during electrodeposition of silver-indium alloys. For the observation of these structures the conventional laboratory equipment and DC power supply are sufficient.

In this work an attempt was made:

- to present the pattern formation during electrodeposition of Ag-In alloys as a typical example of a non-linear process and
- to determine the influence of magnetic field onto the appearance of these structures.

2 Experimental

The composition of the electrolyte for deposition of alloy coatings is given in Table1.

Table 1

Electrolyte composition	Concentration	
	g dm^{-3}	mol dm^{-3}
In as $InCl_3$ /Alfa Aesar/	5.6 – 22.4	0.05 – 0.2
Ag as $KAg(CN)_2$ /Degussa/	4-8	0.04 – 0.08
D(+)-Glucose / Fluka/	20	0.1
KCN /Merck/	16 – 65	0.25 – 1
Electrolysis conditions		
J, A/dm^2	0.07 - 0.3	
Deposition time, min	20 - 180	

The electrolytes were prepared using chemicals of *pro analisi* purity and distilled water. The procedure of preparation of the electrolyte is published elsewhere [15,20].

The alloy coatings with thickness between 1 and 40 μm were deposited in a glass cell under galvanostatic conditions. Platinum anodes were used. Copper cathodes mostly with an area of 5 x 3, 5 x 5 or 2 x 1 cm were used. The preliminary preparation of the copper cathodes includes a standard procedure of electrochemical degreasing followed by pickling in a 20% solution of sulphuric acid. In order to avoid the contact deposition of silver, the cathode was immersed into the electrolyte under current.

The experiments were carried out at room temperature by means of standard DC power supply.

The elemental composition on the coating surface was measured by EDAX and the surface morphology was studied by SEM and optical microscopy.

A magnetic field has been superimposed during the experiments in parallel to the electrode surface directions. The field was generated by a water cooled electromagnet (The Lake Shore EM4 series electromagnet) with flux densities of up to 900 mT. The field flux intensity was measured by the Model 455 digital signal processing gaussmeter equipped with a standard Lake Shore Hall probe.

3 Results and Discussion

Figure 1 shows an optical image of an Ag-In electrodeposited alloy coating. This sample shows two rounded single spirals with up to 25 turns. These spirals are obtained onto copper substrate (8 x 5 cm) at a current density of 0.07A/dm^2 (this is quite low current density for the conventional alloy electrodeposition) and a deposition time of 3 h corresponding to a thickness of the coating of about 30 μm

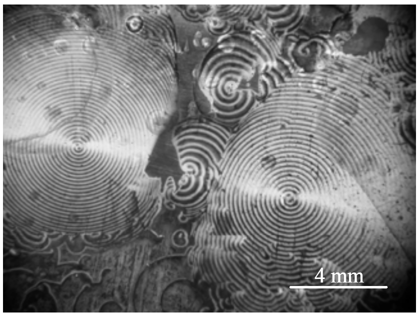

Figure 1. Optical image of an Ag-In electrodeposited alloy coating

. The heterogeneity of the silver-indium coatings is better visible in the optical, than in the SEM images (Figures 2 a, b).

Figures 2 and 3 show SEM images, obtained from the left spiral, shown in Figure 1. The indium contents in the different areas are quite similar – 17 wt. % in the light zones and 19 wt. % in the dark zones and they have similar surface morphology. In previous studies [15] it have been concluded that the wave fronts move with sufficiently high speed forming a layered coating, so that the thickness of the formed during deposition dark and light sublayes is substantially smaller than the penetration depth of the electron beam during EDAX analysis. As a result the beam penetrations through several light and dark sublayers and the estimated average content of indium in both zones on the surface is almost the same. That is the reason for the observation of the both dark and light zones with high quality only at low accelerating voltages (5keV) of the electron beam (Figure 2 a, b).

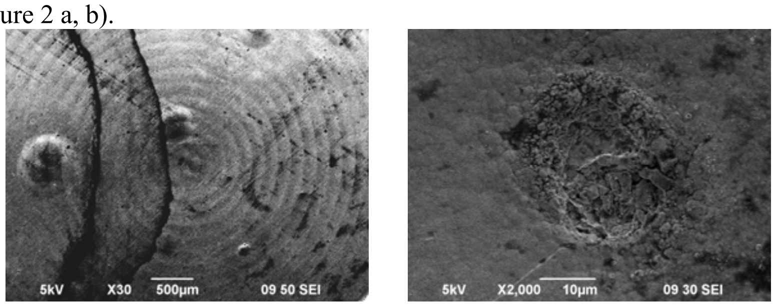

a) b)

Figure 2. a,b SEM images of a surface area of Figure 1 at different magnifications.

At higher voltages the different areas of the spatio–temporal structures are not well discernable.

Figure 2 b shows the morphology of the center of the spiral. In the Belousov–Zhabotinsky reaction the rotating spiral waves with many turns could be created by breaking of a circular wave. In the case of silver-indium electrodeposited coatings some “initial” defect is observed in the core of the rotating spiral waves. It could be possibly formed by adsorption of some impurities or hydrogen evolution on this position of the surface.

The distance between the fronts of the observed spatio-temporal structures in the different samples is in the range between 20 and 200 μm) [24] and the angular velocity of the spiral rotation is determined in the range of about 1- 10 deg $^{1-}$s.

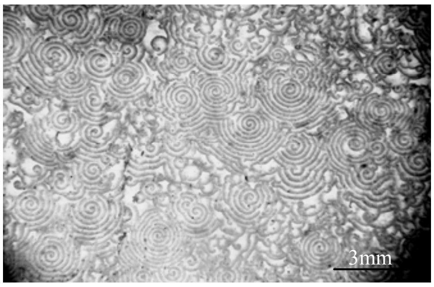

Figure 3. Optical image of a Ag-In electrodeposited alloy.

A typical coatings surface is shown in Figure 3. The left and right handed spirals could be seen almost in every patterned sample of the silver-indium electrodeposited alloy and in present sample more than 15 pairs of the such spirals are detectable.

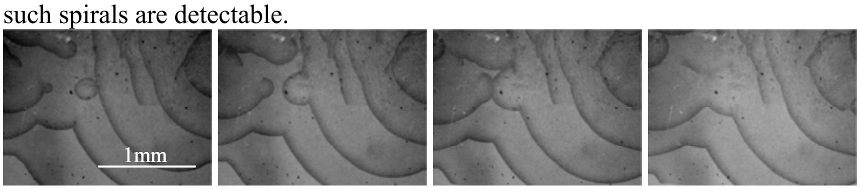

a) b) c) d)

Figure 4. Optical snapshots during the process of electrodeposition of Ag-In alloys.

Figure 4a-d shows optical snapshots during the process of electrodeposition of the silver-indium alloy taken in the interval of 60 sec. The collision of a target and a wave (Fig. 4a) leads to annihilation of the front in the collision zone (Fig. 4b) and after the next annihilation process (Fig. 4c) to a spreading and growing of the new formed wave front (Fig. 4d).

It has been supposed, that the main driving force for the formation of spatio-temporal structures is based on the reaction–diffusion mechanism, coupled with a natural convection, when the process of electrodeposition is performed on a vertical situated electrode [24].

Magnetic field was used in order to influence the hydrodynamic conditions of the natural convection with respect of their impact on the pattern formation.

Figure 5 shows the experimental set for electrodeposition of Ag-In coatings in a magnetic field imposed horizontally parallel to the electrode surface. Snapshots were taken every 3 minutes. The width of the sample was 6 cm. The imposed magnetic field during electrodeposition is 0.3 T. Pictures a) and c) represent the same status under different magnification.

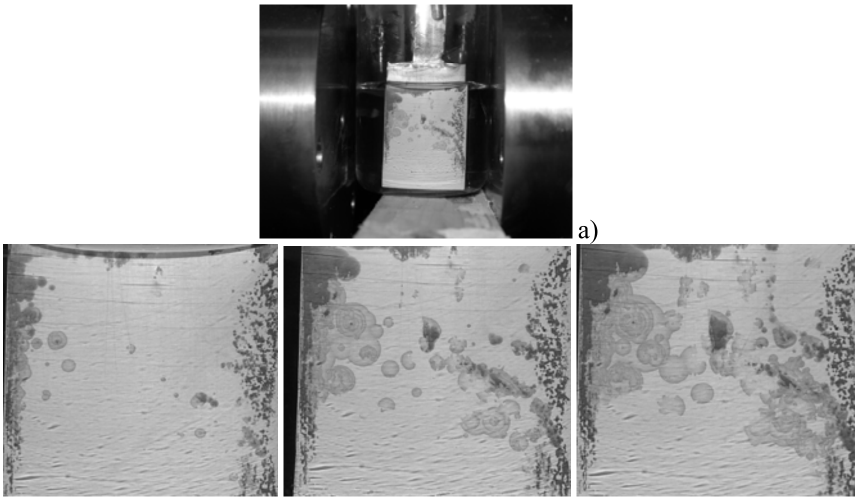

a)

b) c) d)

Figure 5. Optical images of the surface of the alloy coating during deposition in magnetic field.

It is widely accepted that during deposition of non-ferromagnetic metals in a magnetic field, the Lorentz force competes with the other possible forces in the system such as the field gradient force, and concentration gradient force [25,26]. Most probably, the applied magnetic field during the electrodeposition of the alloy contributes to the increase of the diffusion limited current densities, but not enough effectively and the conditions are still appropriate for the observation of the structures.

Figure 5e shows the sample after imposing of a magnetic field with an intensity of 0.5 T. The surface looks like that if only silver is deposited.

Figure 5 e. The appearance of the same area of electrode shown in Figure 5 b-d.

The effect of the magnetic field is similar to the influence of stirring of the electrolyte during electrodeposition, leading to an increase of the diffusion limiting current densities. Fig. 5e shows the effect of the preffered silver deposition under the same conditions but in the magnetic field.

In the work of Nakabayashi et al.[27] it has been established that the propagation direction of the moving bands changes under strong magnetic field

(5 T) in a different oriented experimental setup. These approaches are not reached in this work due to used weak magnetic fields.

4 Conclusions

Electrodeposited silver-indium patterned coatings show spatio-temporal structures similar to those observed during Belousov-Zhabotinsky reaction and this electrochemical system could be used as a model in the investigations of the non-linear dynamic behavior of complex systems.

The applied magnetic filed with a intensity of up to 0.3 T parallel to the electrode surface does not influence significantly the formation and the growth of the observed spatio-temporal structures of Ag-In electrodeposited alloy.

Acknowledgment The authors express their gratitude to the Deutsche Forschungsgemeinschaft (Project 436 BUL 113/97/0-4) for financial support of this work.

References

1. A. M. Turing, "The chemical basis of morphogenesis," *Philos. Trans. R. Soc. London, Ser. B* 237, 37-72 (1952).
2. M. C. Cross and P. C. Hohenberg, "Pattern formation outside of equilibrium," *Rev. Mod. Phys.* 65, 851-1112 (1993).
3. J. J. Tyson and J. P. Keener, "Singular perturbation theory of traveling waves in excitable media (a review)," *Physica D* 32, 327-361 (1988).
4. I. R. Epstein, J. A. Pojman, and O. Steinbock, "Introduction: Self-organization in nonequilibrium chemical systems," *Chaos* 16, 037101-1-037101-6 (2006).
5. F. I. Ataullakhanov, V. I. Zarnitsyna, A. Y. Kondratovich, V. I. Sarbash, and E. S. Lobanova, "A new class of stopping self-sustained waves: A factor determining the spatial dynamics of blood coagulation," *Uspekh. Fizich. Nauk* 172, 689-690 (2002).
6. M. Orlik, "Self-organization in nonlinear dynamical systems and its relation to the materials science," *J. Solid State Electrochem.* 13, 245-261 (2009).
7. A. S. Mikhailov and G. Ertl, "Nonequilibrium microstructures in reactive monolayers as soft matter systems," *ChemPhysChem* 10, 86-100 (2009).
8. G. Ertl, "Pattern formation at electrode surfaces," *Electrochim. Acta* 43, 2743-2750 (1998).
9. K. Krischer, "Spontaneous formation of spatiotemporal patterns at the electrode," *J. Electroanal. Chem* 501, 1-21 (2001).
10. P. Strasser, "Electrochemistry in self-organized dynamical states - Current oscillations and potential patterns in electrocatalytic reactions," *Electrochem. Soc. Interface* 9, 46-52 (2000).
11. E. Raub and A. Schall, *Z. Metallkd.* 30, 149-151 (1938).

12. I. Kristev and M. Nikolova, "Structural effects during the electrodeposition of silver-antimony alloys from ferrocyanide-thiocyanate electrolytes," *J. Appl. Electrochem.* 16, 875-878 (1986).

13. I. Krastev, M. E. Baumgartner, and C. Raub, *Metalloberflache* 46, 115-120 (1992).

14. I. Krastev and M. T. M. Koper, "Pattern formation during the electrodeposition of a silver-antimony alloy," *Physica A* 213, 199-208 (1995).

15. Ts. Dobrovolska, L. Veleva, I. Krastev, and A. Zielonka, "Composition and structure of silver-indium alloy coatings electrodeposited from cyanide electrolytes," *J Electrochem Soc* 152, C137-C142 (2005).

16. Ts. Dobrovolska, I. Krastev, and A. Zielonka, "Electrodeposition of silver-indium alloy from cyanide-hydroxide electrolytes," *Russ. J. Electrochem.* 44, 676-682 (2008).

17. I. Krastev, T. Valkova, and A. Zielonka, "Effect of electrolysis conditions on the deposition of silver-bismuth alloys," *J. Appl. Electrochem.* 33, 1199-1204 (2003).

18. A. Hrussanova and I. Krastev, "Electrodeposition of silver-tin alloys from pyrophosphate-cyanide electrolytes," *J. Appl. Electrochem.* 39, 989-994 (2009).

19. T. Dobrovolska, I. Krastev, and A. Zielonka, "Pattern formation in electrodepostied silver-cadmium alloys," *ECS Transactions* 25, (2010).

20. Ts. Dobrovolska, I. Krastev, and A. Zielonka, "Effect of the electrolyte composition on in and Ag-In alloy electrodeposition from cyanide electrolytes," *J. Appl. Electrochem.* 35, 1245-1251 (2005).

21. I. Krastev, T. Dobrovolska, R. Kowalik, P. Zabinski, and A. Zielonka, "Properties of silver-indium alloys electrodeposited from cyanide electrolytes," *Electrochim. Acta* 54, 2515-2521 (2009).

22. Ts. Dobrovolska, V. D. Jovic, B. M. Jovic, and I. Krastev, "Phase identification in electrodeposited Ag-In alloys by ALSV technique," *J. Electroanal. Chem* 611, 232-240 (2007).

23. Ts. Dobrovolska, G. Beck, I. Krastev, and A. Zielonka, "Phase composition of electrodeposited silver-indium alloys," *J. Solid State Electrochem.* 12, 1461-1467 (2008).

24. T. Dobrovolska and I. Krastev, "Electrodeposition of silver-indium alloys," in *Electrolysis: Theory, Types and Applications,* K. Shing and M. Ji, eds., (Nova Science Publishers, Inc., 2010).

25. A. Bund, S. Koehler, H. H. Kuehnlein, and W. Plieth, "Magnetic field effects in electrochemical reactions," *Electrochim. Acta* 49, 147-152 (2003).

26. J. A. Koza, M. Uhlemann, A. Gebert, and L. Schultz, "The effect of magnetic fields on the electrodeposition of CoFe alloys," *Electrochim. Acta* 53, 5344-5353 (2008).

27. S. Nakabayashi, I. Krastev, R. Aogaki, and K. Inokuma, "Electrochemical instability of Ag/Sb co-deposition coupled with a magnetohydrodynamic flow," *Chem. Phys. Lett.* 294, 204-208 (1998).

JOURNAL OF APPLIED FUNCTIONAL ANALYSIS, VOL.6, NO.1, 65-69, COPYRIGHT 2011 EUDOXUS PRESS, LLC

NUMERICAL-ANALYTICAL METHOD FOR SOLVING FRACTIONAL CHAOTIC SYSTEM

A.K. ALOMARI

ABSTRACT. Nonlinear differential equations with fractional derivative give the most general representation of the real live phenomena. In this paper, modification of differential transform method (DTM) solution within time step for solving nonlinear fractional differential equation is introduced. The algorithm is simple and gives accurate solution. Moreover the new solution is continuous and analytic on each subinterval. Fractional Liu system is considered to demonstrate the efficiency of the algorithm.

1. INTRODUCTION

In the last few decades many authors pointed out that derivatives and integrals of non–integer order are very suitable for the description of properties of various real materials [1]. The advantage of fractional derivatives become apparent in modelling mechanical and electrical properties of real materials as well as fractional Liu system [2]

$$D_t^\alpha x = -ax - ey^2, \tag{1.1}$$
$$D_t^\alpha y = by - kxz, \tag{1.2}$$
$$D_t^\alpha z = -cz + mxy, \tag{1.3}$$
$$x(0) = c_1 \qquad y(0) = c_2, \qquad z(0) = c_3, \tag{1.4}$$

where D^α is Caputo fractional derivative $a = 1, e = 1, b = 2.5, k = 4, c = 5, m = 4$ and $0 < \alpha \leq 1$.

Numerical solution of differential equations satisfies only part of the conditions of the problem: for example the differential equation may be satisfied only at a few position rather than at each point [3]. Finding accurate and efficient methods for solving fractional differential equations (FDEs) has been an active research undertaking. Exact solutions of most of the FDEs cannot be found easily, thus analytical and numerical methods must be used [4]. Zhou [5] introduce the powerful analytical technique namely differential transform method (DTM) Arikoglu and Ozkol [5] and Odibat et al.[6] extended the algorithm to solve fractional differential equations. Fractional chaotic system is one of the systems can not be solved by that extension. Thus, new algorithm should be presented to overcome this limitation.

The aim of this paper is to obtain the solution of the fractional Liu system using DTM when we hybrid the numerical with analytical in a sequence of intervals (i.e. time step) for finding accurate approximate solutions to the nonlinear FDEs. This

1991 *Mathematics Subject Classification.* 04.25.-g, 02.30.Hq, 02.30.Mv, 02.60.Cb.

Key words and phrases. Chaotic system and Fractional Liu system and Differential transform method.

new algorithm will call modify differential transform method (MDTM). To the best of our knowledge, this is also the first time that the analytical solution is obtained for fractional chaotic system by DTM.

2. Preliminaries and notations

In this section, we give some definitions and properties of the fractional calculus.

2.1. **Fractional calculus.** The following properties can found in [1, 5].

Definition 2.1. A real function $f(t)$, $t > 0$, is said to be in the space C_μ, $\mu \in \Re$, if there exists a real number $p > \mu$, such that $f(t) = t^p f_1(t)$, where $f_1(t) \in C(0, \infty)$, and it is said to be in the space C_μ^n if and only if $h^{(n)} \in C_\mu$, $n \in N$.

Definition 2.2. The Riemann-Liouville fractional integral operator (J^α) of order $\alpha \geq 0$, of a function $f \in C_\mu$, $\mu \geq -1$, is defined as

$$J^\alpha f(t) = \frac{1}{\Gamma(\alpha)} \int_0^t (t-s)^{\alpha-1} f(t) \d{s} \quad (\alpha > 0), \tag{2.1}$$

$$J^0 f(t) = f(t), \tag{2.2}$$

where $\Gamma(\alpha)$ is the well-known gamma function.

2.2. **Differential transform method.** Firstly, expand the analytical function $f(t)$ in terms of a fractional power series as follows:

$$f(t) = \sum_{k=0}^{\infty} F(k)(t-t_0)^{k\alpha} \tag{2.3}$$

where $0 < \alpha \leq 1$ is the order of the fractional derivative and $F(k)$ is the fractional differential transform of $f(t)$ as

$$F(k) = \frac{1}{\Gamma(\alpha k + 1)} [(D_{t_0}^\alpha)^k (f(t))]_{t=t_0}. \tag{2.4}$$

where $[(D_{t_0}^\alpha)^k (f(t))]_{t=t_0}$ is the k–time Caputo fractional derivative of $f(t)$ at $t = t_0$.

In the applications we will approximate the function $f(t)$ as a finite series so

$$f(t) = \sum_{i=0}^{N} F(i)(t-t_0)^{(\alpha)}$$

The following are basic properties of the Caputo fractional derivative and differential transformation are given below [6]:

(1) Let $f \in C_{-1}^n, n \in N$, then $D^\alpha f, 0 \leq \alpha \leq n$ is well defined and $D_{t_0}^\alpha f \in C_{-1}$.
(2) If $f(t) = g(t) \pm h(x)$, then $F(k) = G(k) \pm H(k)$.
(3) If $f(t) = g(t)h(t)$, then $F(k) = \sum_{l=0}^{k} G(l)H(k-l)$.
(4) If $f(t) = D_{t_0}^\alpha [g(t)]$, then $F(k) = \frac{\Gamma(\alpha(k+1)+1)}{\Gamma(\alpha k+1)} G(\alpha + 1)$

3. Solution approaches

In this section, we apply DTM and its modification for fractional Liu system.

3.1. **Solution by DTM.** Consider fractional Liu system (1.1–1.4). The differential transformation for this system is

$$\frac{\Gamma(\alpha(k+1)+1)}{\Gamma(\alpha k+1)}X(k+1) = aX(k) - e\sum_{i=0}^{k} Y(k)Y(k-i), \tag{3.1}$$

$$\frac{\Gamma(\alpha(k+1)+1)}{\Gamma(\alpha k+1)}Y(k+1) = bY(k) - k\sum_{i=0}^{k} X(k)Z(k-i), \tag{3.2}$$

$$\frac{\Gamma(\alpha(k+1)+1)}{\Gamma(\alpha k+1)}Z(k+1) = m\sum_{i=0}^{k} X(k)Y(k-i) - cZ(k), \tag{3.3}$$

where

$$X(0) = c_1, \qquad Y(0) = c_2, \qquad Z(0) = c_3. \tag{3.4}$$

Equations (3.1)–(3.3) give recursion formula for the differential transformation of the fractional Liu system which starting from $X(0), Y(0)$ and $Z(0)$ of Eq. (3.4).

Figure 1 present the DTM solution for Liu system, it is clear that the solution going to be unbounded which is not agree with the dynamical property of the system. Thus the DTM solution is not effective for longer time span.

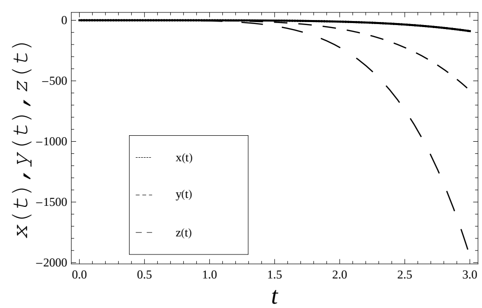

FIGURE 1. DTM solution for Liu system when $\alpha = 0.99$

3.2. **Solution by MDTM.** The solution for Eqs. (1.1)–(1.3) is not effective for larger t. In case if we need the solution for $[0, 7]$, then the simple idea is to divide the interval $[0, 7]$ to subintervals with time step Δt and we get the solution at each subinterval. So in this case we have to satisfy the initial condition at each of the subinterval. Accordingly, the initial values $x(0), y(0), z(0)$ will be changed for each subinterval, i.e. $x(t_0) = c_1^* = X(0), y(t_0) = c_2^* = Y(0)$ and $z(t_0) = c_3^* = Z(0)$.

So, the solution will be as follows:

$$x(t) = c_1^* + \sum_{m=1}^{N} X(m)(t-t_0)^{(m\alpha)}, \tag{3.5}$$

$$y(t) = c_2^* + \sum_{m=1}^{N} Y(m)(t-t_0)^{(m\alpha)}, \tag{3.6}$$

$$z(t) = c_3^* + \sum_{m=1}^{N} Z(m)(t-t_0)^{(m\alpha)}, \tag{3.7}$$

where t_0 starting from $t_0 = 0$ until $t_n = T = 20$. To carry out the solution on every subinterval of equal length Δt, we need to know the values of the following initial conditions:

$$c_1 = x(t_0), \quad c_2 = y(t_0), \quad c_3 = z(t_0).$$

In general, we do not have these information at our clearance except at the initial point $t^* = t_0 = 0$, but we can obtain these values by assuming that the new initial condition is the solution in the previous interval. (i.e. If we need the solution in interval $[t_j, t_{j+1}]$, then the initial conditions of this interval will be as

$$c_1 = x(t_i) = \sum_{m=0}^{N} X(m)(t_i - t_{i-1})^{m\alpha}, \tag{3.8}$$

$$c_2 = y(t_i) = \sum_{m=0}^{N} Y(m)(t_i - t_{i-1})^{m\alpha}, \tag{3.9}$$

$$c_3 = z(t_i) = \sum_{m=0}^{N} Z(m)(t_i - t_{i-1})^{m\alpha}, \tag{3.10}$$

where c_1, c_2 and c_3 are the initial conditions in the interval $[t_j, t_{j+1}]$).

4. Results and discussion

In this part, we take the initial conditions $x(0) = 0.2$, $y(0) = 0$ and $z(0) = 0.5$ at the case $(0.99, 0.99, 0.99)$. To observe the convergent of the solution, we plot the 4-order and 6-order of MDTM solution with $\Delta t = 0.0025$ in Fig. 2. It is clear that

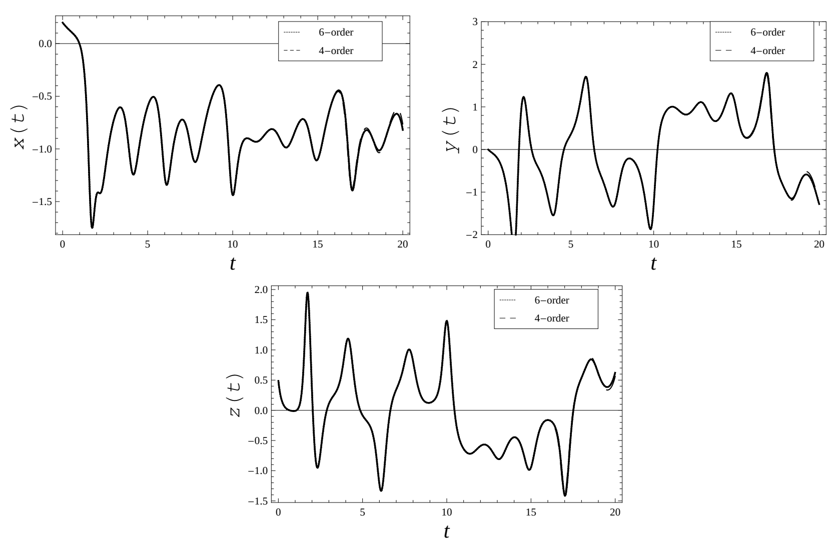

Figure 2. $\hbar$-curves of 8th-order approximation for (0.99,0.99,0.99)

the solution of 4-order like the solution of 6-order then we can consider 6-order as good approximate solution. The phase portraits of the MDTM solution is given in Fig. 3 at different fractional derivative.

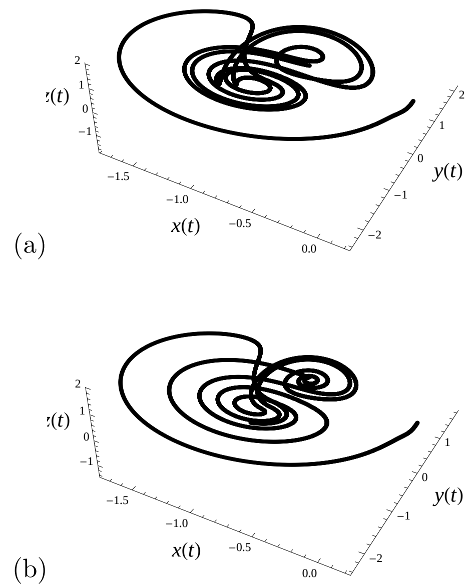

Figure 3. Comparison the phase portraits of $x - y - z$ using 8-order MDTM in (b) with GABMM in (a) when $\alpha = 1$

References

[1] Podlubny I. Fractional differential equations, Academic Press, New York (1999)
[2] Daftardar-Gejji V, Bhalekar S. Chaos in fractional ordered Liu system. Comput Math Appl, in press. doi: 10.1016/j.camwa.2009.07.003.
[3] Finlayson B A. The method of weighted residuals and variational principles. New York: Academic Press (1972)
[4] Bataineh AS, Alomari AK, Noorani MSM, Hashim I, Nazar R. Series solutions of sysytems of nonlinear fractional differential equations. Acta Appl Math 105:18998 (2009).
[5] Arikoglu A, Ozkol I. Solution of fractional differential equations by using differential transform method. Chaos Solitons & Fractals 34: 1473-1481 (2007)
[6] Odibat Z, Momani S, Erturk V, Generalized differential transform method: Application to differential equations of fractional order, Applied Mathematics and Computation 197: 467-477 (2008)

Department of science, faculty of nursing and sciences, Jerash privet university, 26150 Jerash, Jordan
E-mail address: abdomari2008@yahoo.com

JOURNAL OF APPLIED FUNCTIONAL ANALYSIS, VOL.6, NO.1, 70-76, COPYRIGHT 2011 EUDOXUS PRESS, LLC

A Model Representing Biochemical Substances Exchange Between Cells. Part I: Model Formalization

Igor Balaz and Dragutin T. Mihailović

Faculty of Agriculture, University of Novi Sad, Novi Sad, Serbia, ibalaz@polj.uns.ac.rs

Exchange of biochemical substances is essential way in establishing the communication between cells. Despite great diversity among organisms in specific mechanisms, proteins and small molecules involved, general scheme of the communication process remains fairly universal. It is noticeable that all phases of the process are heavily influenced by noise, either internal or external. Therefore, the question is how the system, which is almost stochastic at the basic molecular level, is able to establish and maintain functionality. Here, we investigate what biological constraints are given for the underlying random events, which are their properties and what is the most appropriate way of its formalization. In that sense, we propose a form of coupled difference equations as a suitable approach for modelling exchange of biochemical substances between cells.

Keywords: cellular communication, substance exchange, difference equation, synchronization

1 Introduction

Communication between cells is ubiquitous in biological world. From single cell bacteria to complex eukaryotic organisms, cellular communication is a way for creating more complex structures through integration and maintaining of functioning. Organisms evolved various auxiliary ways for ensuring that transfer of signals can be performed timely and efficiently (e.g. development of vascular systems starting from early chordates). However, at the molecular level, basic scheme of signals exchange remains in the same shape: signaling molecules should reach cellular receptor, which in turn activates regulatory response, modulating production of targeted molecular species. These species then either directly or indirectly influence production of arriving signals. In this general scenario, several points should be noted. Since communication is established by exchange of biochemical substances (substances in the further text) through surrounding environment, this process is heavily influenced by the state of environmental factors. In single cell organisms environmental fluctuations are even more prominent since substances had to be released into external environment, which is not included into homeostasis created by the organism. Additionally, even in clonal population, and under heavily controlled environment, significant level of fluctuations of constituting parameters will remain, due to protein disorder [2,3] and so called intrinsic noise [4,12]. Finally, due to thermal and conformational fluctuations, biochemical processes are inherently random [7]. Although the biological "noise" is not strictly defined, in this paper we will use it in the context of variations in functioning of a biological system that results from the presence of random internal as well as the external fluctuations.

If described process of substances exchange between cells we consider as a complex system, that should maintain its functionality under strong influence of both internal and external fluctuations, we are approaching the problem of robustness [1,5,6]. Although, the robustness and stability are not the main focus of consideration, in [8] we touched how the system can avoid functional collapse by switching between several stable states. Some elaborated formal treatments of this problem are still in infancy. One of the main reasons for that is the fact that its focus is beyond already developed tools of dynamical systems theory. It indicates that a new, more general approach for describing the system had to be developed.

In this paper, our focus is only a segment of the problem, for the specific group of cases. Our question is: how the system which is basically stochastic, and is inherently influenced by noise, can maintain its functioning? In Section 2 we give a short overview of general mechanism for substances exchange between two cells, representing cooperative communication process. In Section 3 we identify main parameters of the process and derive a system of two coupled logistic equations as an appropriate model of the given process. In [8] we investigate synchronization of the model and its sensitivity to fluctuations of environmental parameters. Some concluding remarks are given in Section 4. It should be emphasized that our goal is not development of an accurate quantitative model of substances exchange between cells. Rather, we are interested for formalization of the basic shape of the process, and creating the appropriate strategy, that allows further investigation of robustness and influence of noise induced by external fluctuations of environmental parameters.

2 Empirical background

Communication between cells is one of the main prerequisites for assembling them into the higher organized structures. Starting from bacteria where quorum sensing [13] and colony formation [11] are efficient mechanism for rapid switching between different phenotypes to sophisticated humoral control in vertebrates which ensures proper functioning of the organism as an integrated

system. Despite great variety of specific mechanisms and even greater number of molecules included, the general scheme remains fairly universal (see for example: [10]) as is seen in Fig. 1.
Signaling molecules are ones which are deliberately extracted by the cell into extracellular environment, and which can affect behavior of other cells of the same or different type (species or phenotype) by means of active uptake and subsequent changes in genetic regulations. They can be excreted as either a side product of other metabolic processes, or as purposefully synthesized and transported from the cell. Once appeared in extracellular environment, they can be transported to other cells that can be affected. Since active uptake is one of the milestones of the process, a very important factor is a current set of receptors and transporters in cellular membrane, during the communication process. At the same time they constitute backbone of the whole process, while simultaneously are very important source of perturbations of the process due to protein disorder and intrinsic noise. As a result, the process of exchange is constantly under inherent fluctuations of the aforementioned parameters. Another important factor is surrounding environment which could interfere with the process of exchange. It includes: distance between cells, mechanical and dynamical properties of the fluid which serves as a channel for exchange and various abiotic and biotic factors which influence physiology of the involved cells. Final requisite phase is induction of change in genetic regulations. Signaling molecules can influence production of a number of different genes but synthesis of molecules that are able to directly or indirectly affect production of arriving signals is necessity, to call this process a communication. Therefore, concentration of signaling molecules inside of the cell, that are destined to be extracted, can serve as an indicator of dynamics of the whole process of communication. These signaling molecules can be either the same for all involved cells or they can be different, acting directly or indirectly on production of arriving signals. Additionally, the influence of affinities in functioning of living systems is also an important issue. It can be divided into following aspects: (a1) affinity of genetic regulators towards arriving signals which determine intensity of cellular response and (a2) affinity for uptake of signaling molecules. First aspect is genetically determined and therefore species specific. Second aspect is more complex and is influenced by: affinity of receptors to binding specific signaling molecule, number of active receptor and their conformational fluctuations (protein disorder).

3 Model description

As it is obvious from the empirical description, we can infer successfulness of the communication process by monitoring: (i) number of signaling molecules, both inside and outside of the cell and (ii) their mutual influence. Concentration of signaling molecules in extracellular environment is subject to various environmental influences, and taken alone often can indicate more about state of the environment then about the communication itself. Therefore, we choose to follow concentration of signaling molecules inside of the cell as the main indicator of the process. In that case, parameters of the system are: (i) affinity by which cells perform uptake of signaling molecules (a1), that depends on number and state of appropriate receptors, (ii) concentration of signaling molecules in extracellular environment within the radius of interaction, (iii) intensity of cellular response (a2) and (iv) influence of other environmental factors which can interfere with the process of communication. In this case we postulate that third parameter can be taken collectively, inside of the one variable, indicating overall disposition of the environment to the communication process.

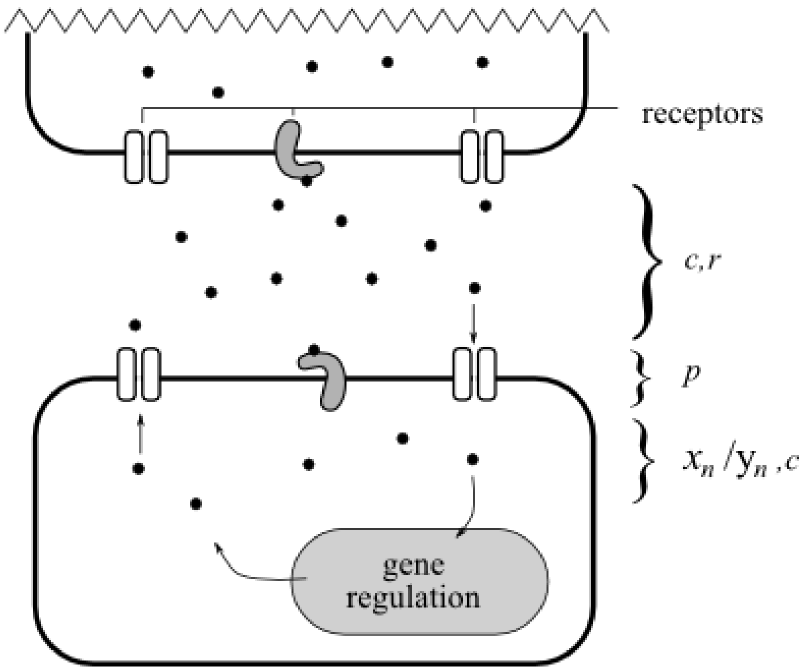

Fig. 1. Schematic representation of cellular communication. Here, *c* represents concentration of signaling molecule in extracellular environment coupled with intensity of response they can provoke while *r* includes collective influence of environmental factors which can interfere with the process of communication. X_n /Y_n represents concentration of signaling molecules in intracellular environment, while *p* denotes cellular affinity to uptake the substance.

Since concentration of signaling molecules can be regarded as their population for fixed volume, and since we are focused on mutual influence of these populations, it points out to use the coupled logistic equations. In that case investigation of conditions under which two equations are synchronized and how this synchronization behave under continuous noise can give some answers on the question of maintaining functionality in the system which is inherently influenced by noise and where elementary events are basically stochastic.

Therefore, having in mind that cellular events are discrete [1], we consider system of difference equations of the form

$$\mathbf{X}_{n+1} = \mathbf{F}(\mathbf{X}_n) \equiv \mathbf{L}(\mathbf{X}_n) + \mathbf{P}(\mathbf{X}_n)\,, \tag{1}$$

with notation

$$\mathbf{L}(\mathbf{X}_n) = ((1-c)rx_n(1-x_n),(1-c)ry_n(1-y_n)), \qquad \mathbf{P}(\mathbf{X}_n) = (cy_n^p, cx_n^{1-p})\,, \tag{2}$$

where $\mathbf{X}_n = (x_n, y_n)$ is a vector representing concentration of signaling molecules inside of the cell, while $\mathbf{P}(\mathbf{X}_n)$ denotes stimulative coupling influence of members of the system which is here restricted only to positive numbers in the interval (0,1). The starting point $\mathbf{X}_0$ is determined so that $0 < x_0, y_0 < 1$. Parameter r is in this case so-called logistic parameter, which in logistic difference equation determines an overall disposition of the environment to the given population of signaling molecules and exchange processes. Affinity to uptake signaling molecules is indicated by p. Since fixed point is $\mathbf{F}(0) = 0$, in order to ensure that zero is not at the same time the point of attraction we defined $p \in (0,1)$ as an exponent. Finally, c represents coupling of two factors: concentration of signaling molecules in extracellular environment and intensity of response they can provoke. This form is taken because the effect of the same intracellular concentration of signaling molecules can vary greatly with variation of affinity of genetic regulators for that signal, which is further reflected on the ability to synchronize with other cells. Therefore, c influence both, rate of intracellular synthesis of signaling molecules, as well as synchronization of signaling processes between two cells so the parameter c is taken to be a part of both $\mathbf{L}(\mathbf{X}_n)$ and $\mathbf{P}(\mathbf{X}_n)$. However, relative ratio of these two influences depends on current empirical setting. For example, if for both cells $\mathbf{X}_n$ is strongly influenced by extracellular concentration of signals, while they can provoke relatively smaller response then the form of equation will be

$$x_{n+1} = (1-c)rx_n(1-x_n) + cy_n^p\,, \tag{3a}$$
$$y_{n+1} = (1-c)ry_n(1-y_n) + cx_n^p\,. \tag{3b}$$

where $0 < c < 1$, $0 < p < 1$ and $r > 0$. Using the fact that for $0 \le x \le 1$ and $1 > p > 0$ we have $x \le x^p \le 1$, then it is possible to consider system (3a)-(3b) in a simpler form. After its majorisation and minorisation, respectively we reach the systems

$$x_{n+1} = (1-c)rx_n(1-x_n) + c \tag{4a}$$
$$y_{n+1} = (1-c)ry_n(1-y_n) + c \tag{4b}$$

and

$$x_{n+1} = (1-c)rx_n(1-x_n) + cy_n , \tag{5a}$$
$$y_{n+1} = (1-c)ry_n(1-y_n) + cx_n . \tag{5b}$$

System (4) is uncoupled system of logistic difference equations defined on domain $D = (I \times I)$ where $I = (-\delta, 1+\delta)$, and $\delta < 0$ is the smallest solution of the equation $x = (1-c)ax(1-x) + c$. In this system, all information about bifurcations and chaotic behavior we get by its comparison with the standard form $x_{n+1} = \rho x_n(1-x_n)$ where $\rho = (a(1-c)+4c)/(1-2\delta)$. A comprehensive analysis of the system (5) in more details can be found in [9].

4 Conclusions

Modeling of cellular processes usually takes the form of explicit kinetic or stoichiometric models. Due to their specificity, they fail to treat some phenomena common for the whole class of different empirical cases. Analyzing general scheme of communication between cells we focused on persistence of the process under constant and significant presence of parameter fluctuations. Following discreteness of cellular processes, we developed model based on coupled difference equations in order to further investigate stability of their synchronization. Additionally, we had in mind that described class of problems is now considered under the notion of robustness. We expect that in the future more abstract mathematical tools will be developed to treat that problem. However, they should be incorporated with already existing formulations from dynamical systems theory in order to connect more abstract notion of functionality preserving with its underlying dynamics. We believe that approach offered here, could serve as one of the connecting links.

Acknowledgement

The research described here was funded by the Serbian Ministry of Science and Technology under the project “Study of climate change impact on environment: monitoring of impact, adaptation and moderation”, for 2011-2014.

References

[1] N. Barkai, B.-Z. Shilo, Variability and Robustness in Biomolecular systems. *Mol. Cell*, 28, 755-760 (2007)

[2] A.K. Dunker, J.D. Lawson, C.J. Brown, R.M. Williams, P. Romero, J.S. Oh, C.J. Oldfield, A.M. Campen, C.M. Ratliff, K.W. Hipps, J. Ausio, M.S.

Nissen, R. Reeves, C. Kang, C.R. Kissinger, R.W. Bailey, M.D. Griswold, W. Chiu, E.C. Garner, Z. Obradovic, Intrinsically disordered protein. *J. Mol. Graph. Model.*, 19, 26-59 (2001)

[3] A.K. Dunker, Brown, C.J., Lawson, J.D., L.M. Iakoucheva, Z. Obradovic, Intrinsic Disorder and Protein Function. *Biochemistry*, 41, 6573–6582 (2002)

[4] M.B. Elowitz, A.J. Levine, E.D. Siggia, P.S. Swain, Stochastic gene expression in a single cell. *Science*, 297, 1183-1186 (2002)

[5] H. Kitano, Biological robustness. *Nat Rev Genet* 5: 826–837 (2004)

[6] H. Kitano, Towards a theory of biological robustness. *Mol. Syst. Biol.*3:137 doi:10.1038/msb4100179 (2007)

[7] D. Longo, J. Hasty, Dynamics of single-cell gene expression. *Mol. Syst. Biol.* 4:64 doi:10.1038/msb4100110 (2006)

[8] D.T. Mihailovic, I. Balaz, A Model Representing Biochemical Substances Exchange Between Cells. Part II: Effect of Fluctuations of Environment parameters to Behavior of the Model. *J. App. Funct. Anal.* (2010) (**accepted**)

[9] D.T. Mihailovic, M. Budinčević, I. Balaz, D. Perišić, Emergence of Chaos and Synchronization in Coupled Interactions in Environmental Interfaces Regarded as Biophysical Complex Systems, in *Advances in Environmental Modeling and Measurements* (D.T. Mihailovic and B. Lalić, eds.) Nova Science Publishers, Inc., New York, 2010, pp. 89-100.

[10] W.K. Purves, D. Sadava, G.H. Orians, C. Heller, *Life – The Science of Biology*, Sinauer Associates and W.H. Freeman (7^{th} ed.), Sunderland, 2003

[11] P. Stoodley, K. Sauer, D.G. Davies, J.W. Costerton, Biofilms as Complex Differentiated Communities. *Annu. Rev. Microbiol.* 56, 187-209 (2002)

[12] P.S. Swain, M.B. Elowitz, E.D. Siggia, Intrinsic and extrinsic contributions to stochasticity in gene expression. *PNAS*, 99, 12795-12800 (2002)

[13] C.M. Waters, B.L. Bassler, Quorum Sensing: Cell-to-Cell Communication in Bacteria. *Annu. Rev. Cell Dev. Biol.* 21, 319-346 (2005)

JOURNAL OF APPLIED FUNCTIONAL ANALYSIS, VOL.6, NO.1, 77-84, COPYRIGHT 2011 EUDOXUS PRESS, LLC

A Model Representing Biochemical Substances Exchange Between Cells. Part II: Effect of Fluctuations of Environmental Parameters to Behavior of the Model

Dragutin T. Mihailović and Igor Balaz

Faculty of Agriculture, University of Novi Sad, Novi Sad, Serbia, 21000
guto@polj.uns.ac.rs

A continuing interest problem in nonlinear science is the interplay between chaos and perturbation. It comes from the fact that complex systems are often under fluctuations of different magnitude, and it is important to assess how the dynamics of deterministic chaotic system is affected by noise. It is well known that chaos, in general, is robust under stochastic fluctuations, which can induce chaos for parameters just before a bifurcation to chaos. Intention of this paper is to study the sensitivity of the model proposed representing biochemical substances exchange between cells [1] to fluctuations of environment parameters of different order of magnitude using maximal Lyapunov exponent and cross sample entropy.

Key words: Substance exchange, cell, chaos, robustness

1 Introduction

The effort towards formalizing a model of process of material exchange between cells is still in its infancy and much remains to be completed to build a mature theory. For a model to be useful, it must be able to predict characteristics and behaviors of the system. This means that the model has to be framed to explicitly describe constraints that bind the system. That effort is still going up over stairways that have no a complete structure. One of the hard tasks in building those stairways is the issue related to stability and robustness. Exploring the deference between “stable” and “robust” touches on essentially every aspect of what we instinctively find interesting about robustness, not only in natural, but also in engineering, and social systems. It is argued here that robustness is a measure of feature persistence in a system that compels us to focus on fluctuations, and often assemblages of perturbations, qualitatively deferent in nature from those addressed by stability theory. Moreover, to address feature persistence under these sorts of perturbations, we are naturally led to study issues including: the coupling of dynamics with organizational architecture, implicit assumptions of the environment, the role of a system's evolutionary history in determining its current state and thereby its future state, the sense in which robustness characterizes the fitness of the set of "strategic options" open to the system and the capability of the system to switch among multiple functionalities [6, 9]. Defining any scientific term is a nontrivial issue, but in this paper, the following definition will be used "robustness" is a property that allows a system to maintain its functions against internal and external perturbations. It important to realize that robustness is concerned with maintaining functions of a system rather than system states, which distinguishes robustness from stability or homeostasis [8]. A continuing interest problem in nonlinear science is the interplay between chaos and noise. This is so because complex systems are often under noise, and it is important to assess how the dynamics of deterministic chaotic system is affected by noise. Some pioneering works on this problem comprise physics, biology and biophysics [2, 11, 13, 14]. It is well known that chaos, in general, is robust under stochastic fluctuations that can induce chaos for parameters just before a bifurcation to chaos. Namely, stochastic perturbations can induce chaotic dynamics where there is no naturally occurring chaos, far away from any bifurcation leading to chaos. This is possible due to the complex topology associated with two nearby unstable orbits [14]. Intention of this paper is to explore the sensitivity of model representing biochemical substance exchange between cells [1] to fluctuations of the environment parameters of different scale using maximal Lyapunov exponent and cross sample entropy.

2 Short Model Background

Following the model introduced by Balaž and Mihaiović [1], we investigate behaviors of two cells, exchanging biochemical substances, using methods of non linear dynamics – calculating maximal Lyapunov exponent and cross sample entropy. In the above paper we derived two-dimensional mapping that describes communicative interaction between two cells having the form

$$x_{n+1} = (1-c)r\, x_n(1-x_n) + cy_n^p \tag{1a}$$

$$y_{n+1} = (1-c)r\, y_n(1-y_n) + cx_n^{1-p} \tag{1b}$$

where the logistic parameter r is such that $0 \le r \le 4$ and the coupling parameter c (intercellular concentration of biochemical substance); x_n and y_n denote the concentrations in cells exchanging the substance while p $(0 < p < 1)$ is the cell affinity to uptake the substance. We considered a two-cell system, where each of them is able to release and uptake the same biochemical substance. According to the assumption in model design, the dynamical behavior of the substance concentrations x_n and y_n depends on three factors: (i) its own concentration c

within radius of interaction in surrounding environment [1], (ii) parameter r and (iii) affinity p for binding on cellular receptors. First factor if determined by underlying feedback mechanism of intracellular regulations, while the second one represents level of the suitability of the environment to the communication between two cells [12]. The third factor depends on protein disorder [3, 4] which is used to be constant in this model. The map displays a wide range of behavior as the parameters r and c are varied including periodic, quasiperiodic, and chaotic motion. The variation of Lyapunov exponent λ as a function of concentration c is depicted in Fig. 1 for $p = 0.2$ and $r = 3.95$. The part of this curve in elliptic area is chosen for analysis of the effect of fluctuations on synchronization of the system.

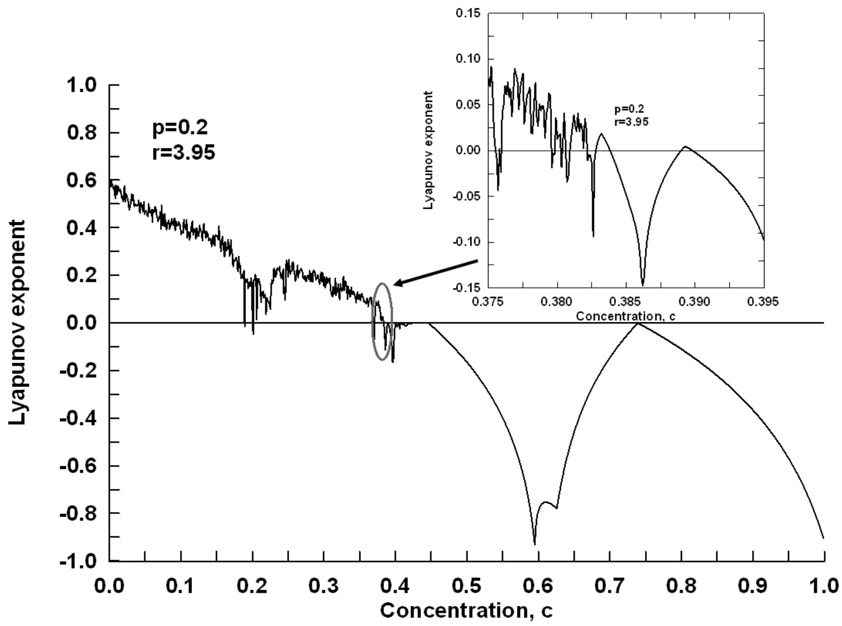

Fig. 1 Lyapunov exponent of coupled maps with no fluctuations [Eq. (1)] as a function of concentration c ranging from 0 to 1. Ellipsis indicates the region used for analysing the effect of fluctuations.

In order to characterize the asymptotic behavior of the orbits, we need to calculate the largest Lyapunov exponent λ, which is given for the initial point $\mathbf{X}_0$ in the attracting region by

$$\lambda = \lim_{n\to\infty}(\ln \| \mathbf{J^n}(\mathbf{X}_0) \| / n) . \tag{2}$$

where $\mathbf{J}$ is the Jacobi matrix. With this exponent, we measure how rapidly two nearby orbits in an attracting region converge or diverge. In practice, using

$\mathbf{J}^k(\mathbf{X}_k)=\mathbf{J}^k(\mathbf{X}_0)=\mathbf{J}(\mathbf{X}_{k-1})...\ \mathbf{J}(\mathbf{X}_1)\mathbf{J}(\mathbf{X}_0)$, we compute the approximate value of λ by substituting in (2) successive values from $\mathbf{X}_{n_0}$ to $\mathbf{X}_{n_1}$, for n_0, n_1 large enough to eliminate transient behaviors and provide good approximation. If $\mathbf{X}_0$ is part of a stable periodic orbit of period k, then $\|\mathbf{J}^k(\mathbf{X}_0)\|<1$ and the exponent λ is negative, which characterizes the rate at which small perturbations from the fixed cycle decay, and we can call such a system synchronised.

3 Effect of Fluctuations

In this section we will investigate the behavior of the coupled maps given by Eqs. (1a) and (1b) in the presence of fluctuations of environmental parameters or other noise. As has been shown in the case of uncoupled non-linear oscillators, the addition of parametric fluctuations has a pronounced effect on the dynamics of such systems [5]. In particular, the presence of noise introduces a gap in the bifurcation sequence of period-doubling systems and renormalizes the threshold of the appearance of chaotic behavior in the model considered. It is therefore of interest to investigate the effect of noise on the exchange substances between two cells. This is because cells are intrinsically noisy biochemical reactors: low reactant numbers can lead to significant statistical fluctuations in molecule numbers and reaction rates [16].

The effect of fluctuations was modeled by adding uniformly distributed random numbers to the map of Eq. (1). Specifically, we considered the map

$$x_{n+1}=(1-c)r(1+\tau\delta_n^{(1)})x_n(1-x_n)+cy_n^p+\xi\mathbf{D}\delta_n^{(1)} \tag{3a}$$

$$y_{n+1}=(1-c)r(1+\tau\delta_n^{(2)})y_n(1-y_n)+cx_n^p+\xi\mathbf{D}\delta_n^{(2)} \tag{3b}$$

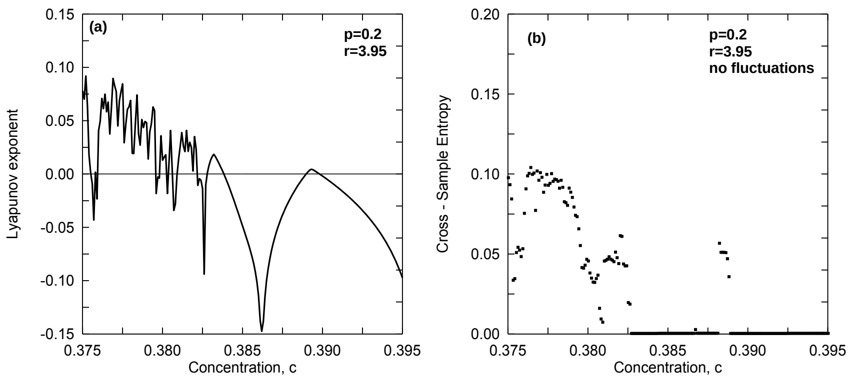

Fig. 2 Lyapunov exponent (a) and cross sample entropy (b) for coupled maps with no fluctuations (Eq. (1)) as a function of concentration c ranging from 0.375 to 0.395.

where τ and ξ take value 0 or 1 while $\delta_n^{(1)}$ and $\delta_n^{(2)}$ are random numbers uniformly distributed in the interval [-1, 1] and $\mathbf{D}$ is the amplitude of the fluctuations. In numerical simulations we used three kind of fluctuations: (1) $(\tau = 0, \xi = 1)$ – fluctuations of c; (2) $(\tau = 1, \xi = 0)$ – fluctuations of r and (3) fluctuations in both c and r. The case $(\tau = 1, \xi = 1)$ corresponds to one with no fluctuations [Eq. (1)]. These fluctuations can destroy the fine scale detail of the transitions and the quasiperiodic regions. For the amplitude $\mathbf{D}$ we used the following values 0.00001, 0.0001, 0.001 and 0.01. Figure 2a shows Lyapunov exponent for coupled maps with no fluctuations [Eq. (1)] as a function of concentration c ranging from 0.375 to 0.395, while Figs. 3a–3c depict this exponent for the largest amplitude of the fluctuation $\mathbf{D} = 0.01$ and the same ranging interval for c. Obviously, those fluctuations remarkably change the Lyapunov exponent if they occur in c and r. That disturbance is highly emphasized for the case when fluctuations are occurred in both parameter r and c.

Cross sample entropy $(Cross-SampEn)$ - measure of asynchrony is a recently introduced technique for comparing two different time series to assess their degree of asynchrony or dissimilarity [7, 10, 15]. Let $u = [u(1), u(2), ...u(N)]$ and $v = [v(1), v(2), ...v(N)]$ fix input parameters m and r. Vector sequences: $x(i) = [u(i), u(i+1), ...u(i+m-1)]$ and $y(j) = [v(j), v(j+1), ...v(j+m-1]$ and N is the number of data points of time series, $i, j = N - m + 1$. For each $i \le N - m$ set $B_i^m(r)(v \,||\, u) =$ (number of $j \le N - m$ such that $d\,[x_m(i), y_m(j)] \le r]\,)\,/(N - m)$, where j ranges from 1 to $N - m$. And then

$$B^m(r)(v \,||\, u) = \sum_{i=1}^{N-m} B_i^m(r)(v \,||\, u) \,/\, N - m \tag{4}$$

which is the average value of $B_i^m(v \,||\, u)$. Similarly we define A^m and A_i^m as $A_i^m(r)(v \,||\, u) =$ (number of such $j \le N - m$ that $d\,[x_m(i), y_m(j)] \le r]\,)\,/(N - m)$.

$$A^m(r)(v \,||\, u) = \sum_{i=1}^{N-m} A_i^m(r)(v \,||\, u) \,/\, N - m \tag{5}$$

which is the average value of $A_i^m(v \,||\, u)$. And then

$$Cross - SampEn\,(m, r, n) = -\ln\left\{\, A^m(r)(v \,||\, u) \,/\, B^m(r)(v \,||\, u)\right\} \tag{6}$$

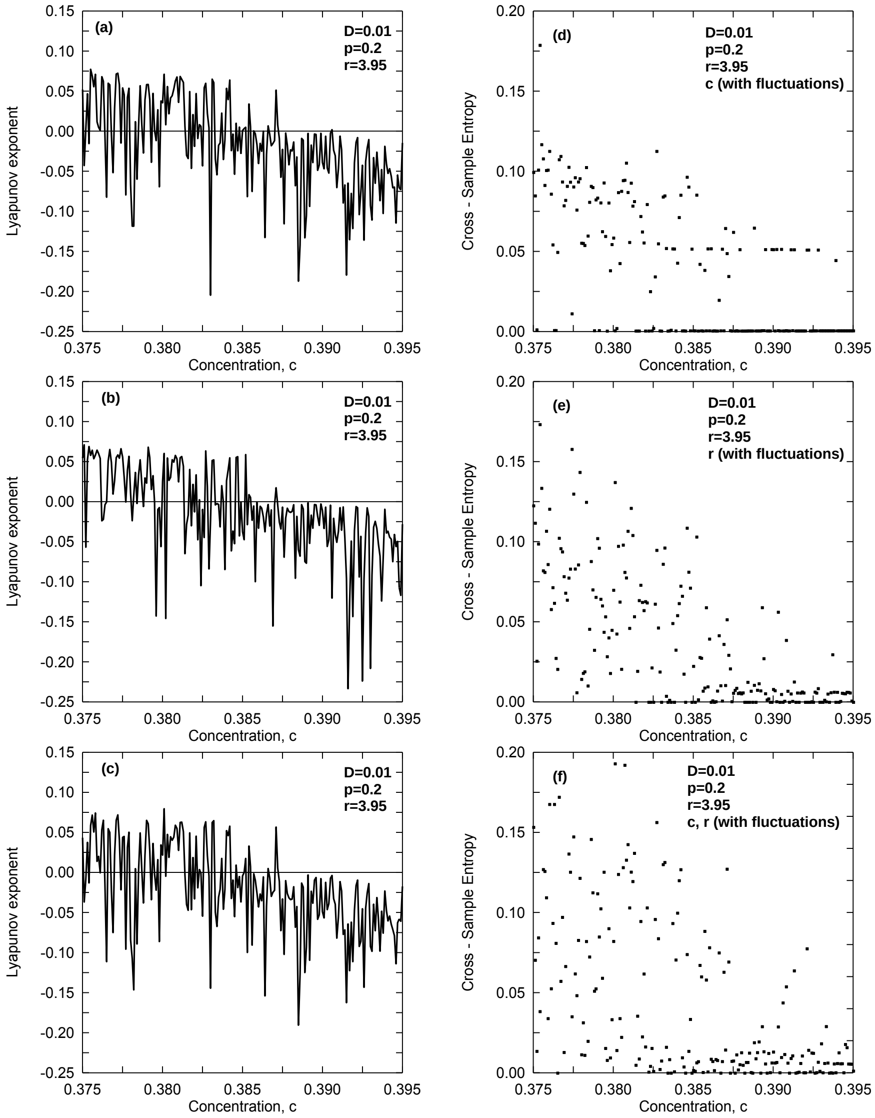

Fig. 3 Lyapunov exponent (a)-(c) and cross sample entropy (d)-(f) for coupled maps [Eq. (3)] for fluctuation with amplitude $\mathbf{D} = 0.01$ as a function of concentration c ranging from 0.375 to 0.395.

We applied $Cross-SampEn$ with $m = 5$ and $r = 0.05$ for x_n and y_n time series. Figures 3d-3f show high disorder between them, particularly when fluctuations occur in the logistic parameter r and the both r and c. Apparently, that the disorder in the entropy is growing up when the amplitude of the fluctuations increases. We calculated the RMSE (root-mean-square-error) of the cross sample entropy with the state without fluctuations as a referent one.

The cross sample entropy for coupled maps [Eq. (3)] for fluctuation as a function of the amplitude $\mathbf{D}$ of fluctuations ranging from 0.00001 to 0.01 is shown in Fig. 4. From this figure is seen that the highest increase of RMSE of the cross sample entropy is obtained when the fluctuations are occurred in the both environment parameters, r and c.

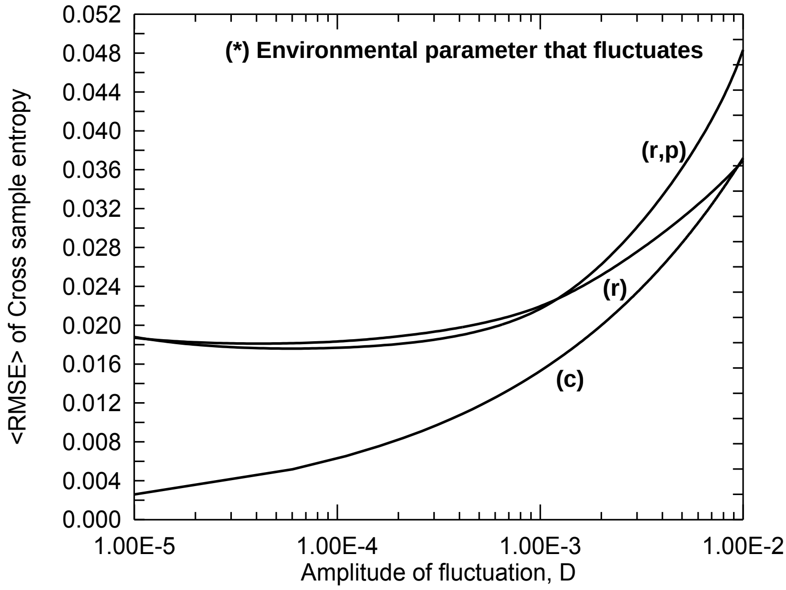

Fig. 4 RMSE of the cross sample entropy for coupled maps [Eq. (3)] for fluctuation as a function of the amplitude $\mathbf{D}$ of fluctuations ranging from 0.00001 to 0.01. The letters next to curves indicate fluctations in: (c) concentration, (r) logistic parameter and both (r , c).

4 Conclusion

Following the model introduced by Balaz and Mihailović [1], we investigate behaviors of two cells, exchanging substances by two-dimensional mapping that describes communicative interaction between two cells. Further, we explore the sensitivity of model proposed to fluctuations in environment parameter of different scale using methods of non linear dynamics – calculating maximal Lyapunov exponent and cross sample entropy.

Acknowledgement

The research described here was funded by the Serbian Ministry of Science and Technology under the project “Study of climate change impact on environment: monitoring of impact, adaptation and moderation”, for 2011-2014.

References

[1] I. Balaz, D.T. Mihailovic, A model representing biochemical substances exchange between cells. Part I: Model formalization. *J. App. Funct. Anal.* (2010) (accepted).

[2] L. Billings, I.B. Schwartz, Exciting chaos with noise: unexpected dynamics in epidemic outbreaks, *J. Math. Biol.*, 44, 31-48 (2002).

[3] A.K. Dunker, J.D. Lawson, C.J. Brown, R.M. Williams, P. Romero, J.S. Oh, C.J. Oldfield, A.M. Campen, C.M. Ratliff, K.W. Hipps, J. Ausio, M.S. Nissen, R. Reeves, C. Kang, C.R. Kissinger, R.W. Bailey, M.D. Griswold, W. Chiu, E.C. Garner, Z. Obradovic, Intrinsically disordered protein. *J. Mol. Graph. Model.*, 19, 26-59 (2001).

[4] A.K. Dunker, C.J. Brown, J.D. Lawson, L.M. Iakoucheva, Z. Obradovic, Intrinsic Disorder and Protein Function. *Biochemistry*, 41, 6573–6582 (2002).

[5] T. Hogg, B.A. Huberman, Generic behavior of coupled oscillators, *Phys. Rev. A*, 29, 275-281 (1984).

[6] E. Jen, Stable or robust? What's the rifference? *Complexity*, 8, 12-18 (2003).

[7] M.B. Kennel, R. Brown, H.D.I. Abarbanel, Determining embedding dimension for phase-space reconstruction using a geometrical construction, *Phys. Rev. A*, 45, 3403–3411 (1992).

[8] H. Kitano, Biological robustness. *Nat. Rev. Genet.*, 5, 826–837 (2004)

[9] H. Kitano, Towards a theory of biological robustness. *Mol. Syst. Biol.* 3, 137, (2007).

[10] D.E. Lake, J.S. Richman, M.P. Griffin, J.R. Moorman, Sample entropy analysis of neonatal heart rate variability, *Am. J. Physiol.- Reg. I,* 283**,** R789–R797 (2002).

[11] Z. Liu, W. Ma, Noise induced destruction of zero Lyapunov exponent in coupled chaotic systems, *Phys. Lett. A*, 343, 300–305 (2005).

[12] D.T. Mihailović, M. Budinčević, I. Balaz, M. Perišić, Emergence of chaos and synchronization in coupled interaction in environmental interfaces regarded as biophysical complex systems, in *Advances in environmental modelling and measurements* (D.T. Mihailović and B. Lalić eds.), Nova Sciences Publishers, New York, 2010, pp. 89-100.

[13] B. Schwartz, D.S. Morgan, L. Billings, Y.-C. Lai, Multi-scale continuum mechanics: From global bifurcations to noise induced high dimensional chaos, *CHAOS*, 14:2, 373-386 (2004).

[14] W.M. Schaffer, B.E. Kendall, C.W. Tidd, L.F. Olsen, Transient periodicity and episodic predictability in biological dynamics, IMA *J. Math. Appl. Med*., 10, 227–247 (1993).

[15] J.S. Richman, J.R. Moorman, Physiological time-series analysis using approximate entropy and sample entropy, *Am. J. Physiol-Heart C,* 278, H2039–H2049 (2000).

[16] M. Thattai, A. van Oudenaarden, Intrinsic noise in gene regulatory networks, *PNAS*, 98, 8614-8619 (2001).

JOURNAL OF APPLIED FUNCTIONAL ANALYSIS, VOL.6, NO.1, 85-90, COPYRIGHT 2011 EUDOXUS PRESS, LLC

Explicate Series Solution for Prey-Predator Problem

N. Alshibly*, A.K. Alomari

March 4, 2010

In this paper, an analytical expression for the solution of the ratio-dependent predator-prey system with constant effort harvesting by an adaptation of the homotopy perturbation method (HPM) is presented. The HPM is treated as an algorithm for approximating the solution of the problem in a sequence of time intervals, i.e HPM is converted into a hybrid numeric–analytic method. Residual error for the solution is presented.

1 Introduction

Most modelling of biological problems are characterized by systems of ordinary differential equations (ODEs). The prey is subjected to constant effort harvesting with r, a parameter that measures the effort being spent by a harvesting agency. The harvesting activity does not affect the predator population directly. It is obvious that the harvesting activity does reduce the predator population indirectly by reducing the availability of the prey to the predator. Adopting a simple logistic growth for prey population with $e > 0, b > 0$, and $c > 0$ standing for the predator death rate, capturing rate, and conversion rate, respectively, we formulate the problem as [1]

$$\frac{dx(t)}{dt} = x(t)(1-x(t)) - \frac{bx(t)y(t)}{y(t)+x(t)} - rx(t), \quad x(t_0) = c_1, \tag{1}$$

$$\frac{dy(t)}{dt} = \frac{cx(t)y(t)}{y(t)+x(t)} - ey(t), \quad y(t_0) = c_2, \tag{2}$$

where $x(t)$ and $y(t)$ represent the fractions of population densities for prey and predator at time t, respectively. Equations (1–2) are to be solved according to biologically meaningful initial conditions $x(t) \geq 0$ and $y(t) \geq 0$.

Authors in [3] and [4] used the Adomian decomposition method (ADM) to handle the systems of prey-predator problem. Yusufoğlu and Erbaş [5] and Rafei et al. [6] employed the variational iteration method (VIM) to compute an approximation to the solution of the system of nonlinear differential equations governing the problem. Biazar [7] used the power series method (PSM) to handle the systems.

In recent years, a great deal of attention has been devoted to study HPM, which was first invented by Prof Ji-Huan He [8] for solving a wide range of problems whose mathematical models yield differential equation or system of differential equations. HPM has successfully been applied to many situations. Chowdhury et al. present new modification of HPM by dividing the solution interval to finite number of subintervals [4].

In this paper, we are interested to find the approximate analytic solution of the system of coupled nonlinear ODEs (1) and (2) by treated the HPM as an algorithm for approximating the solution of the problem in a sequence of time intervals. Residual error for the present solution is introduced.

2 Solution procedure

Firstly, consider (1) and (2) subject to

$$x(t^*) = c_1, \quad y(t^*) = c_2. \tag{3}$$

We note that when $t^* = 0$ we have the initial condition of Eq. (1) and (2). It is straightforward to choose

$$x_0(t) = c_1, \quad y_0(t) = c_2, \tag{4}$$

as our initial approximations of $x(t)$ and $y(t)$, and the linear operator should be

$$L[\phi(t;q)] = \frac{\partial \phi(t;q)}{\partial t}, \tag{5}$$

with the property

$$L[A] = 0, \tag{6}$$

where A is the integration constant, which will be determined by the initial condition.

If $q \in [0,1]$ indicate the embedding parameter, then the *zeroth-order deformation* problems are of the following form:

$$(1-q)L[\hat{x}(t;q) - x_0(t)] = qN_x[\hat{x}(t;q), \hat{y}(t;q)], \tag{7}$$

$$(1-q)L[\hat{y}(t;q) - y_0(t)] = qN_y[\hat{x}(t;q), \hat{y}(t;q)], \tag{8}$$

subject to the initial conditions

$$\hat{x}(t^*;q) = c_1, \quad \hat{y}(t^*;q) = c_2, \tag{9}$$

in which we define the nonlinear operators N_x and N_y as

$$N_x[\hat{x}(t;q), \hat{y}(t;q)] = \frac{\partial \hat{x}(t;q)}{\partial t} - \hat{x}(t;q)(1-\hat{x}(t;q)) + \frac{b\hat{x}(t;q)\hat{y}(t;q)}{\hat{y}(t;q)+\hat{x}(t;q)} + r\hat{x}(t;q),$$

$$N_y[\hat{x}(t;q), \hat{y}(t;q)] = \frac{\partial \hat{y}(t;q)}{\partial t} - \frac{c\hat{x}(t;q)\hat{y}(t;q)}{\hat{y}(t;q)+\hat{x}(t;q)} + e\hat{y}(t;q).$$

For $q=0$ and $q=1$, the above *zeroth-order deformation* equations (7) and (8) have the solutions

$$\hat{x}(t;0)=x_0(t), \quad \hat{y}(t;0)=y_0(t), \tag{10}$$

and

$$\hat{x}(t;1)=x(t), \quad \hat{y}(t;1)=y(t). \tag{11}$$

When q increases from 0 to 1, then $\hat{x}(t;q)$ and $\hat{y}(t;q)$ vary from $x_0(t)$ and $y_0(t)$ to $x(t)$ and $y(t)$. Expanding $\hat{x}$ and $\hat{y}$ in Taylor series with respect to q, we have

$$\hat{x}(t;q) = x_0(t)+\sum_{m=1}^{\infty} x_m(t)q^m, \tag{12}$$

$$\hat{y}(t;q) = y_0(t)+\sum_{m=1}^{\infty} y_m(t)q^m, \tag{13}$$

in which

$$x_m(t)=\frac{1}{m!}\frac{\partial^m \hat{x}(t;q)}{\partial q^m}\bigg|_{q=0}, \quad y_m(t)=\frac{1}{m!}\frac{\partial^m \hat{y}(t;q)}{\partial q^m}\bigg|_{q=0}. \tag{14}$$

Therefore, we have through Eq. (11) that

$$x(t) = x_0(t)+\sum_{m=1}^{\infty} x_m(t), \tag{15}$$

$$y(t) = y_0(t)+\sum_{m=1}^{\infty} y_m(t). \tag{16}$$

Define the vectors

$$\vec{x}(t) = \{x_0(t), x_1(t), ..., x_n(t)\}, \tag{17}$$

$$\vec{y}(t) = \{y_0(t), y_1(t), ..., y_n(t)\}. \tag{18}$$

Differentiating the *zeroth-order* equations (7) and (8) m times with respect to q, then setting $q=0$, and finally dividing by $m!$, we have the *mth-order deformation* equations

$$L[x_m(t)-\chi_m x_{m-1}(t)] = R_{x,m}(\vec{x}(t),\vec{y}(t)), \tag{19}$$

$$L[y_m(t)-\chi_m y_{m-1}(t)] = R_{y,m}(\vec{x}(t),\vec{y}(t)), \tag{20}$$

with the following boundary conditions:

$$x_m(t^*)=0, \quad y_m(t^*)=0, \tag{21}$$

for all $m\geq 1$, where

$$R_{x,m}(\vec{x}(t),\vec{y}(t)) = \frac{1}{(m-1)!}\frac{\partial^{m-1}N_x[\hat{x}(t;q),\hat{y}(t;q)]}{\partial q^{m-1}}\bigg|_{q=0}, \tag{22}$$

$$R_{y,m}(\vec{x}(t),\vec{y}(t)) = \frac{1}{(m-1)!}\frac{\partial^{m-1}N_y[\hat{x}(t;q),\hat{y}(t;q)]}{\partial q^{m-1}}\bigg|_{q=0}. \tag{23}$$

This way, it is easy to solve the linear non-homogeneous Eqs. (19) and (20) at general initial conditions by using Maple, one after the other in the order $m = 1, 2, 3, \ldots$. Thus we successfully have

$$
\begin{aligned}
x_1(t) &= -\frac{c_1\left(-c_1 + 7c_2 + 10c_1^2 + 10c_1c_2\right)(t - t^*)}{10(c_1 + c_2)}, \\
y_1(t) &= -\frac{c_2\,(3c_1 + 5c_2)(t - t^*)}{10(c_1 + c_2)}, \\
x_2(t) &= \frac{1}{200\,(c_1 + c_2)^3}\, c_1\left(c_1^3 - 30c_1^4 + 200c_1^5 + 19c_1^2c_2\right. \\
&\quad +19c_1c_2^2 + 49c_2^3 + 70c_1^3c_2 + 310c_1^2c_2^2 + 210c_1c_2^3 \\
&\quad \left.+600c_1^4c_2 + 600c_1^3c_2^2 + 200c_1^2c_2^3\right)(t - t^*)^2 \\
y_2(t) &= -\frac{1}{200\,(c_1 + c_2)^3}\, c_2\left(-25c_2^3 - 9c_1^3 - 47c_1^2c_2\right. \\
&\quad \left.-51c_1c_2^2 + 20c_1^3c_2 + 20c_1^2c_2^2\right)(t - t^*)^2, \\
&\quad \vdots
\end{aligned}
$$

By the same way we can get the first fourth term to be as analytical approximate solution as $x(t) \simeq \sum_{i=0}^{4} x_i(t)$ and $y(t) \simeq \sum_{i=0}^{4} y_i(t)$ terms. Now we divide the interval $[0, T]$ to subintervals by time step $\Delta t = 0.01$. Then we start from the initial conditions and we get the solution on the interval $[0, 0.01)$. Further, we take $c_1 = x(0.01)$ and $c_2 = y(0.01)$ and $t^* = 0.01$, so we get the solution on the new interval $[0.01, 0.02)$, and so on. Therefore, by choosing this initial approximation on the starting of each interval, the solution on the whole interval should be continuous. It is worth mentioning that if we take $t^* = 0$ and we fixed c_1 and c_2, then the solution will be the standard HPM solution which is not effective at large value of t.

3 Analysis of results

In this section, we compute the result using above algorithm for $x(0) = 0.5, y(0) = 0.3, b = 0.8, c = 0.2, e = 0.5$ and $r = 0.9$. Figure 1 presents the population fraction versus time for prey population fraction $(x(t))$ and predator population fraction $(y(t))$. Moreover the residual error using this algorithm is given in Fig.2 (a)and (b). It is clear that the error within the range 10^{-15} which mean that is very small and it is not be possible in the standard HPM which give error 10^6 using the same interval as in Fig. 2(c).

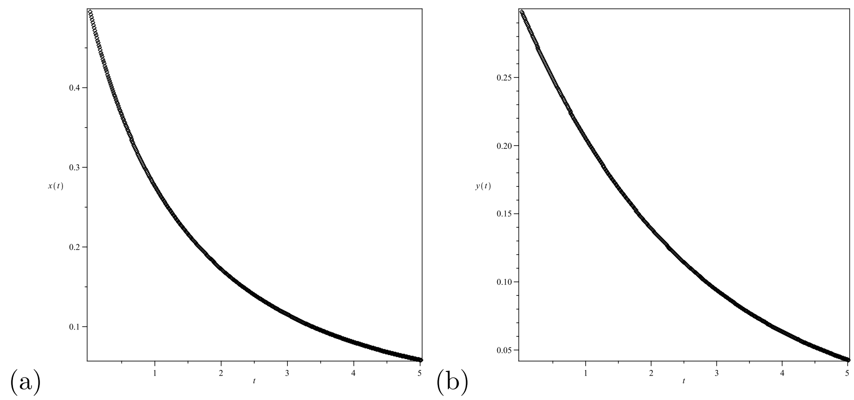

Figure 1: Population fraction versus time(a) prey population fraction; (b) predator population fraction.

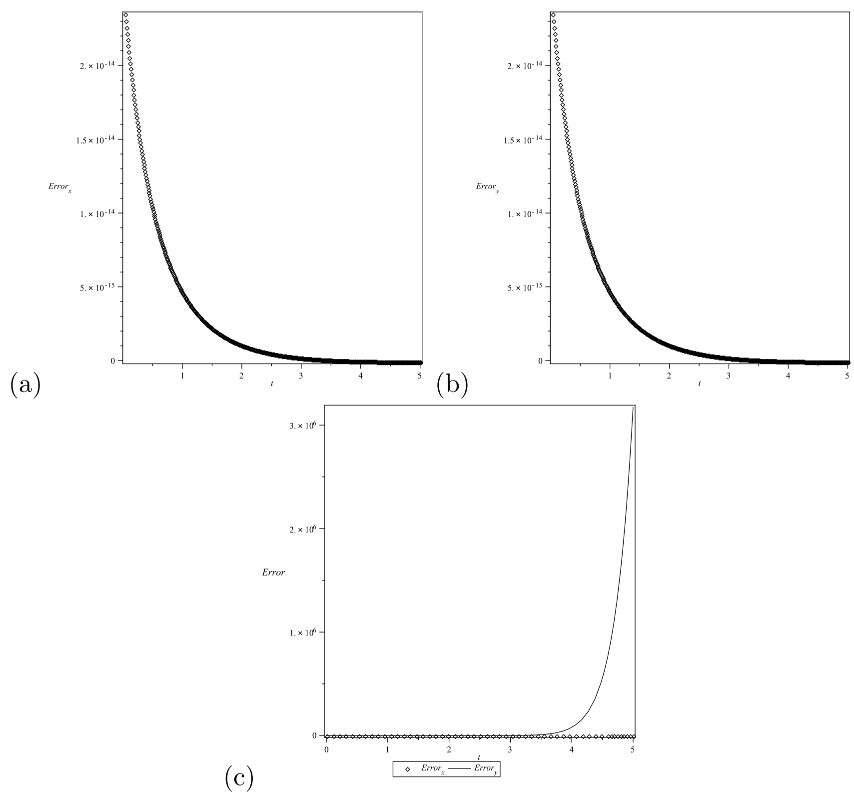

Figure 2: Residual error for (a) MHPM solution of x (b) MHPM solution of y (c) HPM solution

References

[1] Abdoul R. Ghotbi, A. Barari, D. D. Ganji,Solving Ratio-Dependent Predator-Prey System with Constant Effort Harvesting Using Homotopy Perturbation Method,Mathematical Problems in Engineering 2008, Article ID 945420, 8 pages

[2] G.F.C. Simmons, Differential Equations with Applications and Historical Notes, McGraw–Hill, Ohio (1972)

[3] J. Biazar, R. Montazeri, A computational method for solution of the prey and predator problem, Appl. Math. Comput. 163, 841–847 (2005)

[4] M.S.H. Chowdhury, I. Hashim, S. Mawa, Solution of prey-predator problem by numeric-analytic technique, Commun. Nonlinear Sci. Numer. Simul. 14, 1008–1012 (2009)

[5] E. Yusufoğlu, B. Erbaş, He's variational iteration method applied to the solution of the prey and predator problem with variable coefficients,Phys. Lett. A .372, 3829-3835 (2008)

[6] M. Rafei, H. Daniali, D.D. Ganji, Variational iteration method for solving the epidemic model and the prey and predator problem, Appl. Math. Comput. 186, 1701–1709 (2007)

[7] J. Biazar, M. Ilie, A. Khoshkenar, A new approach to the solution of the prey and predator problem and comparison of the results with Adomian decomposition method. Appl. Math. Comput. 173, 486–8491 (2005)

[8] J. He, Homotopy perturbation method: a new nonlinear analytical technique. Applied Mathematics and Computation, 135,73–79 (2003)

Department of science, faculty of nursing and sciences, Jerash privet university, 26150 Jerash, Jordan
nasserayasrah@yahoo.com (N. Alshibly)

The Modern Firm: A Strange Chaotic oscillator

Safieddine Bouali
University of Tunis, Management Institute, Department of Economics
41, rue de la Liberté 2000 Le Bardo, Tunisia,
Safieddine.Bouali@isg.rnu.tn

Abstract:

Corporate arrangement between owners and managers governs modern firm. In the contemporary context of persistent financial crisis, they self-impose a strong distribution of earnings when profits exceed the optimal reinvestment amount. Dividend payout and capitalization are the two items of this financial trade-off. To identify the dynamical outcome of such financial governance, we define a 3D system of differential equations modelling a representative firm under the best standard of management principles and rules. The numerical simulations reveal that state variables of the firm follow a wide spectrum of dynamics amongst them singular strange attractors. The main results show that chaotic oscillation is an intrinsic and endogenous characteristic of the modern firm, not derived from (exogenous) market failure.

Key words*: Firm, Dynamical model, Nonlinearity, Chaos, Strange attractors*

1. Introduction

Profits sharing between dividends and self-financing investment constitutes a main focus of the firm. However, after the revelation of accounting scandals and frauds [1], the actual period spreads generalized and deep lack of trust between owners and managers. In this context, the shareholders intend the immediate conversion of the free cash flow into dividends [2, 3, 4].

Triggering payout beyond a particular threshold of earning express the corporate arrangement between owners and managers to improve the creation of wealth by the firm, enhances its share value in the stock market and, simultaneously, allows incomes to the shareholders.

The paper aims to the determination of a dynamical model of a representative firm managed with the standard financial principles and rules of the corporate governance. The three dimensional system of ordinary differential equations is defined and simulated to investigate the outcome of a particular nonlinear mechanism to pay free cash flows as dividends (sec. 2). We explore by several numerical computations, the dynamics of the firm and their periodicity in the phase portraits of the state variables (sec. 3). The concluding remarks report some implications of this heuristic research to the modern firm behaviour (sec. 4).

2. The model

In our 3D model of autonomous O.D.Es, all variables are endogenous. In the first equation, the capital allows the creation of profits **P**. It is made up of capitalization of the profits **R** (or the re-investments) and financed also by an external capital inflow (i.e. loans and bonds) **F**.

$$\mathbf{dP/dt = (R + F)/v} \qquad (1)$$

1/v: rate of profits.

Moreover, the rule of the self-financing investments determined by the managers is:

$$\mathbf{dR/dt = m}$$

with ***m***: mass of reinvestments *when* the level of profits reaches the “optimal” value **P = 1**. On the other hand, to push managers to apply the corporate arrangement of payout, a strong mechanism is released when dividends are delayed. The complete equation holds a regulation automaton to reach this selected level of capitalization of profits if **P ≠ 1**.

$$\mathbf{dR/dt = m\,P + n\,(1- P^{2})\,R} \qquad (2)$$

n: rate of recapitalization

This specification indicate to the managers, the imperative distribution of earnings to shareholders immediately since the second, and nonlinear, item of the equation allows the strong increase of the dividends when the level of profits is **P > 1.** Expelling earnings outside firm at the maximum speed is the function of this mechanism of convergence. It is similar to a rule of punishment of the managers when excess cash is accumulated.

Symmetrically, it allows fast increase of the capitalization when the mass of Profits is at the level **P < 1.**

In the first case, the dividend distribution is accelerated and the capitalization falls at an accelerated rate according the gap between 1 and P. In the second case, beyond the "normal" profit, the capitalization is reduced by the growth of the dividend distribution.

Eventually, the final equation is the account of the net capital inflow of the firm:

$$\mathbf{dF/dt = - r P + s R} \qquad (3)$$

After deducting the refunding of the debts with the **r** ratio, the corporate borrowing is obtained by loans according to the proportion **s** of the self-financing.

Written in three first-order differential equations, our heuristic model represents the first principles and rules of the best finance of the modern firms [5, 6] and leads to the simulations of the state variables of the firm. Theoretically, the 3D system connects a feedback equation to the van der Pol oscillator [7]. We investigate the implications of the dividend policy when nonlinear decisions are made.

3. Computational Results

The basic study of the system begins with the detection of the solutions.

$$\begin{cases} \mathbf{dP/dt = (R + F)/v} & \mathbf{(1)} \\ \mathbf{dR/dt = m P + n (1 - P^2) R} & \mathbf{(2)} \\ \mathbf{dF/dt = - r P + s R} & \mathbf{(3)} \end{cases}$$

The steady-state equilibriums are obtained for dP/dt = dR/dt = dF/dt= 0.

We get R = -F from Eq.(1), R = m P/n (P^2 - 1) from Eq.(2) and P = s R/r from Eq.(3). The last two relations yielded the following equality: P (nrP^2 - nr – ms) = 0.

Indeed, the three roots of P are: $P_1 = 0$, $P_2 = [(nr + ms) /nr]^{1/2}$ and $P_3 = - P_2$. Let $[(nr + ms) /nr]^{1/2}= k$, the three equilibriums become: E_1 (P, R, F) = (0, 0, 0), E_2 (P, R, F) = (k, rk/s, -rk/s) and E_3 (P, R, F) = - E_2.

The numerical computations are carried out with the fifth-order Runge-Kutta integration method and 10^{-6} accuracy. The initial conditions are CI (P, R, F) = (0.01, 0.01, 0.01).

3.1. The periodic oscillation

We choose a set of parameters in accordance with the real financial data of the firms C_1 (v, m, n, r, s) = (4, 0.04, 0.02, 0.1, 0.2). The simulation displays a periodic motion (Fig. 1) wherein the orbit is centred on the equilibrium: E_2 (P, R, F) = (2.23, 1.11, -1.11).The behaviour of the state variables is cyclical. The other equilibriums are E_1 (P, R, F) = (0, 0, 0) and $E_3 = - E_2$. We notice that anti-symmetric initial condition leads to an anti-symmetric attractor. Moreover, the Jacobean matrix of the 3D system gives a positive $|J| = [nr(1 - P^2) + ms - 2\,nPRs]/v$, since all these equilibriums are unstable.

The firm as a dynamical system oscillates periodically in the phase space of the variables: profits, reinvestments and capital inflow. It oscillates infinitely and don't converge to any steady state equilibrium. We notice that Profits reach a low level of losses but it is not critical.

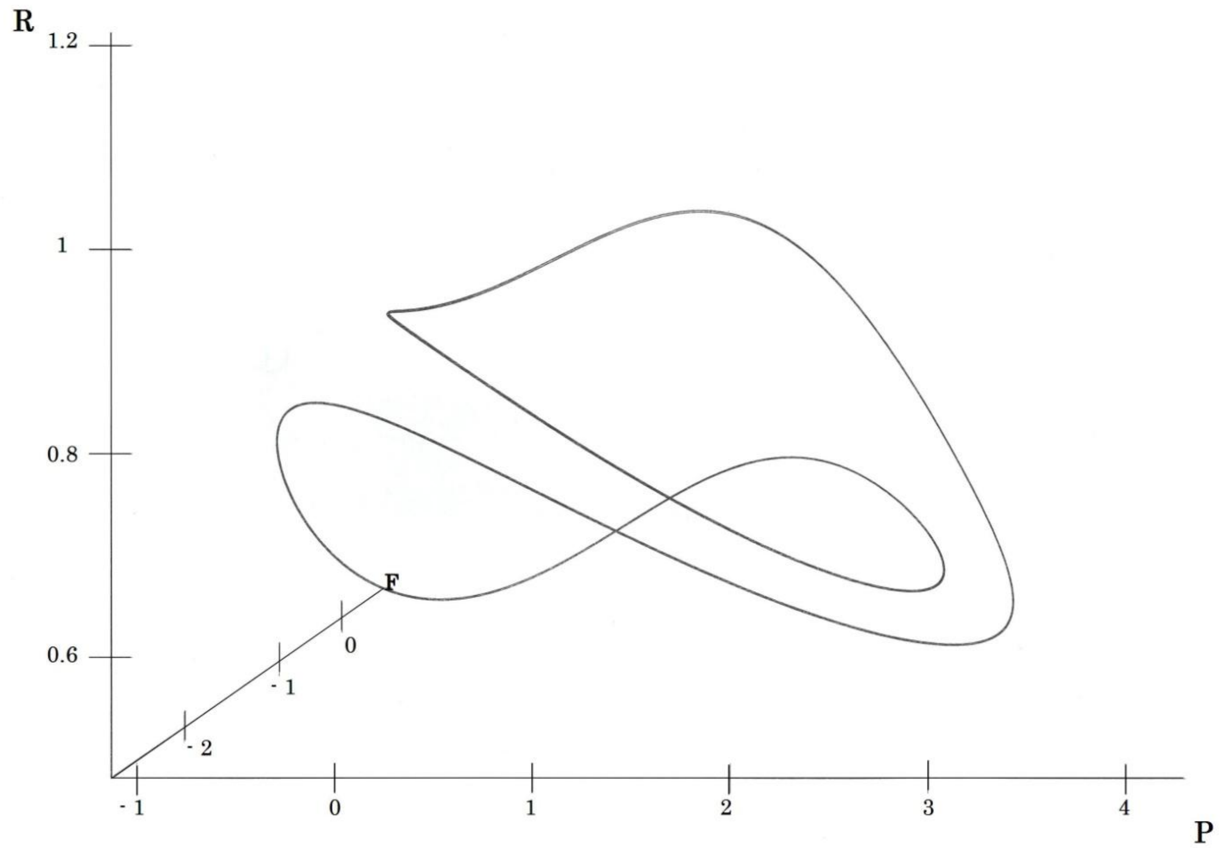

Fig. 1. Period-4 solution for the set of parameters C_1

The dynamic of the firm oscillates between (low) negative values and high levels of profits P.

We notice the particular shape of the orbit.

At this stage, the owners and the management staff can choose a more significant capital flow with a greater **s** parameter to push the profit variable.

3.2. The strange chaos

When the corporate borrowing increases, for instance when C_2 (v, m, n, r, **s**) = (4, 0.04, 0.02, 0.1, **0.3**), the equilibriums become E_1 (P, R, F) = (0, 0, 0), E_2 (P, R, F) = (2.64, 0.88, -0.88) and $E_3 = - E_2$.

The parameters C_2 characterize a chaotic attractor [8] and the model is conservative for the trajectories that are close to E_1 and dissipative particularly at the neighbourhood of E_2 and E_3. The strange chaos indicates that firm follows an infinite number of dynamics, non-periodic and non-predictable behavior (Fig. 2a). Paradoxically, the attractor as a dynamical “object” confined in a limited set of the phase portrait prevents predictions of the future values of the variable. Moreover, for anti-symmetric initial conditions, the 3D system creates another strange attractor but in an anti-symmetric posture (Fig. 2b).

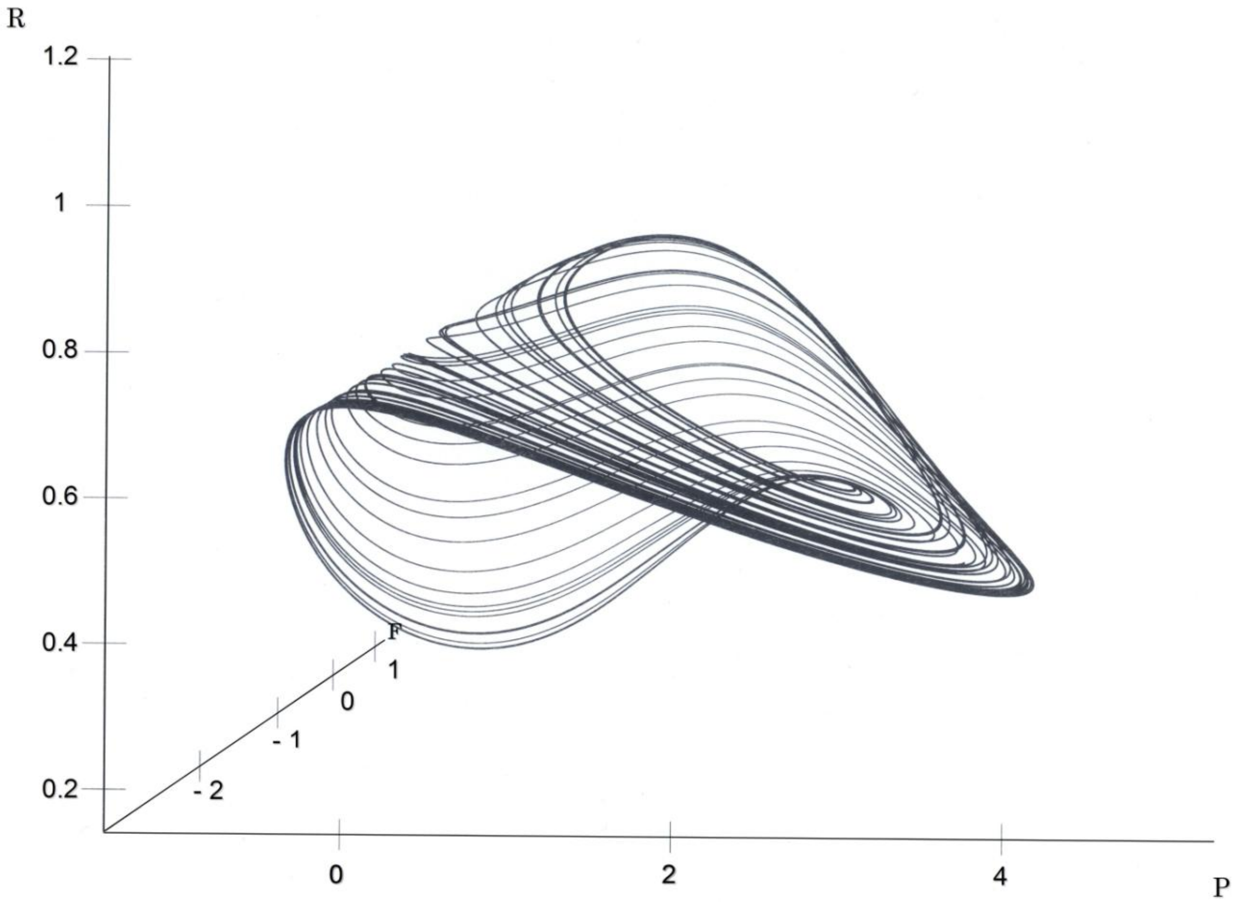

Fig. 2 (a). Chaotic attractors for the set of parameters C_2

Strange attractor displayed with positive initial conditions.

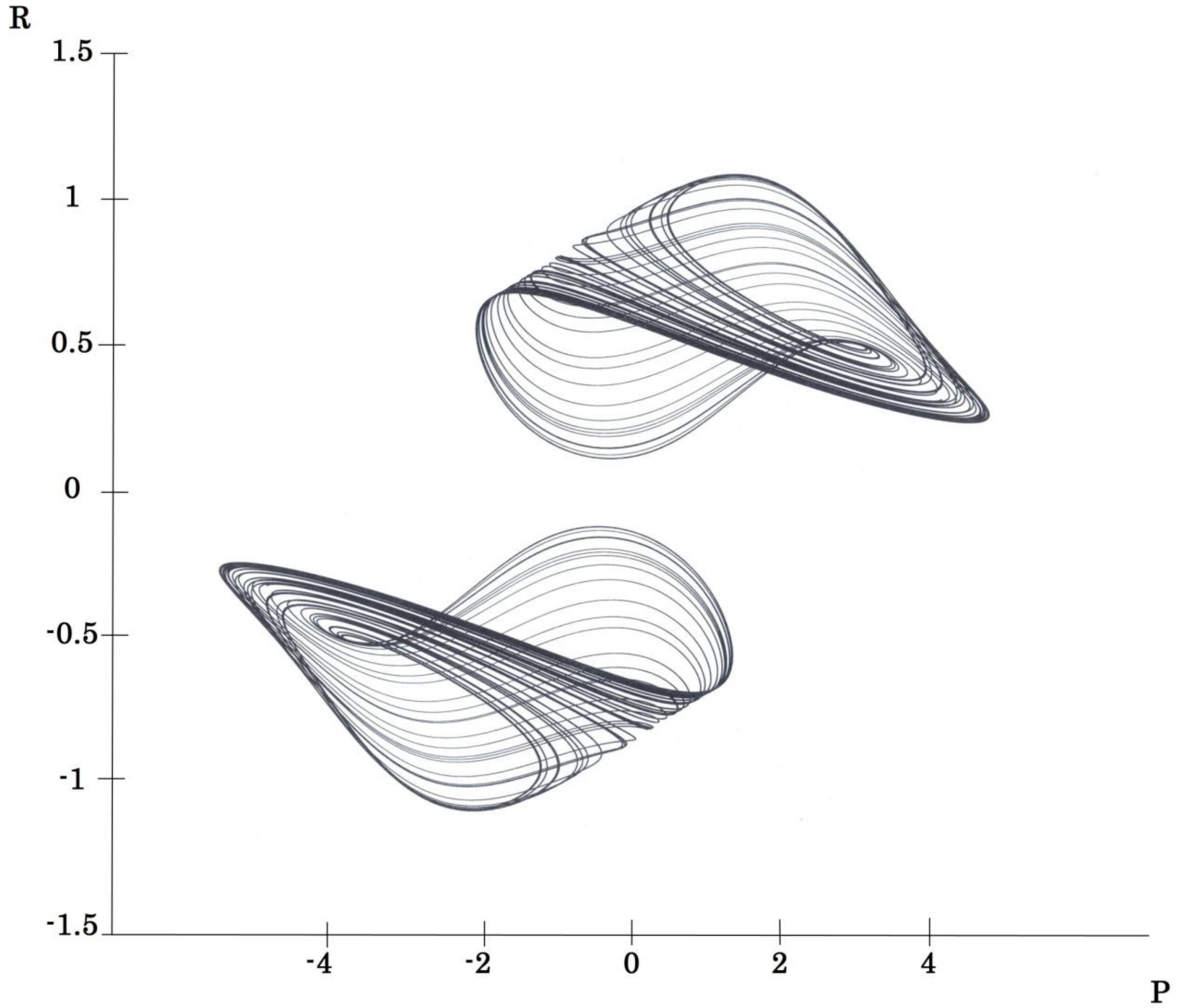

Fig. 2 (b). Two chaotic attractors for the set of parameters C_2

The second attractor emerges in the sub-basin with a negative initial condition. In these anti-symmetric positions, the strange attractors demonstrate the Sensitive Dependency on Initial Conditions (SDIC) of the 3D system.

The numerical simulations of the 3D system display a wide range of dynamics since with the parameters C_3 (v, m, n, r, s) = (1.02, 0.02, 0.3, 0.1, 10), a new shape of the chaotic attractor appears (Fig. 3). Its phase portrait unifies the previous separated sub-basins.

We notice that several dynamical patterns are obtained with only one nonlinear equation in the system. Eventually, the simultaneous presence of SDIC and SDP are proofs of the strange chaos of our heuristic dynamical model of the firm.

Chaotic and permanent oscillations appear as an intrinsic and endogenous characteristic of the modern firm when nonlinear mechanism of payout policy is implemented.

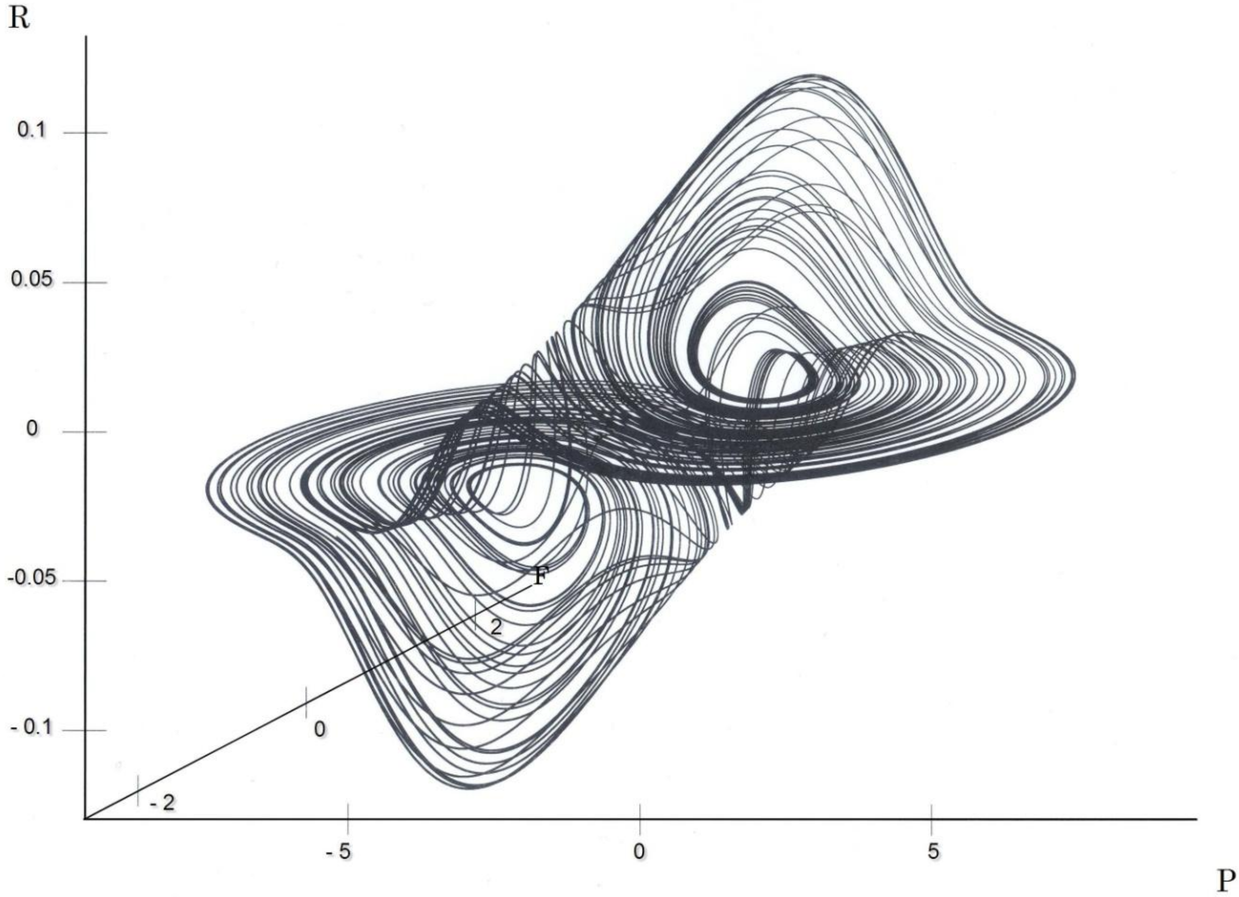

Fig. 3. Chaotic attractor for C_3

A modification of the parameters displays the morphological plasticity of the attractors and demonstrates the Sensitive Dependency on Parameters (SDP) of the 3D system.

4. Concluding Remarks

Our heuristic model of corporate finance serves as a framework to detect the dynamics of the profits in the context of distinction between ownership and management.

Managers and owners fix together the strategy of the modern firm and choose the best direction to boost the corporate activity and its profits. Therefore, the choice itself to divide profits between incomes and self-financing assets injects turbulence when a rigorous and rational mechanism in implemented. Paradoxical conclusions?

Wherein a dynamic perspective, rules and principles of finance governance built in static and *linear* framework may lose their validity. The numerical computations of our nonlinear and *ab initio* financial model show the implications of an embedded automaton of disciplining payout. The disordered dynamics of the modern firm is injected by a main function of the management itself: the sharing of profits.

References

1. D. B. Farber, Restoring trust after fraud: does corporate governance matter? *Accounting Review*, 80, 539-561(2005).

2. J. Lintner, Distribution of Incomes of Corporations among Dividends, Retained Earnings and Taxes, *American Economic Review*, 61, 97-113 (1956).

3. M.C. Jensen, Agency Cost of Free Cash Flow, Corporate Finance and Takeovers, *American Economic Review*, 76, 2, 323-329 (1986).

4. T.W., Bates K.M. Kahle and R.M. Stulz, Why Do U.S. Firms Hold So Much More Cash than They Used To? *Journal of Finance*, 64, 5, 1985-2021 (2009).

5. S. Bouali, Feedback Loop in Extended van der Pol Equation Applied to an Economic Model of Cycles, *International Journal of Bifurcation and Chaos*, 9, 4, 745- 756 (1999),

6. S. Bouali, Targeting Fixed Reinvestment Rate: A "Strange" Path to Financial Distress, *Corporate Ownership & Control*, 7, 2, 311-318 (2009).

7. B. Van der Pol and J. Van der Mark, Frequency demultiplication, *Nature*, 120, 363-364 (1927).

8. D. Ruelle and F. Takens, On the nature of turbulence, *Communication in Mathematical Physics*, 20, 3, 167-192 (1971).

Instructions to Contributors
Journal of Applied Functional Analysis

A quartely international publication of Eudoxus Press, LLC of TN.

Editor in Chief: George Anastassiou

Department of Mathematical Sciences
University of Memphis
Memphis, TN 38152-3240, U.S.A.

1. Manuscripts, hard copies in quadruplicate and in English,should be submitted by regular, unregistered mail, to the Editor in Chief.

Authors may want to recommend an associate editor most related to the submission to possibly handle it. In addition, to assist the Editor and speed the decision process, authors may include a PDF file of the paper on disk with the submitted copies of the manuscript.

Also authors may want to submit a list of six possible referees, to be used in case we cannot find related referees by ourselves.

2. Manuscripts should be typed using any of TEX,LaTEX,AMS-TEX,or AMS-LaTEX and according to EUDOXUS PRESS, LLC. LATEX STYLE FILE. (Click HERE to save a copy of the style file.)They should be carefully prepared in all respects. Submitted copies should be brightly printed (not dot-matrix), double spaced, in ten point type size, on one side high quality paper 8(1/2)x11 inch. Manuscripts should have generous margins on all sides and should not exceed 24 pages.

3. Submission is a representation that the manuscript has not been published previously in this or any other similar form and is not currently under consideration for publication elsewhere. A statement transferring from the authors(or their employers,if they hold the copyright) to Eudoxus Press, LLC, will be required before the manuscript can be accepted for publication.The Editor-in-Chief will supply the necessary forms for this transfer.Such a written transfer of copyright,which previously was assumed to be implicit in the act of submitting a manuscript,is necessary under the U.S.Copyright Law in order for the publisher to carry through the dissemination of research results and reviews as widely and effective as possible.

4. The paper starts with the title of the article, author's name(s) (no titles or degrees), author's affiliation(s) and e-mail addresses. The affiliation should comprise the department, institution (usually university or company), city, state (and/or nation) and mail code.

The following items, 5 and 6, should be on page no. 1 of the paper.

5. An abstract is to be provided, preferably no longer than 150 words.

6. A list of 5 key words is to be provided directly below the abstract. Key words should express the precise content of the manuscript, as they are used for indexing purposes.

The main body of the paper should begin on page no. 1, if possible.

7. All sections should be numbered with Arabic numerals (such as: 1. INTRODUCTION) .
Subsections should be identified with section and subsection numbers (such as 6.1. Second-Value Subheading).
If applicable, an independent single-number system (one for each category) should be used to label all theorems, lemmas, propositions, corrolaries, definitions, remarks, examples, etc. The label (such as Lemma 7) should be typed with paragraph indentation, followed by a period and the lemma itself.

8. Mathematical notation must be typeset. Equations should be numbered consecutively with Arabic numerals in parentheses placed flush right,and should be thusly referred to in the text [such as Eqs.(2) and (5)]. The running title must be placed at the top of even numbered pages and the first author's name, et al., must be placed at the top of the odd numbed pages.

9. Illustrations (photographs, drawings, diagrams, and charts) are to be numbered in one consecutive series of Arabic numerals. The captions for illustrations should be typed double space. All illustrations, charts, tables, etc., must be embedded in the body of the manuscript in proper, final, print position. In particular, manuscript, source, and PDF file version must be at camera ready stage for publication or they cannot be considered.

Tables are to be numbered (with Roman numerals) and referred to by number in the text. Center the title above the table, and type explanatory footnotes (indicated by superscript lowercase letters) below the table.

10. List references alphabetically at the end of the paper and number them consecutively. Each must be cited in the text by the appropriate Arabic numeral in square brackets on the baseline.
References should include (in the following order):
initials of first and middle name, last name of author(s)
title of article,
name of publication, volume number, inclusive pages, and year of publication.

Authors should follow these examples:

Journal Article

1. H.H.Gonska,Degree of simultaneous approximation of bivariate functions by Gordon operators, (journal name in italics) *J. Approx. Theory*, 62,170-191(1990).

Book

2. G.G.Lorentz, (title of book in italics) *Bernstein Polynomials* (2nd ed.), Chelsea,New York,1986.

Contribution to a Book

3. M.K.Khan, Approximation properties of beta operators,in(title of book in italics) *Progress in Approximation Theory* (P.Nevai and A.Pinkus,eds.), Academic Press, New York,1991,pp.483-495.

11. All acknowledgements (including those for a grant and financial support) should occur in one paragraph that directly precedes the References section.

12. Footnotes should be avoided. When their use is absolutely necessary, footnotes should be numbered consecutively using Arabic numerals and should be typed at the bottom of the page to which they refer. Place a line above the footnote, so that it is set off from the text. Use the appropriate superscript numeral for citation in the text.

13. After each revision is made please again submit four hard copies of the revised manuscript. And after a manuscript has been accepted for publication submit four hard copies of the final revised manuscript. Additionally, two copies of the final version of the TEX/LaTex source file and a PDF file, are to be submitted to the Editor's Office on personal 3.5 inch computer disks. Label the disks individually with clearly written identifying information, e.g. :

Your name, title of article, kind of computer used, kind of software and version number, disk format and files names of article, as well as abbreviated journal name.

Package the disks in a disk mailer or protective cardboard. Make sure contents of disks are identical with the ones of final hard copies submitted!

Note: The Editor's Office cannot accept the disks without the accompanying matching hard copies of manuscript. No e-mail final submissions are allowed! File submission on disk must be used.

14. Effective 1 Nov. 2009 for current journal page charges, contact the Editor in Chief. Upon acceptance of the paper an invoice will be sent to the contact author. The fee payment will be due one month from the invoice date. The article will proceed to publication only after the fee is paid. The charges are to be sent, by money order or certified check, in US dollars, payable to Eudoxus Press, LLC, to the address shown on the Eudoxus homepage.

No galleys will be sent and the contact author will receive one(1) electronic copy of the journal issue in which the article appears.

15. This journal will consider for publication only papers that contain proofs for their listed results.

TABLE OF CONTENTS, JOURNAL OF APPLIED FUNCTIONAL ANALYSIS, VOLUME 6, NO.1, 2011

Volume 6, Number 2 April 2011

ISSN:1559-1948 (PRINT), 1559-1956 (ONLINE)

EUDOXUS PRESS,LLC

JOURNAL OF APPLIED FUNCTIONAL ANALYSIS

GUEST EDITORS: HIKMET CAGLAR, LEVENT CUHACI, GURSEL HACIBEKIROGLU and MEHMET OZER

SPECIAL ISSUE II: "CHAOS and COMPLEX SYSTEMS 2010"

SCOPE AND PRICES OF

JOURNAL OF APPLIED FUNCTIONAL ANALYSIS

A quartely international publication of **EUDOXUS PRESS,LLC**

ISSN:1559-1948(PRINT),1559-1956(ONLINE)

Editor in Chief: George Anastassiou
Department of Mathematical Sciences
The University of Memphis
Memphis, TN 38152,USA
E mail: ganastss@memphis.edu

The purpose of the "Journal of Applied Functional Analysis"(JAFA) is to publish high quality original research articles, survey articles and book reviews from all subareas of Applied Functional Analysis in the broadest form plus from its applications and its connections to other topics of Mathematical Sciences. A sample list of connected mathematical areas with this publication includes but is not restricted to: Approximation Theory, Inequalities, Probability in Analysis, Wavelet Theory, Neural Networks, Fractional Analysis, Applied Functional Analysis and Applications, Signal Theory, Computational Real and Complex Analysis and Measure Theory, Sampling Theory, Semigroups of Operators, Positive Operators, ODEs, PDEs, Difference Equations, Rearrangements, Numerical Functional Analysis, Integral equations, Optimization Theory of all kinds, Operator Theory, Control Theory, Banach Spaces, Evolution Equations, Information Theory, Numerical Analysis, Stochastics, Applied Fourier Analysis, Matrix Theory, Mathematical Physics, Mathematical Geophysics, Fluid Dynamics, Quantum Theory. Interpolation in all forms, Computer Aided Geometric Design, Algorithms, Fuzzyness, Learning Theory, Splines, Mathematical Biology, Nonlinear Functional Analysis, Variational Inequalities, Nonlinear Ergodic Theory, Functional Equations, Function Spaces, Harmonic Analysis, Extrapolation Theory, Fourier Analysis, Inverse Problems, Operator Equations, Image Processing, Nonlinear Operators, Stochastic Processes, Mathematical Finance and Economics, Special Functions, Quadrature, Orthogonal Polynomials, Asymptotics, Symbolic and Umbral Calculus, Integral and Discrete Transforms, Chaos and Bifurcation, Nonlinear Dynamics, Solid Mechanics, Functional Calculus, Chebyshev Systems. Also are included combinations of the above topics.

Working with Applied Functional Analysis Methods has become a main trend in recent years, so we can understand better and deeper and solve important problems of our real and scientific world.

JAFA is a peer-reviewed International Quarterly Journal published by Eudoxus Press,LLC.

We are calling for high quality papers for possible publication. The contributor should send four copies of the contribution to the EDITOR in CHIEF in TEX,LATEX double spaced,in ten point type size. They should be sent BY REGULAR MAIL ONLY, NOT REGISTERED MAIL, AND NO E-MAIL SUBMISSIONS [See: Instructions to Contributors]

Journal of Applied Functional Analysis(JAFA)
is published in January,April,July and October of each year by

EUDOXUS PRESS,LLC,
1424 Beaver Trail Drive,Cordova,TN38016,USA,
Tel.001-901-751-3553
anastassioug@yahoo.com
http://www.EudoxusPress.com visit also http://www.msci.memphis.edu/~ganastss/jafa.

Webmaster:Ray Clapsadle

Annual Subscription Current Prices:For USA and Canada,Institutional:Print $400,Electronic $250,Print and Electronic $450.Individual:Print $ 150, Electronic $80,Print &Electronic $200.For any other part of the world add $50 more to the above prices for Print.
Single article PDF file for individual $15.Single issue in PDF form for individual $60.

No credit card payments.Only certified check,money order or international check in US dollars are acceptable.
Combination orders of any two from JoCAAA,JCAAM,JAFA receive 25% discount,all three receive 30% discount.

JAFA is reviewed and abstracted by AMS Mathematical Reviews,MATHSCI,and Zentralblaat MATH.

JAFA IS A JOURNAL OF RAPID PUBLICATION

Journal of Applied Functional Analysis
Editorial Board
Associate Editors

Operators on Banach spaces,
Tensor products of Banach spaces,
Polymeasures, Function spaces.

8) Michele Campiti
Department of Mathematics "E.De Giorgi"
University of Lecce
P.O. Box 193
Lecce,ITALY
Tel. +39 0832 297 432
Fax +39 0832 297 594
michele.campiti@unile.it
Approximation Theory,
Semigroup Theory, Evolution problems,
Differential Operators.

9)Domenico Candeloro
Dipartimento di Matematica e Informatica
Universita degli Studi di Perugia
Via Vanvitelli 1
06123 Perugia
ITALY
Tel +39(0)75 5855038
+39(0)75 5853822,
+39(0)744 492936
Fax +39(0)75 5855024
candelor@dipmat.unipg.it
Functional Analysis, Function spaces,
Measure and Integration Theory in
Riesz spaces.

10) Pietro Cerone
School of Computer Science and
Mathematics, Faculty of Science,
Engineering and Technology,
Victoria University
P.O.14428,MCMC
Melbourne,VIC 8001,AUSTRALIA
Tel +613 9688 4689
Fax +613 9688 4050
Pietro.cerone@vu.edu.au
Approximations, Inequalities,
Measure/Information Theory,
Numerical Analysis, Special Functions.

11)Michael Maurice Dodson
Department of Mathematics
University of York,
York YO10 5DD, UK
Tel +44 1904 433098
Fax +44 1904 433071
Mmd1@york.ac.uk
Harmonic Analysis and Applications to
Signal Theory,Number Theory and
Dynamical Systems.

Almost Periodicity & Almost Automorphy.

32) Vassilis Papanicolaou
Department of Mathematics
National Technical University of Athens
Zografou campus, 157 80
Athens, Greece
tel:: +30(210) 772 1722
Fax +30(210) 772 1775
papanico@math.ntua.gr
Partial Differential Equations,
Probability.

33) Pier Luigi Papini
Dipartimento di Matematica
Piazza di Porta S.Donato 5
40126 Bologna
ITALY
Fax +39(0)51 582528
papini@dm.unibo.it
Functional Analysis, Banach spaces,
Approximation Theory.

34) Svetlozar T.Rachev
Chair of Econometrics,Statistics
and Mathematical Finance
School of Economics and
Business Engineering
University of Karlsruhe
Kollegium am Schloss, Bau II,20.12, R210
Postfach 6980, D-76128,
Karlsruhe,GERMANY.
Tel +49-721-608-7535,
+49-721-608-2042(s)
Fax +49-721-608-3811
Zari.Rachev@wiwi.uni-karlsruhe.de
Second Affiliation:
Dept.of Statistics and Applied Probability
University of California at Santa Barbara
rachev@pstat.ucsb.edu
Probability,Stochastic Processes and
Statistics,Financial Mathematics,
Mathematical Economics.

35) Paolo Emilio Ricci
Department of Mathematics
Rome University "La Sapienza"
P.le A.Moro,2-00185
Rome,ITALY
Tel ++3906-49913201 office
++3906-87136448 home
Fax ++3906-44701007
Paoloemilio.Ricci@uniroma1.it
riccip@uniroma1.it
Special Functions, Integral and Discrete

12) Sever S.Dragomir
School of Computer Science and Mathematics, Victoria University,
PO Box 14428,
Melbourne City,
MC 8001,AUSTRALIA
Tel. +61 3 9688 4437
Fax +61 3 9688 4050
sever@csm.vu.edu.au
Inequalities,Functional Analysis, Numerical Analysis, Approximations, Information Theory, Stochastics.

13) Paulo J.S.G.Ferreira
Department of Electronica e Telecomunicacoes/IEETA
Universidade de Aveiro
3810-193 Aveiro
PORTUGAL
Tel +351-234-370-503
Fax +351-234-370-545
pjf@ieeta.pt
Sampling and Signal Theory, Approximations, Applied Fourier Analysis, Wavelet, Matrix Theory.

14) Gisele Ruiz Goldstein
Department of Mathematical Sciences
The University of Memphis
Memphis,TN 38152,USA.
Tel 901-678-2513
Fax 901-678-2480
ggoldste@memphis.edu
PDEs, Mathematical Physics, Mathematical Geophysics.

15) Jerome A.Goldstein
Department of Mathematical Sciences
The University of Memphis
Memphis,TN 38152,USA
Tel 901-678-2484
Fax 901-678-2480
jgoldste@memphis.edu
PDEs,Semigroups of Operators, Fluid Dynamics,Quantum Theory.

16) Heiner Gonska
Institute of Mathematics
University of Duisburg-Essen
Lotharstrasse 65
D-47048 Duisburg
Germany
Tel +49 203 379 3542
Fax +49 203 379 1845
gonska@math.uni-duisburg.de
Approximation and Interpolation Theory, Transforms, Symbolic and Umbral Calculus, ODE, PDE,Asymptotics, Quadrature, Matrix Analysis.

36) Silvia Romanelli
Dipartimento di Matematica
Universita' di Bari
Via E.Orabona 4
70125 Bari, ITALY.
Tel (INT 0039)-080-544-2668 office
080-524-4476 home
340-6644186 mobile
Fax -080-596-3612 Dept.
romans@dm.uniba.it
PDEs and Applications to Biology and Finance, Semigroups of Operators.

37) Boris Shekhtman
Department of Mathematics
University of South Florida
Tampa, FL 33620,USA
Tel 813-974-9710
boris@math.usf.edu
Approximation Theory, Banach spaces, Classical Analysis.

38) Rudolf Stens
Lehrstuhl A fur Mathematik
RWTH Aachen
52056 Aachen
Germany
Tel ++49 241 8094532
Fax ++49 241 8092212
stens@mathA.rwth-aachen.de
Approximation Theory, Fourier Analysis, Harmonic Analysis, Sampling Theory.

39) Juan J.Trujillo
University of La Laguna
Departamento de Analisis Matematico
C/Astr.Fco.Sanchez s/n
38271.LaLaguna.Tenerife.
SPAIN
Tel/Fax 34-922-318209
Juan.Trujillo@ull.es
Fractional: Differential Equations-Operators-
Fourier Transforms, Special functions, Approximations,and Applications.

40) Tamaz Vashakmadze
I.Vekua Institute of Applied Mathematics
Tbilisi State University,
2 University St. , 380043,Tbilisi, 43,
GEORGIA.
Tel (+99532) 30 30 40 office

Computer Aided Geometric Design, Algorithms.

22) Hubertus Th. Jongen
Department of Mathematics
RWTH Aachen
Templergraben 55
52056 Aachen
Germany
Tel +49 241 8094540
Fax +49 241 8092390
jongen@rwth-aachen.de
Parametric Optimization, Nonconvex
Optimization, Global Optimization.

45) Richard A. Zalik
Department of Mathematics
Auburn University
Auburn University,AL 36849-5310
USA.
Tel 334-844-6557 office
678-642-8703 home
Fax 334-844-6555
zalik@auburn.edu
Approximation Theory,Chebychev Systems,
Wavelet Theory.

Preface

These **four** special issues, which constitute the proceedings of the symposium 3rd International Interdisciplinary Chaos Symposium on CHAOS and COMPLEX SYSTEMS - CCS2010 (21-24 May 2010), have tried to create a forum for the exchange of information and experience in the exciting interdisciplinary field of chaos. However the conference was more in the Applied Mathematics, Social Sciences and Physics direction centered.

The view of the organizers concerning international resonance of the conference has been fulfilled: approximatelly 200 scientists from 21 diffrent countries (Algeria, Bulgaria, Croatia, Denmark, France, Germany, Greece, Iran, Italy, Jordan, Lebanon, Malaysia, Pakistan, Republic of Serbia, Russia, Sultanate of Oman, Tunisia, Turkey, Ukraine, United Kingdom and United States of America) have participated. Good relations to research institutes of these countries might be of great importance for science and applications in different fields of Chaos.

On behalf of the Organizing Committee we would like to express our thanks to the Scientific Committee, the Program Committee and to all who have contributed to this conference for their support and advice. We are also grateful to the invited lecturers Prof. Henry D.I. Abarbanel, Prof. David S. Byrne, Prof. George Anastassiou, Prof. Zidong Wang, Prof. Turgut Ozis and Prof. Markus J. Aschwanden.

Special thanks are due to Rector Prof. Dursun Kocer and Vice Rector Prof. Cetin Bolcal for their close support, advice and incentive encouraging.

Our thanks are also due to the Istanbul Kultur University, which was hosting this symposium and provided all of its facilities.

Finally, we are grateful to the Editor-in-Chief, Prof. George Anastassiou for accepting this volume for publication.

Hikmet Caglar, PhD in Mathematics, s.caglar@iku.edu.tr
Levent Cuhaci, PhD in Computer Science, l.cuhaci@iku.edu.tr
Gursel Hacibekiroglu, PhD in Physics, g.hacibekiroglu@iku.edu.tr
Mehmet Ozer, PhD in Physics, m.ozer@iku.edu.tr

Istanbul Kultur University, Faculty of Science and Letters, Istanbul, Turkey

JOURNAL OF APPLIED FUNCTIONAL ANALYSIS, VOL.6, NO.2, 115-121, COPYRIGHT 2011 EUDOXUS PRESS, LLC

Conformational Behaviour of Tunable Biopolymers: Elastin-Like Polypeptides

Handan Arkın, Mustafa Bilsel
Ankara University, Department of Physics Engineering
Tandoğan, 06100, Ankara, Turkey
Handan.Olgar@eng.ankara.edu.tr; mfbilsel@gmail.com

ABSTRACT

$(VPGXG)_n$ polypeptides known as elastin-like polypeptides with different biological, biomechanical, biochemical and biophysical properties stand out suitable structures appropriate for production of several biomaterials, in the first instance, tissue, microtube and nanotube in tissue engineering. Therefore, understanding the structural properties of such peptides comes into prominence. For this purpose, structural properties of elastin-like polypeptides have been investigated by computer simulation methods in our study. Our simulations have been carried out by multicanonical algorithm having a wide range of application area from solid state to biophysics, the most powerful algorithm in generalized ensemble family.
By taking n=1 and changing amino acid X, hydrophobicity scale has been established in the forepart of our study, afterwards the effect on structural transition temperature has been determined in a solvent (SCH2) and vacuum. In the second part, choosing VPGVG, which is the most repeating pentapeptide sequence in elastin-like proteins, and taking n=1, 2, 3, 4, change in structural transition temperature and secondary structure formation caused by the transition from smaller molecule to larger one have been determined.

1. INTRODUCTION

Protein folding is one of the most intensively studied and still unsolved problems in biology. The process by which a protein folds into its biologically active state cannot be traced in all details solely by experiments. Therefore, many theoretical and experimental studies focus on determination of the three-dimensional structure of these molecules. Recently, molecular modelling has attracted considerable attention for applications in designing and fabrication of nanostructures leading to the development of advanced materials. In a newly growing field of research, synthetic peptides are investigated for their use in nano-devices, by exploiting their self-assembly properties [1]. The self-assembly of biomolecular building blocks plays an increasingly important role in the discovery of new materials, with a wide range of applications in nanotechnology and medical technologies such as drug delivery systems [2]. In these studies, several types of biomaterials are developed, ranging from models for studying protein folding to molecular materials for producing peptide nanofibers, peptide surfactants by designing various classes of self-assembling peptides [3]. These experiments reveal many different interesting and important problems, which are related to general aspects of the question why and how proteins fold. In this context, modern simulation techniques have opened another window to give a new insight to protein folding problem [4, 5].
In this paper, structural properties of peptides $(VPGVG)_n$ known as elastin-like polypeptides (ELPs) have been investigated. Generally, the simulated sequences, the ELPs are important in tissue engineering so they arouse interest due to some of their important and attractive properties. One of the most important property is the self-assembling potential. Because of the self-assembling property, ELPs are fairly convenient for the production of microtubes and nanotubes. Other biomaterials produced from ELPs are hydro gels [6], plates [7], nanoparticles [8], sponge-like isotropic isotropic networks [9] and nanoporous materials [10]. ELPs are not soluble in water and are the most stable proteins with 70-year half-life [11].
Polypeptides known as elastin like polypeptides (ELPs) come into prominence in tissue engineering. The most important reason for this is that elastin-like polypeptides and proteins can be used in designing biomaterials. On the one hand, biomaterials composed of ELPs have a wide range of application fields, one of the most important ones

are skin reconstruction [12], tissue and vascular transportation [13], heart valves [14], elastic crosslink tissue [15]. On the other hand, ELPs are also used in biomedical applications. The principal reasons for this; (1) Since conformational transition temperatures of ELPs can be arranged between 0 and 100 ^{0}C, they can be used in drug delivery and protein purification. (2) ELPS can be synthesized. (3) ELPs can be used as gram/liter in laboratories, hence they bring less cost compared to synthetic polymers. (4) ELPs in biological applications do not have side effects such as toxical and hazardous. (5) They can be implemented in living tissue applications.
Elastin-like polypeptides (ELPs) are a family of polypeptides derived from a portion of the primary sequence of elastin, $(VPGXG)_n$ polypeptide, where V:valine, P:proline, G:glycine, and X:any amino acid except praline and n refers to the length of the chain.
In present study, by taking n=1 and changing amino acid X with different hydrophobic and polar ones, hydrophobicity scale has been established. Then, by choosing n=1, 2, 3, 4 and X=Val conformational transition temperature and secondary structure formation changes have been determined when progression from small molecules to larger ones.

2. THE SIMULATION METHOD

The multicanonical ensemble is based on a probability function in which the different energies are equally probable. The advantage of this algorithm lies in the fact that it not only alleviates the multiple-minima problem but also allows the calculation of various thermodynamic quantities as functions of temperature from one simulation run [16]. This demonstrates the superiority of the method. However, the implementation of MUCA is not straightforward because the density of states, n(E), is unknown a priori. In practice, one needs to know only the weights, ω:

$$\omega \sim \frac{1}{n(E)} = exp\left[\frac{E - F_T(E)}{k_B T(E)}\right] \tag{1}$$

These weights are calculated in the first stage of the simulation process by an iterative procedure, in which the temperatures, T(E), are built recursively together with the microcanonical free energies, $F_T(E)=k_BT(E)$, up to an additive constant. The iterative procedure is followed by a long production run based on the fixed ω, where equilibrium configurations are sampled. Reweighting techniques [17] enable one to obtain the Boltzmann averages of various thermodynamic properties over a wide range of temperatures. Average value of a physical quantity A is

$$\langle A\rangle(T) = \frac{\int dx A(x) e^{-E(x)/k_B T} \;/\; \omega_{MU}[E(x)]}{\int dx e^{-E(x)/k_B T} \;/\; \omega_{MU}[E(x)]} \tag{2}$$

where ω_{MU} is the multicanonical weight factor and $e^{-E(x)/k_B T}$ is the energy distribution of the simulation.
As pointed out above, calculation of the a priori unknown MUCA weights is not trivial, as it requires experienced human intervention. For lattice models, this problem was addressed in a sketchy way by Berg and Çelik [18] and, later, by Berg [19].
In the present work, simulations have been carried on an open-source with a free code software package called SMMP (Simple Molecular Mechanics for Proteins) [20]. We have implemented the multicanonical algorithm with ECEPP/3 force field supplemented in SMMP, which includes electrostatic energy E_{ee}, Lennard-Jones term E_{lj}, hydrogen-bonding term E_{hb} and torsion energy E_{tor} with constant dielectric constant ε=2:

$$ECEPP/3 = E_{ee} + E_{lj} + E_{hb} + E_{tor} \tag{3}$$

$$= \sum \frac{332 q_i q_j}{\varepsilon r_{ij}} + \sum\left(\frac{A_{ij}}{r_{ij}^{12}} - \frac{B_{ij}}{r_{ij}^{6}}\right) + \sum\left(\frac{C_{ij}}{r_{ij}^{12}} - \frac{D_{ij}}{r_{ij}^{10}}\right) + \sum U_l\left(1 \mp cos(n_l \alpha_l)\right) \tag{4}$$

Where i and j correspond to the different atoms, r_{ij} is the distance between atoms. A_{ij}, B_{ij}, C_{ij}, and D_{ij} are the parameters that define Lennard-Jones or Hydrogen bond interaction, and α_i is the ith torsion angle. The conversion factor to determine the energy in kcal/mol is 332.

In all simulations, NH2 and COOH were chosen as the N- and C- terminal groups, respectively. For simplicity, the peptide bond angles ω were kept fixed at 180◦, which leaves independent degrees of freedom between 13-17 depending on the fourth amino acid of the pentapeptide sequence.

All proteins exist in an solvent environment. Explicit solvent models increase the CPU time because of the larger number of degrees of freedom. Instead, it is possible to include the effect of the solvent by using implicit solvent models due to their simplicity and ease of applications. Protein-water interactions are approximated by an accessible surface area (ASA) term,

$$E_{solv} = \sigma_i A_i \tag{5}$$

where A_i is the area of atoms and σ_i is the solvation parameter, both of which change depending on the atom type. All the molecules were simulated in vacuum and in the SCH2 implicit solvation model [21]. The reason why we choose the SCH2 parameter is that it is classified as in the fast class according to their integrated autocorrelations times by Berg and Hsu [22]. The solvation model SCH2 is implemented in the SMMP package.

Specific heat, total energy (data not shown) and Ramachandran plots have been plotted. Specific heat can be defined as the fluctuation of the energy. Here, it is defined as

$$C(T) = (k_B T)^2 \frac{\left(\langle E^2 \rangle_T - \langle E \rangle_T^2\right)}{N} \tag{6}$$

where N is the number of amino acid residues in the peptide.

To determine multicanonical parameters of X= Trp, His, Ala, Lys and Glu residues, 200,000 sweeps with 6000-7000 recalculation of multicanonical parameter have been performed. For the simulation run 2,000,000 sweeps with 20,000 thermalisation factor were used. In all cases, each multicanonical simulation started from completely random initial conformation. No a priori information about the conformation is used in simulations. For the present molecules, a relatively fast approach from the high to the low energy region are achieved by imposing small conformational change of our procedure at each MC step which has a high chance to visit a neighbouring lower energy segment. The superiority of the multicanonical approach lies in the fact that it provides the sampling of conformations at all temperatures from one simulation run, therefore enables one to study thermodynamics of the system under consideration.

3. RESULTS AND DISCUSSION

In the forepart of our study, structural properties of 5 different elastin sequences obtained by taking n=1 and substituting Trp, His, Ala, Lys, Glu instead of X in VPGXG chain, have been determined in both vacuum and in a solvation model (SCH2). Then, the most repeating sequence in ELPs called VPGVG has been studied. By increasing n from one to four so that the chain length has been increased, on the contrary change in conformational transition temperature and differentiation in secondary structure formation has been utilized.

3.1. Effect of Amino Acid X on Conformational Transition Temperature

Firstly, the specific heat plots as a function of temperature to determine transition temperatures of X= Trp, His, Ala, Lys and Glu in vacuum and SCH2 solvation model are shown in Figure 1(a) and (b), respectively. As seen in the figure, transition temperatures decrease in the solvation model when compared to vacuum.

In previous studies [23, 24], it is stated that conformational transition temperature is inversely proportional to hydrophobicity. Transition temperatures (T_t) of peptide sequences under consideration including Trp, His, Ala, Lys and Glu amino acids are in increasing order 302, 314, 317, 341, 344 in vacuum (see Fig.1 (a)) and 210, 230, 280, 290, 300 in SCH2 (see Fig.1 (b)). Since T_t(trp)< T_t(his)<T_t(ala)<T_t(lys)<T_t(glu), the hydrophobicity order from the most hydrophobic to least is predicted as Trp, His, Ala, Lys and Glu. These results are in good agreement with experimental results [23].

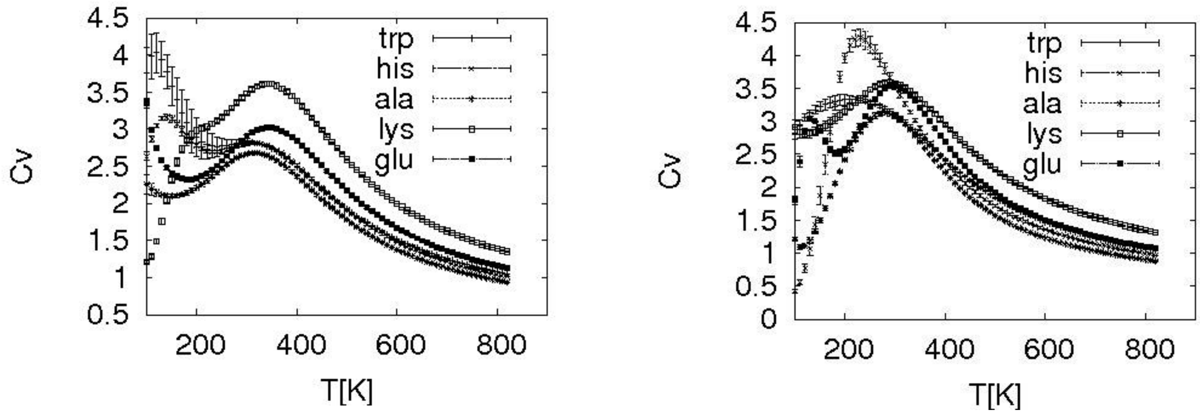

(a) (b)

Figure 1: Specific heat values in (a) vacuum and (b) solvent (SCH2)

3.2. Effect of Chain Length on Conformational Transition Temperature

In Fig. 2 the specific heat as a function of temperature is plotted to determine the transition temperatures for the residue numbers N = 5, 10, 15 and 20. Related conformational transition temperatures for residues N= 5, 10, 15 and 20 are depicted from the specific heat curves and are 435, 425, 410 and 350 K, respectively. Increasing residue number decreases conformational transition temperatures of the polypeptides. Obtained inverse relation between residue number and conformational transition temperature is consistent with experimental results [25] in which it is stated that increasing residue number increases molecular weight but decreases conformational transition temperature. One important point, as seen in the figure, is that: For the peptide N = 5 the specific heat curve has only one pronounced peak which means the peptide has two-state folding channel. The protein changes from an unstructured, extended configuration above the specific heat peak to a compact one with secondary structure below the specific heat peak. When we increase the residue length for N= 10, 15, there appear a shoulder in the specific heat which signal intermediate states in the folding channel. Finally in the N=20 a second peak come into being which points that the folding is two-step process [26, 27]. Firstly, the protein changes from random, unstructured conformations to highly ordered secondary structures and then in the second step the native state is selected out from the ensemble of compact configurations with synchronous formation of secondary structure [28].

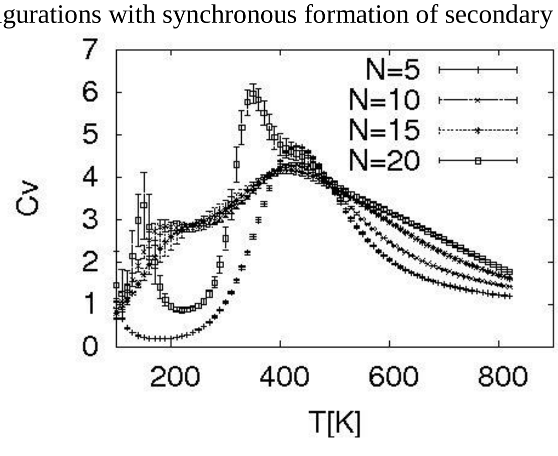

Figure 2: Specific heat for N=5, 10, 15, 20 residues

3.3. Secondary Structure Analysis

In order to check the secondary structures, the distribution of ϕ and ψ dihedral angles of polypeptides with different residue lengths at room temperature 300±10 K is analyzed by Ramachandran plots, which estimate the secondary structure of polypeptides. There are various experimental methods (spectroscopic, viscosimetric, microscopic etc.) used to recognize the secondary structure formation. These methods give an indication of conformations dominant in the structure of a protein. On the other hand, MUCA is the most important as being a thermodynamic method that enables simulating a system over a large range of temperatures. This aspect is used to prepare Ramachandran plots, which provide the distributions of the dihedral angles and allow distinguishing different types of highly ordered segments. Ramachandran plot in figure 3 describes VPGVG polypeptide for Val1, Gly3 and Val4 amino acids. To be able to compare simulation results with experimental ones, room temperature is chosen.

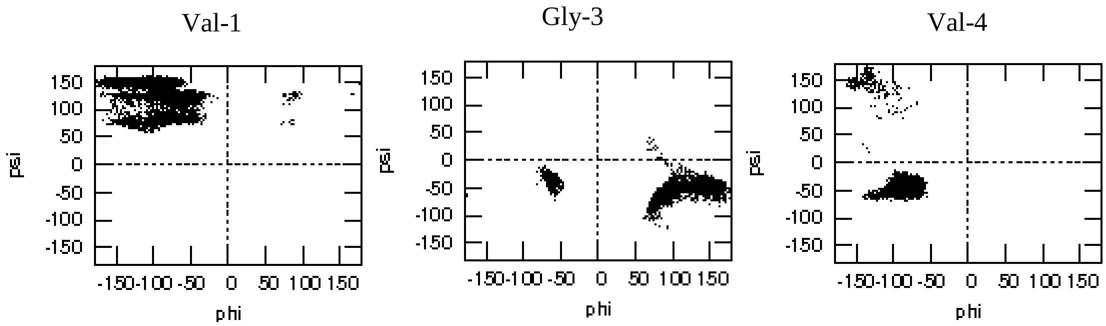

Figure 3: Ramachandran plot for VPGVG at T=300±10 K

When Ramachandran plots are analysed, it is observed that βII-turn is the dominant structure between Val1-Pro2 and Gly3-Val4-Gly5 bridges except for Pro2-Gly3 bridge. βII-turn has characteristics dihedral angle set (ϕ, ψ)=(-60,120). These results are in agreement with previous studies, both experimental [29] and simulation (Villani and Tamburro 1998) approaches, which suggest that main secondary structure in elastin is short β-turns. Circular dichroism (CD) and NMR measurements gave evidence of flexible β-turns as the dominant structural feature [30]. In addition, the literature on protein structure indicate that the occurrence of high probability β-turns in proline at the second and glycine at the third position are consistent with the results of the present study [31].
Ramachandran plot in figure 4 is plotted to determine the secondary structure of $(VPGVG)_2$ polypeptide. $(VPGVG)_2$ polypeptide obtained by increasing the residue number of VPGVG has higher order βII-turns in its secondary structure. Formation of βII-turns has been observed in all residue bridges.

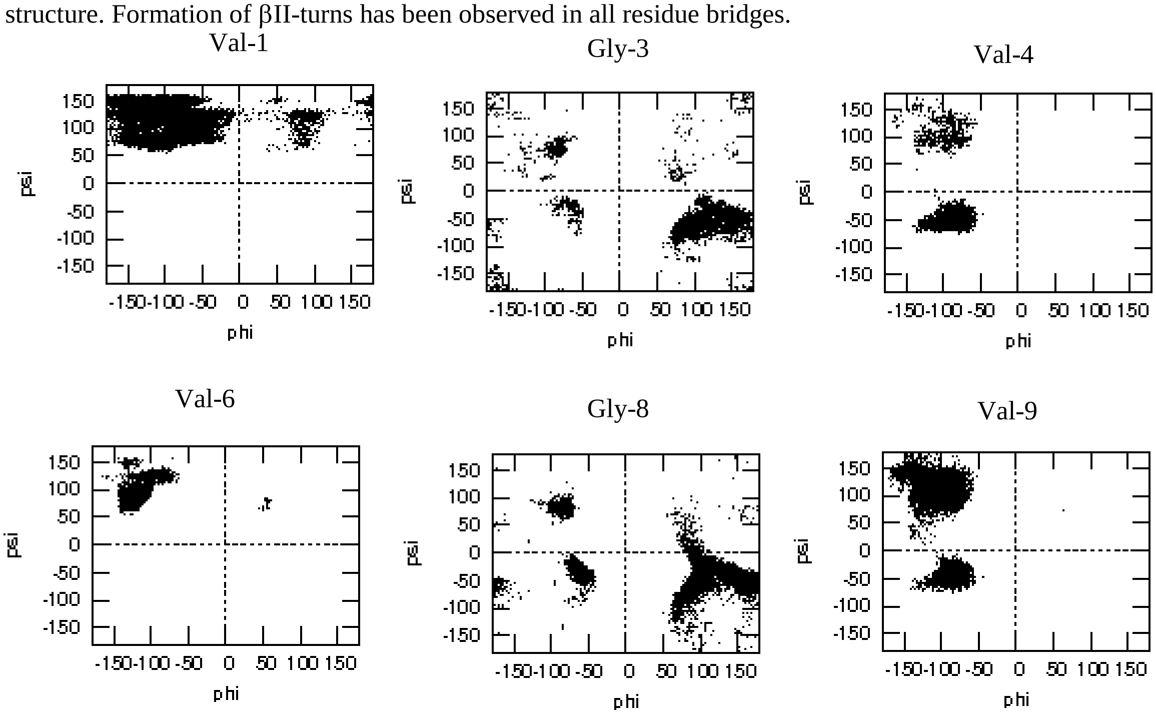

Figure 4: Ramachandran plot for $(VPGVG)_2$ at T=300±10 K

4. CONCLUSION

In summary, five pentapeptide sequences of elastin-like peptides, VPGXG have been simulated by using the multicanonical simulation procedure. By substituting different amino acids in the fourth position of the sequence the thermodynamical variables are calculated in vacuo and in solvent to determine the hydrophobicity dependency of the conformational transition temperatures of the peptides. Our results agree with various hydrophobicity scales [23].

We have analyzed conformational transition temperature and secondary structure formation mechanisms for the sequences VPGVG, $(VPGVG)_2$, $(VPGVG)_3$ and $(VPGVG)_4$ of ELPs. Increasing residue number causes conformational transition temperature to decrease. Obtained inverse relation between residue number and conformational transition temperature is consistent with experimental results [25].

Employing an all-atom model based on the ECEPP/3 force field with different implicit solvation parameter sets and applying the implementation of the Multicanonical Monte Carlo method in the SMMP package, we found βII-turn is the dominant structure between VPGVG bridges except for Pro2-Gly3 bridge. These results are in agreement with previous studies, both experimental [29] and simulation [32] approaches, which suggest that main secondary structure in elastin is short β-turns. Circular dichroism (CD) and NMR measurements gave evidence of flexible β-turns as the dominant structural feature [30];[33].

ACKNOWLEDGEMENTS

H.A. acknowledges support by The Scientific and Technological Research Council of Turkey under the project number 104T150 and The Turkish Academy of Sciences under the programme to Reward Successful Young Scientists.

REFERENCES

1. Santosa S., Hwang W., Hartman H. and Zhang S. 2002. Self-assembly of surfactant-like peptides with variable glycine tails to form nanotubes and nanovesicles. Nano Lett., 2 (7), 687-691.
2. Hubbell J.A. 1999. Bioactive biomaterials. Curr. Opin. Biotechnol. 10, 123-129.
3. Holmes T., De Lacella S., Su X., Rich A. and S. Zhang, 2000. Extensive neurite outgrowth and active synapse formation on self-assembling peptide scaffolds. Proc. Natl. Acad. Sci. USA, 97, 6728-6733.
4. Arkın H. and Çelik T. 2003. A fast and effective conformational search method for peptides. Int. J. Mod. Phys. C 14, 985-991.
5. Gökoğlu G., Bachmann M., Çelik T. and Janke W. 2006. Structural properties of small semiconductor-binding synthetic peptides. Phys. Rev. E. 74, 041802-041812.
6. Wright E.R., McMillan R.A., Cooper A., Apkarian R.P. and Conticello V.P. 2002. Thermoplastic elastomer hydrogels via self-assembly of an elastinmimetic triblock polypeptide. Adv. Funct. Mater. 12,149-154.
7. Mithieux S.M., Rasko J.E. and Weiss A.S. 2004. Synthetic elastin hydrogels derived from massive elastic assemblies of self-organized human protein monomers. Biomaterials. 25, 4921-4927.
8. Herrero-Vanrell R., Rincon A.C., Alonso M., Reboto V., Molina-Martinez I.T. and Rodriguez-Cabello J.C. 2005. Self-assembled particles of an elastin-like polymer as vehicles for controlled drug release. J. Control Release. 102, 113-122.
9. Bellingham C.M., Lillie M.A., Gosline J.M., Wright G.M., Starcher B.C. and Bailey A.J. 2003. Recombinant human elastin polypeptides self-assemble into biomaterials with elastin-like properties. Biopolymers. 70, 445-455.
10. Reguera J., Fahmi A., Moriarty P., Girotti A. and Rodriguez-Cabello J.C. 2004. Nanopore formation by self-assembly of the model genetically engineered elastin-like polymer [(VPGVG)2(VPGEG)(VPGVG)2]15. J. Am. Chem. Soc. 126, 13212-13213.
11. Powell, J.T., Vine, N. and Crossman, M. 1992. On the accumulation of D-aspartate in elastin and other proteins of the ageing aorta. Atherosclerosis. 97, 201-208.

12. Lame E.N., Van Leeuwen R.T., Jonker A., Van Marle J. and Middelkoop E. 1998. Living skin substitutes: survival and function of fibroblasts seeded in a dermal substitute in experimental wounds. J. Invest Dermatol. 111, 989-995.
13. Boland E.D., Matthews J.A., Pawlowski K.J., Simpson D.G., Wnek G.E. and Bowlin G.L. 2004. Electrospinning collagen and elastin: preliminary vascular tissue engineering. Front Biosci. 9,1422-1432.
14. Neuenschwander S. and Hoerstrup S.P. 2004. Heart valve tissue engineering. Transpl. Immunol. 12, 359-365.
15. Xu J.W., Johnson T.S., Motarjem P.M., Peretti G.M., Randolph M.A. and Yaremchuk M.J. 2005. Tissue-engineered flexible ear-shaped cartilage. Plast. Reconstr. Surg. 115, 1633-1641.
16. Arkın H. 2004. Searching low-energy conformations of two elastin sequences. Eur. Phys. J. B. 37, 223–228.
17. Ferrenberg A.M. and Swendsen R.H. 1988. New Monte Carlo technique for studying phase transitions. Phys. Rev. Lett. 61, 2635-2638.
18. Berg B.A. and Çelik T. 1992. New approach to spin-glass simulations. Phys. Rev. Lett. 69, 2292-2295.
19. Berg B.A. 1998. Algorithmic aspects of multicanonical Monte Carlo simulations. Nucl. Phys. B (Proc. Suppl.) 63, 982.
20. Eisenmenger F., Hansmann U.H.E., Hayryan Sh. and Hu C.K. 2001. [SMMP] A modern package for simulation of proteins. Comp. Phys. Comm. 138, 192-21.
21. Juffer, A.H. 1995. Comparison of atomic solvation parametric sets: Applicability and limitations in protein folding and binding. Protein Science 4, 2499-2509.
22. Berg, B.A. and Hsu, H.P. 2004. Metropolis simulations of Met-Enkephalin with solvent-accessible area parametrizations. Phys. Rev. E. 69, 026703 (1-9).
23. Urry D.W. et al. 1991. Hydrophobicity scale for proteins based on inverse temperature transitions. J. Am. Chem. Soc. 113, 4346-4348.
24. Urry D. W. 2004. The change in Gibbs free energy for hydrophobic association: Derivation and evaluation by means of inverse temperature transitions. Chem. Phy. Letters 399, 177–183.
25. Glodberg S. 1988. Opthalmology Made Rediculously Simple, MedMaster Inc., Miami Fl .
26. Trebst S. and Hansmann U.H.E. 2007. Optimized folding simulations of protein A. Eur. Phys. J. E, 24, 311-316.
27. Wei Y. et al. 2008. Backbone and side-chain ordering in a small protein. J. Chem. Phys,128, 025105(1-6).
28. Meinke J.H. and Hansmann U.H.E. 2009. Free-Energy-Driven Folding and Thermodynamics of the 67-Residue Protein GS-α3W—A Large-Scale Monte Carlo Study. J. Comp. Chem. 30, 1642-1648.
29. Li B., Alonso D.O. and Daggett V. 2001. The molecular basis of the inverse temperature transition of elastin. J. Mol. Biol. 305, 581-592.
30. Tamburro A.M., Guantieri V., Pandolfo L. and Scopa A. 1990. Synthetic Fragments and Analogues of Elastin. II. Conformational Studies. Biopolymers. 29, 855-870.
31. Creighton T. E. 1993. Proteins: Structures and Molecular Properties. Freeman & Worth Publishing Group.
32. Villani V. and Tamburro A.M. 1998. Simulated annealing and molecular dynamics of an elastin-related tetrapeptide in aqueous solution. J. Mol. Struc. (Theochem) 431, 205-218.
33. Urry D.W. 1997. Physical chemistry of biological free energy transduction as demonstrated by elastic protein-based polymers. J. Phys. Chem. B, 101, 11007-11028.

JOURNAL OF APPLIED FUNCTIONAL ANALYSIS, VOL.6, NO.2, 122-129, COPYRIGHT 2011 EUDOXUS PRESS, LLC

Nonlinear Behavior Identification of a Gas-Solid Fluidized Bed Using S-Statistics

M. Karimi, N. Mostoufi, R. Zarghami[1],R. Sotudeh-Gharebagh

Multiphase Systems Research Lab., Department of Chemical Engineering, University of Tehran, Tehran, Iran, P.O. Box 11155/4563

Abstract

A novel technique was developed to identify whether a gas-solid fluidized bed system is nonlinear. In order to achieve this objective, attractors of two dependent pressure signals were compared in the state-space domain using the S-statistic. Comparison between two reconstructed attractors of evaluation and reference time series was performed based on the null hypothesis. The null hypothesis that the evaluation and reference time series are similar is rejected if the two time series significantly differ. Evaluation series were measured during the bed operation and reference time series were generated according to phase randomized surrogate data series from evaluation series. Pressure fluctuations were measured in a three-dimensional bubbling fluidized bed of sand particles with different mean diameters. The method was used in two continuous nonlinear systems called Lorenz and Rossler models to determine nonlinearity. The test showed that the nonlinearity is where the contribution of macro structures are more import than micro and mezzo structures. This conclusion can eventually help choose the proper control system.

Keywords: Nonlinearity; Surrogate data series; Pressure fluctuation time series; S-statistic; Chaotic State Space; Fluidized bed

1. Introduction

All nonlinearity tests in the state-space are based on comparison between two reconstructed attractors of two time series. These tests are based on generating a surrogate data series by a stochastic process from the original data set which has

[1] Corresponding author, Tel.: (+98-21)6696-7797, Fax: (+98-21)6646-1024, Email:rzarghami@ut.ac.ir

some of the attributes of the reference or original data series. Depending on the assumptions one is willing to make on the underlying process, different original data set might be proposed. There are different techniques to generate a surrogate series such as shuffled [1], phase randomized [1], target distribution [1], amplitude adjusted Fourier transform [1] (AAFT) and iterative amplitude adjusted Fourier transform [2] (IAAFT) surrogate data. In this work, phase randomized surrogate data was applied which has the same power spectrum as the original time series. To generate a phase randomized surrogate, the first step is the calculation of the fast Fourier transform of the original time series. In the second step, the created series is randomly multiplied by a phase and finally, the surrogate data is generated as the real part of the inverse fast Fourier transform. Then, the surrogate data series and reference signal must be compared by a null hypothesis. The null hypothesis is rejected if the outcome of the nonlinear analysis is significantly different from the original time series [1].

A number of methods have been proposed for comparing two delay vector distributions. Kantz [3] introduced a cross-correlation for this purpose. Schouten and van den Bleek [4] proposed to base a monitoring method on the short-term predictability of pressure fluctuations in fluidized beds. They used a discriminating statistics to compare an original time series of pressure fluctuation with successive time series of pressure fluctuations which are measured in the fluidized bed. The original time series represented the optimum and desired state of fluidization behavior of the bed. The difference between two reconstructed attractors was indicated as the Z-value by using a null hypothesis. Diks et al. [5] stated that the discriminating statistics is based on a general distance concept between two multidimensional distributions that provides a consistent test for the null hypothesis. They demonstrated that the null hypothesis showed whether two sets of independent vectors were obtained from the same probability distributions or not. The S-statistic has been applied for monitoring some phenomena (e.g., agglomeration) and provided a control tool for the drying of granular material. van Ommen et al. [6] applied the S-statistic to monitor the changes in particle size distribution and early detection of the agglomeration by measured pressure fluctuations. Diks et al. [5] found out that their method can be applied where two pairs are mutually independent. In this work, it was checked whether the method can still be applied if the series are dependent on each other, i.e. surrogate and original time series. Nonlinearity was utilized in two nonlinear chaotic systems which called Rossler and Lorenz. They are appropriate to use proposed method. Lorenz and Rossler equations are addressed by Addison [7]. Subsequently, nonlinearity test was applied to determine the nonlinearity in a fluidized bed system.

2. Experimental

The experimental set up is schematically shown in Fig. 1. Experiments were carried out in a gas-solid fluidized bed made of a Plexiglas-pipe of 15 cm inner diameter and 2 m height. Air at ambient temperature entered the column through perforated plate distributor with 435 holes of 7 mm triangle pitch. Cyclone was used to separate air from particles at high superficial gas velocities. Pressure probe (model SEN-3248 (B075), Kobold Company) was screwed onto the gluing studs located at 5 and 10 cm above the distributor. Pressure fluctuations were recorded in approximately 164 sec corresponding to 65535 data points with a sampling frequency of 400 Hz. Sand particles (Geldart B) with mean sizes of 150, 280 and 490 μm and a particle density of 2640 kg/m^3 were used in the experiments.

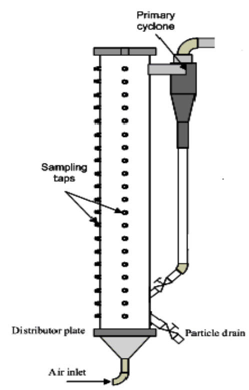

Fig. 1. Schematic of the fluidized bed

3. Methods of analysis

3.1. Attractor reconstruction

To characterize the nonlinearity of the underlying process, it is necessary to first reconstruct a phase space from the time series. There are three domains to analysis pressure signals including time domain, frequency domain and state-space. In this case, the first step refers to transfer a time series from time domain to phase-space by attractor reconstruction. Several method have been applied to reconstrust an attractor. In this work, the method of delay was used which is the simplest method. The state-space was reconstructed from a scalar time series by copying time delayed components of the original time series in the reconstructed state space. Suppose that there is a sampled time series (e.g., pressure signals) $x(i)$ with i=1, 2, 3,.., N, consisting of N values into a set of N-(d-1)τ vectors $s(i)$ which could be represented as:

$$S(i) = (x(i), x(i+\tau), \ldots, x(i+(d-1)\tau) \qquad (1)$$

τ and d are called time delay and embedding dimension, respectively. The time delay was estimated based on mutual information function which was applied by Zarghami et al. [8]. The embedding dimension is equal to the number of elements in the state vectors. Embedding parameters were determined based on the method which is adressed by Zarghami et al. [8].

Time delay was estimated regard to mutual information function criterion which is addressed by Zarghami et al. [8]. The minimum of the embedding dimension could be approximated to correlation dimension of the reconstructed attractor in steady state status. The correlation dimension was calculated from the power law relation ($C(\varepsilon)$ α ε^{Dc}). $C(\varepsilon)$ and ε are called the correlation integral and neighborhood radius, respectively. The correlation dimension is specified by the slop of the log plot of $C(\varepsilon)$ versus ε [8]. This technique was applied to determine embedding dimension for Lorenz and Rossler models. In this work, however, embedding parameters were estimated using the time window method [8] in fluidized beds. Optimum value of the embedding dimension was estimated as one-quarter of the dominant or average cycle time. Average cycle time is defined as the length of the time series (in time units) devided by half of the number of crossing with the average time series.

3.2. S-Statistics

Reconstructed attractors from two dependent time series were compared using a discriminating statistic proposed by Diks et al. [5] to reject or approve the null hypothesis. The time series data were referred to reference (surrogate data) and evaluation time series. An evaluation time set was measured during the operation of the bed. A reference series was randomly generated from an evaluation series. Phase randomized surrogate data was chosen as a reference set. The length of the reference and evaluation series were chosen so that a good representation of the fluidized bed hydrodynamic was obtained [6]. The length of the reference series was taken one-fifth of the length of evaluation series in fluidized bed. The evaluation time series was divided into five segments and each of them was compared with the reference series using S-statistics. The difference was expressed as the S-statistics is defined as:

$$S = \frac{\hat{Q}}{\sqrt{V_c(\hat{Q})}} \qquad (2)$$

The S-statistic is a random variable with zero mean and standard deviation equal to unity according to the null hypothesis. The null hypothesis rejects when estimated value of S is larger than three with 95% confidence level which represents these two delay vector distributions do not originate from the same systems. More information can be found in earlier works and complete details of mathematical aspects of the S-statistic in Diks et al. [5]. This algorithm was applied to detect early warning of agglomeration in the fluidized beds [6].

4. Result and discussion

4.1. Determination of nonlinearity in Lorenz and Rossler systems

In Lorenz and Rossler models, $x(t)$ was taken as an evaluation time series. Reference time series was generated from evaluation series according to phase randomized surrogate data series. Time delays of mentioned systems were specified by mutual information function. Time delay is 16 in Lorenz system with time step corresponds to 0.01. Time delay is 20 in Rossler systems according to time step equal to 0.05 s. Embedding dimension was approximated based on the the slop of the log plot of $C(\varepsilon)$ versus ε, which is 2 in both systems based on inequality of $d>D_C$.

Phase randomized surrogate data series was generated from $x(t)$. Then, the attractor of the surrogate data and $x(t)$ time series were reconstructed to compare two dependent signals using S-statistics. The method of Diks et al. [5] has two parameters which should be optimized based on maximum values of S-statistics. The main reason of this choice refers to the most deviation from the expected zero value. The bandwidth is one of these parameters and the other one is segment length. Fig. 2 indicates average of S values versus bandwidth and segment length in Lorenz system. S values increase by bandwidth to reach a maximum value which is equal to the largest standard deviation. Fig. 2 indicates that with increasing segment length and bandwidth, the S value approaches to an approximately constant value and there is a correlation between reference points at segment lengths smaller than 8. As shown in Fig. 2, S values are more than three and, therefore, indicates that Lorenz and Rossler are two nonlinear deterministic systems. The optimal value of d is 0.03 in Lorenz system and 0.05 in Rossler model.

4.2. Determination of nonlinearity in fluidized bed

Attractors were reconstructed using the method of delay and embedding parameters were determined by the time window method. The optimal segment length and bandwidth were chosen according to recommendations made by van Ommen et al. [6]. They found that for fluidized bed pressure signals, the optimal bandwidth lies between 0.2 and 0.7 times the standard deviation of the signal. İn the present work, the factor 0.5 was selected. Also, they proposed a segment length of about 3 s for yielding good test results. Fig. 3 shows S values against gas velocity at a specific embedding dimension and time window. As can be seen in this figure, by increasing the gas velicity, S value increases to reach a maximum and then begins to decrease.

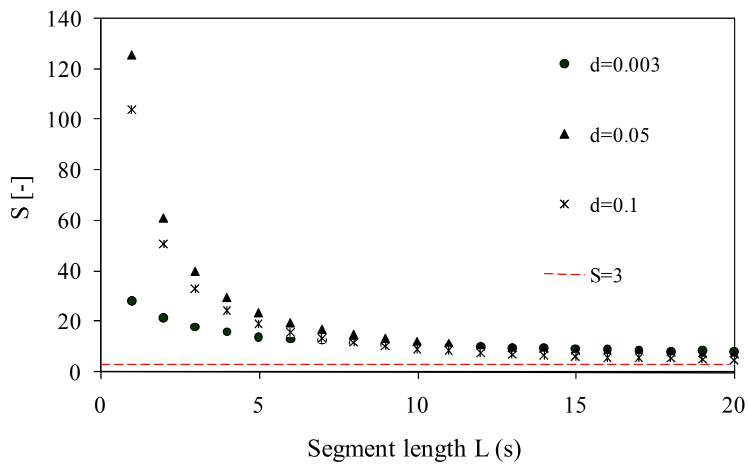

Fig. 2. S values versus bandwidth (*d*) and segment length(*L*)

Zarghami et al. [8] addressed three different structures in fluidized bed, namely macro, mezo and micro, that correspond to different phenomena. The energy of macro strctures has the same behavioure as the S-value. However, the energy of micro and mezo structures shows inverse behaviour. At first, the energy of these structures decreases and after a minimum point increases and becomes more significant.When S value is smaller than 3, fluidized bed behavior is close to stochastic systems where the energy of micro and mezzo structures has more important contribution which is related to some phenomena like particles impacts. In other words, nonlinearity behaviors were mostly seen in where the energy of macro structures is close to the maximum value. The energy was transferred first from micro and mezzo structures to macro structures when velocity is increased and then it is transfered slowly from macro structures to finer structures. However, the contribution of macro structures is higher and fluidized bed behavioure trends to nonlinear deterministic systems where S value is greater than 3.

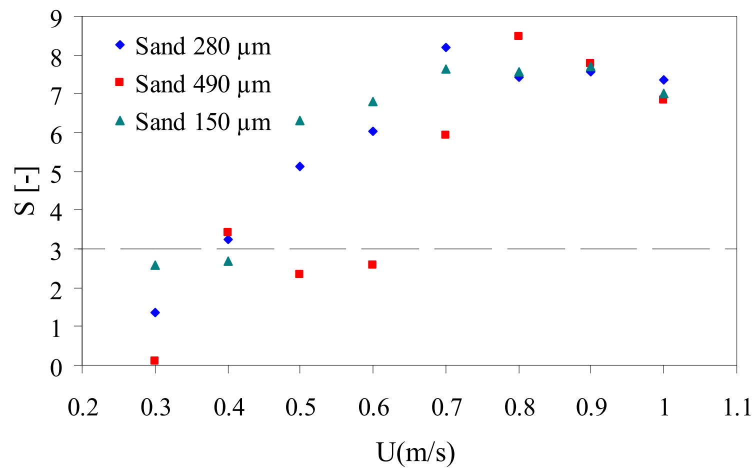

Fig. 3. S value versus superficial gas velocity for three types of snad.

5. Conclusion

A technique was proposed and applied based on comparison between two dependent time series in state-space using the S-Statistics to determine if fluidized beds are nonlinear deterministic or linearly correlated stochastic systems. Nonlinearity was used in Lorenz and Rossler systems. The obtained results from a bubbling fluidized bed showed that the fluidized bed behaviour approximated to nonlinear deterministic behaviour where the energy of macro structure is more import than other structures. This conclusion is important to choose control systems and evaluatation methods of signals in fluidized bed.

Nomenclature

S	state vector, point on state space attractor
d	embedding dimension and bandwith
ACF	Autocorrelation function
MIF	mutual information function
C	correlation Integral
L	segment length,s
Q	squared distance between two attractors
V_c	conditional variance
S	estimator for the normalized squared distance between two attractors.

D_c correlation dimension

Greek Symbols

τ time delay,s
ε neighborhood radius a point on attractor

References

1. J. Theiler, S. Eubank, A. Longtin, B. Galdrikian, J. D. Farmer, Testing for nonlinearity in time series: the method of surrogate data, *Physica D*. 58 (1992) 77-94.

2. T. Schreiber, A. Schmitz, Improved surrogate data for nonlinearity tests. *Physical Review Lett*. 77, 635-638(1996).

3. H. Kanz, Qualitifying the closeness of fractal measures, *Phys. Rev. E*,49,5091 (1994).

4. J. C. Schouten, C. M. van den Bleek, Monitoring the quality of the fluidization using the short-term predictability of pressure fluctuations, *AIChE J.* 44,48-60 (1998).

5. C. Diks, W. R. van Zwet, F. Takens, J. DeGoede, Detecting differences between delay vector distributions, *Phys. Rev. E.* 53,2169-2174 (1996).

6. J. R. van Ommen,M. O. Coppens,C. M. van den Bleek, J. C. Schouten, Early warning of agglomeration in fluidized beds by attractor comparison, *AIChE J.* 46,2183-2197 (2000).

7. P. S. Addison, *Fractal and Chaos*, An illustrated Course; IOP Publishing Ltd., London, UK, 2005.

8. R. Zarghami, N. Mostoufi, R. Sotudeh-Gharebagh, Nonlinear characterization of pressure fluctuations in fluidized beds, *Ind. Eng. Chem*., 47,9497-9499 (2008)

JOURNAL OF APPLIED FUNCTIONAL ANALYSIS, VOL.6, NO.2, 130-137, COPYRIGHT 2011 EUDOXUS PRESS, LLC

SOME ASPECTS OF THE GENERALIZED QUANTUM KICKED ROTATOR

Abdolrasoul Gharaati[1] and Hossain Boroumandy

Physics Departments, Payame Noor University, Shiraz, Iran
1-agharaati@pnu.ac.ir

Abstract: We have studied some aspects of a generalized quantum kicked rotator model which its classical counterpart is chaotic. The model that we have considered is a one dimensional rotator for a special potential which an impulse is applied at equal time intervals T. We obtain time evolution of the wave function between two successive impulses by an evolution matrix. The matrix that evolves the wave function from one impulse to another exponentially falls off away from the main diagonal. We compare time variation of expectation values of energy in quantum version with their classical counterparts. For quantum systems, there are three different cases: Completely periodic case, resonance case and non-resonance case. We derive analytically the time evolution of the energy for the first and second cases where there are fundamental resonances. We show that the energy in fundamental resonances grows up as the time square. This is in contrast to the classical counterpart one.

Keywords: Quantum chaos; kicked rotator; chaos; chaotic system; nonlinear system

1. INTRODUCTION

The classical model of kicked rotator is chaotic at special conditions and so it is the most extensively investigated systems in the field of classical chaos theory [1-3]. Different aspects of the model of kicked rotator have been studied both classically and quantum mechanically by many authors theoretically [4-8] and experimentally [9-10]. This model is applicable in many different branches of physics. For example, related model with the Anderson localization of solid-state physics, (localization problem for a particle on a one-dimensional lattice with a pseudorandom potential) [11-13].

One of the most striking aspects of the quantum kicked rotator behavior is the existence of quantum resonances [14]. Casati et al have considered the quantum mechanical counterpart of the standard map analytically and computationally for $V(\theta) = kcos(\theta)\sum_{n=-\infty}^{\infty}\delta(t-nT)$ and have compared their results with classical ones [1]. There are important differences. They have observed that in fundamental resonances ($T = 4\pi m$, m is an integer) the energy of the rotator grows quadratically with time. Izrailiev and Sheplyansky have extended the work of Casati et al [15]. For resonances in general they observed a similar behavior of energy with time. Dorizzi et al have studied the potential for quantum kicked rotator of the form $V(\theta) = 2\arctan(k\cos(\theta)/2)$ and $k \in R$, in which their numerical results indicate quadratic growth of energy with time in resonances [16].

In this paper, we study a novel quantum system for Hamiltonians whose classical counterparts are chaotic. In this model we consider a one-dimension of potential as

$$V(x) = 2\arctan\left(\frac{k\cos(x)}{2(1-b\cos(x))}\right), \quad |b| < 1,\ k \in R \tag{1}$$

This potential has the remarkable property as: (a) it approaches to a delta-function when $b \to 1$

and (b) it takes the standard kicked rotator form when $b \to 0$. Fig.1.

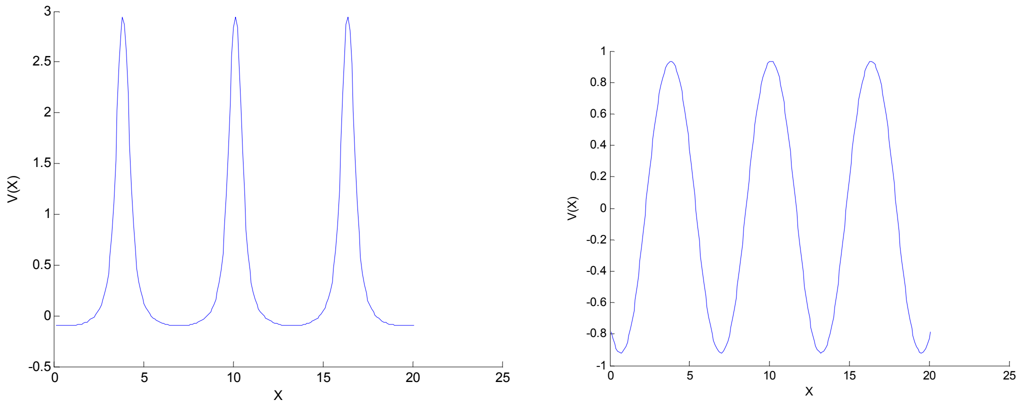

(a) (b)

Fig. 1, Variation of potential $V(x)$ for (a) k = 0.1, b = 0.99 and (b) k = 0.5, b = 0.01

The organization of the paper is as follows. In section 2, we calculate the general form of the wave function analytically and in section 3, for a special potential we find time evolution matrix between two successive impulses and we prove the unitary property of the evolution matrix. In section 4 we study time evolution of the energy and obtain an analytical expression for periodic cases. In section 5 we discuss the non-resonance case numerically and finally section 6 is devoted to conclusion and numerical results.

2. CALCULATION OF THE WAVE FUNCTION OF THE GENERALIZED KICKED ROTATOR

We consider the Hamiltonian equation for the quantum kicked rotator model as

$$H = \frac{p^2}{2} + V(\theta)\sum_n \delta(t - nT), \tag{2}$$

where θ and p are angle and angular momentum variables and potential V(θ) is the periodic function. The wave function at time t_0 and t is related through the following integral form of [17],

$$\psi(t) = \exp\left[-i\int_{t_0}^{t} H(t')dt'\right]\psi(t_0) \tag{3}$$

Where Plank's constant is taken to be 1. For $t = nT^+$ and $t = (n+1)T^-$, where "-" and "+" signs indicate the times immediately before and after the impulses respectively, Eqs. (2) and (3) give

$$\psi(nT^+) = \exp[-iV(\theta)]\psi(nT^-)\,, \qquad nT^- < t < nT^+ \tag{4a}$$

$$\psi[(n+1)T^-] = \exp[-iH_0T]\psi(nT^+), \qquad nT^+ < t < (n+1)T^- \tag{4b}$$

By combining Eqs. (4), the wave function after the (n+1)th impulse, in terms of that after the nth, one obtains

$$\psi[(n+1)T^+] = U(k,\theta,T)\psi(nT^+), \tag{5}$$

where

$$U(k,\theta,T) = e^{-iH_0T}e^{-iV(\theta)}, \tag{6}$$

We expand this wave function in terms of the eigenfunction of free particle, $\varphi_n = (1/\sqrt{2\pi})e^{in\theta}$. Thus

$$\psi(nT^+) = \sum_{j=-\infty}^{\infty} C_j(nT^+)\varphi_j(\theta), \tag{7}$$

Inserting Eq. (7) in Eq. (5), multiplying both sides by $\varphi_m^*(\theta)$ and integrating over the interval $(0,2\pi)$, gives

$$C_j[(n+1)T^+] = \sum_j U_{mj} C_j(nT^+) = A_{ml}\Omega_{lj} C_j(nT^+) \tag{8}$$

Where U_{mj}, A_{ml} and Ω_{lj} are the matrix elements of the form

$$U_{mj} = <\varphi_m \left| e^{-iH_0 T} e^{-iV(\theta)} \right| \varphi_j > \tag{9}$$

$$A_{ml} = \int_0^{2\pi} \varphi_m^*(\theta) e^{-iV(\theta)} \varphi_l(\theta) d\theta \tag{10}$$

$$\Omega_{lj} = \int_0^{2\pi} \varphi_l^*(\theta) e^{-iH_0 T} \varphi_j(\theta) d\theta = e^{-i\omega_j T} \delta_{lj} \tag{11}$$

and $\omega_j = j^2/2$. By considering the wave function of particle of the form $\psi(0) = \sum_j C_j(0)\varphi_j$, and convert $C_m(nT^+)$ in term of wave vector $C(nT\,)$, the Eq. (8) gives

$$C(n) = U^n C(0) = (A\Omega)^n C(0) \tag{12}$$

Where $C(0)$ and $C(n)$ are the initial wave vector and after the n[th] impulse respectively. Hereafter for simplification we suppress plus-sign on T.

3. THE MATRIX ELEMENTS OF THE EVOLUTION OPERATOR

In this section we are going to derive the elements of matrix U by considering special potential (1) for Eq. (2), and obtain analytically the wave function of the kicked rotator.
Inserting Eq. (1) into (9) and using Eqs. (10) and (11) the matrix element between pulses becomes

$$U_{mj} = A_{ml}\Omega_{lj} = < m \left| e^{-iV(\theta)} \right| j > e^{-i(\frac{j^2}{2})T} = \left\langle m \left| \frac{1 - \mathrm{i}(\mathrm{k}\cos(\theta)/2(1-\mathrm{b}\cos(\theta))}{1 + i(k\cos(\theta)/2(1-b\cos(\theta))} \right| j \right\rangle e^{-i(\frac{j^2}{2})T} \tag{13}$$

By calculating the integral (13), the elements of A_{mj} is given by

$$A_{mj} = \begin{cases} (-\dfrac{ir^*}{2\sqrt{1+r^2}})[z(r)^2 + \dfrac{2i}{r^*} z(r) + 1] z(r)^{|m-j|-1} & m \neq j \\ (\dfrac{1}{\sqrt{1+r^2}})(1 + \dfrac{r^*}{r}) - \dfrac{r^*}{r} & m = j \end{cases} \tag{14}$$

Where $z(r) = (i/r)(1-\sqrt{1+r^2})$ and $r = k/2 + ib$. In order to obtain a compact formula we define

$$\frac{1}{r} = \sinh(\gamma + i\mu) \tag{15}$$

Then

$$z(r) = -ie^{-(\gamma + i\mu)} \quad \text{and} \quad z(r)z^*(r) = e^{-2\gamma} \tag{16}$$

Where γ and μ are real numbers [18]. From Eq. (16) we conclude that $|z| = e^{-\gamma}$ this means that the matrix elements of U exponentially fall off away from main diagonal. This is related to the Anderson localization length that we are going to discuss elsewhere.
Inserting Eqs. (15) and (16) in Eq. (14), gives

$$U_{mj} = (\frac{\sinh(\gamma + i\mu)}{\sinh(\gamma - i\mu)})(\frac{2\cos\mu\sinh\gamma}{\cosh(\gamma - i\mu)} - \delta_{mj}) z_-^{|m-j|} e^{-i\frac{j^2}{2}T} \tag{17}$$

By considering the Eqs. (12), (14) and (17) and substituting $n = m - j$ we could analytically obtain the wave function of the generalized quantum kicked rotator.
The matrix U is unitary. To show this, from Eq. (9) one can reads the (l,m)-element of the UU^+ as

$$U_{mj}U_{lj}^{+} = \langle\varphi_m \left|e^{-iV(\theta)}e^{-iH_0T}\right|\varphi_j\rangle\langle\varphi_j\left|e^{+iH_0T}e^{+iV(\theta)}\right|\varphi_l\rangle = \langle\varphi_m\|\varphi_l\rangle = \delta_{ml} = \begin{cases}1 & m=l\\ 0 & m\neq l\end{cases} \tag{18}$$

Hence if $C(0)$ is normalized, then $C(n)$ remain normalized for after n$^{\text{th}}$-pulses and $C^{+}(n)C(n)=1$. We have used this property as a criterion for checking the precision of our numerical computations.

4. EVOLUTION OF THE ENERGY

The expectation value of the energy at $t = nT$ is

$$E(n) = \int_0^{2\pi}\psi^{\bullet}(\theta,n)\frac{p^2}{2}\ \psi(\theta,n)d\theta = \frac{1}{2}\sum_{j=-\infty}^{\infty} j^2\left|C_j(n)\right|^2 = C^{+}(n)H_0C(n) \tag{19}$$

Where the element of H_0 are $H_{kj} = (1/2)j^2\delta_{kj}$. The classical counterpart of Eq. (19) has chaotic behavior for $k > k_c = 0.971635$, $b=0$ [4-7 , 19-20] and for $b\neq 0,\ k\in R$, as it shown in Fig. 2.

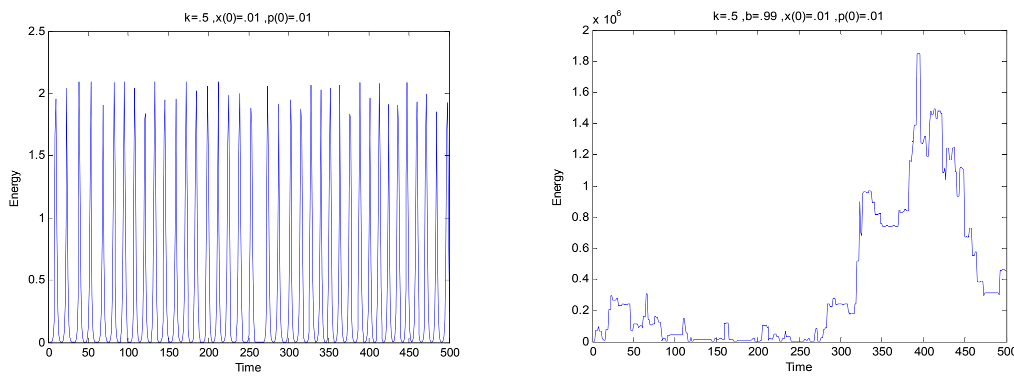

(a) (b)

Fig. 2. Classical evolution of the energy with respect to kicked numbers, (a) $x(0) = 0.01$, $p(0) = 0.01$, $b=0$ and $k=0.5$. (b) $x(0) = 0.1$, $p(0) = 0.1$ $b = 0.99$, *and* $k = 0.5$.

But in the quantum system three different cases can be recognized. In Fig. 2b we can observe that the system has chaotic behavior in the classical case.

4.1. The Periodic Cases

For $T/4\pi = 1/2$ the matrix elements of U of Eq. (17) reduces to

$$U_{mj} = \left(\frac{\sinh(\gamma+i\mu)}{\sinh(\gamma-i\mu)}\right)\left(\frac{2\cos\mu\sinh\gamma}{\cosh(\gamma-i\mu)} - \delta_{mj}\right)Z(r)^{|m-j|}(-1)^j \tag{20}$$

The system for all k and $b=0$, returns to its initial state after every two impulses, and $U^2=1$, [21]. For every k and $b\neq 0$ the system grows with time and $U^2\neq 1$. This analytical feature has been checked numerically by using Eq. (19), as it is shown in Figs. 3, with $T/4\pi = 1/2$, $n=50$, $k=0.5$ and $b=0,\ 0.01,\ 0.1$, *and* $0.99.$. In the case (a), the system for all k and $b=0$, returns to its initial state after every two impulses. But for every k and $b\neq 0$, in the cases (b), (c) and (d), the energy of the system grows with time.

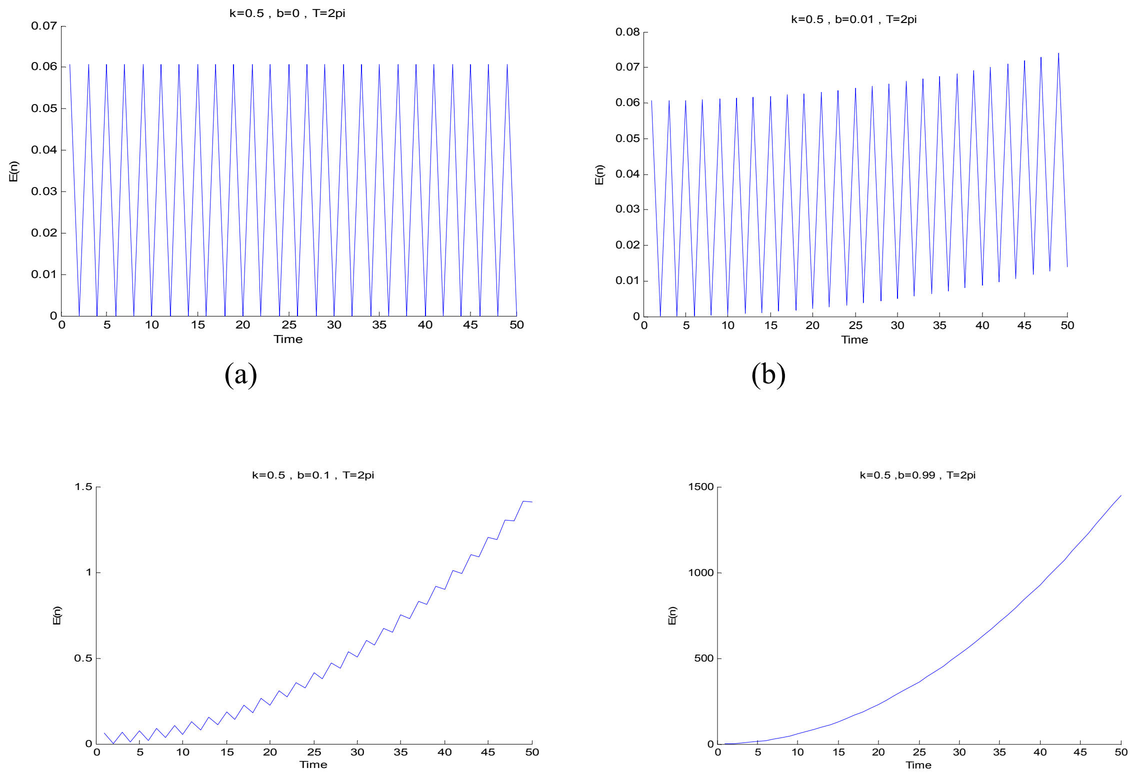

(c) (d)

Fig. 3. Evolution of the energy with respect to kick number, for $T/4\pi = 1/2$, k=0.5 for (a) b=0, (b) b=0.01, (c) b=0.1, and (d) b=0.99.

4.2. Resonance Cases

The cases $T/4\pi = p/q \neq 1/2$, p and q are integers, are known as resonances. The special cases of $T/4\pi = m$, m *is* an integer, are the fundamental resonances. We have numerically verified for $b = 0$ and $b \neq 0$, in all resonance cases that the energy grows quadratically with time. For special case $= 0$, all numerical computations are compatible with refs [4, 21].

Here, we prove this feature for fundamental resonances analytically. For $T/4\pi = m$ the evolution operator of Eq. (6) reduces to $exp[-iV(\theta)]$. For the wavefunction after the n^{th} impulse one finds

$$\psi(\theta,n) = e^{-inV(\theta)}\psi(\theta,0) \tag{21}$$

By considering Eqs. (19) and (21) the expectation value of the energy will be

$$\begin{aligned} E(n) &= \int_0^{2\pi} \psi^*(\theta,n) H_0 \psi(\theta,n) d\theta = -\frac{1}{2}\int_0^{2\pi} \left|\frac{\partial \psi(\theta,n)}{\partial\theta}\right|^2 d\theta \\ &= \eta(k,b)n^2 + \xi(k,b)n + E(0) \end{aligned} \tag{22}$$

Where

$$\eta(k,b) = -\frac{1}{4\pi}\int_0^{2\pi} \frac{k^2 \sin^2\theta \, d\theta}{\left[(b^2 + k^2/4)\cos^2\theta - 2b\cos\ \theta + 1\right]^2} \tag{23a}$$

$$\xi(k,b) = -i\frac{k}{2}\int_0^{2\pi} \frac{\sin\theta}{\left[(b^2 + k^2/4)\cos^2\theta - 2b\cos\theta + 1\right]}(\psi^{\bullet}(\theta,0)\frac{\partial\psi(\theta,0)}{\partial\theta} - \psi(\theta,0)\frac{\partial\psi^{\bullet}(\theta,0)}{\partial\theta})d\theta \tag{23b}$$

$$E(0) = \frac{1}{2}\int_0^{2\pi} \left|\frac{\partial\psi(\theta,n)}{\partial\theta}\right|^2 d\theta \tag{23c}$$

If the initial wave function is the ground state, $\psi(\theta,0)=1/\sqrt{2\pi}$, then $E(0)$ and $\xi(k,b)$ vanish. The integral (23a) can be evaluated by the change of variable $t=\cos(\theta)$. Eq. (22) then becomes

$$E(n)=\left\{\frac{(b^2+k^2/4)^2-(b^2-ibk/2)}{k\sqrt{(b^2+k^2/4)^2-(b-ik/2)^2}}+\frac{(b^2+k^2/4)^2-(b^2+ibk/2)}{k\sqrt{(b^2+k^2/4)^2-(b+ik/2)^2}}\right\}n^2 \tag{24}$$

Moreover, Eq. (24) can be expressed in term of limited conditions of the form:

$$E(n)\approx\frac{k^2}{4}n^2 \quad ; \quad where \quad k<<1, b=0 \tag{25}$$

$$E(n)\approx\frac{k}{2}n^2 \quad ; \quad where \quad k>>1,\ b=0 \tag{26}$$

$$E(n)\approx\left[\frac{[(b^2+k^2/4)^2-(b-ikb/2)]\sqrt{b^4-b^2+k^2/4-ikb}}{k\sqrt{(b^4-b^2+k^2/4)^2+k^2b^2}}\right.$$
$$\left.+\frac{[(b^2+k^2/4)^2-(b+ikb/2)]\sqrt{b^4-b^2+k^2/4+ikb}}{k\sqrt{(b^4-b^2+k^2/4)^2+k^2b^2}}\right]n^2 \quad where \quad k<<1, \quad b\neq 0 \tag{27}$$

and

$$E(n)\approx\left[\frac{b^2+k^2/4}{k/2}\right]n^2 \quad ; \quad where \quad k>>1,\ b\neq 0 \tag{28}$$

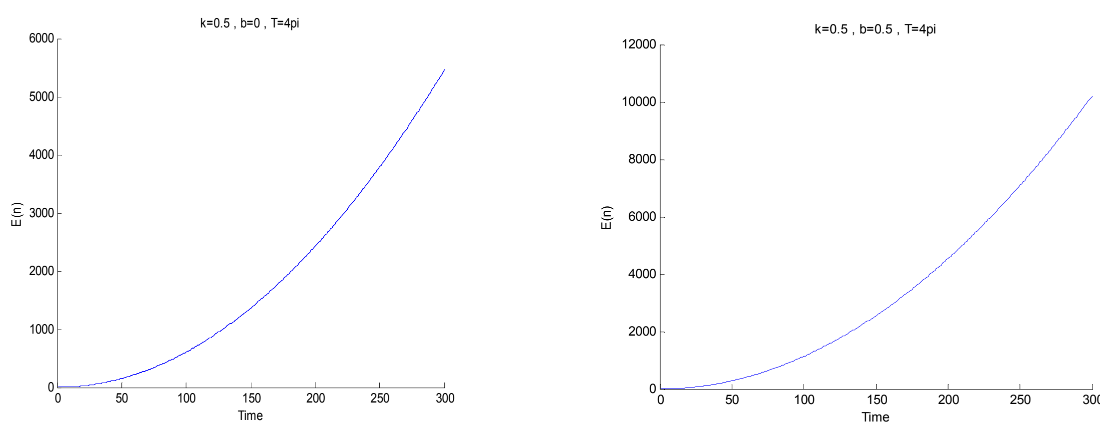

(a) (b)

Fig. 4. Evolution of the energy as a function of kick number, and $T/4\pi=1$, k=0.5 for (a) b = 0 and (b) b=0.5.

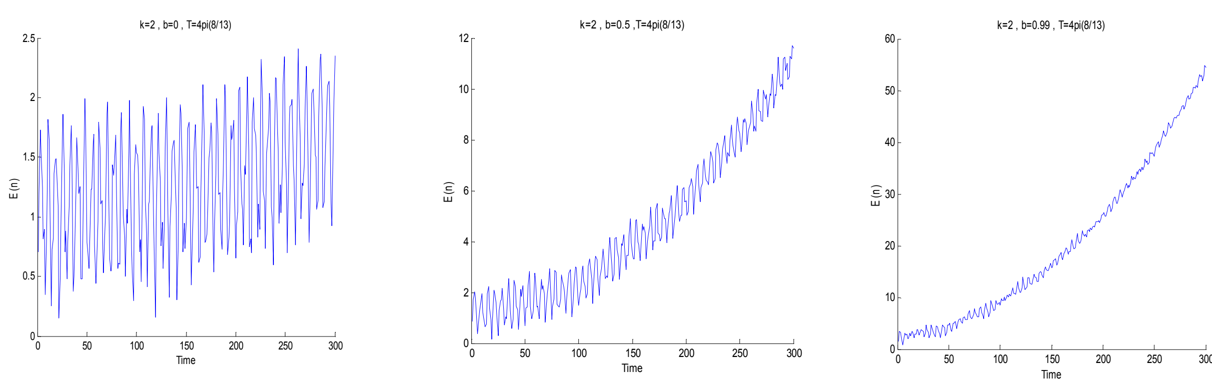

(a) (b) (c)

Fig. 5. Evolution of the energy as a function of kick number, and $T/4\pi=p/q=8/13$, k = 2, (a) $b=0$, (b) $b=0.5$, and (c) $b=0.99$.

Gharaati has analytically obtained Eq. (24) for special case $b = 0$, [21] and the limiting values of analytical computation of this equation, for small and large k's and $b=0$ that is Eqs. (25) and (26) were predicted numerically by Dorizzi et al, [16]. In Fig. 4, we have shown the variation of energy in term of kicked number for $k=0.5$ and $T/4\pi=1$.
We verified numerically the limiting values for $b \neq 0$, that shown in Eqs. (27) and (28). In three cases it can be observed that the variation of energy grows quadratically with time and increase energy by increasing the value of b.
Also for cases $T/4\pi = p/q =$ rational, the energy for example, for $T/4\pi = p/q = 8/13$, increases with time. An analytical study of system in this case is complicated. The results in various stages of numerical computations are shown that the energy grows with time. The variation of energy in term of kick number for $p/q = 8/13$, $k=2$ and (a) $b=0$, (b) $b=0.5$, and (c) $b=0.99$. is shown in Figs. 5.

5. NON-RESONANCE CASES

Non resonance cases occur for $T/4\pi =$ irrational. An analytical study of the system is very complicated. For small k and $b=0$, however, It was verified numerically by Hogg and Huberman [21-23]. In this case, we verified numerically the expectation value of the energy by using Eq. (19) for $b \neq 0$. For this case it can be observed that the energy is oscillating around a mean value and it becomes difficult to decide whether the system becomes chaotic or not. In the numerical study the larger the k *and* b the larger the dimension of the U matrix. The results of numerical computation are shown in Fig. 6.

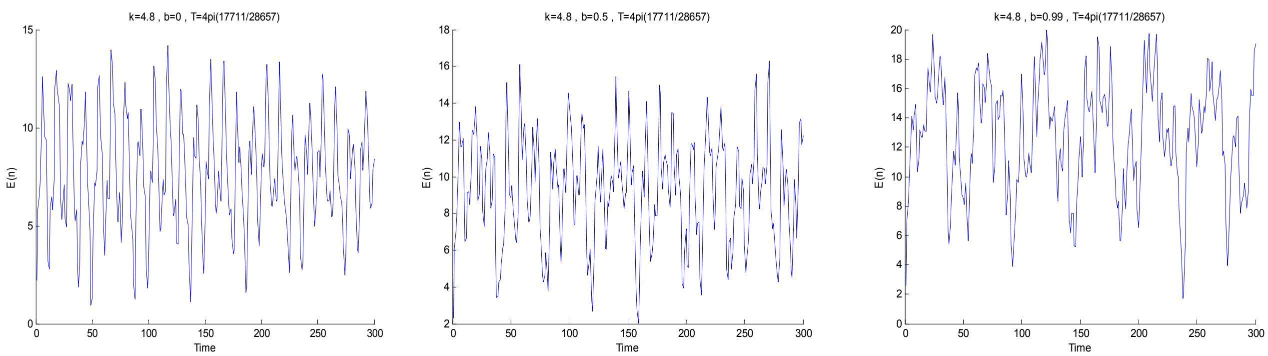

(a) (b) (c)

Fig. 6. Evolution of the energy as a function of kick number, and $T/4\pi = 17711/28657 \cong [\sqrt{5}-1]/2$, k=4.8, (a) $b=0$, (b) $b=0.5$ and (c) $b=0.99$.

6. CONCLUSION AND NUNERICAL RESULTS

By introducing a novel potential for the kicked rotator model (Eq. (1)), we have analytically derived the wave function of the system after each impulse, (Eqs. (6) and (11)). We have shown that the evolution operator of the wave function U is a unitary matrix and the elements of U are periodic in T. This is in contrast to classical case. Also, we have shown the matrix elements of U fall off exponentially.
The time evolution of the energy of the generalized quantum kicked rotator with potential (12) is obtained for various cases. For $T/4\pi = 1/2$ *and* $b=0$ then $U^2 = 1$ and the system returns to its initial state after every two impulses. For $T/4\pi = 1/2$, $b \neq 0$, the energy of system grows with time. For cases $T/4\pi = p/q \neq 1/2$, for all $b's$ and $k's$ the energy grows quadratically with time, as expressed in Eqs. (22) and (24). The coefficients of the quadratic expression for $T/4\pi =$ $=integer$, is explicitly given. For $T/4\pi =$ irrational, the behavior of the system depends on the

strength of the impulses, b and k. In this case numerical computations show upper bound for the energy. The unitary of the truncated matrix U was used to check the accuracy of the numerical results in various stages of the computations.

Acknowledgments

This work has been financially supported by the Payame Noor University (PNU) under Grant No. 1388/3/0/14/185.

References

[1] G. Casati, B. V. Chirikov, F. M. and J. Ford, *Lecture Notes in Physics,* ed. G. Casati, J. Ford, Springer, New York, **93**, 334 (1979).

[2] S. J. Chang and G. Perez, *Chin. J. Phys.* **30**, 479 (1992).

[3] A. L. Lichtenberg and M. A. Lieberman, *Regular and Chaotic Dynamics,* (Springer- Verlag, Berlin, 1992).

[4] B. V. Chirikov, *Phys. Rep.* **52**, 293 (1979).

[5] J. V. Jose, and E. J. Saletan, *Classical Dynamics: A Contemporary Approach*, (Cambridge University Press, 1998),Chap. 7.

[6] T. Tel, and M. Gruitz*, Chaotic Dynamics:An Introduction Based on Classical Mechanics, (Cambridge University Press, 2006), Chap. 7.*

[7] P. Sulkowski, and K. Sokalski, *Acta Physica Polonica B***. 29,** 1943 (1998).

[8] B. Lvi, B. Georgeot and D. L. Shepelyansky, *Phys. Rev. E,* **67**, 046220 (2003).

[9] P. Szriftgiser, H. Lingier. J. Ringot, J. C. Garreau and D. Delaude, *Comm. in Nonlinear Scince and Numerical Simulation*, **8,** 301 (2003).

[10] J. Ringot, P. Szriftgiser, and J. C. Garreau, *Phys. Rev. Letts,* **85,** 2741 (2000).

[11] S. Fishman, D. R. Grempl and R. E. Prange, *Phys. Rev. lett*. **49**, 509 (1982).

[12] P. W. Anderson, *Phys. Rev*. **109**, 1492 (1958).

[13] A. M. Garcia-Garcia, *Proceedings of the 3rd Workshop on Quantum and Localization Phenomena, Warsaw,* Poland, May 25-27, 635 (2007).

[14] F. M. Izrailev, and D. L. Shepelyansky, *Sov. Phys. Dokl*. **24**, 996 (1979).

[15] F. M. Izrailev, and D. L. Shepelyansky, *Theor. Math. Phys*. **43**, 553 (1980).

[16] B. Dorizzi, B. Grammaticos and Y. Pomeau, J. *Stat. Phys.* **37**, 93 (1984).

[17] V. B. Berestetskii, E. M. Lifshitz, and L. P. Pitaevskii, *Relativistic Quantum Theory* (Pergamon Press, Oxford, (1971).

[18] S. Fishman, D. R. Grempl and R. E. Prange, *Phys. Rev. lett*. **49**, 833 (1982).

[19] J. M. Greene*, J. Math. Phys.* **20**,1183 (1979).

[20] G. M. Zaslavsky, *Hamiltonian Chaos and Fractal Dynamics*, (Oxford University Press, 2006), Chaps. 5-6.

[21] A. Gharaati, Behavior of transition amplitude and evolution of the energy of quantum Kicked rotator, *Turkish J. Phys.* **33**, No. 4, 235 (2009).

[22] T. Hogg, and B. A. Huberman, *Pheys. Rev. Lett*. **48**, 711 (1982).

[23] T. Hogg, and B. A. Huberman, *Pheys. Rev. A*. **28**, 22 (1983).

JOURNAL OF APPLIED FUNCTIONAL ANALYSIS, VOL.6, NO.2, 138-144, COPYRIGHT 2011 EUDOXUS PRESS, LLC

Solution of sixth-order boundary value problem using Non-polynomial spline in off step points

Karim.Farajeyan[a],Leila.khayyati[b]
[a]Department of Mathematics, Islamic Azad University of Bonab, Iran.
[b]Payame Noor University (PNU)Tabriz, Iran
karim_faraj@yahoo.com

March 2, 2010

We use non-polynomial spline in off step points to develop a numerical method for the solution of sixth-order boundary-value problems. End conditions of the spline are derived.We compare our results with the results produced by Non-polynomial splines method [2]. However, it is observed that our approach produce better numerical solutions in the sense that max$|e_i|$ is minimum.

Keywords: Sixth-order B.V.P; non-polynomial spline functions; end conditions; convergence analysis; numerical results.

1 Introduction

We consider sixth-order boundary-value problem of type

$$y^{(6)}(x) + f(x)y(x) = g(x), \quad x \in [a, b], \tag{1}$$

with boundary conditions

$$\begin{aligned} &y(a) = A_0, y^{(2)}(a) = A_1, y^{(4)}(a) = A_2, \\ &y(b) = B_0, y^{(2)}(b) = B_1, y^{(4)}(b) = B_2. \end{aligned} \tag{2}$$

where,$g(x)$ and $f(x)$ are continuous on $[a, b]$ and A_i, B_i,$(i = 0, 1, 2)$ are real finite constants. Caglar et al.in [1] solved third order boundary value problems using fourth degree B-spline functions.El-Gamel et al.[3] used Sinc-Galerkin method for the solution of sixth-order boundary value problems. S.S.Siddiqi.G.Akram [4] presented the solutions of sixth-order boundary value problems using Septic spline. Farajeyan and jafari in [5] applied spline approximate to the solution of eight-order boundary-value problems. In this paper we used non-polynomial spline approximation to develop a family of new numerical methods to obtain smooth approximations to the solution of sixth-order differential equation.The spline functions proposed in this paper have the form $T_7 =$

$span\{1, x, x^2, x^3, x^4, x^5, cos(kx), sin(kx)\}$where k is the frequency of the trigonometric part of the spline functions which can be real or pure imaginary and which will be used to raise the accuracy of the method.Thus in each subinterval $x_i \le x \le x_{i+1}$, we have

$$\text{span}\{1, x, x^2, x^3, x^4, x^5, \cos(|k|x), \sin(|k|x)\},$$

or

$$\text{span}\{1, x, x^2, x^3, x^4, x^5, x^6, x^7\}, \quad (\text{when} k \to 0).$$

2 Numerical method

To develop the spline approximation to the sixth-order boundary-value problem (1)-(2), the interval [a,b] is divided into the following subintervals using the grids

$$x_0 = a, \quad x_{i-\frac{1}{2}} = a + (i - \frac{1}{2})h, \quad h = \frac{b-a}{n}, \quad i = 1, 2, ..., n, \quad x_n = b.$$

where $h = \frac{b-a}{n}$. Consider the following non-polynomial spline $S_i(x)$ is each subinterval $[x_{i-\frac{1}{2}}, x_{i+\frac{1}{2}}], i = 1, ..., n-1$,

$$S_i(x) = a_i \text{cos} k(x - x_i) + b_i \text{sin} k(x - x_i) + c_(x - x_i)^5 + d_i(x - x_i)^4 +$$
$$e_i(x - x_i)^3 + f_i^*(x - x_i)^2 + g_i^*(x - x_i) + q_i, \tag{3}$$

where $a_i, b_i, c_i, d_i, e_i, f_i^*, g_i^*$ and q_i, are real finite constants and k is free parameter.The spline S is defined in terms of its 2th and 4th derivatives and we denote these values at knots as:

$$S_i(x_{i-\frac{1}{2}}) = y_{i-\frac{1}{2}} \ , \ S_i^{(2)}(x_{i-\frac{1}{2}}) = m_{i-\frac{1}{2}} \ , \ S_i^{(4)}(x_{i-\frac{1}{2}}) = M_{i-\frac{1}{2}}, \ , \ S_i^{(6)}(x_{i-\frac{1}{2}}) = L_{i-\frac{1}{2}},$$

$$S_i(x_{i+\frac{1}{2}}) = y_{i+\frac{1}{2}} \ , \ S_i^{(2)}(x_{i+\frac{1}{2}}) = m_{i+\frac{1}{2}}, \ , \ S_i^{(4)}(x_{i+\frac{1}{2}}) = M_{i+\frac{1}{2}} \ , \ S_i^{(6)}(x_{i+\frac{1}{2}}) = L_{i+\frac{1}{2}}$$
$$\text{for } \ i = 1, 2, ..., n. \tag{4}$$

Assuming $y(x)$ to be the exact solution of the boundary value problem (1) and y_i be an approximation to $y(x_i)$, using the continuity conditions we obtain the following spline relations:

$$y_{i-\frac{7}{2}} - 6y_{i-\frac{5}{2}} + 15y_{i-\frac{3}{2}} - 20y_{i-\frac{1}{2}} + 15y_{i+\frac{1}{2}} - 6y_{i+\frac{3}{2}} + y_{i+\frac{5}{2}}$$
$$= h^6[\alpha L_{i-\frac{7}{2}} + \beta L_{i-\frac{5}{2}} + \gamma L_{i-\frac{3}{2}} + \delta L_{i-\frac{1}{2}} + \gamma L_{i+\frac{1}{2}} + \beta L_{i+\frac{3}{2}} + \alpha L_{i-\frac{5}{2}}],$$
$$i = 4, 5, ..., n-4. \tag{5}$$

Where

$$\alpha = \frac{120hk - 20h^3k^3 + h^5k^5 - 120Sin(\theta)}{120\theta^6 Sin(\theta)},$$

$$\beta = \frac{-(240hk + 20h^3k^3 - 13h^5k^5 + hk(120 - 20h^2k^2 + h^4k^4)Cos(\theta) - 360Sin(\theta))}{60\theta^6 Sin(\theta)},$$
$$\gamma = \frac{-(240hk + 20h^3k^3 - 13h^5k^5 + 3hk(120 + 20h^2k^2 + 11h^4k^4)Cos(\theta) - 600Sin(\theta))}{30\theta^6 Sin(\theta)},$$
$$\delta = \frac{-(-hk(840 + 100h^2k^2 + 67h^4k^4) + 4hk(-240 - 20h^2k^2 + 13h^4k^4)Cos(\theta) + 1800Sin(\theta))}{120\theta^6 Sin(\theta)}.$$

3 Development of the boundary formulas

The relation (5) forms a system of $(N-7)$ linear equations in the $(N-1)$ unknowns $(y_i, i = 1, 2, ..., N-1)$,while l_i is taken from BVP(1)to be equal to $(-f_i y_i + g_i)$. six equation (end conditions) are required to be associated with the system (5) to determine a unique solution of y_is .In order to obtain the sixth-order boundary formula we define the following identity:

$$d'_0 y_0 + \sum_{k=0}^{5} a'_{k+1} y_{k+\frac{1}{2}} + c' h^2 y_0^{(2)} + p' h^4 y_0^{(4)} = h^6 \sum_{k=0}^{5} b'_{k+1} y^{(5)}_{k+\frac{1}{2}} + t_1, \tag{6}$$

$$d''_0 y_0 + \sum_{k=0}^{6} a''_{k+1} y_{k+\frac{1}{2}} + c'' h^2 y_0^{(2)} + p'' h^4 y_0^{(4)} = h^6 \sum_{k=0}^{6} b''_{k+1} y^{(5)}_{k+\frac{1}{2}} + t_2, \tag{7}$$

$$d'''_0 y_0 + \sum_{k=0}^{7} a'''_{k+1} y_{k+\frac{1}{2}} + c''' h^2 y_0^{(2)} + p''' h^4 y_0^{(4)} = h^6 \sum_{k=0}^{7} b'''_{k+1} y^{(5)}_{k+\frac{1}{2}} + t_3, \tag{8}$$

$$d^\circ_0 y_0 + \sum_{k=0}^{7} a^\circ_{k+1} y_{k+n-\frac{11}{2}} + c^\circ h^2 y_0^{(2)} + p^\circ h^4 y_0^{(4)} = h^6 \sum_{k=0}^{7} b^\circ_{k+1} y^{(5)}_{k+n-\frac{11}{2}} + t_{n-3}, \tag{9}$$

$$d^\star_0 y_0 + \sum_{k=0}^{6} a^\star_{k+1} y_{k+n-\frac{9}{2}} + c^\star h^2 y_0^{(2)} + p^\star h^4 y_0^{(4)} = h^6 \sum_{k=0}^{6} b^\star_{k+1} y^{(5)}_{k+n-\frac{9}{2}} + t_{n-2}, \tag{10}$$

$$d^{\star\star}_0 y_0 + \sum_{k=0}^{5} a^{\star\star}_{k+1} y_{k+n-\frac{7}{2}} + c^{\star\star} h^2 y_0^{(2)} + p^{\star\star} h^4 y_0^{(4)} = h^6 \sum_{k=0}^{5} b^{\star\star}_{k+1} y^{(5)}_{k+n-\frac{7}{2}} + t_{n-1} \tag{11}$$

where all of the coefficients are arbitrary parameters to be determined.By using Taylors expansion and by solving the corresponding linear system we obtain:

$$(a'_1, a'_2, a'_3, a'_4, a'_5) = (1, -\frac{847476}{464945}, \frac{589659}{464945}, -\frac{11907}{20215}, \frac{152793}{929890}, -\frac{19327}{929890}),$$
$$(d'_0, c', p') = (1, -\frac{114723}{743912}, \frac{1407483}{59512960}),$$
$$(b'_1, b'_2, b'_3, b'_4, b'_5) =$$

$$(\frac{199935287}{30470635520}, -\frac{220288121}{152353177600}, -\frac{774211293}{152353177600}, \frac{17670329}{152353177600}, -\frac{629599}{15235317760}),$$

$$(a_1'', a_2'', a_3'', a_4'', a_5'', a_6'') = (-\frac{1503231188725049}{23782817280}, \frac{1867935336508597}{7927605760},$$

$$-\frac{4247624920328657}{11891408640}, \frac{3323910594809683}{11891408640}, -\frac{903030585746583}{7927605760}, \frac{91184360931935}{4756563456}),$$

$$(d_0'', c'', p'') = (1, \frac{128703046919}{12386884}, -\frac{2210375095681}{3963802880}),$$

$$(b_1'', b_2'', b_3'', b_4'', b_5'', b_6'') = (1, \frac{12683929093362529}{2853938073600}, \frac{215355320923364639}{19977566515200},$$

$$\frac{41648028557578489}{9988783257600}, \frac{20633161916767}{133183776768}, 1),$$

$$(a_1''', a_2''', a_3''', a_4''', a_5''', a_6''', a_7''') = (-\frac{31797138715241899}{71348451840}, \frac{39510888135471647}{23782817280},$$

$$-\frac{89842909122366067}{35674225920}, \frac{70301996244994553}{35674225920}, -\frac{19098605121088453}{23782817280}, \frac{1928394545986333}{14269690368}, 1),$$

$$(d_0''', c''', p''') = (1, \frac{2722869100309}{37160652}, -\frac{46967954595971}{11891408640}),$$

$$(b_1''', b_2''', b_3''', b_4''', b_5''', b_6''', b_7''') = (1, \frac{268058128650415139}{8561814220800}, \frac{4555312284197913949}{59932699545600},$$

$$\frac{880203713205739499}{29966349772800}, \frac{442606459030301}{399551330304}, 1, 1),$$

$$(a_1^\circ, a_2^\circ, a_3^\circ, a_4^\circ, a_5^\circ, a_6^\circ, a_7^\circ) = (-\frac{31797138715241899}{71348451840}, \frac{39510888135471647}{23782817280},$$

$$-\frac{89842909122366067}{35674225920}, \frac{70301996244994553}{35674225920}, -\frac{19098605121088453}{23782817280}, \frac{1928394545986333}{14269690368}, 1),$$

$$(d_0^\circ, c^\circ, p^\circ) = (1, \frac{2722869100309}{37160652}, -\frac{46967954595971}{11891408640}),$$

$$(b_1^\circ, b_2^\circ, b_3^\circ, b_4^\circ, b_5^\circ, b_6^\circ, b_7^\circ) = (1, \frac{268058128650415139}{8561814220800}, \frac{4555312284197913949}{59932699545600},$$

$$\frac{880203713205739499}{29966349772800}, \frac{442606459030301}{399551330304}, 1, 1),$$

$$(a_1^\star, a_2^\star, a_3^\star, a_4^\star, a_5^\star, a_6^\star) = (-\frac{1503231188725049}{23782817280}, \frac{1867935336508597}{7927605760},$$

$$-\frac{4247624920328657}{11891408640}, \frac{3323910594809683}{11891408640}, -\frac{903030585746583}{7927605760}, \frac{91184360931935}{4756563456}),$$

$$(d_0^\star, c^\star, p^\star) = (1, \frac{128703046919}{12386884}, -\frac{2210375095681}{3963802880}),$$

$$(b_1^\star, b_2^\star, b_3^\star, b_4^\star, b_5^\star, b_6^\star) =$$

$$(1, \frac{12683929093362529}{2853938073600}, \frac{215355320923364639}{19977566515200}, \frac{41648028557578489}{9988783257600}, \frac{20633161916767}{133183776768}, 1),$$

$$(a_1^{\star\star},a_2^{\star\star},a_3^{\star\star},a_4^{\star\star},a_5^{\star\star})=(1,-\frac{847476}{464945},\frac{589659}{464945},-\frac{11907}{20215},\frac{152793}{929890},-\frac{19327}{929890}),$$
$$(d_0^{\star\star},c^{\star\star},p^{\star\star})=(1,-\frac{114723}{743912},\frac{1407483}{59512960}),$$
$$(b_1^{\star\star},b_2^{\star\star},b_3^{\star\star},b_4^{\star\star},b_5^{\star\star})=(\frac{199935287}{30470635520},-\frac{220288121}{152353177600},-\frac{774211293}{152353177600},$$
$$\frac{17670329}{152353177600},-\frac{629599}{15235317760}),$$

$$\begin{cases} t_1=\frac{16627547407}{804424777728000}h^{12}y_0^{(12)},\\ t_2=-\frac{53312770232930830091}{607573734913474560000}h^{12}y_0^{(12)},\\ t_3=-\frac{130278123730391934288 1}{18227212047404236800 0}h^{12}y_0^{(12)},\\ t_{n-3}=-\frac{1302781237303919342881}{182272120474042368000}h^{12}y_0^{(12)},\\ t_{n-2}=-\frac{53312770232930830091}{607573734913474560000}h^{12}y_0^{(12)},\\ t_{n-1}=\frac{16627547407}{804424777728000}h^{12}y_0^{(12)}, \end{cases} \tag{12}$$

At the mesh point x_i the proposed differential equation (1) may be discretized by:

$$L_i=g_i-f_iy_i, \tag{13}$$

where $L_i=S_i^{(8)}(x_i), f_i=f(x_i), g_i=g(x_i)$ and $y_i=y(x_i)$.
The local truncation error corresponding to the method (5) is given by

$$t_i=(1-2(\alpha+\beta+\gamma)-\delta))h^6y_i^{(6)}+(-\frac{1}{2}+\alpha+\beta+\gamma+\frac{1}{2}\delta)h^7y_i^{(7)}+$$
$$\frac{1}{8}(3-74\alpha-34\beta-10\gamma-\delta)h^8y_i^{(8)}+\frac{1}{48}(-7+218\alpha+98\beta+26\gamma+\delta)h^9y_i^{(9)}+$$
$$\frac{1}{1920}(121-15130\alpha-3530\beta-410\gamma-5\delta)h^{10}y_i^{(10)}+$$
$$\frac{1}{3840}(-77+13682\alpha+2882\beta+242\gamma+\delta)h^{11}y_i^{(11)}+$$
$$\frac{1}{967680}(6227-2798754\alpha-343434\beta-15330\gamma-21\delta)h^{12}y_i^{(12)}+$$
$$\frac{1}{1935360}(-3353+2236254\alpha+227814\beta+6558\gamma+3\delta)h^{13}y_i^{(13)}+$$
$$\frac{1}{10321920}(4681-6155426\alpha-397186\beta-6562\gamma-\delta)h^{14}y_i^{(14)}+$$
$$O(h^{15}),i=4,5,...,(n-4). \tag{14}$$

By using the above truncation error to eliminate the coefficients of various powers h we can obtain classes of the methods. For any choice of α,β,γ and δ

whose $2\alpha+2\beta+2\gamma+\delta=1$, , We obtain the following methods.

Remark(i): Second-order method
For $(\alpha,\beta,\gamma,\delta)=(\frac{1}{5040},\frac{120}{5040},\frac{1191}{5040},\frac{2416}{5040})$ we obtain the second-order method with truncation error $t_i=-\frac{1}{12}h^8y_i^{(8)}+O(h^9)$.
Remark(ii):Fourth-order method
For $(\alpha,\beta,\gamma)=(0,0,\frac{1}{4})$ and $\delta=\frac{1}{2}$, we obtain the fourth-order method with truncation error $t_i=\frac{1}{120}h^{10}y_i^{(10)}+O(h^{11})$.
Remark(iii): Sixth-order method
For $(\alpha,\beta,\gamma)=(0,\frac{1}{120},\frac{13}{60})$ and $\delta=\frac{11}{20}$, we obtain the sixth-order method with truncation error $t_i=\frac{1}{30240}h^{12}y_i^{(12)}+O(h^{13})$.
Remark(iv): Eight-order method
For $(\alpha,\beta,\gamma)=(\frac{1}{30240},\frac{41}{5040},\frac{2189}{10080})$ and $\delta=\frac{4153}{7560}$, we obtain the eight-order method with truncation error $t_i=\frac{-1}{57600}h^{14}y_i^{(14)}+O(h^{15})$.

4 Numerical results

Example 1. We Consider the following boundary-value problem

$$y^{(6)}(x)+y(x)=6(2xCos(x)+5Sin(x)),\quad -1\leq x\leq 1,$$

$$y(-1)=0, y''(-1)=-4Cos(-1)+2Sin(-1), y^{(4)}(-1)=8Cos(-1)-12sin(-1),$$
$$y(1)=0, y''(1)=4Cos(1)+2Sin(1), y^{(4)}(1)=-8Cos(1)-12sin(1) \qquad (15)$$

The exact solution for this problem is $y(x)=(x^2-1)Sin(x)$. We solved this example by different values of $h=\frac{1}{7},\frac{1}{15},\frac{1}{31}$ .The maximum absolute errors associated with y_i for the system (15) are summarized in Table 1 and compared with [2].

Example 2. We Consider the following boundary-value problem

$$y^{(6)}(x)+xy(x)=-(24+11x^3)e^x,\quad 0\leq x\leq 1,$$

$$y(0)=0, y''(0)=0, y^{(4)}(0)=-8,$$
$$y(1)=0, y''(1)=-4e, y^{(4)}(1)=-16e \qquad (16)$$

The exact solution for this problem is $y(x)=x(1-x)e^x$. We solved this example by different values of $h=\frac{1}{7},\frac{1}{15},\frac{1}{31}$ .The maximum absolute errors associated with y_i for the system (16) are summarized in Table 2 and compared with [2].

Table 1: Observed maximum absolute errors for example (1)

h	$\alpha=\frac{1}{30240},\beta=\frac{41}{5040}$, $\gamma=\frac{2189}{10080},\delta=\frac{4153}{7560}$	$\alpha=0,\beta=\frac{1}{120}$, $\gamma=\frac{13}{60},\delta=\frac{11}{20}$	[2]
$\frac{1}{7}$	4.3599×10^{-13}	7.4353×10^{-10}	1.78×10^{-8}
$\frac{1}{15}$	6.7431×10^{-14}	1.9817×10^{-11}	1.37×10^{-10}
$\frac{1}{31}$	1.5438×10^{-14}	2.6639×10^{-12}	9.45×10^{-11}

Table 2: Observed maximum absolute errors for example (2)

h	$\alpha=\frac{1}{30240},\beta=\frac{41}{5040}$, $\gamma=\frac{2189}{10080},\delta=\frac{4153}{7560}$	$\alpha=0,\beta=\frac{1}{120}$, $\gamma=\frac{13}{60},\delta=\frac{11}{20}$	[2]
$\frac{1}{7}$	2.69×10^{-14}	5.71×10^{-12}	1.15×10^{-9}
$\frac{1}{15}$	2.49×10^{-15}	3.61×10^{-12}	3.95×10^{-12}
$\frac{1}{31}$	4.57×10^{-13}	8.44×10^{-11}	4.41×10^{-11}

Conclusion

The new methods of orders 2,4,6 and 8 based on non-polynomial spline in off step points are developed for the solution of special sixth-order boundary-value problems.Tables 1and 2 shows that our methods produced better in the sense that max$|e_i|$ is minimum in comparison with the existing methods.

References

[**1**] H.N.Caglar,S.H.Caglar,E.H.Twizell,The numerical solution of third-order boundary-value problems with fourth-degree B-spline functions,*Int.J. Comput. Math.***71**,373-381(1999).

[**2**] Siraj-ul-Islam,Ikram A. Tirmizi, Fazal-i-Haq,M. Azam Khan, Non-polynomial splines approach to the solution of sixth-order boundary-value problems,*Appl. Math. Comput.***195**,270-284(2008).

[**3**] M. El-Gamel, J.R. Cannon, J. Latour, A.I. Zayed, Sinc-Galerkin method for solving linear sixth order boundary-value problems,*Mathematics of Computation.***73** (247),1325-1343(2003).

[**4**] S.S.Siddiqi.G.Akram,Septic spline solutions of sixth-order boundary value problems,*J.Comput.Appl. Math.*in press.

[**5**] K.Farajiyan,M.jafari,Spline approximate solution of eighth-order boundary-value problems,*38th AIMC,University of Zanjan*,3-6 September, 338-340(2007).

[**6**] J. Rashidinia, R. Jalilian and K. Farajeyan,Spline approximate solutions of fifth-order boundary value problems,*Appl.Math.Comput.***192**,107-112(2007).

JOURNAL OF APPLIED FUNCTIONAL ANALYSIS, VOL.6, NO.2, 145-154, COPYRIGHT 2011 EUDOXUS PRESS, LLC

Chaotic Structure Test and Predictability Analysis on Traffic Time Series in the City of Istanbul

Ugur Yankaya, H. Murat Celik
Izmir Institute of Technology, Architecture Faculty, City and Regional Planning, URLA / İZMİR
Tel: (0232) 750 70 54 / 750 70 30
uguryankaya@iyte.edu.tr, muratcelik@iyte.edu.tr

Serhan Ozdemir, Hakki Erhan Sevil
Izmir Institute of Technology, Engineering Faculty, Mechanical Engineering, URLA / İZMİR
Tel: (0232) 750 67 54 / 750 67 73
serhanozdemir@iyte.edu.tr, erhansevil@iyte.edu.tr

Abstract

Empirical studies suggest that traffic flow generally exhibits irregular and complex behavior. Modeling of traffic flow characteristics is difficult and needs new techniques. In this study, we analyzed chaotic structure in traffic time series data collected from an urban arterial in Istanbul over a period of about 1 week. Nonlinear techniques (correlation dimension and metric entropy) are used to identify chaotic structure. After detecting chaotic characteristics, the predictability of time series data was examined. It is found that the traffic flow at the main road of Ikitelli – Mahmutbey location displayed a periodicity close to 24 hrs, and a 100 minute long prediction interval which is indicative of low dimensional chaos as found from the computed metric entropy. Traffic time series data included speed, occupancy rates, and volume at each lane on the main road of Ikitelli – Mahmutbey on the European side.

Keywords: Chaotic systems, Traffic flow, Time series analysis, Correlation dimension, Metric entropy

1. INTRODUCTION

Many systems may exhibit complex, multi-dimensional, and irregular behaviors. For example, a system that may be known as a stochastic system may represent different characteristics such as chaotic and fractal. Therefore, different techniques need to be used to expand our understanding about the systems. In the last decade, nonlinear techniques to model and predict such complex systems have been applied by many researchers in various fields of natural - social sciences and engineering. Also, these techniques may give better results rather than deterministic techniques.

Recent studies have shown that transportation systems may exhibit chaotic or fractal behaviors (Lan et al., 2003; Nair et al. 2001; Li and Shang 2007; Shang et al., 2007; Frazier and Kockelman, 2004; Shang, Li, and Kamae, 2005; Xu et al., 2008; Shang et al., 2008). In spite of growing interest and voluminous empirical literature, there is no consensus that traffic flow exhibits fractal or chaotic behavior. Chaos theory implies system determinism. Transportation systems are affected from many factors such as human and weather factors. Therefore, the methods based on chaos theory may not be applied in the modeling of transportation systems, since these factors can be random rather than deterministic (Frazier and Kockelman, 2004).

Complex phenomena in general present a nonlinear behavior. Such systems are generally known as deterministic chaotic system. Traffic flow exhibits irregular and complex behavior (Nair et al., 2001; Shang, Li and Kamae, 2005). It is expected that nonlinear methods based on chaos theory (e.g. Lyapunov exponent, Correlation dimension, and Kolmogorov entropy) may provide better model performance for understanding behavioral structure of traffic and transportation systems. Nonlinear methods needs time series data set over a long time period. There is a lack of empirical studies in Turkey due to the lack of time series data for traffic flow characteristics. On the other hand, there is a growing interest about nonlinear analysis for traffic time series data in the literature. Therefore, gaining more contributions to the traffic flow from different cases and techniques needs to be explored. These contributions may provide information about predicting traffic flow dynamics and application in intelligent transportation systems. If we can understand the factors that produce chaos in a traffic flow, it can be possible to build new kinds of traffic models.

To determine the fractal or chaotic characteristics of a data set, different methods can be used. Power spectrum analysis (Shang et al. 2007 and Frazier and Kockelman 2004), Hurst exponent (Lan et al. 2003, Shang et al. 2007, Li and Shang 2007), correlation dimension (Lan et al. 2003, Frazier and Kockelman 2004, Shang et al. 2005, Shang et al. 2006), and the Lyapunov exponent (Lan et al. 2003, Shang et al. 2005, and Nair et al. 2001) are mostly used techniques. Since traffic flow has complex dimension, chaotic approaches are suitable for complex and multidimensional systems.

In the literature, there are a large amount of chaos and fractal studies in the last decade for communication networks like the internet and other fields. Many of these are related to network traffic. In the case of transportation systems, traffic time series data has been analyzed for only one location. Also, the outcomes of the studies in the literature differ substantially. Frazier and Kockelman (2004) applied chaotic data analysis techniques to traffic flow data for Freeway in California. Traffic flow data were analyzed by Fourier power series, the correlation dimension, and the largest Lyapunov exponent. In their study, traffic flow exhibits chaotic characteristics. Lan et al. (2003) tested the presence of chaos for traffic flow time series data. Hurst exponent, Lyapunov exponent, correlation dimension, and Kolmogorov entropy were calculated from the automatic traffic count records (different time scale) for 20 selected stations out of Miami Freeway in the United States. They found that there is a strong evidence of chaotic structure, rather than random. Shang et al. (2005) applied non-linear time series modeling techniques such as correlation dimension and Lyapunov exponent in order to analyze the traffic data collected from the Beijing Xizhimen Highway in China. The results indicated that chaotic characteristics exist in the traffic system. Xu and Gao (2007) investigated the dynamical behavior of network traffic flow, which is based on the dynamical gravity model in the case of origin – destination trip network. They found chaos in the traffic network. Shang et al. (2006) tested the presence of chaos in the traffic time series by employing the correlation dimension method for the highway in Beijing, China. They did not find strong evidence for the evidence of chaotic behavior in the dynamics of traffic time series. Shang et al. (2008) investigated multi-fractal behavior and long-range correlations in traffic time series for Highway data in China. It is realized that traffic time series has an almost mono-fractal behavior. Also, traffic speed fluctuation is turned out to be a multi-fractal. Shang et al. (2007) investigated the presence of fractal in the traffic data for Beijing Yuquanying Highway in China. The power spectrum, the empirical probability distribution function, the statistical moment scaling function, and the autocorrelation functions were used. Traffic time series data exhibited fractal behavior. Li and Shang (2007) studied to determine whether multi-fractal parameters could be used to classify of traffic flow for Beijing Yuquanying Highway. Their analysis was mainly based on Hurst exponent. They found that multi-fractal process is appropriate in the analysis of the traffic flow. Belomestny and Siegel (2003) investigated statistical properties of highway velocity time series data obtained from German highways. There is a strong evidence of a long-range dependence. Also, they found that time series data set has stochastic nature. Wang et al. (2005) tried to forecast the traffic flow in a short-term based on theory of chaos and to identify the chaos in traffic flow time series for Shangai City in China. There is chaos in traffic flow. Also, approaches based on deterministic chaos can be effective in short-term traffic flow forecast. Nair et al. (2001) analyzed traffic flow data and characterized it as chaotic.

Traffic system management is an important tool to use transportation system capacity efficiently in recent years. The tool needs to predict condition of the system from a time to another time with real-time data. Therefore, it is known how the factors such as traffic signals directing the system will behave in the next position. There may be differences between prediction and observation. However, we should have prior information about the probable condition at t+1 time. What signal times should be is important for effective usage of existing capacity. In addition, the determination of the flexibility of the system against unexpected situations is important. It is worthwhile Whether or not the data relate to the system at a time have reliable information about the condition of the system at the next time. This study examines system predictability considering traffic flow characteristics for continental crossing in Istanbul.

2. NONLINEAR TIME SERIES ANALYSIS

In general, dimension is the number of parameters is needed to identify of an object. The dimension of a line is 1, and for a plane it is 2. However, as in many examples in everyday life, all objects are not smooth as geometrically. Complex, non-integer dimensions are called fractal dimensions. Considering that the most of naturally observed phenomena, or scientific researches have nonlinear dynamics and due to the fact that non-linear dynamics (especially chaotic systems) have fractal dimensions, the importance of fractal dimension analysis methods have increased, especially in recent years.

In this study, the variation in non-linear dynamical quantities of Istanbul traffic data was analyzed. In short, the purpose of this study is to test the predictability of traffic flow data through nonlinear time series analysis techniques, and to provide accurate forecasting information for advanced signaling systems.

2.1. Correlation Dimension

Correlation dimension is used to determine the geometry and complexity of an attractor. Correlation dimension is calculated via correlation sum. The correlation sum of a certain point s_n in a vector space is simply the sum of the all points in a "epsilon" (ε) neighborhood. In this study, calculation methods, which were introduced by Kantz and Schreiber (Kantz and Schreiber, 1997) will be the used for nonlinear invariants. More information on nonlinear invariants and their calculation methods can be found in previous works of the authors (Sevil, 2006).

The correlation sum of a time series can be found by the following equation:

$$C(\varepsilon) = \frac{2}{N(N-1)} \sum_{i=1}^{N} \sum_{j=i+1}^{N} H(\varepsilon - \|\mathbf{s}_i - \mathbf{s}_j\|) \qquad (1)$$

Where N is the total number of points and H Heaviside is the step function.

In equation (1), the variable **s** represents the vectors that are obtained through embedding the scalar values to a phase space. The embedding method is nothing but creating m dimensional vectors from one dimensional data by using method of delay, which can be calculated as

$$\mathbf{s}_n = \left(s_n, s_{n-v}, \ldots, s_{n-(m-2)v}, s_{n-(m-1)v}\right) \qquad (2)$$

where $\mathbf{s}_n$ is the vector, m is the dimension of the vector and s_i represent the real time series data. In equation (2), the parameter v is the optimal lag and can be obtained either using autocorrelation function or average mutual information function. In this study, average mutual information function is used for determining optimal lag v.

Correlation sum, basically, is equal to the total number of neighbor points (s_i ,s_j) which are closer than a distance ε. Considering infinite number of data points with ε is approaching to zero, it is expected that correlation sum has an exponential relation with the parameter ε

$$C(\varepsilon) \propto \varepsilon^D \qquad (3)$$

From equation (3), a dimension value D based on the behavior of a correlation sum, can be defined (Eqn 4). This dimension is called correlation dimension and it is quantitative value for time series.

$$D = \lim_{\varepsilon \to 0} \lim_{N \to \infty} \frac{\log C(N, \varepsilon)}{\log \varepsilon} \qquad (4)$$

2.2. Metric Entropy (Kolmogorov – Sinai Entropy)

Metric entropy is quantitative measure used to characterize the chaotic behavior of the systems in multi-dimensional phase space. Metric entropy is proportional to loss of information of a dynamical system for a certain time. In other words, metric entropy represents the predictability of a given system, and it originates from information theory. Considering the observation of a system as a source of information, metric entropy gives a quantity about its predictability while entire past of the system has been observed. The lower limit of informational metric entropy can be defined by using time series analysis.

In the literature, the relation between metric entropy and the predictability of a system, and the real life implementation of this relation was presented (Sevil and Ozdemir, 2006). Metric entropy of a time series is equal to

$$K_2 = \lim_{m\to\infty} \lim_{\varepsilon\to 0} \log \frac{C(m,\varepsilon)}{C(m+1,\varepsilon)} \tag{5}$$

In equation (5), the subscript 2 represents that the metric entropy value that is calculated by time series analysis is the lower limit of the metric entropy value determined from information theory.

3. TRAFFIC FLOW DATA and DATA ANALYSIS

In this study, we use the traffic flow data observed on the urban arterial in European site in Istanbul over a period of about 1 week, from 11/24/2008 to 11/30/2008 (24 h for each day). Our testing data come from the automatic traffic count records called as RTMs for each lane of the selected roads. The data were obtained from Istanbul Metropolitan Municipality, Department of Transportation and Directorate of Traffic. The raw data includes speed, volume, and occupancy rates. They are collected every ten minutes for each lane. We analyzed mainly speed data in the concept of this study. Some studies in the literature analyzed different time scales of 1 minute, 3 minute, 5 minute, 10 minute. In Istanbul, traffic counts are only recorded in the time scales of 10 and 30 minutes. In the concept of the study, we only analyze traffic speed data at second lane (s2) collected from RTMS22 reading the traffic flow crossing from Ikitelli to Mahmutbey (Figure 1 / RTMS22).

Figure 2 represents the time series plot of the speed data observed over a period of about 1 week. The fluctuations can only be seen in speed data. The detecting chaotic structure is difficult. Therefore, we need additional methods identifying behavior of time series data.

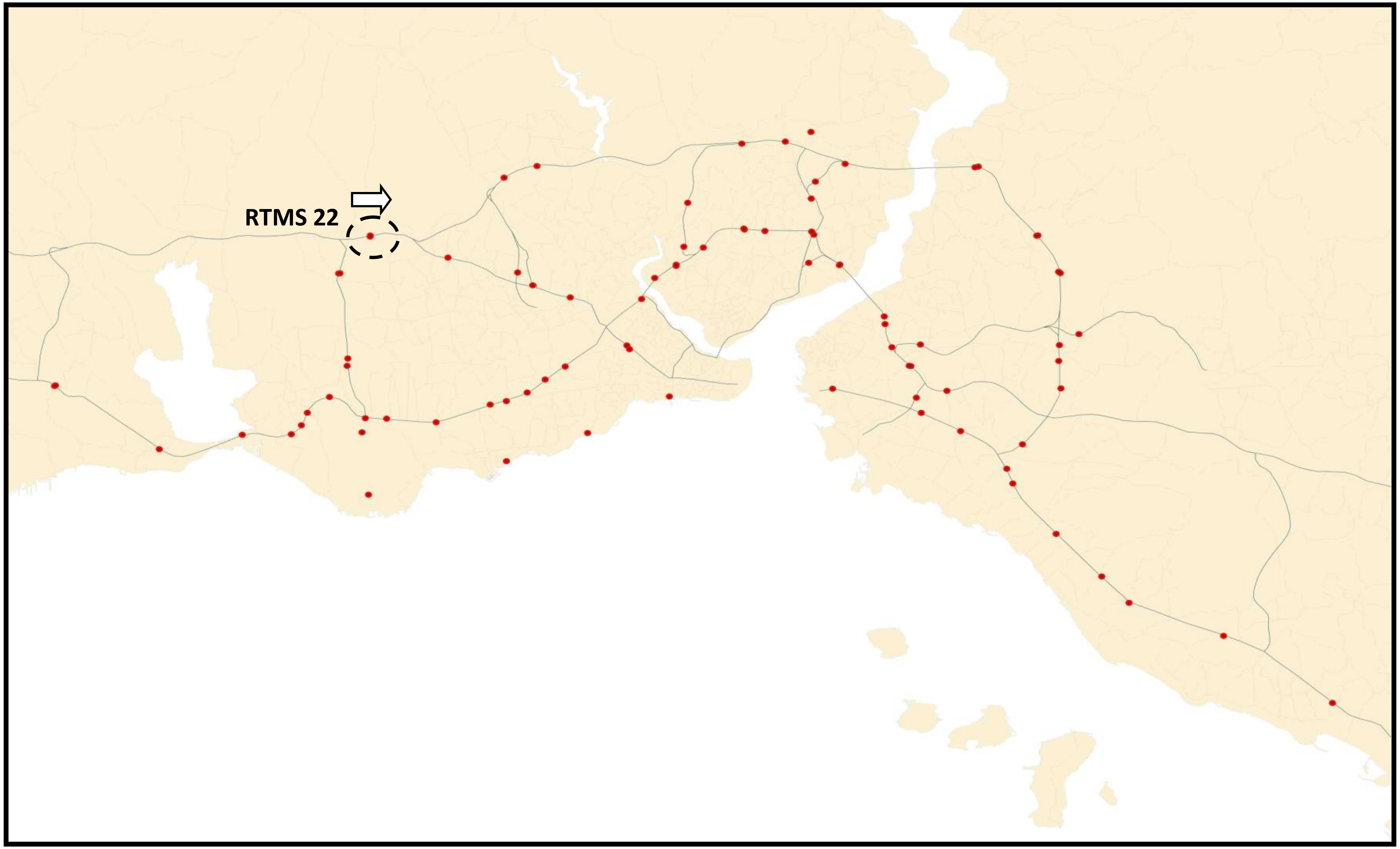

Figure 1: The sensor locations on the main roads in Istanbul

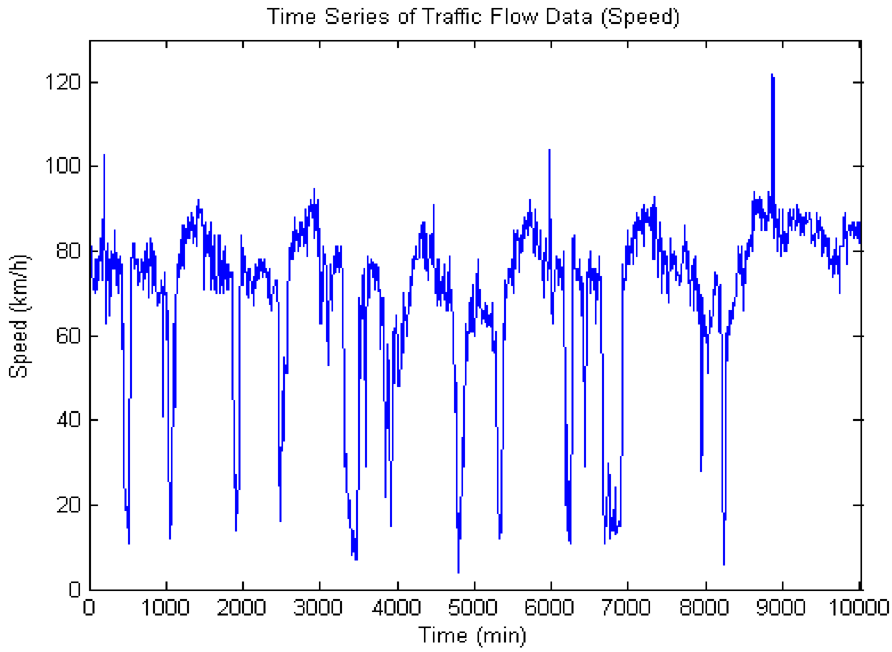

Figure 2: Traffic Flow data (speed) of the direction through Ikitelli – Mahmutbey (rtms22/s2)

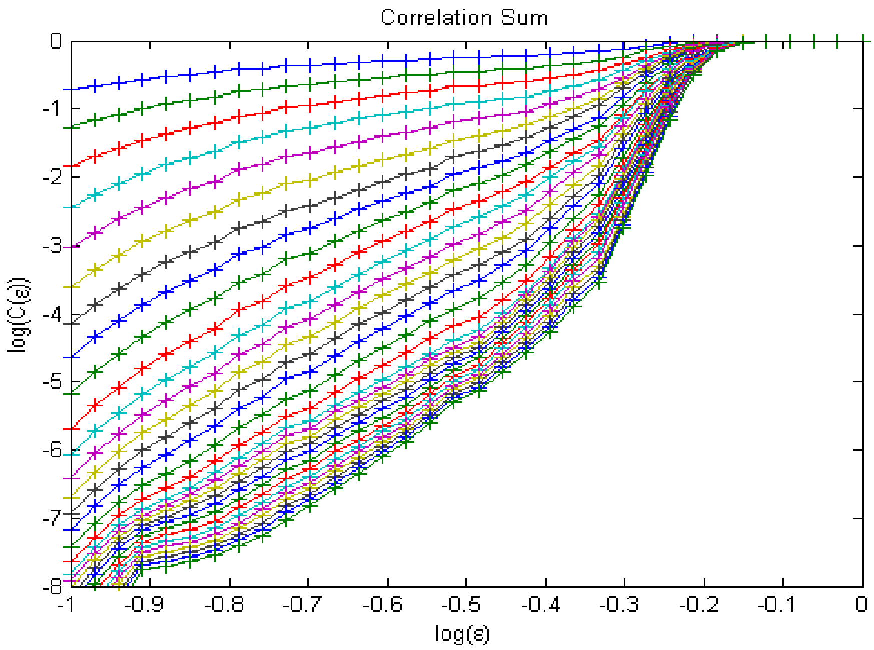

Figure 3: Correlation Sum of Traffic Flow data

Primarily, the scalar data has been normalized and transformed into phase space using method of delay-reconstruction. Then, for different embedding dimensions (m=1-30), correlation sum values were calculated (Figure 3). As shown in equation (4), the slope of correlation sum graph gives the correlation dimension plot (Figure 4 - Left). Due to the limit property, linear part (plateau) of the correlation dimension plot indicates the final dimension which is a characteristic value for the system. In that region, the correlation dimension values can be represented due to changing embedding dimension and after a certain point the value will be constant. (Figure 4-Right, D ~ = 3.17).

For scalar time series, the correlation dimension is a value that used to characterize the series. For instance, using correlation dimension, two traffic data in different times or different locations can be compared and be commented about their behaviors. Additionally, if correlation dimension values are rated (Eqn. 5), metric entropy graph is obtained (Fig. 5 - left). Likewise, the linear part can be plotted with respect to variable embedding dimensions, the steady state value indicates the metric entropy (K ~ = 0.1) of the particular system.

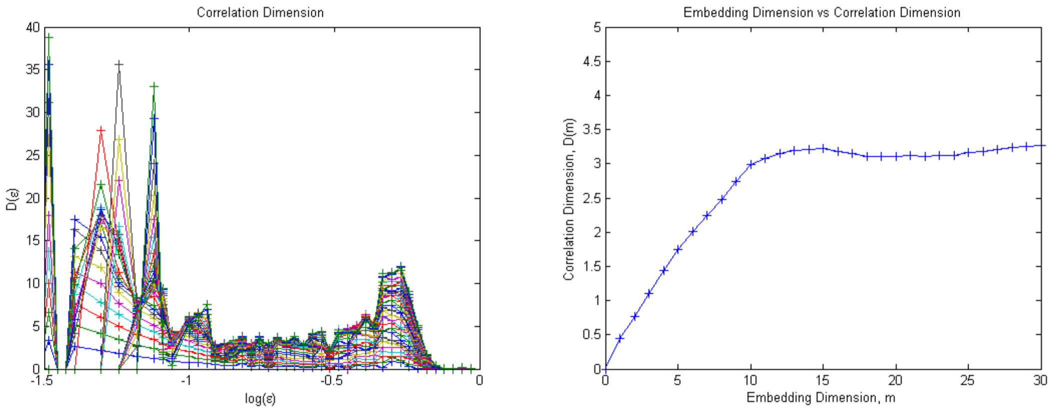

Figure 4: Correlation Dimension and Correlation Dimension variation plots for traffic flow data

Predictability of traffic data can be found by taking the inverse of metric entropy. For the particular implementation of this study, predictability is obtained as 10 (Δt_{max}=1/0.1) according to metric entropy value. Considering the sampling time of the data, it can be said that the predictions up to 100 minutes will have high level of accuracy. In the literature, a similar application was made for the Beijing Highways (Shang, Li, and Kaman, 2005) and predictability was calculated via maximum Lyapunov exponent. We believe that these results are unreliable, due to fact that the research of Shang and his colleagues was based only on largest Lyapunov exponent. According to Pesin's Identity, Metric Entropy is equal to sum of the positive Lyapunov exponents, where K_2 is the lower limit for this summation. Predictions that are only based on the largest Lyapunov exponent could be misleading. In case of multiple positive Lyapunov exponent existence, the prediction times would be greater than actual values.

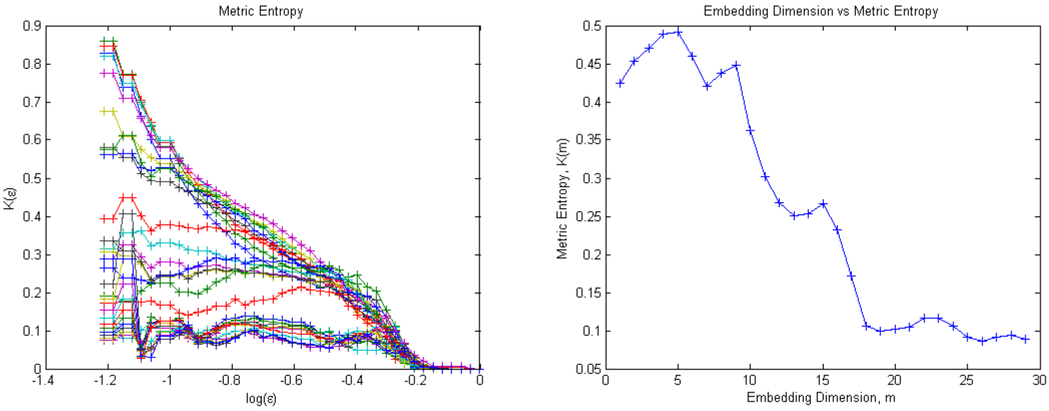

Figure 5: Metric Entropy and Metric Entropy variation plots for traffic flow data

4. CONCLUSION

In this study, on the traffic flow data collected from one of the major traffic artery of Istanbul, the direction of Ikitelli – Mahmutbey, a series of nonlinear analysis have been performed and exhibit of chaotic behavior is shown. Although not given here, the average mutual information analysis also has been made and the data was determined as almost periodic (23.33 hours). The reason of the result is just under 24 hours may depend on computational sensitivity. This almost periodicity led to a low K_2 value. The data is therefore highly deterministic, but it has a low-dimensional chaotic characteristic. In almost all chaos literature, it is recommended to approach low K_2 values with suspicion. The basis of this concern relies on the fact that real- K_2 values could be blocked under the noise. The authors think that it is important to place this warning here.

The effect of noise on traffic flow data as well as determining the type and magnitude of that noise is left as a future work. Obtained value of $K_2 = 0.1$ leads to a 100 min predictability, which provides a longer time frame for prediction and reaction by the authorities compared to highway sections around the world. If it is assumed that the results are accurate, it can be compared with the result of 8 min found by Shang and his colleagues as mentioned above. The predictability value of 8 min indicates that the analyzed dynamic of Beijing Highways segment traffic is more complex and less predictable, in contrast to the traffic in the direction Ikitelli-Mahmutbey. Relatively low predictability values are not beneficial for traffic planners. As a future study, the parameters, which affect the predictability, can be investigated and be adjusted in such way to increase the predictability time.

Acknowledgments

We would like to thank to Department of Transportation of Istanbul Greater Municipality for making the data available.

References

Journal Article

1. C. Fraizer and Kara M. Kockelman, Chaos theory and transportation systems: an instructive example, *Transportation Research Record*, 1897, 9-17 (2004).

2. L. W. Lan, Feng-Yu Lin, and A. Y. Kuo, Testing and prediction of traffic flow dynamics with chaos. *Journal of the Eastern Asia Society for Transportation Studies*, 5, (2003).

3. X. Li and P. Shang, Multifractal classification of road traffic flows. *Chaos, Solitons & Fractals*, 31, 1089-1094 (2007).

4. P. Shang, X. Li, and S. Kamae, Chaotic analysis of traffic time series. *Chaos, Solutions and Fractals*, 25, 121-128 (2005).

5. P. Shang, X. Li, and S. Kamae, Nonlinear analysis of traffic time series at different temporal scales, *Physics Letters A*, 357, 314-318 (2006).

6. P. Shang, Y. Lu, and S. Kama, The application of hölder exponent to traffic congestion warning. *Physica A*, 370, 769 – 776 (2006).

7. P. Shang, Y. Lu, and and S. Kamae, Detecting long-range correlations of traffic time series with multifractal detrended fluctuation analysis, *Chaos, Solutions and Fractals*, 36, 82-90 (2008).

8. P. Shang, M. Wan, and S. Kama, Fractal nature of highway traffic data, *Computers and Mathematics with Applications*, 54, 107-116 (2007).

9. Na Xu, P. Shang, and S. Kamae, Minimizing the effect of exponential trends in detrended fluctuation analysis, *Chaos, Solutions and Fractals*, Article in Press (2008).

Book

10. H. Kantz and T. Schreiber, *Nonlinear Time Series Analysis*, Cambridge University Press, 1997.

Conferences

11. D. Belomestny and H. Siegel, Stochastic and self-similar nature of highway traffic data, ISBN 3-88722-568-6 (2003).

12. H. E. Sevil and S. Ozdemir, Prediction of a Small Diameter Drill Bit Breakage Using Metric Entropy. Proceedings of Int. Colloquium on Math. in Eng. and Num. Physics, Bucharest, Romania, pp. 120-123, 2006.

13. Attoor Sanju Nair, Jyh-Charn Liu, Laurence Rilett and Saurabh Gupta, Non-Linear Analysis of Traffic Flow, IEEE Intelligent Transportation systems Conference Proceedings, Oakland, USA, (2001).

Thesis

14. H. E. Sevil, On *the Predictability of Time Series by Metric Entropy*. M.Sc. Thesis, Izmir Institute of Technology, Izmir, Turkey, 2006.

JOURNAL OF APPLIED FUNCTIONAL ANALYSIS, VOL.6, NO.2, 155-164, COPYRIGHT 2011 EUDOXUS PRESS, LLC

Algebraic structures arising in statistical mechanics

A.M. Scarfone

Dipartimento di Fisica and
Istituto Nazionale per la Fisica della Materia (CNR–INFM)
Sezione del Politecnico di Torino, I-10129, Italy.
Email: antonio.scarfone@polito.it

March 2, 2010

Complex systems have statistical proprieties that differ greatly from those of classical systems governed by the Boltzmann-Gibbs entropy. Often, the probability distribution observed in these systems deviate from the Gibbs one, showing asymptotic behavior with stretched exponential, power law or log-oscillating tails. Recently, several entropic forms have been introduced in the literature to take into account the new phenomenologies observed in such systems. In this paper, we show that for any trace-form entropy one can introduce a pair of algebraic structures with a generalized sum and a generalized product, each forming a commutative groups. These generalized operations may be useful in developing the corresponding statistical theory. We specify our results to some entropic forms already known in literature presenting the related algebraic structures.

Keywords: Entropic forms, Algebraic structures, Anomalous statistical systems, Power-law distributions, Generalized logarithms and exponentials

1 Introduction

A method for introducing generalized entropies is to replace the logarithmic function in the Shannon-Boltzman-Gibbs entropy, that, for convenience, we rewrite as

$$S^{\mathrm{SBG}}[p] = -\sum_{i=1}^{W} \int_0^{p_i} \ln x \, dx + \int_0^1 \ln x \, dx \ , \tag{1}$$

with its generalized version: $\ln x \to \widetilde{\ln}\, x$. In this way, we obtain the following entropic form

$$S[p] = -\sum_{i=1}^{W} \int_{0}^{p_i} \widetilde{\ln}\, x\, dx + \int_{0}^{1} \widetilde{\ln}\, x\, dx \ , \tag{2}$$

where $p \equiv \{p_i \in I\!R^+\}_{1,\ldots,W}$ is a set of probabilities for the W possible outcomes of a given observable.
In the following, we require that $\widetilde{\ln}\, x$ is a monotonically increasing and concave function

$$\frac{d}{d\,x}\,\widetilde{\ln}\, x > 0 \ , \qquad\qquad \frac{d^2}{d\,x^2}\,\widetilde{\ln}\, x < 0 \ . \tag{3}$$

Without lost of generality, we can impose $\widetilde{\ln}\, 1 = 0$ which assures the condition $S[1] = 0$, namely that entropy vanishes for a perfectly ordered system. Moreover, we assume $\widetilde{\ln}\, x \in (-\infty,\, x_{\rm max})$ for $x \in (0,\, +\infty)$, with $x_{\rm max} \leq +\infty$.
In this way, the inverse function of $\widetilde{\ln}\, x$ certainly exist and appears to be a monotonically increasing and convex function

$$\frac{d}{d\,x}\,\widetilde{\exp}\, x > 0, \qquad\qquad \frac{d^2}{d\,x^2}\,\widetilde{\exp}\, x > 0, \tag{4}$$

with $\widetilde{\exp}\, 0 = 1$ and $\widetilde{\exp}\, x \in (0,\, +\infty)$ for $x \in (-\infty,\, x_{\rm max})$.
According to the maximal entropy principle, the equilibrium distribution is the one that maximizes the entropic form constrained by appropriate boundary conditions

$$\sum_{i=1}^{W} p_i\, \phi_{ij} = \mathcal{O}_j \ , \tag{5}$$

with $j = 0,\, 1,\, \ldots M$. Thay fix the values of various observable related to the system under inspection whose possible outcomes are given by ϕ_{ij}.
This can be accomplished through the following variational problem

$$\delta \left(S[p] + \sum_{j=0}^{M} \mu_j \sum_{i=1}^{W} p_i\, \phi_{ij} \right) = 0 \ . \tag{6}$$

Quite often, the constraints represent the moments of a given order of the possible outcomes in an experimental measure. For instance, $\phi_{i0} = 1$, with $\mathcal{O}_0 = 1$, fixes the normalization of the distribution, $\phi_{i1} = x_i$, with $\mathcal{O}_1 \equiv \mu$, fixes its mean value, $\phi_{i2} = x_i^2$, with $\mathcal{O}_2 \equiv \sigma^2$, fixes the variance, and so on.
In this way, from the problem (6) we obtain the generalized distribution function

$$p_i \equiv p(\tilde{x}_i) = \widetilde{\exp}(-\tilde{x}_i) \ , \tag{7}$$

with $\tilde{x}_i = \sum_{j=0}^{M} \mu_j\, \phi_{ij}$.

In Ref. [1], in the framework of the κ-deformed statistical mechanics, it has been suggested to introduce some generalized operations with the purpose of extending some proprieties of logarithm and exponential to the corresponding κ-deformed functions. Shortly afterwards, another generalized algebraic structure has been introduced in the picture of the q-deformed statistical mechanics [2, 3]. These algebraical formalisms are results useful in various applications ranging from the Laplace transformations [4], the Fourier transformation [5], the central limit theorem [6], the combinatorial analysis [7, 8], the Gauss law of error [9] and more.

More recently, in [10], it has been advanced a method to unify these already known mathematical structures starting from an arbitrary bijective function. In this paper, we show that this bijective function can be actually derived from a given trace-form entropy afford to construct two different algebraic structures having the Abelian group structure. In this way, we can establish a link between the statistical mechanics based on a generalized entropic form and the emerging algebraic structures.

2 Generalized algebras

Starting from the functions $f(x) \equiv \widetilde{\exp}\, x$ and $g(x) \equiv \widetilde{\ln}\, x$ we can construct two pairs of operations consisting of a generalized sum and product forming two distinct algebras.
To begin with, we define the following operations

$$x \oplus y = f\big(\ln\big(\exp g(x) + \exp g(y)\big)\big), \tag{8}$$

$$x \otimes y = f\big(g(x) + g(y)\big), \tag{9}$$

for any x, $y \in I\!\!R^+$, although their extension to negative numbers can be easily accomplished.

Theorem 1. The algebraic structure $\mathcal{A} \equiv (I\!\!R^+, \oplus, \otimes)$ forms an Abelian field where sum $\oplus : I\!\!R^+ \times I\!\!R^+ \to I\!\!R^+$ and product $\otimes : I\!\!R^+ \times I\!\!R^+ \to I\!\!R^+$ fulfill the following proprieties

1. Commutative : $x \oplus y = y \oplus x$;
   $x \otimes y = y \otimes x$;
2. Associative : $x \oplus (y \oplus z) = (x \oplus y) \oplus z$;
   $x \otimes (y \otimes z) = (x \otimes y) \otimes z$;
3. Null and identity : $x \oplus 0 = 0 \oplus x = x$;
   $x \otimes 1 = 1 \otimes x = x$;
4. Opposite and inverse : $x \oplus (-x) = (-x) \oplus x = 0$;
   $x \otimes (1/x) = (1/x) \otimes x = 1$;
5. Distributive : $x \otimes (y \oplus z) = (x \otimes y) \oplus (x \otimes z)$.

where $1/x = f\big(-g(x)\big)$, while the sum with negative numbers is defined as

$$x \oplus (-y) \equiv x \ominus y = f\Big(\ln\big(\exp g(x) - \exp g(y)\big)\Big) \ . \tag{10}$$

Proof. For the sum $\oplus$ we have

1. Commutative :
$$\begin{aligned} x \oplus y &= f\Big(\ln\big(\exp g(x) + \exp g(y)\big)\Big) \\ &= f\Big(\ln\big(\exp g(y) + \exp g(x)\big)\Big) = y \oplus x \ . \end{aligned}$$
2. Associative :
$$\begin{aligned} x \oplus (y \oplus z) &= x \oplus f\Big(\ln\big(\exp g(y) + \exp g(z)\big)\Big) \\ &= f\Big(\ln\big(\exp g(x) + \exp g(y) + \exp g(z)\big)\Big) \\ &= f\Big(\ln\big(\exp g(x) + \exp g(y)\big)\Big) \oplus z = (x \oplus y) \oplus z \ . \end{aligned}$$
3. Null element :
$$\begin{aligned} x \oplus 0 &= f\Big(\ln\big(\exp g(x) + \exp g(0)\big)\Big) \\ &= f\Big(\ln\big(\exp g(x)\big)\Big) = f\big(g(x)\big) = x \ . \end{aligned}$$
4. Opposite :
$$x \oplus (-x) = f\Big(\ln\big(\exp g(x) - \exp g(x)\big)\Big) = f(-\infty) = 0 \ .$$

In the same way, for the product $\otimes$ we have

1. Commutative :
$$x \otimes y = f\big(g(x) + g(y)\big) = f\big(g(y) + g(x)\big) = y \otimes x \ .$$
2. Associative :
$$\begin{aligned} x \otimes (y \otimes z) &= x \otimes f\big(g(y) + g(z)\big) \\ &= f\big(g(x) + g(y) + g(z)\big) \\ &= f\big(g(x) + g(y)\big) \otimes z = (x \otimes y) \otimes z \ . \end{aligned}$$
3. Identity element :
$$x \otimes 1 = f\big(g(x) + g(1)\big) = f\big(g(x)\big) = x \ .$$
4. Inverse :
$$x \otimes (1/x) = f\big(g(x) + g(1/x)\big) = f(0) = 1 \ .$$

Finally

5. Distributive :
$$\begin{aligned} x \otimes (y \oplus z) &= x \otimes f\Big(\ln\big(\exp g(y) + \exp g(z)\big)\Big) \\ &= f\Big(g(x) + \ln\big(\exp g(y) + \exp g(z)\big)\Big) \\ &= f\Big(\ln\big(\exp g(x)\big) + \ln\big(\exp g(y) + \exp g(z)\big)\Big) \\ &= f\Big(\ln\Big(\exp\big(g(x) + g(y)\big) + \exp\big(g(x) + g(z)\big)\Big)\Big) \\ &= f\Big(\ln\Big(\exp\big(g(x \otimes y)\big) + \exp\big(g(x \otimes z)\big)\Big)\Big) \\ &= (x \otimes y) \oplus (x \otimes z) \ . \end{aligned}$$
$\diamond$

It is worthily to observe that the product $\otimes$ fulfills the further two relations

$$f(x)\otimes f(y)=f(x+y)\ , \tag{11}$$
$$g(x\otimes y)=g(x)+g(y)\ , \tag{12}$$

that mimic the similar proprieties of the standard logarithm and exponential: $\exp x\cdot\exp y=\exp(x+y)$ and $\ln(xy)=\ln x+\ln y$.

A second pair of operations can be defined as follows

$$x\tilde{\oplus}y=g\big(f(x)\,f(y)\big), \tag{13}$$
$$x\tilde{\otimes}y=g\big(\exp\big(\ln f(x)\,\ln f(y)\big)\big), \tag{14}$$

for any $x,\,y\in\widetilde{I\!R}$, where $\widetilde{I\!R}\in(-\infty,\,x_{\rm min})$.

Theorem 2. The algebraic structure $\widetilde{\mathcal{A}}\equiv(\widetilde{I\!R},\,\tilde{\oplus},\,\tilde{\otimes})$ forms an Abelian field where the sum $\tilde{\oplus}:\,\widetilde{I\!R}\times\widetilde{I\!R}\to I\!R^+$ and the product $\tilde{\otimes}:\,\widetilde{I\!R}\times\widetilde{I\!R}\to I\!R^+$ fulfill the following proprieties

1. Commutative : $x\tilde{\oplus}y=y\tilde{\oplus}x$;
   $x\tilde{\otimes}y=y\tilde{\otimes}x$;
2. Associative : $x\tilde{\oplus}(y\tilde{\oplus}z)=(x\tilde{\oplus}y)\tilde{\oplus}z$;
   $x\tilde{\otimes}(y\tilde{\otimes}z)=(x\tilde{\otimes}y)\tilde{\otimes}z$;
3. Null and identity : $x\tilde{\oplus}0=0\tilde{\oplus}x=x$;
   $x\tilde{\otimes}I=I\tilde{\otimes}x=x$;
4. Opposite and inverse : $x\tilde{\oplus}(-x)=(-x)\tilde{\oplus}x=0$;
   $x\tilde{\otimes}(1/x)=(1/x)\tilde{\otimes}x=I$;
5. Distributive : $x\tilde{\otimes}(y\tilde{\oplus}z)=(x\tilde{\otimes}y)\tilde{\oplus}(x\tilde{\otimes}z)$.

where $-x=g\big(1/f(x)\big)$, $1/x=g\big(\exp\big(1/\ln f(x)\big)\big)$ and $I=g(e)$.

Proof. For the sum $\tilde{\oplus}$ we have

1. Commutative :
   $$x\tilde{\oplus}y=g\big(f(x)\,f(y)\big)=g\big(f(y)\,f(x)\big)=y\tilde{\oplus}x\ .$$
2. Associative :
   $$x\tilde{\oplus}(y\tilde{\oplus}z)=x\tilde{\oplus}g\big(f(y)\,f(z)\big)=g\big(f(x)\,f(y)\,f(z)\big)$$
   $$=g\big(f(x)\,f(y)\big)\tilde{\oplus}z=(x\tilde{\oplus}y)\tilde{\oplus}z\ .$$
3. Null element :
   $$x\tilde{\oplus}0=g\big(f(x)\,f(0)\big)=g\big(f(x)\big)=x\ .$$
4. Opposite :
   $$x\tilde{\oplus}(-x)=g\big(f(x)\,f(-x)\big)=g(1)=0\ .$$

In the same way, for the product $\tilde{\otimes}$ we have

1. Commutative :
$$\begin{aligned} x\tilde{\otimes}y &= g\Big(\exp\big(\ln f(x)\ \ln f(y)\big)\Big) \\ &= g\Big(\exp\big(\ln f(y)\ \ln f(x)\big)\Big) = y\tilde{\otimes}x\ . \end{aligned}$$
2. Associative :
$$\begin{aligned} x\tilde{\otimes}(y\tilde{\otimes}z) &= x\tilde{\otimes}g\Big(\exp\big(\ln f(y)\ \ln f(z)\big)\Big) \\ &= g\Big(\exp\big(\ln f(x)\ \ln f(y)\ \ln f(z)\big)\Big) \\ &= g\Big(\exp\big(\ln f(x)\ \ln f(y)\big)\Big)\tilde{\otimes}z = (x\tilde{\otimes}y)\tilde{\otimes}z\ . \end{aligned}$$
3. Identity element :
$$\begin{aligned} x\tilde{\otimes}I &= g\Big(\exp\big(\ln f(x)\ \ln f(I)\big)\Big) \\ &= g\big(f(x)\big) = x\ . \end{aligned}$$
4. Inverse :
$$\begin{aligned} x\tilde{\otimes}(1/x) &= g\Big(\exp\big(\ln f(x)\ \ln f(1/x)\big)\Big) \\ &= g(e) = I\ . \end{aligned}$$

Finally

5. Distributive :
$$\begin{aligned} x\tilde{\otimes}(y\tilde{\oplus}z) = x\tilde{\otimes}g\big(f(y)\,f(z)\big) &= g\Big(\exp\big(\ln f(x)\ \ln\big(f(y)\,f(z)\big)\big)\Big) \\ &= g\Big(\exp\big(\ln f(x)\ln f(y) + \ln f(x)\ln f(z)\big)\Big) \\ &= g\Big(\exp\big(\ln f(x)\ln f(y)\big)\exp\big(\ln f(x)\ln f(z)\big)\Big) \\ &= g\big(f(x\tilde{\oplus}y)\,f(x\tilde{\oplus}z)\big) = (x\tilde{\otimes}y)\tilde{\oplus}(x\tilde{\otimes}z)\ . \end{aligned}$$ ◇

Remarkably, the sum $\tilde{\oplus}$ fulfills the following relations

$$f(x\tilde{\oplus}y) = f(x)\,f(y)\ , \tag{15}$$
$$g(x)\tilde{\oplus}g(y) = g(xy)\ , \tag{16}$$

which are the dual of Eqs. (11) and (12).

3 Examples

Let us specialize algebras studied in the previous Section to the case of some distributions known in literature.

3.1 Student distribution

Consider the following entropic form

$$S_\nu[p] = -\frac{1}{\nu}\sum_{i=1}^{W}\left(p_i - p_i^{1-\nu}\right)\ . \tag{17}$$

Its maximization, with the constraints of the normalization and the variance $\sigma^2 = (2-\nu)/(2-3\,\nu)$, with $0 < \nu < 2/3$, gives the well-know Student distribution

$$p(x_i) = \sqrt{\frac{\nu}{\pi\,(2-\nu)}}\,\frac{\Gamma\left(\frac{1}{\nu}\right)}{\Gamma\left(\frac{1}{\nu}-\frac{1}{2}\right)}\,\left(1+\frac{\nu}{2-\nu}\,x_i^2\right)^{-1/\nu} \quad , \tag{18}$$

that can be rewritten as

$$p(\tilde{x}_i) = (1+\nu\,\tilde{x}_i)^{-1/\nu} \quad , \tag{19}$$

with $\tilde{x}_i = (1+\mu_0+\mu_2\,x_i^2)/(1-\nu)$ and $\tilde{x}_{\rm max} = -1/\nu$.
Entropy (17) follows from Eq. (2) by posing

$$f(x) = (1-\nu\,x)^{-1/\nu} \quad , \tag{20}$$

where

$$g(x) = \frac{1}{\nu}\,\left(1-x^{-\nu}\right) \quad , \tag{21}$$

is its inverse function.
The related algebraic structures are generated by the operations

$$x\oplus y = \nu\,\left[h_+(x,\,y)-\ln\left(2\,\cosh h_-(x,\,y)\right)\right]^{-1/\nu} \quad , \tag{22}$$

$$x\otimes y = \left(x^{-\nu}+y^{-\nu}-1\right)^{-1/\nu} \quad , \tag{23}$$

where we posed

$$h_\pm(x,\,y) = \frac{x^{-\nu}\pm y^{-\nu}}{2\,\nu} \quad , \tag{24}$$

and

$$x\tilde{\oplus}y = x+y-\nu\,x\,y \ , \tag{25}$$

$$x\tilde{\otimes}y = \frac{1}{\nu}\left[1-\exp\left(-\frac{1}{\nu}\,\ln(1-\nu\,x)\,\ln(1-\nu\,y)\right)\right] \quad . \tag{26}$$

3.2 Cauchy-Lorentz distribution

In the $\nu\to 1$ limit, Eq. (18) reduces to the Cauchy-Lorentz distribution

$$p(\tilde{x}_i) = \frac{1}{\pi}\,\frac{1}{1+x_i^2} = \frac{1}{1+\tilde{x}_i} \quad , \tag{27}$$

with $\tilde{x}_i = \pi-1+\pi\,x_i^2$. Although Eq. (27) cannot be obtained from the variational problem (6)[1], we can still derive the corresponding algebras by posing

$$f(x) = \frac{1}{1-x} \ , \qquad \text{and} \qquad g(x) = 1-\frac{1}{x} \ , \tag{28}$$

[1] In the $\nu\to 1$ limit entropy (17) vanishes.

so that

$$x \oplus y = \frac{1}{h_+(x,\,y) - \ln\big(2\,\cosh h_-(x,\,y)\big)}\ , \tag{29}$$

$$x \otimes y = \frac{x\,y}{x + y - x\,y}\ , \tag{30}$$

with

$$h_\pm(x,\,y) = \frac{x \mp y}{2\,xy}\ , \tag{31}$$

and

$$x\tilde{\oplus} y = x + y - x\,y\ , \tag{32}$$

$$x\tilde{\otimes} y = 1 - \exp\big(-\ln(1-x)\,\ln(1-y)\big)\ , \tag{33}$$

respectively.

3.3 κ-distribution

As a further example, let us consider the κ-entropy [11] that we rewrite here in the form

$$S_\kappa[p] = -\frac{1}{2\,|\kappa|}\sum_{i=1}^{W}\left(\frac{p_i^{1+|\kappa|} - p_i}{1+|\kappa|} - \frac{p_i^{1-|\kappa|} - p_i}{1-|\kappa|}\right)\ , \tag{34}$$

with $|\kappa| < 1$. The corresponding distribution, constrained by the normalization and by the mean value, reads

$$p(\tilde{x}_i) = \left(-|\kappa|\,\tilde{x}_i + \sqrt{1+\kappa^2\,\tilde{x}_i^2}\right)^{1/|\kappa|}\ , \tag{35}$$

where $\tilde{x}_i = -1/(1-\kappa^2) + \mu_0 + \mu_1\,x_i$, with μ_0 and μ_1 the Lagrange multipliers whose values are fixed by the corresponding constraint equations and $\tilde{x}_{\min} = +\infty$.

The related algebras can be obtained by posing

$$f(x) = \left(|\kappa|\,x + \sqrt{1+\kappa^2\,x^2}\right)^{1/|\kappa|}\ , \tag{36}$$

and

$$g(x) = \frac{x^{|\kappa|} - x^{-|\kappa|}}{2\,|\kappa|}\ , \tag{37}$$

that generate the operations

$$x \oplus y = \exp\left(\frac{1}{\kappa}\,\mathrm{arcsinh}\left(\big[h_+(x,\,y) + \ln\big(2\,\cosh h_-(x,\,y)\big)\big]\right)\right)\ , \tag{38}$$

$$x \otimes y = \exp\left(\frac{1}{\kappa}\mathrm{arcsinh}\big[\sinh(\kappa\,\ln x) + \sinh(\kappa\,\ln y)\big]\right)\ , \tag{39}$$

where

$$h_\pm(x,\, y) = \frac{x^{|\kappa|} \pm y^{|\kappa|} - x^{-|\kappa|} \mp y^{-|\kappa|}}{4\,|\kappa|} \ , \tag{40}$$

and

$$x \tilde{\oplus} y = x\,\sqrt{1+\kappa^2\,y^2} + y\,\sqrt{1+\kappa^2\,x^2} \ , \tag{41}$$

$$x \tilde{\otimes} y = \frac{1}{\kappa}\,\sinh\left(\frac{1}{\kappa}\,\mathrm{arcsinh}(\kappa\,x)\,\mathrm{arcsinh}(\kappa\,y)\right) \ , \tag{42}$$

respectively.

3.4 Zip-Pareto distribution

As a final example, let us consider the Zip-Pareto distribution given by a simple power-law

$$p(x) = x^{-s} \ . \tag{43}$$

It can be obtained as the limit of the distribution (35) for $x \gg 1$, with $s = 1/|\kappa|$. In this case, we can derive the corresponding operations although some algebraic feature does not hold since these algebras are obtained from the ones introduced in the only in the Section 3.3 for large value of x.
Therefor, the related operations can be obtained formally through the functions

$$f(x) = x^s \ , \qquad \text{and} \qquad g(x) = x^{1/s} \ , \tag{44}$$

and are given by

$$x \oplus y = \left[\ln\left(\exp x^{1/s} + \exp y^{1/s}\right)\right]^s \ , \tag{45}$$

$$x \otimes y = (x^{1/s} + y^{1/s})^s \ , \tag{46}$$

where $h_\pm(x,\, y) = x^{1/s} \pm y^{1/s}$ and

$$x \tilde{\oplus} y = x\,y \ , \tag{47}$$

$$x \tilde{\otimes} y = \exp\left(s\,\ln x \cdot \ln y\right) \ , \tag{48}$$

respectively.

4 Conclusion

Summarizing, we have shown that starting from a very general trace-form entropy one can introduce two Abelian groups whose composition laws allow the generalization the well-known algebraic proprieties of the ordinary logarithm and exponential functions to the case of the generalized logarithm and exponential employed in the construction of a generalized statistical mechanics. In particular, we can rewrite Eqs. (11) and (15) in the form of

$$p(\tilde{x}_i + \tilde{y}_j) = p(\tilde{x}_i)\tilde{\otimes}p(\tilde{y}_j) \ , \tag{49}$$

$$p(\tilde{x}_i \oplus \tilde{y}_j) = p(\tilde{x}_i)\, p(\tilde{y}_j) \ , \tag{50}$$

that clarify the relevance of these operations in the manipulation of the generalized distributions and their role in the development of the mathematical formalism underlying the corresponding statistical theory.

References

[1] G. Kaniadakis, A.M. Scarfone, A new one-parameter deformation of the exponential function, *Physica A*, 305, 69-75 (2002).

[2] L. Nivanen, A. Le Mehaute, Q.A. Wang, Generalized algebra within a nonextensive statistics, *Rep. math. Phys.*, 52, 437-444 (2003).

[3] E.P. Borges, A possible deformed algebra and calculus inspired in nonextensive thermostatistics, *Phisica A*, 340, 95-101 (2004).

[4] E.K. Lenzi, E.P. Borges, R.S. Mendes, A q-generalization of Laplace transforms, *J. Phys. A: Math. Gen.*, 32, 8551-8561 (1999).

[5] S. Umarov, C. Tsallis, On a representation of the inverse F_q-transform, *Phys. Lett. A*, 372, 4874-4876 (2008).

[6] S. Umarov, C. Tsallis, S. Steinberg, On a q-central limit theorem consistent with nonextensive statistical mechanics, *Milan J. Math.*, 76, 307-328 (2008).

[7] R.K. Niven, H. Suyari, Combinatorial basis and non-asymptotic form of the Tsallis entropy function, *Eur. Phys. J. B*, 61, 75-82 (2008).

[8] H. Suyari, T. Wada, Multiplicative duality, q-triplet and $(\mu,\, \nu,\, q)$-relation derived from the one-to-one correspondence between the $(\mu,\, \nu)$-multinomial coefficient and Tsallis entropy S_q, *Physica A*, 387, 71-83 (2008).

[9] A.M. Scarfone, H. Suyari, T. Wada, Gauss' law of error revisited in the framework of Sharma-Taneja-Mittal information measure, *Centr. Eur. J. Phys.*, 7, 414-420 (2009).

[10] A. El Kaabouchi, et al, A mathematical structure for the generalization of conventional algebra, *Centr. Eur. J. Phys.*, 7, 549-554 (2009).

[11] G. Kaniadakis, P. Quarati, A.M. Scarfone, Kinetical foundations of nonconventional statistics, *Physica A*, 305, 76-83 (2002).

JOURNAL OF APPLIED FUNCTIONAL ANALYSIS, VOL.6, NO.2, 165-172, COPYRIGHT 2011 EUDOXUS PRESS, LLC

The Chaotic Point Works as Qubits in High Temperature Superconductors

Zeynep Güven Özdemir

Physics Department, Faculty of Science and Arts, Yıldız Technical University, Davutpaşa Campus, Esenler 34210, İstanbul, Turkey.
(E-mail: zguvenozdemir@yahoo.com)

March 02, 2010

The basic element of quantum computer is a qubit that corresponds to a quantum two level system. In recent years, low temperature superconductors have been utilized in the research of quantum computation, since they intrinsically provide the requirement of quantum computation such as a reliable tolerance to decoherence, efficient qubit interaction and scalability. In this work, the mercury based high temperature superconductors are proposed to be the most possible candidate for the bulk flux qubit for the first time due to the presence of $\left|0\right\rangle$ and $\left|1\right\rangle$ states at the same time on the Paramagnetic Meissner effect (PME) point. The PME leads to develop spontaneous currents in the opposite direction with the diamagnetic Meissner current in superconductors at the PME temperature, T_{PME} which is referred to the quantum chaotic point [1,2]. From this respect, the existence of both the clockwise and anti-clockwise currents at T_{PME} enables to design a qubit by the mercury cuprate superconductors.

Key words: Mercury cuprates, Paramagnetic Meissner Effect, Flux qubit, Chaotic Point

1 Introduction

Quantum computers have an increasing attention due to their high advantage for solving very difficult problems more easily in a short time relative to conventional computers. A quantum bit or "qubit", which represents the quantum information, is the basis of the quantum computation. Qubit can carry data in two quantum states at the same time and is described by a state vector in a two level quantum system. There are naturally exist and man-made qubit materials such as atomic elements, semi-conductors and superconductors etc. In

recent years, superconductors have been extensively investigated by means of their capability of being qubits. The performance of the quantum two-level system namely qubit is determined in terms of some criteria such as the tolerance to decoherence, efficient qubit interaction and scalability. The superconducting energy gap between the condensed Cooper pair state and the excited quasi-particle state protects the qubit system from unexpected excitations that destroy qubit coherence and hence cause decoherence that results in the information loss. In this point of view, superconductors can be considered as the most promising candidate of condensed matter qubit systems [3]. Superconducting qubits are based on the Josephson tunnel junctions that are combined with superconducting inductors and capacitors. In scientific literature, Josephson qubit circuits can be considered as artificial macroscopic atoms and their Hamiltonian can be controlled by applying electric or magnetic fields and bias currents [4].
The formation of two level quantum system in superconductors has been expressed gradually in the context of energy gap as follows:

- The quantum energy levels in the superconducting gap, which is located above the Fermi energy, can be used by making superconducting inductor-capacitor (*LC*) circuits (Figure 1-(a)).
- The *LC* circuit behaves as harmonic oscillator so that the energy levels have a same spacing value which equals to $h/\left(2\pi\sqrt{LC}\right)$. All the quantum energy levels can be excited by microwave frequency. This system can not be worked as a two level quantum system.
- In order to achieve two level quantum system, the Josephson junction is added to the superconducting LC circuit. In this condition, the spacings between the energy levels are not equal anymore due to the phase difference between superconducting layers in the Josephson junction. The lowest two quantum energy levels namely “qubit” can be manipulated by the resonant microwaves (Figure 1-(b)).

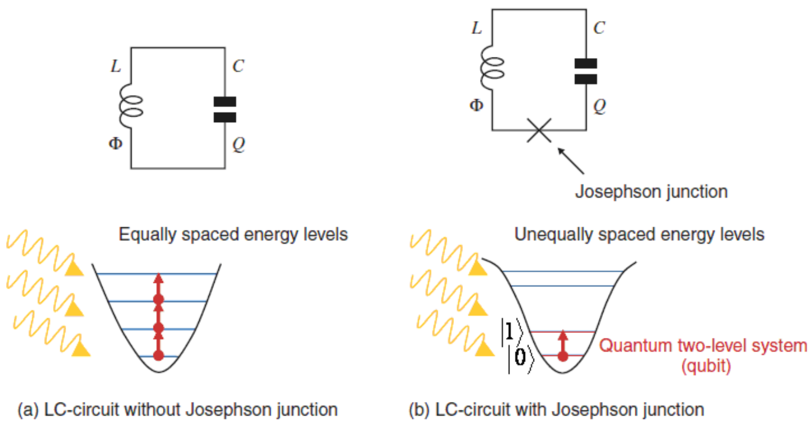

Figure 1. Schematic energy levels of superconducting LC-circuit with or without Josephson junction [5].

One of the superconducting qubits is the flux qubit, which is composed of a superconducting loop that incorporates multiple (generally three) Josephson junctions (Figure 2). If an appropriate magnetic field is applied to the superconducting loop, two superconducting persistent currents in opposite direction, which refer to clockwise $|0\rangle$ and anti-clockwise $|1\rangle$ current state, become stable at the same time thereby two-level quantum system namely "qubit" is realized [5].

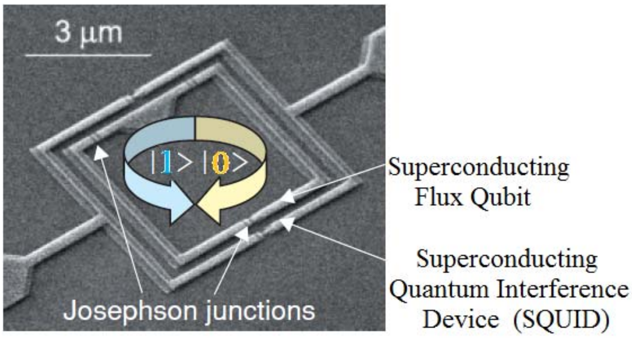

Figure 2. The SEM (Scanning Electron Microscopy) photograph of the micrometer sized superconducting flux qubit made by superconducting metal. Arrows indicate the current flow in the two qubit states.

Two classical persistent current states with opposite direction in the flux qubit indicated the symmetric and anti-symmetric quantum superposition of macroscopic states [6]. Under the illumination of microwaves corresponding to the energy difference between $|0\rangle$ and $|1\rangle$ states, the qubit reiterates between absorption and emission of one photon and it oscillates between $|0\rangle$ and $|1\rangle$ states coherently. In other words, the quantum superposition of two states is also manipulated by resonant microwave pulses and applying strong microwave to the system induces hundreds of coherent oscillations [7]. This phenomenon is known as "Rabi oscillations" and it is the basis of quantum gate operations.

2 Mercury Cuprates as a Candidate of Bulk Flux Qubit

In this work, the mercury cuprate high temperature superconductors have been investigated by means of bulk flux qubit due to their properties that satisfy the general requirement of the quantum computation. In this section, the mentioned features related to quantum two level system of mercury cuprates are summarized.

As is known, copper oxide ceramic high temperature superconductors have a common structure in which superconducting copper oxide layers are separated by thin insulating layers (Figure 3). Copper oxide layers are coupled together by Josephson tunneling between adjacent layers. According to the experimental evidences of cuprates such as $Bi_2Sr_2CaCu_2O_8$, $Tl_2Ba_2Ca_2Cu_3O_{10}$ and, $YBa_2Cu_3O_{7-x}$, the cuprate systems behave like stack of superconductor-insulator-superconductor intrinsic Josephson junctions [8]. In this context, $HgBa_2Ca_2Cu_3O_{8+x}$ (Hg-1223) superconductors can be considered as an array of intrinsic Josephson junctions [9]. It is known that the fabricated superconducting Josephson junctions are used in the qubit circuits [10,11]. In this respect, since the multiply connected intrinsic Josephson junction arrays is an inherent property of the mercury cuprates, there is no need to make an effort to fabricate individual Josephson junctions for the construction of a qubit.

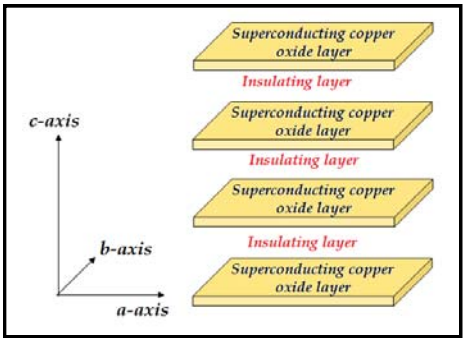

Figure 3. The schematic representation of the intrinsic Josephson structure in the layered high temperature superconductors.

The another advantage is the $d_{x^2-y^2}$ -wave symmetry of the order (or energy gap) parameter of the Hg-1223 superconductors [12,13]. According to Taffuri et. al, the qubit proposals basically exploit the fact that the Josephson junctions with a π -shift in phase can be produced by a d-wave order parameter symmetry. This may lead to intrinsically doubly degenerated system, i.e. the systems based on Josephson junctions with an energy-phase relation with two minima [14]. This condition is intrinsically occurs in mercury cuprates due to the d-wave symmetry of its order parameter.

There have been several problems related to the conventional superconducting qubits from fabrication techniques to the decoherence which is based on the insulating layer and that is limited to the performance of the qubit [15,16]. In this study, bulk Hg-1223 superconductors are proposed to resolve these problems easily due to their properties such as inherent Josephson junction structure, d-wave symmetric order parameter, occurrence of the plasma resonance mode with the infrared or microwave frequency depending on the temperature, the three dimensional (spatial) BEC etc [1,9,17]. Since, Hg-1223 sample exhibits three dimensional BEC at the Josephson plasma resonance frequency [17], the system represents itself a unique macroscopic quantum wave function regardless of the insulating material. In this point of view, both the electromagnetic wave cavity character of Hg-1223 and the spatial BEC can be considered as a spontaneous natural source of forming the coherent temporal oscillations between macroscopic quantum states in the system.

3 The Paramagnetic Meissner Effect and Flux Qubit

In this work, the bulk flux qubit character of Hg-1223 superconductors has been discussed in terms of Paramagnetic Meissner Effect, which emanates itself both d.c. (direct current) and a.c. (alternative current) magnetic moment-temperature experimental data. The Paramagnetic Meissner Effect is a special quantum phenomenon which is based on the alteration of the orbital current's direction. Some low temperature superconductors and very cleanly prepared poly crystalline high temperature superconductors exhibit a net paramagnetic moment in a certain temperature interval, which is close to T_c, under d.c. or a.c. magnetic fields [18-27]. This effect is known as Paramagnetic Meissner Effect (PME). One of the main explanations of PME is as follows; the π -junctions between weakly coupled superconducting grains cause spontaneous orbital currents in arbitrary directions and an applied very weak magnetic field (1 Gauss) aligns the spontaneous loop currents in such a way that the system gains a net positive magnetic moment [18].
In this work, the flux qubit character of the optimally oxygen annealed Hg-1223 superconductors has been examined by the temperature dependence of a.c. magnetic measurements (Figure 4).

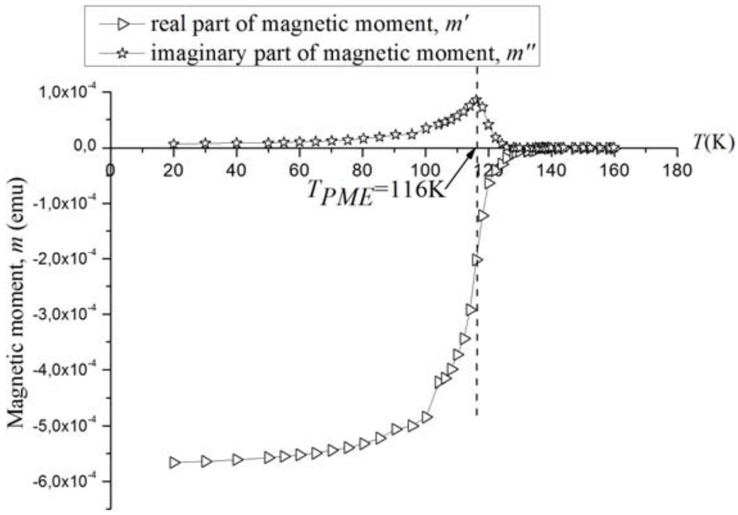

Figure 4. a.c. magnetic moment versus temperature response taken by quantum design SQUID magnetometer model MPMS-5S for the optimally oxygen doped Hg-1223 superconductor.

The diamagnetic response of the system to external magnetic field is represented by the real part of magnetic moment whereas the paramagnetic tendency can be seen from the imaginary part of the magnetic moment in Figure 4. The maximum paramagnetic signal has been observed at the paramagnetic Meissner effect temperature (T_{PME}) of 116K for the optimally oxygen doped mercury cuprate superconductor (Figure 4). Since the orbital currents flow in the opposite direction above and below T_{PME}, both the clockwise and anti-clockwise orbital currents exist at the T_{PME} chaotic point. From this respect, the achievement of the maximum paramagnetic signal has a crucial importance for the flux qubit investigations. In this point of view, it has been proposed that the mercury cuprate high temperature superconducting system can work as a bulk flux qubit at the T_{PME} chaotic point. The term "bulk" is attributed to the fact that this phenomenon is realized by the response of the bulk mercury cuprate sample to the applied magnetic field. However, it is possible to fabricate the single flux qubit with mercury cuprates in the length of 2.3 nm which corresponds to the thickness of three intrinsic Josephson junctions in the mercury cuprates*. As is known for technical applications three layered system is required for the construction of the flux qubit.

4 Conclusions

Up till now, some low temperature conventional superconductors such as Nb and Al have been used to produce two-level quantum system. On the other hand, some high temperature superconductors such as Bi-Sr-Ca-Cu-O, Y-Ba-Cu-O etc. have not give good results for qubits due to their high decoherence problem. As is known, mercury cuprate family has remarkable features such as intrinsic Josephson junction arrays, the spatial resonance that results to resolve the decoherence problem in the system with the highest Meissner critical temperature. In this context, by utilizing the Hg-1223 superconductors at the T_{PME} chaotic point may give some acceleration to the research of the flux qubits.

5 References

[1] Ü. Onbaşlı, Z.Güven Özdemir, Ö. Aslan, Symmetry breakings and topological solitons in mercury based d-wave superconductors, *Chaos Solitons and Fractals*, 42, 1980-1989 (2009).

[2] Ö. Aslan, Z. Güven Özdemir, S.S. Keskin, Ü. Onbaşlı, The chaotic points and XRD analysis of Hg-based superconductors, *Journal of Physics: Conference Series*, 153 Number 1/ 012002 (2009).

[3] H. Takayanagi, H.Tanaka, S. Saito, H. Nakano, Observation of qubit state with a dc-SQUID and dissipation effect in the SQUID, *Physica Scripta*, T102 95-102 (2002).

* The Hg-1223 superconductor primitive cell contains two intrinsic Josephson junctions in the approximately 1.5 nm size.

[4] G. Ithier, F. Nguyen, E. Collin, N. Boulant, P.J. Meeson, P. Joyez, D. Vion, D. Esteve, Solid-state quantum bit circuits, in *Proceedings of the International School of Physics "Enrico Fermi" Course CLXII Quantum Computer, Algorithms and Chaos* ed (G. Casati, D. Shepelyansky, P. Zoller and G. Benenti eds.), IOS Publishing Amsterdam, The Netherlands, 2006, pp 447-469.

[5] K. Semba, Entanglement control of superconducting qubit single photon system, *NTT Technical Review*, Vol. 6 no:1, 1-6 (2008), NTT Basic Research Laboratories Qubit Reports.

[6] C. H. van der Wal, A.C.J.T. Haar, F.K. Wilhelm, R.N. Schouten, C.J.P.M. Harmans, T.P. Orlando, S. Lloyd, J.E. Mooij, Quantum superposition of macroscopic persistent-current states, *Science*, 290, 773-777 (2000).

[7] I. Chiorescu, Y. Nakamura, C.J.P.M. Harmans and J.E. Mooij Coherent quantum dynamics of a superconducting flux qubit, *Science*, 299, 1869-1871 (2003).

[8] R. Kleiner, P. Müller, Intrinsic Josephson effects in high-T_c superconductors, *Phys. Rev. B*, 49,1327-1341 (1994).

[9] Z. G. Özdemir, Ö. Aslan, Ü. Onbaşlı, Determination of c-axis electrodynamics parameters of mercury cuprates, *Journal of Physics and Chemistry of Solids*, 67, 453-456 (2006).

[10] M. Wallquist, J. Lantz, S. Shumeiko, G. Wendin, Superconducting qubit network with controllable nearest-neighbour coupling, *New Journal of Physics*, **7**, 178/1-178/23 (2005).

[11] D. Vion, A. Aassime, A. Cottet, P. Joyez, H. Pothier, C. Urbina, D. Esteve, M.H. Devoret, Manipulating the quantum state of an electrical circuit, *Science*, 296, 886-889 (2002).

[12] C. Panagopoulos, J.R. Cooper, G.B. Peacock, L. Gameson, P.P. Edwards, W. Schmidbauer, J.W. Hodby, Anisotropic magnetic penetration depth of grain-aligned $HgBa_2Ca_2Cu_3O_{8+\delta}$,*Phys. Rev B*, 53, R2999-R3002 (1996).

[13] C. Panagopoulos, T. Xiang, Relationship between the Superconducting Energy Gap and the Critical Temperature in High-T_c Superconductors *Phys. Rev. Lett.*, 81 2336-2339 (1998).

[14] F. Tafuri, J.R. Kirtley, F. Lombardi, T. Bauch, E. Il'ichev, F. Miletto Granozio, D.Stornaiuolo, U. Scotti di Uccio, Flavours of intrinsic d-wave induced effects in $YBa_2Cu_3O_{7-\delta}$ grain boundary Josephson junctions, in *Institute of Physics Conference Series Number 181: Proceedings of the Sixth European Conference on Applied Superconductivity*, (A Andreone, G.P. Pepe, R. Cristiano, G. Masullo eds.), IOP Publishing, United Kingdom, 2004, pp. 273-282.

[15] R.W. Simmonds, D.A. Hite, R. McDermott, M. Steffen, K.B. Cooper, K.M. Lang, J.M. Martinis, D.P. Pappas, Josephson junction materials research using phase qubits, in *Quantum Computation: Solid State Systems*, (B. Ruggiero, P. Delsing, C. Granata, Y. Pashkin, P. Silvestrini eds.), Springer, NewYork, 2006,pp. 86-94.

[16] J.M. Martinis, K.B. Cooper, R. McDermott, M. Steffen, M. Ansmann, K.D. Osborn, K. Cicak, S. Oh, D.P. Pappas, R.W. Simmonds, C.C. Yu, Decoherence in Josephson qubits from dielectric loss, *Phys. Rev. Lett.*, 95, 210503-1-210503-4 (2005).

[17] Z. G. Özdemir, Ö. Aslan, Ü. Onbaşlı, Calculation of microwave plasma oscillations in high temperature superconductors, in *The Seventh International Conference on Vibration Problems ICOVP 2005 Springer Proceedings in Physics* vol. 111, (E. İnan, A. Kırış eds.), Springer Verlag ,Berlin, Heidelberg, 2007 pp. 377-382.

[18] W. Braunisch, N. Knauf, V. Kataev, S. Neuhause, A. Grütz, A. Kock, B. Roden, D. Khomskii, D. Wohlleben, Paramagnetic Meissner effect in Bi high-temperature superconductors, *Phys. Rev. Lett.*, 68, 1908-1911 (1992).

[19] B. Schliepe, M. Stindtmann, I. Nikolic, K. Baberschke, Positive field-cooled susceptibility in high-T_c superconductors, *Physical Review B*, 47, 8331-8334 (1993).

[20] W. Braunisch, N. Kanuf, G. Bauer, A. Kock, A. Becker, B. Freitag, A. Grütz, V. Kataev, S. Neuhausen, B. Roden, D. Khomskii, D. Wohlleben, J. Bock, E. Preisler, Paramagnetic Meissner effect in high-temperature superconductors *Phys. Rev. B*, 48, 4030-4042 (1993).

[21] D. I. Khomskii, Wohlleben effect (Paramagnetic Meissner effect) in high-temperature superconductors, *Journal of Low Temp. Physics*, 95, 205-223 (1994).

[22] S. Riedling, G. Brauchle, R. Lucht, K. Röhberg, H.V. Löhneysen, H. Claus, A. Erb, G. Müler-Vogt, Observation of the Wohlleben effect in $YBa_2Cu_3O_{7-\delta}$ single crystals, *Phys. Rev. B*, 49 13283-13286 (1994).

[23] D.J. Thompson, M.S.M. Minhaj, L.E. Wenger, J.T. Chen, Observation of Paramagnetic Meissner effect in niobium disks, *Phys. Rev. Lett.*, 75, 529-532 (1995).

[24] Ü. Onbaşlı, Y.T. Wang, A. Naziripour, R. Tello, W. Kiehl, A.M. Hermann, Transport properties of high-T_c mercury cuprates, *Phys. Stat. Sol. (b)*, 194 371-382 (1996).

[25] J. Magnusson, E. Papadopoulou, P. Svedlindh, P. Nordblad, Ac susceptibility of a paramagnetic Meissner effect sample, *Physica C,* 297, 317-325 (1998).

[26] P. V. Patanjali, V. Seshu Bai, R.M. Kadam, M.D. Sastry, Anomalous microwave absorption in GdBCO powder: π junctions and the paramagnetic Meissner effect, *Physica C*, 296, 188-194 (1998).

[27] A. P. Nielsen, A.B. Cawthorne, P. Barbara, F.C. Wellstood, C.J. Lobb, R.S. Newrock, M.G. Forrester, Paramagnetic Meissner effect in multiply-connected superconductors, *Phys. Rev. B*, 62, 14380-14383(2000).

JOURNAL OF APPLIED FUNCTIONAL ANALYSIS, VOL.6, NO.2, 173-181, COPYRIGHT 2011 EUDOXUS PRESS, LLC

Approximate solutions of eighth-order BVPs by homotopy analysis method and its modification

A. Sami Bataineh *

Department of Basic Science
Al-Huson University College
Al-Balqa' Applied University
Al Huson 50, Jordan

Abstract

In this paper, approximate and/or exact analytical solutions of a class of linear and nonlinear eighth-order boundary value problems (BVPs) are obtained by the standard and modified homotopy analysis methods, in short, HAM and MHAM respectively. Numerical comparisons against the modified Adomian decomposition method (MDM) show the reliability of the HAM and MHAM.

Key words: Homotopy analysis method; Modified homotopy analysis method; Boundary value problem; series solutions

1 Introduction

In this work, we consider a class of eighth-order BVP of the form

$$y^{(viii)}(t) = f(t, y), \quad a \leq t \leq b, \tag{1}$$

with boundary conditions as an even-order derivatives on both edges of the domain

$$\begin{aligned} &y(a) = \alpha_0, \quad y''(a) = \alpha_2, \quad y^{(iv)}(a) = \alpha_4, \quad y^{(vi)}(a) = \alpha_6, \\ &y(b) = \beta_0, \quad y''(b) = \beta_2, \quad y^{(iv)}(b) = \beta_4, \quad y^{(vi)}(b) = \beta_6, \end{aligned} \tag{2}$$

or with boundary conditions given for the starting point

* Corresponding author.
Email address: a_s_bataineh@yahoo.com (A. Sami Bataineh).

$$y(a) = \alpha_0, \quad y'(a) = \alpha_1, \quad y''(a) = \alpha_2, \quad y'''(a) = \alpha_3,$$
$$y^{(iv)}(a) = \alpha_4, \quad y^{(v)}(a) = \alpha_5, \quad y^{(vi)}(a) = \alpha_6, \quad y^{(vii)}(a) = \alpha_7, \tag{3}$$

where f is a continuous function on $[a, b]$ and the parameters $\alpha_i, (i = 0, 1 \ldots, 7)$ and $\beta_i, (i = 0, 2, 4, 6)$ are real constants.

Eq. (1) describes some hydrodynamic stability problems. When an infinite horizontal layer of fluid is heated from below and under the action of rotation, instability sets in. When this instability is as ordinary convection, the problem is expressed as a sixth-order BVP. When the instability sets in as overstability, the problem is modelled by an eighth-order BVP [1].

Several numerical methods including spectral Galerkin and collocation methods [2,3], sixth B-spline method [4], decomposition method [5], and others have been developed for solving the problem of type (1).

The aim of this paper is to apply the standard homotopy analysis method (HAM) [6] and modified homotopy analysis method (MHAM) [7] for the first time to obtain approximate solutions of the eighth-order BVP (1) directly. The HAM, initially proposed by Liao in his Ph.D. thesis [6], is a powerful method to solve non-linear problems. In recent years, this method has been successfully employed to solve many types of nonlinear problems in science and engineering.

2 Solution approaches

For the convenience of the reader, we will first present a brief account of the HAM [6] and MHAM [7].

2.1 Standard HAM

To describe the basic ideas of the *standard* HAM and to achieve our goal for the modification of HAM, we consider the differential equations

$$N[y(t)] = g(t), \tag{4}$$

where N is a nonlinear operators, t denotes the independent variable, $y(t)$ is an unknown functions and $g(t)$ is a known analytic functions representing the nonhomogeneous terms. If $g(t) = 0$, Eq. (4) reduces to the homogeneous equations. By means of generalizing the traditional homotopy method, Liao [8] constructs the so-called *zeroth-order deformation equation*

$$(1 - q)L[\phi(t; q) - y_0(t)] = q\hbar \left\{ N[\phi(t; q)] - g(t) \right\}, \tag{5}$$

where $q \in [0, 1]$ is an embedding parameter, $\hbar$ is a nonzero auxiliary operator, L is an auxiliary linear operator, $y_0(t)$ is the initial guesses of $y(t)$ and $\phi(t; q)$ is an unknown functions. It is important to note that one has great freedom to choose the auxiliary objects such as $\hbar$ and L in HAM. Obviously, when $q = 0$ and $q = 1$ both

$$\phi(t;0) = y_0(t) \quad \text{and} \quad \phi(t;1) = y(t),$$

hold. Thus as q increases from 0 to 1, the solutions $\phi(t;q)$ varies from the initial guesses $y_0(t)$ to the solutions $y(t)$. Expanding $\phi(t;q)$ in Taylor series with respect to q, one has

$$\phi(t;q) = y_0(t) + \sum_{m=1}^{+\infty} y_m(t)q^m, \tag{6}$$

where

$$y_m = \frac{1}{m!}\frac{\partial^m \phi(t;q)}{\partial q^m}\bigg|_{q=0}. \tag{7}$$

If the auxiliary linear operator, the initial guesses and the auxiliary parameters $\hbar$ are so properly chosen, then the series (6) converges at $q = 1$ and

$$\phi(t;1) = y_0(t) + \sum_{m=1}^{+\infty} y_m(t),$$

which must be one of the solutions of the original nonlinear equations, as proved by Liao [8]. As $\hbar = -1$, Eq. (5) becomes

$$(1-q)L[\phi(t;q) - y_0(t)] + q\left\{N[\phi(t;q)] - g(t)\right\} = 0, \tag{8}$$

which is used mostly in the homotopy-perturbation method [9].

According to (7), the governing equations can be deduced from the *zeroth-order deformation equations* (5). Define the vectors

$$\vec{y}_n = \{y_0(t), y_1(t), \ldots, y_n(t)\}.$$

Differentiating (5) m times with respect to the embedding parameter q and then setting $q = 0$ and finally dividing them by $m!$, we have the so-called *mth-order deformation equation*

$$L[y_m(t) - \chi_m y_{m-1}(t)] = \hbar R_m(\vec{y}_{m-1}), \tag{9}$$

where

$$R_m(\vec{y}_{m-1}) = \frac{1}{(m-1)!} \frac{\partial^{m-1}\left\{N\left[\phi(t;q)\right] - g(t)\right\}}{\partial q^{m-1}}\bigg|_{q=0}, \tag{10}$$

and

$$\chi_m = \begin{cases} 0, & m \leq 1, \\ 1, & m > 1. \end{cases}$$

It should be emphasized that $y_m(t)$ $(m \geq 1)$ is governed by the linear equations (9) with the linear boundary conditions that come from the original problem, which can be easily solved by symbolic computation softwares such as Maple and Mathematica.

2.2 Modified HAM

In this section, a modification of the HAM is established. It is assumed that the "coefficients" and/or nonhomogeneous terms $g(t)$ in Eq. (4) can be expressed in Taylor series based on a kind of a continuous homotopy mapping with respect to q, $g(t) \to \varphi(t;q)$ as,

$$\varphi(t;q) = \sum_{m=0}^{\infty} g_m(t) q^m.$$

We also expand the coefficients of the linear or nonlinear equation using the Taylor series with respect to the embedding parameter q when the notion of coefficient is clear in these equations.

According to (5), the new *zeroth-order deformation equation* given by the Taylor series expansion is

$$(1-q)L[\phi(t;q) - y_0(t)] = q\hbar\{N[\phi(t;q)] - \varphi(t;q)\}, \tag{11}$$

and the *mth-order deformation equation* is

$$L[y_m(t) - \chi_m y_{m-1}(t)] = \hbar R_m(\vec{y}_{m-1}), \tag{12}$$

where $R_m(\vec{y}_{m-1})$ same as in 10 and

$$R_m(\vec{y}_{m-1}) = \frac{1}{(m-1)!} \frac{\partial^{m-1}\{N[\phi(t;q)] - \varphi(t;q)\}}{\partial q^{m-1}}\bigg|_{q=0}, \tag{13}$$

and

$$\chi_m = \begin{cases} 0, & m \leq 1, \\ 1, & m > 1. \end{cases}$$

It should be emphasized that $y_m(t)$ $(m \geq 1)$ is governed by the linear equation (12) with the linear boundary conditions that come from the original problem.

3 Numerical experiments

To illustrate the effectiveness of the HAM and MHAM we shall consider four examples of eighth-order BVPs.

3.1 Example 1.

We first consider the linear BVP,

$$y^{(viii)}(t) = y(t) + g(t), \quad 0 \leq t \leq 1, \tag{14}$$

with boundary conditions at starting points

$$\begin{aligned} &y(0) = 1, \quad y'(0) = 0, \quad y''(0) = -1, \quad y'''(0) = -2, \\ &y^{(iv)}(0) = -3, \quad y^{(v)}(0) = -4, \quad y^{(vi)}(0) = -5, \quad y^{(vii)}(0) = -6. \end{aligned} \tag{15}$$

The exact solution of (14) subject to (15) in the case $g(t) = -8\mathrm{e}^t$ is

$$y(t) = (1 - t)\mathrm{e}^t. \tag{16}$$

To solve (14)–(15) by means of MHAM [7], we choose the initial boundary approximation

$$y_0(t) = 1 - \frac{1}{2}t^2 - \frac{1}{3}t^3 - \frac{1}{8}t^4 - \frac{1}{30}t^5 - \frac{1}{144}t^6 - \frac{1}{840}t^7, \tag{17}$$

and the linear operator

$$L[\Phi(t;q)] = \frac{\partial^8 \phi(t;q)}{\partial t^8}, \tag{18}$$

with the property

$$L\left[\sum_{i=1}^{8} c_i t^{i-1}\right] = 0, \tag{19}$$

where c_i $(i = 1, \ldots, 8)$ are constants of integration.

Now expand the homotopy $\varphi(t;q) = g(t)$ in powers of the embedding parameter q as follows:

$$g(t) = -8\mathrm{e}^t = -8\sum_{m=0}^{\infty} \frac{t^m}{m!},$$

which implies

$$\varphi(t;q) = -8\sum_{m=0}^{\infty} \frac{t^m}{m!} q^m.$$

Eq. (14) suggests that we define a nonlinear operator

$$N[\phi(x;q)] = \frac{\partial^8 \phi(t;q)}{\partial t^8} - \phi(t;q) \tag{20}$$

Using the above definition, we construct the *zeroth-order deformation equation* as in (11) and the *mth-order deformation equation* for $m \geq 1$ is as in (12) with the initial conditions

$$y_m^{(j)}(0) = 0, \quad j = 1, \ldots, 7, \tag{21}$$

where

$$R_m(y_{m-1}) = y_{m-1}^{(8)}(t) - y_{m-1}(t) - 8\frac{t^{m-1}}{(m-1)!},$$

etc. Now, the solution of (12) for $m \geq 1$ becomes

$$y_m(t) = \chi_m y_{m-1}(t) + \hbar L^{-1} R_m(\vec{y}_{m-1}). \tag{22}$$

We now successively obtain

$$\begin{aligned} y_1(t) = {} & \frac{\hbar}{5760} t^8 + \frac{\hbar}{3628800} t^{10} + \frac{\hbar}{19958400} t^{11} + \frac{\hbar}{159667200} t^{12} \\ & + \frac{\hbar}{1556755200} t^{13} + \frac{\hbar}{17435658240} t^{14} + \frac{\hbar}{217945728000} t^{15}, \\ & \vdots \end{aligned} \tag{23}$$

Then the series solution expression can be written in the form

$$y(t) = y_0(t) + y_1(t) + y_2(t) + \cdots. \tag{24}$$

Hence, the series solution when $\hbar = -1$ is

$$y(t) \simeq 1 - \frac{1}{2}t^2 - \frac{1}{3}t^3 - \frac{1}{8}t^4 - -\frac{1}{30}t^5 - \frac{1}{144}t^6 - \frac{1}{840}t^7 - \frac{1}{5760}t^8 - \cdots, \tag{25}$$

which converges to the closed-form solution (16).

3.2 Example 2.

Finally we consider again the non-linear BVP,

$$y^{(viii)}(t) = g(t)y^2(t), \quad 0 < t < 1, \tag{26}$$

with boundary conditions with even-order derivatives at the boundary points

$$\begin{aligned} &y(0) = y''(0) = y^{(iv)}(0) = y^{(vi)}(0) = 1, \\ &y(1) = y''(1) = y^{(iv)}(1) = y^{(vi)}(1) = \mathrm{e}. \end{aligned} \tag{27}$$

The exact solution of (26) subject to (27) in the case $g(t) = \mathrm{e}^{-t}$ is

$$y(t) = \mathrm{e}^t. \tag{28}$$

To solve (26)–(27) by means of HAM [6], we choose the initial boundary approximation

$$\begin{aligned} y_0(t) = 1 &- \frac{1241}{945}t + \frac{12863\mathrm{e}}{15120}t + \frac{1}{2}t^2 - \frac{59}{270}t^3 + \frac{307\mathrm{e}}{2160}t^3 + \frac{1}{24}t^4 - \frac{1}{90}t^5 + \frac{\mathrm{e}}{144}t^5 \\ &+ \frac{1}{720}t^6 - \frac{1}{5040}t^7 + \frac{\mathrm{e}}{5040}t^7. \end{aligned} \tag{29}$$

Now construct the *zeroth-order deformation equation* as in (5) and the *mth-order deformation equation* as in (9) with the initial approximation (29) and linear operator (18) with the property (19), where c_i $(i = 1, \ldots, 8)$ are constants of integration.

The boundary conditions are

$$\begin{aligned} &y_m(0) = 0, \quad y_m''(0) = 0, \quad y_m^{(iv)}(0) = 0, \quad y_m^{(vi)}(0) = 0, \\ &y_m(1) = 0, \quad y_m''(1) = 0, \quad y_m^{(iv)}(1) = 0, \quad y_m^{(vi)}(1) = 0, \end{aligned} \tag{30}$$

where

$$R_m(\vec{y}_{m-1}) = y_{m-1}^{(8)}(t) - \mathrm{e}^{-t} \sum_{i=0}^{m-1} y_i(t) y_{m-1-i}(t).$$

Table 1
Absolute errors for Example 2.

t	2-term HAM, $\hbar = -1$	3-term MDM [5]
0.25	2.16 E-06	4.91 E-05
0.5	4.88 E-07	7.04 E-05
0.75	1.86 E-07	4.98 E-05

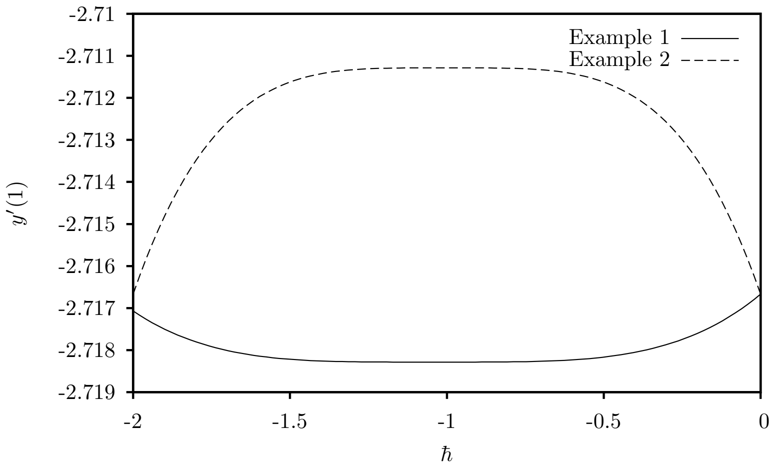

Fig. 1. The $\hbar$-curve of $y'(1)$ given by (14) and (26): 5th-order approximation of $y'(1)$.

Now, the solution of (9) for $m \geq 1$ is the same as (22).

We now successively obtain

$$y_1(t) = \frac{80489998892401\hbar}{33075} - \frac{22398711220261e\hbar}{33075} + \frac{501269004951823e^2\hbar}{1058400} + \frac{22398711220261e^{1-t}\hbar}{33075} - \cdots, \tag{31}$$

$$\vdots$$

Then the series solution of $y(t)$ is found to be as an approximation with first two components

$$y(t) = y_0(t) + y_1(t). \tag{32}$$

In Table 1 we present the absolute errors of the two-term HAM and three-term MDM solutions [5]. Again, in this case HAM is more accurate than MDM [5].

The series solutions of Eqs. (14) and (26) given by HAM and MHAM contains the auxiliary parameter $\hbar$. The validity of the method is based on such an assumption that the series (6) converges at $q = 1$. It is the auxiliary parameter $\hbar$ which ensures that this assumption can be satisfied. In general, by means of the so-called $\hbar$-curve, it is straightforward to choose a proper value of $\hbar$ which ensures that the solution series is convergent. Fig. 1 show the $\hbar$-curves obtained from the 5th-order HAM and MHAM approximate solutions of Eqs. (14) and (26). From these figures, the valid regions of $\hbar$ corresponds to the line segments nearly parallel to the horizontal axis.

4 Conclusions

In this paper, the standard and modified homotopy analysis methods (HAM and MHAM) were applied to solve a class of linear and non-linear BVPs. The HAM and MHAM provide us with a convenient way of controlling the convergence of approximation series, which is a fundamental qualitative difference in analysis between HAM and the other methods. Comparison of the result obtained by the HAM with that obtained by the modified decomposition method (MDM) [5] reveals that the present method is very effective and convenient.

Acknowledgments

The authors would like to acknowledge the financial support received from the Irbid National University.

References

[1] Chandrasekhar S. Hydrodynamic and hydromagnetic stability. Dover, New York; 1981.

[2] Davies AR, Karageoghis A, Phllips TN. Spectral Galerkin methods for the primary two-point boundary-value problems in modelling viscoelastic flows. Int J Numer Methods Eng 1988;26:647–662.

[3] Karageoghis A, Phllips TN, Davies AR. Spectral collocation methods for the primary two-point boundary-value problems in modelling viscoelastic flows. Int J Numer Methods Eng 1998;26:805–813.

[4] Caglar HN, Caglar SH, Twizel EE. The numerical solution of fifth-order boundary value problems with sixth degree B-spline functions. Appl Math Lett 1999;12:25–30.

[5] Mestrovic M. The modified decomposition method for eighth-order boundary value problems. Appl Math Comput 2007;188:1437–1444

[6] Liao SJ. The proposed homotopy analysis techniques for the solution of nonlinear problems. Ph.D. Dissertation, Shanghai Jiao Tong University, Shanghai; 1992 (in English).

[7] Bataineh AS, Noorani MSM, Hashim I. On a new reliable modification of homotopy analysis method. Commun Nonlinear Sci Numer Simul 10.1016/j.cnsns.2007.10.007 [in press].

[8] Liao SJ. Beyond perturbation: introduction to the homotopy analysis method. CRC Press, Boca Raton, Chapman and Hall; 2003.

[9] He JH. Homotopy perturbation method: a new nonlinear analytical technique. Appl Math Comput 2003;135:73–79.

THEAPPROXIMATE ANALYTIC SOLUTIONS FOR FREE VIBRATIONS OF A MASS GROUNDED BY LINEAR AND NONLINEAR SPRINGS IN SERIES

M. Bayat[1a], G.R.Abdollahzade[b], M. Shahidi[a]

[a] *Civil engineering Department, Shomal University, Amol, Iran, P.O.Box731*

[b] *Civil Engineering Department, Babol University of Technology, Babol, Iran, P.O.Box484*

ABSRACT

In many technical applications, spring-like flexible elements or real springs connected in series are used. The applicable range of these components determines whether or not the system behavior has a linear or nonlinear characteristic. This study is concerned to a system that consists of a mass grounded two springs which one of those springs is linear and the other is nonlinear. Two methods are studied to analyze the dynamic system behavior. One method makes use of a set of Energy Balance Method (EBM) and the other is Homotopy Perturbation Method (HPM). The results indicate that the present analysis is accurate, and provides us a unified and systematic procedure which is simple and more straightforward than the other modal analysis. The main objective of present study is to obtain highly accurate analytical solutions for free vibrations of a conservative oscillator with inertia and static type cubic nonlinearities.

KEYWORDS: Energy Balance Method, Homotopy Perturbation Method, Nonlinear Oscillation, Equation of motion, Nonlinear springs.

1. INTRODUCTION

We all know nonlinear functions are crucial points in engineering problems, so solving these equations are in the circle of most scientists and engineers' priority and requirements. In addition, many physical phenomena are modeled by nonlinear differential equations in order to we have more opportunities to handle the real objects in our real world. As an example, vibration of mechanical systems associated with nonlinear properties is in this category. Therefore, scientists tried to solve the problem and find some

[1] Corresponding Author: Tell/Fax: (0098 511 6635253)
E-mail: mbayat@shomal.ac.ir , Mahmoud_Bayat@hotmail.com (M. Bayat)

solutions which finally a number of approaches for solving nonlinear equations are emerged for the range of completely analytical to completely numerical ones. Besides all advantages of using numerical methods, closed form solutions appear more appealing because they reveal physical insights through the physics of the problem. Also, parametric studies become more convenient with applying analytical methods. Traditional perturbation methods which were methods for solving nonlinear equations have many shortcomings and they are not valid for strongly nonlinear equations .To overcome the shortcomings, many new techniques have appeared in the open literature, such as, Delta-perturbation [1], Bookkeeping Parameter Perturbation [2], Decomposition [3-4],Homotopy Perturbation [5-12],Energy Balance [13–16] and etc. Recently, Telli and Kopmaz [17] attempted to solve the motion of a mechanical system associated with linear and nonlinear properties using analytical and numerical techniques. It dealt with vibration of a conservative oscillation system with attached mass grounded by linear and nonlinear springs. The linkage of the linear and nonlinear springs in series has been derived with cubic nonlinear characteristics in the equations of motion [18]. The general equation of motion can be formed by transforming intermediate variables into a set of differential algebraic equations and it may be further transformed into a nonlinear ordinary differential equation. The resulted nonlinear differential equation was separately solved by using the EBM and HPM methods and compared with numerical integration solutions using Maple or MATLAB. Moreover, analytical solutions are generally required for the validation of numerical methods and software's approving.

2. GOVERNING EQUATION OF MOTION

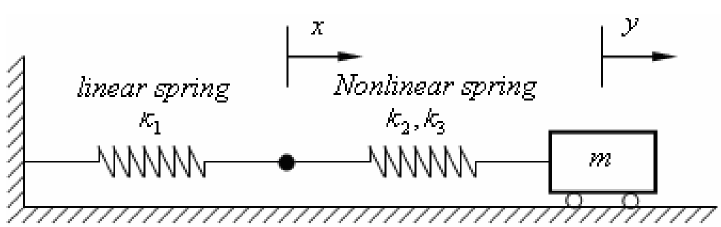

Fig. 1. Nonlinear free vibration of a system of mass with serial linear and Nonlinear stiffness on a frictionless contact surface.

Consider a mechanical system with single-degree-of freedom shown in Fig. 1, which has a mass m grounded by linear and nonlinear springs in series [18-20]. In this figure, the stiffness coefficient of the first linear spring is k_1, the coefficients associated with the linear and nonlinear portions of spring force in the second spring with cubic nonlinear characteristic are described by k_2 and k_3, respectively. Let ε be defined as:

$$\varepsilon = k_2/k_3 \tag{2.1}$$

The case of $k_3 > 0$ corresponds to a hardening spring while $k_3 < 0$ indicates a softening one.

Let x and y denote the absolute displacements of the connection point of two springs, and the mass m, respectively. By introducing two new variables

$$u = y - x\,,\ r = x\,. \tag{2.2}$$

Telli and Kopmaz [17] obtained the following governing equation for u and r:

$$(1+3\varepsilon\eta u^2)\,u'' + 6\varepsilon\eta u\,u'^2 + \omega_0^2(u+\varepsilon u^3) = 0, \tag{2.3}$$

$$r = x = \xi(1+\varepsilon u^2)u,\ y = (1+\xi+\xi\,\varepsilon u^2)u, \tag{2.4}$$

Where a prime denotes differentiation with respect to time t and

$$\xi = k_2/k_1,\quad \eta = \frac{\xi}{1+\xi},\quad \omega_0^2 = \frac{k_2}{m(1+\xi)}. \tag{2.5}$$

Eq. (3) is an ordinary differential equation in u .For Eq. (2.3), we consider the following initial conditions:

$$u(0) = A\,,\quad \dot{u}(0) = 0. \tag{2.6}$$

3. SOLUTUION PROCUDERS

Let us consider the general nonlinear oscillators as follows:

$$\ddot{u} + N(u,\dot{u},\ddot{u},t) = 0, \qquad u(0) = A, \quad \dot{u}(0) = 0. \tag{3.1}$$

Where $N(u,\dot{u},\ddot{u},t)$ is a function with the nonlinear term. There exists no small parameter in Eq. (3.1), so the traditional perturbation methods cannot be applied directly, moreover the equation involves discontinuity. Due to the fact that these methods requires neither a small parameter nor a linear term in a differential equation, we can approximately solve Eq. (3.1) using these solution procedures. In these methods, an artificial perturbation equation is constructed by embedding an artificial parameter $p = [0,1]$, which is used as an expanding parameter. These technique yields a very rapid convergence of the solution series; in most cases, only one iteration leads to high accuracy of the solution. These methods provide an effective and convenient mathematical tool for nonlinear differential equations.

3.1 BASIC CONCEPT OF EBM

In the present paper, we consider a general nonlinear oscillator in the Form:

$$u''+f(u(t))=0 \tag{3.1.1}$$

In which u and t are generalized dimensionless displacement and time variables, respectively. Its variational principle can be easily obtained:

$$J(u)=\int_0^t\left(-\frac{1}{2}u'^2+F(u)\right)dt \tag{3.1.2}$$

Where $T=\dfrac{2\pi}{\omega}$ is period of the nonlinear oscillator, $F(u)=\int f(u)du$.

Its Hamiltonian, therefore, can be written in the form;

$$H=\frac{1}{2}u'^2+F(u)+F(A) \tag{3.1.3}$$

Or

$$R(t)=-\frac{1}{2}u'^2+F(u)-F(A)=0 \tag{3.1.4}$$

Oscillatory systems contain two important physical parameters, i.e.,
The frequency ω and the amplitude of oscillation. A . So let us consider such initial conditions:

$$u(0)=A, \qquad u'(0)=0 \tag{3.1.5}$$

We use the following trial function to determine the angular frequency ω

$$u(t)=A\cos\omega t \tag{3.1.6}$$

Substituting (3.1.6) into u term of (3.1.4), yield:

$$R(t)=\frac{1}{2}\omega^2A^2\sin^2\omega t+F(A\cos\omega t)-F(A)=0 \tag{3.1.7}$$

If, by chance, the exact solution had been chosen as the trial function, then it would be possible to make R zero for all values of t by appropriate choice of ω. Since Eq. (3.1.6) is only an approximation to the exact solution,

R cannot be made zero everywhere. Collocation at $\omega t=\dfrac{\pi}{4}$ gives:

$$\omega=\sqrt{\frac{2(F(A))-F(A\cos\omega t)}{A^2\sin^2\omega t}} \tag{3.1.8}$$

Its period can be written in the form:

$$T=\frac{2\pi}{\sqrt{\dfrac{2(F(A))-F(A\cos\omega t)}{A^2\sin^2\omega t}}} \tag{3.1.9}$$

3.2 BASIC CONCEPT OF HPM

In order to, Eq. (3.1) can be rewritten:

$$\ddot{u}+1u=u-N(u,\dot{u},\ddot{u},t). \tag{3.2.1}$$

We, therefore, can establish the following homotopy:

$$\ddot{u} + 1u = p.\left(u - N(u, \dot{u}, \ddot{u}, t)\right), \qquad p \in [0,1]. \tag{3.2.2}$$

The homotopy parameter p always changes from zero to unity. In case $p = 0$, Eq. (3.2.2) becomes the linearized equation $\ddot{u}_0 + \omega^2 u_0 = 0$, and when it is one, Eq. (3.2.2) turns out to be the original one (Eq. (3.2.1)).Applying the HPM solution we expand the solution v, and 1 as a coefficient of u, the series of p introduce as follows [9]:

$$u = \sum_{i=0}^{n} p^i u_i \tag{3.2.3}$$

$$1 = \omega^2 - \sum_{i=1}^{n} p^i \gamma_i \tag{3.2.4}$$

Substituting Eqs. (3.2.3) and (3.2.4) into Eq. (3.2.2) and equating the terms with the identical powers of p, we can obtain a series of linear equations, and we write only the first two linear equations:

$$p^0: \quad \ddot{u}_0 + \omega^2 u_0 = 0 \tag{3.2.5}$$

$$p^1: \quad \ddot{u}_1 + \omega^2 u_1 = \left(1 + \gamma_1\right) u_0 - \psi(u_0, \dot{u}_0, \ddot{u}_0, t), \tag{3.2.6}$$

.

.

.

Where $\psi(u_0, \dot{u}_0, \ddot{u}_0, t)$ is a function with the nonlinear term in Eq. (3.2.6). The solution of Eq. (3.2.5) is $u_0 = A \cos \omega t$. Substituting u_0 into Eq. (3.2.6), we obtain:

$$\begin{aligned} p^1: \quad \ddot{u}_1 + \omega^2 u_1 &= \left(1 + \gamma_1\right) A \cos \omega t \\ &\quad - \psi(A \cos \omega t, -A\omega \sin \omega t, -A\omega^2 \cos \omega t, t) \end{aligned} \tag{3.2.7}$$

For achieving the secular term, we use Fourier expansion series as follows:

$$\begin{aligned} &\psi(A \cos \omega t, -A\omega \sin \omega t, -A\omega^2 \cos \omega t, t) = \\ &\sum_{n=0}^{\infty} b_{2n+1} \cos\left[\left(2n+1\right)\omega t\right] = b_1 \cos(\omega t) + b_3 \cos(3\omega t) \\ &\qquad + \ldots \approx b_1 \cos(\omega t) \end{aligned} \tag{3.2.8}$$

Substituting Eq. (3.2.8) into Eq. (3.2.7) yields:

$$p^1: \quad \ddot{u}_1 + \omega^2 u_1 = \left(1 + \gamma_1 - b_1\right) A \cos(\omega t) \tag{3.2.9}$$

For avoiding secular term, we have:

$$1+\gamma_1-b_1=0 \tag{3.2.10}$$

Setting $p=1$ in Eq. (3.2.3), we have:

$$1=\omega^2-\gamma_1 \tag{3.2.11}$$

Substituting Eqs. (3.2.11) into Eq. (3.2.10), we can achieve the first-order frequency of Duffing equation, Eq. (3.2.6), as follow:

$$\omega_{HHPM}=\sqrt{b_1}. \tag{3.2.12}$$

4. APPLICATION OF SOLUTUION PROCUDERS

4.1 APPLYING EBM

In Eq. (2.3) , Its Variational principle can be easily obtained:

$$J(u)=\int_0^t\left(-\frac{1}{2}\dot{u}^2\left(1+\frac{3}{2}\varepsilon\eta u^2\right)+\omega_0{}^2\left(\frac{1}{2}u^2+\frac{1}{4}\varepsilon u^4\right)\right)dt \tag{4.1.1}$$

Its Hamiltonian, therefore, can be written in the form:

$$\begin{aligned}H&=\frac{1}{2}\dot{u}^2\left(1+\frac{3}{2}\varepsilon\eta u^2\right)+\omega_0{}^2\left(\frac{1}{2}u^2+\frac{1}{4}\varepsilon u^4\right)\\&=\frac{1}{2}\omega_0{}^2A^2+\frac{1}{4}\omega_0{}^2\varepsilon A^4\end{aligned} \tag{4.1.2}$$

or

$$\begin{aligned}R(t)=&\frac{1}{2}\dot{u}^2\left(1+\frac{3}{2}\varepsilon\eta u^2\right)+\omega_0{}^2\left(\frac{1}{2}u^2+\frac{1}{4}\varepsilon u^4\right)\\&-\frac{1}{2}\omega_0{}^2A^2-\frac{1}{4}\omega_0{}^2\varepsilon A^4=0\end{aligned} \tag{4.1.3}$$

Oscillatory systems contain two important physical parameters, i.e. the frequency ω and the amplitude of oscillation, A. So let us consider such initial conditions:

$$u(0)=A,\qquad \dot{u}(0)=0 \tag{4.1.4}$$

Assume that its initial approximate guess can be expressed as:

$$u(t)=A\cos\omega t \tag{4.1.5}$$

Substituting Eq. (4.1.5) into Eq. (4.1.3), yields:

$$\begin{aligned}R(t)=&\frac{1}{2}(-A\omega\sin\omega t)^2\left(1+\frac{3}{2}\varepsilon\eta(A\cos\omega t)^2\right)+\omega_0{}^2\left(\frac{1}{2}(A\cos\omega t)^2\right.\\&\left.+\frac{1}{4}\varepsilon(A\cos\omega t)^4\right)-\frac{1}{2}\omega_0{}^2A^2-\frac{1}{4}\omega_0{}^2\varepsilon A^4=0\end{aligned} \tag{4.1.6}$$

Which trigger the following results:

$$\omega = \frac{\omega_0\sqrt{2}}{A\sin\omega t}\sqrt{\frac{-(\frac{1}{2}(A\cos\omega t)^2+\frac{1}{4}\varepsilon(A\cos\omega t)^4)+\frac{1}{2}A^2+\frac{1}{4}\varepsilon A^4}{\left(1+\frac{3}{2}\varepsilon\eta(A\cos\omega t)^2\right)}} \tag{4.1.7}$$

If we collocate at $\omega t = \dfrac{\pi}{4}$, we obtain:

$$\omega_{EBM} = \frac{\omega_0\sqrt{\left(4+3A^2\varepsilon\eta\right)\left(4+3A^2\varepsilon\right)}}{4+3A^2\varepsilon\eta}, \tag{4.1.8}$$

Its period can be written in the form:

$$T_{EBM} = \frac{2\pi\left(4+3A^2\varepsilon\eta\right)}{\omega_0\sqrt{\left(4+3A^2\varepsilon\eta\right)\left(4+3A^2\varepsilon\right)}}. \tag{4.1.9}$$

4.2 APPLYING HPM

Eq. (2.3) can be rewritten as the following form:

$$\ddot{u}+1u = p.\left[-3\ddot{u}\,\varepsilon\eta u^2-6\varepsilon\eta u\dot{u}^2-\omega_0^2\varepsilon u^3-\omega_0^2 u+u\right]=0,\quad p\in[0,1]. \tag{4.2.1}$$

Substituting Eqs. (3.2.3) and (3.2.4) into Eq. (4.2.1) and expanding, we can write the first two linear equations as follows:

$$p^0:\quad \ddot{u}_0+\omega^2 u_0 = 0 \tag{4.2.2}$$

$$p^1:\quad \ddot{u}_1+\omega^2 u_1 = -3u_0''\eta\varepsilon u_0^2-6\eta\varepsilon u_0 u_0'^2-\omega_0^2\varepsilon u_0^3+\left(1+\gamma_1-\omega_0^2\right)u_0, \tag{4.2.3}$$

.

.

.

Solving Eq. (4.2.2) gives: $u_0 = A\cos\omega t$. Substituting u_0 into Eq. (4.2.3), yield:

$$p^1:\quad \ddot{u}_1+\omega^2 u_1 = 9A^3\eta\varepsilon\omega^2\cos^3\omega t-6\eta\varepsilon\omega^2 A^3\cos\omega t+\left(1+\gamma_1-\omega_0^2\right)A\cos\omega t-\omega_0^2\varepsilon A^3\cos^3\omega t, \tag{4.2.4}$$

For achieving the secular term, we use Fourier expansion series as follows:

$$9A^3\eta\varepsilon\omega^2\cos^3\omega t - 6\eta\varepsilon\omega^2 A^3\cos\omega t - \omega_0^2\varepsilon A^3\cos^3\omega t$$
$$\begin{aligned} &= \sum_{n=0}^{\infty} b_{2n+1}\cos\left[(2n+1)\,\omega t\right] \\ &= b_1\cos(\omega t) + b_3\cos(3\omega t) + \ldots \\ &\approx \frac{3A^3\varepsilon}{4}\left(\eta\omega^2 - \omega_0^2\right)\cos(\omega t) + \ldots. \end{aligned} \tag{4.2.5}$$

Substituting Eq. (4.2.5) into Eq. (4.2.4) yields:

$$p^1: \quad \ddot{u}_1 + \omega^2 u_1 = \left[\frac{3A^2\varepsilon}{4}\left(\eta\omega^2 - \omega_0^2\right) + \left(1 + \gamma_1 - \omega_0^2\right)\right] \times A\cos(\omega t) \tag{4.2.6}$$

Avoiding secular term, gives:

$$\gamma_1 = \frac{3A^2\varepsilon}{4}\left(\omega_0^2 - \eta\omega^2\right) + \left(\omega_0^2 - 1\right) \tag{4.2.7}$$

From Eq. (3.2.3) and setting $p = 1$, we have:

$$\gamma_1 = \omega - 1 \tag{4.2.8}$$

Comparing Eqs. (4.2.7) and (4.2.8), we can obtain:

$$\omega^2 = \frac{3A^2\varepsilon}{4}\left(\omega_0^2 - \eta\omega^2\right) + \omega_0^2 \tag{4.2.9}$$

Solving Eq. (4.2.9), gives:

$$\omega_{HPM} = \frac{\omega_0\sqrt{\left(4 + 3A^2\varepsilon\eta\right)\left(4 + 3A^2\varepsilon\right)}}{4 + 3A^2\varepsilon\eta}, \tag{4.2.10}$$

Its period can be written in the form:

$$T_{HPM} = \frac{2\pi\left(4 + 3A^2\varepsilon\eta\right)}{\omega_0\sqrt{\left(4 + 3A^2\varepsilon\eta\right)\left(4 + 3A^2\varepsilon\right)}}. \tag{4.2.11}$$

5. RESULTS AND DISCUSSIONS

To illustrate and verify accuracy of these approximate analytical approaches, comparisons of angular frequencies for different parameters via numerical and other approaches is presented in Table. 1. The parameter ε is linearly dependent on the coefficient of nonlinear spring force k_3 as given in Eq. (2.3). The latter can be positive or negative depending on whether the nonlinear spring has hard or soft-spring properties. The results for ω_n is numerically obtained from Eq. (2.3) using the Runge–Kutta [18] numerical integration method in combination with the bisection method. The results for ω_{LP} , and ω_{HB} are solutions of Eq. (2.3) using the second-order of Linearized Perturbation (LP) method [20] , and harmonic balance (HB) technique [17], respectively.

Table 1
Comparison of frequency corresponding to various parameters of system

No.	m	A	ε	k_1	k_2	ω_{LP} [20]	ω_{HB} [17]	$\omega_{HPM} = \omega_{EBM}$	ω_n [17]
1	1	0.5	0.5	50	5	2.220197	2.220239	2.220265	2.220231
2	1	2	0.5	50	5	3.134986	3.257248	3.162277	3.175501
3	1	2	0.5	5	5	1.838180	1.726619	1.889822	1.903569
4	1	2	0.5	5	50	2.144360	2.145708	2.192645	2.195284
5	3	5	1	8	16	$**$	1.176927	1.612706	1.615107
6	3	5	1	10	5	$**$	1.052717	1.739775	1.749115
7	3	10	2	12	16	$**$	$**$	1.545360	1.545853
8	3	30	5	15	5	$**$	$**$	1.731282	1.731382
9	10	200	5	5	250	$**$	$**$	0.707107	0.707107
10	10	100	10	5	25	$**$	$**$	0.707106	0.707106
11	1	0.5	-0.5	50	5	2.038254	2.038207	2.038315	2.038209
12	2	2	-0.1	10	10	1.444007	1.458194	1.434860	1.446389
13	3	4	-0.02	30	10	1.320867	1.336111	1.313064	1.318370
14	10	5	-0.01	8	16	0.705078	0.706817	0.703731	0.705412

$**$ Invalid numerical solutions in complex values.

Also, then percentage errors between the presenting methods (EBM and HPM) and other approximate approaches (LP and HB) is shown in Table 2. As wee can see in this table, wee can find that in many instances, the error percentages of the first order approximation of presenting methods are less than the second order of LP, except examples in rows 1- which the percentage errors are equal to presenting methods -,11, 13 and 14.

Note that in some cases which exist in rows 5-10, LP method could not to get any result, while the presenting methods yield the perfect results with the maximal error 0.53398 %. Also, for HB solution, the presenting methods errors are more less that HB, except examples in rows 1- which the percentage errors are equal to presenting methods- 11 and 14. Similar to LP, HB too not achieves any results which are existed in the rows 7-10. The first order approximation of EBM and HPM for the parameters $m = 3, A = 10, \varepsilon = 2$, $k_1 = 12$, $k_2 = 16$ is 0.03189 %, and for other cases in rows 8-10, is 0.00%.To further illustrate and verify the accuracy of the presenting analytical approach, comparison of EBM and HPM with other approximate methods and numerical solution [18] are presented in Figs. 2 (a-b). Apparently, it is confirmed that the analytical approximations shows excellent agreement with the numerical solutions.

Table 2
Comparison of error percentages corresponding to various parameters of system

No.	m	A	ε	k_1	k_2	$\frac{\lvert\omega_{LP}-\omega_n\rvert}{\omega_n}$	$\frac{\lvert\omega_{HB}-\omega_n\rvert}{\omega_n}$	$\frac{\lvert\omega_{HPM=EBM}-\omega_n\rvert}{\omega_n}$
1	1	0.5	0.5	50	5	0.00153	0.00036	0.00153
2	1	2	0.5	50	5	1.27586	2.57430	0.41644
3	1	2	0.5	5	5	3.43507	9.29570	0.72170
4	1	2	0.5	5	50	2.31970	2.25829	0.12021
5	3	5	1	8	16	**	27.1301	0.14866
6	3	5	1	10	5	**	34.8206	0.53398
7	3	10	2	12	16	**	**	0.03189
8	3	30	5	15	5	**	**	0.00
9	10	200	5	5	250	**	**	0.00
10	10	100	10	5	25	**	**	0.00
11	1	0.5	-0.5	50	5	0.00221	0.00010	0.00520
12	2	2	-0.1	10	10	0.16469	0.81617	0.00520
13	3	4	-0.02	30	10	0.18940	1.34568	0.40247
14	10	5	-0.01	8	16	0.04735	0.19917	0.23830

** Invalid numerical solutions in complex values.

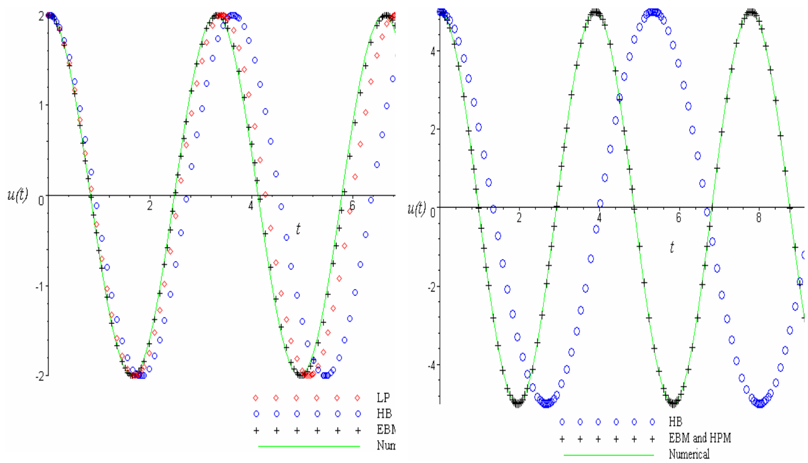

(a) **(b)**

$m=1,\ A=2,\ \varepsilon=0.5,\ k_1=5,\quad m=3,\ A=5,\ \varepsilon=1,\ k_1=8,\ k$

Fig. 2. Comparison between approximate solutions for different parameters.

6. CONCLUSION

Energy Balance and Homotopy perturbation methods are applied to nonlinear oscillators which are useful in so many branches of sciences such as: fluid mechanics, electromagnetic and waves, telecommunication, civil and its structures and all so-called majors' applications, etc. The Energy Balance Method is a well-established method for the analysis of nonlinear systems, can be easily extended to any nonlinear equation. We demonstrated the accuracy and efficiency of the presenting method with some strong nonlinear problems. We can suggest HPM as strongly nonlinear method and EBM as novel and simple method for oscillation systems which provide easy and direct procedures for determining approximations to the periodic solutions. Eventually, this paper suggests to readers to apply the methods for solving nonlinear oscillations because of their accuracy, reliability and simplicity.

REFRENCES

1. J.H. He; A note on delta-perturbation expansion method, Applied Mathematics and Mechanics 23 (6) (2002) 634–638.
2. J.H. He, Bookkeeping parameter in perturbation methods, International Journal of Non-Linear Sciences and Numerical Simulation 2 (3) (2001) 257.
3. G. Adomian, Solving frontier problems of physics: the composition method, Boston: kluwer: 1994.

4. J.I. Ramos, Piecewise-adaptive decomposition methods, Chaos & Soliton and Fractals, In press.
5. J.H. He, The homotopy perturbation method for nonlinear oscillators with discontinuities, Applied Mathematics and Computation; 151 (1) (2004) 287.
6. J. H. He, Homotopy perturbation method for bifurcation on nonlinear problems, International Journal of Non-Linear Science and Numerical Simulation 6 (2005) 207.
7. M. Bayat, D.D. Ganji, M. Shahidi, H. Ebrahim khah. Application of some approximate methods for strongly nonlinear oscillators with external, International Journal of Modern Physics B.(2010)(In press).
8. M. Shahidi, D. D. Ganji1, M. Bayat, "The Analytic Solution for Parametrically Excited Oscillators of Complex Variable in Nonlinear Dynamic Systems with Forcing". International Journal of Modern Physics B,(2010)(In press).
9. T. O zis, A. Yildirim, A comparative study of He' homotopy perturbation method for determining frequency–amplitude relation of a nonlinear oscillator with discontinuities, International Journal of Nonlinear Sciences and Numerical Simulation 8 (2) (2007) 243.
10. A. Beléndez , C. Pascual, S. Gallego, M. Ortuño, C. Neipp, Application of a modified He's homotopy perturbation method to obtain higher-order approximations of an $x^{1/3}$ force nonlinear oscillator, Physics Letters A, 371 (2007) 421.
11. J. H. He, Non-perturbative methods for strongly nonlinear problems, Dissertation. de-Verlag im Internet GmbH, 2006.
12. S. R. Seyed Alizadeh.G, G. Domairry, S. Karimpour, An approximation of the analytical solution of the linear and nonlinear integro-differential equations by homotopy perturbation method, Acta Applicandae Mathematicae.doi: 10.1007/s10440-008-9261-z.
13. S. S. Ganji, S. Karimpour, D. D. Ganji , Z. Z. Ganji, Periodic Solution for Strongly Nonlinear Vibration Systems by Energy Balance Method, Acta Applicandae Mathematicae, doi: 10.1007/s10440-008-9283-6.
14. J. H. He, Preliminary report on the energy balance for nonlinear oscillations, Mechanics Research Communications 29 (2002) 107.
15. T. $\ddot{O}$ zis, A. Yildirim, Determination of the frequency–amplitude relation for a Duffing-harmonic oscillator by the energy balance method, Computers and Mathematics with Applications 54 (2007) 1184.
16. S. S. Ganji, D. D. Ganji, S. Karimpour, Determination of the frequency–amplitude relation for nonlinear oscillators with fractional potential using He's energy balance method, Progress In Electromagnetics Research C 5 (2008) 21.

17. S. Telli, O. Kopmaz, Free vibrations of a mass grounded by linear and nonlinear springs in series, Journal of Sound and Vibration 289 (2006) 689.
18. S. K. Lai, C. W. Lim, Accurate approximate analytical solutions for nonlinear free vibration of systems with serial linear and nonlinear stiffness, Journal of Sound and Vibration 307 (2007) 720–736.
19. W. P. Sun, B. S. Wu, Large amplitude free vibrations of a mass grounded by linear and nonlinear springs in series, Journal of Sound and Vibration, (2008) In press.
20. N. Minorsky, Nonlinear Oscillations, Huntington, R.E. Krieger, New York, 1974.

Instructions to Contributors
Journal of Applied Functional Analysis

A quartely international publication of Eudoxus Press, LLC of TN.

Editor in Chief: George Anastassiou

Department of Mathematical Sciences
University of Memphis
Memphis, TN 38152-3240, U.S.A.

1. Manuscripts, hard copies in quadruplicate and in English,should be submitted by regular, unregistered mail, to the Editor in Chief.

Authors may want to recommend an associate editor most related to the submission to possibly handle it. In addition, to assist the Editor and speed the decision process, authors may include a PDF file of the paper on disk with the submitted copies of the manuscript.

Also authors may want to submit a list of six possible referees, to be used in case we cannot find related referees by ourselves.

2. Manuscripts should be typed using any of TEX,LaTEX,AMS-TEX,or AMS-LaTEX and according to EUDOXUS PRESS, LLC. LATEX STYLE FILE. (Click HERE to save a copy of the style file.)They should be carefully prepared in all respects. Submitted copies should be brightly printed (not dot-matrix), double spaced, in ten point type size, on one side high quality paper 8(1/2)x11 inch. Manuscripts should have generous margins on all sides and should not exceed 24 pages.

3. Submission is a representation that the manuscript has not been published previously in this or any other similar form and is not currently under consideration for publication elsewhere. A statement transferring from the authors(or their employers,if they hold the copyright) to Eudoxus Press, LLC, will be required before the manuscript can be accepted for publication.The Editor-in-Chief will supply the necessary forms for this transfer.Such a written transfer of copyright,which previously was assumed to be implicit in the act of submitting a manuscript,is necessary under the U.S.Copyright Law in order for the publisher to carry through the dissemination of research results and reviews as widely and effective as possible.

4. The paper starts with the title of the article, author's name(s) (no titles or degrees), author's affiliation(s) and e-mail addresses. The affiliation should comprise the department, institution (usually university or company), city, state (and/or nation) and mail code.

The following items, 5 and 6, should be on page no. 1 of the paper.

5. An abstract is to be provided, preferably no longer than 150 words.

6. A list of 5 key words is to be provided directly below the abstract. Key words should express the precise content of the manuscript, as they are used for indexing purposes.

The main body of the paper should begin on page no. 1, if possible.

7. All sections should be numbered with Arabic numerals (such as: 1. INTRODUCTION) .
Subsections should be identified with section and subsection numbers (such as 6.1. Second-Value Subheading).
If applicable, an independent single-number system (one for each category) should be used to label all theorems, lemmas, propositions, corrolaries, definitions, remarks, examples, etc. The label (such as Lemma 7) should be typed with paragraph indentation, followed by a period and the lemma itself.

8. Mathematical notation must be typeset. Equations should be numbered consecutively with Arabic numerals in parentheses placed flush right,and should be thusly referred to in the text [such as Eqs.(2) and (5)]. The running title must be placed at the top of even numbered pages and the first author's name, et al., must be placed at the top of the odd numbed pages.

9. Illustrations (photographs, drawings, diagrams, and charts) are to be numbered in one consecutive series of Arabic numerals. The captions for illustrations should be typed double space. All illustrations, charts, tables, etc., must be embedded in the body of the manuscript in proper, final, print position. In particular, manuscript, source, and PDF file version must be at camera ready stage for publication or they cannot be considered.

Tables are to be numbered (with Roman numerals) and referred to by number in the text. Center the title above the table, and type explanatory footnotes (indicated by superscript lowercase letters) below the table.

10. List references alphabetically at the end of the paper and number them consecutively. Each must be cited in the text by the appropriate Arabic numeral in square brackets on the baseline.
References should include (in the following order):
initials of first and middle name, last name of author(s)
title of article,
name of publication, volume number, inclusive pages, and year of publication.

Authors should follow these examples:

Journal Article

1. H.H.Gonska,Degree of simultaneous approximation of bivariate functions by Gordon operators, (journal name in italics) *J. Approx. Theory*, 62,170-191(1990).

Book

2. G.G.Lorentz, (title of book in italics) *Bernstein Polynomials* (2nd ed.), Chelsea,New York,1986.

Contribution to a Book

3. M.K.Khan, Approximation properties of beta operators,in(title of book in italics) *Progress in Approximation Theory* (P.Nevai and A.Pinkus,eds.), Academic Press, New York,1991,pp.483-495.

11. All acknowledgements (including those for a grant and financial support) should occur in one paragraph that directly precedes the References section.

12. Footnotes should be avoided. When their use is absolutely necessary, footnotes should be numbered consecutively using Arabic numerals and should be typed at the bottom of the page to which they refer. Place a line above the footnote, so that it is set off from the text. Use the appropriate superscript numeral for citation in the text.

13. After each revision is made please again submit four hard copies of the revised manuscript. And after a manuscript has been accepted for publication submit four hard copies of the final revised manuscript. Additionally, two copies of the final version of the TEX/LaTex source file and a PDF file, are to be submitted to the Editor's Office on personal 3.5 inch computer disks. Label the disks individually with clearly written identifying information, e.g. :

Your name, title of article, kind of computer used, kind of software and version number, disk format and files names of article, as well as abbreviated journal name.

Package the disks in a disk mailer or protective cardboard. Make sure contents of disks are identical with the ones of final hard copies submitted!

Note: The Editor's Office cannot accept the disks without the accompanying matching hard copies of manuscript. No e-mail final submissions are allowed! File submission on disk must be used.

14. Effective 1 Nov. 2009 for current journal page charges, contact the Editor in Chief. Upon acceptance of the paper an invoice will be sent to the contact author. The fee payment will be due one month from the invoice date. The article will proceed to publication only after the fee is paid. The charges are to be sent, by money order or certified check, in US dollars, payable to Eudoxus Press, LLC, to the address shown on the Eudoxus homepage.

No galleys will be sent and the contact author will receive one(1) electronic copy of the journal issue in which the article appears.

15. This journal will consider for publication only papers that contain proofs for their listed results.

TABLE OF CONTENTS, JOURNAL OF APPLIED FUNCTIONAL ANALYSIS, VOLUME 6, NO.2, 2011

Volume 6, Number 3 July 2011

ISSN:1559-1948 (PRINT), 1559-1956 (ONLINE)

EUDOXUS PRESS,LLC

JOURNAL OF APPLIED FUNCTIONAL ANALYSIS

GUEST EDITORS: HIKMET CAGLAR, LEVENT CUHACI, GURSEL HACIBEKIROGLU and MEHMET OZER

SPECIAL ISSUE III: "CHAOS and COMPLEX SYSTEMS 2010"

SCOPE AND PRICES OF

JOURNAL OF APPLIED FUNCTIONAL ANALYSIS

A quartely international publication of **EUDOXUS PRESS,LLC**

ISSN:1559-1948(PRINT),1559-1956(ONLINE)

Editor in Chief: George Anastassiou
Department of Mathematical Sciences
The University of Memphis
Memphis, TN 38152,USA
E mail: ganastss@memphis.edu

The purpose of the "Journal of Applied Functional Analysis"(JAFA) is to publish high quality original research articles, survey articles and book reviews from all subareas of Applied Functional Analysis in the broadest form plus from its applications and its connections to other topics of Mathematical Sciences. A sample list of connected mathematical areas with this publication includes but is not restricted to: Approximation Theory, Inequalities, Probability in Analysis, Wavelet Theory, Neural Networks, Fractional Analysis, Applied Functional Analysis and Applications, Signal Theory, Computational Real and Complex Analysis and Measure Theory, Sampling Theory, Semigroups of Operators, Positive Operators, ODEs, PDEs, Difference Equations, Rearrangements, Numerical Functional Analysis, Integral equations, Optimization Theory of all kinds, Operator Theory, Control Theory, Banach Spaces, Evolution Equations, Information Theory, Numerical Analysis, Stochastics, Applied Fourier Analysis, Matrix Theory, Mathematical Physics, Mathematical Geophysics, Fluid Dynamics, Quantum Theory. Interpolation in all forms, Computer Aided Geometric Design, Algorithms, Fuzzyness, Learning Theory, Splines, Mathematical Biology, Nonlinear Functional Analysis, Variational Inequalities, Nonlinear Ergodic Theory, Functional Equations, Function Spaces, Harmonic Analysis, Extrapolation Theory, Fourier Analysis, Inverse Problems, Operator Equations, Image Processing, Nonlinear Operators, Stochastic Processes, Mathematical Finance and Economics, Special Functions, Quadrature, Orthogonal Polynomials, Asymptotics, Symbolic and Umbral Calculus, Integral and Discrete Transforms, Chaos and Bifurcation, Nonlinear Dynamics, Solid Mechanics, Functional Calculus, Chebyshev Systems. Also are included combinations of the above topics.

Working with Applied Functional Analysis Methods has become a main trend in recent years, so we can understand better and deeper and solve important problems of our real and scientific world.

JAFA is a peer-reviewed International Quarterly Journal published by Eudoxus Press,LLC.

We are calling for high quality papers for possible publication. The contributor should send four copies of the contribution to the EDITOR in CHIEF in TEX,LATEX double spaced,in ten point type size. They should be sent BY REGULAR MAIL ONLY, NOT REGISTERED MAIL, AND NO E-MAIL SUBMISSIONS [See: Instructions to Contributors]

Journal of Applied Functional Analysis(JAFA)
is published in January,April,July and October of each year by

EUDOXUS PRESS,LLC,
1424 Beaver Trail Drive,Cordova,TN38016,USA,
Tel.001-901-751-3553
anastassioug@yahoo.com
http://www.EudoxusPress.com visit also http://www.msci.memphis.edu/~ganastss/jafa.

Webmaster:Ray Clapsadle

Annual Subscription Current Prices:For USA and Canada,Institutional:Print $400,Electronic $250,Print and Electronic $450.Individual:Print $ 150, Electronic $80,Print &Electronic $200.For any other part of the world add $50 more to the above prices for Print.
Single article PDF file for individual $15.Single issue in PDF form for individual $60.

No credit card payments.Only certified check,money order or international check in US dollars are acceptable.
Combination orders of any two from JoCAAA,JCAAM,JAFA receive 25% discount,all three receive 30% discount.

JAFA is reviewed and abstracted by AMS Mathematical Reviews,MATHSCI,and Zentralblaat MATH.

JAFA IS A JOURNAL OF RAPID PUBLICATION

Journal of Applied Functional Analysis
Editorial Board
Associate Editors

Operators on Banach spaces,
Tensor products of Banach spaces,
Polymeasures, Function spaces.

8) Michele Campiti
Department of Mathematics "E.De Giorgi"
University of Lecce
P.O. Box 193
Lecce,ITALY
Tel. +39 0832 297 432
Fax +39 0832 297 594
michele.campiti@unile.it
Approximation Theory,
Semigroup Theory, Evolution problems,
Differential Operators.

9)Domenico Candeloro
Dipartimento di Matematica e Informatica
Universita degli Studi di Perugia
Via Vanvitelli 1
06123 Perugia
ITALY
Tel +39(0)75 5855038
+39(0)75 5853822,
+39(0)744 492936
Fax +39(0)75 5855024
candelor@dipmat.unipg.it
Functional Analysis, Function spaces,
Measure and Integration Theory in
Riesz spaces.

10) Pietro Cerone
School of Computer Science and
Mathematics, Faculty of Science,
Engineering and Technology,
Victoria University
P.O.14428,MCMC
Melbourne,VIC 8001,AUSTRALIA
Tel +613 9688 4689
Fax +613 9688 4050
Pietro.cerone@vu.edu.au
Approximations, Inequalities,
Measure/Information Theory,
Numerical Analysis, Special Functions.

11)Michael Maurice Dodson
Department of Mathematics
University of York,
York YO10 5DD, UK
Tel +44 1904 433098
Fax +44 1904 433071
Mmd1@york.ac.uk
Harmonic Analysis and Applications to
Signal Theory,Number Theory and
Dynamical Systems.

Almost Periodicity & Almost Automorphy.

32) Vassilis Papanicolaou
Department of Mathematics
National Technical University of Athens
Zografou campus, 157 80
Athens, Greece
tel:: +30(210) 772 1722
Fax +30(210) 772 1775
papanico@math.ntua.gr
Partial Differential Equations,
Probability.

33) Pier Luigi Papini
Dipartimento di Matematica
Piazza di Porta S.Donato 5
40126 Bologna
ITALY
Fax +39(0)51 582528
papini@dm.unibo.it
Functional Analysis, Banach spaces,
Approximation Theory.

34) Svetlozar T.Rachev
Chair of Econometrics,Statistics
and Mathematical Finance
School of Economics and
Business Engineering
University of Karlsruhe
Kollegium am Schloss, Bau II,20.12, R210
Postfach 6980, D-76128,
Karlsruhe,GERMANY.
Tel +49-721-608-7535,
+49-721-608-2042(s)
Fax +49-721-608-3811
Zari.Rachev@wiwi.uni-karlsruhe.de
Second Affiliation:
Dept.of Statistics and Applied Probability
University of California at Santa Barbara
rachev@pstat.ucsb.edu
Probability,Stochastic Processes and
Statistics,Financial Mathematics,
Mathematical Economics.

35) Paolo Emilio Ricci
Department of Mathematics
Rome University "La Sapienza"
P.le A.Moro,2-00185
Rome,ITALY
Tel ++3906-49913201 office
++3906-87136448 home
Fax ++3906-44701007
Paoloemilio.Ricci@uniroma1.it
riccip@uniroma1.it
Special Functions, Integral and Discrete

12) Sever S.Dragomir
School of Computer Science and
Mathematics, Victoria University,
PO Box 14428,
Melbourne City,
MC 8001,AUSTRALIA
Tel. +61 3 9688 4437
Fax +61 3 9688 4050
sever@csm.vu.edu.au
Inequalities,Functional Analysis,
Numerical Analysis, Approximations,
Information Theory, Stochastics.

13) Paulo J.S.G.Ferreira
Department of Electronica e
Telecomunicacoes/IEETA
Universidade de Aveiro
3810-193 Aveiro
PORTUGAL
Tel +351-234-370-503
Fax +351-234-370-545
pjf@ieeta.pt
Sampling and Signal Theory,
Approximations, Applied Fourier Analysis,
Wavelet, Matrix Theory.

14) Gisele Ruiz Goldstein
Department of Mathematical Sciences
The University of Memphis
Memphis,TN 38152,USA.
Tel 901-678-2513
Fax 901-678-2480
ggoldste@memphis.edu
PDEs, Mathematical Physics,
Mathematical Geophysics.

15) Jerome A.Goldstein
Department of Mathematical Sciences
The University of Memphis
Memphis,TN 38152,USA
Tel 901-678-2484
Fax 901-678-2480
jgoldste@memphis.edu
PDEs,Semigroups of Operators,
Fluid Dynamics,Quantum Theory.

16) Heiner Gonska
Institute of Mathematics
University of Duisburg-Essen
Lotharstrasse 65
D-47048 Duisburg
Germany
Tel +49 203 379 3542
Fax +49 203 379 1845
gonska@math.uni-duisburg.de
Approximation and Interpolation Theory,
Transforms, Symbolic and Umbral Calculus,
ODE, PDE,Asymptotics, Quadrature,
Matrix Analysis.

36) Silvia Romanelli
Dipartimento di Matematica
Universita' di Bari
Via E.Orabona 4
70125 Bari, ITALY.
Tel (INT 0039)-080-544-2668 office
080-524-4476 home
340-6644186 mobile
Fax -080-596-3612 Dept.
romans@dm.uniba.it
PDEs and Applications to Biology and
Finance, Semigroups of Operators.

37) Boris Shekhtman
Department of Mathematics
University of South Florida
Tampa, FL 33620,USA
Tel 813-974-9710
boris@math.usf.edu
Approximation Theory, Banach spaces,
Classical Analysis.

38) Rudolf Stens
Lehrstuhl A fur Mathematik
RWTH Aachen
52056 Aachen
Germany
Tel ++49 241 8094532
Fax ++49 241 8092212
stens@mathA.rwth-aachen.de
Approximation Theory, Fourier Analysis,
Harmonic Analysis, Sampling Theory.

39) Juan J.Trujillo
University of La Laguna
Departamento de Analisis Matematico
C/Astr.Fco.Sanchez s/n
38271.LaLaguna.Tenerife.
SPAIN
Tel/Fax 34-922-318209
Juan.Trujillo@ull.es
Fractional: Differential Equations-
Operators-
Fourier Transforms, Special functions,
Approximations,and Applications.

40) Tamaz Vashakmadze
I.Vekua Institute of Applied Mathematics
Tbilisi State University,
2 University St. , 380043,Tbilisi, 43,
GEORGIA.
Tel (+99532) 30 30 40 office

22) Hubertus Th. Jongen
Department of Mathematics
RWTH Aachen
Templergraben 55
52056 Aachen
Germany
Tel +49 241 8094540
Fax +49 241 8092390
jongen@rwth-aachen.de
Parametric Optimization, Nonconvex Optimization, Global Optimization.

45) Richard A. Zalik
Department of Mathematics
Auburn University
Auburn University,AL 36849-5310
USA.
Tel 334-844-6557 office
678-642-8703 home
Fax 334-844-6555
zalik@auburn.edu
Approximation Theory,Chebychev Systems, Wavelet Theory.

Preface

These **four** special issues, which constitute the proceedings of the symposium 3rd International Interdisciplinary Chaos Symposium on CHAOS and COMPLEX SYSTEMS - CCS2010 (21-24 May 2010), have tried to create a forum for the exchange of information and experience in the exciting interdisciplinary field of chaos. However the conference was more in the Applied Mathematics, Social Sciences and Physics direction centered.

The view of the organizers concerning international resonance of the conference has been fulfilled: approximatelly 200 scientists from 21 diffrent countries (Algeria, Bulgaria, Croatia, Denmark, France, Germany, Greece, Iran, Italy, Jordan, Lebanon, Malaysia, Pakistan, Republic of Serbia, Russia, Sultanate of Oman, Tunisia, Turkey, Ukraine, United Kingdom and United States of America) have participated. Good relations to research institutes of these countries might be of great importance for science and applications in different fields of Chaos.

On behalf of the Organizing Committee we would like to express our thanks to the Scientific Committee, the Program Committee and to all who have contributed to this conference for their support and advice. We are also grateful to the invited lecturers Prof. Henry D.I. Abarbanel, Prof. David S. Byrne, Prof. George Anastassiou, Prof. Zidong Wang, Prof. Turgut Ozis and Prof. Markus J. Aschwanden.

Special thanks are due to Rector Prof. Dursun Kocer and Vice Rector Prof. Cetin Bolcal for their close support, advice and incentive encouraging.

Our thanks are also due to the Istanbul Kultur University, which was hosting this symposium and provided all of its facilities.

Finally, we are grateful to the Editor-in-Chief, Prof. George Anastassiou for accepting this volume for publication.

Hikmet Caglar, PhD in Mathematics, s.caglar@iku.edu.tr
Levent Cuhaci, PhD in Computer Science, l.cuhaci@iku.edu.tr
Gursel Hacibekiroglu, PhD in Physics, g.hacibekiroglu@iku.edu.tr
Mehmet Ozer, PhD in Physics, m.ozer@iku.edu.tr

Istanbul Kultur University, Faculty of Science and Letters, Istanbul, Turkey

JOURNAL OF APPLIED FUNCTIONAL ANALYSIS, VOL.6, NO.3, 211-218, COPYRIGHT 2011 EUDOXUS PRESS, LLC

Absolute Stability of Uncertain Fractional Order Control Systems

Celaleddin Yeroglu and Nusret Tan

Electrical and Electronics Engineering Department,
Inonu University , Malatya, 44280 TURKEY
(cyeroglu@inonu.edu.tr; ntan@inonu.edu.tr).

March 07, 2010

The paper present extensions of some results developed for absolute stability of the system with parametric uncertainty structure to the fractional order interval control systems (FOICS). Nyquist envelopes of FOICS whose numerator and denominator polynomials are fractional order polynomials with interval uncertainty structure, are calculated using the geometric structure of the value set of fractional order interval polynomials (FOIP). Absolute stability of the system is analyzed using Nyquist envelopes in the light of Lur'e, Popov and Circle criterion. A numerical example is included to illustrate the benefit of the method presented.
Keywords: Absolute stability, fractional order control system, parametric uncertainty, Nyquist envelope.

1 Introduction

The real world systems can be described by fractional order differential equations more adequately than the integer order one [1, 2]. Therefore, in recent years considerable attention has been given to the fractional order control systems (FOCS) due to the better understanding of fractional calculus. As a result, some important studies dealing with the applications of the fractional calculus to the control systems have been done in [3-6]. This field of research is still new and there is not much work dealing with nonlinear FOCS with parametric uncertainty. The frequency domain analysis of systems is an important topic in control theory. There are some powerful graphical tools in classical control, such as the Nyquist plot, Bode plots and Nichols charts, which are widely used to evaluate the frequency domain behaviours of systems. Motivated by the results especially the Kharitonov and the Edge theorems [7, 8] obtained in the parametric robust control, there have been several studies on the computation of the frequency responses of control systems under parametric uncertainty [9]. However, these results are related to the integer order control systems with parametric uncertainty. Therefore, extensions of these results to FOCS with parametric uncertainty will be very important.

The robust stability analysis of a control system in the presence of uncertainties is important and well-developed subject in control theory. The well-known absolute stability problem [10] which was formulated in the 1950's is an important stability problem regarding nonlinear systems. The robust absolute stability for systems with parametric uncertainty was studied in [11-13]. The main idea of this approaches are based on the boundary results developed in parametric robust control.

The purpose of this paper is to present extensions of the methods for absolute stability analysis of integer order systems to the nonlinear fractional order control system. The Nyquist envelope of fractional order control system with parametric uncertainty structure is calculated. Based on the Nyquist envelopes, the robust versions of Lur'e, Papov and Circle criterion are derived for nonlinear FOCS with parametric uncertainty.

The paper is organized as follows: In Section 2, the computation of Nyquist envelope is given. Absolute stability is discussed in Section 3. A numerical example is given in Section 4. Section 5 includes concluding remarks.

2 Nyquist Envelope of FOITF

The numerator and denominator polynomials of a fractional order interval transfer function (FOITF) are a FOIP of the form,

$$P(s,q) = q_0 s^{\alpha_0} + q_1 s^{\alpha_1} + q_2 s^{\alpha_2} + q_3 s^{\alpha_3} + \cdots + q_n s^{\alpha_n} \tag{1}$$

where $\alpha_0 < \alpha_1 < \cdots < \alpha_n$ are generally real numbers, $q = [q_{0,} q_1, q_2, ..., q_n]$ is the uncertain parameter vector and the uncertainty box is $Q = \{q : q_i \in [\underline{q_i}, \overline{q_i}], i = 0,1,2,...,n\}$. Here $\underline{q_i}$ and $\overline{q_i}$ are specified lower and upper bounds of i^{th} perturbation q_i, respectively. Thus, a FOITF can be represented as,

$$G(s,a,b) = \frac{N(s,b)}{D(s,a)} = \frac{b_0 s^{\alpha_0} + b_1 s^{\alpha_1} + b_2 s^{\alpha_2} + ... + b_m s^{\alpha_m}}{a_0 s^{\beta_0} + a_1 s^{\beta_1} + a_2 s^{\beta_2} + ... + a_n s^{\beta_n}} \tag{2}$$

where $\alpha_0 < \alpha_1 < ... < \alpha_m$ and $\beta_0 < \beta_1 < .... < \beta_n$ are generally real numbers, $a = [a_0, a_1, ..., a_n]$ and $b = [b_0, b_1, ..., b_m]$ are uncertain parameter vectors, $A = \{a : a_i \in [\underline{a_i}, \overline{a_i}],\ i = 0,1,2,...,n\}$ and $B = \{b : b_i \in [\underline{b_i}, \overline{b_i}],\ i = 0,1,2,...,m\}$ are uncertainty boxes. It is first shown that the value set of the family of polynomial of Eq. (1) can be constructed using the upper and lower values of uncertain parameters. Then, using the geometric structure of the value set the Nyquist envelopes of FOITF represented by Eq. (2) can be computed. For FOIP of Eq. (1), substituting $s = j\omega$ gives,

$$\begin{aligned} P(j\omega, q) &= q_0 (k_{0r} + jk_{0i})\omega^{\alpha_0} + \cdots + q_n (k_{nr} + jk_{ni})\omega^{\alpha_n} \\ &= (q_0 k_{0r}\omega^{\alpha_0} + \cdots + q_n k_{nr}\omega^{\alpha_n}) + j(q_0 k_{0i}\omega^{\alpha_0} + \cdots + q_n k_{ni}\omega^{\alpha_n}) \end{aligned} \tag{3}$$

where k_{lr} and k_{li} , $l = 1,2,...,n$ are constants. From Eq. (3), it is clear that the uncertain parameters appearing both in the real and imaginary parts are linearly dependent to each other. The value set of such a polynomial in the complex plane is a polygon. Thus the corresponding polytope of a family of Eq. (1) in the coefficient space has $2^{(n+1)}$ vertices and $(n+1)2^n$ exposed edges since the polynomial family has $(n+1)$ uncertain parameters. For example, the uncertainty box in the parameter space and image of the exposed edges in the complex plane for a polynomial of the form of Eq. (1) with 3 uncertain parameters are shown in Fig. 1.

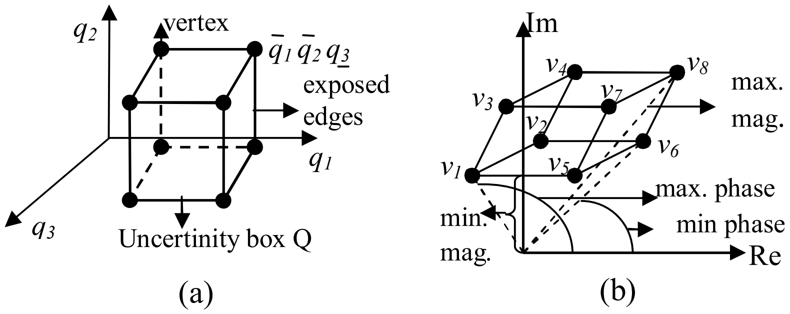

Fig. 1: For a polynomial of the form of (1) with 3 uncertain parameters
a) Uncertainty box in the parameter space b) Images of exposed edges in the complex plane

Using the upper and lower values of the uncertain parameters, all the 2^{n+1} vertex polynomials of $P(s,q)$ can be written in the following pattern

$$
\begin{aligned}
& v_1(s) = \underline{q_0} s^{\alpha_0} + \underline{q_1} s^{\alpha_1} + \underline{q_2} s^{\alpha_2} + \cdots + \underline{q_n} s^{\alpha_n} \\
& v_2(s) = \overline{q_0} s^{\alpha_0} + \underline{q_1} s^{\alpha_1} + \underline{q_2} s^{\alpha_2} + \cdots + \underline{q_n} s^{\alpha_n} \\
& \vdots \\
& v_{2^{(n+1)}}(s) = \overline{q_0} s^{\alpha_0} + \overline{q_1} s^{\alpha_1} + \overline{q_2} s^{\alpha_2} + \cdots + \overline{q_n} s^{\alpha_n}
\end{aligned}
\tag{4}
$$

From these vertex polynomials the exposed edges can be obtained. For example, the vertex polynomial $v_1(s)$ and $v_2(s)$ have the same structure except the parameter (q_0) is its lower value $(\underline{q_0})$ in $v_1(s)$ and its upper value $(\overline{q_0})$ in $v_2(s)$. Thus one of the exposed edges can be expressed as $e(v_1, v_2) = (1-\lambda)v_1(s) + \lambda v_2(s)$ where $\lambda \in [0,1]$. The numerator and denominator polynomials of FOITF of Eq. (2) are in the form of $P(s,q)$ of Eq. (1). Therefore, the results given above can be used to obtain the Nyquist envelope of FOITF. Consider the transfer function given in Eq. (2), and let $n_1, n_2, ..., n_{2^{m+1}}$ and $d_1, d_2, ..., d_{2^{n+1}}$ be the vertex polynomials of $N(s,b)$ and $D(s,a)$ polynomials respectively. Define the sets N_V and N_E, which contain the vertices and edges of $N(s,b)$, as $N_V = \{n_1, n_2, ..., n_{2^{m+1}}\}$ and $N_E = \{ne_1, ne_2, ..., ne_{(m+1)2^m}\}$. Similarly define D_V and D_E for the $D(s,a)$ as $D_V = \{d_1, d_2, ..., d_{2^{n+1}}\}$ and $D_E = \{de_1, de_2, ..., de_{(n+1)2^n}\}$. Define the extremal system as,

$$
G_E(s) = \frac{N_V(s)}{D_E(s)} \cup \frac{N_E(s)}{D_V(s)}
\tag{5}
$$

where N_V, N_E, D_V and D_E are defined above. Thus, at $s = j\omega$, $\partial G(j\omega, a, b) \subset G_E(j\omega)$ where G_E is defined in Eq. (5) and ∂ denotes the boundary [14].

3 Absolute Stability Analysis

In this section, the robust versions of classical absolute stability criterion namely, Lur'e, Popov and Circle criterion are obtained for FOCS with parametric uncertainty using the boundary results explained in previous section which is $\partial G(j\omega, a, b) \subset G_E(j\omega)$. The proofs of the theorems given below are omitted in the paper due to the space limitations.

Theorem 1: (*Lur'e Criterion*) if $G(s,a,b)$ of Fig. 2 is a stable transfer function and the nonlinearity ϕ belongs to the sector $[0,k_l]$ then the condition for absolute stability is defined for G_E given in Eq. (5) as,

$$\frac{1}{k_l}+\mathrm{Re}[G_E(j\omega)]>0, \quad \forall\omega\geq 0 \tag{6}$$

Theorem 2: (*Popov Criterion*) if $G(s,a,b)$ of Fig. 2 is a stable transfer function and ϕ is a time-invariant nonlinearity, which belongs to the sector $[0,k_p]$, then the condition for absolute stability for G_E given in Eq. (5) is that there exist a real number θ such that ,

$$\frac{1}{k_p}+\mathrm{Re}[(1+\theta j\omega)\,G_E(j\omega)]>0, \quad \forall\omega\geq 0 \tag{7}$$

Theorem 3: (*Circle criterion*) if $G(s,a,b)$ of Fig. 2 is a stable transfer function and ϕ is a time-invariant nonlinearity, which belongs to the sector $[k_1,k_2]$, then the condition for absolute stability is that the Nyquist plot of $G_E(s)$ of Eq. (5) stays out of the circle C which is centered on the negative real axis at the point $(-(k_1+k_2)/2k_1k_2,0)$ and cutting the negative real axis at $-1/k_1$ and $-1/k_2$ where $k_1>0$, $k_2>0$ and $k_1<k_2$.

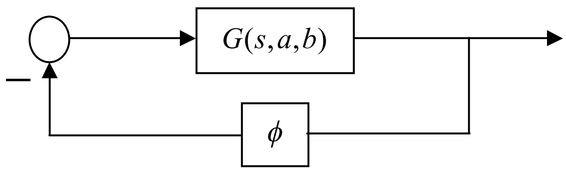

Fig. 2: A fractional order control system with nonlinear feedback perturbations.

4 A Numerical Example

In this example the Nyquist envelope and robust Lur'e, Popov Circle criterion for Fig. 2 with the following transfer function is studied.

$$G(s,a,b)=\frac{N(s,b)}{D(s,a)}=\frac{b_0+b_1s^{0.9}}{a_0+a_1s^{0.8}+a_2s^{2.2}+a_3s^{3.1}} \tag{8}$$

where, $a_0 \in [0.4,0.8]$, $a_1 \in [2,3]$, $a_2 \in [3,6]$, $a_3 = 1$, $b_0 \in [1,1.2]$, $b_1 = 1$. Thus, the transfer function has four uncertain parameters. It can be seen that the $N(s,b)$ has one uncertain parameters. Therefore $N(s,b)$ have $2^1 = 2$ vertex polynomials and $1x2^0 = 1$ exposed edge. $D(s,a)$ have 3 uncertain parameters. So, there are $2^3 = 8$ vertex polynomials and $3x2^2 = 12$ exposed edges for $D(s,a)$. The vertex polynomials of $N(s,b)$ are $n_1(s) = 1 + s^{0.9}$ and $n_2(s) = 1.2 + s^{0.9}$. Thus, $N_V = \{n_1, n_2\}$ and $N_E = \{ne_1\} = \{e(n_1, n_2)\}$. The vertex polynomials of $D(s,a)$ are

$$\begin{aligned} d_1(s) &= 0.4 + 2s^{0.8} + 3s^{2.2} + s^{3.1}, \quad d_2(s) = 0.8 + 2s^{0.8} + 3s^{2.2} + s^{3.1} \\ d_3(s) &= 0.4 + 3s^{0.8} + 3s^{2.2} + s^{3.1}, \quad d_4(s) = 0.8 + 3s^{0.8} + 3s^{2.2} + s^{3.1} \\ d_5(s) &= 0.4 + 2s^{0.8} + 6s^{2.2} + s^{3.1}, \quad d_6(s) = 0.8 + 2s^{0.8} + 6s^{2.2} + s^{3.1} \\ d_7(s) &= 0.4 + 3s^{0.8} + 6s^{2.2} + s^{3.1}, \quad d_8(s) = 0.8 + 3s^{0.8} + 6s^{2.2} + s^{3.1} \end{aligned} \tag{9}$$

Thus, $D_V = \{d_1, d_2, \cdots, d_8\}$ and the set of exposed edges of $D(s,a)$ is

$$\begin{aligned} &D_E = \{de_1, de_2, ..., de_{12}\} = \\ &\left\{ \begin{matrix} e(d_1,d_2), e(d_1,d_3), e(d_1,d_5), e(d_2,d_4), e(d_2,d_6), e(d_3,d_4), \\ e(d_3,d_7), e(d_4,d_8), e(d_5,d_6), e(d_5,d_7), e(d_6,d_8), e(d_7,d_8) \end{matrix} \right\} \end{aligned} \tag{10}$$

Using explanations in section 2, Nyquist envelope of the system can be calculated. Using the theorem 1 and Fig. 3, the robust Lur'e gain is computed as $k_l = 0.8558$. From theorem 2 and Fig. 4, the robust Popov gain is calculated as $k_p = 16.1390$. From Fig. 5, the radius of the smallest circle centered at (-1, 0) and touching to the Nyquist envelope is 0.43. Using theorem 3, the robust absolute stability sector for circle C is calculated as $[k_1, k_2] = [0.8749, 1.7544]$.

5 Conclusion and Remarks

In this paper, the absolute stability problem of the fractional order control system whose numerator and denominator are in the form of FOIP, has been studied. Nyquist envelope of the system is obtained. Absolute stability is analyzed using Nyquist envelope of the system and new robust Lur'e, Popov and Circle criterion have been obtained. These results will be important for the stability analysis of uncertain nonlinear fractional order systems. It can be concluded that extensions of the results obtained for integer order control systems is possible for FOCS. Further results can be obtained in this direction.

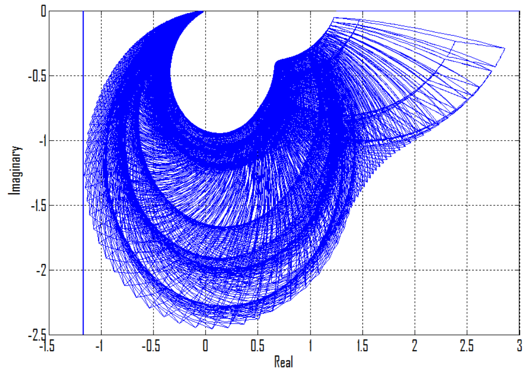

Fig. 3: Lur'e criterion

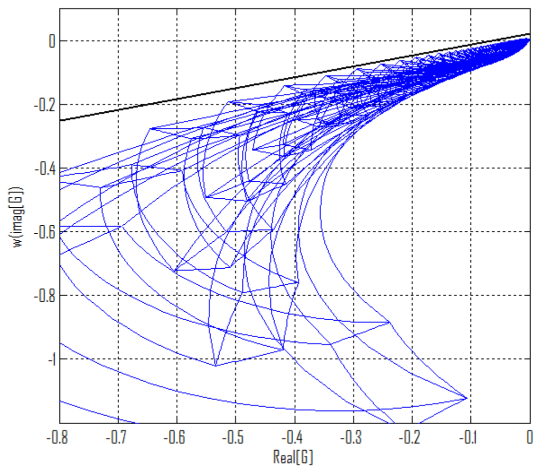

Fig. 4: Popov criterion

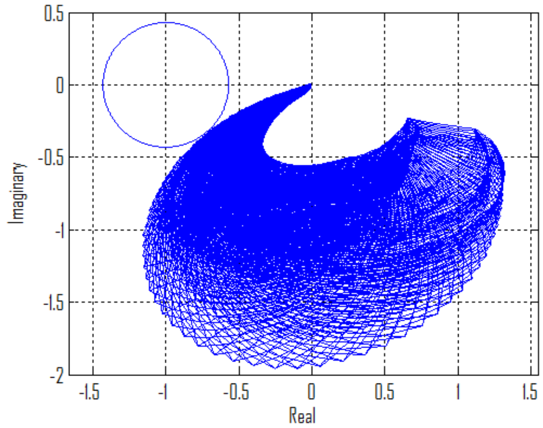

Fig. 5: Circle criterion

6 References

1. T.F. Nonnenmacher and W.G. Glöckle, “A fractional model for mechanical stress relaxation,” *Philosophical Magazine Lett*., vol. 64,(2) pp: 89-93, 1991.
2. S Westerlund,. “Capacitor theory”. *IEEE Trans. Dielectrics Electron Insulation,* vol.1 (5), pp. 826-839, 1994 .
3. J Sabatier, S. Poullain, P. Latteux, J. L. Thomas and A. Oustaloup “Robust speed control of a low damped electromechanical system based on CRONE control: application to a four mass experimental test bench”. *Nonlinear Dynamics,* vol. 38, pp. 383-400, 2004.
4. I Podlubny, “Fractional-order systems and $PI^{\lambda}D^{\mu}$ controllers”. *IEEE Trans. on Automatic Control*, vol. 44, (1), pp. 208-214, 1999.
5. D Valério and J.S. da Costa. “Time domain implementation of fractional order controllers” *IEEProc., Control Theory Appl*., vol. 152, (5), pp. 539-552, 2005.
6. C.A Monje, B. M. Vinagre and V. Feliu; et al “Tuning and auto-tuning of fractional order controllers for industry applications”. *Control Engineering Practice*, vol. 16, pp. 798-812, 2008.
7. V. L. Kharitonov, “Asymptotic stability of an equilibrium position of a family of systems of linear differential equations”, *Differantial Equations*, vol. 14, pp. 1483-1485, 1979.
8. A. C. Bartlett, C. V. Hollot and H. Lin, “Root location of an entire polytope of polynomials: it suffices to check edges”, *Mathematics of controls, Signals and Systems*, vol. 1, pp. 61-71, 1988.
9. S. P. Bhattacharyya, H. Chapellat, and L. H. Keel, “Robust Control: The Parametric Approach”, Prentice Hall, 1995.
10. M. Vidyasagar, “*Nonlinear System Analysis*” Engle-wood Cliffs, Prentice-Hall, 1978.
11. L. T. Grujic and D. Petkovski, “On robustness of Lurie systems with multiple nonlinearities”, *Automatica*, vol. 23, pp. 327-334, 1987.
12. Y. K. Foo and Y. C. Soh, “Closed loop hyperstabilityof interval plants”, *IEEE Trans. Automat. Contr*., vol. 39, pp. 151-154, 1994.
13. T. Mori, T. Nishimura and H. Kokame, “Comments on “on the robust Popov criterionfor interval Lur’e systems””, *IEEE Trans. Automat. Contr*., vol. 40, pp. 136-137, 1995.
14. N. Tan, M.M. Ozyetkin and C. Yeroglu, “Nyquist Envelope of Fractional order transfer function with parametric uncertainty”, *New Trends in Nanotechnology and Fractional Calculus Application* (D. Baleanu et. al. eds.), Springer Science +Businness Media, pp. 487-494, 2010.

JOURNAL OF APPLIED FUNCTIONAL ANALYSIS, VOL.6, NO.3, 219-224, COPYRIGHT 2011 EUDOXUS PRESS, LLC

Stokes fluid Surrounding a Viscoelastic Suspension with Short Memory

Fadila Bentalha
Laboratory LTM, University Hadj-Lakhdar of Batna , Algeria
Laboratory LEM2I, Laboratoire Euromaghebin des Mathématiques et ses Intractions
fbentalha@hotmail.com

Abstract

We study the flow of Stokes fluid surrounding solid suspension. The suspension is periodically distributed and made of an heterogeneous viscoelastic material with short memory. By homogenization methods, we show that the limit behavior of the mixture is that of a viscoelastic medium with fading memory.
Key Words: Homogenization; multi-scale method; Short memory; Stokes fluid.

1 Formulation of the problem

Let $Y = [0, l_1[\times[0, l_2[\times[0, l_3[$ $(l_i > 0, i = 1, 3)$ be the reference cell.. Let Y_s an open subset $\left(\overline{Y_s} \subset Y\right)$ with sufficiently smooth boundary, locally in one side of its boundary, and $Y_f = Y - \overline{Y_s}$. $\mathbb{R}^3$ is cover in a periodic manner by cells obtained by translating εY, $\varepsilon > 0$. Let Ω be an open bounded and connected subset of $\mathbb{R}^3$. The fluid (respectively the solid) part denoting by Ω_f^ε (respectively Ω_s^ε) is the translates of εY_f (respectively εY_s) in Ω. One supposes that $\partial\Omega_s^\varepsilon \cap \partial\Omega = \emptyset$.

In the solid part the strain tensor is given by

$$\sigma_{ij}^\varepsilon(w) = a_{ijkh}^{0\varepsilon} e_{kh}(w) + a_{ijkh}^{1\varepsilon} \frac{\partial e_{kh}(w)}{\partial t}, \tag{1}$$

where $e_{kh}(v) = \frac{1}{2}\left(\frac{\partial v_k}{\partial x_h} + \frac{\partial v_h}{\partial x_k}\right)$ is the deformation tensor. The coefficients $a_{ijkh}^{0\varepsilon}$ and $a_{ijkh}^{1\varepsilon}$ are respectively the elasticity and visco-elasticity ones, and are such that

$$a_{ijkh}^{l\varepsilon}(x) = a_{ijkh}^{l}\left(\frac{x}{\varepsilon}\right), \quad x \in \Omega_s^\varepsilon,\ l = 0, 1,$$

with a^{l}_{ijkh} being $Y-$periodic, bounded and measurable in Y_s and satisfying the usual conditions of symmetry and ellipticity. Note that the functions $a^{l\varepsilon}_{ijkh}$ are $\varepsilon Y-$periodic.

We denote by u^ε and p^ε respectively the fluid velocity and the fluid pressure, w^ε the solid displacement, and f the exterior forces.

We shall consider Q^ε the following system:

$$\begin{cases} \frac{\partial u^\varepsilon}{\partial t} - \mu\Delta u^\varepsilon = f - \nabla p^\varepsilon & \text{in } \Omega^\varepsilon_f \times]0,T[\,, \\ div u^\varepsilon = 0 & in\, \Omega^\varepsilon_f \times]0,T[\,, \\ \frac{\partial^2 w^\varepsilon_i}{\partial t^2} - \sigma^\varepsilon_{ij,,j}(w^\varepsilon) = f_i\ ,\ i = \overline{1,3} & in\, \Omega^\varepsilon_s \times]0,T[\,, \end{cases} \tag{2}$$

with the initial and boundary conditions:

$$\begin{cases} u^\varepsilon = \frac{\partial w^\varepsilon}{\partial t}, & on\, \partial\Omega^\varepsilon_s \times]0,T[\,, \\ \mu\frac{\partial u^\varepsilon_i}{\partial n} = \sigma^\varepsilon_{ij}(w^\varepsilon)n_j + p^\varepsilon n_i, \quad i = \overline{1,3} & on\, \partial\Omega^\varepsilon_s \times]0,T[\,, \\ u^\varepsilon = 0 & on\ \partial\Omega \times]0,T[\,, \end{cases} \tag{3}$$

$$\begin{cases} u^\varepsilon(0) = 0 & in\ \Omega^\varepsilon_f \\ w^\varepsilon(0) = 0 \qquad {w'}^\varepsilon(0) = 0 & in\ \Omega^\varepsilon_s, \end{cases} \tag{4}$$

n being the exterior unit normal on $\partial\Omega^\varepsilon_s$ and $\mu > 0$ is the viscosity of the fluid.

One supposes that

$$f \in L^2\left(0, T, \left(L^2\left(\Omega\right)\right)^3\right). \tag{5}$$

Using $(3)_1$, one extends w^ε at the whole Ω by: $u^\varepsilon = \frac{\partial w^\varepsilon}{\partial t}$ on Ω^ε_f. The system Q^ε has the following variational formulation:

$$\begin{gathered} \frac{d^2}{dt^2}\left(w^\varepsilon, v\right)_{(0,\Omega)} + \mu\frac{d}{dt}\left(\nabla w^\varepsilon, \nabla v\right)_{(0,\Omega^\varepsilon_f)} + \left(a^{1\varepsilon}_{ijkh} e_{kh}\left(\frac{\partial w^\varepsilon}{\partial t}\right), e_{ij}\left(v\right)\right)_{(0,\Omega^\varepsilon_s)} \\ + \left(a^{0\varepsilon}_{ijkh} e_{kh}\left(w^\varepsilon\right), e_{ij}\left(v\right)\right)_{(0,\Omega^\varepsilon_s)} = \left(f, v\right)_{(0,\Omega)}\ \ \forall v \in V_\varepsilon, \end{gathered} \tag{6}$$

$$\begin{cases} w^\varepsilon\left(x, 0\right) = 0\ on\,\Omega \\ \frac{\partial w^\varepsilon}{\partial t}\left(x, 0\right) = 0\ on\,\Omega, \end{cases} \tag{7}$$

with

$$V_\varepsilon = \left\{v \in \left(H^1_0\left(\Omega\right)\right)^3, div v = 0\ on\,\Omega^\varepsilon_f\right\}.$$

Using the Faedo Galerkin method (see [8], [1]) and some priori estimates, one proves the following:

Proposition 1 *Under the previous hypothesis there exists a unique solution of the problem* (6) (7) *such that:*

$$\begin{cases} w^{\varepsilon} \in L^{\infty}(0,T,(H_0^1(\Omega))^3), \\ \frac{\partial w^s}{\partial t} \in L^2(0,T,(H_0^1(\Omega))^3) \cap L^{\infty}(0,T,(L^2(\Omega))^3), \\ \|w^{\varepsilon}\|_{L^{\infty}(0,T,(H_0^1(\Omega))^3)} \leq c \end{cases} \tag{8}$$

where c is strictly positive constant independent of ε.

2 Multiscale methode

In the following, one use Saint Jean Paulin and Cioranescu's process [3]. One looks for a formal asymptotic expansions of the form:

$$\begin{cases} u^{\varepsilon}(x,t) = u^0(x,y,t) + \varepsilon u^1(x,y,t) + \varepsilon^2 u^2(x,y,t) + ... \\ w^{\varepsilon}(x,t) = w^0(x,y,t) + \varepsilon w^1(x,y,t) + \varepsilon^2 w^2(x,y,t) + ... \\ p^{\varepsilon}(x,t) = p^0(x,y,t) + \varepsilon p^1(x,y,t) + \varepsilon^2 p^2(x,y,t) + ..., \end{cases} \tag{9}$$

where $y = x/\varepsilon$ and u^j, w^j, p^j are smooth functions $Y-$periodic in the variable y. Substituting (9) into (2)..(4) , and identifying the coefficients of the powers of ε, one shows that u^0 and w^0 are independent of y. Because of the transmission conditions, looking for u^1 and w^1 requires us to take the Laplace transform with respect to time $(denoted\widehat{\cdot})$. Extending w^0 and w^1 at the whole Ω by $u^l = \frac{\partial w^l}{\partial t}$ $(l = 0,1)$ on Ω_f, one looks for $\widehat{w^1}$ and $\widehat{p^0}$ with the form $(\lambda \in \mathbb{C})$

$$\begin{cases} \widehat{w}^1(x,y,\lambda) = -\chi^{kh}(y,\lambda) \frac{\partial \widehat{w}_k^0}{\partial x_h}(x,\lambda) \\ \hat{p}^0(x,y,\lambda) = r^{kh}(y,\lambda) \frac{\partial \widehat{w}_k^0}{\partial x_h}(x,\lambda). \end{cases} . \tag{10}$$

If one denotes by $\pi_i^{kh}(y) = y_h \delta_{ki}$ and $A_{ijlm}(y,\lambda) = a_{ijlm}^0(y) + \lambda a_{ijlm}^1(y)$, one proves (see [1]) the following:

Proposition 2 *There is a unique* $\left(\chi^{kh}, r^{kh}\right) \in \left(H_{per}^1(Y)^3 \times L_{per}^2(Y_f)\right)$ *solution of the local system*

$$\begin{cases} -\mu\lambda \triangle_y \left(-\chi_i^{kh} + \pi_i^{kh}\right) = -\frac{\partial r^{kh}}{\partial y_i} \quad on\, Y_f \\ div\left(-\chi^{kh} + \pi^{kh}\right) = 0 \qquad on\, Y_f \\ -\frac{\partial}{\partial y_j} A_{ijlm} e_{lm}^y \left(-\chi^{kh} + \pi^{kh}\right) = 0 \quad on\, Y_s \\ \mu\lambda \frac{\partial}{\partial y_j}\left(-\chi_i^{kh} + \pi_i^{kh}\right) n_j - r^{kl} n_i - \\ -A_{ijlm} e_{lm}^y \left(-\chi^{kh} + \pi^{kh}\right) n_j = 0 \quad in\, \partial Y_s, \end{cases} \tag{11}$$

such that $\int_Y \chi^{kh} dy = 0$.

By using Fredholm alternative one proves that $\widehat{w}^0$ is solution of the following equation (see [1] or [3])

$$\begin{cases} \lambda^2 \widehat{w}_i^0 (x,p) - q_{ijkh}(\lambda) \frac{\partial^2 \widehat{w}_k^0 (x,\lambda)}{\partial x_h \partial x_j} = \hat{f}_i (x) \;\; in\, \Omega, \forall i \in \left\{ \overline{1,3} \right\} \\ \widehat{w}_i^0 (x,p) = 0 \qquad on\, \partial\Omega, \end{cases} \tag{12}$$

where

$$q_{ijkh}(\lambda) = \begin{array}{c} \frac{1}{|Y|} \left\{ \mu\lambda \int_{Y_f} \frac{\partial \left(\chi_m^{kh} - \pi_m^{kh} \right)}{\partial y_l} \frac{\partial \left(\chi_m^{ij} - \pi_m^{ij} \right)}{\partial y_l} dy + \right. \\ \left. + \int_{Y_s} A_{\alpha\beta lm} e_{\alpha\beta}^y \left(\chi^{kh} - \pi^{kh} \right) e_{lm} \left(\chi^{ij} - \pi^{ij} \right) dy \right\}. \end{array} \tag{13}$$

Proposition 3 *If $Re\lambda > 0$ is sufficiently large, the coefficients q_{ijkh} are coercive, holomorphic and*

$$|q_{ijkh}(\lambda)| \le poly\, |\lambda| .$$

3 Convergence-Energy method

Theorem 4 *Under the previous hypotheses and if $Re\lambda > 0$ is sufficiently large*

$$\widehat{w^\varepsilon} \rightharpoonup \widehat{w^*} \; weakly\, in \left(H_0^1 (\Omega) \right)^3 , \tag{14}$$

where $\widehat{w^*} \in \left(H_0^1 (\Omega) \right)^3 \cap \left(H^2 (\Omega) \right)^3$ is the unique solution of (12) (13).

Proof. The same as in [3], but for the pressure one doesn't use the extension proposed by L.Tartar in the appendix of [9], but the one proposed in [7] ,defined by:

$$\tilde{p}^\varepsilon = \begin{cases} \hat{p}^\varepsilon - \frac{1}{|\Omega|} \int_{\Omega_f^\varepsilon} \hat{p}^\varepsilon dx \;\; on\, \Omega_f^\varepsilon \\ -\frac{1}{|\Omega|} \int_{\Omega_f^\varepsilon} \hat{p}^\varepsilon dx \;\; on\, \Omega_s^\varepsilon, \end{cases} \tag{15}$$

which insure the continuity of the stress tensor on fluid-solid interface, and have the mean value equal to zero, and the following properties (see [7]):

$$\nabla \tilde{p}^\varepsilon = \nabla \hat{p}^\varepsilon \;\; in\, \Omega_f^\varepsilon, \;\; and \;\; \nabla \tilde{p}^\varepsilon = 0 \;\; in\, \Omega_s^\varepsilon.$$
$$\|\tilde{p}^\varepsilon\|_{L_0^2(\Omega)} \le c, \text{ c constant independent of } \varepsilon \; .$$

than up to a subsequence, one has: $\tilde{p}^\varepsilon \rightharpoonup \hat{p}^*$ weakly in $L^2(\Omega)$. ■

Remark 5 *One has $p^\varepsilon \in \mathcal{D}' \left( ]0,T[, \Omega_f^\varepsilon \right)$ (see [12]), but under the Laplace transform the problem Q^ε becomes a stationary problem for which there exists a unique $\hat{p}^\varepsilon \in L^2 \left(\Omega_f^\varepsilon \right)$ (see[12]). Then $\tilde{p}^\varepsilon$ is well defined.*

By using the proposition 3, the Theorem 1, and by applying the inverse Laplace transformed to (12) one deduces the following (*see* [1]) .
.

Lemma 6 *Under the previous hypotheses, w^* is the solution of the equation*

$$\frac{\partial^2 w_i^*}{\partial t^2} - \sum_{jkh} c_{ijkh} * \frac{\partial^2 w_k^*}{\partial x_h \partial x_k} = f_i \ in \Omega, i = \overline{1,3}, \tag{16}$$

where c_{ijkh} is the inverse Laplace transformed of q_{ijkh}, and $(*)$ is the convolution product.

Remark 7 *The equation* (16) *is the Q^ε's homogeneous equation, which is of a viscoelastic medium with fading memory.*

References

[1] F. Bentalha, Etude mathématique de quelques problèmes en mécanique des fluides, *thèse d'état, université de Constantine*, 2006.

[2] C. Conca, On the application of the homogenization theory to a class of problems arising in fluid mecanics, *J.Math.pures et appl.*, 64, p. 31-75, 1985.

[3] D. Cioranescu; J. Saint Jean Paulin, Particules Déformables en Suspension dans un Fluide Visqueux, *E.D.F. Bull. de la dir. d'Etudes et Recherches, Série C Math. Info.*.N^{0}1, pp 53-76, 1991.

[4] D. Cioranescu; P. Donato, An introduction to homogenization, *Oxford Lecture Series in Math. App., Vol. 17, Oxford University Press*, 1999.

[5] V. Girault; P.A. Raviart, Finite Elements Methods for Navier-Stokes Equations. *Springer Series in computational Mathematics, 5, Berlin*, 1986.

[6] H.I. Ene; M.L. Mascarenhas ;J.Saint Jean Paulin, Fading memory effects in elastic-viscoelastic composites. *RAIRO, modélisation Math. Anal.*, numér.31,No.7, 927-952, 1997.

[7] I.A.E. Ene; J. Saint Jean Paulin, Homogenization and two-scale convergence for a Stokes or Navier-Stokes flow in an elastic thin porous medium. *Prépublications Mathématiques, Département de mathématiques, Université de Metz*, 1996.

[8] J.L. Lions, Quelques méthodes de résolution des problèmes aux limites non linéaires. *Dunod, Gautier-Villars, Paris* 1969.

[9] E. Sanchez-Palancia, Non homogenous media and vibration theory, *Lecture notes in physics, Springer*, 127, 1980.

[10] L. Tartar, Topic in non linear analysis. *Publication d'Orsay*, 78.13, 1978.

[11] L. Tartar, Memory Effects and Homogenization. *Arch Ration. Mech Anal* , 111, No 2, 121-133, 1990.
[12] R. Temam, Navier Stokes Equations, *North holland*, 1979.

JOURNAL OF APPLIED FUNCTIONAL ANALYSIS, VOL.6, NO.3, 225-232, COPYRIGHT 2011 EUDOXUS PRESS, LLC

Approximate Analytical Solutions for Non-Natural and Non-Linear Vibration Systems Using He's Variational Approach Method

I. Pakar[1,*], M. Shahidi[1], D. D. Ganji[2], M. Bayat[1]

[1] Department of Civil Engineering, Shomal University, P.O. Box 731, Amol, Iran
[2] Department of Mechanical Engineering, Mazandaran University, P.O. Box 484, Babol, Iran

Abstract

This paper applied, He's Variational Approach Method (VAM) to solve the non-natural vibrations and oscillations. We find this method (VAM) works very well for the whole range of initial amplitudes and does not demand small perturbation and also sufficiently accurate to both linear and nonlinear physics and engineering problems. Some examples are given to illustrate the effectiveness and convenience of the method. He's energy balance method as approximate method and Runge-Kutta's [RK] algorithm was also implemented to solve the governing equation through a numerical method. Finally, the accuracy of the solution obtained by the approximate method (VAM), has been shown graphically and compared with that of the numerical solution.

Keywords: Variational Approach; Nonlinear Oscillators; Mathematical Pendulum; Runge-Kutta's algorithm; Energy balance

Introduction

Nonlinear oscillation in engineering and applied mathematics has been a topic to intensive research for many years. Nonlinear oscillator models have been widely considered in physics and engineering. Many authors used various analytical methods for solving nonlinear oscillation systems. The traditional perturbation methods have many shortcomings, and they are not valid for strongly nonlinear equations. [1,2]. To handle the nonlinear problems, many new mathematical methods have appeared in open literatures recently, for example: Lindstedt-Poincaré [3] Parameterized Perturbation Method, Homotopy Perturbation Method [4,5]. Parameter-Expanding (Expansion) [6] ,Energy Balance Method [7-9], Harmonic Balance Method [10], Variational Iteration Method [11], and also Variational Approach Method [12,13]. In this paper, we will show how to solve the problems of nonlinear oscillators by a new variational approach proposed by He [12], which is an easy, effective and convenient mathematical tool and analytical formulas for the period and periodic solution.

In this paper, At the first, we describe basic idea of he's variational approach method and then Runge-Kutta's [RK] algorithm will be introduced to solve the governing equation [14]. The VAM will be applied to the Mathieu-Duffing equations. Finally, The frequency of the oscillator obtained by He's Energy balance method and numerical solution is given to demonstrate the validity of the proposed method (VAM).

The comparison shows the efficiency of these methods. As we can see, the results presented in this Letter reveal that the method (VAM) is very effective and convenient for nonlinear oscillators.

1. Basic idea of He's Variational Approach Method

He [12] suggested a variational approach which is different from the known variational methods in open literature. Hereby we give a brief introduction of the method:

$$u'' + f(u) = 0 \tag{1}$$

Its variational principle can be easily established using the semi-inverse method

$$J(u) = \int_0^{T/4} \left(-\frac{1}{2} u'^2 + F(u) \right) dt \tag{2}$$

Where T is period of the nonlinear oscillator, $\partial F / \partial u = f$. Assume that its solution can be expressed as

* Corresponding author: Tel/Fax: +98 111 3234205
E–mail: iman.pakar@yahoo.com (I. pakar)

$$u(t) = A\cos(\omega t) \tag{3}$$

Where A and ω are the amplitude and frequency of the oscillator, respectively. Substituting Eq.(3) into Eq.(2) results in:

$$\begin{aligned} J(A,\omega) &= \int_0^{T/4}\left(-\frac{1}{2}A^2\omega^2\sin^2\omega t + F(A\cos\omega t)\right)dt = \frac{1}{\omega}\int_0^{\pi/2}\left(-\frac{1}{2}A^2\omega^2\sin^2(\omega t) + F\left(A\cos(\omega t)\right)\right)dt \\ &= -\frac{1}{2}A^2\omega\int_0^{\pi/2}\sin^2 t\,dt + \frac{1}{\omega}\int_0^{\pi/2}F\left(A\cos t\right)dt \end{aligned} \tag{4}$$

Applying the Ritz method, we require:

$$\frac{\partial J}{\partial A} = 0 \tag{5}$$

$$\frac{\partial J}{\partial \omega} = 0 \tag{6}$$

But with a careful inspection, for most cases He find that

$$\frac{\partial J}{\partial \omega} = -\frac{1}{2}A^2\int_0^{\pi/2}\sin^2 t dt - \frac{1}{\omega^2}\int_0^{\pi/2}F\left(A\cos(\omega t)\right)dt < 0 \tag{7}$$

Thus, He modify conditions Eq.(5) and Eq.(6) into a simpler form:

$$\frac{\partial J}{\partial A} = 0 \tag{8}$$

From which the relationship between the amplitude and frequency of the oscillator can be obtained.

2. Basic idea of Runge-Kutta's method (RKM)

Here we apply the fourth-order RK algorithm to solve governing equation subject to the given boundary conditions. RK iterative formulae for the second-order differential equation are [14]:

$$\dot{u}_{(i+1)} = \dot{u}_i + \frac{\Delta t}{6}\left(k_1 + 2k_2 + 2k_3 + k_4\right), \qquad u_{(i+1)} = u_i + \Delta t\left[\dot{u}_i + \frac{\Delta t}{6}\left(k_1 + k_2 + k_3\right)\right], \tag{9}$$

Where Δt is the increment of the time and k_1, k_2, k_3 and k_4 are determined from the following formula:

$$\begin{aligned} &k_1 = f\left(t_i, u_i, \dot{u}_i\right), && k_2 = f\left(t_i + \frac{\Delta t}{2}, u_i + \frac{\Delta t}{2}, \dot{u}_i + \frac{\Delta t}{2}k_1\right), \\ &k_3 = f\left(t_i + \frac{\Delta t}{2}, u_i + \frac{\Delta t}{2}\dot{u}_i, \frac{1}{4}\Delta t^2 k_1, \dot{u}_i + \frac{\Delta t}{2}k_2\right), && k_3 = f\left(t_i + \Delta t,\ u_i + \Delta t\ \dot{u}_i + \frac{1}{2}\Delta t^2 k_2,\ \dot{u}_i + \Delta t\ k_3\right), \end{aligned} \tag{10}$$

The numerical solution starts from the boundary at the initial time, where the first value of the displacement function and its first-order derivative is determined from initial condition. Then, with a small time increment [Δt], the displacement function and its first-order derivative at the new position can be obtained using (3). This process continues to the end of time.

3. Applications

In this section, we will present three examples to illustrate the applicability, accuracy and effectiveness of the proposed approach.

4.1. Example 1

In this example, we consider the following nonlinear oscillator [1]:

$$\left(\frac{1}{12}l^2 + r^2\theta^2\right)\ddot{\theta} + r^2\theta\,\dot{\theta}^2 + r\,g\,\theta\,cos\left(\theta\right) = 0 \tag{11}$$

With the boundary conditions of:

$$\theta(0) = A, \qquad \dot{\theta}(0) = 0 \tag{12}$$

In order to apply the variational approach method to solve the above problem, the approximation $\cos\theta \approx 1 - \frac{1}{2}\theta^2 + \frac{1}{24}\theta^4$ is used.

Its variational formulation is:

$$J(\theta) = \int_0^{T/4} \left(-\frac{1}{24} l^2 \dot{\theta}^2 - \frac{1}{2} r^2 \theta^2 \dot{\theta}^2 + \frac{1}{2} r\, g\, \theta^2 - \frac{1}{8} r\, g\, \theta^4 + \frac{1}{144} g\, r\, \theta^6 \right) dt \tag{13}$$

Choosing the trial function $\theta(t) = A\cos(\omega t)$ into Eq.(13) we obtain

$$J(A,\omega) = \int_0^{T/4} \left(\begin{aligned} & -\frac{1}{24} l^2 \left(\mathrm{A}\,\omega \sin(\omega \mathrm{t})\right)^2 - \frac{1}{2} r^2 \left(A \cos(\omega t)\right)^2 \left(\mathrm{A}\,\omega \sin(\omega \mathrm{t})\right)^2 \\ & + \frac{1}{2} r\, g \left(A \cos(\omega t)\right)^2 - \frac{1}{8} r\, g \left(A \cos(\omega t)\right)^4 + \frac{1}{144} g\, r \left(A \cos(\omega t)\right)^6 \end{aligned} \right) dt \tag{14}$$

The stationary condition with respect to A reads:

$$\frac{\partial J}{\partial A} = \int_0^{T/4} \left(-\frac{1}{12} l^2 \omega^2 A\, sin^2(\omega t) - 2 r^2 \omega^2 A^3 sin^2(\omega t) cos^2(\omega t) + r\, g\, A\, cos^2(\omega t) - \frac{1}{2} r\, g\, A^3 cos^4(\omega t) + \frac{1}{24} r\, g\, A^5 cos^6(\omega t) \right) dt = 0 \tag{15}$$

Or

$$\frac{\partial J}{\partial A} = \int_0^{\pi/2} \left(-\frac{1}{12} l^2 A\, sin^2 t\, \omega^2 - 2 r^2 \omega^2 A^3 sin^2 t\, cos^2 t + r\, g\, A\, cos^2 t - \frac{1}{2} r\, g\, A^3 cos^4 t + \frac{1}{24} r\, g\, A^5 cos^6 t \right) dt = 0 \tag{16}$$

Then we have ;

$$\omega^2 = \frac{\int_0^{\pi/2} \left(r\, g\, A\, cos^2 t - \frac{1}{2} r\, g\, A^3 cos^4 t + \frac{1}{24} r\, g\, A^5 cos^6 t \right) dt}{\int_0^{\pi/2} \left(\frac{1}{12} l^2 A\, sin^2 t + 2 r^2 A^3 sin^2 t\, cos^2 t \right) dt} \tag{17}$$

Solving Eq. (17), according to ω, we have:

$$\omega = \frac{1}{4} \sqrt{\frac{r\, g\, \left(192 - 72A^2 + 5A^4\right)}{6A^2 r^2 + l^2}} \tag{18}$$

Hence, the approximate solution can be readily obtained:

$$\theta(t) = A \cos\left(\frac{1}{4} \sqrt{\frac{r\, g\, \left(192 - 72A^2 + 5A^4\right)}{6A^2 r^2 + l^2}}\; t \right) \tag{19}$$

For comparison of the approximate solution, frequency obtained from solution of nonlinear equation with the Energy Balance method is:

$$\omega_{EBM} = \frac{\sqrt{6}}{12} \sqrt{\frac{r\, g \left(288 - 108A^2 + 7A^4\right)}{6A^2 r^2 + l^2}} \tag{20}$$

The numerical solution (with Runge-Kutta method of order 4) for nonlinear equation is:

$$\dot{\theta} = y \qquad \theta(0)=A$$
$$\dot{y} = -\frac{r^2\theta u^2 + r\,g\,\theta cos(\theta)}{\frac{1}{12}l^2 + r^2\theta^2} \qquad y(0)=0 \tag{21}$$

For the following value parameters, we compared the numerical solution and Energy Balance method with the variational approach method in Figs (1-3):
l=2.5,   r=0. 5,   g=10 ,   A=1

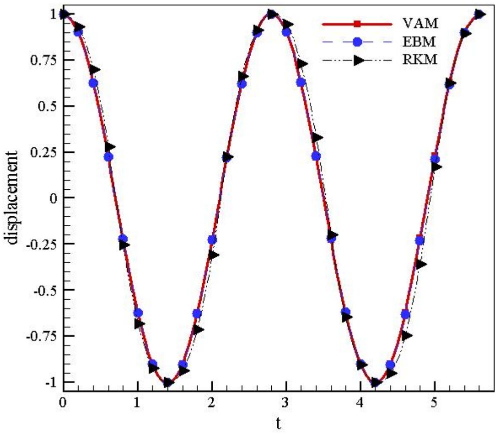

Fig. 1. Comparison of displacement (θ) of the VAM solution with the EBM and RKM solution

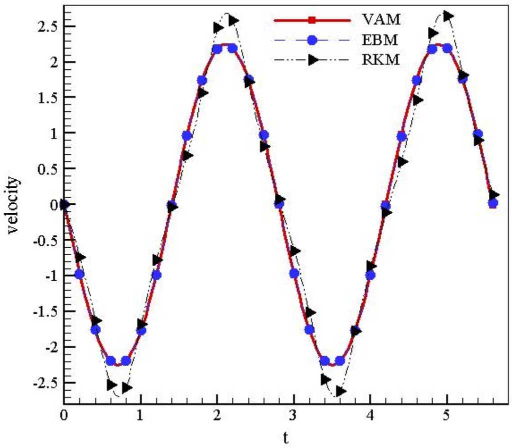

Fig. 2. Comparison of velocity ($\dot{\theta}$) of the VAM solution with the EBM and RKM solution

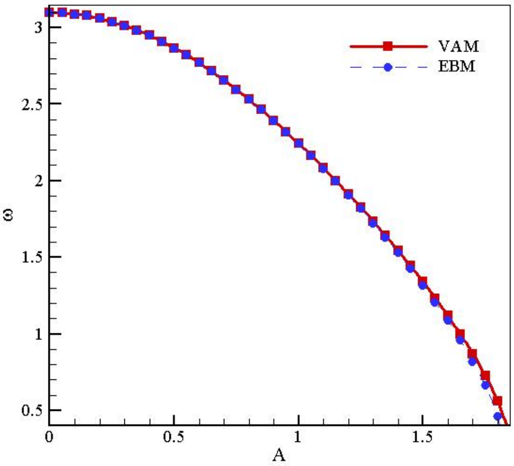

Fig. 3. Comparison of frequency corresponding to various parameters of amplitude (A)
l=2.5,   r=0. 5,   g=10

4.2. Example 2

We consider the mathematical pendulum. the differential equation governing for the free oscillation of the mathematical pendulum is given by [1].

$$\ddot{\theta} - \Omega^2 cos\left(\theta\right) sin\left(\theta\right) + \frac{g}{r} sin\left(\theta\right) = 0 \tag{22}$$

With the boundary conditions of:

$$\theta\left(0\right) = A, \qquad \dot{\theta}\left(0\right) = 0 \tag{23}$$

In order to apply the variational approach method to solve the above problem, the approximation $\cos\theta \approx 1-\frac{1}{2}\theta^2+\frac{1}{24}\theta^4$ and $\sin\theta \approx \theta-\frac{1}{6}\theta^3$ is used.

Its variational formulation can be readily obtained as follows:

$$J(\theta)=\int_0^{T/4}\left(-\frac{1}{2}\dot{\theta}^2-\frac{1}{2}\Omega^2\theta^2+\frac{1}{6}\Omega^2\theta^4-\frac{1}{48}\Omega^2\theta^6+\frac{1}{1152}\Omega^2\theta^8+\frac{1}{2}\frac{g}{r}\theta^2-\frac{1}{24}\frac{g}{r}\theta^4\right)dt \tag{24}$$

Choosing the trial function $\theta(t)=A\cos(\omega t)$ into Eq.(24) we obtain

$$J(A,\omega)=\int_0^{T/4}\left(\begin{array}{l}-\frac{1}{2}\left(\mathrm{A}\,\omega\sin(\omega \mathrm{t})\right)^2-\frac{1}{2}\Omega^2\left(A\cos(\omega t)\right)^2+\frac{1}{6}\Omega^2\left(A\cos(\omega t)\right)^4-\frac{1}{48}\Omega^2\left(A\cos(\omega t)\right)^6\\+\frac{1}{1152}\Omega^2\left(A\cos(\omega t)\right)^8+(\frac{1}{2})\frac{g}{r}\left(A\cos(\omega t)\right)^2-(\frac{1}{24})\frac{g}{r}\left(A\cos(\omega t)\right)^4\end{array}\right)dt \tag{25}$$

The stationary condition with respect to A reads:

$$\frac{\partial J}{\partial A}=\int_0^{T/4}\left(\begin{array}{l}-A\,\omega^2 sin^2(\omega t)-\Omega^2 A\,cos^2(\omega t)+\frac{2}{3}\Omega^2A^3cos^4(\omega t)-\frac{1}{8}\Omega^2A^5cos^6(\omega t)\\+\frac{1}{144}\Omega^2A^7cos^8(\omega t)+\frac{g}{r}A\,cos^2(\omega t)-\frac{1}{6}\frac{g}{r}A^3cos^4(\omega t)\end{array}\right)dt=0 \tag{26}$$

Or

$$\frac{\partial J}{\partial A}=\int_0^{\pi/2}\left(\begin{array}{l}-A\,\omega^2 sin^2 t-\Omega^2 A\,cos^2 t+\frac{2}{3}\Omega^2A^3cos^4 t-\frac{1}{8}\Omega^2A^5cos^6 t\\+\frac{1}{144}\Omega^2A^7cos^8 t+\frac{g}{r}A\,cos^2 t-\frac{1}{6}\frac{g}{r}A^3cos^4 t\end{array}\right)dt=0 \tag{27}$$

Then we have ;

$$\omega^2=\frac{\int_0^{\pi/2}\left(-\Omega^2A\,cos^2t+\frac{2}{3}\Omega^2A^3cos^4t-\frac{1}{8}\Omega^2A^5cos^6t+\frac{1}{144}\Omega^2A^7cos^8t+\frac{g}{r}A\,cos^2t-\frac{1}{6}\frac{g}{r}A^3cos^4t\right)dt}{A\int_0^{\pi/2}sin^2t\,dt} \tag{28}$$

Solving Eq. (28), according to ω, we have:

$$\omega=\frac{1}{96}\sqrt{-9216\Omega^2+4608\Omega^2A^2-720\Omega^2A^4+35\Omega^2A^6+9216\frac{g}{r}-1152\frac{g}{r}A^2} \tag{29}$$

Hence, the approximate solution can be readily obtained:

$$\theta(t)=A\cos\left(\frac{1}{96}\sqrt{-9216\Omega^2+4608\Omega^2A^2-720\Omega^2A^4+35\Omega^2A^6+9216\frac{g}{r}-1152\frac{g}{r}A^2}\;t\right) \tag{30}$$

For comparison of the approximate solution, frequency obtained from solution of nonlinear equation with the Energy Balance method is:

$$\omega_{EBM}=\frac{\sqrt{6}}{96}\sqrt{-1536\Omega^2+768\Omega^2A^2-112\Omega^2A^4+5\Omega^2A^6+1536\frac{g}{r}-192\frac{g}{r}A^2} \tag{31}$$

The numerical solution (with Runge-Kutta method of order 4) for nonlinear equation is:

$$\begin{array}{ll}\dot{\theta}=\mathrm{y} & \theta(0)=\mathrm{A}\\ \dot{y}=\Omega^2cos(\theta)sin(\theta)-\frac{g}{r}sin(\theta) & y(0)=0\end{array} \tag{32}$$

For the following value parameters, we compared the numerical solution and Energy Balance method with the variational approach method in Figs (4-6):

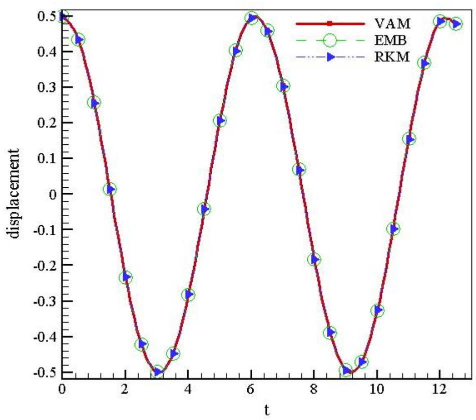

Fig. 4. Comparison of displacement (θ) of the VAM solution with the EBM and RKM solution
Ω =1, r= 5, g=10, A=0.5

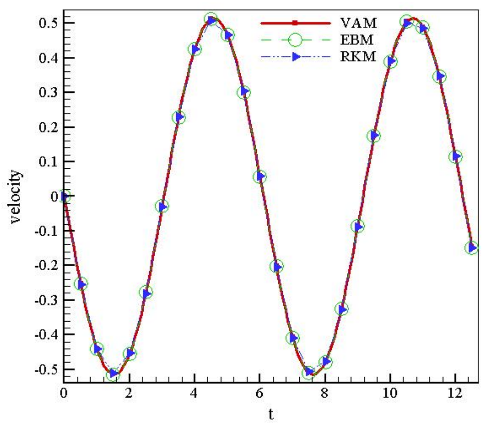

Fig. 5. Comparison of velocity ($\dot{\theta}$) of the VAM solution with the EBM and RKM solution
Ω =1, r= 5, g=10, A=0.5

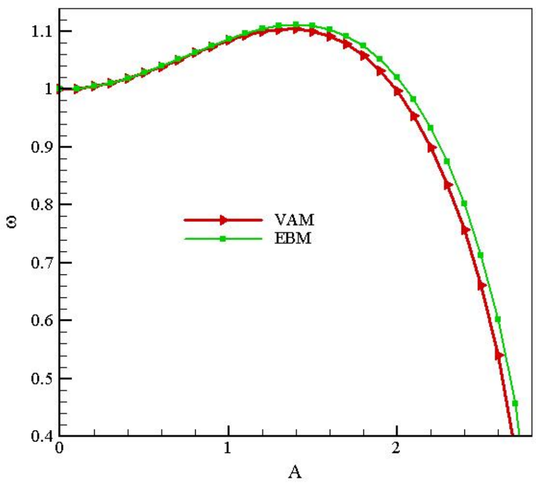

Fig. 6. Comparison of frequency corresponding to various parameters of amplitude (A)
Ω =1, r= 5, g=10

4.3. Example 3

The motion of a particle on a rotating parabola. The governing equation of motion and can be expressed as:

$$\ddot{u} + a\,u\left(\dot{u}^{2} + u\,\ddot{u}\right) + b\,u + c\,u^{3} + d\,u^{5} = 0 \tag{33}$$

With the boundary conditions of:

$$u(0) = A, \qquad \dot{u}(0) = 0 \tag{34}$$

Its variational formulation can be readily obtained as follows:

$$J(u) = \int_0^{T/4}\left(-\frac{1}{2}\dot{u}^2 - \frac{1}{2}a\dot{u}^2u^2 + \frac{1}{2}b\,u^2 + \frac{1}{4}c\,u^4 + \frac{1}{6}d\,u^6\right)dt \tag{35}$$

Choosing the trial function $\theta(t) = A\,\cos(\omega t)$ into Eq. (35) we obtain

$$J(A,\omega) = \int_0^{T/4}\left(\begin{array}{l} -\frac{1}{2}\left(\mathrm{A}\omega\sin(\omega t)\right)^2 - \frac{1}{2}a\left(\mathrm{A}\omega\sin(\omega t)\right)^2\left(\mathrm{A}\cos(\omega t)\right)^2 + \frac{1}{2}b\left(\mathrm{A}\cos(\omega t)\right)^2 \\ +\frac{1}{4}c\left(\mathrm{A}\cos(\omega t)\right)^4 + \frac{1}{6}d\left(\mathrm{A}\cos(\omega t)\right)^6 \end{array}\right)dt \tag{36}$$

The stationary condition with respect to A reads:

$$\frac{\partial J}{\partial A}=\int_0^{T/4}\left(-A\,\omega^2 sin^2(\omega t)-2a\,\omega^2A^3 sin^2(\omega t)cos^2(\omega t)+b\,A\,cos^2(\omega t)+c\,A^3cos^4(\omega t)+d\,A^5cos^6(\omega t)\right)dt=0 \quad (37)$$

Or

$$\frac{\partial J}{\partial A}=\int_0^{\pi/2}\left(-A\,\omega^2 sin^2t-2a\,\omega^2A^3sin^2t\,cos^2t+b\,A\,cos^2t+c\,A^3cos^4t+d\,A^5cos^6t\right)dt=0 \quad (38)$$

Then we have;

$$\omega^2=\frac{\int_0^{\pi/2}\left(b\,A\,cos^2t+c\,A^3cos^4t+d\,A^5cos^6t\right)dt}{\int_0^{\pi/2}\left(A\,sin^2t+2a\,A^3sin^2t\,cos^2t\right)dt} \quad (39)$$

Solving Eq. (39), according to ω, we have:

$$\omega=\frac{1}{2}\sqrt{\frac{8b+6cA^2+5d\,A^4}{aA^2+2}} \quad (40)$$

Hence, the approximate solution can be readily obtained:

$$\theta(t)=A\cos\left(\frac{1}{2}\sqrt{\frac{8b+6cA^2+5d\,A^4}{aA^2+2}}\;t\right) \quad (41)$$

For comparison of the approximate solution, frequency obtained from solution of nonlinear equation with the Energy Balance method is:

$$\omega_{EBM}=\frac{1}{\sqrt{6}}\sqrt{\frac{12b+9cA^2+7dA^4}{a\,A^2+2}} \quad (42)$$

The numerical solution (with Runge-Kutta method of order 4) for nonlinear equation is:

$$\begin{aligned}&\dot{u}=y && u(0)=A\\ &\dot{y}=-\frac{1}{1+au^2}\left(a\,u\,\dot{u}^2+bu+cu^3+d\,u^5\right) && y(0)=0\end{aligned} \quad (43)$$

For the following value parameters, we compared the numerical solution and Energy Balance method with the variational approach method in Figs (7-9):

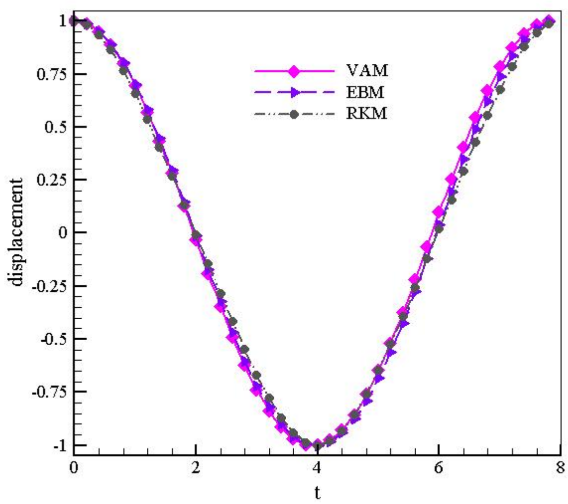

Fig. 7. Comparison of displacement (θ) of the VAM solution with the EBM and RKM solution
a=0.1, b= 0.2, c=0.3, d=0.4, A=1

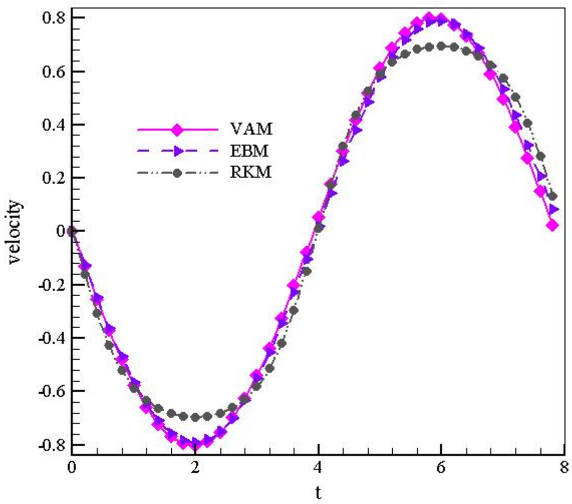

Fig. 8. Comparison of velocity ($\dot{\theta}$) of the VAM solution with the EBM and RKM solution
a=0.1, b= 0.2, c=0.3, d=0.4, A=1

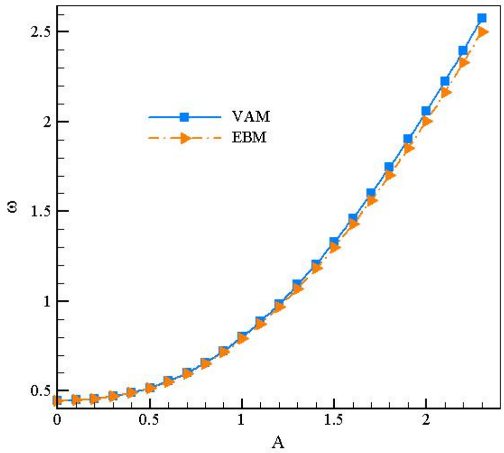

Fig. 9. Comparison of frequency corresponding to various parameters of amplitude (A)
a=0.1, b= 0.2, c=0.3, d=0.4

4. Conclusion

In this paper, the variational approach method has been successfully used to study the nonlinear vibrating equations. The method, which is proved to be a powerful mathematical tool to study nonlinear vibrating equations, can be easily extended to any nonlinear equation. We find that the variational approach method is very effective, convenient and adequately accurate in engineering problems.

These examples have shown that the approximate analytical solutions are in excellent agreement between of two other methods. The obtained results from this method have been compared with those obtained from Runge-Kutta's method (RKM) and Energy Balance method (EBM).VAM can be easily extended to any nonlinear equation for the analysis of nonlinear systems.

References

[1]. A. H. Nayfeh," Introduction to Perturbation Techniques", John Wiley & Sons, New York, 1981.
[2]. A. H. Nayfeh, "Problems in Perturbation",John Wiley, New York, 1985.
[3]. J. H. He, "Modified Lindstedt–Poincare methods for some strongly nonlinear oscillations, Part I: a new transformation", International Journal of Non–linear Mechanics, Vol.37 , 315-320,2002.
[4]. J. H. He, "Homotopy perturbation method:a new nonlinear analytical technique, Applied Mathematics and Computation Vol.135 , 73-79,2003.
[5]. N. Tolou, I. Khatam, B. Jafari and D.D. Ganji, "Analytical Solution of Nonlinear Vibrating Systems", American Journal of Applied Sciences ,Vol.5 (9), 1219-1224, 2008.
[6]. L. Xu ,"Determination of limit cycle by He's parameter expanding method for strongly nonlinear oscillators," Journal of Sound and Vibration ,Vol. 302(1-2),178-184,2007.
[7]. J.H. He, "Preliminary report on the energy balance for nonlinear oscillations," Mechanics Research Communications , Vol. 29, 107-111, 2002.
[8]. S. S. Ganji, D. D. Ganji, S. Karimpour, "He's energy balance and He's variational methods for nonlinear oscillations in engineering", International Journal of Modern Physics B, Vol. 23, 461-471, 2009.
[9]. H. Babazadeh, D. D. Ganji, and M. Akbarzade," He's energy balance method to evaluate the effet of amplitude on the natural frequency in nonlinear vibration systems", Progress In Electromagnetics Research M, Vol. 4, 143-154, 2008.
[10]. A. Bel´endez, A. Hern´andez, T. Bel´endez, M. L. ´Alvarez, S. Gallego, M. Ortu˜no, and C. Neipp, "Application of the harmonic balance method to a nonlinear oscillator typified by a mass attached to a stretched wire," Journal of Sound and Vibration., Vol. 302, 1018-1029, 2007.
[11]. J.H. He, "Variational iteration method: a kind of non-linear analytical technique: some examples", International Journal of Non-Linear Mechanics, Vol. 34, 699-708, 1999.
[12]. J.H. He, "Variational approach for nonlinear oscillators," Chaos, Solitons & Fractals, Vol. 34, 1430-1439, 2007.
[13]. Jun-Fang Liu, "He's variational approach for nonlinear oscillators with high nonlinearity", Computers and Mathematics with Applications Vol.58 2423_2426, 2009.
[14]. M. L. James, G. M. Smith, and J. C.Wolford, "Applied Numerical Methods for Digital Computation", Harper& Row, New York, NY, USA, 1985.

JOURNAL OF APPLIED FUNCTIONAL ANALYSIS, VOL.6, NO.3, 233-240, COPYRIGHT 2011 EUDOXUS PRESS, LLC

Simulation of The Behaviour Dynamics of a Diesel Engine Under Load

Enco Tireli[1], Joško Dvornik[2], Srđan Dvornik[2]

[1] University of Rijeka, Faculty of Maritime Studies
Studentska 2 51000 Rijeka, Croatia
[2] University of Split, Faculty of Maritime Studies,
Zrinsko frankopanska 38, 21000 Split, Croatia

Abstract

The purpose of this paper is to present the efficiency of the application of the system dynamics simulation modelling in investigating the behaviour dynamics of the diesel engine complex system. The marine diesel engine is defined by a set of non-linear differential equations, i.e. by a continuous simulation model of a higher order and the so-called equations of state. At the same time, the simulation model is discrete as it strictly satisfies the chosen value of the fundamental integration time step DT. The paper presents a mathematical model of the system consisting of a marine diesel engine model, which forms the basis for designing a system dynamic qualitative model (mental-verbal, structural and schematic model) and a quantitative model (system dynamic mathematical and information simulation model). A scenario of mixed propulsion states has been presented. Parameters obtained with the aid of the hardware simulator Kongsberg ERS-L11 MAN B&W-5L90MC–VLCC Version MC90-IV have been used in conducting the simulation.
The results presented in the paper have been derived from the scientific research project „SHIPBOARD ENERGY SYSTEMS, ALTERNATIVE FUEL OILS AND REDUCTION OF POLLUTANTS EMISION“ supported by the Ministry of Science, Education and Sports of the Republic of Croatia.

Keywords:
Simulation, System Dynamics, Diesel Engine, Simulator, Heuristic Optimisation.

1. Introduction

As there are a large number of various diesel engines in use, it appears that designing a universal model applicable to each individual type of engine would be very useful and effective, particularly in the case of designing complex mathematical models of diesel engines that include all essential sub-processes:

- description of the working medium (fuel, air),
- mechanical system dynamics,
- cooling system,
- lubrication system,

as well as their mutual interactions.

However, such a complex model is not suitable for the computer-supported simulation modelling of a diesel engine. Other sub-processes of the universal model are indirectly involved through the values of the various parameters that have been defined for given stationary states.

Some of the features of the diesel engine operation process have a discrete quality (injection process, ignition, burning and combustion of the air and fuel mixture) so that a discrete model of the engine is undoubtedly more exact. Since in high-speed diesel engines the time of discretisation (injection period) is much shorter than the dominant time constants of the very process, the discrete model of the engine closely approaches the continuous one, so that only the latter will be analysed in this paper.

Figure 1. shows a generic scheme of a marine turbocharged diesel engine. The following basic functional units can be noticed:

- engine mechanism (M),
- exhaust gas receiver (KIP),
- turbine (T) and the compressor (K) of the turbocharger,
- scavenge air receiver (KZ),
- high-pressure fuel pump (VTSg).

Each of the above functional units has been allocated input and output variables, variables of states and disorders, which are relevant for the model. They connect the units into a unique multivariable system.

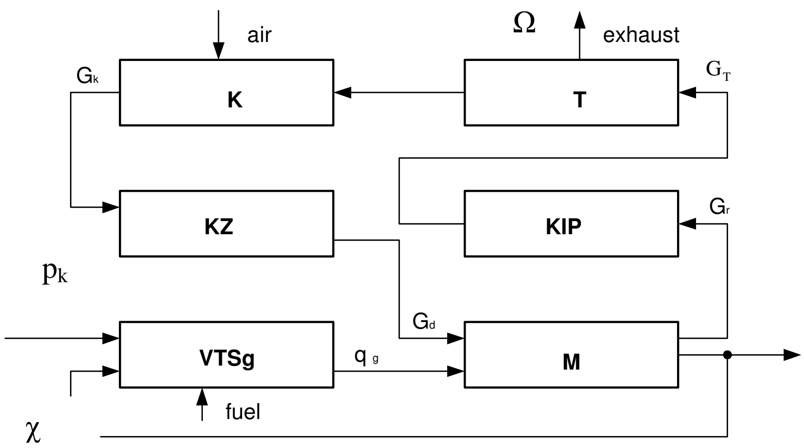

Figure 1. Generic scheme of a marine diesel engine

Ω

Where:

M – engine,

KIP – exhaust gas receiver,
T – turbine,
K – compressor,
KZ – scavenge air receiver,
VTSg – high-pressure fuel pump,
Ω – angular speed of the engine crankshaft (KV),
G_r – amount of the exhaust gas from the engine, entering the KIP,
p_r – exhaust gas pressure in the KIP,
ρ_r – exhaust gas density,
G_T – amount of the exhaust gas flowing through the turbine,
Ω_T – angular speed of the turbocharger,
G_k – amount of air that the turbocharger supplies to the KZ,
p_k – air pressure in the receiver,
ρ_k – specific air mass in the KZ,
χ – regulator action,
q_g – amount of fuel supplied to the engine by VTS.

2. Computer simulation model for a marine diesel engine

2.1.System dynamic mathematical model for a marine diesel engine

The system dynamic mathematical model for a turbocharged diesel engine can be defined by the expression:

$$\frac{d^2\varphi}{dt^2} = -\frac{d\varphi}{dt}\frac{T_{DH}}{T_H^{\ 2}} - \varphi\frac{k_{DH}}{T_H^{\ 2}} + \frac{d\chi}{dt}\frac{T_S}{T_H^{\ 2}} + \chi\frac{k_S}{T_H^{\ 2}} - \frac{d\alpha_D}{dt}\frac{T_u}{T_H^{\ 2}} - \alpha_D\frac{k_u}{T_H^{\ 2}}$$

where:

$d^2\ \varphi$= D2FI - acceleration of the angular speed of the engine crankshaft (KV)
$d\ \varphi$= D1F1- angular speed change rate of the engine crankshaft (KV) (speed gradient)
T_{DH}= TDH- time characterising the sluggishness of the engine as a regulated object
$T_H^{\ 2}$= TH2- square of the time characterising the sluggishness of the engine as a regulated object
T_S= TS- time characterising the engine sluggishness

d χ =DKAPA- speed of moving the *rack lever* high – fuel pressure pump (VTS)
χ = KAPA- relative movement of the rack lever of the fuel pressure pump (VTS)
k_S= KS- coefficient of the engine gain
d α_D= DALFAD - change rate of the relative consumer load
α_D= ALFAD- relative change of the consumer load
T_u= TU- time characterising the generator sluggishness
k_u= KU- coefficient of the gain of the external engine load
φ= FI- relative change of the angular speed of the KV
k_{DH}= KDH- factor depending on the self-equalisation coefficient and engine gain coefficient
ALFAD- external engine load
SLOPE - subroutine of the first derivation (KAPA and ALFAD)

.2.2.System-dynamic structural model for marine diesel engine

Based on the described mental-verbal model, it is possible to make a structural diagram as shown in Figure 2.

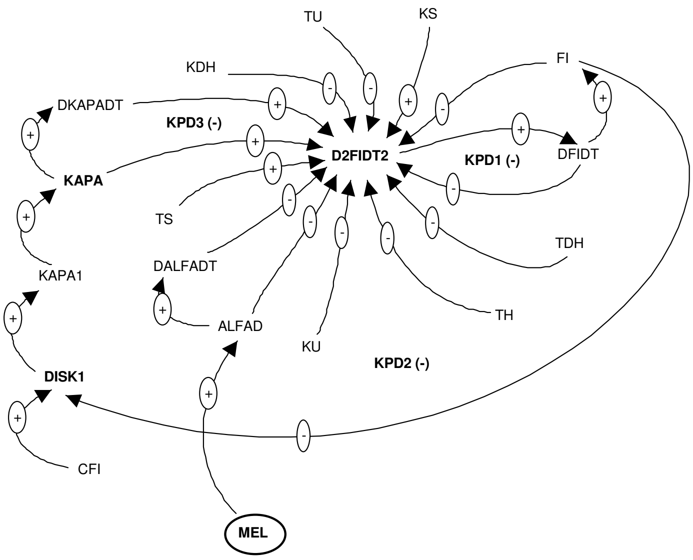

Figure 2. Structural model for a marine diesel engine

There are several feedback loops (KPD) in the observed system:
1. KPD1(-):D2FIDT2(+)=>DFIDT(+)=>FI=>D2FIDT2
2. KPD2(-):FI()=>DISK1(+)=>KAPA1(+)=>KAPA(+)=>D2FIDT2(+)=> DFIDT(+)=>FI

3. KPD3(-):FI(-)=>DISK1(+)=>KAPA1(+)=>KAPA(+)=>DKAPADT(+)=>
D2FIDT2(+)=>DFIDT(+)=>FI

2.3. System-dynamic flowchart diagram of a marine diesel engine

The flowchart diagram has been created in line with the previously made mental-verbal and structural models, as shown in Figure 3.

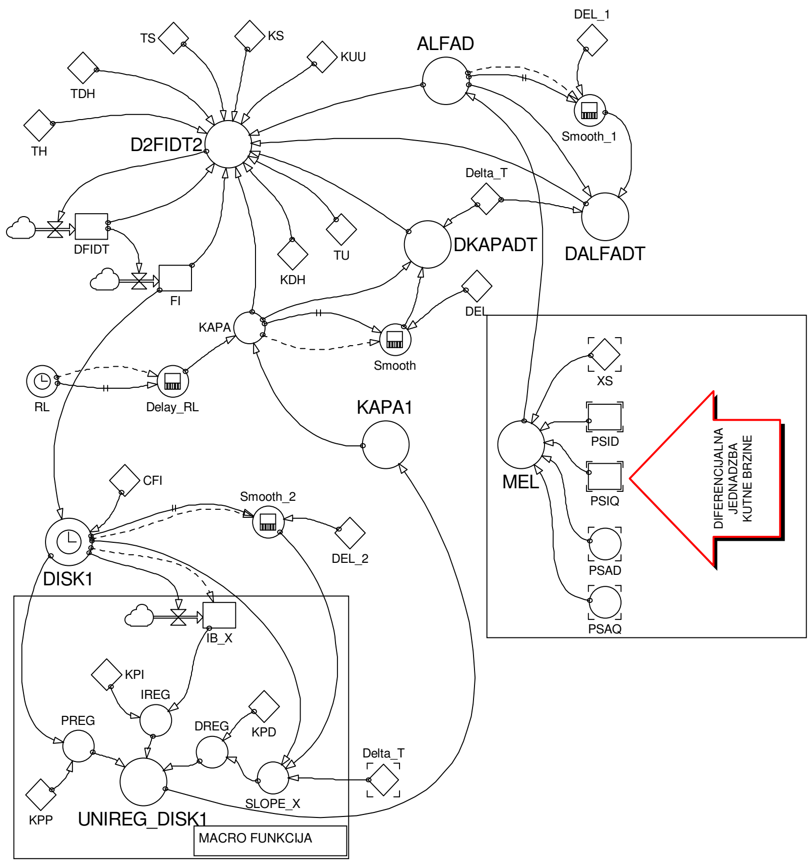

Figure 3. Flowchart diagram of a marine diesel engine with UNIREG regulator

3. SIMULATION SCENARIOS OF THE MARINE DIESEL ENGINE MODEL

3.1. Simulation scenario of the start-up of an idling marine diesel engine – starting

The marine diesel engine is started at TIME=0 at zero load.

The diesel engine system is fitted with an electronic universal (UNIREG_DISK1) regulator. After a series of scenarios, we have obtained coefficients of the electronic universal PID regulator for the start-up of the idling marine diesel engine. The coefficients have been obtained with the aid of the heuristic optimisation. The latter implies the use of all familiar methods, including the ones that cannot be expressed in a mathematically exact way, so that expertise in modelling is necessary. Heuristic optimisation in system dynamics involves the "retry and error" method, a method that could be described as trying to obtain results gradually, i.e. "step by step"

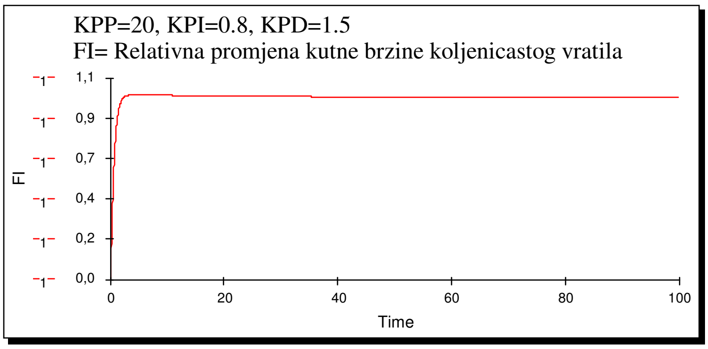

Figure 4. KPP=20, KPI=0.8, KPD=1.5

Relative change of the crankshaft angular speed

Comments on the obtained results from the Scenario:

The behaviour dynamics of an idling marine diesel engine is entirely in accordance with its model, i.e. with the second order differential equation. The revolution speed regulation has been performed by the electronic universal PID regulator whose elements' coefficients have been changing. The heuristic optimisation of the PID regulator parameters has been carried out, resulting in the following combination of coefficients:

KPP=20, KPI=0.8, KPD=1.5

This combination entirely meets the criteria of the revolution speed of a marine diesel engine. The same results have been obtained in the Kongsberg hardware simulator at the University of Split.

4. CONCLUSION

The presentation and the results of the simulation of the system-dynamic models for a marine diesel engine lead to the conclusion that applying System Dynamics, a modern scientific discipline, in the research of behaviour dynamics of complex ship systems is an exceptionally effective, rational, and prospective methodology. It is extraordinarily useful in education of both engineering faculty students and graduate engineers of all profiles as it provides a cost-effective, fast and accurate method of acquiring new insights and skills in the field of engineering systems and processes. This brief presentation gives to an expert all the necessary data and the opportunity to collect further information on the same system using a fast and scientific method of investigation of a complex system.

Which means:

Do not simulate the behaviour dynamics of complex systems using the research method of the "black box", because the education and designing practice of complex systems has confirmed that it is much better to simulate using the research approach of the “white box”, i.e. the System Dynamics methodology.

Authors

REFERENCES

1. R. A. Nalepin, O.P. Demeenko, *Avtomatizacija sudovljih energetskih ustanovok*,Sudostroennie, in Russian, 1975.
2. L.I. Isakov, L.I. Kutljin, *Kompleksnaja avtomatizacija sudovljlh dizeljnih i gazoturbinmljih ustanovok*, in Russian, Leningrad, Sudostreonnie, 1984.
3. L.P. Veretenikov, *Isledovanie procesov v sudovljih elektro-energetieeskih sistemah-teorija i metodlji*, in Russian, Sudostroennie, 1975.
4. G.F. Suprun, *Sintezsistem elektroenergetiki sudov,* in Russian; Leningrad, Sudostroenie, 1972.
5. A. Munitić, R. Antonić, J. Dvornik, *System Dynamics Simulation Modeling of Ship Gas-turbine generator,* ICCC'03, International Carpathian Control Conference,26-29 May, 2003, KOŠICE, SLOVAK, pp. 357-360, 2003.
6. A. Munitić, M. Oršulić, J. Dvornik, *Computer Simulation of Complex Ship System"Gas turbine - Synchronous generator"*, ISC 2003, The Industrial

Simulation Conference, 9-12 June, 2003, VALENCIA, SPAIN, ISBN: 90-77381-03-1, pp. 192197, 2003.

7. A. Munitić, L. Milić, *System Dynamics Simulation Modelling of the Diesel-drive Generating Set,,* 9th EUROPEAN SIMULATION SYMPOSIUM ESS 97, pp. 679 684, Simulation in Energy Systems I, Passau, Germany, October 19-23, 1997.
8. A. Munitić, I. Kuzmanić, M. Krčum, *System Dynamics Simulation Modelling of the Marine Synchronous Generator Set,* INTERNATIONAL CONFERENCE:MODELLING AND SIMULATION, May 13-16, 1998, Pittsburgh, USA, 1998.

Minimum Entropy Control of Chaos via Application of Particle Swarm Optimization Method

Mehdi Sadeghpour [a], Hassan Salarieh [b], Mehrdad Boroushaki [c], Aria Alasty [b]

[a] Department of Mechanical Engineering, Sharif University of Technology,Tehran, Iran.
sadeghpour@mech.sharif.ir

[b] Center of Excellence in Design, Robotics and Automation, Department of Mechanical Engineering, Sharif University of Technology, PO Box 11365-9567, Tehran, Iran.
salarieh@sharif.edu
aalasti@sharif.edu

[c] Department of Energy Engineering, Sharif University of Technology,Tehran, Iran.
boroushaki@sharif.edu

Abstract

One of the recently developed approaches for controlling chaos is the minimum entropy control technique. In this method an entropy function based on the Shannon definition, is defined for a chaotic system. The entropy of the system is a function of control action and it has been shown that by applying appropriate control action to the chaotic system the entropy of that system can be minimized which means that the chaotic behavior be stabilized [7]. In this paper the particle swarm optimization technique is used for minimizing the entropy function of the system from which the appropriate control action is obtained. The application of this technique is studied in two case studies: The chaotic logistic map which is controlled by an error feedback controller and the chaotic Hénon map which is controlled by a delayed feedback controller form. Simulation results show very good effectiveness of this method in chaos elimination.
Keywords: chaos, PSO, minimum entropy control, delayed feedback, error feedback

1. Introduction

There are considerable number of chaotic systems in nature and the engineering world. Researchers and engineers who are dealing with the chaotic systems, have tried to develop effective methods to control chaotic behavior in such systems especially in the recent decades. The problem of chaos control is first introduced by Ott et al. [5] who demonstrated that a significant change in the behavior of a chaotic system can be made by a tiny adjustment of its parameters. In general, control of chaos can be carried out by changing the physical parameters of the system or by means of some physical inputs to the system such as forces, torques, etc [2]. In fact controlling of chaotic systems means controlling of their behavior in a way that they show a regular behavior. The typical purpose in controlling of chaotic systems is stabilizing the unstable periodic orbits (UPOs). Since 1990, when the OGY method for controlling chaos was proposed [5], many control techniques have been introduced. In 1992, Pyragas presented a linear delayed feedback control law [10]. Also several nonlinear control methods such as feedback linearization [1,4], variable structure control [6,9,13] and feedback linearization in discrete time systems [3,14] have been developed. One of the control techniques for the chaotic systems is the minimum entropy control method which is based on the stochastic concept of entropy for chaotic maps. In this method an entropy function is defined for the system as a measure of irregularity of the chaotic map. Salarieh and Alasty [7] used the definition of entropy in the sense of Shannon and developed an entropy minimization approach for controlling chaos. One important advantage of this method is that there is no need for mathematical model of the system and only the measured states of the system are enough for calculating the control action. They used the gradient descent algorithm for minimizing the entropy function. The gradient descent algorithm usually has trouble with local minimums of functions and cannot pass over them easily. As a result, it may not be an effective minimization tool to be used in the minimum entropy control method.

In this paper, the particle swarm optimization (PSO) technique is used for minimizing the entropy function of the chaotic system. This optimization technique, has exhibited remarkable results in various optimization problems and resolved the problem of being trapped in local minimums to some good extent. Despite its simplicity over the other optimization methods, the PSO technique has presented satisfying performances, particularly in dynamic problems. In this paper, the minimum entropy control method based on the PSO algorithm, is applied for stabilizing the first order fixed points of the Logistic map and the Hénon map. In the first case an error feedback controller and in the second example a delayed feedback controller is used while in each case the feedback gain is obtained from the minimum entropy strategy via PSO algorithm.

2. Problem statement

Consider the following nonlinear map which generates a chaotic motion

$$x(n+1) = f(x(n), u(n)) \tag{1}$$

where $x(n)$ is the state vector, $u(n)$ is the control action and f is a nonlinear map. If the fixed point of the chaotic system is denoted by x_F, it would satisfy the following equation

$$x_F = f(x_F, 0) \tag{2}$$

The purpose of controlling the chaos in such a system is to obtain a control law $u(n)$ that stabilizes the fixed point of the nonlinear map, x_F. To achieve this goal, the entropy minimization technique is used to design a stabilizing feedback controller. According to this method the control action $u(n)$ is designed such that the entropy of the chaotic system be minimized. The chaotic system will show a regular and stable behavior if its entropy is minimized [7]. Hence, the entropy of the system can be considered as an objective function for minimizing.
The entropy function of a chaotic system in the sense of Shannon could be defined as follows [7]

$$E(u) = -\int_{x\in\Omega} p(x,u)\ln p(x,u)dx \tag{3}$$

where E is the entropy, p is the probability density function and Ω is a D-dimensional region in which the state variables lie (D is the dimension of the state variables). If p is not known, it is usually estimated by numerical methods. In the minimum entropy control technique the region Ω is divided to N sub-regions Ω_i, $i = 1, 2, \dots, N$. Thus, each new state generated from Eq. (1), i.e. $x(n+1)$, lies in one of these sub-regions. Then the probability density function in the $N_{iter}{}^{\text{th}}$ iteration may be defined as follows

$$p(x,u) = P_i(x,u) = \frac{N_i}{N_{iter}}, \quad if\ x \in \Omega_i \tag{4}$$

where N_i is the number of points (states) lie in sub-region Ω_i and N_{iter} is the number of all points in region Ω which is equal to the number of iterations of Eq. (1), that is, $N_{iter} = \sum_{i=1}^{N} N_i$.
Using Eq. (4) the entropy function of the system can be written as

$$E(u) = -\sum_{i=1}^{N} P_i(x,u)\ln P_i(x,u) \tag{5}$$

Now we must produce a control action u so that the entropy function of Eq. (5) is minimized. We use the two forms of error feedback and delayed feedback for the control action. The error feedback form is $u(n) = \varphi(x(n) - x_F, \mu)$ and the delayed feedback form is $u(n) = \varphi(x(n) - x(n-1), \mu)$. In each form μ is a controlling parameter which is to be determined from the PSO algorithm.

2. Particle swarm optimization (PSO) technique

Particle Swarm Optimization or PSO is an optimization technique introduced by Kennedy and Eberhart [8] in 1995. This method was inspired from some patterns of natural life such as swarms of bird or fish trying to find food.
This optimization algorithm begins with an initial population of particles with random positions and velocities. In the next iterations every particle (bird) updates its position by information it gets from other particles of the group. The information consists of the best position obtained by the same particle until that iteration (P_{best}) and the best position among all positions obtained by all particles until that iteration (g_{best}). Thus, in each iteration the position of each particle (which can potentially be a solution of the problem) changes by adding a combination of the following terms:

- Current velocity of the particle (inertia term)
- Motion toward the best position of the particle (P_{best}) (cognitive term)
- Motion toward the best position among all particles (g_{best}) (social learning term)

Therefore, if the position and velocity of particle i are denoted, respectively, by $X_i = (x_{i1}, x_{i2}, \ldots, x_{iD})$ and $V_i = (v_{i1}, v_{i2}, \ldots, v_{iD})$, (D is the dimension of the solution), then its velocity and position are updated as follows [12]

$$V_{i,t+1} = \omega\, V_{i,t} + c_1 r_{1,t}\left(P_{best,i,t} - X_{i,t}\right) + c_2 r_{2,t}\left(g_{best,t} - X_{i,t}\right) \tag{6}$$

$$X_{i,t+1} = X_{i,t} + k\, V_{i,t+1} \tag{7}$$

where t is the iteration number, ω is the inertia weight, $r_{1,t}$ and $r_{2,t}$ are random numbers between 0 and 1, c_1 and c_2 are constants and k is the constriction coefficient. Suitable values of quantities ω, c_1, c_2 and k may be depended on the problem.
The algorithm consists of the following steps:

1. *Initialization:* generation of a population of particles with random D-dimensional positions and velocities using a uniform probability distribution function.

2. *Evaluation:* computation of fitness value (objective function) for each particle.

3. *Comparison:* for each particle its fitness value is compared with its best fitness value obtained in previous iterations (the fitness value of P_{best}) and if the new position has better fitness value (for example less fitness value in a minimization problem), P_{best} is replaced with the new position. Also, the fitness value of each particle is compared with the best fitness value of the group obtained until the previous iteration (the fitness value of g_{best}) and if the particle has better fitness value, g_{best} is replaced with that particle's position.

4. *Convergence:* if a sufficiently good fitness value is achieved or a maximum number of iterations is reached, the algorithm could be stopped. Otherwise it will continue to step 5.

5. *Updating:* calculating of new velocity and position of each particle from Eqs. (6,7) and returning to step 2.

4. Description of case studies and simulation results

Suppose a chaotic map under control has the equation:

$$x(n+1) = f(x(n)) + u(n) \tag{8}$$

For controlling of this map we use the error feedback control law for the control action in the form of:

$$u(n) = \mu(n)[x(n) - x_F] \tag{9}$$

and the delayed feedback control law in the form of:

$$u(n) = \mu(n)[x(n) - x(n-1)] \tag{10}$$

The position X in Eqs. (6,7) is replaced by $\mu(n)$. The PSO algorithm is applied in the offline form in all simulations in this paper. The control procedure is as follows:
In each iteration, we have N_{pso} control parameters μ (according to N_{pso} birds). Each $\mu(n)$ is substituted in Eq. (9) or Eq. (10) to produce the corresponding $u(n)$. Then, $u(n)$ is substituted in Eq. (8) to generate $x(n+1)$. Afterwards, the entropy function $E(n+1)$ is calculated. After that the corresponding entropy of all μ's is computed, P_{best} and g_{best} are obtained. Then the control parameters ($\mu's$) are updated from Eqs. (6,7). The new control parameters are used to generate $x(n+1)$ again and this loop repeats J times. In each repetition g_{best} is updated and after J^{th} repetition of the loop,

$\mu(n)$ is set equal to the last updated g_{best} and $x(n+1)$ and $E(n+1)$ are computed based on it. The same approach is applied for obtaining $x(n+2)$ and etc. J is an arbitrary parameter .It is better for J to be chosen small enough for reducing computations time. The initial values of $\mu's$ are taken randomly in the initialization step of the PSO algorithm.

4.1. Stabilizing the 1-cycle fixed point of the Logistic map

Consider the Logistic map as given below

$$x(n+1) = \lambda\, x(n)\big(1 - x(n)\big) + u(n) \tag{11}$$

For $\lambda = 3.7$ the behavior of this system without applying control action $u(n)$ is chaotic. The 1-cycle fixed point of this system is $x_F = 0.72973$.
In the two simulations in this paper the inertia weight is chosen in the form of a decreasing function $\omega(t+1) = k_\omega\,.\,\omega(t)$ where t represents the iteration number and k_ω is a positive constant between 0 and 1 [11].
Fig. (1) shows the stabilizing of the 1-cycle fixed point of the Logistic map using error feedback control form of Eq. (9). For the first 200 iterations the control action is not applied to the system. In this case, the constriction coefficient k is set equal to 1. c_1 and c_2 are set equal to 2. k_ω is chosen equal to 0.95. The initial value of ω is $\omega(1) = 0.95$. The number of particles of the algorithm is $N_{pso} = 30$. $J = 5$ is chosen. The region Ω is the interval $[0,1]$ which is divided to N sub-region $\Omega_i = [\frac{i-1}{N}, \frac{i}{N}]$, $i = 1, 2, \dots, N$, when $N = 20$ [7].

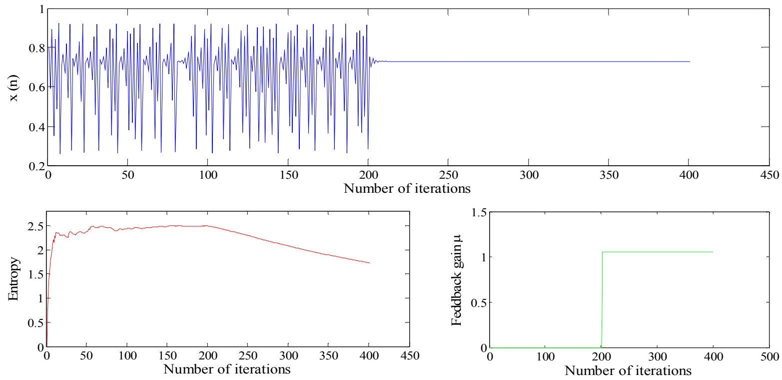

Figure 1: Stabilizing the 1-cycle fixed point of the Logistic map using error feedback controller.

As seen from Fig. (1), after applying control action, the chaotic behavior of the system gradually vanishes in about 20 iterations. The entropy of the system begins to decrease after the controller begins to apply. Finally the control action $u(n)$ becomes zero when $x(n) = x_F$.

4.2. Stabilizing the 1-cycle fixed point of the Hénon map

Another example of a chaotic map is the Hénon map given by the following equations:

$$x(n+1) = 1 - ax(n)^2 + by(n) + u(n)$$
$$y(n+1) = x(n) \tag{12}$$

The behavior of the map depends on two parameters a and b. For values of $a = 1.4$ and $b = 0.3$ (canonical values of the Hénon map) the behavior of the map is chaotic. The region Ω in this case is the interval $[-1.5, 1.5]$ which is uniformly divided to $N = 20$ sub-regions. The 1-cycle fixed point of this system is $x_F = y_F = 0.63135$. Moreover, in calculation of the entropy function of the Hénon map only 250 last points (states) of the system are considered for reducing of the computations time. As a result, the entropy decreases more rapidly with respect to the previous cases.
By using the delayed feedback control law of Eq. (10) (Pyragas method) for the control action and substituting in Eq. (12), the following equation is obtained:

$$x(n+1) = 1 - ax(n)^2 + bx(n-1) + \mu(n)[x(n) - x(n-1)] \tag{13}$$

In this case, in the first 500 iterations the system is uncontrolled. The results of the proposed approach for this case are shown in Fig. (2).

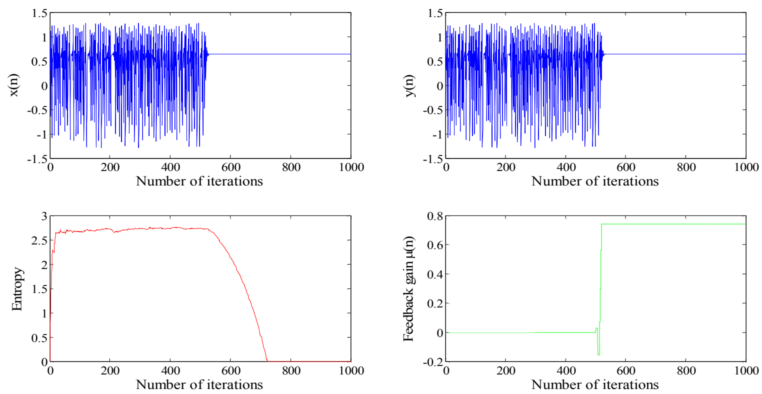

Figure 2: Stabilizing the 1-cycle fixed point of the Hénon map using delayed feedback controller.

The parameters of the PSO algorithm are: $k = 1$, $c_1 = c_2 = 2.05$, $N_{pso} = 35$, $k_\omega = .98$, $\omega(1) = .98$ and $J = 1$. The stabilization of the fixed point of the Hénon map is achieved about 25 iterations after the controller begins to work. The entropy becomes zero after about 220 iterations.

5. Conclusions

The entropy minimization approach for controlling chaos and stabilizing the fixed points of chaotic systems is implemented by using PSO algorithm as a minimization tool. Two control techniques are used: the error feedback and the delayed feedback (Pyragas) method. In both methods the PSO algorithm is used to produce an appropriate feedback gain such that the corresponding control action be able to decrease the entropy of the system. The proposed method is applied for stabilizing the 1-cycle fixed points of the Logistic map and the Hénon map. Simulation results of the studied cases show that the proposed approach has a good effectiveness on eliminating chaos and regulating the behavior of a chaotic system by conducting it toward its fixed points. The high ability in finding the global extremum of a function and good functionality in dynamic problems, made the PSO algorithm able to show very good results as a minimizing tool in the minimum entropy control technique.

References

[1] A. Alasty, H. Salarieh, Nonlinear feedback control of chaotic pendulum in presence of saturation effect, *Chaos, Solitons & Fractals*, 31(2), 292–304 (2007).

[2] A.L. Fradkov, R.J. Evans, Control of chaos: Methods and applications in engineering, *Annual Reviews in Control*, 29, Issue 1, 33-56 (2005).

[3] C.C. Fuh, H.H. Tsai, Control of discrete-time chaotic systems via feedback linearization, *Chaos, Solitons & Fractals,* 13, 285–294 (2002).

[4] C.C. Hwang, R.F. Fung, J.Y. Hsieh, W.J. Li, Nonlinear feedback control of the Lorenz equation, *Int J Eng Sci*, 37, 1893–1900 (1999).

[5] E. Ott, C. Grebogi, J.A. Yorke, Controlling chaos, *Phys Rev Lett*, 64, 1196–1199 (1990).

[6] H.H. Tsai, C.C Fuh, C.N. Chang, A robust controller for chaotic systems under external excitation, *Chaos, Solitons & Fractals*, 14, 627–632 (2002).

[7] H. Salarieh, A. Alasty, Stabilizing unstable fixed points of chaotic maps via minimum entropy control, *Chaos, Solitons and Fractals*, 37, 763–769 (2008).

[8] J. Kennedy, R.C. Eberhart, Particle Swarm Optimization, *Proceedings of IEEE International Conference on Neural Networks*, IV, 1942-1948 (1995).

[9] K. Konishi, M. Hirai, H. Kokame, Sliding mode control for a class of chaotic systems, *Phys Lett A*, 245, 511–517 (1998).

[10] K. Pyragas, Continuous control of chaos by self-controlling feedback, *Phys Lett A*, 170, 421–428 (1992).

[11] P.C. Fourie, A.A. Groenwold, The particle swarm optimization algorithm in size and shape optimization, *Structural Optimization*, 23, 259-267 (2002).

[12] R.C. Eberhart, Y. Shi, Particle Swarm Optimization: Developments, Applications and Resources, *Proceedings of the 2001 congress on evolutionary Computation*, 81-86 (2001), Seoul, Korea.

[13] X. Yu, Variable structure control approach for controlling chaos, *Chaos, Solitons & Fractals*, 8(9), 1577–1586 (1997).

[14] Y.M. Liaw, P.C. Tung, Controlling chaos via state feedback cancellation under a noisy environment, *Phys Lett A*, 211, 350–356 (1996).

JOURNAL OF APPLIED FUNCTIONAL ANALYSIS, VOL.6, NO.3, 250-257, COPYRIGHT 2011 EUDOXUS PRESS, LLC

Bifurcation analysis of resource coupled Rössler systems

J. L. Laugesen and E. Mosekilde
Complex Systems Group and
Department of Physics, The Technical University of Denmark

March 8, 2010

Abstract

Nephrons in the kidney interact via different mechanisms that involve mutual readjustments in the distribution of the blood flow. At the same time, the flow of blood controls the dynamics of the individual nephron, including its ability to produce complex nonlinear oscillations, synchronization of various internal modes, and deterministic chaos. In order to better understand a variety of phenomena that are specific to this type of coupling we have studied a system of two interacting Rössler oscillators with a coupling that reproduces essential aspects of the biological mechanism. We have performed detailed one- and two-dimensional bifurcation analyses of the 1:1 resonance tongue in this system. These analyses have disclosed an unusual substructure with cascades of period-doubling bifurcations unfolding along the edges of the tongue. This structure is typical of interacting period-doubling systems. However, while associated with the so-called C-type critical behavior, it appears that the bifurcation structure has not previously been examined in detail.

Keywords: Nephron, resource coupling, Rössler system, resonance, synchronization, bifurcation analysis.

1 Introduction

The human kidney contains approximately 1.2 million functional units, called nephrons. Each of these units possesses a certain ability to protect its own function against fluctuations in the arterial blood pressure by regulating the flow resistance of the incoming arteriole. As experiments on anesthetized rats have shown [2, 1], this regulation tends to be unstable and produce interacting oscillatory modes, period-doubling bifurcations, and other complicated dynamic phenomena in the tubular pressures and flows. The nephrons interact with one another through different mechanisms of which the so-called vascular propagated coupling involves waves of muscular contractions that travel along the common structure of blood vessels. This coupling tends to produce in-phase synchronization among the interacting nephrons. An alternative mechanism, denoted hemodynamic coupling, arises from the simple fact that as one nephron reduces its incoming blood flow, more blood will flow to its neighbors. This mechanism generally causes the interacting nephrons to show out-of-phase oscillations in their pressures and flows. Both in-phase and anti-phase synchronization of neighboring nephrons have been observed experimentally [3].

Figure 1 shows a sketch of two nephrons with their afferent arterioles branching off from a common larger arteriole. Under the control of a variety of regulatory feedback mechanisms, water and salt filtered out from the capillary system in the glomerulus is processed as the fluid flows through the tubular system. As mentioned above, interaction between the nephrons arises from the influence that contraction of the afferent arteriole of one nephron has on the blood flow to neighboring nephrons.

Despite its simplicity, the hemodynamic coupling is of significant interest both from a theoretical point of view and in view of its relevance to a range of other systems, including coupled electronic oscillators [12] and coupled population dynamic systems [13]. The peculiar aspect of this interaction is that it is mediated directly through variations in the supply (or distribution) of those resources that cause the individual subsystem to oscillate or, in other words, the coupling takes place through a main bifurcation parameter rather than through the system variables as for the more commonly studied diffusive coupling.

The purpose of the present paper is to examine some of the bifurcation phenomena that are characteristic for the resource distributed type of coupling. The hemodynamic interaction between neighboring nephrons is almost immediate such that the, displacement of the blood flow away from one nephron immediately leads to an increasing blood flow to its neighbors. Besides involving regulation of a main bifurcation parameter, the coupling between our two Rössler oscillators should therefore be designed such that growing oscillations in one system leads to declining amplitudes in the other.

To better understand the generic aspects of this type of coupling, we have performed detailed one-and two-dimensional bifurcation analyses of a pair of coupled Rössler systems with resource mediated coupling. These analyses have revealed an unusual structure with cascades of period-doubling bifurcations that unfold along the edges of the resonance tongues. This structure is related to the so-called C-type criticality [5, 6]. It appears, however, that a detailed bifurcation analysis of the structures has not previously been performed [8].

2 Coupled Rössler systems

Detailed mechanism-based modeling is often possible for physiological systems, and over the years we have developed increasingly advanced models of the blood flow regulation for the individual nephron [1, 7]. We have used these models to study both the synchronization of neighboring nephrons [3] and the interaction of a large number of nephrons in a so-called nephron tree [10]. This physiology-based modeling approach has the advantage of providing significant insight into the biological processes and their mutual interaction. However to shed light on some of the more generic phenomena it is obviously preferable to choose a simpler system, even if it has no direct physiological interpretation. Hence we shall

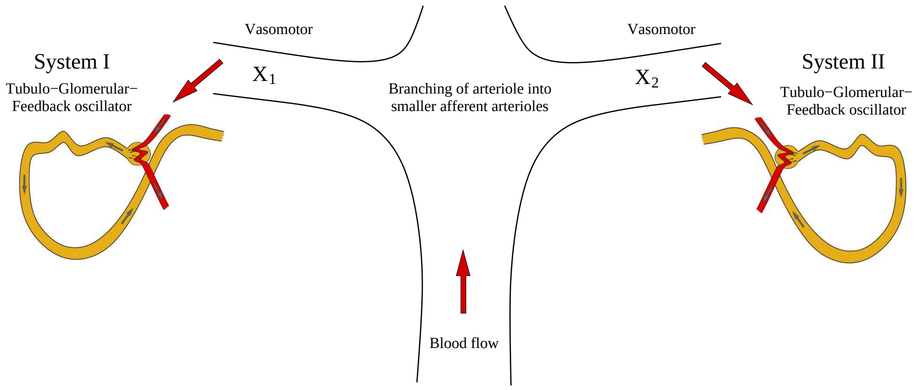

Figure 1: Sketch of two interaction nephrons with their afferent arterioles branching off from a common larger arteriole. Coupling between the nephrons arises from phenomena that play out via the vascular system that connect them. At the same time this system provides the individual nephron with the flow of blood it needs to maintain its complicated dynamics.

consider a system of two coupled Rössler oscillators where the coupling is introduced via the parameter a that can be considered as a main control of the dissipation of the individual oscillator. To a certain extent the Rössler system displays a dynamics similar to the dynamics of our more detailed physiological models: For part of the time the Rössler system exhibits a relatively fast expanding oscillatory dynamics close to the (x, y)-plane. This may be interpreted as representing the relatively fast so-called myogenic oscillations that arise in the blood flow regulation from periodic contractions of the smooth muscle cells surrounding the afferent arteriole. When the amplitude of these oscillations becomes sufficiently large, the trajectories are folded back towards the unstable equilibrium point to start a new outwards spiral. This may be interpreted as representing the slower component of nephron oscillations that arise through a feedback from variations in the sodium concentration in the tubular fluid [9, 2]. Our system thus takes the form:

$$I: \quad \begin{cases} \dot{x}_1 &= -y_1 - z_1 \\ \dot{y}_1 &= x_1 + a[1 - \alpha(x_2 - x_1 - c)]y_1 \\ \dot{z}_1 &= b + z_1(x_1 - c) \end{cases} \tag{1}$$

$$II: \quad \begin{cases} \dot{x}_2 &= -\omega y_2 - z_2 \\ \dot{y}_2 &= \omega x_2 + a[1 - \alpha(x_1 - x_2 - c)]y_2 \\ \dot{z}_2 &= b + z_2(x_2 - c) \end{cases} \tag{2}$$

where the parameter values throughout this paper are taken to be $a = 0.057258$, $b = 0.2$ and $c = 5.7$. ω is a bifurcation parameter that controls the frequency of system II. The value of a is defined as the mean value between the Hopf bifurcation point and the first period-doubling. As described above the coupling takes place via the variable y, and the coupling term for system I take the form

$$a_{eff} y_1 = a[1 - \alpha(x_2 - x_1 - c)]y_1, \tag{3}$$

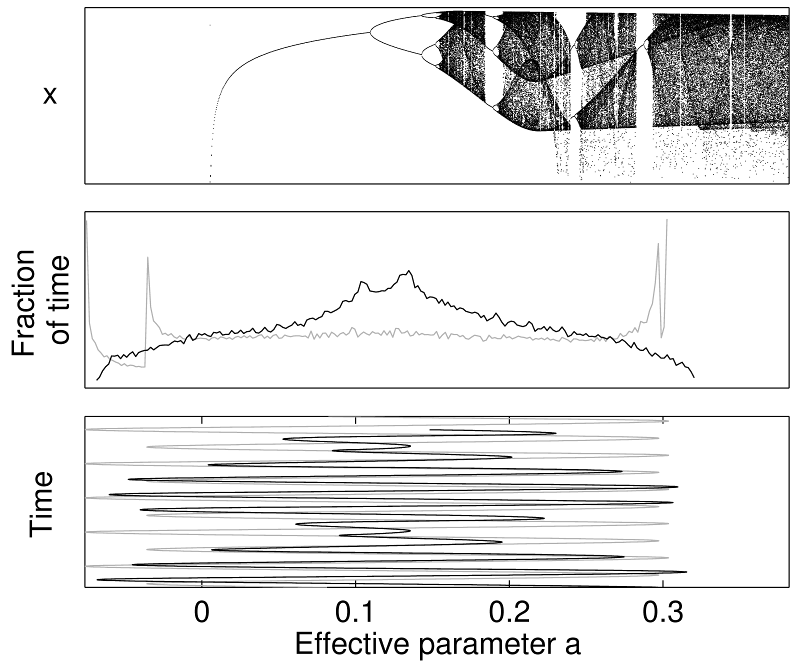

Figure 2: The period-doubling cascade to chaos in two coupled Rössler systems together with the fraction of time spent at different values of a_{eff} and the time evolution of a_{eff} at two different situations: $(\omega, \alpha) = (1.001, 0.2)$ (gray) and $(\omega, \alpha) = (1.2, 0.2)$ (black).

where α is a coupling parameter and a_{eff} may be considered as an effective, time-dependent value of parameter a. When $\Delta x = x_2 - x_1 > c$ the effective a in system I reduces linearly and thus the rate of change in y due to the coupling change non-linearly by $a_{eff}y_1$. In accordance with our previous comments, this type of coupling may be called a resource mediated coupling [11], since parameter a may be considered to describe the flow of resources that maintain the dynamics of the system. The system may be interpreted as a single Rössler system, where a is oscillating over the period-doubling cascade and eventually into the chaotic region. This is illustrated in Figure 2. The top panel of this figure shows a one-dimensional bifurcation diagram for the single Rössler system with a as parameter. The middle panel shows two examples of the fraction of time that the effective a on average spend at specific values for a period two orbit at $(\omega, \alpha) = (1.001, 0.2)$ and for an ergodic torus at $(\omega, \alpha) = (1.2, 0.2)$. Note, that the period two orbit shows four spikes, two at the maxima and two at the minima, where the rate of change of a_{eff} is slow. The lower panel shows the time evolution of a_{eff} for the two cases.

3 Bifurcation analysis

Continuation methods represent a unique tool to follow bifurcations and thus to understand how the two systems interact. We have applied this method to study the resonnance and synchronization mechanisms in the 1:1 Arnold' tongue. Figure 3 shows the main bifurcations with the coupling parameter α and the forcing frequency ω as bifurcation parameters. For low values of α the system is in a 1:1 resonant state and saddle-node bifurcation (labelled SN_1^L and SN_1^R) form the borders of the tongue. As α increases two different bifurcations occur, depending on ω. At the borders of the resonance zone, period-doubling bifurcations take

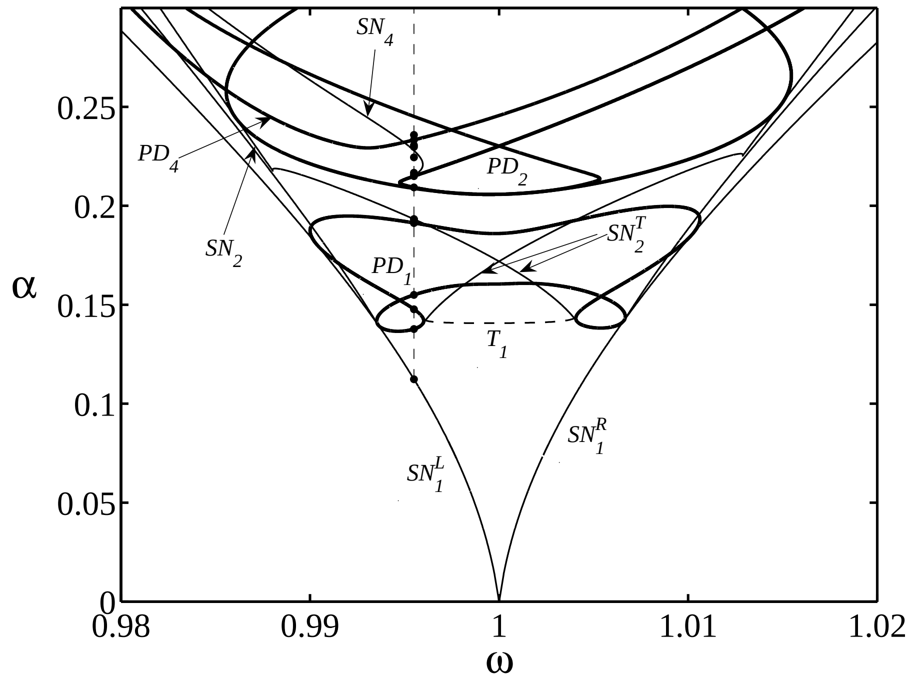

Figure 3: Main Arnold' tongue (1:1) with part of the bifurcation structure. The torus bifurcation inside the tongue give rise to quasi-periodic dynamics. It is terminated by saddle node bifurcations (SN_2^T) of a period-2 cycle, which exist only in the region above $SN_{2,T}$. Period-doubling bifurcations are drawn with thick lines.

place, while around the center a torus bifurcation (T_1) leads to the formation of an ergodic torus. The torus is later destroyed by the birth of a period-2 cycle in the saddle-node bifurcations ($SN_{2,T}^L$ and $SN_{2,T}^R$). The saddle-node bifurcations extend towards the borders of the resonant region and become the new borders for the 2:2 resonant region. At the point of contact between PD_1 and SN_1^L a new saddle-node bifurcation is born, which becomes the border for the period-2 cycle that co-exist with the period-2 cycle emerging at $SN_{2,T}$. Figure 4 shows the bifurcations along the dashed line at $\omega = 0.9955$. Starting from the period-1 cycle a period-doubling bifurcation (PD_1) takes place, and the period-2 subsequently undergoes a second period-doubling at (PD_2). The period-4 then suffers a cusp bifurcation (SN_4) and leaves the cascade to follow a second period-doubling cascade (labelled with superscript 2). The new attractor undergoes a full period-doubling cascade to chaos (not shown). A third attractor co-exist in the range $\alpha > 0.19$. This is the cycle that terminated the torus mentioned

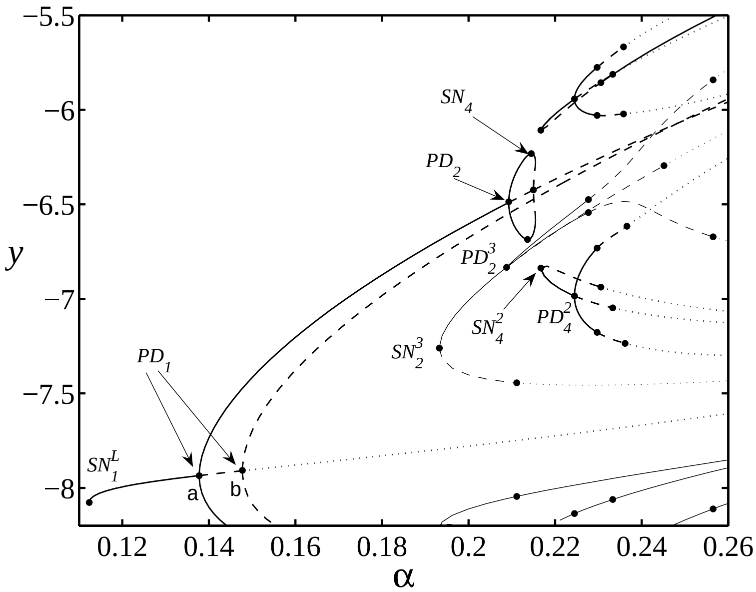

Figure 4: Bifurcations on the **stable** branch of the 1:1 resonance cycle along the dashed line at $\omega = 0.9955$ in Figure 3.

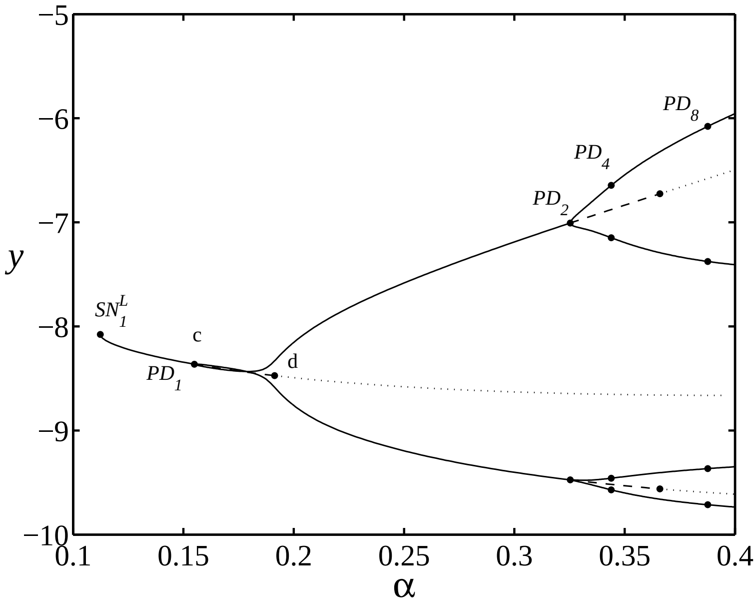

Figure 5: Bifurcations on the **unstable** branch of the 1:1 resonance cycle along the dashed line at $\omega = 0.9955$ in Figure 3. Note, that in this figure saddles are drawn with solid lines, doubly unstable nodes are dashed lines and triply unstable nodes are dotted lines.

above. It is born as a period-2 cycle. The first period-doubling (PD_2^3) taking place on this 2-cycle behaves in an unusual way, but this is likely to be due the Poincaré section chosen, i.e. the projection of the orbit. The further evolution shows a period-doubling cascade to chaos.

The looping of the period-doubling PD_1 is typical for systems, where a parameter is replace by a variable that span over a period-doubling cascade and similar loops of other higher period-doublings exist. As we follow the stable period-1 cycle it undergoes a period-doubling at (a) and turns into a saddle. The saddle then undergoes a period-doubling at (b) and turns into an unstable node. The remaining two intersections with PD_1 take place on the unstable branch of the period-1 cycle. Figure 5 shows the bifurcations on the unstable branch. Similar, as for the stable branch, the 1-cycle undergoes two succesive period-doublings at (c) and (d).

4 Conclusion

The coupling used here is a first attemp to approach the mechanisms involved in the coupling between nephrons. Although the study is preliminary it has brought valuable information on the bifurcation structure. This may be useful in interpreting a larger study of a complete nephron tree with physiologically more correct models. The dynamics of the two Rössler systems with the special resource coupling are out of phase for all parameter ranges explored, because of the symmetry of the coupling. The bifurcation structure show a termination of a period-doubling cascade followed by a second period-doubling cascade, due to a cusp bifurcation. A co-existing period-doubling structure was also found.

5 Acknowledgement

This work was supported by the European Union through the Network of Excellence BioSim (LSHB-CT-2004 005137). We acknowledge inspiring discussions with Zh. T. Zhusubaliyev.

References

[1] M. Barfred, E. Mosekilde and N.-H. Holstein-Rathlou, Bifurcation analysis of nephron pressure and flow regulation, *Chaos*, 6, 280-287, 1996.

[2] N.-H. Holstein-Rathlou, Oscillations and Chaos in Renal Blood Flow Control, *Journal of the American Society of Nephrology*, 4, 1275-1287, 1993.

[3] N.-H. Holstein-Rathlou, K.-P. Yip, O. V. Sosnovtseva and E. Mosekilde, Synchronization phenomena in nephron-nephron interaction, *Chaos*, 11, 417-426, 2001.

[4] K. S. Jensen, E. Mosekilde and N.-H. Holstein-Rathlou, Self-sustained oscillations and chaotic behavior in kidney pressure regulation, *Mondes en Developpement*, 54/55, 91-109, 1986.

[5] S. P. Kuznetsov, A. P. Kuznetsov and I. R. Sataev, Multiparameter Critical Situations, Universality and Scaling in Two-Dimensional Period-Doubling Maps, *Journal of Statistical Physics*, 121, 697-748, 2005.

[6] S. P. Kuznetsov and I. R. Sataev, Universality and scaling for the breakup of phase synchronization at the onset of chaos in a periodically driven Rössler oscillator,*Physical Review E (Statistical, Nonlinear, and Soft Matter Physics)*, 64, 046214/1-7, 2001.

[7] J. L. Laugesen, O. V. Sosnovtseva, E. Mosekilde, N.-H. Holstein-Rathlou and D. J. Marsh,Coupling induced complexity in nephron models of renal blood flow regulation, *Am J Physiol Regul Integr Comp Physiol*, 2010.

[8] J. L. Laugesen, E. Mosekilde and Zh. Zhusubaliyev, Bifurcation structure of the C-type period-doubling transition, *Submitted to Physica D*, 2010.

[9] P. P. Leyssac and N.-H. Holstein-Rathlou, Tubulo-glomerular feedback response: Enhancement in adult spontaneously hypertensive rats and effects of anaesthetics, *Pflügers Archive*, 413, 267-272, 1989.

[10] D. J. Marsh, O. V. Sosnovtseva, E. Mosekilde and N.-H. Holstein-Rathlou, Vascular coupling induces synchronization, quasiperiodicity, and chaos in a nephron tree, *Chaos*, 17, 15114-1-10, 2007.

[11] D. E. Postnov, O. V. Sosnovtseva and E. Mosekilde, Oscillator clustering in a resource distribution chain, *Chaos*, 15, 13704-1-12, 2005.

[12] D. E. Postnov, O. V. Sosnovtseva, P. Scherbakov and E. Mosekilde, Multimode dynamics in a network with resource mediated coupling, *Chaos*, 18, 015114-1-9, 2008.

[13] D. E. Postnov, A. G. Balanov and E. Mosekilde, Synchronization phenomena in an array of population dynamic systems, *Advances in Complex Systems*, 1, 181-202, 1998.

[14] O. E. Rössler, An equation for continuous chaos, *Physics Letters A*, 57, 397-398, 1976.

JOURNAL OF APPLIED FUNCTIONAL ANALYSIS, VOL.6, NO.3, 258-265, COPYRIGHT 2011 EUDOXUS PRESS, LLC

Multiple Scales Lindstedt Poincare Method for Strongly Nonlinear Forced Oscillations

Mehmet Pakdemirli and M.M. Fatih Karahan
Celal Bayar University, Department of Mechanical Engineering
45140, Muradiye, Manisa, Turkiye
fatih.karahan@bayar.edu.tr

March 06, 2010

Forced vibrations of duffing equation with damping is considered. Recently developed Multiple Scales Lindstedt-Poincare (MSLP) technique for free vibrations is applied for the first time to the forced vibration problem in search of approximate solutions. For the case of weak and strong nonlinearities, approximate solutions of the new method are contrasted with the numerical simulations. For weakly and strongly nonlinear systems, frequency response curve of MSLP method and numerical solutions are in good agreement.

Keywords: MSLP Method, Lindstedt Poincare method, Multiple Scales method, Numerical Solutions, Forced Vibrations, Strongly Nonlinear Systems.

1 Introduction

Perturbation methods are well established and used for over a century to determine approximate analytical solutions for mathematical models. Algebraic equations, integrals, differential equations, difference equations and integro-differential equations can be solved approximately with these techniques. The direct expansion method (pedestrian expansion) does not produce physically valid solutions for most of the cases and depending on the nature of the equation, many different perturbation techniques such as Lindstedt-Poincare technique, Renormalization method, Method of Multiple Scales, Averaging methods, Method of Matched Asymptotic Expansions etc. are developed within time.
One of the deficiencies in applying perturbation methods is that a small parameter is needed in the equations or the small parameter should be introduced artificially to the equations. Nevertheless, the problem solved is a weak nonlinear problem and it becomes hard to obtain an approximate solution valid for strongly nonlinear systems.

There have been a number of attempts recently to validate perturbation solutions for strongly nonlinear systems also. Hu and Xiong [1] contrasted two different approaches of Lindstedt-Poincare methods using the duffing equation. First, they solved the equation with classical method and then they made a slight modification in the expansions. Instead of expanding the transformation frequency, they expanded the natural frequency and obtained solutions with excellent convergence properties for the duffing equation. The time histories of solutions agree with the numerical solutions for arbitrarily large perturbation parameters. In a similar paper, the approximate and exact frequencies are contrasted for the duffing equation [2]. The case of vanishing restoring force was also treated for the same equation [3]. The periods obtained are contrasted with the exact period with good convergence properties for large parameters.
While a complete review of the attempts to validate perturbation solutions for strongly nonlinear oscillators is beyond the scope of this work, a partial list will be given. Among the many developed methods, Linearized perturbation method [4-6], parameter expanding method [7, 8], new time transformations as modifications of Lindstedt-Poincare method [9-11], iteration methods [12, 13] are some examples.
Very recently, Pakdemirli *et al.* [14] proposed a new perturbation method to handle strongly nonlinear systems. The method combines Multiple Scales and Lindstedt Poincare method with a frequency expansion suggested in references [1,2]. The justification for combining both methods is that Multiple Scales is better in determining transient solutions while Lindstedt Poincare method may be better under some circumstances in determining steady state solutions [15]. The new method, namely the Multiple Scales Lindstedt Poincare method (MSLP), is applied to free vibrations of a linear damped oscillator, undamped and damped duffing oscillator. It is shown that exact analytical solution can be retrieved by the new method for the linear damped oscillator. For undamped and damped duffing oscillators, results of the new method are in good agreement with the numerical simulations for strong nonlinearities.

In this work, MSLP method is applied for the first time to a forced vibration problem. Primary resonances are considered in this study. The expansions of natural and external frequencies to obtain valid solutions are nontrivial and the outline of the method is given for the forced vibrations of a duffing equation with damping. Frequency response curve of MSLP is contrasted with direct numerical simulations. For weakly and strongly nonlinear systems; result of MSLP and numerical solutions are consistent with each other.

2 Multiple Scales Lindstedt Poincare Method

In this section, the forced vibrations of the damped duffing oscillator

$$\ddot{u} + {\omega_0}^2 u + 2\varepsilon^2 \mu \dot{u} + \varepsilon \alpha u^3 = \varepsilon^2 f \cos \Omega t \tag{1}$$

will be treated with recently developed Multiple Scales Lindstedt Poincare method [14] for the first time.
First, the time transformation

$$\tau = \omega t \tag{2}$$

is applied to Eq.(1)

$$\omega^2 u'' + \omega_0^2 u + 2\varepsilon^2 \mu\omega u' + \varepsilon\alpha u^3 = \varepsilon^2 f \cos\frac{\Omega}{\omega} T_0 \tag{3}$$

Note that a time transformation involving $\tau = \Omega t$ instead of ω would not be appropriate. Prime represents derivative with respect to time variable τ. Fast and slow time scales are

$$T_0 = \tau, \qquad T_1 = \varepsilon\tau, \qquad T_2 = \varepsilon^2\tau \tag{4}$$

Using

$$\frac{d^2}{d\tau^2} = D_0^2 + 2\varepsilon D_0 D_1 + \varepsilon^2 (D_1^2 + 2D_0 D_2) + \ldots \tag{5}$$

where $D_n = \partial/\partial T_n$ and substituting the expansions

$$u = u_0(T_0, T_1, T_2) + \varepsilon u_1(T_0, T_1, T_2) + \varepsilon^2 u_2(T_0, T_1, T_2) + \ldots \tag{6}$$

$$\omega_0^2 = \omega^2 - \varepsilon\omega_1 - \varepsilon^2\omega_2 \tag{7}$$

into Eq.(3) yields after separation

$$O(1):\ \omega^2 D_0^2 u_0 + \omega^2 u_0 = 0 \tag{8}$$

$$O(\varepsilon):\ \omega^2 D_0^2 u_1 + \omega^2 u_1 = -2\omega^2 D_0 D_1 u_0 + \omega_1 u_0 - \alpha u_0^3 \tag{9}$$

$$O(\varepsilon^2):\ \begin{aligned} \omega^2 D_0^2 u_2 + \omega^2 u_2 &= -2\omega^2 D_0 D_1 u_1 - \omega^2 (D_1^2 + 2D_0 D_2) u_0 + \omega_1 u_1 \\ &\quad + \omega_2 u_0 - 2\mu\omega D_0 u_0 - 3\alpha u_0^2 u_1 + f \cos\frac{\Omega}{\omega} T_0 \end{aligned} \tag{10}$$

Note that following [1,2], in Eq. (7), instead of transformation frequency, the natural frequency is expanded. The solution at the first order is

$$u_0 = A e^{iT_0} + cc = a\cos(T_0 + \beta) \tag{11}$$

This solution is substituted into the right hand side of Eq.(9) and secular terms are eliminated

$$-2i\omega^2 D_1 A + \omega_1 A - 3\alpha A^2 \overline{A} = 0 \tag{12}$$

In MSLP as outlined in [14], first $D_1A=0$ is selected and if the frequency correction is real, this choice is admissible. If ω_1 turns out to be complex, then $D_1A \neq 0$ which implies $\omega_1=0$ and secularities are eliminated by choosing D_1A. A complex ω_1 implies that there is amplitude variation and LP method fails to produce physical solutions [16]. The method allows switching back and forth with MS and LP type of eliminating secularities thereby augmenting the advantages of both methods. For Eq.(12), selection of

$$D_1 A = 0 \ \Rightarrow \qquad A = A(T_2) \tag{13}$$

produces

$$\omega_1 = 3\alpha A\overline{A} = \frac{3}{4}\alpha a^2 \tag{14}$$

which is suitable because ω_1 is real. The solution at order ε is

$$u_1 = \frac{\alpha}{8\omega^2} A^3 e^{3iT_0} + cc = \frac{\alpha}{32\omega^2} a^3 \cos(3T_0 + 3\beta) \tag{15}$$

For the last order of approximation, the nearness of excitation frequency to the transformation frequency is expressed as follows

$$\Omega = \omega\,(1 + \varepsilon^2 \sigma) \tag{16}$$

Substitution of Eqs.(11), (15) and (16) into the right hand side of Eq.(10) and elimination of secularities yield

$$-2i\omega^2 D_2 A + \omega_2 A - 2\mu i\omega A - \frac{3\alpha^2}{8\omega^2} A^3 \overline{A}^2 + \frac{f}{2} e^{i\sigma T_2} = 0 \tag{17}$$

D_2A cannot be selected as zero, since ω_2 would then be complex. Therefore the admissible choice is

$$\omega_2 = 0 \tag{18}$$

and

$$-2i\omega^2 D_2 A - 2\mu i\omega A - \frac{3\alpha^2}{8\omega^2} A^3 \overline{A}^2 + \frac{f}{2} e^{i\sigma T_2} = 0 \tag{19}$$

The polar form $A = \frac{1}{2} a e^{i\beta}$ is substituted, real and imaginary parts are separated

$$D_2 a = -\frac{\mu}{\omega} a + \frac{f}{2\omega^2} \sin\gamma \tag{20}$$

$$D_2 \gamma = \sigma - \frac{3\alpha^2}{256\omega^4} a^4 + \frac{f}{2a\omega^2} \cos\gamma \tag{21}$$

where

$$\gamma = \sigma T_2 - \beta \tag{22}$$

For steady state solutions, $D_2a=0$, $D_2\gamma=0$ and elimination of γ between Eqs.(20) and (21) yields

$$\sigma = \frac{3\alpha^2}{256\omega^4} a^4 \pm \sqrt{\frac{f^2}{4a^2\omega^4} - \left(\frac{\mu}{\omega}\right)^2} \tag{23}$$

From Eq.(16), frequency-response relation is

$$\Omega = \omega \left[1 + \varepsilon^2 \left(\frac{3\alpha^2}{256\omega^4} a^4 \pm \sqrt{\frac{f^2}{4a^2\omega^4} - \left(\frac{\mu}{\omega}\right)^2} \right) \right] \tag{24}$$

where

$$\omega = \sqrt{\omega_0^{\,2} + \varepsilon \frac{3}{4} \alpha a^2} \tag{25}$$

Eq.(25) is obtained by substituting Eqs.(18) and (14) into Eq.(7). The approximate solution is

$$u = a\cos(\Omega t - \gamma) + \varepsilon \frac{\alpha}{32\omega^2} a^3 \cos[3(\Omega t - \gamma)] + O(\varepsilon^2) \tag{26}$$

The amplitude and phases are governed by

$$\dot{a} = \varepsilon^2 \left(-\mu a + \frac{f}{2\omega} \sin\gamma \right) \tag{27}$$

$$\dot{\gamma} = \varepsilon^2 \left(\omega\sigma - \frac{3\alpha^2}{256\omega^3} a^4 + \frac{f}{2a\omega} \cos\gamma \right) \tag{28}$$

3 Comparisons with the Numerical Solutions

Frequency response relations obtained by MSLP method will be contrasted by direct numerical integrations of the equation. For perturbation solutions to be valid, the correction term should be much smaller than the leading term. For MSLP method, the requirement is

$$\frac{\varepsilon\alpha a^2}{32\omega^2} << 1 \tag{29}$$

For strong nonlinearities, α should be arbitrarily large. For MSLP method, taking the limit yields as follows

$$\lim_{\alpha\to\infty} \frac{\varepsilon\alpha}{32\omega^2} a^2 = \frac{\varepsilon\alpha a^2}{32\left(\omega_0^2 + \varepsilon \dfrac{3\alpha}{4} a^2 \right)} = \frac{1}{24} << 1 \tag{30}$$

which satisfies the perturbation requirement for arbitrarily large nonlinearities.
Frequency response relations are contrasted with the numerical simulations as a next step. In Figure 1, all parameters are selected within the preordered range with a weak nonlinearity (α=1). As expected, frequency response curve of MSLP method and numerical solutions are in good agreement. The numerical simulation results are obtained by integrating the original Eq.(1) and determining the steady state amplitudes by taking a sufficient interval of time history. Numerical results are labeled by dots on the graphs. In Figure 2, the cubic nonlinearity is increased substantially (α=100). Result of MSLP and numerical solutions are consistent with each other. Taking α=1000 in Figure 3 still shows the same trend, that is MSLP and numerical simulations being in good agreement.

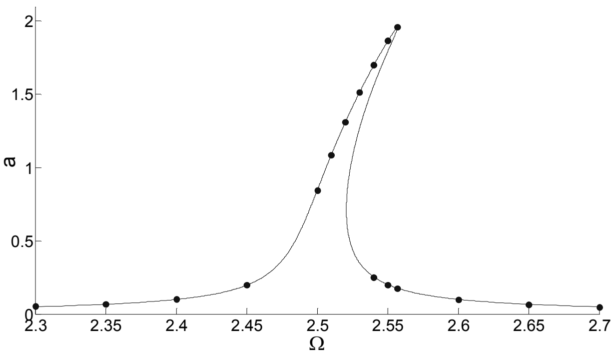

Figure 1- Comparison of frequency response curve of the MSLP Method and Numerical Simulations (Represented by dots) (ε=0.1, α=1, f=5, ω_0=2.5, μ=0.5)

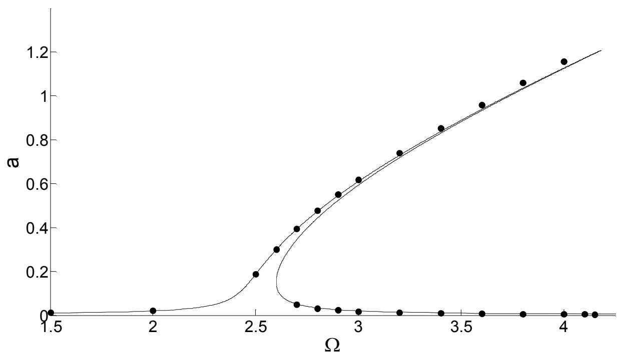

Figure 2- Comparison of frequency response curve of the MSLP Method and Numerical Simulations (Represented by dots) (ε=0.1, α=100, f=5, ω_0=2.5, μ=0.5)

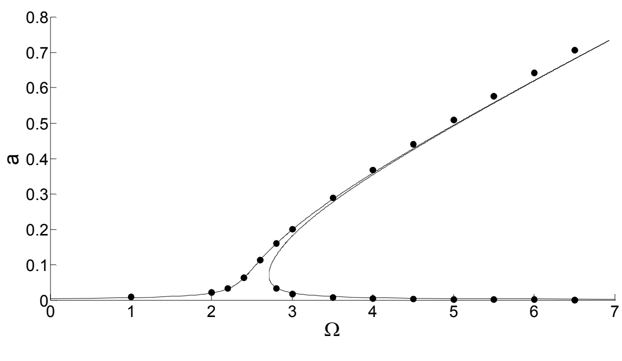

Figure 3- Comparison of frequency response curves of the MSLP Method and Numerical Simulations (Represented by dots) (ε=0.1, α=1000, f=5, ω_0=2.5, μ=0.5)

3 Concluding Remarks

The new perturbation technique combining the Multiple Scales and Lindstedt Poincare method developed in [14] is applied to forced vibrations for the first time. Primary resonances are considered in the study and frequency expansions are outlined for the new method. Approximate solutions and frequency response curves are derived for the new Multiple Scales Lindstedt Poincare method. To test the solutions, direct numerical integrations of the equations are done.
For weakly and strongly nonlinear systems, frequency response curve of the MSLP method are contrasted with numerical solutions. Comparison of the obtained results with numerical simulations provides confirmation for the validity of MSLP method.
A further study would be to apply this new technique to partial differential equations. The nonlinearities arising in partial differential equations are classified using a suitable operator notation and general solution algorithms were developed for the models previously [17-19].

Acknowledgement- This work is supported by The Scientific and Technical Research Council of Turkey under project number 108M490

References

[1] H. Hu and Z. G. Xiong, Comparison of two Lindstedt-Poincare type perturbation methods, *Journal of Sound and Vibration* 278, 437-444 (2004).
[2] H. Hu, A classical perturbation technique which is valid for large parameters, *Journal of Sound and Vibration* 269, 409-412 (2004).
[3] H. Hu, A classical perturbation technique that works even when the linear part of restoring force is zero, *Journal of Sound and Vibration* 271, 1175-1179 (2004).
[4] J. H. He, Linearized perturbation technique and its applications to strongly nonlinear oscillators, *Computers and Mathematics with Applications* 45, 1-8 (2003).
[5] H. Hu, A modified method of equivalent linearization that works even when the non-linearity is not small, *Journal of Sound and Vibration* 276, 1145-1149 (2004).
[6] J. H. He, Modified straightforward expansion, *Meccanica* 34, 287-289 (1999).
[7] J. H. He, Some asymptotic methods for strongly nonlinear equations, *International Journal of Modern Physics B* 20, 1141-1199 (2006).
[8] L. Xu, Determination of limit cycle by He's parameter-expanding method for strongly nonlinear oscillators, *Journal of Sound and Vibration* 302, 178-184 (2007).
[9] S. Q. Dai, On a generalized PLK method and its applications, *Acta Mechanica Sinic*a 6, 111-118 (1990).

[10] J. H. He, Modified Lindstedt-Poincare methods for some strongly nonlinear oscillations Part I: expansion of a constant, *International Journal of Non-Linear Mechanics* 37, 309-314 (2002).
[11] J. H. He, Modified Lindstedt-Poincare methods for some strongly nonlinear oscillations Part II: a new transformation, *International Journal of Non-Linear Mechanics* 37, 315-320 (2002).
[12] V. Marinca and N. Herisanu, A modified iteration perturbation method for some nonlinear oscillation problems, *Acta Mechanica* 184, 231-242 (2006).
[13] H. Hu, Solutions of a quadratic nonlinear oscillator: Iteration procedure, *Journal of Sound and Vibration* 298, 1159-1165 (2006).
[14] M. Pakdemirli, M. M. F. Karahan and H. Boyacı, A New Perturbation Algorithm with Better Convergence Properties: Multiple Scales Lindstedt Poincare Method, *Mathematical and Computational Applications* 14, 31-44 (2009).
[15] M. Pakdemirli, Comparison of higher order versions of the method of multiple scales for an odd nonlinearity problem, *Journal of Sound and Vibration* 262, 989-998 (2003).
[16] A. H. Nayfeh, *Introduction to Perturbation Techniques*, John Wiley and Sons, New York 1981.
[17] M. Pakdemirli, A comparison of two perturbation methods for vibrations of systems with quadratic and cubic nonlinearities, *Mechanics Research Communications* 21, 203-208, (1994).
[18] M. Pakdemirli and H. Boyaci, Comparison of direct-perturbation methods with discretization-perturbation methods for nonlinear vibrations, *Journal of Sound and Vibration* 186, 837-845, (1995).
[19] M. Pakdemirli, Vibrations of continuous systems with a general operator notation suitable for perturbative calculations, *Journal of Sound and Vibration* 246(5), 841-851, 2001.

JOURNAL OF APPLIED FUNCTIONAL ANALYSIS, VOL.6, NO.3, 266-271, COPYRIGHT 2011 EUDOXUS PRESS, LLC

Exact Travelling Wave Solutions for (2+1)-dimensional cupling Boiti-Leon-Pempinelli system

Ahmad Neirameh[1],Nasir Taghizadeh[2]

March 5, 2010

Abstract

The objective of this paper is to construct explicit travelling wave solutions involving parameters of the cupling Boiti-Leon-Pempinelli system . When the parameters are taken special values, the solitary waves are derived from the travelling waves.

MSC 2000: 35j05
Keywords:cupling Boiti-Leon-Pempinelli system ,($\frac{G'}{G}$)-Expansion Method,travelling wave solutions

1 Introduction

In this letter we consider the cupling Boiti-Leon-Pempinelli system

$$\begin{aligned} u_{ty} &= (u^2 - u_x)_{xy} + 2v_{xxx} \\ v_t &= v_{xx} + 2uv_x \end{aligned}$$

Seeking the exact solutions of the nonlinear partial differential equations play an important role in the nonlinear problems.A number of this methods have been developed such as the tanh-method [1,2,3,4,5],homogeneous balance[6,7] method.The objective of this paper is to use a method which is called the $\frac{G'}{G}$-expansion method [8,9,10,11].The main idea of this method is that the traveling wave solutions of non-linear equations can be expressed by a polynomial in $\frac{G'}{G}$ where $G = G(\xi)$ satisfies the second order linear ordinary differential equation $G'' + \lambda G' + \mu G = 0$, where $\xi = x + ly - wt$.The paper is arranged as follows. In Section 2, we describe briefly the $\frac{G'}{G}$-expansion method. In Sections 3, we apply the method to the cupling Boiti-Leon-Pempinelli system. In Section 4 some conclusions are given.

[1]Department of Mathematics Islamic Azad University of Gonbad,Iran
[2]Department of Mathematics Faculty of science University of Guilan,Rasht,Iran

2 Description of The $\frac{G'}{G}$-expansion method

Suppose that a nonlinear equation, say in two independent variables x and t, is given by

$$P(u, u_x, u_y, u_t, u_{tt}, u_{xt}, u_{xx}, \cdots) = 0 \tag{1}$$

where $u = u(x, y, t), v = v(x, y, t)$ is an unknown function, P is a polynomial in $u = u(x, y, t), v = v(x, y, t)$ and its various partial derivatives,in which the highest order derivatives and nonlinear terms are involved.In the following we give the main steps of the $\frac{G'}{G}$-expansion method.

step 1:Combining the independent variables x and t into one variable $\xi = x - vt$, we suppose that

$$u(x, y, t) = u(\xi), v = v(x, y, t), \quad \xi = x + ly - wt \tag{2}$$

The travelling wave variable (2) permits us to reduce Eq.(1) to an ODE for $u = u(\xi)$, namely

$$P(u, u', lu', -wu', u'', l^2u'', w^2u'', \cdots) = 0 \tag{3}$$

step 2:Suppose that the solution of ODE (3) can be expressed by a polynomial in $\frac{G'}{G}$ as follows

$$u(\xi) = \alpha_m(\frac{G'}{G})^m + \cdots, \tag{4}$$

where $G = G(\xi)$ satisfies the second order LODE in the form

$$G'' + \lambda G' + \mu G = 0 \tag{5}$$

$\alpha_m, \cdots, \lambda$ and μ are constants to be determined later, $\alpha_m \neq 0$, the unwritten part in (4) is also a polynomial in $\frac{G'}{G}$, but the degree of which is generally equal to or less than $m - 1$, the positive integer m can be determined by considering the homogeneous balance between the highest order derivatives and nonlinear terms appearing in ODE (3).

step 3:By substituting (4) into Eq. (3) and using the second order linear ODE (5), collecting all terms with the same order of $\frac{G'}{G}$ together, the left-hand side of Eq. (3) is converted into another polynomial in $\frac{G'}{G}$. Equating each coefficient of this polynomial to zero yields a set of algebraic equations for $\alpha_m, \cdots, \lambda$ and μ.

step 4:Assuming that the constants $\alpha_m, \cdots, \lambda$ and μ can be obtained by solving the algebraic equations in Step 3, since the general solutions of the second order LODE (5) have been well known for us, then substituting $\alpha_m, \cdots, v$ and the general solutions of Eq. (5) into (4) we have more travelling wave solutions of the nonlinear evolution equation (1).

3 cupling Boiti-Leon-Pempinelli system

In this section we consider the cupling Boiti-Leon-Pempinelli system as

$$\begin{aligned} u_{ty} &= (u^2 - u_x)_{xy} + 2v_{xxx} \\ v_t &= v_{xx} + 2uv_x \end{aligned} \tag{6}$$

Using the wave variable $u(x, y, t) = u(\xi)$ and $v(x, y, t) = v(\xi)$ where $\xi = x + ly - wt$ carries the BLp system Eq.(6) into asystem of ODEs

$$\begin{aligned} -wlu'' &= 2l(uu')' - lu''' + 2v''' \\ -wv' &= v'' + 2uv' \end{aligned} \tag{7}$$

By integrating twice the first equation above we find

$$v' = \frac{1}{2}(lu' - lu^2 - wlu) \tag{8}$$

Substituting Eq.(8) into the second equation of Eq.(6), we obtain

$$u'' - 2u^3 - 3wu^2 - w^2u = 0 \tag{9}$$

Integrating (8) and taking the integral constant be zero, we have

$$v = \frac{1}{2}lu - \int (lu^2 + wlu)d\xi. \tag{10}$$

Suppose that the solution of O.D.E (9) can be expressed by a polynomial in $(\frac{G'}{G})$ as follows:

$$u(\xi) = \alpha_m(\frac{G'}{G})^m + \cdots, \tag{11}$$

Where $G = G(\xi)$ satisfies the second order LODE in the form

$$G'' + \lambda G' + \mu G = 0 \tag{12}$$

$\alpha_0, \alpha_1, \cdots, \lambda$ and μ are to be determined later.Considering the homogeneous balance between u'' and u^3 in Eq.(9) we required that $3m = m+2$ then $m = 1$.So we can write (11) as

$$u(\xi) = \alpha_1(\frac{G'}{G}) + \alpha_0 \tag{13}$$

And therefore

$$u^3 = \alpha_1^3(\frac{G'}{G})^3 + 3\alpha_1^2\alpha_0(\frac{G'}{G})^2 + 3\alpha_1\alpha_0^2(\frac{G'}{G}) + \alpha_0^3 \tag{14}$$

$$u^2 = \alpha_1^2(\frac{G'}{G})^2 + 2\alpha_1\alpha_0(\frac{G'}{G}) + \alpha_0^2 \tag{15}$$

By using (12) and (13) it is derived that

$$u'' = 2\alpha_1(\frac{G'}{G})^3 + 3\alpha_1\lambda(\frac{G'}{G})^2 + (\alpha_1\lambda^2 + 2\alpha_1\mu)(\frac{G'}{G}) + \alpha_1\lambda\mu \tag{16}$$

By substituting $(13) - (16)$ into Eq. (9) and collecting all terms With the same power of $(\frac{G'}{G})$ together, the left-hand side of Eq. (9) is converted into another polynomial in $(\frac{G'}{G})$. Equating each coefficient of this polynomial to zero, yields a set of simultaneous algebraic equations for $\alpha_1, \alpha_0, w, \lambda, \mu$ as follows:

$$2\alpha_1 - 2\alpha_1^3 = 0$$

$$3\alpha_1\lambda - 6\alpha_1^2\alpha_0 - 3w\alpha_1^2 = 0$$
$$\alpha_1\lambda^2 + 2\alpha_1\mu - 6\alpha_1\alpha_0^2 - 6w\alpha_1\alpha_0^2 - w^2\alpha_1 = 0$$
$$\alpha_1\lambda\mu - 2\alpha_0^3 - 3w\alpha_0^2 - w^2\alpha_0 = 0$$

Solving the algebraic equations above by using the maple, yields

$$\alpha_1 = \pm 1$$

$$\alpha_1 = 1, \quad \alpha_0 = \frac{1}{2}\lambda \pm \frac{1}{2}\sqrt{-\lambda^2 - 4\mu} \tag{17}$$

$$w = \mp\frac{1}{2}\sqrt{-\lambda^2 - 4\mu}$$

By using (17), expression (13) can be written as

$$u(\xi) = (\frac{G'}{G}) + \frac{1}{2}\lambda \pm \frac{1}{2}\sqrt{-\lambda^2 - 4\mu} \tag{18}$$

Where $\xi = x \pm (\frac{1}{2}\sqrt{-\lambda^2 - 4\mu})t$. Eq. (18) is the formula of a solution of Eq. (9). On solving the Eq. (12), we deduce after some reduction that

$$\frac{G'}{G} = \frac{1}{2}\sqrt{\lambda^2 - 4\mu} \times (\frac{C_1 sinh\frac{1}{2}\sqrt{\lambda^2 - 4\mu}\xi + C_2 cosh\frac{1}{2}\sqrt{\lambda^2 - 4\mu}\xi}{C_1 cosh\frac{1}{2}\sqrt{\lambda^2 - 4\mu}\xi + C_2 sinh\frac{1}{2}\sqrt{\lambda^2 - 4\mu}\xi}) - \frac{\lambda}{2}$$

where C_1 and C_2 are arbitrary constants. Substituting the general solutions of Eq. (12) into (18) we have three types of travelling wave solutions of cupling Boiti-Leon-Pempinelli system (6) as follows:

When $\lambda^2 - 4\mu > 0$

$$u(\xi) = \frac{1}{2}(\frac{C_1 sinh\frac{1}{2}\sqrt{\lambda^2 - 4\mu}\xi + C_2 cosh\frac{1}{2}\sqrt{\lambda^2 - 4\mu}\xi}{C_1 cosh\frac{1}{2}\sqrt{\lambda^2 - 4\mu}\xi + C_2 sinh\frac{1}{2}\sqrt{\lambda^2 - 4\mu}\xi}) \pm \frac{1}{2}\sqrt{-\lambda^2 - 4\mu} \tag{19}$$

Where $\xi = x \pm (\frac{1}{2}\sqrt{-\lambda^2 - 4\mu})t$. C_1 and C_2,are arbitrary constants.And by Substituting (19), into (10) we have solution of v.

In particular, if $C_1 \neq 0, C_2 = 0, \lambda > 0, \mu = 0$,u become

$$u(\xi) = \lambda tgh\frac{1}{2}\lambda\xi \pm \frac{1}{2}\lambda i$$

When $\lambda^2 - 4\mu < 0$

$$u(\xi) = \frac{1}{2}\sqrt{4\mu - \lambda^2} \times (\frac{-C_1 sin\frac{1}{2}\sqrt{4\mu - \lambda^2}\xi + C_2 cos\frac{1}{2}\sqrt{4\mu - \lambda^2}\xi}{C_1 cos\frac{1}{2}\sqrt{4\mu - \lambda^2}\xi + C_2 sin\frac{1}{2}\sqrt{4\mu - \lambda^2}\xi}) \pm \frac{1}{2}\sqrt{-\lambda^2 - 4\mu} \quad (20)$$

Also in this case we obtain v by substituting (20),into (10).
When $\lambda^2 - 4\mu = 0$

$$u(\xi) = \frac{C_2}{C_1 + C_2\xi}$$

where C_1 and C_2 are arbitrary constants.
And for $\alpha_1 = -1$ we have

$$\alpha_0 = -\frac{1}{2}\lambda \pm \frac{1}{2}\sqrt{-\lambda^2 - 4\mu}, w = -\frac{3}{2}\lambda \mp \frac{1}{2}\sqrt{-\lambda^2 - 4\mu} \quad (21)$$

By using (21) we obtain three types of travelling wave solutions of the cupling Boiti-Leon-Pempinelli system (6) as follows When $\lambda^2 - 4\mu > 0$

$$u(\xi) = -\frac{1}{2}\sqrt{\lambda^2 - 4\mu} \times (\frac{C_1 sinh\frac{1}{2}\sqrt{\lambda^2 - 4\mu}\xi + C_2 cosh\frac{1}{2}\sqrt{\lambda^2 - 4\mu}\xi}{C_1 cosh\frac{1}{2}\sqrt{\lambda^2 - 4\mu}\xi + C_2 sinh\frac{1}{2}\sqrt{\lambda^2 - 4\mu}\xi}) - \lambda \pm \frac{1}{2}\sqrt{-\lambda^2 - 4\mu} \quad (22)$$

Where $\xi = x - (-\frac{3}{2}\lambda \mp \frac{1}{2}\sqrt{-\lambda^2 - 4\mu})t$. C_1 and C_2,are arbitrary constants.And by Substituting (22), into (10) we have solution of v.

In particular, if $C_1 \neq 0, C_2 = 0, \lambda > 0, \mu = 0$,u become

$$u(\xi) = -\lambda tgh\frac{1}{2}\lambda\xi - \lambda \pm \frac{1}{2}\lambda i$$

When $\lambda^2 - 4\mu < 0$

$$u(\xi) = -\frac{1}{2}\sqrt{4\mu - \lambda^2} \times (\frac{-C_1 sin\frac{1}{2}\sqrt{4\mu - \lambda^2}\xi + C_2 cos\frac{1}{2}\sqrt{4\mu - \lambda^2}\xi}{C_1 cos\frac{1}{2}\sqrt{4\mu - \lambda^2}\xi + C_2 sin\frac{1}{2}\sqrt{4\mu - \lambda^2}\xi}) - \lambda \pm \frac{1}{2}\sqrt{-\lambda^2 - 4\mu} \quad (23)$$

When $\lambda^2 - 4\mu = 0$

$$u(\xi) = \frac{-C_2}{C_1 + C_2\xi}$$

where C_1 and C_2 are arbitrary constants.Also in this cases we obtain v by substituting u into (10)

4 Conclusions

These equations are very difficult to be solved by traditional methods.The performance of this method is reliable, simple and gives many new exact solutions. The $\frac{G'}{G}$-expansion method has its own advantages: direct, concise, elementary that the general solutions of the second order LODE have been well known for many researchers and effective that it can be used for many other nonlinear evolution equations.

References

[1] E.G. Fan, Extended tanh-function method and its applications to nonlinear equations, Phys. Lett. A 277 (2000) 212-218.

[2] W. Maliet, Solitary wave solutions of nonlinear wave equations, Am. J. Phys. 60 (1992) 650- 654.

[3] E.J. Parkes, B.R. Duy, An automated tanh-function method for nding solitary wave solutions to nonlinear evolution equations, Comput. Phys. Commun. 98 (1996) 288-300.

[4] M.L. Wang, X.Z. Li, Applications of F-expansion to periodic wave solutions for a new Hamil- tonian amplitude equation, Chaos, Solitons and Fractals 24 (2005) 1257-1268.

[5] K.W. Chow, A class of exact periodic solutions of nonlinear envelope equation, J. Math. Phys. 36 (1995) 4125-4137.

[6] M.Wang,phys.letter. A 216(1995)67.

[7] L.Wang, Z.Zhu,Y.Wang .phys.letter. A 260(1999) 55

[8] A. Bekir, Application of the -expansion method for nonlinear evolution equations, Phys. Lett. A 372 (2008) 3400-3406.

[9] M.L. Wang, X.Z. Li, J.L. Zhang, The -expansion method and travelling wave solutions of nonlinear evolution equations in mathematical physics, Phys. Lett. A 372 (2008) 417-423.

[10] S.Zhang, J.L. Tong, W. Wang, A generalized -expansion method for the mKdV equation with variable coecients, Phys. Lett. A 372 (2008) 2254-2257.

[11] J. Zhang, X. Wei, Y. Lu, A generalized -expansion method and its applications, Phys. Lett. A 372 (2008) 3653-3658

JOURNAL OF APPLIED FUNCTIONAL ANALYSIS, VOL.6, NO.3, 272-279, COPYRIGHT 2011 EUDOXUS PRESS, LLC

Solving Fractional Disturbance Equation of Distributed Order Using the $\mathcal{L}_A$-Transform

A.Aghili and A.Ansari
Department of Mathematics, Faculty of Sciences
University of Guilan, P.O.Box 1841, Rasht, Iran
armanaghili@yahoo.com, alireza_1038@ yahoo.com

Abstract

In this article, authors introduce the $\mathcal{L}_A$-transform and derive the complex inversion formula and a convolution theorem for the transform. Furthermore, the fundamental solution of the Cauchy type fractional diffusion equation on fractals is given by means of the $\mathcal{L}_A$-transform in terms of the Wright functions. Also, the Cauchy fractional disturbance equation with continuous or discrete distribution of time fractional derivative is introduced and by using the $\mathcal{L}_2$-transform its solution is expressed in terms of the Laplace type integral.

Key words: The $\mathcal{L}_A$-transform, Fractional derivatives, Fractional diffusion equation, Fractional disturbance equation, The Wright function

Mathematics Subject Classification: 26A33; 44A10; 44A15; 44A35

1 Introduction

We consider the Laplace-type integral transform called the $\mathcal{L}_A$-transform as follows

$$\mathcal{L}_A\{f(x);p\} = \int_0^\infty A'(x)e^{-\Phi(p)A(x)}f(x)dx, \tag{1}$$

where, $f(x)$ is piecewise continuous and of the exponential order (i.e. $|f(x)| \le Me^{\Phi(c)A(x)}$) for some constants c, M, and p is complex parameter. Also, Φ, A are invertible and increasing functions respectively with boundary condition $A(0)=0$.

By the definition (1), it is obvious that, the $\mathcal{L}_A$ - transform is a generalization of the following well known transforms.

i) The Laplace transform [21] (in the case $\Phi(x) = A(x) = x$, and the abscissa of convergence c_0)

$$\begin{aligned} \mathcal{L}\{f(x);p\} &= F(p) = \int_0^\infty e^{-px}f(x)dx, \\ f(x) &= \frac{1}{2\pi i}\int_{c-i\infty}^{c+i\infty} F(p)e^{px}dp, \qquad c = \Re(p) > c_0. \end{aligned} \tag{2}$$

ii) The Mellin transform [21] (in the case $\Phi(x) = -x, A(x) = \ln(x)$)

$$\begin{aligned} \mathcal{M}\{f(x);p\} &= F(p) = \int_0^\infty x^{p-1}f(x)dx, \\ f(x) &= \frac{1}{2\pi i}\int_{c-i\infty}^{c+i\infty} F(p)x^{-p}dp, \qquad c = \Re(p). \end{aligned} \tag{3}$$

iii) The $\mathcal{L}_2$-transform[1] [1-3], [30,31,32] (in the case $\Phi(x) = A(x) = x^2$)

$$\mathcal{L}_2\{f(x);p\} = \int_0^{\infty} 2xe^{-p^2x^2} f(x)dx,$$
$$f(x) = \frac{1}{2\pi i}\int_{c-i\infty}^{c+i\infty} F(\sqrt{p})e^{px^2}dp, \qquad \Re(p^2) > c. \tag{4}$$

In recent years, Mainardi et al. [14,19], Gorenflo et al. [10,11,12],[17,18] and other researchers have investigations on the diffusion- wave type equations and other equations of this type with constant coefficients containing fractional derivatives (in the Riemann–Liouville or Caputo sense) in time and/or in space to describe the models of anomalous transport in physics. They applied the joint transform method to boundary value problems to find the fundamental solutions of these equations in terms of higher transcendental functions such as Fox H-function and the Wright function[26-29]..

For the linear partial fractional differential equations (LPFDEs) with non-constant coefficients the existing integral transform methods (such as the joint Laplace-Fourier transform) are not applicable, therefore, importance of the $\mathcal{L}_A$-transform for solving some fractional-type equations with non-constant coefficients is emphasized.

In this work, we focus our attention on the LPFDEs with non-constant coefficients which occur in physical phenomena such as *fractional diffusion* on fractals and *fractional disturbance* and can be easily solved by applying the $\mathcal{L}_A$-transform by choosing the appropriate $A(x)$. Furthermore, effectiveness of the $\mathcal{L}_A$-transform for solving these LPFDEs in terms of the ${}_A\delta_x$-derivatives is treated.

In this regard, in section 2, we derive a new inversion formula for the $\mathcal{L}_A$-transform in terms of the Bromwich's integral. Two theorems in the $\mathcal{L}_A$-transform of the ${}_A\delta_x$-derivatives and the convolution property are also established. These properties can be useful for obtaining the solutions of fractional diffusion on fractals and fractional disturbance.

In sections 3 we find the fundamental solution of the fractional diffusion equation on fractals introduced by Giona and Roman [9,22] by applying the $\mathcal{L}_{\frac{x^{\beta+1}}{\beta+1}}$- transform $(\beta \geq 0)$. These solutions can be expressed in terms of the higher transcendental functions of the Wright type

In section 4, a fractional disturbance equation of distributed order is introduced and by using the $\mathcal{L}_2$-Laplace transform (as a special case of the $\mathcal{L}_A$-transform) the fundamental solution of this equation is given as an integral representation in terms of the Laplace type integral. Finally, in section 5, the main conclusions are drawn .

2 Some Properties of the $\mathcal{L}_A$-Transform

In this section, we establish theorems on the $\mathcal{L}_A$-transform which can be useful for solving LPFDEs. First, we derive a complex inversion formula for this transform in terms of the Bromwich's integral.

Theorem 2.1 (The Complex Inversion Formula for The $\mathcal{L}_A$-transform)

Let $F(\Phi^{-1}(p))$ be analytic function of p (assuming that $F(\Phi^{-1}(p))$ has not the branch point) except at finite number of poles and each of poles lies to the left of the vertical line $\Re p = c$. If $F(\Phi^{-1}(p)) \to 0$ as $p \to \infty$ through the left plane $\Re p \leq c$, and

[1] Yurekli and Sadek introduced this transform and showed the Parseval-Goldstein theorems involving the $\mathcal{L}_2$-transform and the Laplace transform can be used to yield identities involving several well-known integral transforms and infinite integrals of elementary and special functions. Also, authors applied this transform to solve some systems of ODEs , PDEs and singular integral equations with the special kernels[1-2].

$$\mathcal{L}_{\mathcal{A}}\{f(x);p\} = F(p) = \int_0^{\infty} A'(x)e^{-\Phi(p)A(x)}f(x)dx$$

then

$$\mathcal{L}_{\mathcal{A}}^{-1}\{F(p)\} = f(x) = \frac{1}{2\pi i}\int_{c-i\infty}^{c+i\infty} F(\Phi^{-1}(p))e^{pA(x)}dp\,. \tag{5}$$

Proof: By definition of the $\mathcal{L}_{\mathcal{A}}$ -transform (1) and letting $\Phi(p) = r$, we have

$$F(\Phi^{-1}(r)) = \int_0^{\infty} A'(x)e^{-rA(x)}f(x)dx$$

now, by setting $t = A(x)$ in the above relation, we obtain

$$F(\Phi^{-1}(r)) = \int_0^{\infty} e^{-rt}f(A^{-1}(t))dt = \mathcal{L}\{f(A^{-1}(t));r\}.$$

At this point, by the complex inversion formula for the Laplace-Transform and setting back $A^{-1}(t) = x, r = p$, we get finally

$$f(x) = \frac{1}{2\pi i}\int_{c-i\infty}^{c+i\infty} F(\Phi^{-1}(p))e^{pA(x)}dp.$$

Theorem 2.2 (The $\mathcal{L}_{\mathcal{A}}$ -transform of ${}_A\delta_x$ -derivatives)

Let $f, f', \ldots, f^{(n-1)}$ are continuous functions with piecewise continuous derivative $f^{(n)}$ on the interval $x \geq 0$ and if all functions are of exponential order $e^{\Phi(c)A(x)}$ as $x \to \infty$ (i.e. $|f(x)| \leq Me^{\Phi(c)A(x)}$) for some constants c, M ,then for $n = 1, 2, \ldots$

$$\begin{aligned}\mathcal{L}_{\mathcal{A}}\{{}_A\delta_x^n f(x);p\} &= \Phi^n(p)\mathcal{L}_{\mathcal{A}}\{f(x);p\} - \Phi^{n-1}(p)f(0^+) \\ &\quad - \Phi^{n-2}(p)({}_A\delta_x f)(0^+) - \cdots - ({}_A\delta_x^{n-1}f)(0^+)\end{aligned} \tag{6}$$

where the ${}_A\delta_x$ -derivative operator is defined as follows

$${}_A\delta_x = \frac{1}{A'(x)}\frac{d}{dx}$$

and by notation

$${}_A\delta_x^2 = {}_A\delta_x\,{}_A\delta_x = \frac{1}{A'^2(x)}\frac{d^2}{dx^2} - \frac{A''(x)}{A'^3(x)}\frac{d}{dx}$$

the ${}_A\delta_x$ -derivative for any positive integer power can be found.

Proof: Using the definitions of the $\mathcal{L}_{\mathcal{A}}$ -transform (1) and the ${}_A\delta_x$ -derivative, by integration by parts, we obtain

$$\mathcal{L}_{\mathcal{A}}\{{}_A\delta_x f(x);p\} = \int_0^{\infty} e^{-\Phi(p)A(x)}f'(x)dx = e^{-\Phi(p)A(x)}f(x)\big|_0^{\infty} + \Phi(p)\int_0^{\infty} A'(x)e^{-\Phi(p)A(x)}f(x)dx.$$

Since f is of exponential order $e^{\Phi(c)A(x)}$ as $x \to \infty$,it follows that

$$\lim_{x\to\infty} e^{-\Phi(p)A(x)}f(x) = 0$$

consequently

$$\mathcal{L}_{\mathcal{A}}\{{}_A\delta_x f(x);p\} = \Phi(p)\mathcal{L}_{\mathcal{A}}\{f(x);p\} - f(0^+).$$

Similarly by repeated application of the above relation once again, we get

$$\begin{aligned}\mathcal{L}_{\mathcal{A}}\{{}_A\delta_x^2 f(x);p\} &= \Phi(p)\mathcal{L}_{\mathcal{A}}\{{}_A\delta_x f(x);p\} - ({}_A\delta_x f)(0^+) \\ &= \Phi^2(p)\mathcal{L}_{\mathcal{A}}\{f(x);p\} - \Phi(p)f(0^+) - ({}_A\delta_x f)(0^+),\end{aligned}$$

and by repeating the above scheme for ${}_A\delta_x^n f(x)$, we can readily arrive at (6).

Theorem 2.3 (The Convolution Theorem for The $\mathcal{L}_A$ -transform)

If $F(p), G(p)$ be the $\mathcal{L}_A$ -transform of the functions $f(x), g(x)$ respectively, then

$$F(p)G(p) = \mathcal{L}_A\{f * g\} = \mathcal{L}_A\{\int_0^x A'(t)g(t)f(A^{-1}(A(x) - A(t)))dt\} \qquad (7)$$

Proof: Using the definition of the $\mathcal{L}_A$ -transform for $F(p), G(p)$, we have

$$F(p)G(p) = (\int_0^\infty A'(y)e^{-\Phi(p)A(y)}f(y)dy)(\int_0^\infty A'(t)e^{-\Phi(p)A(t)}g(t)dt)$$
$$= \int_0^\infty \int_0^\infty A'(y)A'(t)e^{-\Phi(p)(A(t)+A(y))}f(y)g(t)dydt.$$

Now, by substitution $A(t) + A(y) = A(x)$ and changing the order of integration in the double integral ,we get

$$F(p)G(p) = \{\int_0^\infty A'(x)e^{\Phi(p)A(x)}dx \int_0^x A'(t)g(t)f(A^{-1}(A(x) - A(t)))dt\}$$
$$= \mathcal{L}_A\{\int_0^x A'(t)g(t)f(A^{-1}(A(x) - A(t)))dt\}.$$

In view of the theorems of the $\mathcal{L}_A$ -transform expressed in this section we may apply this transform to LPFDEs in the next sections.

3 The time-fractional diffusion equation of single order on fractals

In connection with initial-value problems in fractals, Giona and Roman [9, 22] state the partial fractional differential equation in the Riemann–Liouville sense [13,21,23] in the form

$${}_tD_{0^+}^\alpha u(x,t) = -Cx^{-\beta}\frac{\partial u(x,t)}{\partial x}, \qquad C > 0, \beta \geq 0, 0 < \alpha \leq \frac{1}{2}, \qquad (8)$$

with Cauchy type initial and boundary conditions as

$${}_tD_{0^+}^{\alpha-1}u(x,0^+) = f(x), \quad u(0,t) = 0, \quad x,t \in \mathbb{R}^+, \qquad (9)$$

since, the equation (8) is a LPFDE with non-constant coefficients we set $A(x) = \dfrac{x^{\beta+1}}{\beta+1}, \Phi(p) = p^{\beta+1}$ in the integral (1) and apply this new integral transform (the $\mathcal{L}_{\frac{x^{\beta+1}}{\beta+1}}$ -transform) in space and the Laplace transform in time as follows

$$\mathcal{L}\{u(x,t);s\} = \tilde{u}(x,s) = \int_0^\infty e^{-st}u(x,t)dt, \quad \Re s > 0$$

$$\mathcal{L}_{\frac{x^{\beta+1}}{\beta+1}}\{u(x,t);p\} = \hat{u}(p,t) = \int_0^\infty x^\beta e^{-p^{\beta+1}\frac{x^{\beta+1}}{\beta+1}}u(x,t)dx, \;\; \Re p^{\beta+1} > 0.$$

Then ,by using the Laplace transform of the Riemann-Liouville derivative (A.8) and the $\mathcal{L}_{\frac{x^{\beta+1}}{\beta+1}}$ -transform of the equation (8), we obtain

$$\mathcal{L}\{{}_tD_{0^+}^\alpha u(x,t);s\} = s^\alpha\tilde{u}(x,s) - {}_tD_{0^+}^{\alpha-1}u(x,0^+),$$

$$\mathcal{L}_{\frac{x^{\beta+1}}{\beta+1}}\{u(x,t);p\} = p^{\beta+1}\hat{u}(p,t) - u(0,t)$$

where by utilizing the Cauchy type initial conditions (9) ,we arrive at

$$\hat{\tilde{u}}(p,s)=\frac{1}{s^{\alpha}+Cp^{\beta+1}}F(p) \tag{10}$$

where $F(p)$ is the $\mathcal{L}_{\frac{x^{\beta+1}}{\beta+1}}$-transform of the initial condition $f(x)$.

At this point, by considering the complex inversion formula for the $\mathcal{L}_{\frac{x^{\beta+1}}{\beta+1}}$-transform (5) and the convolution theorem (7), we obtain

$$\tilde{u}(x,s)=\frac{1}{2\pi i}\int_{c-i\infty}^{c+i\infty}\hat{\tilde{u}}(\sqrt[\beta+1]{p},s)e^{p\frac{x^{\beta+1}}{\beta+1}}dp=\frac{1}{C}\mathcal{L}^{-1}_{\frac{x^{\beta+1}}{\beta+1}}\{\frac{1}{\frac{s^{\alpha}}{C}+p}\}*f(x)=\frac{1}{C}e^{-s^{\alpha}\frac{x^{\beta+1}}{C(\beta+1)}}*f(x)$$

where the convolution of the two functions f,g for the $\mathcal{L}_{\frac{x^{\beta+1}}{\beta+1}}$-transform ,can be expressed by the relation (7) as follows

$$f*g=\int_0^x t^{\beta}g(t)f(\sqrt[\beta+1]{x^{\beta+1}-t^{\beta+1}})dt.$$

Now, in regard to the inverse Laplace transform of the functions $e^{-s^{\alpha}\frac{x^{\beta+1}}{C(\beta+1)}}$ via the Wright functions

$$\mathcal{L}^{-1}\{e^{-s^{\alpha}\frac{x^{\beta+1}}{C(\beta+1)}}\}=\frac{1}{t}W(-\alpha,0;-\frac{x^{\beta+1}}{C(\beta+1)}t^{-\alpha}),$$

we get the explicit solution of the Cauchy type problem (8)-(9) as follows

$$u(x,t)=\int_0^x \tau^{\beta}G^{\alpha}(x^{\beta+1}-\tau^{\beta+1},t)f(\tau)d\tau, \tag{11}$$

where the Green function G^{α} is given by [19,21]

$$G^{\alpha}(x,t)=\frac{1}{Ct}W(-\alpha,0;-\frac{x}{C(\beta+1)}t^{-\alpha}), \tag{12}$$

provided that the integral on the right-hand side of (11) is convergent.

4. The time-fractional disturbance equation of distributed order

The earlier idea of fractional derivative of distributed order was developed by Caputo [4-6] and later, Umarov et.al [25] and Gorenflo et al. [19] study the fractional diffusion equation of distributed order by analyzing some interesting cases of the order-density function. In this paper by the notion of fractional derivative of distributed order, we consider a generalization of Shankar equation [24] which estimates disturbances at an inviscid interface. The following equation

$$\int_0^1 b(\alpha)[{}_t^C D_{0^+}^{\alpha}u(x,t)]d\alpha+\frac{1}{x}\frac{\partial u(x,t)}{\partial x}=f(x),\quad x,t>0, b(\alpha)\geq 0, \int_0^1 b(\alpha)d\alpha=1 \tag{13}$$

is called the *fractional disturbance* equation subject to initial and boundary conditions $u(x,0)=u(0,t)=0$ and the order-density function $b(\alpha)$ which enables us to determine the intensity of disturbances.

In order to solve the equation (13), we extend the approach by Naber [20] and Mainardi et al.[12] to find a general representation of the fundamental solution related to a generic order-density function $b(\alpha)$. In this respect, by applying the Laplace transform with respect to t,

$\mathcal{L}\{{}_t^C D_{0^+}^{\alpha}u(x,t);s\}=s^{\alpha}\tilde{u}(x,s)-u(x,0^+)$

and the $\mathcal{L}_2$-transform (by the notion (4) we call the $\mathcal{L}_{x^2}$-transform as the $\mathcal{L}_2$-transform) with respect to x and setting $n = 1$ in (6)

$$\mathcal{L}_2\{\delta_x u(x,t); p\} = p^2 \hat{u}(p,t) - u(0,t)$$

we obtain

$$\left(\int_0^1 b(\alpha) s^\alpha d\alpha\right)\hat{\tilde{u}}(p,s) + p^2 \hat{\tilde{u}}(p,s) = F(p)$$

from which

$$\hat{\tilde{u}}(p,s) = \frac{F(p)}{B(s) + p^2}, \quad \Re s, \Re p > 0 \tag{14}$$

where $F(p)$ is the $\mathcal{L}_2$-transform of the function $f(x)$ and

$$B(s) = \int_0^1 b(\alpha) s^\alpha d\alpha.$$

By inverting the $\mathcal{L}_2$-transform of (14) ,we get the remaining Laplace transform as the following expression

$$\tilde{u}(x,s) = f(x) * e^{-x^2 B(s)} \tag{15}$$

where the convolution of the two functions f, g for the $\mathcal{L}_2$-transform by (7) can be written as

$$f * g = \int_0^x 2t g(t) f(\sqrt{x^2 - t^2}) dt. \tag{16}$$

By virtue of Titchmarsh's theorem for inversion of the Laplace transform [7] of the function $\tilde{u}_1(x,s) = e^{-x^2 B(s)}$,we have the following

$$u_1(x,t) = -\frac{1}{\pi}\int_0^\infty e^{-rt} \Im\{\tilde{u}_1(x, re^{i\pi})\} dr, \tag{17}$$

In order to simplify the above relation (17), we need to evaluate the imaginary part of the function $-\tilde{u}_1(x, re^{i\pi})$ (i.e. $-\Im\{e^{-x^2 B(s)}\}$) along the ray $s = re^{i\pi}$, $r > 0$ where the branch cut of the function s^β is defined .

In this regard ,by writing

$$B(re^{i\pi}) = \rho\cos\gamma\pi + i\rho\sin\gamma\pi, \quad \begin{cases} \rho = \rho(r) = \left|B(re^{i\pi})\right| \\ \gamma = \gamma(r) = \dfrac{1}{\pi}\arg[B(re^{i\pi})] \end{cases}$$

Substitution of the above relation in the equation (17) leads to the following

$$u_1(x,t) = \frac{1}{\pi}\int_0^\infty e^{-rt - x^2\rho\cos(\pi\gamma)} \sin(x^2 \rho \sin(\pi\gamma)) dr$$

and finally by using the convolution product given by relation (16) $u(x,t)$ is expressed as an integral representation

$$\begin{aligned} u(x,t) &= \frac{1}{\pi} f(x) * \{\int_0^\infty e^{-rt - x^2\rho\cos(\pi\gamma)} \sin(x^2\rho\sin(\pi\gamma)) dr\} \\ &= \frac{1}{\pi}\int_0^\infty e^{-rt} dr \int_0^x e^{-(x^2-\tau^2)\rho\cos(\pi\gamma)} \sin((x^2 - \tau^2)\rho\sin(\pi\gamma)) f(\tau)\, d\tau \end{aligned} \tag{18}$$

provided that the integrals on the right-hand side of (18) are convergent.

The explicit solution (18) of the time-fractional disturbance equation of distributed order (13) can be simplified in particular cases. For example if we set $b(\alpha) = \delta(\alpha - n),\ \ 0 < n < 1$

the time-fractional disturbance equation of distributed order (13) is converted to time-fractional disturbance equation of single order n , so that

$B(s) = s^n$, $\rho = \rho(r) = r^n$, $\gamma = n$

and the desired solution $u(x,t)$ (18) takes the form

$$u(x,t) = \frac{1}{\pi} f(x) * \{\int_0^\infty e^{-rt - x^2 r^n \cos(n\pi)} \sin(x^2 r^n \sin(n\pi)) dr\}. \quad (19)$$

Since, the inverse Laplace transform of $e^{-x^2 s^n}$ in (15) can be easily obtained as the Wright functions

$$\mathcal{L}^{-1}\{e^{-x^2 s^n}\} = \frac{1}{t} W(-n, 0; -x^2 t^{-n})$$

the relation (19) can be written as follows [19, 21]

$$u(x,t) = \frac{1}{\pi t} \int_0^x W(-n, 0; -(x^2 - \tau^2) t^{-n}) f(\tau) d\tau. \quad (20)$$

5 Conclusion

This paper provides some new results in the area of fractional calculus. In this work a new integral transform ($\mathcal{L}_{\mathcal{A}}$ - transform) was implemented to solve

1- Cauchy type fractional diffusion equation on fractals
2- Cauchy fractional disturbance equation with continuous or discrete distribution of time fractional derivative.

It may be concluded that the $\mathcal{L}_{\mathcal{A}}$ transform method is very powerful efficient technique in finding exact solution for P.F.D.Es.

Although the $\mathcal{L}_{\mathcal{A}}$ transform method described in this paper is well – suited to solve the time fractional diffusion equations in terms of higher transcendental functions, the method could lead to a promising approach for many applications in applied sciences.

References

[1] A.Aghili, A.Ansari, Complex Inversion Formula for Stieltjes and Widder Transforms with Applications, J. Contemp. Math. Sciences, Vol.2, 2008, no.16, 761-770.

[2] A.Aghili, A.Ansari, A.Sedghi, An inversion technique for the $\mathcal{L}_2$–transform with applications, Int. J. Contemp. Math. Sciences, Vol.2, 2007, no.28, 1387-1394.

[3] D.Brown , N.Dernek, O.Yurekli, Identities for the $\mathcal{E}_{2,1}$-transform and their applications, Appl. Math.Comput.187 (2007) 1557-1566.

[4] M. Caputo, Linear models of dissipation whose Q is almost frequency independent. II, Geophys. J. Roy. Astronom. Soc. 13 (1967) 529–539.

[5] M. Caputo, Elasticita e Dissipazione, Zanichelli, Bologna, 1969 (in Italian).

[6]M. Caputo, Distributed order differential equations modeling dielectric induction and diffusion, Fract. Calc. Appl. Anal. 4 (2001) 421–442.

[7] D.G. Duffy, Transform Methods for Solving Partial Differential Equations, CRC Press, 1994.

[8]A. Erdelyi, W. Magnus, F. Oberhettinger, F.G. Tricomi, Higher Transcendental Functions, Bateman Project, vols. 1–3, McGraw-Hill, New York, 1953–1955.

[9] M. Giona, H. E. Roman, Fractional diffusion equation on fractals: One-dimensional case and asymptotic behaviour, J. Phys. A: Math. Gen., 25(8), (1992) 2107-2117.

[10] R. Gorenflo, Yu. Luchko, F. Mainardi, Analytical properties and applications of the Wright function, Fract. Calc. Appl. Anal. 2 (1999) 383–414.

[11] R. Gorenflo,Yu. Luchko, F. Mainardi, Wright functions as scale-invariant solutions of the diffusion-wave equation, J. Comput.Appl. Math. 118 (2000) 175–191.

[12] R. Gorenflo, F. Mainardi, Simply and multiply scaled diffusion limits for continuous time random walks, in: S. Benkadda, X.Leoncini, G. Zaslavsky (eds.), Proceedings of the International Workshop on Chaotic Transport and Complexity in Fluids and Plasmas Carry LeRouet (France)20–25June2004,IOP (Institute of Physics)Journal of Physics: Conference Series 7,2005,pp.1–16.

[13] A.A. Kilbas, H.M. Srivastava, J.J. Trujillo, Theory and Applications of Fractional Differential Equations, North-Holland Mathematics Studies, 204, Elsevier Science Publishers, Amsterdam, Heidelberg and New York, 2006.
[14]F. Mainardi, Fractional calculus: some basic problems in continuum and statistical mechanics, in: A. Carpinteri, F. Mainardi (Eds.), Fractals and Fractional Calculus in Continuum Mechanics, Springer Verlag, Wien and New York, 1997, pp. 291–348. Reprinted in NEWS 011201. Available from <http://www.fracalmo.org>.
[15] F. Mainardi, The fundamental solutions for the fractional diffusion-wave equation, Applied Mathematics Letters 9 (6) (1996) 23–28.
[16]F. Mainardi, Yu. Luchko, G. Pagnini, The fundamental solution of the space–time fractional diffusion equation, Fractional Calculus and Applied Analysis 4 (2) (2001) 153–192, Reprinted with permission in NEWS 010401.Available from <http://www.fracalmo.org>.
[17] F. Mainardi , G.Pagnini, The role of the Fox–Wright functions in fractional sub-diffusion of distributed order, J. Comput.Appl. Math. 207 (2007) 245–257.
[18] F. Mainardi , G.Pagnini, The Wright functions as solutions of the time-fractional diffusion equation, J. Comput.Appl. Math. 141 (2003) 51–62.
[19]F. Mainardi , G.Pagnini, R. Gorenflo, Some aspects of fractional diffusion equations of single and distributed order, . Comput.Appl. Math. 187 (2007) 295–305.
[20] M. Naber, Distributed order fractional subdiffusion, Fractals 12 (2004) 23–32.
[21] I.Podlubny, Fractional Differential Equations, Academic Press, San Diego, 1999.
[22] H. E. Roman, M. Giona, Fractional diffusion equation on fractals: three-dimensional case and scattering function, J. Phys. A: Math. Gen., 25(8), (1992) 2107-2117.
[23] S.G. Samko, A.A. Kilbas, O.I. Marichev, Fractional Integrals and Derivatives: Theory and Applications, Gordon and Breach, NewYork, 1993, Translation from the Russian edition, Nauka i Tekhnika, Minsk, 1987.
[24] P.N., Shankar, On the evolution of disturbances at an inviscid interface. J. Fluid Mech., 108, (1981) 159-170.
[25] S. Umarov, R. Gorenflo, Cauchy and nonlocal multi-point problems for distributed order pseudo-differential equations: Part one, Z.Anal. Anwendungen 24 (2005) 449–466.
[26] E.M.Wright,On the coefficients of power series having exponential singularities, J. London Math.Soc.8 (1933) 71–79.
[27] E.M.Wright, The asymptotic expansion of the generalized Bessel function, Proc. London Math. Soc. (Ser.II) 38 (1935) 257–270.
[28] E.M.Wright, The asymptotic expansion of the generalized hypergeometric function, J. London Math.Soc.10 (1935)287–293.
[29] E.M.Wright, The generalized Bessel function of order greater than one, Quart. J.Math.Oxford Ser.11 (1940) 36–48.
[30] O.Yurekli, Theorems on $\mathcal{L}_2$-transforms and its applications, complex Variables Theory Appl.38 (1999) 95-107.
[31] O.Yurekli, New identities involving the Laplace and the $\mathcal{L}_2$–transforms and their applications, Appl.Math.Comput.99 (1999)141-151.
[32] O.Yurekli, I.Sadek,A Parseval-Goldstein type theorem on the Widder potential transform and its applications, International Journal of Mathematics and Mathematical Sciences, 14 (1991) 517-524.

JOURNAL OF APPLIED FUNCTIONAL ANALYSIS, VOL.6, NO.3, 280-292, COPYRIGHT 2011 EUDOXUS PRESS, LLC

MAXIMUM PRINCIPLES FOR NONHOMOGENEOUS ELLIPTIC SYSTEMS

M. ALMAHAMEED

Department of Mathematics
Irbid National University
Irbid, Jordan

Abstract

In this paper we discuss a classical maximum principle for weakly coupled second order homogeneous elliptic systems

$$Lu + Au = 0 \qquad in \qquad \Omega \subset \mathbf{R}^n$$

Where $\quad L[u(x)] = \sum_{i,j=1}^{n} a_{ij}(x) \dfrac{\partial^2 u}{\partial x_i \partial x_j} + \sum_{i=1}^{n} a_i(x) \dfrac{\partial u}{\partial x_i}$, $a_{ij} = a_{ji}$

is a second order real elliptic operator, $u=(u_1, u_2, \ldots, u_n)^T$, *and A is an* $n \times n$ *matrix with entries which are all complex valued functions.*

We find a sufficient condition for the classical maximum principle which extend the result of Winter and Wong [14] *for A being negative semidefinite to a more general form of A.*

We also prove uniqueness theorems for various boudary value problems with bounded and unbounded domains,and extend the generalized maximum principles obtained in [1] to nonhomogeneous elliptic systems.

Keywords and Phrases. Maximum Principles, Elliptic systems
2000 Mathematics subject classification. 35B50, 35 J60.

1. Introduction

Generalized maximum principles for weakly coupled second order elliptic systems have been obtained by Dow [2], Hile and Protter [5], and Wasowski [13] under different conditions on the coefficients.

In [1] we find a generalized maximum principle for second order homogeneous elliptic systems, in this paper we extend these results to nonhomogeneous elliptic systems. Also we prove uniqueness theorems for various boundary value problems as applications of the maximum principles .

Consider a second order operator

$$L\,[u(x)] = \sum_{i,j=1}^{n} a_{ij}(x)\,\frac{\partial^2 u}{\partial x_i\,\partial x_j} + \sum_{i=1}^{n} a_i\,(x)\,\frac{\partial u}{\partial x_i}\ ,\ a_{ij} = a_{ji} \qquad \ldots\ldots\ldots (1.1)$$

in a bounded domain Ω in $\boldsymbol{R}^n$. We assume that L is elliptic in Ω, i.e., for all $x \in \Omega$ and all $y=(y_1, y_2, \ldots, y_n) \in \boldsymbol{R}^n \setminus \{0\}$.

$$a_{ij}\,(x)\,y_i\,y_j > 0 \qquad \ldots\ldots\ldots (1.2)$$

holds, we also suppose that the coefficients a_{ij} and a_i are bounded and real-valued functions in Ω.

Now consider the following weakly coupled second order elliptic system,

$$Lu_s(x) + a_{sk}\,(x)\,u_k(x) = 0\ ,\ s = 1,2,\ \ldots,\ n \quad in\ \ \Omega,$$

or in matrix from,

$$Lu(x) + A(x)\,u(x) = 0 \qquad in\ \ \Omega \qquad \ldots\ldots\ldots (1.3)$$

Here $A(x) = (a_{sk}\,(x))$ is an $n \times n$ complex matrix function and u is a $C^2\,[\,n \times 1]$complex vector function.

Associated with (1.3) the following characteristic equation of A,

$|\lambda I - A| = 0.$

In [1] we use the idea of Liapunov's Second Method to find a generalized maximum principle for a class of weakly coupled second order homogeneous elliptic systems.

$$Lu + Au = 0 \quad in \quad \Omega \subset \boldsymbol{R}^n$$

Where L is the second order elliptic operator

$$L\,[u(x)] = \sum_{i,j=1}^{n} a_{ij}(x)\,\frac{\partial^2 u}{\partial x_i\,\partial x_j} + \sum_{i=1}^{n} a_i(x)\,\frac{\partial u}{\partial x_i}\ ,\ a_{ij} = a_{ji},\ u = (u_1, u_2, \ldots, u_n)^T.$$

Theorem (1.1): *Assume that there exists a constant complex matrix $B > 0$ such that*

$$A^*(x)\,B + BA(x) \le 0, \quad x \in \Omega \qquad \ldots\ldots\ldots (1.4)$$

Then for all solutions $u \in C^2(\Omega) \cap C(\overline{\Omega})$ of (1.3) there exist a constant $k > 0$ such that

$$\|u\|_{0,\Omega} \le k\ \|u\|_{0,\partial\Omega} \qquad \ldots\ldots\ldots (1.5)$$

Here $k = (\lambda_n / \lambda_1)^{1/2}$, where λ_1 and λ_n are the smallest and biggest eigenvalues of B, respectively.

Theorem (1.2): *Let $A(x) = g(x)\,I + D$ in (1.3), where $g(x) \le 0$ in Ω and D is a constant matrix over* **C**. *Assume that none of the eigenvalues of D has a positive real part, and moreover that the elementary divisors of D corresponding to eigenvalues with vanishing real part are linear. Then there exit a constant $k > 0$ such that for all solutions $u \in C^2(\Omega) \cap C(\overline{\Omega})$ of (1.3).*

$$\|u\|_{0,\Omega} \le k\,\|u\|_{0,\partial\Omega}.$$

From the proof of Theorem (1.1) , and from Protter and Weinberger [9], we have the following maximum principles for system (1.3),[1].

***Theorem(1.3)**: if $u \in C^2(\Omega) \cap C(\overline{\Omega})$ is a solution of (2.3), and if u^*Bu attains a maximum in Ω for some positive definite matrix B such that $A^*(x)B+BA(x)$ is negative semidefinite in Ω, then u is a complex constant vector in Ω. Moreover, if $A^*(x)B+BA(x)$ is negative definite at some $x \in \Omega$ or, if $A(x)$ is invertible for some $x \in \Omega$ then*

$u=0$ in Ω.

***Theorem (1.4)**: Let $u \in C^2(\Omega) \cap C(\overline{\Omega})$ be a solution of 2.3 Suppose that $u^*Bu \le M$ in Ω and that $u^*Bu=M$ at a point $P \in \partial\Omega$ for some positive definite B such that A^*B+BA is negative semidefinite. Here M is a nonnegative constant. Assume that P lies on the boundary of a ball in Ω, and that the outward directional derivative $\partial u/\partial v$ exists at P. Then*

$$\frac{\partial\left(u^* Bu\right)}{\partial v} = 2\mathrm{Re}\left[u^* B\frac{\partial u}{\partial v}\right] = 2\ \mathrm{Re}\left[\left(B^{1/2}u\right)^* \frac{\partial\left(B^{1/2}u\right)}{\partial v}\right] > 0 \qquad \text{at } P$$

Unless u is a complex constant vector such that $u^*Bu \equiv M$; equivalently,

$$\frac{\partial\left|B^{1/2}u\right|}{\partial v} > 0 \qquad\qquad \text{at } P$$

Unless u is constant and $|B^{1/2}u| = M^{1/2}$

2. The Classical Maximum Principle

In this section we will consider the case k=1 in (1.5) for any matrix A ,which corresponds to the classical maximum principle.

Theorem (2.1):

(a) A sufficient condition that:

$$||u||_{0,\Omega} \leq ||u||_{0,\partial\Omega} \qquad \text{……….} \ (2.1)$$

holds , for all solutions $u \in C^2(\Omega) \cap C(\overline{\Omega})$ *of (2.3) is*

$$A^*(x) + A(x) \leq 0. \qquad \text{……….} \ (2.2)$$

(b) Assume that the variable matrix $A=A(x)$ *in (1.3) is normal (i.e.,* $A^*(x)\, A(x) = A(x)\, A^*(x)$, $x \in \Omega$*), and all its eigenvalues have nonpositive real parts for all* $x \in \Omega$*.*

Then (2.1) holds for all solutions $u \in C^2(\Omega) \cap C(\overline{\Omega})$ *of (1.3) .*

Proof. (a) By choosing $B=I$ in Theorem (1.1), (1.5) with $k=1$ (i.e., 2.1) follows from the condition (2.2)

(b) suppose

$$\lambda_1(x)\ \lambda_2(x),\ \dots,\ \lambda_n(x)$$

are all the eigenvalues of $A(x)$. Since $A(x)$ is normal, there exists a unitary matrix $U(x)$ such that

$$U^*(x)\, A\,(x)\, U(x) = \begin{bmatrix} \lambda_1(x) & & & \\ & \lambda_2(x) & & \\ & & \ddots & \\ & & & \lambda_n(x) \end{bmatrix}$$

Therefore, by the assumption,

$$U^*(x)\, (A^*(x) + A(x))\, U(x) = \begin{bmatrix} 2\,\mathrm{Re}\lambda_1(x) & & \\ & \ddots & \\ & & 2\,\mathrm{Re}\,\lambda_n(x) \end{bmatrix} =: \Lambda(x) \leq 0.$$

Hence $A^* + A = U\Lambda U^* \leq 0;$ and then(2.1) follows from (a). □

Example: For the system

$$Lu(x) + \begin{bmatrix} a(x) & b(x) \\ c(x) & d(x) \end{bmatrix} u(x) = o,$$

Where a, b, c, and d are complex – valued functions, by Theorem(2.1), the classical maximum principle(2.1) holds if

$$\begin{bmatrix} a & b \\ c & d \end{bmatrix}^* + \begin{bmatrix} a & b \\ c & d \end{bmatrix} = \begin{bmatrix} 2R\{a\} & b+\bar{c} \\ \overline{(b+\bar{c})} & 2R\{d\} \end{bmatrix} \leq 0$$

which is equivalent to

Re $\{a\} \leq 0$, Re $\{d\} \leq 0$; and

$|b + \bar{c}|^2 \leq 4$ Re $\{a\}$ Re $\{d\}$ ………. (2.3)

3. Applications

As applications of the maximum principles in sections 1,2, we will prove uniqueness theorems for various boundary value problems.

As a first example, consider the following mixed boundary value problem with bounded domain :

$$Lu\,(x) + A(x)\,u(x) = f(x) \qquad in \qquad \Omega \subset \boldsymbol{R}^n \qquad \ldots(3.1)$$

$$\begin{cases} u(x) = g_1(x) & on \ \Gamma_1 \\ \dfrac{\partial u(x)}{\partial v} + \alpha(x)u = g_2(x) & on \ \Gamma_2 \end{cases} \qquad ……….\ (3.2)$$

where $v = v(x)$ is a given outward direction on Γ_2, and $\Gamma_2 = \dfrac{\partial\Omega}{\Gamma_1}$.

Theorem (3.1): *Suppose that u_1 and u_2 satisfy (3.1) and (3.2) in a bounded domain in $\Omega \subset \boldsymbol{R}^n$ and A satisfies the assumption of Theorem (1.1) assume that each point of Γ_2 lies on the boundary of a ball in Ω. If L is elliptic as defined by (1.1) and $\alpha(x) \geq 0$ on Γ_2, then $u_1 = u_2$, except when $\alpha=0$, Γ_1 is vacuous and A(x) is singular for all $x \in \Omega$, in which case $u_1 - u_2$, is a complex constant vector.*

Proof: Define $u = u_1 - u_2$. Then u satisfies

$$Lu + Au = 0 \quad in \;\; \Omega, \qquad \text{……….} (2.1)$$

$$\begin{cases} u = o & on \;\; \Gamma_1, \\ \dfrac{\partial u}{\partial v} + \alpha u & on \;\; \Gamma_2 \end{cases} \qquad \text{……….} (3.3)$$

Choose positive definite B, as in the proof of Theorem(1.1), such that $A^*B + BA$ is negative semidefinite, and let $v = u^*Bu$; then we have

$$v(x) \leq \max_{y \in \partial\Omega} v(y), \quad \forall x \in \Omega \; . \qquad \text{………}(3.4)$$

If v is not a constant, by Theorem(1.3), a nonzero maximum of v must occur at a point P on Γ_2; and by Theorem(1.4),

$$Re\left[u^* B \frac{\partial u}{\partial v}\right] > 0 \qquad at \;\; P.$$

Hence

$$Re\left[u^* B\left(\frac{\partial u}{\partial v} + \alpha u\right)\right] \qquad at\, P \in \Gamma_2 \, .$$

Which contradicts the boundary condition (3.3). Thus $v = u^*Bu$ must be a constant. From (3.4), by the proof of Theorem(1.3), u must be a complex constant vector. Then, from (1.3) and (3.3), we know that $u = 0$, i.e., $u_1 = u_2$, in Ω, except when $\alpha = 0$, Γ_1 is vacuous, and $A(x)$ is singular for $x \in \Omega$.□

Remark: Besides having applications to some boundary value problems with bounded domain Ω, the maximum principle we obtained in sections 1,2 can be used to establish uniqueness theorems for various boundary value problems with unbounded domain $\Omega \subset \boldsymbol{R}^n$. In this case, the point ∞ is called the exceptional boundary points; and an appropriate growth restriction on the solution at ∞ is required. Moreover, by using a recent result of Hile and Yeh [7], we even obtain uniqueness for the boundary value problem with an exceptional boundary at Γ is less than n-1.

As another example, we have uniqueness for the following boundary value problem with unbounded domain $\Omega \subset \boldsymbol{R}^n$:

$$Lu\,(x) + A(x)\,u\,(x) = f(x) \qquad in\ \ \Omega, \qquad \ldots\ldots\ldots (3.1)$$

$$\begin{cases} u\,(x) = g(x) & on\ \partial\Omega \\ |u(x)|\ \ is\ bounded\ in\ \Omega \end{cases} \qquad \ldots\ldots\ldots (3.5)$$

Theorem (3.2): *Let Ω be an unbounded domain contained inside a cone, let L be given in Ω by (1.1), with*

$$a_i\,(x) = \delta\,(r^{-1}) \qquad as \quad x \to \infty \qquad in\ \Omega,$$

$$i = 1,\ \ldots,\ n,\ (r = 1x1),$$

and with the uniform ellipticity condition

$$\delta\,|y|^2 \le a_{ij}\,(x)\,y_i\,y_j \le \Lambda\,|y|^2, \qquad x \in \Omega, \qquad y \in \boldsymbol{R}^n,$$

holding for some positive constant δ and Λ.Suppose u_1 and u_2 satisfy (3.1), (3.4) in Ω and matrix A satisfies the assumption of theorem(1.1).

Then $u_1 = u_2$ in Ω.

Proof: Let $u = u_1 - u_2$ and $v = u^*Bu$, where B, as in Theorem (1.1), is positive definite such that $A^*(x)\,B + B\,A\,(x)$ is negative semidefinite for all $x \in \Omega$. .Then v is nonnegative, and the proof of Theorem (1.1) gives:

$$\begin{cases} Lv = -\ u^*\,(A^*B + BA)u + 2\,\alpha_{ij}\,B^{1/2}\,u.\,B^{1/2}\,u \ge 0 & in\ \ \Omega \\ v\,(x) = 0 \qquad on\ \partial\,\Omega, \\ v(x) \quad is\ bounded\ in\ \Omega \end{cases}$$

Hence, by the Phragmen- Lindelof principle [6],

$$lim\ v(x) = 0\,, \qquad as \quad x \to \infty \qquad in\ \Omega\,.$$

Therefore, the maximum principle in Theorem(1.1) implies that $v = 0$ in Ω;

i.e., $u_1 = u_2$, in Ω.

4. An Extension of Maximum Principles to Nonhomogeneous Elliptic System:

In sections 1,2 we obtained maximum principles for some homogeneous elliptic systems. Now we extend these results to the nonhomogeneous elliptic system.

$$Lu(x) + A(x)\,u(x) = f(x), \quad x \in \Omega \qquad \ldots(3.1)$$

Under the restriction of A being a real matrix function such that:

$$\overset{T}{\zeta}\, A\, \zeta \leq - c_o\, |\zeta|^2 \quad \text{in } \Omega, \qquad \text{for some } c_o > 0$$

and for any $\zeta \in \mathbf{R}^n$, Miranda [8] obtained a bound for solutions of the elliptic system (3.1):

$$||u||_{0,\Omega} \leq ||u||_{0,\partial\Omega} + c_0^{-1}\, ||f||_{0,\Omega}.$$

In this section we obtain a similar result for more general complex matrix function A in the elliptic system (3.1).

Theorem (4.1): *Suppose, for $A = A(x)$, there exist two complex constant matrices $B > 0$, $E > 0$ such that $A^*(x)\, B + B\, A(x) \leq - E$. Then for all solutions $u \in C^2(\Omega) \cap C(\overline{\Omega})$ of (3.1), there exist positive constants k_1 and k_2 such that:*

$$||u||_{0,\Omega} \leq k_1\, ||u||_{0,\partial\Omega} + k_2\, ||f||_{0,\Omega} \qquad \ldots\ldots\ldots (4.1)$$

Here $k_1 = \left(\dfrac{\lambda_n}{\lambda_1}\right)^{1/2}$ and $k_2 = \dfrac{2\,\lambda_n^{1/2}}{\mu_1 \lambda_1^{1/2}}$, *where λ_1 and λ_n are the smallest and biggest eigenvalues of B respectively, and μ_1 is the smallest eigenvalue of EB^{-1}.*

Proof: Define $v = B^{1/2}u$; *i.e.*, $u = B^{-1/2}v$. First we will prove that (for v),

$$||v||_{0,\Omega} \leq k_1\, ||v||_{0,\partial\Omega} + k\, ||f||_{0,\Omega}, \quad k > 0 \qquad \ldots\ldots\ldots (4.2)$$

It is sufficient to show that at an internal relative maximum of $|v|$

(or of $|v|^2 = |B^{1/2}u|^2 = Bu.u$),

$$|v(x)| \leq k\, |f(x)| \qquad \ldots\ldots\ldots (4.3)$$

We assume $v(x) \neq 0$ at such a maximum; otherwise the inequality is trivial.

At a relative maximum of $|v|^2 = Bu.u$, we have

$$\frac{\partial}{\partial x_K} \; |v|2 \; = \; 2\, Re\, (Bu.uk) = 0,$$

and the matrix of second derivatives is negative semidefinite; i.e.,

$$\left[\frac{\partial^2 |v|^2}{\partial x_i \; \partial x_K}\right]_{n\times n} \; = \; \Big[2\,\mathrm{Re}\,(\mathrm{v_i}\,.\,\mathrm{v_k} \; + \; \mathrm{v.v_{ik}})\Big]_{n\times n} \; \leq 0.$$

Hence,

$$Re\,(Bu.u_k) = Re\,(v.v_k) = 0,$$

$$\Big[Re\,(v_i\,.\,v_k \; + \; v.v_{ik})\Big]_{n\times n} \leq 0.$$

Since $(a_{ik}) > 0$, we have that

$$a_{ik}\,(v_i\,.\,v_k \; + Re\,(v.v_{ik})) \leq 0.$$

Into this inequality we substitute the system (3.1) and $Re\,(Bu.u_k) = 0$ to get

$$0 \geq a_{ik}\, v_i\, v_k + Re\,(Bu.\; a_{ik}\, u_{ik})$$

$$= a_{ik}\, v_i\, v_k + Re\,[Bu.(-\,a_i\, u_i - Au + f)]$$

$$= a_{ik}\, v_i\, v_k - ½\;\; (A^*B + BA)\; u.\; u + Re\,(Bu.\, f)$$

Therefore $\qquad \lambda_n^{1/2}\, |v|\; |f| \geq -Re(Bu.f) \geq \; a_{ik}\, v_i\, v_k - ½\;\; (A^*B + BA)\; u.\; u$

$$\geq ½\; Eu.\; u = ½\; (B^{-½}\; EB^{-½})\; v.v$$

Since $B^{-½}\; EB^{-½}$ *and* EB^{-1} have the same eigenvalues, it follows that

$$\lambda_n^{1/2}\, |v|\; |f| \geq \frac{\mu_1}{2}\; |\mathrm{v}|^2$$

and then (4.3) holds with

$$\mathrm{k} = \frac{2\; \lambda_n^{1/2}}{\mu_1}$$

Hence we have proved (4.2).

By using *(4.2)* and substituting $v = B^{1/2} u$, we have

$$\lambda_n^{1/2} \, ||u||_{0,\Omega} \leq \lambda_n^{1/2} \, ||u||_{0,\partial\Omega} + k \, ||f||_{0,\Omega},$$

so (4.1) holds with

$$k_1 = \left(\frac{\lambda_n}{\lambda_1}\right)^{1/2} \text{ and } k_2 = \frac{k}{\lambda_1^{1/2}} = \frac{2\lambda_n^{1/2}}{\mu_1 \lambda_1^{1/2}} \quad \square.$$

From the liapunov lemma [1], the following theorem is easily obtained.

Theorem (4.2): *Assume that $A(x) = r(x) I + \bar{A}$ in (3.1), where $r \leq 0$ in Ω and each eigenvalue of the complex constant matrix $\bar{A}$ has negative real part. Then for all solutions $u \in C^2(\Omega) \cap C(\overline{\Omega})$ of (3.1), there exist positive constants k_1 and k_2 such that (4.1) holds.*

Theorem (4.3): *(a) A sufficient condition that*

$$||u||_{0,\Omega} \leq ||u||_{0,\partial\Omega} + c_0^{-1} \, ||f||_{0,\Omega} \qquad \text{……… (4.4)}$$

holds, for all solutions $u \in C^2(\Omega) \cap C(\overline{\Omega})$ of (3.1), is

$$A^*(x) + A(x) \leq -2 c_0 I < 0, \quad \text{for some } c_0 \in R \qquad \text{……… (4.5)}$$

(b) Suppose that the variable matrix $A = A(x)$ is normal, and all its eigenvalues $\{\lambda_i(x)\}_{i=1}^n$ have uniformly negative real parts in Ω; i.e., Re $\lambda_i(x) \leq - c_0 < 0$ in Ω, for $1 \leq i \leq n$. Then (4.4) holds for all solutions $u \in C^2(\Omega) \cap C(\overline{\Omega})$ of (3.1).

Proof: (a) By choosing $B = I$ in Theorem(4.1), the inequality (4.4) follows from the condition (4.5).

(b) Since A(x) is normal, there exist a unitary matrix U(x) such that

$$U^*(x)\,[A^*(x) + A(x)]\,U(x)$$

$$= \begin{bmatrix} 2\operatorname{Re}\lambda_1(x) & & \\ & \ddots & \\ & & 2\operatorname{Re}\lambda_n(x) \end{bmatrix} \le -2\ c_0 I < 0$$

Hence $A^*(x) + A(x) \le -2\ c_0 I$; and then (4.4) follows from (a)□.

5. Concluding Remarks

1. The condition (3.2) is also necessary for the proof of the classical maximum principle by the method imposed here.
2. Theorem (3.1) contains the result of winter and Wong [14] for real negative semidefinite $A=A(x, u, \nabla u)$ as a special case; one may view, for given u, $A(x, u(x), \nabla u(x))$ as a matrix function $A_1(x)$.

REFERENCES

[1] M.M.Al-Mahameed, " Generalized Maximum Principles for a Class of Homogeneous Elliptic Systems",*Inter.J.of Math.Game Theory and Algebra*, 13(2003).

[2] M. A. Dow, "Maximum Principles for Weakly Coupled Systems of Quasilinear Parabolic Inequalities", *J. Austral. Math. Soc*. 19 (1975), 79-83.

[3] L.E. Fraenkel, " An Introduction to Maximum Principles and Symmetry in Elliptic Problem", Cam. Tracts. in Math., Cam University Press., Cambridge,128(2000).

[4] M. Franciosi, "Maximum Principles for Second Order Elliptic Equations and Applications" , *J.Math.Anal.Appl*.**138**(2)(1989), 343-348.

[5] G. N. Hille and M. H. Protter, "Maximum Principles for a Class of First Order Elliptical Systems", *J.Diff. Eqs*. 24(1977),136-151.

[6] G.N.Hille and R.Z. Yeh, "Phrngmen- Lindelof Priciples for Solutions of Elliptic Differentil Inequalities", *J.Math.Anal.Appl*.107(1985), 478-497.

[7] G.N.Hille and R.Z. Yeh, " Exceptional Boundary Set for Solutions of Elliptic Partial Inequalities", *Indiana .Univ.Math.J*.35(1986), 611-621.

[8] C.Miranda, " Partial Differential Equations of Elliptic Type", 2nd Rev.Ed., Springer- Verlag, Berlin, 1970.

[9] M. H. Protter and H. F. Weinberger," Maximum Principles in Differential Equations" Springer – verlag, Berlin, 1984.

[10] J. Snyders and M. Zakai, "On Nonnegative Solutions of the Equation $AD+DA^{*}= -C$", *SIAM J. Appl. Math*. **18** (1970), 704-714.

[11] R. Sperb, "Maximum Principles and Their Applications". Academic Press, New York, 1981.

[12] P.Takac,"An Abstract Form of Maximum and Anti-Maximum Principles of Hopfs Type" , *J, Math. Anal. Appl*.(2)201(1996) , 339-364.

[13] J. Wasowski, "Maximum Principles for a Certain Strongly Elliptic System of Linear Equations of Second Order", *Bull. Acad. Polon. Sci* 18 (1972), 741-745.

[14] M. J. Winter and Pui – Kei. Wong, "Comparison and Maximum Theorems for System of Quasilinear Elliptic Differential Equations", *J. Math. Anal. Appl*. 40 (1972), 634-642.

[15] T. Yoshizaea, "Stability Theory by Liapunov's Second Method", *The Math. Society of Japan*, 1966.

Instructions to Contributors
Journal of Applied Functional Analysis

A quartely international publication of Eudoxus Press, LLC of TN.

Editor in Chief: George Anastassiou
Department of Mathematical Sciences
University of Memphis
Memphis, TN 38152-3240, U.S.A.

1. Manuscripts, hard copies in quadruplicate and in English,should be submitted by regular, unregistered mail, to the Editor in Chief.

Authors may want to recommend an associate editor most related to the submission to possibly handle it. In addition, to assist the Editor and speed the decision process, authors may include a PDF file of the paper on disk with the submitted copies of the manuscript.

Also authors may want to submit a list of six possible referees, to be used in case we cannot find related referees by ourselves.

2. Manuscripts should be typed using any of TEX,LaTEX,AMS-TEX,or AMS-LaTEX and according to EUDOXUS PRESS, LLC. LATEX STYLE FILE. (Click HERE to save a copy of the style file.)They should be carefully prepared in all respects. Submitted copies should be brightly printed (not dot-matrix), double spaced, in ten point type size, on one side high quality paper 8(1/2)x11 inch. Manuscripts should have generous margins on all sides and should not exceed 24 pages.

3. Submission is a representation that the manuscript has not been published previously in this or any other similar form and is not currently under consideration for publication elsewhere. A statement transferring from the authors(or their employers,if they hold the copyright) to Eudoxus Press, LLC, will be required before the manuscript can be accepted for publication.The Editor-in-Chief will supply the necessary forms for this transfer.Such a written transfer of copyright,which previously was assumed to be implicit in the act of submitting a manuscript,is necessary under the U.S.Copyright Law in order for the publisher to carry through the dissemination of research results and reviews as widely and effective as possible.

4. The paper starts with the title of the article, author's name(s) (no titles or degrees), author's affiliation(s) and e-mail addresses. The affiliation should comprise the department, institution (usually university or company), city, state (and/or nation) and mail code.

The following items, 5 and 6, should be on page no. 1 of the paper.

5. An abstract is to be provided, preferably no longer than 150 words.

6. A list of 5 key words is to be provided directly below the abstract. Key words should express the precise content of the manuscript, as they are used for indexing purposes.

The main body of the paper should begin on page no. 1, if possible.

7. All sections should be numbered with Arabic numerals (such as: 1. INTRODUCTION) .
Subsections should be identified with section and subsection numbers (such as 6.1. Second-Value Subheading).
If applicable, an independent single-number system (one for each category) should be used to label all theorems, lemmas, propositions, corrolaries, definitions, remarks, examples, etc. The label (such as Lemma 7) should be typed with paragraph indentation, followed by a period and the lemma itself.

8. Mathematical notation must be typeset. Equations should be numbered consecutively with Arabic numerals in parentheses placed flush right,and should be thusly referred to in the text [such as Eqs.(2) and (5)]. The running title must be placed at the top of even numbered pages and the first author's name, et al., must be placed at the top of the odd numbed pages.

9. Illustrations (photographs, drawings, diagrams, and charts) are to be numbered in one consecutive series of Arabic numerals. The captions for illustrations should be typed double space. All illustrations, charts, tables, etc., must be embedded in the body of the manuscript in proper, final, print position. In particular, manuscript, source, and PDF file version must be at camera ready stage for publication or they cannot be considered.

Tables are to be numbered (with Roman numerals) and referred to by number in the text. Center the title above the table, and type explanatory footnotes (indicated by superscript lowercase letters) below the table.

10. List references alphabetically at the end of the paper and number them consecutively. Each must be cited in the text by the appropriate Arabic numeral in square brackets on the baseline.
References should include (in the following order):
initials of first and middle name, last name of author(s)
title of article,
name of publication, volume number, inclusive pages, and year of publication.

Authors should follow these examples:

Journal Article

1. H.H.Gonska,Degree of simultaneous approximation of bivariate functions by Gordon operators, (journal name in italics) *J. Approx. Theory*, 62,170-191(1990).

Book

2. G.G.Lorentz, (title of book in italics) *Bernstein Polynomials* (2nd ed.), Chelsea,New York,1986.

Contribution to a Book

3. M.K.Khan, Approximation properties of beta operators,in(title of book in italics) *Progress in Approximation Theory* (P.Nevai and A.Pinkus,eds.), Academic Press, New York,1991,pp.483-495.

11. All acknowledgements (including those for a grant and financial support) should occur in one paragraph that directly precedes the References section.

12. Footnotes should be avoided. When their use is absolutely necessary, footnotes should be numbered consecutively using Arabic numerals and should be typed at the bottom of the page to which they refer. Place a line above the footnote, so that it is set off from the text. Use the appropriate superscript numeral for citation in the text.

13. After each revision is made please again submit four hard copies of the revised manuscript. And after a manuscript has been accepted for publication submit four hard copies of the final revised manuscript. Additionally, two copies of the final version of the TEX/LaTex source file and a PDF file, are to be submitted to the Editor's Office on personal 3.5 inch computer disks. Label the disks individually with clearly written identifying information, e.g. :

Your name, title of article, kind of computer used, kind of software and version number, disk format and files names of article, as well as abbreviated journal name.

Package the disks in a disk mailer or protective cardboard. Make sure contents of disks are identical with the ones of final hard copies submitted!

Note: The Editor's Office cannot accept the disks without the accompanying matching hard copies of manuscript. No e-mail final submissions are allowed! File submission on disk must be used.

14. Effective 1 Nov. 2009 for current journal page charges, contact the Editor in Chief. Upon acceptance of the paper an invoice will be sent to the contact author. The fee payment will be due one month from the invoice date. The article will proceed to publication only after the fee is paid. The charges are to be sent, by money order or certified check, in US dollars, payable to Eudoxus Press, LLC, to the address shown on the Eudoxus homepage.

No galleys will be sent and the contact author will receive one(1) electronic copy of the journal issue in which the article appears.

15. This journal will consider for publication only papers that contain proofs for their listed results.

TABLE OF CONTENTS, JOURNAL OF APPLIED FUNCTIONAL ANALYSIS, VOLUME 6, NO.3, 2011

Volume 6, Number 4 October 2011

ISSN:1559-1948 (PRINT), 1559-1956 (ONLINE)

EUDOXUS PRESS,LLC

JOURNAL OF APPLIED FUNCTIONAL ANALYSIS

SCOPE AND PRICES OF

JOURNAL OF APPLIED FUNCTIONAL ANALYSIS

A quartely international publication of **EUDOXUS PRESS,LLC**

ISSN:1559-1948(PRINT),1559-1956(ONLINE)

Editor in Chief: George Anastassiou
Department of Mathematical Sciences
The University of Memphis
Memphis, TN 38152,USA
E mail: ganastss@memphis.edu

The purpose of the "Journal of Applied Functional Analysis"(JAFA) is to publish high quality original research articles, survey articles and book reviews from all subareas of Applied Functional Analysis in the broadest form plus from its applications and its connections to other topics of Mathematical Sciences. A sample list of connected mathematical areas with this publication includes but is not restricted to: Approximation Theory, Inequalities, Probability in Analysis, Wavelet Theory, Neural Networks, Fractional Analysis, Applied Functional Analysis and Applications, Signal Theory, Computational Real and Complex Analysis and Measure Theory, Sampling Theory, Semigroups of Operators, Positive Operators, ODEs, PDEs, Difference Equations, Rearrangements, Numerical Functional Analysis, Integral equations, Optimization Theory of all kinds, Operator Theory, Control Theory, Banach Spaces, Evolution Equations, Information Theory, Numerical Analysis, Stochastics, Applied Fourier Analysis, Matrix Theory, Mathematical Physics, Mathematical Geophysics, Fluid Dynamics, Quantum Theory. Interpolation in all forms, Computer Aided Geometric Design, Algorithms, Fuzzyness, Learning Theory, Splines, Mathematical Biology, Nonlinear Functional Analysis, Variational Inequalities, Nonlinear Ergodic Theory, Functional Equations, Function Spaces, Harmonic Analysis, Extrapolation Theory, Fourier Analysis, Inverse Problems, Operator Equations, Image Processing, Nonlinear Operators, Stochastic Processes, Mathematical Finance and Economics, Special Functions, Quadrature, Orthogonal Polynomials, Asymptotics, Symbolic and Umbral Calculus, Integral and Discrete Transforms, Chaos and Bifurcation, Nonlinear Dynamics, Solid Mechanics, Functional Calculus, Chebyshev Systems. Also are included combinations of the above topics.

Working with Applied Functional Analysis Methods has become a main trend in recent years, so we can understand better and deeper and solve important problems of our real and scientific world.

JAFA is a peer-reviewed International Quarterly Journal published by Eudoxus Press,LLC.

We are calling for high quality papers for possible publication. The contributor should send four copies of the contribution to the EDITOR in CHIEF in TEX,LATEX double spaced,in ten point type size. They should be sent BY REGULAR MAIL ONLY, NOT REGISTERED MAIL, AND NO E-MAIL SUBMISSIONS [See: Instructions to Contributors]

Journal of Applied Functional Analysis(JAFA)
is published in January,April,July and October of each year by

EUDOXUS PRESS,LLC,
1424 Beaver Trail Drive,Cordova,TN38016,USA,
Tel.001-901-751-3553
anastassioug@yahoo.com
http://www.EudoxusPress.com visit also http://www.msci.memphis.edu/~ganastss/jafa.

Webmaster:Ray Clapsadle

Annual Subscription Current Prices:For USA and Canada,Institutional:Print $400,Electronic $250,Print and Electronic $450.Individual:Print $ 150, Electronic $80,Print &Electronic $200.For any other part of the world add $50 more to the above prices for Print.
Single article PDF file for individual $15.Single issue in PDF form for individual $60.

No credit card payments.Only certified check,money order or international check in US dollars are acceptable.
Combination orders of any two from JoCAAA,JCAAM,JAFA receive 25% discount,all three receive 30% discount.

JAFA is reviewed and abstracted by AMS Mathematical Reviews,MATHSCI,and Zentralblaat MATH.

JAFA IS A JOURNAL OF RAPID PUBLICATION

Journal of Applied Functional Analysis
Editorial Board
Associate Editors

Operators on Banach spaces,
Tensor products of Banach spaces,
Polymeasures, Function spaces.

8) Michele Campiti
Department of Mathematics "E.De Giorgi"
University of Lecce
P.O. Box 193
Lecce,ITALY
Tel. +39 0832 297 432
Fax +39 0832 297 594
michele.campiti@unile.it
Approximation Theory,
Semigroup Theory, Evolution problems,
Differential Operators.

9)Domenico Candeloro
Dipartimento di Matematica e Informatica
Universita degli Studi di Perugia
Via Vanvitelli 1
06123 Perugia
ITALY
Tel +39(0)75 5855038
+39(0)75 5853822,
+39(0)744 492936
Fax +39(0)75 5855024
candelor@dipmat.unipg.it
Functional Analysis, Function spaces,
Measure and Integration Theory in
Riesz spaces.

10) Pietro Cerone
School of Computer Science and
Mathematics, Faculty of Science,
Engineering and Technology,
Victoria University
P.O.14428,MCMC
Melbourne,VIC 8001,AUSTRALIA
Tel +613 9688 4689
Fax +613 9688 4050
Pietro.cerone@vu.edu.au
Approximations, Inequalities,
Measure/Information Theory,
Numerical Analysis, Special Functions.

11)Michael Maurice Dodson
Department of Mathematics
University of York,
York YO10 5DD, UK
Tel +44 1904 433098
Fax +44 1904 433071
Mmd1@york.ac.uk
Harmonic Analysis and Applications to
Signal Theory,Number Theory and
Dynamical Systems.

Almost Periodicity & Almost Automorphy.

32) Vassilis Papanicolaou
Department of Mathematics
National Technical University of Athens
Zografou campus, 157 80
Athens, Greece
tel:: +30(210) 772 1722
Fax +30(210) 772 1775
papanico@math.ntua.gr
Partial Differential Equations,
Probability.

33) Pier Luigi Papini
Dipartimento di Matematica
Piazza di Porta S.Donato 5
40126 Bologna
ITALY
Fax +39(0)51 582528
papini@dm.unibo.it
Functional Analysis, Banach spaces,
Approximation Theory.

34) Svetlozar T.Rachev
Chair of Econometrics,Statistics
and Mathematical Finance
School of Economics and
Business Engineering
University of Karlsruhe
Kollegium am Schloss, Bau II,20.12, R210
Postfach 6980, D-76128,
Karlsruhe,GERMANY.
Tel +49-721-608-7535,
+49-721-608-2042(s)
Fax +49-721-608-3811
Zari.Rachev@wiwi.uni-karlsruhe.de
Second Affiliation:
Dept.of Statistics and Applied Probability
University of California at Santa Barbara
rachev@pstat.ucsb.edu
Probability,Stochastic Processes and
Statistics,Financial Mathematics,
Mathematical Economics.

35) Paolo Emilio Ricci
Department of Mathematics
Rome University "La Sapienza"
P.le A.Moro,2-00185
Rome,ITALY
Tel ++3906-49913201 office
++3906-87136448 home
Fax ++3906-44701007
Paoloemilio.Ricci@uniroma1.it
riccip@uniroma1.it
Special Functions, Integral and Discrete

12) Sever S.Dragomir
School of Computer Science and
Mathematics, Victoria University,
PO Box 14428,
Melbourne City,
MC 8001,AUSTRALIA
Tel. +61 3 9688 4437
Fax +61 3 9688 4050
sever@csm.vu.edu.au
Inequalities,Functional Analysis,
Numerical Analysis, Approximations,
Information Theory, Stochastics.

13) Paulo J.S.G.Ferreira
Department of Electronica e
Telecomunicacoes/IEETA
Universidade de Aveiro
3810-193 Aveiro
PORTUGAL
Tel +351-234-370-503
Fax +351-234-370-545
pjf@ieeta.pt
Sampling and Signal Theory,
Approximations, Applied Fourier Analysis,
Wavelet, Matrix Theory.

14) Gisele Ruiz Goldstein
Department of Mathematical Sciences
The University of Memphis
Memphis,TN 38152,USA.
Tel 901-678-2513
Fax 901-678-2480
ggoldste@memphis.edu
PDEs, Mathematical Physics,
Mathematical Geophysics.

15) Jerome A.Goldstein
Department of Mathematical Sciences
The University of Memphis
Memphis,TN 38152,USA
Tel 901-678-2484
Fax 901-678-2480
jgoldste@memphis.edu
PDEs,Semigroups of Operators,
Fluid Dynamics,Quantum Theory.

16) Heiner Gonska
Institute of Mathematics
University of Duisburg-Essen
Lotharstrasse 65
D-47048 Duisburg
Germany
Tel +49 203 379 3542
Fax +49 203 379 1845
gonska@math.uni-duisburg.de
Approximation and Interpolation Theory,

Transforms, Symbolic and Umbral Calculus,
ODE, PDE,Asymptotics, Quadrature,
Matrix Analysis.

36) Silvia Romanelli
Dipartimento di Matematica
Universita' di Bari
Via E.Orabona 4
70125 Bari, ITALY.
Tel (INT 0039)-080-544-2668 office
080-524-4476 home
340-6644186 mobile
Fax -080-596-3612 Dept.
romans@dm.uniba.it
PDEs and Applications to Biology and
Finance, Semigroups of Operators.

37) Boris Shekhtman
Department of Mathematics
University of South Florida
Tampa, FL 33620,USA
Tel 813-974-9710
boris@math.usf.edu
Approximation Theory, Banach spaces,
Classical Analysis.

38) Rudolf Stens
Lehrstuhl A fur Mathematik
RWTH Aachen
52056 Aachen
Germany
Tel ++49 241 8094532
Fax ++49 241 8092212
stens@mathA.rwth-aachen.de
Approximation Theory, Fourier Analysis,
Harmonic Analysis, Sampling Theory.

39) Juan J.Trujillo
University of La Laguna
Departamento de Analisis Matematico
C/Astr.Fco.Sanchez s/n
38271.LaLaguna.Tenerife.
SPAIN
Tel/Fax 34-922-318209
Juan.Trujillo@ull.es
Fractional: Differential Equations-
Operators-
Fourier Transforms, Special functions,
Approximations,and Applications.

40) Tamaz Vashakmadze
I.Vekua Institute of Applied Mathematics
Tbilisi State University,
2 University St. , 380043,Tbilisi, 43,
GEORGIA.
Tel (+99532) 30 30 40 office

Computer Aided Geometric Design, Algorithms.

17) Karlheinz Groechenig
Institute of Biomathematics and Biometry,
GSF-National Research Center
for Environment and Health
Ingolstaedter Landstrasse 1
D-85764 Neuherberg,Germany.
Tel 49-(0)-89-3187-2333
Fax 49-(0)-89-3187-3369
Karlheinz.groechenig@gsf.de
Time-Frequency Analysis, Sampling Theory, Banach spaces and Applications, Frame Theory.

18) Vijay Gupta
School of Applied Sciences
Netaji Subhas Institute of Technology
Sector 3 Dwarka
New Delhi 110075, India
e-mail: vijay@nsit.ac.in;
vijaygupta2001@hotmail.com
Approximation Theory

19) Weimin Han
Department of Mathematics
University of Iowa
Iowa City, IA 52242-1419
319-335-0770
e-mail: whan@math.uiowa.edu
Numerical analysis, Finite element method, Numerical PDE, Variational inequalities, Computational mechanics

20) Tian-Xiao He
Department of Mathematics and Computer Science
P.O.Box 2900,Illinois Wesleyan University
Bloomington,IL 61702-2900,USA
Tel (309)556-3089
Fax (309)556-3864
the@iwu.edu
Approximations,Wavelet, Integration Theory, Numerical Analysis, Analytic Combinatorics.

21) Don Hong
Department of Mathematical Sciences
Middle Tennessee State University
1301 East Main St.
Room 0269, Blgd KOM
Murfreesboro, TN 37132-0001
Tel (615) 904-8339
dhong@mtsu.edu
Approximation Theory,Splines,Wavelet, Stochastics, Mathematical Biology Theory.

(+99532) 30 47 84 office
(+99532) 23 09 18 home
Vasha@viam.hepi.edu.ge
tamazvashakmadze@yahoo.com
Applied Functional Analysis, Numerical Analysis, Splines, Solid Mechanics.

41) Ram Verma
International Publications
5066 Jamieson Drive, Suite B-9,
Toledo, Ohio 43613,USA.
Verma99@msn.com
rverma@internationalpubls.com
Applied Nonlinear Analysis, Numerical Analysis, Variational Inequalities, Optimization Theory, Computational Mathematics, Operator Theory.

42) Gianluca Vinti
Dipartimento di Matematica e Informatica
Universita di Perugia
Via Vanvitelli 1
06123 Perugia
ITALY
Tel +39(0) 75 585 3822,
+39(0) 75 585 5032
Fax +39 (0) 75 585 3822
mategian@unipg.it
Integral Operators, Function Spaces, Approximation Theory, Signal Analysis.

43) Ursula Westphal
Institut Fuer Mathematik B
Universitaet Hannover
Welfengarten 1
30167 Hannover,GERMANY
Tel (+49) 511 762 3225
Fax (+49) 511 762 3518
westphal@math.uni-hannover.de
Semigroups and Groups of Operators, Functional Calculus, Fractional Calculus, Abstract and Classical Approximation Theory, Interpolation of Normed spaces.

44) Ronald R.Yager
Machine Intelligence Institute
Iona College
New Rochelle,NY 10801,USA
Tel (212) 249-2047
Fax(212) 249-1689
Yager@Panix.Com
ryager@iona.edu
Fuzzy Mathematics, Neural Networks, Reasoning,
Artificial Intelligence, Computer Science.

22) Hubertus Th. Jongen
Department of Mathematics
RWTH Aachen
Templergraben 55
52056 Aachen
Germany
Tel +49 241 8094540
Fax +49 241 8092390
jongen@rwth-aachen.de
Parametric Optimization, Nonconvex Optimization, Global Optimization.

45) Richard A. Zalik
Department of Mathematics
Auburn University
Auburn University,AL 36849-5310
USA.
Tel 334-844-6557 office
678-642-8703 home
Fax 334-844-6555
zalik@auburn.edu
Approximation Theory,Chebychev Systems, Wavelet Theory.

JOURNAL OF APPLIED FUNCTIONAL ANALYSIS, VOL.6, NO.4, 308-313, COPYRIGHT 2011 EUDOXUS PRESS, LLC

TRAVELING WAVE SOLUTION FOR A NON - LINEAR DIFFUSIVE PARTIAL DIFFERENTIAL EQUATION

By

Omar M. Abu Ghalyoun and Marwan S. Abualrub

Department of Mathematics / The University of Jordan / P.O.Box 11942 / Amman – Jordan

E- mail : omar_ghalyoun@yahoo.com and abualrubms@yahoo.com

2000 Mathematics Subject Classification code: 92B99

Keywords : Traveling wave solution, Diffusion, Tanh method solution.

Abstract

A non-linear diffusive partial differential equation has been considered, Tanh method solution has been used to obtain a traveling wave solution for the considered equation.

1. Introduction

In recent years, quite a few methods for obtaining explicit traveling wave solutions of non-linear diffusion equations have been proposed. A variety of powerful methods such as Tanh method and Sine-Cosine method were used in the analysis of these problems. In this paper we has been considered the non-linear diffusion partial differential equation

$$au_{xx} - u_{tt} + uu_x - bu + du^3 = 0$$

Tanh method has been used to solve this equation. Stability of the resulting solutions has been discussed using stability rules after transforming the equation into a system of linear differential equations.

2. Traveling wave technique

The considered equation is

$$au_{xx} - u_{tt} + uu_x - bu + du^3 = 0 \qquad (1)$$

To find a possible traveling wave solution (by transforming the partial differential equation into an ordinary differential equation) we introduce the independent wave variable $\xi = x - ct$ that leads to the following ODE:

$$(a - c^2)\, \boldsymbol{u}(\xi)'' + \boldsymbol{u}(\xi)'\, \boldsymbol{u}(\xi) - b\boldsymbol{u}(\xi) + d\, \boldsymbol{u}(\xi)^3 = 0 \qquad (2)$$

For more details about traveling wave technique refer to [4].

3. Tanh method solution

Tanh method introduces the solution of (2) as F(Y); where $F(Y) = \sum_{n=0}^{N} a_n Y^n$; Y = tanh(μξ).

Considering F(Y) as a solution we can replace(2) by:

$$\mu^2(a - c^2)\,(1-Y^2)((1-Y^2)\,F(Y)')' + \mu((1-Y^2)F(Y)'\,F(Y) - b\,F(Y) + d\,F(Y)^3 = 0 \qquad (3)$$

Balancing the most non-linear term with the highest derivative term results in

$$3\,N = N+2 \;\Rightarrow\; N = 2/(3-1) \Rightarrow N = 1$$

$$F(Y) = a_0 + a_1 Y;\; Y = \tanh(\mu\xi) \qquad (4)$$

Substituting F(Y) into equation (3) leads to the following equation:

$$\mu^2(a - c^2)\,(1-Y^2)[(1-Y^2)(a_1)]' + \mu(a_1)\,(1-Y^2)(a_0 + a_1 Y) +$$

$$b(a_0 + a_1 Y) + d\,(a_0 + a_1 Y)^3 = 0 \qquad (5)$$

Expanding and collecting like terms leads to the following values of the constants:

$$\{\, a_0 = 0,\quad a_1 = \frac{1}{bd}\left(-\frac{1}{2}b\sqrt{-\frac{b}{2(a-c^2)} + \frac{b}{8(a-c^2)^2 d} + \frac{b\sqrt{1-8(a-c^2)d}}{8(a-c^2)^2\,d}}\right.$$

$$\left. + \frac{b}{2}\sqrt{1-8(a-c^2)d}\;\sqrt{-\frac{b}{2(a-c^2)} + \frac{b}{8(a-c^2)^2 d} + \frac{b\sqrt{1-8(a-c^2)d}}{8(a-c^2)^2\,d}}\right), \text{ and}$$

$$\mu = -\sqrt{-\frac{b}{2(a-c^2)} + \frac{b}{8(a-c^2)^2 d} + \frac{b\sqrt{1-8(a-c^2)d}}{8(a-c^2)^2\,d}}\;\}$$

Substituting the values of a_0, a_1 and μ into (5) gives the following form of the solution:

$$U(\zeta) = \frac{1}{bd}\left(-\frac{1}{2}b\sqrt{-\frac{b}{2(a-c^2)} + \frac{b}{8(a-c^2)^2 d} + \frac{b\sqrt{1-8(a-c^2)d}}{8(a-c^2)^2\,d}}\right.$$

$$+\ \frac{b}{2}\sqrt{1-8(a-c^2)d}\ \sqrt{-\frac{b}{2(a-c^2)}+\frac{b}{8(a-c^2)^2d}+\frac{b\sqrt{1-8(a-c^2)d}}{8(a-c^2)^2\ d}}\ \Bigg)$$

$$\tanh\left(-\sqrt{-\frac{b}{2(a-c^2)}+\frac{b}{8(a-c^2)^2d}+\frac{b\sqrt{1-8(a-c^2)d}}{8(a-c^2)^2\ d}}\ (\zeta)\right) \tag{6}$$

Or the following form in 3D:

$$U(x,t)=\frac{1}{bd}\Bigg(-\frac{1}{2}\,b\sqrt{-\frac{b}{2(a-c^2)}+\frac{b}{8(a-c^2)^2d}+\frac{b\sqrt{1-8(a-c^2)d}}{8(a-c^2)^2\ d}}\ +$$

$$\frac{b}{2}\sqrt{1-8(a-c^2)d}\ \sqrt{-\frac{b}{2(a-c^2)}+\frac{b}{8(a-c^2)^2d}+\frac{b\sqrt{1-8(a-c^2)d}}{8(a-c^2)^2\ d}}\ \Bigg)$$

$$\tanh\left(-\sqrt{-\frac{b}{2(a-c^2)}+\frac{b}{8(a-c^2)^2d}+\frac{b\sqrt{1-8(a-c^2)d}}{8(a-c^2)^2\ d}}\ (x-ct)\right) \tag{7}$$

For more details about Tanh method refer to [3]&[5].

4. Stability

Now let us discuss stability of (1), first we rewrite it as a system of differential equations by letting $x=u$, $y=\frac{du}{d\zeta}$; therefore $\frac{dx}{d\zeta}=y$, $\frac{dy}{d\zeta}=-\frac{xy}{(a-c^2)}+\frac{bx}{(a-c^2)}-\frac{dx^3}{(a-c^2)}$.

The equivalent system becomes:

$$\begin{cases} \dfrac{dx}{d\zeta} = y \\[2ex] \dfrac{dy}{d\zeta} = -\dfrac{xy}{(a-c^2)}+\dfrac{bx}{(a-c^2)}-\dfrac{dx^3}{(a-c^2)} \end{cases}$$

The equilibrium points are $(x,y)=(0,0)$, and $(x,y)=\left(\sqrt{\frac{b}{d}}\ ,\ 0\right)$.

The Jacobian matrix of the system will be:

$$J = \begin{pmatrix} 0 & 1 \\ -\frac{y}{(a-c^2)} + \frac{b}{(a-c^2)} - \frac{3d\,X^2}{(a-c^2)} & -\frac{x}{(a-c^2)} \end{pmatrix}$$

Let us concentrate on the equilibrium position $\left(\sqrt{\frac{b}{d}}\ ,\ 0\right)$.

For $\left(\sqrt{\frac{b}{d}}\ ,\ 0\right)$ the Jacobian matrix becomes:

$$J = \begin{pmatrix} 0 & 1 \\ \frac{-2b}{(a-c^2)} & -\frac{\sqrt{\frac{b}{d}}}{(a-c^2)} \end{pmatrix}$$

The eigen values of J are $\lambda = \dfrac{\frac{-\sqrt{b}}{\sqrt{d}\ (a-c^2)} \pm \sqrt{\frac{b}{d(a-c^2)^2} - \frac{8ab}{(a-c^2)} + \frac{8bc^2}{(a-c^2)}}}{2}$ (8)

We now have the following three cases for the eigen values:

Case 1) The eigen values are real when:

$$\frac{b}{d(a-c^2)^2} - \frac{8ab}{(a-c^2)} + \frac{8bc^2}{(a-c^2)} \geq 0 \quad \Rightarrow \quad \frac{1}{d} \geq 8(a - c^2)\text{, and } b > 0$$

Case 2) The eigen values are negative real when case 1 is satisfied, and $\frac{-\sqrt{b}}{\sqrt{d}\ (a-c^2)} < 0 \Rightarrow -\sqrt{b} < 0 \Rightarrow \sqrt{b} > 0 \Rightarrow b > 0$ (If $a > c^2$), *or* $b < 0$ (*if* $a < c^2$) which is not the case; since $b < 0$ leads to $\frac{1}{d} < 8(a - c^2)$; which means that the eigen values are not real, and this contradicts case1.

Case 3) The eigen values are imaginary with negative real parts when:
$\frac{b}{d(a-c^2)^2} - \frac{8b}{(a-c^2)} < 0 \Rightarrow \frac{1}{d} < 8(a - c^2)$, b > 0, and $a > c^2$.

Thus as result we have:

1) The critical point $\left(\sqrt{\frac{b}{d}}\ ,\ 0\right)$ is a node point of the system if $\frac{1}{d} \geq 8(a - c^2)$, and b > 0.

2) The critical point $\left(\sqrt{\frac{b}{d}}\ ,\ 0\right)$ is a spiral sink of the system if $\frac{1}{d} < 8(a - c^2)$, and b > 0.

Let us now use a table to organize some values of the constants a, c, b, and d in order to use Mathematica software to plot the solution in stable cases depending on the above study and results of stability.

Case	a	B	c	d
1	1	1	0.5	1/10
2	3	1	2	1

Case 1 -2D

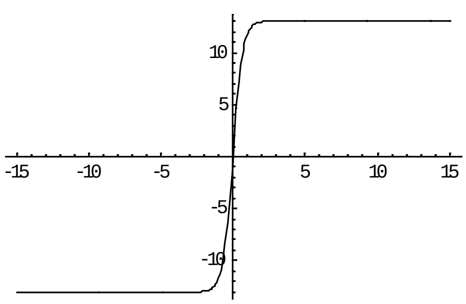

Case 1- 3D

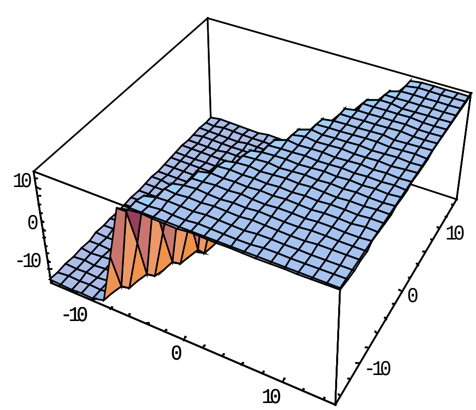

Case 2-2D

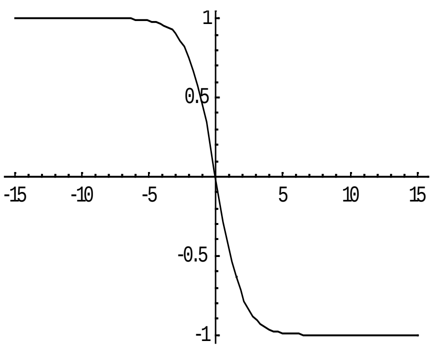

Case 2 - 3D

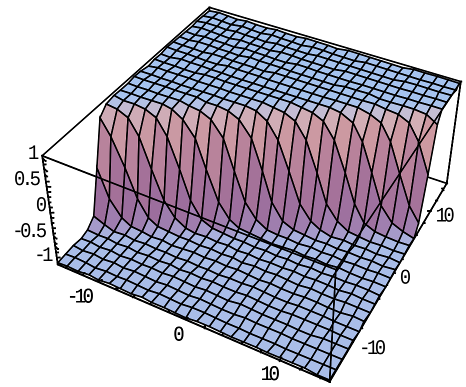

Fore more details about stability refer to [1] &[2].

References:

[1] Abualrub, M.S. (1998). An Analysis to the Traveling Wave Solution of a diffusive Model of an Epidemic. Tamkang Journal of Mathematics, Vol. 29, No.1,pp.65-68.

[2] Burton, T. (1991) The nonlinear wave equation as a Lienard equation. Funkcialaj Ekvacioj, Vol. 34, 529-545.

[3] Malfliet, W. (2004), The tanh method : a tool for solving certain classes of nonlinear evolution and wave equations, *J.* computational and applied mathematics , 529-541.

[4] Wazwaz, A. M. (2004). Traveling wave solutions for the reaction-diffusion equations. International Journal of Applied mathematics, Vol. 16, no.4, pp.497-505.

[5] Wazwaz, A. M. (2004).The tanh method for traveling wave solutions of nonlinear equations.Appl. Math. Comput**,** 154, no 3, pp. 713-723.

JOURNAL OF APPLIED FUNCTIONAL ANALYSIS, VOL.6, NO.4, 314-323, COPYRIGHT 2011 EUDOXUS PRESS, LLC

A STUDY ON SOME NEW q-INTEGRAL INEQUALITIES

W. T. Sulaiman
Department of Computer Engineering
College of Engineering
University of Mosul, Iraq.
waadsulaiman@hotmail.com

Abstract. Many new q-integral inequalities are presented via new ideas.

2000 (MSC) : 26D15
Key words : Integral inequality.

1. Introduction

For $0 < q < 1$, the q-analog of the derivative, denoted by D_q is defined by (see[6])

$$D_q f(x) = \frac{f(x) - f(qx)}{x - qx}, \quad x \neq 0. \tag{1.1}$$

Whenever $f'(0)$ exists, $D_q F(0) = f'(0)$, and as $q \to 1$, the q-derivative reduces to the usual derivative.

The q-analog of integration from 0 to a is given by (see[7])

$$\int_0^a f(x)\, d_q x = a(1-q) \sum_{k=0}^{\infty} f\left(aq^k\right) q^k , \tag{1.2}$$

provided the sum converges absolutely. On a general interval $[a,b]$, the q-integral is defined by (see[2])

$$\int_a^b f(x)\, d_q x = \int_0^b f(x)\, d_q x - \int_0^a f(x)\, d_q x. \tag{1.3}$$

The q-Jackson integral and the q-derivative are related by the fundamental theorem of quantum calculus, which can be stated as follows (see[11, p.73]) :

If F is an anti q-derivative of the function *f*, namely $D_q F = f$, continuous at $x = a$, then

$$\int_a^b f(x)\, d_q x = F(b) - F(a). \tag{1.4}$$

For any function *f*, we have

$$D_q \int_a^x f(t)\, d_q t = f(x). \tag{1.5}$$

For $b > 0$ and $a = bq^n$, $n \in N$, we denote

$$[a,b]_q = \{bq^k : 0 \le k \le n\} \text{ and } (a,b]_q = [aq^{-1}, b]_q. \tag{1.6}$$

In [4] the following results were proved

Theorem 1.1. *If* $f(x)$ *is a non-negative and increasing function on* $[a,b]_q$ *and satisfies*

$$(\alpha - 1) f^{\alpha-2}(qx) D_q f(x) \ge \beta(\beta - 1) f^{\beta-1}(x)(x-a)^{\beta-2} \tag{1.7}$$

for $\alpha \ge 1$ *and* $\beta \ge 1$, *then*

$$\int_a^b f^{\alpha}(x)\, d_q x \ge \left(\int_a^b f(x)\, d_q x \right)^{\beta}. \tag{1.8}$$

Theorem 1.2. *If* $f(x)$ *is a non-negative and increasing function on* $[bq^{n+m}, b]$ *and satisfies*

$$(\alpha - 1) D_q f(x) \ge \beta(\beta - 1) f^{\beta-\alpha+1}(q^m x)(x-a)^{\beta-2} \tag{1.9}$$

on $[a,b]_q$ *and for* $\alpha, \beta \ge 1$, *then*

$$\int_a^b f^{\alpha}(x)\, d_q x \ge \left(\int_a^b f(q^m x)\, d_q x \right)^{\beta}. \tag{1.10}$$

Theorem 1.3. *If* $f(x)$ *is a non-negative function on* $[0,b]_q$ *and satisfies*

$$\int_x^b f^{\beta}(t)\, d_q t \ge \int_x^b t^{\beta}\, d_q t \tag{1.11}$$

for $x \in [0,b]_q$ *and* $\beta > 0$, *then the inequality*

$$\int_0^b f^{\alpha+\beta}(t)\, d_q t \ge \int_0^b t^{\alpha} f^{\beta}(t)\, d_q t \tag{1.12}$$

holds for all positive numbers α *and* β.

The aim of the present paper is to give good generalization for the above results. In fact we give the following

2. Results

We start with the following key lemma

Lemma 2.1. *Let* $p \ge 1$, $f, g, f' > 0$, g, f' *are non-decreasing on* $[a,b]_q$. *Then*

$$p f^{p-1}\big(g(qx)\big) f'\big(g(qx)\big) D_q g(x) \le D_q f^p\big(g(x)\big) \le p f^{p-1}\big(g(x)\big) f'\big(g(x)\big) D_q g(x). \tag{2.1}$$

In particular, for $f(x)=x$,

$$p\,g^{p-1}(qx)\,D_q g(x)\le D_q g^p(x))\le p\,g^{p-1}(x)\,D_q g(x)\ . \tag{2.2}$$

Proof. We have

$$p\,f^{p-1}(g(qx))\,f'(g(qx))(g(x)-g(qx))\le p\int_{g(qx)}^{g(x)} f^{p-1}(t)\,f'(t)\,dt$$

$$\le p\,f^{p-1}(g(x))\,f'(g(x))(g(x)-g(qx)),$$

that is

$$p\,f^{p-1}(g(qx))\,f'(g(qx))(g(x)-g(qx))\le \left(f^p(g(x))-f^p(g(qx))\right)$$
$$\le p\,f^{p-1}(g(x))\,f'(g(x))(g(x)-g(qx)).$$

The result follows by dividing by $(1-q)x$.

Theorem 2.2. *Let* $f,g,f'\ge 0$, g,f' *are non-decreasing on* $[a,b]_q$, $f(g(a))=0$, *and they satisfy*

$$(\alpha-1)\,f^{\alpha-2}(g(qx))\,f'(g(qx))D_q g(x)\ge\beta(\beta-1)\,f^{\beta-1}(g(x))(x-a)^{\beta-2}\,D_q g(x) \tag{2.3}$$

for $\alpha\ge 1$ *and* $\beta\ge 2$. *Then the following inequality it holds*

$$\int_a^x f^{\alpha}(g(t))\,d_q t\ge\left(\int_a^x f(g(t))\,d_q t\right)^{\beta},\quad x\in[a,b]_q\,. \tag{2.4}$$

Proof. Define

$$F(x)=\int_a^x f^{\alpha}(g(t))\,d_q t-\left(\int_a^x f(g(t))\,d_q t\right)^{\beta},\quad x\in[a,b]_q\,,$$

and

$$h(x)=\int_a^x f(g(t))\,d_q t\,.$$

By Lemma 2.1,

$$\begin{aligned}D_q F(x)&=f^{\alpha}(g(x))-D_q h^{\beta}(x)\\&\ge f^{\alpha}(g(x))-\beta\,h^{\beta-1}(x)\,f(g(x))\\&=f(g(x))\left(f^{\alpha-1}(g(x))-\beta\,h^{\beta-1}(x)\right)\\&:=f(g(x))G(x).\end{aligned}$$

Now, $f'\ge 0$ implies that f is non-decreasing. Therefore, we have

$$h(x)\le f(g(x))\int_a^x d_q t=f(g(x))(x-a).$$

The above implies via Lemma 2.1,

$$D_q G(x)\ge(\alpha-1)\,f^{\alpha-2}(g(qx))\,f'(g(qx))D_q g(x)-\beta(\beta-1)\,h^{\beta-2}(x)\,f(g(x))D_q g(x)$$

$$\geq (\alpha-1) f^{\alpha-2}\big(g(qx)\big) f'\big(g(qx)\big) D_q g(x) - \beta(\beta-1)\ f^{\beta-1}\big(g(x)\big)(x-a)^{\beta-2}\ D_q g(x)$$
$$\geq 0.$$

Therefore $G(x)$ is non decreasing on $[a,b]_q$. But $G(a)=0,$ then $G(x)\geq 0,$ which implies $D_q F(x)\geq 0$. Hence $F(x)$ is non-decreasing on $[a,b]_q$. As $F(a)=0,$ then $F(x)\geq 0$. The proof is complete.

Theorem 2.3. *Let* $f, g, f' \geq 0,$ g, f' *are non-decreasing on* $[aq^{-1}, b]_q$, $f\big(g(a)\big)=0,$ *and they satisfy*

$$(\alpha-1) f^{\gamma-2}\big(g(x)\big) f'\big(g(x)\big) D_q g(x) \leq \delta(\delta-1)\ f^{\delta-1}\big(g(q^2x)\big)(q^2x-qa)^{\delta-2}\ D_q g(qx) \tag{2.5}$$

for $\gamma\geq 1$ *and* $\delta\geq 2$. *Then the following inequality is holds*

$$\int_a^x f^{\gamma}\big(g(t)\big) d_q t \leq \left(\int_a^x f\big(g(t)\big) d_q t\right)^{\delta},\quad x\in[a,b]_q. \tag{2.6}$$

Proof. Define

$$H(x) = \int_a^x f^{\gamma}\big(g(t)\big) d_q t - \left(\int_a^x f\big(g(t)\big) d_q t\right)^{\delta},\quad x\in[aq^{-1},b]_q,$$
$$h(qx) = \int_{qa}^{qx} f\big(g(t)\big) d_q t.$$

By Lemma 2.1,

$$\begin{aligned} D_q H(x) &= f^{\gamma}\big(g(x)\big) - D_q h^{\delta}(x) \\ &\leq f^{\gamma}\big(g(x)\big) - \delta\, h^{\delta-1}(qx)\, f\big(g(x)\big) \\ &= f\big(g(x)\big)\Big(f^{\gamma-1}\big(g(x)\big) - \delta\, h^{\delta-1}(qx)\Big) \\ &:= f\big(g(x)\big) K(x). \end{aligned}$$

Now, $f'\geq 0$ implies that f is non-decreasing. Therefore, we have

$$h(q^2x) \leq f\big(g(q^2x)\big)\int_{qa}^{q^2x} d_q t = f\big(g(q^2x)\big)(q^2x-qa).$$

The above implies via Lemma 2.1,

$$D_q K(x) \leq (\gamma-1) f^{\gamma-2}\big(g(x)\big) f'\big(g(x)\big) D_q g(x) - \delta(\delta-1) h^{\delta-2}(q^2x)\, f\big(g(q^2x)\big) D_q g(qx)$$

$$\leq (\alpha-1) f^{\gamma-2}\big(g(x)\big) f'\big(g(x)\big) D_q g(x) - \delta(\delta-1)\ f^{\delta-1}\big(g(q^2x)\big)(q^2x-a)^{\delta-2}\ D_q g(qx)$$
$$\leq 0.$$

Therefore $K(x)$ is non -increasing on $[aq^{-1}, b]_q$. But $K(a) = 0$, then $K(x) \le 0$, which implies $D_q H(x) \le 0$. Hence $H(x)$ is non-increasing on $[aq^{-1}, b]_q$. As $H(a) = 0$, then $H(x) \le 0$.

Theorem 2.4. *Let* $f, g \ge 0$, g *is non-decreasing, and let* $\alpha \ge 1$. *If*

$$\int_x^b f(t)\, d_q t \ge \int_x^b g(t)\, d_q t, \quad \forall\, x \in [a,b]_q, \tag{2.7}$$

then the following inequalities hold

(a)
$$\int_a^b g^{\alpha}(x)\, d_q x \le \int_a^b f(x)\, g^{\alpha-1}(x)\, d_q x \le \int_a^b f^{\alpha}(x)\, d_q x \tag{2.8}$$

(b)
$$\int_a^b f^{\alpha}(x)\, d_q x \ge \int_a^b f^{\alpha-1}(x)\, g(x)\, d_q x \tag{2.9}$$

Proof. (a). Since g is non-decreasing, then $D_q g(x) \ge 0$, and we have

$$\int_a^b g^{\alpha}(x)\, d_q x = \int_a^b g(x)\, g^{\alpha-1}(x)\, d_q x$$

$$= \int_a^b g(x) \left(\int_a^x D_q g^{\alpha-1}(t)\, d_q t + g^{\alpha-1}(a) \right) d_q x$$

$$= \int_a^b D_q g^{\alpha-1}(t) \int_t^b g(x)\, d_q x\, d_q t \;+\; g^{\alpha-1}(a) \int_a^b g(x)\, d_q x$$

$$\le \int_a^b D_q g^{\alpha-1}(t) \int_t^b f(x)\, d_q x\, d_q t \;+\; g^{\alpha-1}(a) \int_a^b g(x)\, d_q x$$

$$\le \int_a^b f(x) \int_a^x D_q g^{\alpha-1}(t)\, d_q t\, d_q x \;+\; g^{\alpha-1}(a) \int_a^b f(x)\, d_q x$$

$$= \int_a^b f(x) \left(\int_a^x D_q g^{\alpha-1}(x)\, d_q x + g^{\alpha-1}(a) \right) d_q x$$

$$= \int_a^b f(x)\, g^{\alpha-1}(x)\, d_q x.$$

The right inequality follows from the AG inequality as follows,

$$\frac{1}{\alpha} f^{\alpha}(x) + \frac{\alpha-1}{\alpha} g^{\alpha}(x) \ge f(x)\, g^{\alpha-1}(x),$$

which implies via the left inequality

$$\int_a^b f^{\alpha}(x)\,d_qx \ge (1-\alpha)\int_a^b g^{\alpha}(x)\,d_qx + \alpha\int_a^b f(x)\,g^{\alpha-1}(x)\,d_qx$$

$$\ge (1-\alpha)\int_a^b f(x)\,g^{\alpha-1}(x)\,d_qx+\alpha\int_a^b f(x)\,g^{\alpha-1}(x)\,d_qx$$

$$= \int_a^b f(x)\,g^{\alpha-1}(x)\,d_qx.$$

(b). As

$$\left(f(x)-g(x)\right)\left(f^{\alpha-1}(x)-g^{\alpha-1}(x)\right)\ge 0,$$

then, we have

$$\int_a^b f^{\alpha}(x)\,d_qx + \int_a^b g^{\alpha}(x)\,d_qx \ge \int_a^b f^{\alpha-1}(x)\,g(x)\,d_qx + \int_a^b f(x)\,g^{\alpha-1}(x)\,d_qx$$

$$\ge \int_a^b f^{\alpha-1}(x)\,g(x)\,d_qx + \int_a^b g^{\alpha}(x)\,d_qx\,,$$

which implies (2.5).

Remark. 2.5. It may be mentioned that inequality (2.5) follows if we are assuming that f is non-decreasing instead of g, as follows

$$\int_a^b f^{\alpha}(x)\,d_qx = \int_a^b f(x)\,f^{\alpha-1}(x)\,d_qx$$

$$= \int_a^b f(x)\left(\int_a^x D_q f^{\alpha-1}(t)\,d_qt+f^{\alpha-1}(a)\right)d_qx$$

$$= \int_a^b D_q f^{\alpha-1}(t)\int_t^b f(x)\,d_qx\,d_qt + f^{\alpha-1}(a)\int_a^b f(x)\,d_qx$$

$$\ge \int_a^b D_q f^{\alpha-1}(t)\int_t^b g(x)\,d_qx\,d_qt + f^{\alpha-1}(a)\int_a^b g(x)\,d_qx$$

$$= \int_a^b g(x)\int_a^x D_q f^{\alpha-1}(t)\,d_qt\,d_qx + f^{\alpha-1}(a)\int_a^b g(x)\,d_qx$$

$$= \int_a^b g(x) \left(\int_a^x D_q f^{\alpha-1}(x)\, d_q x + f^{\alpha-1}(a) \right) d_q x$$

$$= \int_a^b g(x)\, f^{\alpha-1}(x)\, d_q x.$$

Theorem 2.6. *Let* $f, g \geq 0$, *g is non-decreasing. If* (2.7) *is satisfied, then the following inequality it holds*

$$\int_a^b f^{\alpha+\beta}(x)\, d_q x \geq \int_a^b f^{\alpha}(x)\, g^{\beta}(x)\, d_q x, \tag{2.10}$$

for all $\alpha, \beta \geq 0$, $\alpha + \beta \geq 1$.

Proof. By the AG inequality,

$$\frac{\alpha}{\alpha+\beta} f^{\alpha+\beta}(x) + \frac{\beta}{\alpha+\beta} g^{\alpha+\beta}(x) \geq f^{\alpha}(x)\, g^{\beta}(x).$$

q-integrating the above inequality with making use of (2.8) gives

$$\int_a^b f^{\alpha+\beta}(x)\, d_q x \geq \int_a^b \left(\frac{\alpha}{\alpha+\beta} f^{\alpha+\beta}(x) + \frac{\beta}{\alpha+\beta} g^{\alpha+\beta}(x) \right) d_q x \geq \int_a^b f^{\alpha}(x)\, g^{\beta}(x)\, d_q x.$$

Theorem 2.7. *Let* $f, g \geq 0$, *g is non-decreasing. If*

$$\int_x^b f^{-1}(x)\, d_q x \leq \int_x^b g^{-1}(x)\, d_q x \qquad \forall x \in [a,b]_q, \tag{2.11}$$

then the following inequality holds

$$\int_a^b f^{\beta-\alpha}(x)\, d_q x \leq \int_a^b f^{\beta}(x)\, g^{-\alpha}(x)\, d_q x, \tag{2.12}$$

for all α, β, $0 < \alpha < \beta$.

Proof.

$$\int_a^b g^{\beta}(x)\, d_q x = \int_a^b g^{-1}(x)\, g^{\beta+1}(x)\, d_q x$$

$$= \int_a^b g^{-1}(x) \left(\int_a^x D_q g^{\beta+1}(t)\, d_q t + g^{\beta+1}(a) \right) d_q x$$

$$= \int_a^b D_q g^{\beta+1}(t) \int_t^b g^{-1}(x)\, d_q x\, d_q t \,+\, g^{\beta+1}(a) \int_a^b g^{-1}(x)\, d_q x$$

$$\geq \int_a^b D_q g^{\beta+1}(t) \int_t^b f^{-1}(x)\, d_q x\, d_q t \,+\, g^{\beta+1}(a) \int_a^b g(x)\, d_q x$$

$$= \int_a^b f^{-1}(x) \int_a^x D_q g^{\beta+1}(t)\, d_q t\, d_q x \,+\, g^{\beta+1}(a) \int_a^b f(x)\, d_q x$$

$$= \int_a^b f^{-1}(x) \left(\int_a^x D_q g^{\beta+1}(x)\, d_q x + g^{\beta+1}(a)) \right) d_q x$$

$$= \int_a^b f^{-1}(x)\, g^{\beta+1}(x)\, d_q x. \qquad (2.13)$$

By the AG inequality,

$$f^{-1}(x)\, g^{\beta+1}(x) \geq \frac{\beta+1}{\beta} g^{\beta}(x) - \frac{1}{\beta} f^{\beta}(x)$$

or

$$g^{\beta}(x) \leq \frac{\beta}{\beta+1} f^{-1}(x)\, g^{\beta+1}(x) + \frac{1}{\beta+1} f^{\beta}(x).$$

Now, q-integrating the above inequality with making use of (2.13) gives

$$\int_a^b g^{\beta}(x)\, d_q x \leq \frac{\beta}{\beta+1} \int_a^b f^{-1}(x)\, g^{\beta+1}(x)\, d_q x + \frac{1}{\beta+1} \int_a^b f^{\beta}(x)\, d_q x$$

$$\leq \frac{\beta}{\beta+1} \int_a^b g^{\beta}(x)\, d_q x \,+\, \frac{1}{\beta+1} \int_a^b f^{\beta}(x)\, d_q x,$$

which implies

$$\int_a^b g^{\beta}(x)\, d_q x \;\leq\; \int_a^b f^{\beta}(x)\, d_q x. \qquad (2.14)$$

Again, by the AG inequality,

$$f^{\beta}(x)\,g^{-\alpha}(x) \ge \frac{\beta}{\beta-\alpha} f^{\beta-\alpha}(x) - \frac{\alpha}{\beta-\alpha} g^{\beta-\alpha}(x)$$

or

$$f^{\beta-\alpha}(x) \le (1-\alpha/\beta)\, f^{\beta}(x)\, g^{-\alpha}(x) + (\alpha/\beta)\, g^{\beta-\alpha}(x)\,.$$

q-integrating the above inequality with the use of (2.14) implies

$$\int_a^b f^{\beta-\alpha}(x)\,d_qx \le (1-\alpha/\beta)\int_a^b f^{\beta}(x)\,g^{-\alpha}(x)\,d_qx + (\alpha/\beta)\int_a^b g^{\beta-\alpha}(x)\,d_qx$$

$$\le (1-\alpha/\beta)\int_a^b f^{\beta}(x)\,g^{-\alpha}(x)\,d_qx + (\alpha/\beta)\int_a^b f^{\beta-\alpha}(x)\,d_qx$$

which implies (2.12) .

Combining theorems (2.6) and (2.7), we obtain

Theorem 2.8. *Let* $f, g \ge 0$, g *is non-decreasing. If* (2.7) *and* (2.11) *are satisfied, then the following inequality is satisfied.*

$$\frac{\int_a^b f^{\beta-\alpha}(x)\,d_qx}{\int_a^b f^{\alpha+\beta}(x)\,d_qx} \le \frac{\int_a^b f^{\beta}(x)\,g^{-\alpha}(x)\,d_qx}{\int_a^b f^{\alpha}(x)\,g^{\beta}(x)\,d_qx}. \tag{2.15}$$

Proof. Multiplying (2.10) and (2.12), we have

$$\int_a^b f^{\alpha}(x)\,g^{\beta}(x)\,d_qx \int_a^b f^{\beta-\alpha}(x)\,d_qx \le \int_a^b f^{\alpha+\beta}(x)\,d_qx \int_a^b f^{\beta}(x)\,g^{-\alpha}(x)\,d_qx\,,$$

and hence

$$\frac{\int_a^b f^{\beta-\alpha}(x)\,d_qx}{\int_a^b f^{\alpha+\beta}(x)\,d_qx} \le \frac{\int_a^b f^{\beta}(x)\,g^{-\alpha}(x)\,d_qx}{\int_a^b f^{\alpha}(x)\,g^{\beta}(x)\,d_qx}.$$

Theorem 2.9. *If* $p > 1$, $\frac{1}{p} + \frac{1}{q} = 1$ *and if* (2.7) *is satisfied, then the following inequalities hold*

$$\int_a^b f^{\alpha+\beta}(x)\,d_qx \le \frac{1}{2}\int_a^b \left(f^{\alpha}(x)\,g^{\beta}(x) + f^{\beta}(x)\,g^{\alpha}(x)\right)d_qx, \tag{2.16}$$

$$\int_a^b f(x)\,g(x)\,d_qx \le \frac{1}{p}\int_a^b f^{p}(x)\,d_qx + \frac{1}{q}\int_a^b f^{q}(x)\,d_xx\,, \tag{2.17}$$

$$\int_a^b f(x)\,g(x)\,d_qx \le \left(\int_a^b f^{p}(x)\,d_qx\right)^{1/p}\left(\int_a^b f^{q}(x)\,d_qx\right)^{1/q}, \tag{2.18}$$

$$\left(\int_a^b \left(f(x)+g(x)\right)^{p}\right)^{1/p} \le 2\left(\int_a^b f^{p}(x)\,d_qx\right)^{1/p}. \tag{2.19}$$

Proof. (2.16) follows from the inequality

$$\left(f^{\alpha}(x) - g^{\alpha}(x)\right)\left(f^{\beta}(x) - g^{\beta}(x)\right) \ge 0,$$

and the rest follows from AG, Holder's and Minkowski's inequalities respectively.

References

[1] N. S. Hoang, Notes on an inequality, J. Inequal. Pure and Appl. Math., 9 (2) (2009), Art. 42.

[2] V. Kac and P. Cheung, Quantum Calculus, Universitex, Springer-Verlag, New York, 2002.

[3] W. J. Liu, C. C. Li and J. W. Dong, On an problem concerning an integral inequality, J. inequal. Pure and Appl. Math. 8 (3) (2007), Art. 74.

[4] Yu Miao and Feng Qi, Several q-integral inequalities, J.Math. Ineq. 3(1) (2009), 115-121.

[5] Q. A. Ngo, D. D. Thang, T. T. Dat and D. A. Tuan, Notes on an integral inequality, J. Pure and Appl. Math., 7 (4) (2006), Art. 120.

[6] E. W. Weisstein, q-derivative, From Math World- A Wolfram Web Resource, Available online at http://mathworld.wolfram.com/q-Deriative.html.

[7] E. W. Weisstein, q-Integral, From Math World- A Wolfram Web Resource, Available online at http://mathworld.wolfram.com/q-Integral.html.

[8] G. Zabadan, Notes on an open problem, J. Ineq. Pure and Appl. Math., 9 (2) (2007), Art. 37.

JOURNAL OF APPLIED FUNCTIONAL ANALYSIS, VOL.6, NO.4, 324-330, COPYRIGHT 2011 EUDOXUS PRESS, LLC

An Extended Multiple Hardy-Hilbert's Integral Inequality

W. T. Sulaiman
Department of Computer Engineering, College of Engineering, University of Mosul. Iraq.

Abstract. New extended multiple Hardy-Hilbert's integral inequalities are presented.

1. Introduction

If $f, g \geq 0$ are such that

$$0 < \int_0^\infty f^2(x)\,dx < \infty, \quad 0 < \int_0^\infty g^2(x)\,dx < \infty,$$

then the famous Hilbert's integral inequality is given by

$$(1) \qquad \int_0^\infty \int_0^\infty \frac{f(x)\,g(y)}{x+y}\,dx\,dy < \pi \left(\int_0^\infty f^2(x)\,dx \int_0^\infty g^2(x)\,dx \right)^{1/2}.$$

where the constant factor π is the best possible (see [2]) . Inequality (1) has been generalized by Hardy-Riesz [1] as

If p>1, $\frac{1}{p} + \frac{1}{q} = 1$,

$$0 < \int_0^\infty f^p(x)\,dx < \infty, \quad 0 < \int_0^\infty g^q(x)\,dx < \infty,$$

then

$$(2) \qquad \int_0^\infty \int_0^\infty \frac{f(x)\,g(y)}{x+y}\,dx\,dy < \frac{\pi}{\sin(\pi/p)} \left(\int_0^\infty f^p(x)\,dx \right)^{1/p} \left(\int_0^\infty g^q(x)\,dx \right)^{1/q},$$

where the constant factor $\frac{\pi}{\sin(\pi/p)}$ is the best possible. The inequality (2) is called Hardy-Hilbert's integral inequality, and is important in analysis and its applications (see [3]).

Yang [4,5] has extended inequality (2) by proving the following

If $f, g \geq 0,\ p > 1,\ \frac{1}{p} + \frac{1}{q} = 1,\ \lambda > 2 - \min\{p, q\}$ are such that

$$0 < \int_0^\infty x^{1-\lambda} f^p(x)\,dx < \infty, \quad 0 < \int_0^\infty x^{1-\lambda} g^q(x)\,dx < \infty,$$

then the extended Hardy-Hilbert's inequality is given by

$$(3)\qquad \int_0^\infty\int_0^\infty \frac{f(x)\,g(y)}{(x+y)^\lambda}\,dx\,dy < k_\lambda(p)\left(\int_0^\infty t^{1-\lambda} f^p(t)\,dt\right)^{1/p}\left(\int_0^\infty t^{1-\lambda} g^q(t)\,dt\right)^{1/q},$$

and the constant $k_\lambda(p) = B\left(\frac{p+\lambda-2}{p}, \frac{q+\lambda-2}{q}\right)$, where B denotes the Beta function, is the best possible. The aim of this paper is to give new kinds of Hardy-Hilbert's integral inequalities.

We introduce the following symbols :

$$R_n^+ = \{x = (x_1,\dots,x_n) : x_1,\dots,x_n > 0\}$$

$$\|x\|_\alpha = \left(x_1^\alpha + \dots + x_n^\alpha\right)^{1/\alpha}, \quad \alpha > 0.$$

2. Results

We start with the following key Lemma

Lemma 2.1. *If* $c_i,\ p_i,\ q_i > 0,\ i = 1,\dots,n,$ *and* $\Psi(z)$ *is a measurable, then*

$$(4)\quad I = \int\cdots\int_E x_1^{q_1-1}x_2^{q_2-1}\dots x_n^{q_n-1}\,\Psi\left(\left(\frac{x_1}{c_1}\right)^{p_1} + \left(\frac{x_2}{c_2}\right)^{p_2} + \dots + \left(\frac{x_n}{c_n}\right)^{p_n}\right)dx_1\,dx_2\dots dx_n$$

$$\leq \frac{c_1^{q_1}c_2^{q_2}\dots c_n^{q_n}}{p_1 p_2 \cdots p_n}\,\frac{\Gamma\left(\frac{q_1}{p_1}\right)\Gamma\left(\frac{q_2}{p_2}\right)\dots\Gamma\left(\frac{q_n}{p_n}\right)}{\Gamma\left(\left(\frac{q_1}{p_1}\right) + \left(\frac{q_2}{p_2}\right) + \dots + \left(\frac{q_n}{p_n}\right)\right)}\int_0^h z^{\frac{q_1}{p_1}+\frac{q_2}{p_2}+\dots+\frac{q_n}{p_n}-1}\,\Psi(z)\,dz,$$

where

$$E = \left\{(x_1, x_2,\dots,x_n) : \left(\frac{x_1}{c_1}\right)^{p_1} + \left(\frac{x_2}{c_2}\right)^{p_2} + \dots + \left(\frac{x_n}{c_n}\right)^{p_n} \leq h,\quad x_1,\dots,x_n \geq 0\right\}.$$

Proof. Let $z = \left(\frac{x_1}{c_1}\right)^{p_1} + \left(\frac{x_2}{c_2}\right)^{p_2} + \dots + \left(\frac{x_n}{c_n}\right)^{p_n}$, then, we have

$$x_n = c_n\left(z - \left(\frac{x_1}{c_1}\right)^{p_1} - \left(\frac{x_2}{c_2}\right)^{p_2} - \dots - \left(\frac{x_{n-1}}{c_{n-1}}\right)^{p_{n-1}}\right)^{\frac{1}{p_n}},$$

$$dx_n = \frac{c_n}{p_n}\left(z - \left(\frac{x_1}{c_1}\right)^{p_1} - \left(\frac{x_2}{c_2}\right)^{p_2} - \dots - \left(\frac{x_{n-1}}{c_{n-1}}\right)^{p_{n-1}}\right)^{\frac{1}{p_n}-1} dz,$$

$$I = \frac{c_n^{q_n}}{p_n}\int_0^h \Psi(z)\int_0^{c_1 z^{\frac{1}{p_1}}} x_1^{q_1-1}\int_0^{c_2\left(z-\left(\frac{x_1}{p_1}\right)^{p_1}\right)^{\frac{1}{p_2}}} x_2^{q_2-1}\,\dots\dots\int_0^{c_{n-2}\left(z-\left(\frac{x_1}{c_1}\right)^{p_1}-\dots-\left(\frac{x_{n-3}}{c_{n-3}}\right)\right)^{\frac{1}{p_{n-2}}}} x_{n-2}^{q_{n-2}-1}\quad\times$$

$$\int_0^{c_{n-1}\left(z-\left(\frac{x_1}{c_1}\right)^{p_1}-\dots-\left(\frac{x_{n-2}}{c_{n-2}}\right)^{p_{n-2}}\right)^{\frac{1}{p_{n-1}}}} x_{n-1}^{q_{n-1}-1}\left(z-\left(\frac{x_1}{c_1}\right)^{p_1}-\dots-\left(\frac{x_{n-1}}{c_{n-1}}\right)^{p_{n-1}}\right)^{\frac{q_n}{p_n}-1} dx_{n-1}\dots dx_2\, dx_1\, dz$$

$$=\frac{c_n^{q_n}}{p_n}\int_0^h \Psi(z)\int_0^{c_1 z^{\frac{1}{p_1}}} x_1^{q_1-1}\int_0^{c_2\left(z-\left(\frac{x_1}{p_1}\right)^{p_1}\right)^{\frac{1}{p_2}}} x_2^{q_2-1}\,.....\int_0^{c_{n-2}\left(z-\left(\frac{x_1}{c_1}\right)^{p_1}-\dots-\left(\frac{x_{n-3}}{c_{n-3}}\right)^{p_{n-3}}\right)^{\frac{1}{p_{n-2}}}} x_{n-2}^{q_{n-2}-1}\qquad\times$$

$$\int_0^{c_{n-2}\left(z-\left(\frac{x_1}{c_1}\right)^{p_1}-\dots-\left(\frac{x_{n-3}}{c_{n-3}}\right)\right)^{\frac{1}{p_{n-2}}}} x_{n-2}^{q_{n-2}-1}\left(z-\left(\frac{x_1}{c_1}\right)^{p_1}-\dots-\left(\frac{x_{n-2}}{c_{n-2}}\right)^{p_{n-2}}\right)^{\frac{q_n}{p_n}-1}\times$$

$$\int_0^{c_{n-1}\left(z-\left(\frac{x_1}{c_1}\right)^{p_1}-\dots-\left(\frac{x_{n-2}}{c_{n-2}}\right)^{p_{n-2}}\right)^{\frac{1}{p_{n-1}}}} x_{n-1}^{q_{n-1}-1}\left(1-\frac{\left(\frac{x_{n-1}}{c_{n-1}}\right)^{p_{n-1}}}{z-\left(\frac{x_1}{c_1}\right)^{p_1}-\dots-\left(\frac{x_{n-2}}{c_{n-2}}\right)^{p_{n-2}}}\right)^{\frac{q_n}{p_n}-1} dx_{n-1}\, dx_{n-2}\dots dx_1 dz\,.$$

Now, denoting the last integral by I_1 and let

$$y=\left(\frac{x_{n-1}}{c_{n-1}}\right)^{p_{n-1}}\Big/\ z-\left(\frac{x_1}{c_1}\right)^{p_1}-\dots-\left(\frac{x_{n-2}}{c_{n-2}}\right)^{p_{n-2}}$$

to obtain

$$I_1=\frac{c_{n-1}^{q_{n-1}}}{p_{n-1}}\left(z-\left(\frac{x_1}{c_1}\right)^{p_1}-\dots-\left(\frac{x_{n-2}}{c_{n-2}}\right)^{p_{n-2}}\right)^{\frac{q_{n-1}}{p_{n-1}}}\int_0^1 y^{\frac{q_{n-1}}{p_{n-1}}-1}(1-y)^{\frac{q_n}{p_n}-1}\,dy.$$

Therefore

$$I=\frac{c_n^{q_n}c_{n-1}^{q_{n-1}}}{p_n p_{n-1}}\frac{\Gamma\left(\frac{q_n}{p_n}\right)\Gamma\left(\frac{q_{n-1}}{p_{n-1}}\right)}{\Gamma\left(\frac{q_n}{p_n}+\frac{q_{n-1}}{p_{n-1}}\right)}\int_0^h\Psi(z)\int_0^{c_1 z^{\frac{1}{p_1}}} x_1^{q_1-1}\int_0^{c_2\left(z-\left(\frac{x_1}{p_1}\right)^{p_1}\right)^{\frac{1}{p_2}}} x_2^{q_2-1}\,.....\int_0^{c_{n-2}\left(z-\left(\frac{x_1}{c_1}\right)^{p_1}-\dots-\left(\frac{x_{n-3}}{c_{n-3}}\right)\right)^{\frac{1}{p_{n-2}}}} x_{n-2}^{q_{n-2}-1}\qquad\times$$

$$.....\int_0^{c_{n-2}\left(z-\left(\frac{x_1}{c_1}\right)^{p_1}-\dots-\left(\frac{x_{n-3}}{c_{n-3}}\right)\right)^{\frac{1}{p_{n-2}}}} x_{n-2}^{q_{n-2}-1}\left(z-\left(\frac{x_1}{c_1}\right)^{p_1}-\dots-\left(\frac{x_{n-2}}{c_{n-2}}\right)^{p_{n-2}}\right)^{\frac{q_n}{p_n}+\frac{q_{n-1}}{p_{n-1}}-1} dx_{n-2}\,....dx_2 dx_1 dz$$

Proceeding in this manner, we have

$$I=\frac{c_n^{q_n}c_{n-1}^{q_{n-1}}\dots c_2^{q_2}}{p_n p_{n-1}\dots p_2}\frac{\Gamma\left(\frac{q_n}{p_n}\right)\Gamma\left(\frac{q_{n-1}}{p_{n-1}}\right)\dots\Gamma\left(\frac{q_2}{p_2}\right)}{\Gamma\left(\frac{q_n}{p_n}+\frac{q_{n-1}}{p_{n-1}}+\dots+\frac{q_2}{p_2}\right)}\int_0^h\Psi(z)\int_0^{c_1 z^{\frac{1}{p_1}}} x_1^{q_1-1}\left(z-\left(\frac{x_1}{c_1}\right)^{p_1}\right)^{\frac{q_n}{p_n}+\dots\frac{q_2}{p_2}-1} dx_1\,dz\,.$$

Let $(x_1/c_1)^{p_1} = zt$. Then ,

$$I_2 := \int_0^{c_1 z^{\frac{1}{p_1}}} x_1^{q_1-1}\left(z-\left(\frac{x_1}{c_1}\right)^{p_1}\right)^{\frac{q_n}{p_n}+...+\frac{q_2}{p_2}-1} dx_1 = \frac{c_1^{q_1}}{p_1} z^{\frac{q_n}{p_n}+....+\frac{q_1}{p_1}-1}\int_0^1 t^{\frac{q_1}{p_1}-1}(1-t)^{\frac{q_n}{p_n}+...+\frac{q_2}{p_2}-1}\,dt$$

$$= \frac{c_1^{q_1}}{p_1} z^{\frac{q_n}{p_n}+....+\frac{q_1}{p_1}-1} B\left(\frac{q_1}{p_1}, \frac{q_n}{p_n}+...+\frac{q_2}{p_2}\right).$$

The result follows and the proof is complete.

The following is the main result

Theorem 2.2. *If* $p_i > 1$, $\sum_{i=1}^{n}\frac{1}{p_i} = 1$, $n \in Z_+$, $\alpha > 0$, $f_i \geq 0$, $\lambda = 1+\sum_{i=1}^{n}\lambda_i$, $\lambda_i > 0$, $(n-\lambda_i)p_i < n+1$, then

$$(5) \qquad \int_{R_n^+}...\int_{R_n^+}\frac{f_1(x_1)....f_n(x_n)}{\left(\|x_1\|_\alpha + ... + \|x_n\|_\alpha\right)^\lambda}dx_1...dx_n \leq \frac{1}{\Gamma(\lambda)}\prod_{i=1}^{n} K_i\left(\int_{R_n^+}\|x_i\|_\alpha^{(n-\lambda_i)p_i-n-1} f_i^{p_i}(x_i)\,dx\right)^{1/p_i},$$

where

$$K_i = \left(\alpha\, n^{-\alpha}\frac{\Gamma^n(1/\alpha)\Gamma(n)}{\Gamma(n/\alpha)}\right)^{1-1/p_i}\Gamma^{1/p_i}\left((\lambda_i - n)p_i + n + 1\right).$$

Provided the integrals on the RHS do exist.

Proof. Define

$$G_i(t) = \int_{R_n^+} e^{-t\|x_i\|_\alpha} f_i(x_i)\,dx_i\ .$$

Then, we have

$$J := \int_0^\infty t^{\lambda-1}G_1(t)...G_n(t)\,dt$$

$$= \int_0^\infty t^{\lambda-1}\int_{R_n^+} e^{-t\|x_1\|_\alpha} f_1(x_1)\,dx_1 ... \int_{R_n^+} e^{-t\|x_n\|_\alpha} f_n(x_n)\,dx_n\,dt$$

$$= \int_{R_n^+}...\int_{R_n^+} f_1(x_1)\,...\,f_n(x_n)\,dx_1...dx_n\int_0^\infty t^{\lambda-1}e^{-t\left(\|x_1\|_\alpha+...+\|x_n\|_\alpha\right)}dt$$

Let $t\left(\|x_1\|_\alpha + ... + \|x_n\|_\alpha\right) = v$, gives

$$J = \int_{R_n^+}...\int_{R_n^+}\frac{f_1(x_1)\,...\,f_n(x_n)}{\left(\|x_1\|_\alpha + ... + \|x_n\|_\alpha\right)^\lambda}dx_1...dx_n\int_0^\infty v^{\lambda-1}e^{-v}dv$$

$$(6) \qquad = \Gamma(\lambda)\int_0^\infty...\int_0^\infty\frac{f_1(x_1)...f_n(x_n)}{\left(\|x_1\|_\alpha + ... + \|x_n\|_\alpha\right)^\lambda}dx_1...dx_n\,.$$

On the other hand

$$J = \int_0^\infty t^{\lambda_1} G_1(t) \ldots t^{\lambda_n} G_n(t)\, dt$$
$$\leq \left(\int_0^\infty t^{\lambda_1 p_1} G_1^{p_1}(t)\, dt \right)^{1/p_1} \ldots \left(\int_0^\infty t^{\lambda_n p_n} G_n^{p_n}(t)\, dt \right)^{1/p_n}$$
$$= \prod_{i=1}^n \left(\int_0^\infty t^{\lambda_i p_i} G_i^{p_i}(t)\, dt \right)^{1/p_i}.$$

Now,

$$\int_0^\infty t^{\lambda_i p_i} G_i^{p_i}(t)\, dt = \int_0^\infty t^{\lambda_i p_i} \left(\int_{R_n^+} e^{-t\|x_i\|_\alpha} f_i(x_i)\, dx_i \right)^{p_i} dt$$
$$\leq \int_0^\infty t^{\lambda_i p_i} \left(\int_{R_n^+} e^{-t\|x_i\|_\alpha} f_i^{p_i}(x_i)\, dx_i \right) \left(\int_{R_n^+} e^{-t\|x_i\|_\alpha}\, dx_i \right)^{p_i - 1} dt .$$

By making use of Lemma 2.1 with $h = \infty$, we have

$$J_1 := \int_{R_n^+} e^{-t\|x_i\|_\alpha}\, dx_i = n^{-\alpha} \frac{\Gamma^n(1/\alpha)}{\Gamma(n/\alpha)} \int_0^\infty e^{-tu^{\frac{1}{\alpha}}} u^{\frac{n}{\alpha}-1}\, du$$
$$= \alpha^{1-n}\, t^{-n} \frac{\Gamma^n(1/\alpha)}{\Gamma(n/\alpha)} \int_0^\infty u^{n-1} e^{-u}\, du = \alpha^{1-n}\, t^{-n} \frac{\Gamma^n(1/\alpha)\Gamma(n)}{\Gamma(n/\alpha)}.$$

Therefore

$$\int_0^\infty t^{\lambda_i p_i} G_i^{p_i}(t)\, dt \leq \left(\alpha^{1-n} \frac{\Gamma^n(1/\alpha)\Gamma(n)}{\Gamma(n/\alpha)} \right)^{p_i - 1} \int_0^\infty t^{\lambda_i p_i - n(p_i - 1)} \left(\int_{R_n^+} e^{-t\|x_i\|_\alpha} f_i^{p_i}(x_i)\, dx_i \right) dt$$
$$= \left(\alpha^{1-n} \frac{\Gamma^n(1/\alpha)\Gamma(n)}{\Gamma(n/\alpha)} \right)^{p_i - 1} \int_{R_n^+} f_i^{p_i}(x_i)\, dx_i \int_0^\infty e^{-t\|x_i\|_\alpha} t^{(\lambda_i - n)p_i + n}\, dt$$
$$= \left(\alpha^{1-n} \frac{\Gamma^n(1/\alpha)\Gamma(n)}{\Gamma(n/\alpha)} \right)^{p_i - 1} \int_{R_n^+} \|x_i\|_\alpha^{(n-\lambda_i)p_i - n - 1} f_i^{p_i}(x_i)\, dx_i \int_0^\infty t^{(\lambda_i - n)p_i + n} e^{-t}\, dt$$

(7) $$= \left(\alpha^{1-n} \frac{\Gamma^n(1/\alpha)\Gamma(n)}{\Gamma(n/\alpha)} \right)^{p_i - 1} \Gamma((\lambda_i - n)p_i + n + 1) \int_{R_n^+} \|x_i\|_\alpha^{(n-\lambda_i)p_i - n - 1} f_i^{p_i}(x_i)\, dx_i ,$$

which implies

(8) $J \leq$

$$\prod_{i=1}^n \left(\alpha^{1-n} \frac{\Gamma^n(1/\alpha)\Gamma(n)}{\Gamma(n/\alpha)} \right)^{1-1/p_i} \Gamma^{1/p_i}((\lambda_i - n)p_i + n + 1) \left(\int_{R_n^+} \|x_i\|_\alpha^{(n-\lambda_i)p_i - n - 1} f_i^{p_i}(x_i)\, dx_i \right)^{1/p_i}$$

Combining (6) and (8), the result follows. This completes the proof.

We need the following Lemma for the coming result

Lemma 2.3. *Let* $a_i \geq 0$, $p_i > 1$, $i = 1,\ldots,n$, *and let* $\sum_{i=1}^n \frac{1}{p_i} = 1$, then

(9) $$\prod_{i=1}^{m} a_i \le \sum_{i=1}^{m} \frac{a_i^{p_i}}{p_i}.$$

Proof. We have to use mathematical induction. For $m = 2$, the inequality is well-known. Suppose it is true for $m = n-1$. That is

$$\prod_{n=1}^{n-1} a_i \le \sum_{i=1}^{n-1} \frac{a_i^{p_i}}{p_i}, \quad \text{provided} \quad \sum_{i=1}^{n-1} 1/p_i = 1.$$

Now, as

$$\sum_{i=1}^{n} \tfrac{1}{p_i} = 1 \Rightarrow \sum_{i=1}^{n-1} \tfrac{1}{p_i} + \tfrac{1}{p_n} = 1 \Rightarrow \sum_{i=1}^{n-1} \frac{1}{\frac{p_n-1}{p_n} p_i} = 1, \quad \tfrac{1}{p_n} + \frac{1}{\frac{p_n}{p_n-1}} = 1,$$

then we have

$$\prod_{i=1}^{n} a_i = \left(\prod_{i=1}^{n-1} a_i\right) a_n \le \left(\sum_{i=1}^{n-1} \frac{a_i^{\frac{p_n-1}{p_n} p_i}}{\frac{p_n-1}{p_n} p_i}\right) a_n = \tfrac{p_n}{(p_n-1)} \sum_{i=1}^{n-1} a_i^{\frac{p_n-1}{p_n} p_i} a_n$$

$$\le \tfrac{p_n}{(p_n-1)p_i} \sum_{i=1}^{n-1} \left(\tfrac{p_n-1}{p_n p_i} \left(a_i^{\frac{p_n-1}{p_n} p_i} \right)^{\frac{p_n}{p_n-1}} + \tfrac{1}{p_n} a_n^{p_n} \right)$$

$$= \sum_{i=1}^{n-1} \frac{a_i^{p_i}}{p_i} + \frac{a_n^{p_n}}{p_n} = \sum_{i=1}^{n} \frac{a_i^{p_i}}{p_i}.$$

Theorem 2.4. *If* $p_i > 1$, $\sum_{i=1}^{n} \frac{1}{p_i} = 1$, $n \in Z_+$, $\alpha > 0$, $f_i \ge 0$, $\lambda = 1 + \sum_{i=1}^{n} \lambda_i$, $(n-\lambda_i) p_i < n+1$, then

$$\int_{R_n^+} \cdots \int_{R_n^+} \frac{f_1(x_1) \dots f_n(x_n)}{\left(\|x_1\|_\alpha + \dots + \|x_n\|_\alpha\right)^{\lambda}} dx_1 \dots dx_n \le \frac{1}{\Gamma(\lambda)} \sum_{i=1}^{n} C_i \int_{R_n^+} \|x_i\|_\alpha^{(n-\lambda_i)p_i - n-1} f_i^{p_i}(x_i)\, dx_i,$$

where

$$C_i = \frac{1}{p_i} \left(\alpha^{1-n} \frac{\Gamma^n(1/\alpha)\Gamma(n)}{\Gamma(n/\alpha)} \right)^{p_i - 1} \Gamma\big((\lambda_i - n)p_i + n + 1\big),$$

provided the integrals on the RHS do exist.

Proof. By virtue of Lemma 2.3,

$$J = \int_0^\infty t^{\lambda_1} G_1(t) \dots t^{\lambda_n} G_n(t)\, dt$$

$$\le \int_0^\infty \sum_{i=1}^{n} \frac{t^{\lambda_i p_i} G^{p_i}(t)}{p_i} dt = \sum_{i=1}^{n} \int_0^\infty \frac{t^{\lambda_i p_i} G^{p_i}(t)}{p_i} dt,$$

and the above, by (7), implies

(10) $J \le$

$$\sum_{i=1}^{n}\frac{1}{p_i}\left(\alpha^{1-n}\,\frac{\Gamma^n(1/\alpha)\Gamma(n)}{\Gamma(n/\alpha)}\right)^{p_i-1}\Gamma((\lambda_i-n)p_i+n+1)\int_{R_n^+}\|x_i\|_\alpha^{(n-\lambda_i)p_i-n-1}\,f_i^{\,p_i}(x_i)\,dx_i\,.$$

The result follows by combining (6) and (10) .

References

[1] G. H.Hardy, Note on a theorem of Hilbert concerning series of positive terms, Proc. Math. Soc., 23(2) (1925), Records of Proc. XLV-XLVI.

[2] G.H.Hardy, J.E.Littlewood and G.Polya, Inequalities,Cambridge University Press, Cambridge, UK, 1952.

[3] D.S.Mitrinovic, J.E.Pecaric and A.M.Fink, Inequalities Involving Functions and their Integrals and Derivatives, Kluwer Academic Publisher, Bosten, 1991.

[4] B. Yang, On a generalization of Hardy-Hilbert's integrel inequality with a best value Chinese Ann. Math. Ser A 21 (2000) 401-408.

[5] B. Yang, On Hardy-Hilbert's integral inequality, J Math. Anal. Appl. 26 (2001) 295-306.

JOURNAL OF APPLIED FUNCTIONAL ANALYSIS, VOL.6, NO.4, 331-342, COPYRIGHT 2011 EUDOXUS PRESS, LLC

On the Green Function of the Operator $\left(\circledcirc_B + m^4\right)^k$ Related to the Bessel Helmoltz Operator and the Bessel Klien-Gordon Operator.

Wanchak Satsanit

Department of Mathematics,
Regina Coeli College,
166 Charoenprathet Road
Changkran Chiang Mai, 50100 Thailand.
E-mail : aunphue@live.com

Abstract

In this paper, we study the operator $(\circledcirc_B + m^4)^k$ which is iterated $k-$times and m is positive real number. At first we find the Green function of the operator $(\circledcirc_B + m^4)^k$ and after that we apply such a Green function to solve the solution of the equation $(\circledcirc_B + m^4)^k K(x) = f(x)$ where $f(x)$ is a generalized function and $K(x)$ is an unknown function for $x \in \mathbb{R}^n$.

Key Words: Bessel Helmoltz operator, Bessel Klien-Gordon operator, Tempered distribution.

AMS Subject Classification: 44A35, 46F10

1 Introduction

Consider the Ultra-hyperbolic operator iterated $k-$ times is deined by

$$\Box^k = \left(\frac{\partial^2}{\partial x_1^2} + \frac{\partial^2}{\partial x_2^2} + \cdots + \frac{\partial^2}{\partial x_p^2} - \frac{\partial^2}{\partial x_{p+1}^2} - \frac{\partial^2}{\partial x_{p+2}^2} - \cdots - \frac{\partial^2}{\partial x_{p+q}^2}\right)^k, \tag{1.1}$$

S.E. Trione [See 7] has shown that the generalized function $R_{2k}^H(x)$ is defined by (2.2) is the unique solution of the operator $\Box^k$, that is $\Box^k R_{2k}^H(x) = \delta(x)$ where $x \in \mathbb{R}^n$, the

$n-$ dimensional Euclidian space. Also M. Agirre Tellez [See 2, pp.147-149] has proved that $R^H_{2k}(x)$ exists only if n is an odd with p odd.

We also know that the function $R^e_{2k}(x)$ is defined by (2.4) is an elementary solution of the Laplace operator iterated $k-$ times and is defined by

$$\triangle^k = \left(\frac{\partial^2}{\partial x_1^2} + \frac{\partial^2}{\partial x_2^2} + \ldots + \frac{\partial^2}{\partial x_n^2}\right)^k, \tag{1.2}$$

that is $\triangle^k(-1)^k R^e_{2k}(x) = \delta(x)$ where $x \in \mathbb{R}^n$.

Next, Hüseyin Yildirim, M.Zeki Sarikaya and Sermin Öztürk [see 8] first introduced the Bessel Diamond operator iterated $k-$times, and is defined by

$$\diamondsuit^k_B = \left(\left(\sum_{i=1}^{p} B_{x_i}\right)^2 - \left(\sum_{j=p+1}^{p+q} B_{x_j}\right)^2\right)^k \tag{1.3}$$

where $B_{x_i} = \frac{\partial^2}{\partial x_i^2} + \frac{2v_i}{x_i}\frac{\partial}{\partial x_i}$, $2v_i = 2\alpha_i + 1, \alpha_i > -\frac{1}{2}, x_i > 0$. The operator $\diamondsuit^k_B$ can be expressed by $\diamondsuit^k_B = \triangle^k_B \Box^k_B = \Box^k_B \triangle^k_B$, where

$$\triangle^k_B = \left(\sum_{i=1}^{p} B_{x_i}\right)^k \tag{1.4}$$

and

$$\Box^k_B = \left(\sum_{i=1}^{p} B_{x_i} - \sum_{j=p+1}^{p+q} B_{x_j}\right)^k. \tag{1.5}$$

And,Hüseyin Yildirim, M.Zeki Sarikaya and Sermin Öztürk [see 7] has shown that the solution of the convolution form $u(x) = (-1)^k S_{2k}(x) * R_{2k}(x)$ is a unique elementary solution of the $\diamondsuit^k_B$ operator that is

$$\diamondsuit^k_B((-1)^k S_{2k}(x) * R_{2k}(x)) = \delta,$$

where $S_{2k}(x)$ and $R_{2k}(x)$ are defined by (2.7) and (2.8) respectively with $\alpha = \gamma = 2k$.

Furthermore, W.Satsanit [See 6] has first introduced the operator $\circledcirc^k_B$ iterated $k-$

times and can be write

$$
\begin{aligned}
\circledcirc_B^k &= \left[\left(\sum_{i=1}^{p} B_{x_i^2}\right)^2 + \left(\sum_{j=p+1}^{p+q} B_{x_j^2}\right)^2\right]^k \\
&= \left[\left(\frac{\triangle_B + \Box_B}{2}\right)^2 + \left(\frac{\triangle_B - \Box_B}{2}\right)^2\right]^k \\
&= \left(\frac{\triangle_B^2 + \Box_B^2}{2}\right)^k. \qquad (1.6)
\end{aligned}
$$

where $\triangle_B$ and $\Box_B$ are defined by (1.4) and (1.5) respectively with $k = 2$.

The purpose of this work is to study the operator $(\circledcirc_B + m^4)^k$ and the operator can be express in the form $(\circledcirc_B + m^4)^k$

$$
\begin{aligned}
\left(\circledcirc_B + m^4\right)^k &= \left(\frac{\triangle_B^2 + \Box_B^2}{2} + m^4\right)^k \\
&= \left(\frac{1}{2}\left(\triangle_B^2 + m^4\right) + \frac{1}{2}\left(\Box_B^2 + m^4\right)\right)^k \\
&= \left(\frac{1}{2}\left(\triangle_B + m^2\right)^2 - m^2\left(\Box_B + \triangle_B\right) + \frac{1}{2}\left(\Box_B + m^2\right)^2\right)^k, \qquad (1.7)
\end{aligned}
$$

where $\Box_B + m^2$ is the Bessel Klein-Gordon operator and $\triangle_B + m^2$ is the Bessel Helmoltz operator and are defined by

$$\Box_B + m^2 = \sum_{i=1}^{p} \frac{\partial^2}{\partial {x_i}^2} - \sum_{j=p+1}^{p+q} \frac{\partial^2}{\partial {x_j}^2} + m^2 \qquad (1.8)$$

and

$$\triangle_B + m^2 = \sum_{i=1}^{n} \frac{\partial^2}{\partial {x_i}^2} + m^2 \qquad (1.9)$$

Firstly, we find the Green function of the operator $(\circledcirc_B + m^4)^k$ from the equation

$$\left(\circledcirc_B + m^4\right)^k G(x) = \delta(x), \qquad (1.10)$$

where $G(x)$ is the Green function, $\delta(x)$ is the Dirac-delta distribution, k is a nonnegative integer.

Finally, we apply such a Green function to find the solution of the equation

$$\left(\circledcirc_B + m^4\right)^k K(x) = f(x), \qquad (1.11)$$

where $f(x)$ is a generalized function and $K(x)$ is an unknown function.

Before finding the Green function of (1.10), the following definitions and concepts are needed.

2 Preliminaries

Definition 2.1 Let $x = (x_1, x_2, ..., x_n)$ be a point of the n-dimensional Euclidean space $\mathbb{R}^n$. Denoted by

$$\upsilon = x_1^2 + x_2^2 + ... + x_p^2 - x_{p+1}^2 - x_{p+2}^2 - ... - x_{p+q} \tag{2.1}$$

the nondegenerated quadratic form and $p + q = n$ is the dimension of the space $\mathbb{R}^n$.

Let $\Gamma_+ = \{x \in \mathbb{R}^n : x_1 > 0 \text{ and } u > 0\}$ is the interior of forward cone and $\overline{\Gamma}_+$ denotes its closure. For any complex number α, define the function

$$R_\alpha^H(\upsilon) = \begin{cases} \frac{\upsilon^{\frac{\alpha-n}{2}}}{K_n(\alpha)}, & \text{for } x \in \Gamma_+, \\ 0, & \text{for } x \notin \Gamma_+, \end{cases} \tag{2.2}$$

where the constant $K_n(\alpha)$ is given by the formula

$$K_n(\alpha) = \frac{\pi^{\frac{n-1}{2}}\Gamma(\frac{2+\alpha-n}{2})\Gamma(\frac{1-\alpha}{2})\Gamma(\alpha)}{\Gamma(\frac{2+\alpha-p}{2})\Gamma(\frac{p-\alpha}{2})}. \tag{2.3}$$

The function $R_\alpha^H(\upsilon)$ is called the Ultra-hyperbolic kernel of Marcel Riesz and was introduced by Y. Nozaki [see 3].

It is well known that $R_\alpha^H(u)$ is an ordinary function if $Re(\alpha) \geq n$ and is a distribution of α if $Re(\alpha) < n$. Let supp $R_\alpha^H(\upsilon)$ denote the support of $R_\alpha^H(u)$ and suppose supp $R_\alpha^H(u) \subset \bar{\Gamma}_+$, that is supp $R_\alpha^H(\upsilon)$ is compact.

Definition 2.2 Let $x = (x_1, x_2, ..., x_n)$ be a point of $\mathbb{R}^n$ and the function $R_\alpha^e(\omega)$ denoted the elliptic kernel of Marcel Riesz and is defined by

$$R_\alpha^e(\omega) = \frac{\omega^{\frac{\alpha-n}{2}}}{H_n(\alpha)} \tag{2.4}$$

where

$$\omega = x_1^2 + x_2^2 + ... + x_n^2 \tag{2.5}$$

$$H_n(\alpha) = \frac{\pi^{\frac{n}{2}} 2^{\alpha} \Gamma\left(\frac{\alpha}{2}\right)}{\Gamma\left(\frac{n-\alpha}{2}\right)} \tag{2.6}$$

α is a complex parameter and n is the dimension of $\mathbb{R}^n$.

Definition2.3 Let $x = (x_1, x_2, \ldots, x_n), \nu = (\nu_1, \nu_2, \ldots, \nu_n) \in \mathbb{R}_n^+$. For any complex number α, we define the function $S_\alpha(x)$ by

$$S_\alpha(x) = \frac{2^{n+2|\nu|-2\alpha}\Gamma(\frac{n+2|\nu|-\alpha}{2})|x|^{\alpha-n-2|\nu|}}{\prod_{i=1}^{n} 2^{\nu_i - \frac{1}{2}}\Gamma(\nu_i + \frac{1}{2})} \tag{2.7}$$

Definition 2.4 Let $x = (x_1, x_2, \ldots, x_n), \nu = (\nu_1, \nu_2, \ldots, \nu_n) \in \mathbb{R}_n^+$, and $V = x_1^2 + x_2^2 + \cdots + x_p^2 - x_{p+1}^2 - x_{p+2}^2 - \cdots - x_{p+q}^2$ is the nondegenerated quadratic form. Denote the interior of the forward cone by $\Gamma_+ = \{x \in \mathbb{R}_n^+ : x_1 > 0, x_2 > 0, \ldots, x_n > 0, V > 0\}$. The function $R_\gamma(x)$ is defined by

$$R_\gamma(x) = \frac{V^{\frac{\gamma-n-2|\nu|}{2}}}{K_n(\gamma)}. \tag{2.8}$$

where

$$K_n(\gamma) = \frac{\pi^{\frac{n+2|\nu|-1}{2}}\Gamma\left(\frac{2+\gamma-n-2|\nu|}{2}\right)\Gamma\left(\frac{1-\gamma}{2}\right)\Gamma(\gamma)}{\Gamma\left(\frac{2+\gamma-p-2|\nu|}{2}\right)\Gamma\left(\frac{p-2|\nu|-\gamma}{2}\right)},$$

and γ is a complex number.

Definition 2.5 Let $x = (x_1, x_2, \ldots, x_n) \in \mathbb{R}_n^+$, For any complex number α, we define the function

$$T_\alpha(x) = \sum_{r=0}^{\infty} \frac{(-1)^r \Gamma\left(\frac{\eta}{2} + r\right)}{r!\Gamma\left(\frac{\eta}{2}\right)} (m^2)^r (-1)^{\frac{\alpha}{2}+r} S_{\alpha+2r}(x), \tag{2.9}$$

where η is a complex number and $S_{\alpha+2r}(x)$ is defined in definition 2.3.

Definition 2.6 Let $x = (x_1, x_2, \ldots, x_n)$, For any complex number β, we define the function

$$W_\beta(x) = \sum_{r=0}^{\infty} \frac{(-1)^r \Gamma\left(\frac{\eta}{2} + r\right)}{r!\Gamma\left(\frac{\eta}{2}\right)} (m^2)^r R_{\beta+2r}(x), \tag{2.10}$$

where η is a complex number and $R_{\beta+2r}(x)$ is defined in definition 2.4.

Lemma 2.1 *Given the equation* $\triangle_B^k u(x) = \delta(x)$ *for* $x \in \mathbb{R}_n^+$, *where* $\triangle_B^k$ *is defined by (1.5). Then*

$$u(x) = (-1)^k S_{2k}(x)$$

where $S_{2k}(x)$ *is defined by (2.7), with* $\alpha = 2k$.
We obtain $(-1)^k R_{2k}^e(x)$ *is an elementary solution of the operator* $\triangle_B^k$.*That is*

$$\triangle_B^k (-1)^k S_{2k}(x) = \delta(x) \tag{2.11}$$

Proof., [See 8, p.379]. □

Lemma 2.2 *Given the equation* $\square_B^k u(x) = \delta(x)$ *for* $x \in \mathbb{R}_n^+$, *where* $\square_B^k$ *is defined by (1.5). Then*

$$u(x) = R_{2k}(x)$$

where $R_{2k}(x)$ *is defined by (2.8), with* $\gamma = 2k$
We obtain $R_{2k}(x)$ *is an elementary solution of the operator* $\square_B^k$.*That is*

$$\square_B^k R_{2k}(x) = \delta(x) \tag{2.12}$$

Proof. [See 8, p.379]. □

Lemma 2.3 *Let* $S_\alpha(x)$*and* $R_\beta(x)$ *be the function defined by (2.1) and (2.2) respectively.Then*

$$S_\alpha(x) * S_\beta(x) = S_{\alpha+\beta}(x)$$

and

$$R_\beta(x) * R_\alpha(x) = R_{\beta+\alpha}(x)$$

where α *and* β *are a positive even number.*
Proof.*[See 9], [See 1, pp.171-190] .* □

Lemma 2.4 *Given the equation*

$$\left(\triangle_B + m^2\right)^k u(x) = \delta(x), \tag{2.13}$$

for $x \in \mathbb{R}_n^+$ *and* $(\triangle_B + m^2)^k$ *is the Bessel Helmholtz operator iterated* $k-$*times defined by (1.9) then*

$$u(x) = T_{2k}(x)$$

is an elementary solution or Green function of the Bessel Helmholtz operator where $T_{2k}(x)$ *is defined by (2.9) with* $\alpha = 2k$.

Proof. [See 3, pp.10-19].

Lemma 2.5 *Given the equation*

$$\left(\square_B + m^2\right)^k u(x) = \delta(x), \tag{2.14}$$

for $x \in \mathbb{R}_n^+$ *and* $\left(\square_B + m^2\right)^k$ *is the Bessel Klein-Gordon operator iterated* $k-$*times defined by (1.8) then*

$$u(x) = W_{2k}(x)$$

is an elementary solution or Green function of the Bessel Klein-Gordon operator where $W_{2k}(x)$ *is defined by (2.10) with* $\beta = 2k$.

Proof. [See 3, pp.10-19].

Lemma 2.6 *Let* $T_{2k}(x)$ *and* $W_{2k}(x)$ *be defined by (2.3) and (2.4) respectively,where* $\alpha = \beta = 2k$. *Then the convolution* $T_{2k}(x) * W_{2k}(x)$ *exist and it is lie in* $\mathcal{S}'$, *where* $\mathcal{S}'$ *is a space of tempered distribution.*

Proof. From (2.3) and (2.4) with $\alpha = \beta = 2k$, we have

$$\begin{aligned} T_{2k}(x) * W_{2k}(x) &= \left(\sum_{r=0}^{\infty} \frac{(-1)^r \Gamma(k+r)}{r! \Gamma(k)} (m^2)^r (-1)^{k+r} S_{2k+2r}(x)\right) \\ &\quad * \left(\sum_{r=0}^{\infty} \frac{(-1)^r \Gamma(k+r)}{r! \Gamma(k)} (m^2)^r R_{2k+2r}(x)\right) \\ &= \sum_{r=0}^{\infty} \sum_{s=0}^{\infty} \frac{(-1)^s \Gamma(k+s)}{s! \Gamma(k)} (m^2)^s \cdot \frac{(-1)^r \Gamma(k+r)}{r! \Gamma(k)} (m^2)^r \cdot \\ &\qquad (-1)^{k+r} S_{2k+2r}(x) * R_{2k+2r}(x). \end{aligned}$$

Hüseyin Yildirim, M. Zeki Sarikaya and Sermin Öztürk [See 8, p.380] has shown that $S_{2k+2r}(x) * R_{2k+2r}(x)$ exists and is a tempered distribution. It follows that $T_{2k}(x) * W_{2k}(x)$ exists and also is a tempered distribution. $\square$

Lemma 2.7 *Let* $T_4(x)$ *and* $W_4(x)$ *be defined by (2.9) and (2.10) respectively where* $\alpha = \beta = 4$. *Then*

$$\left(\square_B + \triangle_B\right)\left(T_4(x) * W_4(x)\right) = T_2(x) * W_2(x) * \left(\left(T_2(x) + W_2(x) - 2m^2 \left(T_2(x) * W_2(x)\right)\right)\right.$$

Proof.

$$
\begin{aligned}
(\Box_B + \triangle_B)(T_4(x) * W_4(x)) &= \Box_B (T_4(x) * W_4(x)) + \triangle_B (T_4(x) * W_4(x)) \\
&= (\Box_B W_2(x)) * (T_4(x) * W_2(x)) + \\
&\qquad (\triangle_B T_2(x)) * (T_2(x) * W_4(x)) .
\end{aligned}
$$

By Lemma 2.4 and Lemma 2.5, for $k = 1$ we have

$$\left(\triangle_B + m^2\right) T_2(x) = \delta(x) \quad or \quad \triangle_B T_2(x) = \delta(x) - m^2 T_2(x) \tag{2.15}$$

and

$$\left(\Box_B + m^2\right) W_2(x) = \delta(x) \quad or \quad \Box_B W_2(x) = \delta(x) - m^2 W_2(x). \tag{2.16}$$

By (2.15) and (2.16) , we obtain

$$
\begin{aligned}
(\Box_B + \triangle_B)(T_4(x) * W_4(x)) &= \left(\delta(x) - m^2 W_2(x)\right) * T_4(x) * W_2(x) \\
&+ \left(\delta(x) - m^2 T_2(x)\right) * (T_2(x) * W_4(x)) \\
&= T_4(x) * W_2(x) - m^2 T_4(x) * W_4(x) \\
&+ T_2(x) * W_4(x) - m^2 T_4(x) * W_4(x) \\
&= T_2(x) * W_2(x) * (T_2(x) + W_2(x)) \\
&- 2m^2 T_2(x) * W_2(x)
\end{aligned}
$$

Thus

$$
\begin{aligned}
(\Box_B + \triangle_B)(T_4(x) * W_4(x)) &= T_2(x) * W_2(x) * \\
&\qquad \left(T_2(x) + W_2(x) - 2m^2 (T_2(x) * W_2(x))\right) .
\end{aligned}
$$

That complete this proof. □

3 Main Results

Theorem 3.1 *Given the equation*

$$\left(\circledcirc_B + m^4\right)^k G(x) = \delta(x), \tag{3.1}$$

where $(\circledcirc_B + m^4)^k$ *is the operator iterated* $k-$ *times defined by (1.7),* $\delta(x)$ *is the Dirac delta distribution,* $x = (x_1, x_2, \ldots, x_n) \in \mathbb{R}_n^+$ *and* k *is a nonnegative integer. Then we obtain*

$$G(x) = (T_{4k}(x) * W_{4k}(x)) * \left(C^{*k}(x)\right)^{*-1} \tag{3.2}$$

is a Green function for the operator $(\circledcirc_B + m^4)^k$ *iterated* $k-$*times where* $\circledcirc_B$ *is defined by (1.6),* m *is a nonnegative real number and*

$$C(x) = \frac{1}{2}T_4(x) - m^2\left(T_2(x) * W_2(x) * (T_2(x) + W_2(x)) - 2m^2\left(T_2(x) * W_2(x)\right)\right) + \frac{1}{2}W_4(x) \tag{3.3}$$

$C^{*k}(x)$ *denotes the convolution of* $C(x)$ *itself* $k-$*times ,* $\left(C^{*k}(x)\right)^{*-1}$ *denotes the inverse of* $C^{*k}(x)$ *in the convolution algebra. Moreover* $G(x)$ *is a tempered distribution.*

Proof. From (1.7)

$$\left(\circledcirc_B + m^4\right) = \left(\frac{1}{2}\left(\square_B + m^2\right)^2 - m^2\left(\square_B + \triangle_B\right) + \frac{1}{2}\left(\triangle_B + m^2\right)^2\right)^k$$

Taking account into (3.1) we obtain

$$\left(\frac{1}{2}\left(\square_B + m^2\right)^2 - m^2\left(\square_B + \triangle_B\right) + \frac{1}{2}\left(\triangle_B + m^2\right)^2\right)^k G(x) = \delta(x)$$

or we can write

$$\left(\frac{1}{2}\left(\square_B + m^2\right)^2 - m^2\left(\square_B + \triangle_B\right) + \frac{1}{2}\left(\triangle_B + m^2\right)^2\right) \cdot \\ \left(\frac{1}{2}\left(\square_B + m^2\right)^2 - m^2\left(\square_B + \triangle_B\right) + \frac{1}{2}\left(\triangle_B + m^2\right)^2\right)^{k-1} G(x) = \delta(x). \tag{3.4}$$

By Lemma 2.6 with $k = 2$, we have $T_4(x) * W_4(x)$ exists and is a tempered distribution. Convolving both sides of the above equation by $T_4(x) * W_4(x)$, we obtain

$$\left(\frac{1}{2}\left(\square_B + m^2\right)^2 - m^2\left(\square_B + \triangle_B\right) + \frac{1}{2}\left(\triangle_B + m^2\right)^2\right)\left(T_4(x) * W_4(x)\right) * \\ \left(\frac{1}{2}\left(\square_B + m^2\right)^2 - m^2\left(\square_B + \triangle_B\right) + \frac{1}{2}\left(\triangle_B + m^2\right)^2\right)^{k-1} G(x) = \\ \delta(x) * T_4(x) * W_4(x)$$

or

$$(\frac{1}{2}\left(\square_B + m^2\right)^2\left(T_4(x) * W_4(x)\right) - m^2\left(\square_B + \triangle_B\right)\left(T_4(x) * W_4(x)\right) \\ + \frac{1}{2}\left(\triangle_B + m^2\right)^2\left(T_4(x) * W_4(x)\right)) * (\frac{1}{2}\left(\square_B + m^2\right)^2 - m^2\left(\square_B + \triangle_B\right) \\ + \frac{1}{2}\left(\triangle_B + m^2\right)^2)^{k-1} G(x) = T_4(x) * W_4(x). \tag{3.5}$$

By Lemma 2.1 and Lemma 2.2, for $k=2$ we have

$$\left(\Box_B+m^2\right)^2 W_4(x)=\delta(x) \;\; and \;\; \left(\triangle_B+m^2\right)^2 T_4(x)=\delta(x),$$

and by Lemma 2.7 we have

$$\left(\Box_B+\triangle_B\right)\left(T_4(x)*W_4(x)\right)=T_2(x)*W_2(x)*\left(T_2(x)+W_2(x)-2m^2\left(T_2(x)*W_2(x)\right)\right)$$

Hence the equation (3.5) becomes

$$\left(\frac{1}{2}T_4(x)-m^2\left(T_2(x)*W_2(x)*\left(T_2(x)+W_2(x)\right)-2m^2\left(T_2(x)*W_2(x)\right)\right)+\frac{1}{2}W_4(x)\right)*$$
$$\left(\frac{1}{2}\left(\Box_B+m^2\right)^2-m^2\left(\Box_B+\triangle_B\right)+\frac{1}{2}\left(\triangle_B+m^2\right)^2\right)^{k-1}G(x)=T_4(x)*W_4(x)$$

or

$$C(x)*\left(\frac{1}{2}\left(\Box_B+m^2\right)^2-m^2\left(\Box_B+\triangle_B\right)+\frac{1}{2}\left(\triangle_B+m^2\right)^2\right)^{k-1}G(x)=T_4(x)*W_4(x).$$

Keeping on convolving both sides of the above equation by $T_4(x)*W_4(x)$ up to $k-1$ times, we obtain

$$C^{*k}(x)*G(x)=\left(T_4(x)*W_4(x)\right)^{*k}.$$

The symbol $*k$ denotes the convolution of itself $k-$times. By Lemma 2.3, we obtain

$$\left(T_4(x)*W_4(x)\right)^{*k}=T_{4k}(x)*W_{4k}(x).$$

Thus,

$$C^{*k}(x)*G(x)=T_{4k}(x)*W_{4k}(x). \tag{3.6}$$

Now, consider the function $C^{*k}(x)$, since $\delta(x)$, $T_4(x)$, $W_4(x)$ and $T_4(x)*W_4(x)$ are lies in S' where S' is a space of tempered distribution, then $C(x)\in S'$. Moreover by Donoghue[See 6, p.152] we obtain $C^{*k}(x)\in S'$.

Since $T_{4k}(x)*W_{4k}(x)\in S'$, choose $S'\subset D'_R$ where D'_R is the right-side distribution which is a subspace of D' of distribution.

Thus $T_{4k}(x)*W_{4k}(x)\in D'_R$, it follows that $T_{4k}(x)*W_{4k}(x)$ is an element of convolution algebra, that is by method of Zemanian[See 10, pp.150-151], we have (3.6) has a unique solution

$$G(x)=T_{4k}(x)*W_{4k}(x)*\left(C^{*k}(x)\right)^{*-1} \tag{3.7}$$

, where $\left(C^{*k}(x)\right)^{*-1}$ is an inverse of $C^{*k}(x)$ in the convolution algebra, $G(x)$ is called the Green function of the operator $\left(\circledcirc_B + m^4\right)^k$. Since $T_{4k}(x) * W_{4k}(x)$ and $\left(C^{*k}(x)\right)^{*-1}$ are lie in S', then by Donoghue[See 4, p.152] again, we have $T_{4k}(x) * W_{4k}(x)$ and $\left(C^{*k}(x)\right)^{*-1} \in S'$. Hence $G(x)$ is a tempered distribution.

Theorem 3.2 *(An application of green function)*

Given the equation

$$\left(\circledcirc_B + m^4\right)^k K(x) = f(x) \tag{3.8}$$

where $f(x)$ is a generalized function, $K(x)$ is an unknown function and $x \in \mathbb{R}_n^+$. Then

$$K(x) = G(x) * f(x)$$

is a unique solution of the equation (3.8) where $G(x)$ is a Green function for the operator $\left(\circledcirc_B + m^4\right)^k$.

Proof. By convolving both sides of (3.8) by $G(x)$ where $G(x)$ is a Green function for the operator $\left(\circledcirc_B + m^4\right)^k$ in theorem 3.1. we have

$$G(x) * \left(\circledcirc + m^4\right)^k K(x) = G(x) * f(x)$$

$$\left(\circledcirc_B + m^4\right)^k G(x) * K(x) = G(x) * f(x)$$

$$\delta(x) * K(x) = G(x) * f(x).$$

Thus,

$$K(x) = G(x) * f(x).$$

Sine $G(x)$ is unique, by theorem 3.1. It follows that $K(x) = G(x) * f(x)$ is unique.

Acknowledgement

The authors would like to thank Dr. Chalermpon Bunpog, Department of Mathematics, Faculty of Science, Chiang Mai University, for many helpful discussion and also the Thailand Research Fund and Graduate School, Chiang Mai University, Thailand for financial support.

References

[1] M. Aguirre Tellez. *Some properties of Bessel Elliptic kernel and Bessel ultra-hyperbolic kernel*, Thai Journal of Matematics ,Volume 6(2008) Number 1.P 171-190.

[2] M. Aguirre Tellez. *The Distribution Hankel transform of Marcel Riesz's ultra-hyperbolic kernel*, Studies in Applied Matematics 93: 133-162(1994) Massachusetts Institute of Technology, Elsevier Science, Inc.

[3] C. Bunpog, A. Kananthai. *On the Bessel diamond operator*, Journal of Applied Functional Analysis. Volume 4, No.1, 2009, 10-19.

[4] W.F. Donoghue.*Distributions and Fourier transform*, Academic Press, (1969).

[5] Y. Nozaki. *On Riemamn-Liouville integral of Ultra-hyperbolic type*, Kodai Mathematical Seminar Reports, 6(2), 69-87 (1964).

[6] W. Satsanit, A.Kananthai. *On the Green function of the Bessel* $\oplus_B^k$ *operator*, Journal of Advanced Research in Differential Equation, Vol. 2, Issue. 1, 2010, 10-29.

[7] S.E. Trione. *On Marcel Riesz's Ultra-hyperbolic Kernel*, Trabojos de Mathematica, 116 preprint, 1987.

[8] H.Yildirim, M.Zeki Sarikaya and Sermin Öztürk. *The solution of the n-dimensional Bessel diamond operator and the Fourier-Bessel transform of their convolution*, Proc. Indian Acad. Sci. (Math. Sci.) Vol. 114, No.4, November 2004, 375–387.

[9] M.Zeki Sarikaya and H. Yildirim.*On the operator* $\oplus_B^k$ *related to the Bessel-wave equation and Laplacian-Bessel*, Advances in Inequality for special function , Edited by Cerone , P. and Dragomir ,S.S.,(2008) .

[10] A.H. Zemanian. *Distribution Theory and Transform Analysis*, McGraw-Hill, New York, (1965).

JOURNAL OF APPLIED FUNCTIONAL ANALYSIS, VOL.6, NO.4, 343-355, COPYRIGHT 2011 EUDOXUS PRESS, LLC

ON UNCONDITIONAL ATOMIC DECOMPOSITIONS IN BANACH SPACES

S.K. KAUSHIK[1] AND S.K. SHARMA[2]
[1] Department of Mathematics, Kirori Mal College, University of Delhi, Delhi 110 007, India
E-mail: shikk2003@yahoo.co.in
[2] Department of Mathematics, University of Delhi, Delhi 110 007, India
E-mail: sumitkumarsharma@gmail.com

Abstract. Unconditional atomic decompositions in Banach spaces have been defined and studied. It has been proved that a separable Banach space, with a subspace whose conjugate space is weakly complete and non-separable, has no unconditional atomic decomposition. Also, we proved that $L^1[0,1]$ has no unconditional atomic decomposition. Finally, two characterizations of unconditional atomic decompositions have been given.

1. Introduction

Duffin and Schaeffer [8] were first to introduce frames for the Hilbert spaces. Later, in 1986, Daubechies, Grossmann and Meyer [7] reintroduced frames and found a new application to wavelets and Gabor transforms.

Some generalizations of frames for Hilbert spaces have been proposed and studied, namely frame of subspaces [2], pseudo frames [20], bounded quasi-projectors [13, 14], oblique frames [4, 10], g-frames [22]. Frames for Banach spaces were studied in [17, 18] and their generalizations in [19].

Coifman and Weiss [6] introduced the notion of atomic decompositions for certain function spaces. Atomic decompositions have played an important role in wavelet theory and Gabor theory. Frazier and Jawerth [15] constructed wavelet atomic decompositions for Besov spaces and called them ϕ transforms.

2000 *Mathematics Subject Classification.* 42C15, 42A38.
Key words and phrases. Atomic Decompositions, Banach Frames.

Feichtinger [11] constructed Gabor atomic decompositions for the modulation spaces which are Banach spaces similar in many respects to Besov spaces, defined by smoothness and decay condition. Atomic decompositions were further studied in [3, 5, 16].

In the present paper, we define unconditional atomic decompositions and proved that a separable Banach space, with a subspace whose conjugate space is weakly complete and non-separable, has no unconditional atomic decomposition. Also, it has been proved that a Banach space containing subspace with property (P) has no unconditional atomic decomposition and as a corollary it has been deduced that $L^1[0,1]$ has no unconditional atomic decomposition. Further Λ-atomic decompositions have been defined and proved that they are same as unconditional atomic decompositions. Finally, a characterization of unconditional atomic decompositions has been given.

2. Preliminaries

Throughout the paper, E will denote an infinite dimensional Banach space over the scalar field $\mathbb{K}(\mathbb{R}$ or $\mathbb{C})$, E^* and E^{**}, respectively, the first and second conjugate spaces of E, E_d an associated Banach space of scalar-valued sequences, indexed by $\mathbb{N}$, $[f_n]$ the closed linear span of $\{f_n\}$ and $\widetilde{[f_n]}$ the closed linear span of $\{f_n\}$ in the $\sigma(E^*,E)$-topology. A sequence $\{f_n\} \subset E^*$ is said to be complete if $[f_n] = E^*$ and total if $\{x \in E : f_n(x) = 0, n \in \mathbb{N}\} = \{0\}$. A series $\sum\limits_{i=1}^{\infty} x_i$ in a Banach space E is called $\sigma(E,E^*)$-unconditional Cauchy or weakly unconditionally Cauchy, if $\sum\limits_{i=1}^{\infty} |f(x_i)| < \infty$, for all $f \in E^*$. Also, a series $\sum\limits_{i=1}^{\infty} f_i$ in a conjugate Banach space E^* is called $\sigma(E^*,E)$-unconditional Cauchy if $\sum\limits_{i=1}^{\infty} |f_i(x)| < \infty$, for all $x \in E$. A Banach space E is said to satisfy property

(P) if there exists a subspace F of E^* such that for each $\phi \in E^*$ there exists a sequence $\{\beta_n\} \subset F$ satisfying $\phi(x) = \lim_{n\to\infty} \beta_n(x), x \in E$ and $\lim_{n\to\infty} \psi(\beta_n)$ exists for each $\psi \in E^{**}$, is non-separable.

Definition 2.1 ([12])**.** Let E be a Banach space and let E_d be an associated Banach space of scalar-valued sequences, indexed by $\mathbb{N}$. Let $\{x_n\}$ be a sequence in E and let $\{f_n\}$ be a sequence in E^*. Then, the pair $(\{f_n\}, \{x_n\})$ is called an atomic decomposition for E with respect to E_d if

(a) $\{f_n(x)\} \in E_d$, $x \in E$

(b) there exist constants A, B with $0 < A \leq B < \infty$ such that

$$A\|x\|_E \leq \|\{f_n(x)\}\|_{E_d} \leq B\|x\|_E, \quad x \in E$$

(c) $x = \sum_{n=1}^{\infty} f_n(x)x_n$, $x \in E$.

The positive constants A, B are called atomic bounds for the atomic decomposition $(\{f_n\}, \{x_n\})$.

The following results are referred in this paper and are listed in the form of lemmas

Lemma 2.2 ([18])**.** *If E is a Banach space and $\{f_n\} \subset E^*$ is total over E, then E is linearly isometric to the associated Banach space $E_d = \{\{f_n(x)\} : x \in E\}$, where the norm is given by $\|\{f_n(x)\}\|_{E_d} = \|x\|_E$, $x \in E$.*

Lemma 2.3. *Let $\{g_n\}$ be a sequence in $E^*, D_n = \{1, 2, \ldots, n\} \subset \mathbb{N}, n \in \mathbb{N}$ and $\{a_n\}$ be a sequence of scalars such that $a_i = \pm 1, i \in D_n, n \in \mathbb{N}$. Let $C > 0$ be a constant such that $\left\| \sum_{i \in D_n} a_i g_i \right\| \leq C$, $n \in \mathbb{N}$. Then $\sum_{i=1}^{\infty} g_i$ is $\sigma(E^*, E^{**})$-unconditional Cauchy.*

Proof. For any $h \in E^{**}$, define

$$a_i = \begin{cases} \text{sign Real } \ h(g_i), & \text{if Real } \ h(g_i) \neq 0 \\ 1, & \text{otherwise}. \end{cases}$$

Then $a_i = \pm 1$, for all $i \in \mathbb{N}$. Therefore, by hypotheses, we have

$$\begin{aligned} \sum_{i \in D_n} |\text{Real } h(g_i)| &= \text{Real } h\Big(\sum_{i \in D_n} a_i g_i\Big) \\ &\leq \left| h\Big(\sum_{i \in D_n} a_i g_i\Big)\right| \leq C\|h\|. \end{aligned}$$

Thus $\sum\limits_{i=1}^{\infty} |\text{Real } h(g_i)| < \infty$. Similarly, we have $\sum\limits_{i=1}^{\infty} |\text{Imaginary } h(g_i)| < \infty$. Therefore

$$\sum_{i=1}^{\infty} |h(g_i)| \leq \sum_{i=1}^{\infty} |\text{Real } h(g_i)| + \sum_{i=1}^{\infty} |\text{Imaginary } h(g_i)| < \infty.$$

Hence $\sum\limits_{i=1}^{\infty} g_i$ is $\sigma(E^*, E^{**})$-unconditional Cauchy. $\square$

3. Main results

Definition 3.1. Let E be a Banach space and let E_d be an associated Banach space of scalar-valued sequences, indexed by $\mathbb{N}$. Let $\{x_n\}$ be a sequence in E and $\{f_n\}$ be a sequence in E^*. Then, $(\{f_n\}, \{x_n\})$ is said to be an unconditional atomic decomposition for E with respect to E_d if

(1) $\{f_{\sigma(n)}(x)\} \in E_d$, $x \in E$ and σ is any permutation of $\mathbb{N}$

(2) there exist constants A, B with $0 < A \leq B < \infty$ such that

$A\|x\|_E \leq \|\{f_{\sigma(n)}(x)\}\|_{E_d} \leq B\|x\|_E$, $x \in E$ and σ is any permutation of $\mathbb{N}$

(3) $\sum\limits_{i=1}^{\infty} f_i(x) x_i$ converges unconditionally to x in E.

The positive constants A, B are called atomic bounds for the unconditional atomic decomposition $(\{f_n\}, \{x_n\})$.

Regarding existence of unconditional atomic decompositions, we give the following examples

Example 3.2. Let $E = c_0$, $\{e_n\}$ be the sequence of unit vectors in E and $\{f_n\}$ be the sequence of unit vectors in E^*.

(a) By Lemma 2.2, there exists an associated Banach space $E_d = \{\{f_n(x)\} : x \in E\}$ with $\|\{f_n(x)\}\|_{E_d} = \|x\|_E$, $x \in E$. Then, $(\{f_n\}, \{x_n\})$ is an unconditional atomic decomposition for E with respect to E_d.

(b) Define $\{x_n\} \subset E$ and $\{g_n\} \subset E^*$ by

$$x_n = \{\underbrace{1, 1, \ldots, 1}_{n\text{-times}}, 0, 0, \ldots\},$$

$$g_n = \{0, 0, \ldots, \underset{n\text{th position}}{\underset{\downarrow}{1}}, \underset{(n+1)\text{th position}}{\underset{\downarrow}{-1}}, 0, \ldots\}, \ n \in \mathbb{N}.$$

Then, $(\{g_n\}, \{x_n\})$ is an atomic decomposition for E with respect to $E_d = \{\{g_n(x)\} : x \in E\}$. Further

$$\begin{aligned} \sum_{i=m}^{m+p} g_i(x) x_i &= \sum_{i=m}^{m+p} g_i(x) \sum_{j=1}^{i} e_j \\ &= \left(\sum_{i=m}^{m+p} g_i(x)\right) \left(\sum_{j=1}^{m} e_j\right) \\ &\quad + \left(\sum_{i=m+1}^{m+p} g_i(x)\right) (e_{m+1}) + \ldots + g_{m+p}(x) e_{m+p}. \end{aligned}$$

Therefore, we have

$$\left\| \sum_{i=m}^{m+p} g_i(x) x_i \right\| = \sup_{m \le k \le m+p} \left| \sum_{i=k}^{m+p} g_i(x) \right|.$$

Thus, $\sum\limits_{i=1}^{\infty} g_i(x) x_i$ converges if and only if $\sum\limits_{i=1}^{\infty} g_i(x)$ converges. Note that, for $x = \left(0, \frac{1}{2}, 0, \frac{1}{3}, 0, \frac{1}{4}, \ldots\right) \in E$, $\sum\limits_{i=1}^{\infty} g_i(x)$ is conditionally convergent. Hence $\sum\limits_{i=1}^{\infty} g_i(x) x_i$ is conditionally convergent.

Also, we prove the following result concerning existence of unconditional atomic decompositions

Theorem 3.3. *Let E be a separable Banach space containing a subspace F with F^* weakly complete and non-separable. Then, E has no unconditional atomic decomposition.*

Proof. Assume that E has an unconditional atomic decomposition, $(\{f_n\},\{x_n\})$ $(\{f_n\}\subset E^*, \{x_n\}\subset E)$. Let $\phi_n = f_n|_F$, $n\in\mathbb{N}$. Let $\phi\in F^*$ be any arbitrary functional and $f\in E^*$ be an extension of ϕ to E. Since $\sum\limits_{i=1}^{\infty} f_i(x)x_i$ converges unconditionally to x, we have

$$\left(\sum_{i=1}^{\infty} f(x_i)f_i\right)(x) = f(x), \quad f\in E^*.$$

Hence $\sum\limits_{i=1}^{\infty} f(x_i)f_i$ is $\sigma(E^*,E)$-unconditional Cauchy. Define

$$p_n(x) = \sum_{i=1}^{n} |f(x_i)f_i(x)|, \quad x\in E \text{ and } n\in\mathbb{N}.$$

Then, $\{p_n\}$ is a sequence of continuous non-linear functionals on E. So, by Lemma 13, page 53 in [9], there exists a constant $C>0$ such that

$$\sum_{i=1}^{n} |f(x_i)f_i(x)| \le C\|x\|, \quad x\in E \text{ and } n\in\mathbb{N}.$$

This gives

$$|\sum_{i=1}^{n} \beta_i f(x_i)f_i(x)| \le \sum_{i=1}^{n} |f(x_i)f_i(x)| \le C\|x\|, \quad x\in E,$$

where $\{\beta_n\}$ is a sequence of scalars such that $|\beta_n|\le 1, n\in\mathbb{N}$.

So for $\alpha_i = 0$ or $1, i=1,2,\ldots,n$, there exists a constant $C>0$ such that

$$\left\|\sum_{i=1}^{n} \alpha_i f(x_i)f_i\right\| \le C, \qquad \text{for all } n\in\mathbb{N}.$$

Let $\varepsilon_i = \pm 1$, $i=1,2,3\ldots n$. Then, for all $n\in\mathbb{N}$

$$\left\|\sum_{i=1}^{n} \varepsilon_i f(x_i)f_i\right\| \le \left\|\sum_{i=1}^{n} \alpha_i f(x_i)f_i\right\| + \left\|\sum_{i=1}^{n} \alpha_i' f(x_i)f_i\right\|,$$

where $\alpha_i = 1$, $\alpha_i' = 0$ if $\varepsilon_i = 1$ and $\alpha_i = 0$, $\alpha_i' = 1$ if $\varepsilon_i = -1$. Therefore

$$\left\|\sum_{i=1}^{n} \varepsilon_i f(x_i)\phi_i\right\| \le \left\|\sum_{i=1}^{n} \varepsilon_i f(x_i)f_i\right\| \le C, \quad \varepsilon_i = \pm 1, \quad i=1,2,\ldots,n,\ n\in\mathbb{N}.$$

Hence by Lemma 2.3, the series $\sum\limits_{i=1}^{\infty} f(x_i)\phi_i$ is $\sigma(F^*, F^{**})$-unconditional Cauchy. Since F^* is weakly complete, $\sum\limits_{i=1}^{\infty} f(x_i)\phi_i$ is $\sigma(F^*, F^{**})$-convergent to $\psi \in F^*$. Further

$$\sum_{i=1}^{\infty} f(x_i)\phi_i(x) = \sum_{i=1}^{\infty} f(x_i)f_i(x) = \phi(x), \quad x \in F\,.$$

Thus $\left\{ \sum\limits_{i=1}^{n} f(x_i)\phi_i \right\}$ is $\sigma(F^*, F^{**})$-convergent to ϕ. Since $\phi \in F^*$ is arbitrary, this proves that F^* is separable, which is a contradiction. $\square$

Next, we prove a result regarding the existence of an unconditional atomic decomposition in a separable Banach space containing a subspace having property (P).

Theorem 3.4. *A separable Banach space containing a subspace having property* (P) *has no unconditional atomic decomposition.*

Proof. Assume that E is a separable Banach space having an unconditional atomic decomposition $(\{f_n\}, \{x_n\})$ $(\{f_n\} \subset E^*, \{x_n\} \subset E)$. Let F be a subspace of E having property (P). For each $n \in \mathbb{N}$, define $\phi_n = f_n|_F$ and $B = [\phi_n]$. Then, B is a separable subspace of F^*. Let $\phi_0 \in F^*$ be arbitrary and let $f_0 \in E^*$ be an extension of ϕ_0 to E. Since $(\{f_n\}, \{x_n\})$ is an unconditional atomic decomposition of E, $\sum\limits_{n=1}^{\infty} f_0(x_n)f_n$ is $\sigma(E^*, E)$-unconditionally convergent to f_0. Define

$$\beta_n = \sum_{i=1}^{n} f_0(x_i)\phi_i, \quad n \in \mathbb{N}.$$

Then, $\{\beta_n\}$ is a sequence in B such that for each $y \in F$,

$$\lim_{n\to\infty} \beta_n(y) = \lim_{n\to\infty} \sum_{i=1}^{n} f_0(x_i)\phi_i(y) = \phi_0(y).$$

Also, as in the proof of Theorem 3.3, the series $\sum_{i=1}^{\infty} f_0(x_i)\phi_i$ is $\sigma(F^*, F^{**})$-unconditional Cauchy, i.e., $\lim_{n\to\infty} \phi(\beta_n)$ exists for each $\phi \in F^{**}$. This is a contradiction. □

Corollary 3.5. $L^1[0,1]$ has no unconditional atomic decomposition.

Proof. Since the Banach space $L^1[0,1]$ has property (P) [1, 21], the result follows in view of Theorem 3.4. □

The following theorem gives a necessary condition for a weak Cauchy sequence in a Banach space having an unconditional atomic decomposition

Theorem 3.6. *Let E be a Banach space and $(\{f_n\}, \{x_n\})$ $(\{f_n\} \subset E^*, \{x_n\} \subset E)$ be an unconditional atomic decomposition for E. Then, for every weak Cauchy sequence $\{z_n\} \subset E$, there exists a sequence $\{y_n\} \subset E$, such that $\sum_{i=1}^{\infty} y_i$ is weakly unconditionally Cauchy.*

Proof. Assume that $\|x_n\| = 1$, $n \in \mathbb{N}$. Let $\{z_n\}$ be any weak Cauchy sequence in E and $\alpha_i = \lim_{n\to\infty} f_i(z_n)$, $i = 1, 2, \ldots$. Define $y_n = \alpha_n x_n$, $n \in \mathbb{N}$. Then, for every $f \in E^*$, the series $\sum_{i=1}^{\infty} f(x_i) f_i$ is $\sigma(E^*, E)$-unconditional convergent to f. Therefore, as in the proof of Theorem 3.2, for every $f \in E^*$ there exists a constant $C > 0$ such that

$$\left\| \sum_{i=1}^{n} \varepsilon_i f(x_i) f_i \right\| \leq C, \qquad \text{for all } \ n \in \mathbb{N} \ \text{ and } \ |\varepsilon_i| \leq 1\,.$$

Further, since

$$\begin{aligned}
\sum_{i=1}^{n} |f(y_i)| &= \sum_{i=1}^{n} f|\alpha_i x_i| \\
&= \lim_{k\to\infty} \sum_{i=1}^{n} [\text{sign } f(x_i)\alpha_i] f(x_i) f_i(z_k) \\
&\leq \left\| \sum_{i=1}^{n} [\text{sign } f(x_i)\alpha_i] f(x_i) f_i \right\| \left(\sup_{1\leq k<\infty} \|z_k\| \right) \\
&\leq C \sup_{1\leq k<\infty} \|z_k\| < \infty, \qquad f \in E^*, \quad n = 1, 2, 3, \ldots,
\end{aligned}$$

we conclude that

$$\sum_{i=1}^{\infty} |f(y_i)| < \infty, \quad f \in E^* . \qquad \square$$

Next, we obtain a characterization for unconditional atomic decompositions in terms of Λ-atomic decompositions which are defined as

Definition 3.7. Let E be a Banach space and E_d be an associated Banach space of scalar-valued sequences, indexed by $\mathbb{N}$ and $\Lambda = \{\{i_1, i_2, \ldots, i_n\} \subset \mathbb{N} : n \in \mathbb{N}\}$. Let $\{x_n\}$ be a sequence in E and $\{f_n\}$ be a sequence in E^*. Then, $(\{f_n\}, \{x_n\})$ is said to be Λ-atomic decomposition of E with respect to E_d if

(1) $\{f_n(x)\} \in E_d$, $x \in E$

(2) there exist constants A, B with $0 < A \leq B < \infty$ such that

$$A\|x\|_E \leq \|\{f_n(x)\}\|_{E_d} \leq B\|x\|_E, \ x \in E$$

(3) $\lim\limits_{d \in \Lambda} \sum\limits_{i \in d} f_i(x) x_i = x$, $x \in E$.

Theorem 3.8. *Let E be a Banach space, $\{x_n\} \subset E$ and $\{f_n\} \subset E^*$. Then, $(\{f_n\}, \{x_n\})$ is an unconditional atomic decomposition for E with respect to some associated Banach space E_d if and only if $(\{f_n\}, \{x_n\})$ is Λ-atomic decomposition for E with respect to E_d.*

Proof. Let $\varepsilon_0 > 0$ be such that for every $d \in \Lambda$, there exists $d' \in \Lambda$ with $d' \supset d$ and $\left\| x - \sum\limits_{i \in d'} f_i(x) x_i \right\| \geq \varepsilon_0$. Since $x = \sum\limits_{i=1}^{\infty} f_i(x) x_i$, there exists a positive integer n_0 such that $\left\| x - \sum\limits_{i=1}^{n} f_i(x) x_i \right\| < \dfrac{\varepsilon_0}{2}$, for all $n \geq n_0$. Let $d_1 = \{1, 2, \ldots, n_0\}$ and $d_1' \in \Lambda$ with $d_1' \supset d_1$ be such that $\left\| x - \sum\limits_{i \in d_1'} f_i(x) x_i \right\| \geq \varepsilon_0$. Let $d_2 = \{1, 2, 3, \ldots, \max\limits_{i \in d_1'} i\}$ and $d_2' \in \Lambda$ with $d_2' \supset d_2$ be such that $\left\| x - \sum\limits_{i \in d_2'} f_i(x) x_i \right\| \geq \varepsilon_0$. Continuing this way, we get $d_3, d_3', d_4, d_4' \ldots$ with $d_i' \supset d_i$, $i = 1, 2, \ldots$. Define $\{\sigma_n\} \subset \mathbb{N}$, enumerating the elements of the sets

$d_1, d_1' \setminus d_1, d_2 \setminus d_1', d_2' \setminus d_2 \ldots$. Then, for each $n \in \mathbb{N}$, we have

$$\left\| \sum_{i \in d_n' \setminus d_n} f_i(x) x_i \right\| \geq \left| \left\| x - \sum_{i \in d_n} f_i(x) x_i \right\| - \left\| x - \sum_{i \in d_n'} f_i(x) x_i \right\| \right| \geq \frac{\varepsilon_0}{2}.$$

So, the series $\sum\limits_{n=1}^{\infty} f_{\sigma_n}(x) x_{\sigma_n}$ is not convergent, which is a contradiction. The converse part follows from the definition. □

Finally, we give the following characterization of unconditional atomic decompositions

Theorem 3.9. *Let E be a Banach space, $\{x_n\} \subset E$ and $\{f_n\} \subset E^*$. Then, $(\{f_n\}, \{x_n\})$ is an unconditional atomic decomposition for E with respect to some associated Banach space E_d if and only if for every $x \in E$, $\sum\limits_{i=1}^{\infty} |f(x_i)||f_i(x)|$ converges uniformly with respect to $f \in E^*$, $\|f\| \leq 1$.*

Proof. In view of Theorem 3.8, $(\{f_n\}, \{x_n\})$ is Λ-atomic decomposition for E with respect to E_d. Let $\varepsilon > 0$ be given. Then, there exists a set $d \in \Lambda$ such that $\left\| x - \sum\limits_{i \in d'} f_i(x) x_i \right\| < \dfrac{\varepsilon}{4}$ for all $d' \in \Lambda$ with $d' \supset d$. Put $n_0 = \max\limits_{i \in d} i$. For $n \geq n_0$, $m \geq 1$ and $f \in E^*$ with $\|f\| < 1$, define

$$d_1(f) = \{i \in \{n+1, n+2, \ldots, n+m\} : \text{Real } f(x_i) f_i(x) \geq 0\},$$
$$d_2(f) = \{i \in \{n+1, n+2, \ldots, n+m\} : \text{Real } f(x_i) f_i(x) < 0\}$$

Then, for every $x \in E$, we have

$$\begin{aligned}
\sum_{i=n+1}^{n+m} |\text{Real } f(x_i) f_i(x)| &= \sum_{j=1}^{2} \sum_{i \in d_j(f)} |\text{Real } f(x_i) f_i(x)| \\
&= \sum_{j=1}^{2} \left| \text{Real } f\Big(\sum_{i \in d_j(f)} f_i(x) x_i \Big) \right| \\
&\leq \sum_{j=1}^{2} \left\| \sum_{i \in d_j(f)} f_i(x) x_i \right\|
\end{aligned}$$

$$\begin{aligned} &\leq \sum_{j=1}^{2}\Big\|x-\sum_{i\in d\cup d_j(f)} f_i(x)x_i\Big\| + \Big\|x-\sum_{i\in d} f_i(x)x_i\Big\| \\ &< \frac{\varepsilon}{2}\,. \end{aligned}$$

By similar arguments, we obtain

$$\sum_{i=n+1}^{n+m} |\text{Imaginary } f(x_i)f_i(x)| < \frac{\varepsilon}{2}\,.$$

Hence for every $x \in E$, we have

$$\sum_{i=n+1}^{n+m} |f(x_i)f_i(x)| < \varepsilon\,.$$

Conversely, let $\{\beta_i\} \subset \mathbb{K}$ with $|\beta_i| \leq 1$, $i = 1,2,\ldots$, $n \geq 1$, $m \geq 1$. Then, there exists $f_{n,m} \in E^*$ with $\|f_{n,m}\| = 1$ such that

$$\begin{aligned} \Big\|\sum_{i=n+1}^{n+m} \beta_i f_i(x)x_i\Big\| &= \Big\|f_{n,m}\Big(\sum_{i=n+1}^{n+m}\beta_i f_i(x)x_i\Big)\Big\| \\ &\leq \sum_{i=n+1}^{n+m} |f_i(x)|\,|f_{n,m}(x_i)| \\ &< \varepsilon, \quad n \geq n_0 \text{ and } m = 1,2,3,\ldots\,. \end{aligned}$$

Therefore, for every $\{\beta_i\} \subset \mathbb{K}$ with $|\beta_i| \leq 1$, $i = 1,2,\ldots$, $\sum\limits_{i=1}^{\infty}\beta_i f_i(x)x_i$ converges. Hence for every $\{\varepsilon_i\} \subset \mathbb{K}$ with $\varepsilon_i = \pm 1$, $i = 1,2,3,\ldots$, $\sum\limits_{i=1}^{\infty}\varepsilon_i f_i(x)x_i$ converges. Let $\theta = \{\{i_n\} \subset \mathbb{N} : i_1 < i_2 < i_3 \ldots\}$ and let $\{i_j\} \in \theta$, $n \geq 1$ and $m \geq 1$. Then,

$$\sum_{j=n+1}^{n+m} f_{i_j}(x)x_{i_j} = \frac{1}{2}\left(\sum_{i=r}^{r+k}\varepsilon_i f_i(x)x_i + \sum_{i=r}^{r+k}\varepsilon'_i f_i(x)x_i\right),$$

where $r = i_{n+1}$, $r+k = i_{n+m}$, $\varepsilon_{i_j} = \varepsilon'_{i_j} = 1$ for $j = n+1\ldots n+m$ and $\varepsilon_i = 1$, $\varepsilon'_i = -1$ for $i \in \{r,\ldots,r+k\}\setminus\{i_{n+1}, i_{n+2},\ldots,i_{n+m}\}$.

Thus

$$\Big\|\sum_{j=n+1}^{n+m} f_{i_j}(x)x_{i_j}\Big\| < \varepsilon\,, \quad i_{n+1} > n_0,\ n \in \mathbb{N}\,. \tag{3.1}$$

Therefore, for every $\{i_n\} \in \theta$, $\sum\limits_{i=1}^{\infty} f_{i_j}(x)x_{i_j}$ converges in E.

Assume on contrary that $\sum_{i=1}^{\infty} f_i(x)x_i$ does not converge unconditionally to x. Then, there exits a permutation σ of $\mathbb{N}$ for which $\sum_{i=1}^{\infty} f_{\sigma_i}(x)x_{\sigma_i}$ is not convergent. So, there exist an $\varepsilon_0 > 0$ and a sequence $\{m_n\} \in \theta$ such that

$$\left\| \sum_{i=m_n+1}^{m_{n+1}} f_{\sigma_i}(x)x_{\sigma_i} \right\| \geq \varepsilon_0 , \quad n = 1, 2, 3, \dots .$$

Choose an infinite subsequence $\{m_{n_j}\} \subset \{m_n\}$ such that

$$\min_{m_{n_{j+1}}+1 \leq i \leq m_{n_{j+1}+1}} \sigma_i > \max_{m_{n_j}+1 \leq i \leq m_{n_j+1}} \sigma_i , \quad j = 1, 2, 3, \dots$$

and rearrange the integers σ_i, $m_{n_j} + 1 \leq i \leq m_{n_{j+1}}$, $j = 1, 2, 3, \dots$ into an increasing sequence $\{i_j\}$. Then, $\sum_{j=1}^{\infty} f_{i_j}(x)x_{i_j}$ is not convergent, which contradicts (3.1).

References

[1] C. Bessaga and A. Pelczynski, A generalization of results of R.C. James concerning absolute bases in Banach spaces, Studia Math. 17 (1958), 165–174.

[2] P.G. Casazza and G. Kutyniok, Frames of subspaces, in wavelets, frames and operaor theory, Contemp. Math., 345, 87–113, Amer. Math. Soc., Providence, RI, 2004.

[3] O. Christensen, *An introducton to Frame and Riesz Bases*, Birkhäuser, 2003.

[4] O. Christensen and Y.C. Eldar, Oblique dual frames with shift-invariant spaces, Appl. Comput. Harmon. Anal., 17 (2004), 48–68.

[5] O. Christensen and C. Heil, Perturbation of Banach frames and atomic decompositions, Math. Nach. 185 (1997), 33–47.

[6] R.R. Coifman and G. Weiss, Extensions of Hardy spaces and their use in analysis, Bull. Amer. Math. Soc., 83 (1977), 569–645.

[7] I. Daubechies, A. Grossmann and Y. Meyer, Painless non-orthogonal expansions, J. Math. Physics, 27 (1986), 1271–1283.

[8] R.J. Duffin and A.C. Schaeffer, A class of non-harmonic Fourier series, Trans. Amer. Math. Soc., 72 (1952), 341-366.

[9] N. Dufford and J.T. Schwartz, *Linear Operators. Part I: General Theory*, New York: Intersci. Publ. (1958).

[10] Y.C. Eldar, Sampling with arbitrary sampling and reconstruction spaces and oblique dual frame vectors, J. Four. Anal. Appl. 9 (2003), 77-96.

[11] H.G. Feichtinger, Atomic characterizations of Modulation spaces through Gabor-Type Representation, Rocky Mountain J. Math. 19 (1989), 113-126.

[12] H.G. Feichtinger and K. Gröcheing, A unified approach to atomic decompositions via integrable group represnetations, In: Proc. Conf. "Function Spaces and Applications", Lecture Notes Math. 1302, Berlin -Heidelber -New York: Springer (1988), 52-73.

[13] M. Fornasier, Quasi-orthogonal decompositions of structured frames, J. Math. Anal. Appl., 289 (2004), 180–199.

[14] M. Fornasier, Decomposition of Hilbert spaces: Local constructions of global frames, in: B. Bojanorv (Ed.), Proc. In.: Conf. on Constructive Function Theory. Varna. 2002. DARBA. J. Sofia. 2003. pp. 271–281.

[15] M. Frazier and B. Jawerth, Decompositions of Besov spaces, Indiana Univ. Math. J., 34 (1985), 777-799.

[16] K. Gröchenig, Describing functions: Atomic decompositions versus frames, Monatsh. Math., 112 (1991), 1-41.

[17] P.K. Jain, S.K. Kaushik and Nisha Gupta, On near exact Banach frames in Banach spaces, Bull. Aust. Math. Soc., 78 (2008), 335-342.

[18] P.K. Jain, S.K. Kaushik and L.K. Vashisht, On perturbations of Banach frames, Internatioal Jour. of Wavelet, Multiresolution and Information Processing (IJWMIP) (World Scientific), 4 (3) (2006), 559–565.

[19] P.K. Jain, S.K. Kaushik and Varinder Kumar, Frame of subspaces, Internatioal Jour. of Wavelet, Multiresolution and Information Processing (IJWMIP) (World Scientific), (to appear).

[20] S. Li and H. Ogawa, Pseudoframes for subspaces with applications, J. Fourier Anal. Appl., 10 (2004), 409–431.

[21] A. Pelczynski, On the impossibility of embedding of the space L in certain Banach spaces, Colloq. Math. 8 (1961), 199–203.

[22] W. Sun, G-frames and g-Riesz bases, J. Math. Anal. Appl., 322 (2006), 437–452.

JOURNAL OF APPLIED FUNCTIONAL ANALYSIS, VOL.6, NO.4, 356-364, COPYRIGHT 2011 EUDOXUS PRESS, LLC

Complete convergences of rowwise $\tilde{\rho}$-mixing sequences of random variables[1]

Guang-hui Cai [2]

(Department of Mathematics and Statistics, Zhejiang Gongshang University, Hangzhou 310018, P. R. China)

Abstract In this paper, we study the complete convergences and strong law of large numbers of rowwise $\tilde{\rho}$-mixing sequences of random variables. The results obtained not only generalize the results of Hu (1998, Statist. Probab. Lett. 38, 27—31) to $\tilde{\rho}$-mixing sequence, but also improve them.

Key words $\tilde{\rho}$-mixing, Strong law of large numbers, Complete convergences

MSC 60F15

1 Introduction

Let nonempty sets $S, T \subset \mathcal{N}$, and define $\mathcal{F}_S = \sigma(X_k, k \in S)$, and the maximal correlation coefficient $\tilde{\rho}_n = \sup corr(f, g)$ where the supremum is taken over all (S, T) with $dist(S, T) \geq n$ and all $f \in L_2(\mathcal{F}_S)$, $g \in L_2(\mathcal{F}_T)$ and where $dist(S, T) = \inf_{x \in S, y \in T} |x - y|$.

Definition 1.1. a sequence of random variables $\{X_n, n \geq 1\}$ on a probability space $\{\Omega, \mathcal{F}, P\}$ is called $\tilde{\rho}$ -mixing if there exists $k \in N$, such that $\tilde{\rho}(k) < 1$.

As for $\tilde{\rho}$-mixing sequences of random variables, one can refer to Bryc and Smolenski(1993) found bounds for the moments of partial sums for a sequence of random variables satisfying

$$\lim_{n \to \infty} \tilde{\rho}(n) < 1.$$

Peligrad (1996) for CLT, Peligrad (1998) for invariance principles, Peligrad and Gut (1999) for the Rosenthal type maximal inequality, Yang (1998) for the moment inequalities and strong law of large numbers, Utev and Peligrad (2003) for invariance principles of nonstationary sequences. Gan (2004) for almost sure convergence.

As for complete convergences, let $\{X, X_n, n \geq 1\}$ be a sequence of independent indentically distribution random variables (i.i.d) random variables and denote $S_n = \sum_{i=1}^{n} X_i$. The Hsu-Robbins-Erdös law of large numbers (Hsu and Robbins, 1947; Erdös, 1949) states

[1] Research Supported by National Social Science Foundation of China(09BTJ003)

[2] Email address: cghzju@163.com

that

$$\forall \varepsilon > 0, \sum_{n=1}^{\infty} P(|S_n| > \varepsilon n) < \infty$$

is equivalent to $EX = 0$ and $EX^2 < \infty$.

This is a foundamental theorm in probability theory and has been intensively investigated by many authors in the past decades. We can see in Petrov (1995), Chow (1997) and Stout (1974). There have been many extensions in various directions for Hsu-Robbins-Erdös law of large numbers. Two of them are Hu (1998) showed that.

Theorem A Let $\{X, X_{ni}, i \geq 1\}$ be an rowwise independent sequence. If $\{c_n, n \geq 1\}$ be a positive numbers sequence such that $\sum_{n=1}^{\infty} c_n = \infty$. Suppose that $\forall \varepsilon > 0$ and $\forall \delta > 0$ such that

(i) $\sum_{n=1}^{\infty} c_n \sum_{k=1}^{k_n} P(|X_{nk}| > \varepsilon) < \infty$,

(ii) there exists $J \geq 2$ such that $\sum_{n=1}^{\infty} c_n (\sum_{k=1}^{k_n} E|X_{nk}|^2 I(|X_{nk}| \leq \delta))^J < \infty$

(iii) $\sum_{k=1}^{k_n} EX_{nk} I(|X_{nk}| \leq \delta) \to 0$ as $n \to \infty$.

Then

$$\forall \varepsilon > 0, \sum_{n=1}^{\infty} c_n P(|\sum_{k=1}^{k_n} X_{nk}| > \varepsilon) < \infty.$$

Theorem B Let $\{X, X_{ni}, i \geq 1\}$ be an rowwise independent sequence with $EX_{ni} = 0, \forall i \geq 1, n \geq 1$. And $P(|X_{ni}| > x) \leq CP(|X| > x), \forall x > 0, i \geq 1, n \geq 1$. If $\{a_{nk}, k \geq 1\}$ be a real numbers sequence, $\max_k |a_{nk}| = O(n^{-\alpha})$ for some $\alpha > 0$, let $\{a_{nk}, k \geq 1\}$ be a Toeplitz sequence and $E|X|^{1+\frac{1}{\alpha}} < \infty$, $0 < \alpha < 1$. Then $\sum_{i=1}^{n} a_{ni} X_{ni} \to 0$ completely as $n \to \infty$.

The main purpose of this paper is to study study the complete convergences and strong law of large numbers of rowwise $\tilde{\rho}$-mixing sequences of random variables. The results obtained not only generalize the results of Hu (1998, Statist. Probab. Lett. 38, 27—31, see Theorem A, Theorem B) to $\tilde{\rho}$-mixing sequence, but also improve them.

2 The mian results

Throughout this paper, C will represent a positive constant though its value may change from one appearance to the next, and $a_n = O(b_n)$ will mean $a_n \leq Cb_n$. And $a_n \ll b_n$ will mean $a_n = O(b_n)$.

In order to prove our results, we need the following lemma.

Lemma 1 (Utev and Peligrad, 2003) Let $\{X_i, i \geq 1\}$ be a $\tilde{\rho}$-mixing sequence of random variables, $EX_i = 0, E|X_i|^p < \infty$ for some $p \geq 2$ and for every $i \geq 1$. Then there exists $C = C(p)$, such that

$$E \max_{1 \le k \le n} |\sum_{i=1}^{k} X_i|^p \le C\{\sum_{i=1}^{n} E|X_i|^p + (\sum_{i=1}^{n} EX_i^2)^{p/2}\}.$$

Theorem 1 Let $\{X, X_{ni}, i \ge 1\}$ be an rowwise $\tilde{\rho}$-mixing sequence with $EX_{ni} = 0, \forall i \ge 1, n \ge 1$. And $P(|X_{ni}| > x) \le CP(|X| > x), \forall x > 0, i \ge 1, n \ge 1$. If $\{a_{nk}, k \ge 1\}$ be a real numbers sequence, $\max_k |a_{nk}| = O(n^{-\alpha})$ for some $\alpha > 0$ and $E|X|^{1+\frac{1}{\alpha}} < \infty$, $\alpha \ge 1$. Then

$$\forall \varepsilon > 0, \sum_{n=1}^{\infty} P(\max_{1 \le j \le n} |\sum_{i=1}^{j} a_{ni} X_{ni}| > \varepsilon) < \infty. \tag{1}$$

Proof of Theorem 1

$\forall i \ge 1$, define $X_{ni}^{(n)} = X_{ni} I(|X_{ni}| \le n^\alpha)$, $S_{nj}^{(n)} = \sum_{i=1}^{j} (X_{ni}^{(n)} - EX_{ni}^{(n)})$. By $\max_k |a_{nk}| = O(n^{-\alpha})$ for some $\alpha > 0$. $\forall \varepsilon > 0$, Then

$$\begin{aligned}
&P(\max_{1 \le j \le n} |\sum_{i=1}^{j} a_{ni} X_{ni}| > \varepsilon) \\
&\le P(\max_{1 \le j \le n} |\sum_{i=1}^{j} X_{ni}| > \varepsilon C n^\alpha) \\
&\le P(\max_{1 \le j \le n} |X_{nj}| > n^\alpha) + P(\max_{1 \le j \le n} |S_{nj}^{(n)}| > \varepsilon C n^\alpha - \max_{1 \le j \le n} |\sum_{i=1}^{j} EX_{ni}^{(n)}|).
\end{aligned} \tag{2}$$

First we show that, when $n \to \infty$,

$$n^{-\alpha} \max_{1 \le j \le n} |\sum_{i=1}^{j} EX_{ni}^{(n)}| \to 0. \tag{3}$$

In fact, i) If $\alpha > 1$, when $n \to \infty$, then

$$\begin{aligned}
&n^{-\alpha} \max_{1 \le j \le n} |\sum_{i=1}^{j} EX_{ni}^{(n)}| \\
&\le n^{-\alpha} \sum_{i=1}^{n} E|X_{ni}| I(|X_{ni}| \le n^\alpha) \\
&\le n^{-\alpha} CnE|X| I(|X| \le n^\alpha) \\
&= Cn^{1-\alpha} E|X| I(|X| \le n^\alpha) \\
&\to 0.
\end{aligned} \tag{4}$$

ii) If $\alpha = 1$, noting that $EX_{ni} = 0, \forall i \ge 1, n \ge 1$. When $n \to \infty$, it follows that

$$n^{-\alpha} \max_{1 \le j \le n} |\sum_{i=1}^{j} EX_{ni}^{(n)}|$$

3

$$\begin{aligned}
&\le n^{-\alpha}\sum_{i=1}^{n} E|X_{ni}|I(|X_{ni}|>n^{\alpha})\\
&\le Cn^{-\alpha}nE|X|I(|X|>n^{\alpha})\\
&\le Cn^{1-\alpha}E|X|^{1+\frac{1}{\alpha}}I(|X|>n^{\alpha})(n^{\alpha})^{-\frac{1}{\alpha}}\\
&= Cn^{-\alpha}E|X|^{1+\frac{1}{\alpha}}I(|X|>n^{\alpha})\\
&\to 0. \qquad (5)
\end{aligned}$$

From (4) and (5), which imply (3).

From (2) and (3) it follows that for n large enough

$$P(\max_{1\le j\le n}|\sum_{i=1}^{j} a_{ni}X_{ni}|>\varepsilon Cn^{\alpha})\le \sum_{j=1}^{n} P(|X_{nj}|>n^{\alpha})+P(\max_{1\le j\le n}|S_{nj}^{(n)}|>\frac{\varepsilon}{2}Cn^{\alpha}). \qquad (6)$$

Hence we need only to prove that

$$I=:\sum_{n=1}^{\infty}\sum_{j=1}^{n} P(|X_{nj}|>n^{\alpha})<\infty; \qquad (7)$$

$$II=:\sum_{n=1}^{\infty} P(\max_{1\le j\le n}|S_{nj}^{(n)}|>\frac{\varepsilon}{2}Cn^{\alpha})<\infty. \qquad (8)$$

From the fact that $E|X|^{1+\frac{1}{\alpha}}<\infty$, it follows easily that

$$\begin{aligned}
I &\le \sum_{n=1}^{\infty} CnP(|X|>n^{\alpha})\\
&\ll E|X|^{1+\frac{1}{\alpha}}<\infty. \qquad (9)
\end{aligned}$$

By Markov inequality and Lemma 1, it follows that

$$\begin{aligned}
II &\ll \sum_{n=1}^{\infty} n^{-\alpha q}E\max_{1\le j\le n}|S_{nj}^{(n)}|^{q}\\
&\ll \sum_{n=1}^{\infty} n^{-\alpha q}\{\sum_{j=1}^{n} E|X_{nj}^{(n)}|^{q}+(\sum_{j=1}^{n} E|X_{nj}^{(n)}|^{2})^{q/2}\}\\
&=: II_1+II_2. \qquad (10)
\end{aligned}$$

1) If $\alpha>1$, let $q=2$. Then one can show that

$$\begin{aligned}
II_1 &\ll \sum_{n=1}^{\infty} n^{-\alpha q+1}E|X|^{q}I(|X|\le n^{\alpha})\\
&= \sum_{n=1}^{\infty} n^{-\alpha q+1}\sum_{k=1}^{n} E|X|^{q}I(k-1<|X|^{\frac{1}{\alpha}}\le k)
\end{aligned}$$

$$
\begin{aligned}
&= \sum_{k=1}^{\infty}\sum_{n=k}^{\infty} n^{-\alpha q+1} E|X|^q I(k-1 < |X|^{\frac{1}{\alpha}} \le k) \\
&\le \sum_{k=1}^{\infty}\sum_{n=k}^{\infty} n^{-\alpha q+1} P(k-1 < |X|^{\frac{1}{\alpha}} \le k) k^{\alpha q} \\
&\ll \sum_{k=1}^{\infty} k^2 P(k-1 < |X|^{\frac{1}{\alpha}} \le k) \\
&\ll E|X|^{\frac{2}{\alpha}} \\
&\ll E|X|^{1+\frac{1}{\alpha}} < \infty. \qquad (11)
\end{aligned}
$$

2) If $\alpha = 1$, let $q > 2$. Then

$$
\begin{aligned}
II_1 &\ll \sum_{n=1}^{\infty} n^{-\alpha q+1} E|X|^q I(|X| \le n^{\alpha}) \\
&= \sum_{n=1}^{\infty} n^{-\alpha q+1} \sum_{k=1}^{n} E|X|^q I(k-1 < |X|^{\frac{1}{\alpha}} \le k) \\
&= \sum_{k=1}^{\infty}\sum_{n=k}^{\infty} n^{-\alpha q+1} E|X|^q I(k-1 < |X|^{\frac{1}{\alpha}} \le k) \\
&\le \sum_{k=1}^{\infty}\sum_{n=k}^{\infty} n^{-\alpha q+1} P(k-1 < |X|^{\frac{1}{\alpha}} \le k) k^{\alpha q} \\
&\ll \sum_{k=1}^{\infty} k^2 P(k-1 < |X|^{\frac{1}{\alpha}} \le k) \\
&\ll E|X|^{\frac{2}{\alpha}} \\
&= E|X|^{1+\frac{1}{\alpha}} < \infty. \qquad (12)
\end{aligned}
$$

3) If $\alpha > 1$, by $q = 2$. Then

$$
II_2 = II_1 < \infty. \qquad (13)
$$

4) If $\alpha = 1$, by $E|X|^{1+\frac{1}{\alpha}} < \infty$ and $q > 2$. Then

$$
II_2 \ll \sum_{n=1}^{\infty} n^{-\alpha q}(nE|X|^2)^{q/2} \ll \sum_{n=1}^{\infty} n^{-q/2} < \infty. \qquad (14)
$$

Putting (11), (12), (13) and (14) into (10) yields $II < \infty$. Now we complete the prove of Theorem 1.

Remark 1 Using Theorem 1, we can get Corollary 2 in Hu (1998). And Theorem 1 doesnot need the condition of $\{a_{nk}, k \ge 1\}$ be a Toeplitz sequence. So Theorem 1 not only generalizes the results of Hu (1998, Statist. Probab. Lett. 38, 27—31) to $\tilde{\rho}$-mixing sequence, but also improve them.

Remark 2 Let $\alpha = 1$, $a_{ni} = n^{\alpha}, i \geq 1$ in Theorem 1, then we can get Corollary 2.2 in Gan (2004).

Recall that $\{a_{nk}, k \geq 1\}$ be a Toeplitz sequence if $\lim_{n\to\infty} a_{nk} = 0$ for each k and $\sum_{k=1}^{n} |a_{nk}| \leq C$ for each n.

Theorem 2 Let $\{X, X_{ni}, i \geq 1\}$ be an rowwise $\tilde{\rho}$-mixing sequence with $EX_{ni} = 0, \forall i \geq 1, n \geq 1$. And $P(|X_{ni}| > x) \leq CP(|X| > x), \forall x > 0, i \geq 1, n \geq 1$. If $\{a_{nk}, k \geq 1\}$ be a real numbers sequence, $\max\limits_{k} |a_{nk}| = O(n^{-\alpha})$ for some $\alpha > 0$, let $\{a_{nk}, k \geq 1\}$ be a Toeplitz sequence and $E|X|^{1+\frac{1}{\alpha}} < \infty$, $0 < \alpha < 1$. Then

$$\forall \varepsilon > 0, \sum_{n=1}^{\infty} P(\max_{1\leq j\leq n} |\sum_{i=1}^{j} a_{ni} X_{ni}| > \varepsilon) < \infty. \tag{15}$$

Proof of Theorem 2

Because $\{a_{nk}, k \geq 1\}$ be a Toeplitz sequence, then $\sum_{k=1}^{n} |a_{nk}| \leq C$ for each n. And by $\max\limits_{k} |a_{nk}| = O(n^{-\alpha})$. Then for any $q \geq 2$, we have

$$\sum_{k=1}^{n} |a_{nk}|^q = \sum_{k=1}^{n} |a_{nk}||a_{nk}|^{q-1} \ll n^{-\alpha(q-1)} \tag{16}$$

$\forall i \geq 1$, define $X_{ni}^{(n)} = X_{ni} I(|X_{ni}| \leq n^{\alpha})$, $T_{nj}^{(n)} = \sum\limits_{i=1}^{j} (a_{ni} X_{ni}^{(n)} - Ea_{ni} X_{ni}^{(n)})$. By $\max\limits_{k} |a_{nk}| = O(n^{-\alpha})$ for some $\alpha > 0$. $\forall \varepsilon > 0$, Then

$$\begin{aligned} &P(\max_{1\leq j\leq n} |\sum_{i=1}^{j} a_{ni} X_{ni}| > \varepsilon) \\ &\leq P(\max_{1\leq j\leq n} |X_{nj}| > n^{\alpha}) + P(\max_{1\leq j\leq n} |T_{nj}^{(n)}| > \varepsilon - \max_{1\leq j\leq n} |\sum_{i=1}^{j} Ea_{ni} X_{ni}^{(n)}|). \end{aligned} \tag{17}$$

First we show that, when $n \to \infty$,

$$\max_{1\leq j\leq n} |\sum_{i=1}^{j} Ea_{ni} X_{ni}^{(n)}| \to 0. \tag{18}$$

In fact, $EX_{ni} = 0, \forall i \geq 1, n \geq 1$, and $0 < \alpha < 1$, when $n \to \infty$, then

$$\begin{aligned} &\max_{1\leq j\leq n} |\sum_{i=1}^{j} Ea_{ni} X_{ni}^{(n)}| \\ &= \max_{1\leq j\leq n} |\sum_{i=1}^{j} Ea_{ni} X_{ni} I(|X_{ni}| > n^{\alpha})| \end{aligned}$$

$$\begin{aligned}
&\le \sum_{i=1}^{n} |Ea_{ni}X_{ni}I(|X_{ni}| > n^{\alpha})| \\
&\ll \sum_{i=1}^{n} |a_{ni}|E|X|I(|X| > n^{\alpha}) \\
&\le Cn^{-1}E|X|^{1+\frac{1}{\alpha}}I(|X| > n^{\alpha}) \\
&\to 0. \qquad (19)
\end{aligned}$$

From (19), which imply (18).

From (17) and (18) it follows that for n large enough

$$P(\max_{1\le j\le n} |\sum_{i=1}^{j} a_{ni}X_{ni}| > \varepsilon) \le \sum_{j=1}^{n} P(|X_{nj}| > n^{\alpha}) + P(\max_{1\le j\le n} |T_{nj}^{(n)}| > \frac{\varepsilon}{2}). \qquad (20)$$

Hence we need only to prove that

$$I =: \sum_{n=1}^{\infty}\sum_{j=1}^{n} P(|X_{nj}| > n^{\alpha}) < \infty; \qquad (21)$$

$$II =: \sum_{n=1}^{\infty} P(\max_{1\le j\le n} |T_{nj}^{(n)}| > \frac{\varepsilon}{2}) < \infty. \qquad (22)$$

From the fact that $E|X|^{1+\frac{1}{\alpha}} < \infty$, it follows easily that

$$\begin{aligned}
I \quad &\le \sum_{n=1}^{\infty} CnP(|X| > n^{\alpha}) \\
&\ll E|X|^{1+\frac{1}{\alpha}} < \infty. \qquad (23)
\end{aligned}$$

By Markov inequality and Lemma 1, it follows that

$$\begin{aligned}
II \quad &\ll \sum_{n=1}^{\infty} E\max_{1\le j\le n} |T_{nj}^{(n)}|^{q} \\
&\ll \sum_{n=1}^{\infty}\{\sum_{j=1}^{n} E|a_{nj}X_{nj}^{(n)}|^{q} + (\sum_{j=1}^{n} E|a_{nj}X_{nj}^{(n)}|^{2})^{q/2}\} \\
&=: II_1 + II_2. \qquad (24)
\end{aligned}$$

By $0 < \alpha < 1$, let $q > 1 + \frac{1}{\alpha}$. Then one can show that

$$\begin{aligned}
II_1 \quad &= \sum_{n=1}^{\infty}\sum_{j=1}^{n} |a_{ni}|^{q}E|X_{nj}^{(n)}|^{q} \\
&\ll \sum_{n=1}^{\infty} n^{-\alpha(q-1)}E|X|^{q}I(|X| \le n^{\alpha})
\end{aligned}$$

$$\begin{aligned}
&= \sum_{n=1}^{\infty} n^{-\alpha(q-1)} \sum_{k=1}^{n} E|X|^q I(k-1 < |X|^{\frac{1}{\alpha}} \le k) \\
&= \sum_{k=1}^{\infty} \sum_{n=k}^{\infty} n^{-\alpha(q-1)} E|X|^q I(k-1 < |X|^{\frac{1}{\alpha}} \le k) \\
&\le \sum_{k=1}^{\infty} \sum_{n=k}^{\infty} n^{-\alpha(q-1)} P(k-1 < |X|^{\frac{1}{\alpha}} \le k) k^{\alpha q} \\
&\ll \sum_{k=1}^{\infty} k^{\alpha+1} P(k-1 < |X|^{\frac{1}{\alpha}} \le k) \\
&\ll E|X|^{1+\frac{1}{\alpha}} < \infty. \qquad (25)
\end{aligned}$$

By $0 < \alpha < 1$, let $q > 2/\alpha$. Then

$$\begin{aligned}
II_2 &= \sum_{n=1}^{\infty} (\sum_{j=1}^{n} |a_{ni}|^2 E|X_{nj}^{(n)}|^2)^{q/2} \\
&\ll \sum_{n=1}^{\infty} n^{-\alpha q/2} (E|X|^2)^{q/2} \\
&\ll \sum_{n=1}^{\infty} n^{-\alpha q/2} < \infty. \qquad (26)
\end{aligned}$$

Putting (25) and (26) into (24) yields $II < \infty$. Now we complete the prove of Theorem 2.

Theorem 3 Let $\{X, X_{ni}, i \ge 1\}$ be an rowwise $\tilde{\rho}$-mixing sequence. If $\{c_n, n \ge 1\}$ be a positive numbers sequence, $\forall \varepsilon > 0$ and $\exists \delta > 0$ such that
$\sum_{n=1}^{\infty} c_n \sum_{k=1}^{k_n} P(|X_{ni}| > \frac{\varepsilon}{k_n}) < \infty$,
$\sum_{n=1}^{\infty} c_n \sum_{k=1}^{k_n} E|X_{nk}|^2 I(|X_{nk}| \le \delta) < \infty$
and $\sum_{k=1}^{k_n} E|X_{nk}| I(|X_{nk}| \le \delta) \to 0$ as $n \to \infty$.
Then

$$\forall \varepsilon > 0, \sum_{n=1}^{\infty} c_n P(|\sum_{k=1}^{k_n} X_{nk}| > \varepsilon) < \infty. \qquad (27)$$

Proof of Theorem 3

$\forall i \ge 1$, define $X_{ni}^{(n)} = X_{ni} I(|X_{ni}| \le \delta)$, $S_{nj}^{(n)} = \sum_{i=1}^{j} (X_{ni}^{(n)} - EX_{ni}^{(n)})$.
By $\sum_{k=1}^{k_n} E|X_{nk}| I(|X_{nk}| \le \delta) \to 0$ as $n \to \infty$.
Then $\max_{1 \le j \le k_n} |\sum_{k=1}^{j} X_{nk}^{(n)}| \le \max_{1 \le j \le k_n} \sum_{k=1}^{j} |X_{nk}| I(|X_{nk}| \le \delta) \to 0$ as $n \to \infty$.
By Markov inequality and Lemma 1, then

$$\begin{aligned}
&\sum_{n=1}^{\infty} c_n P(|\sum_{k=1}^{k_n} X_{nk}| > \varepsilon) \\
&\le \sum_{n=1}^{\infty} c_n P(\max_{1 \le j \le k_n} |\sum_{k=1}^{j} X_{nk}| > \varepsilon) + \sum_{n=1}^{\infty} c_n P(|\sum_{k=1}^{k_n} X_{ni}^{(n)}| > \varepsilon - \max_{1 \le j \le k_n} |\sum_{k=1}^{j} X_{nk}^{(n)}|)
\end{aligned}$$

8

$$
\begin{aligned}
&\leq \sum_{n=1}^{\infty} c_n P(\sum_{k=1}^{k_n} |X_{nk}| > \varepsilon) + \sum_{n=1}^{\infty} c_n P(|\sum_{k=1}^{k_n} X_{ni}^{(n)}| > \varepsilon/2) \\
&\leq \sum_{n=1}^{\infty} c_n \sum_{k=1}^{k_n} P(|X_{nk}| > \varepsilon/k_n) + \sum_{n=1}^{\infty} c_n \frac{E|\sum_{k=1}^{k_n} X_{ni} I(|X_{nk}| \leq \delta)|^2}{(\varepsilon/2)^2} \\
&\leq \sum_{n=1}^{\infty} c_n \sum_{k=1}^{k_n} P(|X_{nk}| > \varepsilon/k_n) + (\varepsilon/2)^{-2} \sum_{n=1}^{\infty} c_n \sum_{k=1}^{k_n} E|X_{nk}|^2 I(|X_{nk}| \leq \delta) \\
&< \infty. \qquad (28)
\end{aligned}
$$

Now we complete the prove of Theorem 3.

Remark 3 Theorem 3 generalizes Theorem in Hu (1998) to rowwise $\tilde{\rho}$-mixing sequence.

Reference

[1] Bryc,W., Smolenski,W., 1993. Moment conditions for almost sure convergence of weakly correlated random variables. Proc. Amer. Math. Soc. 2, 629—635.

[2] Chow, Y. S. and Teicher, H. 1997. Probability Theory: Independence, Interchangeability, Martingales, Springer-Verlag, New York, 3rd ed.

[3] Erdös, P. 1949. On a theorem of Hsu-Robbins. Ann. Math. Statist. 20, 286—291.

[4] Gan, S. 2004. Almost sure convergence for $\tilde{\rho}$-mixing random variable sequences. Statist. Probab. Lett. 67, 289—298.

[5] Hsu, P. L. and Robbins, H. 1947. Complete convergence and the law of larege numbers. Proc. Nat. Acad. Sci. (USA), 33(2), 25—31.

[6] Hu, T. C., Szynal, D. and Volodin, A. I. 1998. A note on complete convergence for arrays. Stat. Prob. Lett. 38, 27—31.

[7] Peligrad, M. 1996. On the asymptotic normality of sequences of weak dependent random variables. J. Theoret. Probab. 9, 703—715.

[8] Peligrad, M. 1998. Maximum of partial sums and an invariance principle for a class weak depend random variables. Proc. Amer. Math. Soc. 126(4), 1181—1189.

[9] Peligrad, M. and Gut, A. 1999. Almost sure results for a class of dependent random variables. J. Theoret. Probab. 12, 87—104.

[10] Petrove, V. V. 1995. Limit theorems of probability theory sequences of independent random variables, Oxford, Oxford Science Publications.

[11] Stout, W. 1974. Almost sure convergence. New York, Academic Press.

[12] Utev, S. and Peligrad, M., 2003. Maximal inequalities and an invariance principle for a class of weakly dependent random variables. J. Theoret. Probab. 16, 101—115.

Instructions to Contributors
Journal of Applied Functional Analysis

A quartely international publication of Eudoxus Press, LLC of TN.

Editor in Chief: George Anastassiou

Department of Mathematical Sciences
University of Memphis
Memphis, TN 38152-3240, U.S.A.

1. Manuscripts, hard copies in quadruplicate and in English,should be submitted by regular, unregistered mail, to the Editor in Chief.

Authors may want to recommend an associate editor most related to the submission to possibly handle it. In addition, to assist the Editor and speed the decision process, authors may include a PDF file of the paper on disk with the submitted copies of the manuscript.

Also authors may want to submit a list of six possible referees, to be used in case we cannot find related referees by ourselves.

2. Manuscripts should be typed using any of TEX,LaTEX,AMS-TEX,or AMS-LaTEX and according to EUDOXUS PRESS, LLC. LATEX STYLE FILE. (Click HERE to save a copy of the style file.)They should be carefully prepared in all respects. Submitted copies should be brightly printed (not dot-matrix), double spaced, in ten point type size, on one side high quality paper 8(1/2)x11 inch. Manuscripts should have generous margins on all sides and should not exceed 24 pages.

3. Submission is a representation that the manuscript has not been published previously in this or any other similar form and is not currently under consideration for publication elsewhere. A statement transferring from the authors(or their employers,if they hold the copyright) to Eudoxus Press, LLC, will be required before the manuscript can be accepted for publication.The Editor-in-Chief will supply the necessary forms for this transfer.Such a written transfer of copyright,which previously was assumed to be implicit in the act of submitting a manuscript,is necessary under the U.S.Copyright Law in order for the publisher to carry through the dissemination of research results and reviews as widely and effective as possible.

4. The paper starts with the title of the article, author's name(s) (no titles or degrees), author's affiliation(s) and e-mail addresses. The affiliation should comprise the department, institution (usually university or company), city, state (and/or nation) and mail code.

The following items, 5 and 6, should be on page no. 1 of the paper.

5. An abstract is to be provided, preferably no longer than 150 words.

6. A list of 5 key words is to be provided directly below the abstract. Key words should express the precise content of the manuscript, as they are used for indexing purposes.

The main body of the paper should begin on page no. 1, if possible.

7. All sections should be numbered with Arabic numerals (such as: 1. INTRODUCTION) .
Subsections should be identified with section and subsection numbers (such as 6.1. Second-Value Subheading).
If applicable, an independent single-number system (one for each category) should be used to label all theorems, lemmas, propositions, corrolaries, definitions, remarks, examples, etc. The label (such as Lemma 7) should be typed with paragraph indentation, followed by a period and the lemma itself.

8. Mathematical notation must be typeset. Equations should be numbered consecutively with Arabic numerals in parentheses placed flush right,and should be thusly referred to in the text [such as Eqs.(2) and (5)]. The running title must be placed at the top of even numbered pages and the first author's name, et al., must be placed at the top of the odd numbed pages.

9. Illustrations (photographs, drawings, diagrams, and charts) are to be numbered in one consecutive series of Arabic numerals. The captions for illustrations should be typed double space. All illustrations, charts, tables, etc., must be embedded in the body of the manuscript in proper, final, print position. In particular, manuscript, source, and PDF file version must be at camera ready stage for publication or they cannot be considered.

Tables are to be numbered (with Roman numerals) and referred to by number in the text. Center the title above the table, and type explanatory footnotes (indicated by superscript lowercase letters) below the table.

10. List references alphabetically at the end of the paper and number them consecutively. Each must be cited in the text by the appropriate Arabic numeral in square brackets on the baseline.
References should include (in the following order):
initials of first and middle name, last name of author(s)
title of article,
name of publication, volume number, inclusive pages, and year of publication.

Authors should follow these examples:

<u>Journal Article</u>

1. H.H.Gonska,Degree of simultaneous approximation of bivariate functions by Gordon operators, (journal name in italics) *J. Approx. Theory*, 62,170-191(1990).

<u>Book</u>

2. G.G.Lorentz, (title of book in italics) *Bernstein Polynomials* (2nd ed.), Chelsea,New York,1986.

<u>Contribution to a Book</u>

3. M.K.Khan, Approximation properties of beta operators,in(title of book in italics) *Progress in Approximation Theory* (P.Nevai and A.Pinkus,eds.), Academic Press, New York,1991,pp.483-495.

11. All acknowledgements (including those for a grant and financial support) should occur in one paragraph that directly precedes the References section.

12. Footnotes should be avoided. When their use is absolutely necessary, footnotes should be numbered consecutively using Arabic numerals and should be typed at the bottom of the page to which they refer. Place a line above the footnote, so that it is set off from the text. Use the appropriate superscript numeral for citation in the text.

13. After each revision is made please again submit four hard copies of the revised manuscript. And after a manuscript has been accepted for publication submit four hard copies of the final revised manuscript. Additionally, two copies of the final version of the TEX/LaTex source file and a PDF file, are to be submitted to the Editor's Office on personal 3.5 inch computer disks. Label the disks individually with clearly written identifying information, e.g. :

Your name, title of article, kind of computer used, kind of software and version number, disk format and files names of article, as well as abbreviated journal name.

Package the disks in a disk mailer or protective cardboard. Make sure contents of disks are identical with the ones of final hard copies submitted!

Note: The Editor's Office cannot accept the disks without the accompanying matching hard copies of manuscript. No e-mail final submissions are allowed! File submission on disk must be used.

14. Effective 1 Nov. 2009 for current journal page charges, contact the Editor in Chief. Upon acceptance of the paper an invoice will be sent to the contact author. The fee payment will be due one month from the invoice date. The article will proceed to publication only after the fee is paid. The charges are to be sent, by money order or certified check, in US dollars, payable to Eudoxus Press, LLC, to the address shown on the Eudoxus <u>homepage</u>.

No galleys will be sent and the contact author will receive one(1) electronic copy of the journal issue in which the article appears.

15. This journal will consider for publication only papers that contain proofs for their listed results.

TABLE OF CONTENTS, JOURNAL OF APPLIED FUNCTIONAL ANALYSIS, VOLUME 6, NO.4, 2011